xrm2010

the 10th international conference on x-ray microscopy

chicago, illinois, usa

august 15-20, 2010

Conference Information and Abstracts

International Program Committee
Chris Jacobsen (Chair), *APS/ Northwestern University, USA*
Günter Schmahl (Emeritus), University of Göttingen, Germany
Janos Kirz (Emeritus), *Lawrence Berkeley National Laboratory, USA*
Sadao Aoki, *University of Tsukuba, Japan*
David Attwood, *University of California at Berkeley, USA*
Henry Chapman, *University of Hamburg and DESY, Germany*
Hans Hertz, *Royal Institute of Technology, Sweden*
Adam Hitchcock, *McMaster University, Canada*
Maya Kiskinova, *ELETTRA, Italy*
Ian McNulty, *APS, Argonne National Laboratory, USA*
Graeme Morrison, *Kings College, UK*
Keith Nugent, *University of Melbourne, Australia*
Christoph Quitmann, *Paul Scherrer Institut, Switzerland*
Gerd Schneider, *BESSY, Germany*
Hyun-Joon Shin, *Pohang Accelerator Laboratory, South Korea*
Jean Susini, *ESRF, France*
Mau-Tsu Tang, *NSRRC, Taiwan*
Wenbing Yun*, Xradia Inc., USA*
Peiping Zhu, *BSRF, China*

Local Organizing Committee
Ian McNulty, *Chair*
Rose Torres, *Conference Coordinator*
Catherine Eyberger, *Conference Editor*
Constance A. Vanni, *Exhibits Coordinator*
Jonas Downey, *Web Developer*
Ross Harder
Barry Lai
Wenjun Liu
Jörg Maser
Steve Sutton
Stefan Vogt
Robert Winarski

This volume is published by Argonne National Laboratory, a U.S. Department of Energy laboratory managed by UChicago Argonne, LLC.

10th International Conference on X-ray Microscopy

Sheraton Chicago Hotel and Towers
Chicago, Illinois USA

August 15-20, 2010

XRM2010 Gold Sponsors

SKYSCAN
X-RAY MICROTOMOGRAPHY
www.skyscan.be

xradia™
insight in 3D

NORTH STAR IMAGING, INC.

nanoV

XRM2010 Exhibitors

attocube systems
explore your nanoworld

ENERGETIQ

LUXEL

SCANCO MEDICAL

vsg
Visualization Sciences Group

Spectral Instruments

TABLE of CONTENTS

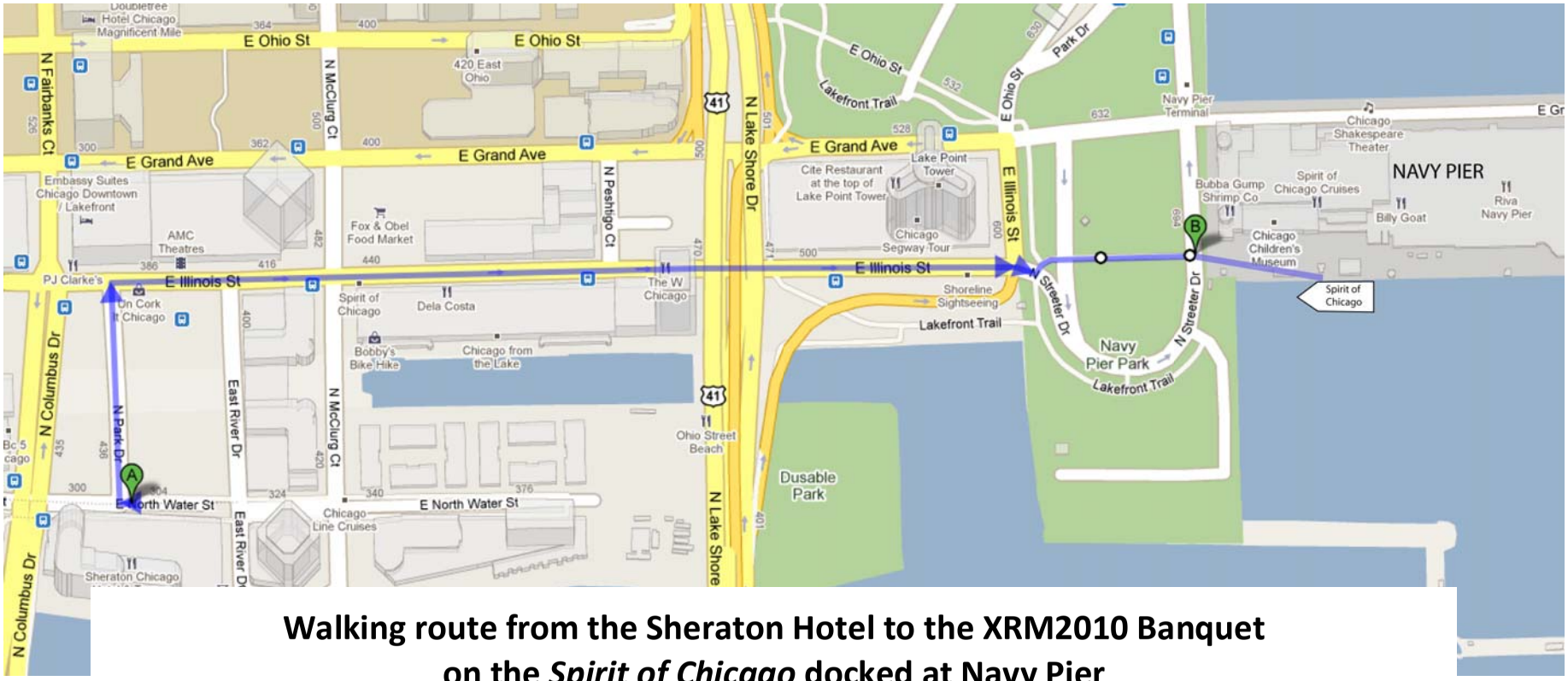

Walking route from the Sheraton Hotel to the XRM2010 Banquet on the *Spirit of Chicago* docked at Navy Pier

A is the Sheraton Hotel; B is the entrance to Navy Pier

General Conference Information

Introduction

The 10th International Conference on X-ray Microscopy, organized by Argonne National Laboratory, is being held at the Sheraton Hotel and Towers in Chicago, Illinois, USA. This international conference is a gathering for the presentation and discussion of advances in high-resolution x-ray imaging and its application to understanding a broad field of scientific questions. The conference aims to present new advances in the capabilities and uses of state-of-the-art, high-resolution x-ray microscopy techniques.

This year's conference has 24 invited speakers, 41 contributed oral speakers, and 13 vendors. Program topics fall into the following seven categories: X-ray Facilities, Instruments, and Optics; X-ray Microscopy Methods; Environmental, Earth, and Space Science; Materials and Condensed Matter; Magnetism and Magnetic Materials; Biological and Biomedical Science; and Emerging Fields in X-ray Microscopy.

The conference opens with a Welcome by Dr. Eric Isaacs, Director of Argonne National Laboratory, at 08:15 on Monday, August 16. Sessions will generally start at 08:30 and finish at 18:00 with morning and afternoon breaks for coffee and a 1½- hour lunch break around 12:00 (see the Program-at-a-Glance on the back cover). This Conference Information and Abstract book contains abstracts of contributions accepted for presentation at the conference, together with some useful information concerning the activities taking place during the conference.

Conference Venue

The address and telephone numbers of the Sheraton Hotel and Towers are:

Sheraton Chicago Hotel & Towers
301 East North Water Street
Chicago, Illinois 60611 USA
Telephone: 1 312.464.1000
Fax: 1 312.464.9140
Email: info@sheratonchicago.com

Registration/Information Desk

Registration materials (i.e., conference badge, banquet tickets) will be available at the registration and information desk located in the hallway outside Chicago Ballrooms VI – X on the 4th floor (see map inside the back cover) during the following times:

Registration and Information Desk hours:

Sunday, August 15	17:00 – 19:00 (at the Welcome Reception on the 3rd floor)
Monday, August 16	07:30 – 17:00
Tuesday, August 17	07:30 – 17:00
Wednesday, August 18	07:30 – 17:00
Thursday, August 19	08:00 – 12:00
Friday, August 20	08:00 – 12:00

The fee for standard registration (after May 1) is $850 (US$). For participants whose registration fees were not received in full prior to the conference, the difference will be requested of them upon registration. Payment at the Registration Desk must be by credit card (VISA, MasterCard), check (US$), or in cash (US$).

The conference fee includes the Sunday Welcome Reception. Tickets for the conference Banquet on Wednesday, August 18, may be purchased for $75 (US$) at the XRM2010 Registration Desk through Wednesday morning.

A Message Board will be located near the Registration Desk. *If you need assistance*, please ask anyone wearing a blue XRM2010 Conference shirt.

Security and Insurance

Participants are asked not to leave their baggage or conference bags unattended and to wear conference badges at all times. The conference organizers cannot accept liability for personal injuries sustained, or for loss of, or damage to, property belonging to conference participants (or accompanying persons), either during or as a result of the conference. Please check the validity of your own insurance.

Conference Social Program

WELCOME RECEPTION, SUNDAY, AUGUST 15 All conference attendees and companions are invited to an *hors d'oeuvres* reception on the third (street level) floor in the Java Bar / Chi Bar area of the Sheraton Hotel from 17:00 to 19:00. See the map inside the back cover.

CONFERENCE BANQUET, WEDNESDAY, AUGUST 18 The XRM2010 banquet will be aboard the *Spirit of Chicago* on Lake Michigan. Departing from Navy Pier, the *Spirit of Chicago* offers a most unique entertainment experience that combines nautical breezes, sumptuous cuisine, and incredible skyline views. The *Spirit of Chicago* will begin boarding from Navy Pier at 18:00 and will set sail at 19:00. A map of the walking route (0.6 miles) to Navy Pier is on page 4.

PLEASE NOTE: For men, appropriate attire includes slacks and a polo or button-down shirt. For women, nice slacks, Capri pants, or a casual dress is recommended. Collarless t-shirts, jeans, shorts, or sneakers are strongly discouraged.

Scientific Program

An overview of the sessions and detailed abstracts of each paper are included in this book. The scientific program is organized as follows:

INVITED PAPERS AND ORAL CONTRIBUTED PAPERS Invited papers and Oral Contributed Papers will be presented in Chicago Ballrooms VIII, IX, and X (4th floor) each day from 08:30 to approximately 17:30.

POSTER SESSIONS Two poster sessions are scheduled for the afternoons of Tuesday, August 17, and Thursday, August 19, from 17:30 to 19:30 in Chicago Ballrooms VI and VII (4th floor). (See the map inside the back cover of this book.) Each poster will be mounted on a cork board with a maximum display area of 47” (119 cm) wide by 44” (111 cm) high. The standard metric size A0 (84.1 cm x 118.9 cm or 33.1" x 46.8") would fit into this area.

Posters can be mounted as early as the day preceding the poster session but no later than one hour before the poster session begins. Each poster must be manned at least through a major part of the session and removed immediately after the end of each session. Conference personnel will be available on Monday and Wednesday afternoons to assist authors.

Speaker Ready Room

A Speaker Ready Room is located in the Arkansas Room on the 2nd floor (see map on page 8). Speakers can test their PowerPoint presentations on these computers prior to giving their talks.

Breaks and Meals

Refreshment breaks are generally at 10:20 and 15:00. Lunch breaks are from 12:00 to 13:30 with the exception of Wednesday, which is from 11:40 to 13:00.

Proceedings

The conference proceedings will be refereed and published as an American Institute of Physics (AIP) Conference Proceedings in both CD and online formats (the CD is included in the conference fee). Invited papers can be up to six pages long; contributed oral and poster papers have a maximum length

of four pages. All manuscripts must be prepared in full accordance with the author guidelines for publication with AIP (8.5" x 11" single-column format). All manuscripts must be submitted electronically to xrm_2010_proceedings@aps.anl.gov. The final deadline for submitting manuscripts is September 15, 2010.

Please see the conference web site at http://xrm2010.aps.anl.gov for more information.

Tour of the Advanced Photon Source

The Advanced Photon Source tour, available by prior registration only, will begin after the close of the conference on Friday, August 20. **NOTE:** Registered participants must bring their passports or other government-issued ID to enter the Argonne site. If you forget to bring this, you will not be allowed on-site for the tour.

Registered tour participants will be able to order a box lunch (to eat on the bus) at the conference Registration Desk through Thursday morning. The cost is $14.00. Tour attendees should pick up their box lunches at the Registration Desk after the conference closeout. The buses will start boarding at 12:00 and depart at 12:30. There is always road construction in Chicago in the summer, so the buses will leave promptly at 12:30 and will not wait for latecomers. Please make every effort to board early.

Conference Exhibitors

The booth assignments for the conference exhibitors are listed below. A complete list of exhibitors and contact information can be found on page 26.

Booth #	Company	Booth #	Company
1	Xradia	8	Energetiq Technology, Inc.
2	North Star Imaging, Inc.	9	VSG – Visualization Sciences Group
3	SkyScan	10	Bruker Advanced Supercon GmbH
4	Nano UV	11	Huber Diffraktionstechnik GmbH & Co. KG
5	Silson Ltd.	12	Spectral Instruments
6	Scanco USA, Inc.	13	Luxel Corporation
7	attocube systems AG		

Tours and Companion Program

Three tours are available for conference attendees and their companions. See the conference web page http://xrm2010.aps.anl.gov/index.php?/xrm2010/companion-program/ for more information.

TOUR 1: Chicago Architectural Tour, Sunday, August 15, 14:30 – 16:00, $25 per person.

TOUR 2: Chicago Highlights Trolley Tour, Monday, August 16, 10:00 – 12:00, $20 per person.

TOUR 3: Chicago Neighborhood Trolley Tour, Tuesday, August 17, 10:00 – 13:00, $20 per person.

Ground Transportation

Around Chicago and to Airports:

Taxicabs are available outside the main hotel entrance. Currently, the base Chicago taxi fare is $2.25 and increases $.20 for each additional 1/9 of a mile (or 36 seconds). Plus, there's a $1 charge for the first additional passenger ages 12–65, $.50 for each additional passenger, and a $1 fuel surcharge. Tips are accepted for good service.

The CTA provides bus and 'L' (subway) service. See http://www.transitchicago.com/ for more information.

Other methods of travel around town can be found on the conference web page http://xrm2010.aps.anl.gov/index.php?/xrm2010/accommodations/.

Tipping

Tipping in the U.S. is generally 15-20% for restaurant service; more for exceptional service. Tips are typically 10% for taxis and $1.00 per bag for luggage.

About Chicago

There is so much to do in Chicago in the summer! The Tall Ships Chicago event will be held on August 24-29, and the Chicago Outdoor Film Festival and Grant Park Music Festival run during most of the summer (through August). You can explore the city by bus, boat, or on foot with world-renowned attractions such as the Hancock and Willis (formerly Sears) Towers, Millenium Park, Navy Pier, The Art Institute of Chicago, the Museum of Science and Industry, the Museum Campus (Field Museum—home of "Sue", the Shedd Aquarium, and the Adler Planetarium), and Lincoln Park Zoo either within walking distance or a short bus ride away.

There are theaters galore, sporting events (two baseball teams, the Cubs and White Sox), and hundreds of restaurants. See the conference web page http://xrm2010.aps.anl.gov/index.php?/xrm2010/excursions/ for more information.

Speaker Ready Room — 2nd Floor (below street level)

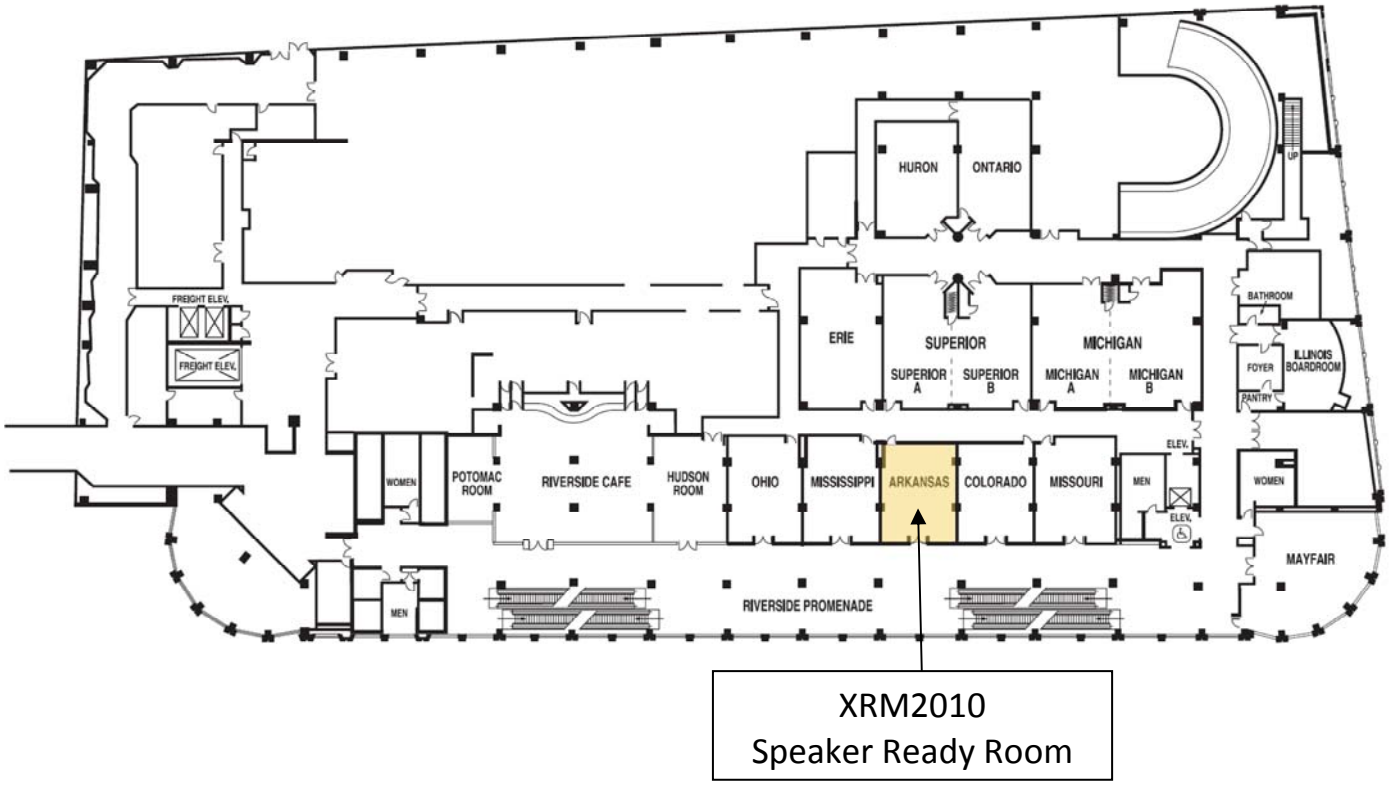

XRM2010 Daily Program

Monday, August 16

		Tuesday Poster Session setup (all day)	
08:15 – 08:30		**Opening and Welcome** Eric Isaacs, Director, Argonne National Laboratory	
Session Mo1: X-ray Facilities, Instruments, and Optics I		**Chicago Ballrooms IX and X**	
08:30 – 09:05	Mo1-Facil-1 *invited*	**Sub-10-nm Focusing of Hard X-rays Using Mirror Optics** Kazuto Yamauchi, *Osaka University*	**Chair:** *David Attwood*
09:05 – 09:40	Mo1-Facil-2 *invited*	**Towards 10-nm Zone-Plate Fabrication** Anders Holmberg, *Royal Institute of Technology*	
09:40 – 10:00	Mo1-Facil-3	**Development of Multilayer Laue Lenses; (1) Linear Type** Takahisa Koyama, *University of Hyogo*	
10:00 – 10:20	Mo1-Facil-4	**Toward One-Nanometer Hard X-Ray Microscopy Using Multilayer Laue Lenses** Hanfei Yan, *Brookhaven National Laboratory*	
10:20 – 10:45		**Break**	
10:45 – 11:20	Mo1-Facil-5 *invited*	**Instruments for Soft X-ray Tomography and Correlated Light Microscopy of Biological Specimens at the National Center for X-ray Tomography** Christian Knoechel, *U. California at San Francisco & Advanced Light Source*	**Chair:** *Albert Macrander*
11:20 – 11:40	Mo1-Facil-6	**Fabrication of Diffractive Optics for Present and Future X-ray Sources** Christian David, *Paul Scherrer Institut*	
11:40 – 12:00	Mo1-Facil-7	**X-ray Talbot Interferometry at ESRF: Applications and Recent Technical Developments** Timm Weitkamp, *ESRF*	
12:00 – 13:30		**Lunch**	
Session Mo2: X-ray Facilities, Instruments, and Optics II		**Chicago Ballrooms IX and X**	
13:30 – 14:05	Mo2-Facil-1 *invited*	**Zone Plate Development at the Helmholtz-Zentrum Berlin: Current Status and Future Possibilities with the New 100-keV e-Beam Writer** Stefan Rehbein, *BESSY*	**Chair:** *Hans Hertz*
14:05 – 14:25	Mo2-Facil-2	**Following Dynamic Processes by X-ray Tomographic Microscopy with Sub-second Temporal Resolution** Rajmund Mokso, *Swiss Light Source, Paul Scherrer Institut*	
14:25 – 14:45	Mo2-Facil-3	**Coherence Measurements and Coherent Diffractive Imaging Experiments at FLASH** Ivan Vartaniants, *DESY*	
15:00 – 15:30		**Exhibits & Refreshments**	
15:30 – 16:05	Mo2-Facil-4 *invited*	**Multilayer-Based Optics for High-Brightness X-ray Sources** Saša Bajt, *CFEL-DESY*	**Chair:** *Tim Salditt*
16:05 – 16:25	Mo2-Facil-5	**Full-Field Microscope for EUVL Mask Characterization** Fernando Brizuela, *Colorado State University*	
16:25 – 16:45	Mo2-Facil-6	**Laboratory Soft X-ray Tomography of Cryo-Fixated Cells** Michael Bertilson, *Royal Institute of Technology/Albanova*	

Tuesday, August 17

Tuesday Poster Session setup (until 17:30)

	Session Tu1: X-ray Microscopy Methods I		**Chicago Ballrooms IX and X**
Chair: *Janos Kirz*	08:30 – 09:05	Tu1-Methods-1 *invited*	**The Application of Electron Microscopy to Nanomaterials** Amanda Petford-Long, *Argonne National Laboratory*
	09:05 – 09:25	Tu1-Methods-2	**3D Chemical and Elemental Imaging by STXM Spectro-tomography** Jian Wang, *Canadian Light Source*
	09:25 – 09:45	Tu1-Methods-3	**Ultrafast X-ray Fluorescence Microscopy: What Does It Enable?** David Paterson, *Australian Synchrotron*
	09:45 – 10:05	Tu1-Methods-4	**MAD Holography** Andreas Scherz, *SLAC National Accelerator Laboratory*
	10:05 – 10:45		**Break**
Chair: *Murray Gibson*	10:45 – 11:20	Tu1-Methods-5 *invited*	**Coherent X-ray Diffraction Microscopy of Frozen-Hydrated Yeast Cells** Johanna Nelson, *Stony Brook University*
	11:20 – 11:40	Tu1-Methods-6	**Lensless Biological Imaging with Waveguides: Holographic, Iterative and Ptychographic Reconstruction** Klaus Giewekemeyer, *Institut für Röntgenphysik, Georg-August-Universität*
	11:40 – 12:00	Tu1-Methods-7	**Wavefront Modulation Coherent Diffractive Imaging** F. Zhang, *University of Sheffield*
	12:00 – 13:30		**Lunch**
	Session Tu2: X-ray Microscopy Methods II		**Chicago Ballrooms IX and X**
Chair: *Keith Nugent*	13:30 – 14:05	Tu2-Methods-1 *invited*	**Scanning Small-Angle X-ray Scattering Microscopy of Biological Tissues** Andreas Menzel, *Paul Scherrer Institut*
	14:05 – 14:25	Tu2-Methods-2	**Hard X-ray Scanning Microscopy with Coherent Diffraction Contrast** Christian Schroer, *Technische Universität Dresden*
	14:25 – 14:45	Tu2-Methods-3	**Scanning Hard X-ray Phase Contrast X-ray Microscopy: Zernike Quantitation and Applications** Christian Holzner, *Stony Brook University*
	15:00 – 15:30		**Exhibits & Refreshments**
Chair: *Alan Michette*	15:30 – 16:05	Tu2-Methods-4 *invited*	**Fresnel Coherent Diffractive Imaging** Andrew Peele, *La Trobe University, Australia*
	16:05 – 16:25	Tu2-Methods-5	**Development and Application of High-Resolution Diffraction Microscopy Using Focused Hard X-ray Beam** Yukio Takahashi, *Osaka University*
	16:25 – 16:45	Tu2-Methods-6	**Bragg Coherent Diffraction Imaging Using <100 nm Focused Hard X-rays** Stephan Hruszkewycz, *Argonne National Laboratory*
	17:30 – 19:30		**Exhibits & Poster Session I**

Wednesday, August 18

Thursday Poster Session setup (all day)

Session We1: X-ray Facilities, Instruments, and Optics III			**Chicago Ballrooms IX and X**
08:30 – 09:05	We1-Facil-1 *invited*	**Latest Development of Ultra-High-Resolution Soft X-ray Zone Plate Microscopy** Weilun Chao, *Lawrence Berkeley National Laboratory*	**Chair:** *Peiping Zhu*
09:05 – 09:40	We1-Facil-2 *invited*	**X-ray Microscopy Beamlines at the SSRF: Present Status and Future Plan** Hongjie Xu, *Shanghai Synchrotron Radiation Facility*	
09:40 – 10:00	We1-Facil-3	**The Nanoscopium Scanning Nanoprobe Beamline at Synchrotron Soleil** Andrea Somogyi, *Synchrotron Soleil*	
10:00 – 10:20	We1-Facil-4	**Nano and Life Sciences with the TwinMic Soft X-ray Transmission and Emission X-ray Spectromicroscope at Elettra** Burkhard Kaulich, *ELETTRA - Sincrotrone Trieste*	
10:20 – 10:45		**Break**	
Session We2: X-ray Microscopy Methods III			**Chicago Ballrooms IX and X**
10:45 – 11:20	We2-Methods-1 *invited*	**Pushing the Resolution Limit of Visible Light Microscopy** Bo Huang, *University of California at San Francisco*	**Chair:** *G. Schmahl*
11:20 – 11:40	We2-Methods-2	**Combined Holographic and Fluorescence Laminography for Three-Dimensional Imaging of Flat Nanostructures** Lukas Helfen, *Karlsruhe Institute of Technology*	
11:40 – 13:00		**Lunch**	
Session We3a: X-ray Microscopy Methods IV			**Chicago Ballroom VIII**
13:00 – 13:20	We3a-Methods-1	**Chemical Imaging of Nanodevices with Zone Plate-Based SPEM** Luca Gregoratti, *Sincrotrone Trieste*	**Chair:** *Hun-Joon Shin*
13:20 – 13:40	We3a-Methods-2	**Polarized X-ray Excited Optical Luminescence Imaging of Nano-LEDs** Gema Martinez-Criado, *ESRF*	
13:40 – 14:00	We3a-Methods-3	**Imaging Interfacial Topography and Reactivity with X-ray Reflection Interface Microscopy (XRIM)** Paul Fenter, *Argonne National Laboratory*	
14:00 – 14:20	We3a-Methods-4	**Hard X-ray Phase-Contrast Tomographic Nanoimaging** Marco Stampanoni, *Paul Scherrer Institut*	
14:20 – 14:40	We3a-Methods-5	**The Maia X-ray Detector Array at the Australian Synchrotron: High-Definition SXRF Trace Element Imaging** Chris Ryan, *CSIRO*	
15:00 – 15:30		**Exhibits & Refreshments**	
Session We4a: Emerging Fields			**Chicago Ballroom VIII**
15:30 – 16:05	We4a-Emerging-1 *invited*	**An Innovative Low-Dose Single-Step Method for Grating-Based X-ray Phase-Contrast Imaging** Ziyu Wu, *NSRL, University of Science & Technology of China*	**Chair:** *Graeme Morrison*
16:05 – 16:40	We4a-Emerging-2 *invited*	**Femtosecond X-ray Imaging Using Free Electron Lasers** Anton Barty, *CFEL-DESY*	
16:40 – 17:00	We4a-Emerging-3	**Cultural Heritage Science at the ESRF** Marine Cotte, *ESRF*	
17:00 – 17:20	We4a-Emerging-4	**One-Nanometer-Scale Elemental Analysis by SR-Based Scanning Tunneling Microscopy** Akira Saito, *Osaka University and RIKEN and JST*	

Wednesday, August 18 (continued)

Thursday Poster Session setup (all day)

Session We3b: Magnetism and Magnetic Materials — **Chicago Ballroom X**

Chair: *Christoph Quitmann*

13:00 – 13:35	We3b-Magnet-1 *invited*	**Imaging of Spin Phenomena in Magnetic Nanostructures Using Magnetic Soft X-ray Microscopy** Mi-Young Im, *Lawrence Berkeley National Laboratory*
13:35 – 14:10	We3b-Magnet-2 *invited*	**Probing Magnetic Domain Structure via Coherent X-ray Diffractive Imaging** Oleg Shpyrko, *University of California at San Diego*
14:10 – 14:30	We3b-Magnet-3	**Spins and Twins: Correlation Between Crystallographic and Magnetic Domains at Co/NiO(001) Interfaces** Hendrik Ohldag, *Stanford Synchrotron Radiation Lightsource*
14:30 – 14:50	We3b-Magnet-4	**Vortex and Vortex Core Dynamics Imaged by Time-Resolved X-ray Microscopy** Bartel Van Waeyenberge, *Ghent University*
15:00 – 15:30		**Exhibits & Refreshments**

Session We4b: Environmental, Earth, and Space Science — **Chicago Ballroom X**

Chair: *Adam Hitchcock*

15:30 – 16:05	We4b-Environ-1 *invited*	**STXM Analysis of Impact Tracks in the Stardust Interstellar Dust Collector Aerogel** Anna Butterworth, *University of California at Berkeley*
16:05 – 16:40	We4b-Environ-2 *invited*	**Nanostructure of Geopolymers** Paulo Monteiro, *University of California at Berkeley*
16:40 – 17:00	We4b-Environ-3	**Hard X-ray Imaging of Mercury Accumulation in Plants** Joy Andrews, *SLAC National Accelerator Laboratory and California State University*
17:00 – 17:20	We4b-Environ-4	**Synchrotron X-ray Fluorescence Microtomography in Geo-, Cosmo-, and Biochemistry** Antonio Lanzirotti, *The University of Chicago*
18:30 – 22:00		**Banquet** aboard the ***Spirit of Chicago*** **(map on page**

Thursday, August 19

		Thursday Poster Session setup (until 17:30)	
Session Th1: Biological and Biomedical Science I			**Chicago Ballrooms IX and X**
08:30 – 09:05	Th1-Biological-1 *invited*	**Tomographic Analysis by X-ray and Electron Microscopy of Vaccinia Virus Structure and Assembly: A.** José Carrascosa, *Centro Nacional de Biotecnologia, CSIC*	**Chair:** *Chris Jacobsen*
09:05 – 09:40	Th1-Biological-2 *invited*	**Use of X-ray Fluorescence Microscopy for Elemental Mapping of Samples Treated with Contrast Agents for Medical Imaging** Tanja Paunescu, *Northwestern University*	
09:40 – 10:00	Th1-Biological-3	**Investigating the Subsellular 3D Structures of the Oldest Found Embryo Fossils Using Synchrotron Hard X-ray Phase Contrast Microtomography** Gang Li, *Beijing Synchrotron Radiation Facility, IHEP*	
10:00 – 10:20	Th1-Biological-4	**High-Resolution Phase-Contrast Imaging of Sub-micron Particles in Unstained Lung Parenchyma** Johannes Schittny, *University of Bern*	
10:20 – 10:45		**Break**	
10:45 – 12:00		**Presentations for XRM 2012** **Vote for XRM 2012 Location**	
12:00 – 13:30		**Lunch**	
Session Th2a: Biological and Biomedical Science II			**Chicago Ballroom VIII**
13:30 – 14:05	Th2a-Biological-1 *invited*	**3-D Cellular Fine Structure Resolved by a Partially Coherent X-ray Microscope** Jim McNally, *NIH National Cancer Institute*	**Chair:** *Sadao Aoki*
14:05 – 14:25	Th2a-Biological-2	**Cryo Transmission X-ray Imaging of the Malaria Parasite *P. falciparum*** Keith Nugent, *ARC Centre of Excellence for Coherent X-ray Science*	
14:25 – 14:45	Th2a-Biological-3	**Cryogenic X-ray Diffraction Microscopy for Biological Samples** Enju Lima, *Brookhaven National Laboratory*	
15:00 – 15:30		**Exhibits & Refreshments**	
15:30 – 16:05	Th2a-Biological-4 *invited*	**Application of XRM to Human Disease and Therapies** Peter Lay, *University of Sydney*	**Chair:** *Gerd Schneider*
16:05 – 16:25	Th2a-Biological-5	**Subcellular X-ray Fluorescence Imaging as a Tool to Better Understand Metal-Induced Pathologies** Martina Ralle, *Argonne National Laboratory*	
16:25 – 16:45	Th2a-Biological-6	**Visualizing a Role for Zinc in Stem Cell Differentiation through X-ray Fluorescence Mapping** Lydia Finney, *Argonne National Laboratory*	
17:30 – 19:30		**Exhibits & Poster Session II**	

Thursday, August 19 (continued)

Thursday Poster Session setup (until 17:30)

Session Th2b: Materials and Condensed Matter		**Chicago Ballroom X**
Chair: *Maya Kiskinova*		
13:30 – 14:05	Th2b-Materials-1 *invited*	***In situ* Nanoscale Chemical Imaging of Catalysts** Emiel de Smit, *Utrecht University*
14:05 – 14:25	Th2b-Materials-2	**Elemental Mapping and Analysis of Solid Oxide Fuel Cells by Transmission X-ray Microscopy** Wilson Chiu, *University of Connecticut*
14:25 – 14:45	Th2b-Materials-3	**Time-Dependent Dealloying and Coarsening Studies of Nanoporous Gold Using Transmission X-ray Microscopy** Yu-chen Chen, *Northwestern University*
15:00 – 15:30		**Exhibits & Refreshments**
Chair: *Michael Feser*		
15:30 – 16:05	Th2b-Materials-4 *invited*	**Coherent X-ray Diffraction Imaging of Strain on the Nanoscale** Ross Harder, *Argonne National laboratory*
16:05 – 16:25	Th2b-Materials-5	**Submicron-Resolution Three-Dimensional Polychromatic X-ray Microdiffraction** Jon Tischler, *Oak Ridge National Laboratory*
16:25 – 16:45	Th2b-Materials-6	**Imaging and Structural Analysis of Ferroelectric Domains Written by Piezoresponse Force Microscopy** Pice Chen, *University of Wisconsin at Madison*
17:30 – 19:30		**Exhibits & Poster Session II**

Friday, August 20

Session Fr1: Panel Discussion	Chicago Ballrooms IX and X
08:30 – 10:15	**Panel Discussion:** **Nanometer Resolution in X-ray Microscopy** **Chair: Qun Shen, *Brookhaven National Laboratory*** **Panelists: Christian David, *Paul Scherrer Institut*** **Chris Jacobsen, *Argonne/Northwestern University*** **Jörg Maser, *Argonne National Laboratory*** **Hidekazu Mimura, *Osaka University*** **Keith Nugent, *University of Melbourne*** **Ian Robinson, *University College London*** **Christian Schroer, *Technical University Dresden*** **Gayle Woloschak, *Northwestern University***
	Refreshments
10:45 – 12:00	**Werner Meyer-Ilse Award and Student Award Presentations** **Chair: Alan Michette, *Kings College London*** **XRM2012 Location Winner** **XRM2010 Closeout**

For APS Tour Participants:	
12:00 – 12:30	**Pick up box lunch and board bus**
12:30	**Buses depart for APS Tour**
17:30	**Buses depart for return to Chicago**
18:30	**Buses return to Sheraton Hotel**

Facilities

PAPER ID	1ST AUTHOR'S NAME	TITLE
Tues-P001	Ray Barrett	A High-Efficiency Dynamically Figured KB System for High-Energy Nanofocusing at the ESRF
Tues-P002	Markus Benk	Gas Discharge Source and Collector Module for Soft X-ray Microscopy in the Water Window Spectral Range
Tues-P003	Matthieu Boone	Preliminary Results of a Combined Laboratory Micro-CT and XRT System
Tues-P004	Nathalie Bouet	Reactive Ion Etching of WSi2/Si Structures for Multilayer Laue Lens Fabrication
Tues-P005	Peter Bruyndonckx	Laboratory 3D Micro XRF - Micro CT Imaging System
Tues-P006	Flavio Capotondi	Coherent Diffraction and Projection imaging at FERMI@ELETTRA
Tues-P007	Pambos Charalambous	Developments in the Fabrication of Zone Plates and Other Nanostructures
Tues-P008	Kwon Su Chon	X-ray Imaging Using Characteristic X-rays Generated from a Conventional X-ray Tube
Tues-P009	Yong Chu	Capabilities of the Hard X-ray Nanoprobe at the NSLS-II
Tues-P010	Raymond Conley	Multilayer Laue Lens Growth at NSLS-II
Tues-P011	Darren Dale	Scanning X-ray Fluorescence Microscopy at CHESS
Tues-P012	Gregory Denbeaux	Large-Area Zone-Plate Fabrication with Optical Lithography
Tues-P013	Reiner Dietsch	Performance of Multilayer Monochromators for Hard X-ray Imaging with Coherent Synchrotron Radiation
Tues-P014	Elizabeth Duke	Biological Imaging at Diamond: The Cryo-Transmission X-ray Microscope Beamline
Tues-P015	Johannes Ewald	Source Size Characterization of a Nanofocus X-ray Tube used for In-Line Phase Contrast Imaging
Tues-P016	Gerald Falkenberg	The Hard X-Ray Micro/Nano-Probe beamline P06 at PETRA III
Tues-P017	Anatoly Firsov	Germanium-Based Circular Zone Plates for Soft and Hard X-rays
Tues-P018	Sergey Gorelick	Diamond Fresnel Zone Plates for High Power X-ray Beams
Tues-P019	Sergey Gorelick	High Efficiency Au Zone Plates for Multi-keV X-ray
Tues-P020	Sergey Gorelick	Investigation of Damage in Diffractive Optics Induced by High Intensity X-ray Beams
Tues-P021	Arshak Grigoryan	X-ray Zone Plate in Combination with Diffraction Reflections
Tues-P022	Robert Gunion	X-Ray Diffractive Optics Simulation Using a GPU, Web Service, and Graphical User Interface
Tues-P023	Vitaliy Guzenko	Efficient EBL Exposure Strategies for Diffractive X-ray Optics
Tues-P024	Martin Holt	Scanning Probe Diffraction Microscopy at the CNM/APS Hard X-ray Nanoprobe Beamline
Tues-P025	Benjamin Hornberger	Cryogenic Transmission X-ray Nano-Tomography in the Water Window with a Z-Pinch Plasma Source
Tues-P026	Steve Horne	Development of the Electrode-less Z-Pinch Soft X-ray Source for Water-Window Microscopy
Tues-P027	Fumihiko Ishida	Development of Wide Field of View EUV Microscope Using Normal-Incident Multilayer Optics with LPP Light Source

Facilities

Tues-P028	Simon James	Preparation and Characterization of Thin Film Elemental Standards for X-ray Fluorescence Microscopy
Tues-P029	Sebastian Kalbfleisch	The Holographic Imaging Setup at the P10 Beamline of PETRA III
Tues-P030	David Kilcoyne	A New Scanning Transmission X-ray Microscope at the Advanced Light Source for Operation from 280 eV to 2500 eV
Tues-P031	Takahisa Koyama	Development of Multilayer Laue Lenses; (2) Circular Type
Tues-P032	Naresh Kujala	Copper Speciation Studies of Biological Samples Using a Compact, Short Focal Distance Bent Crystal Laue Analyzer
Tues-P033	Johannes Lenz	Nanofabrication of Optical Elements for SXR and EUV Applications: Ion Beam Lithography as New Approach
Tues-P034	Adam Leontowich	Approaching Diffraction-Limited Resolution in Zone Plate-Based Soft X-ray Lithography
Tues-P035	Aiguo Li	The Commissioning Results and User Opening of Hard X-Ray Micro-Focus Beamline BL15U1 at SSRF
Tues-P036	Jun Lim	A Compact Sample-in-air Soft-X-ray Microscope at PLS
Tues-P037	Enju Lima	Investigation on High Diffraction Orders of a Fresnel Zone Plate
Tues-P038	Wenjun Liu	X-ray Laue Diffraction 3D Microscopy at the 34-ID Beamline of the Advanced Photon Source
Tues-P039	Derrick Mancini	Hard X-ray Zone Plates Using Ultrananocrystalline Diamond Molds
Tues-P040	Federica Marone	Present and Future X-ray Tomographic Microscopy at TOMCAT
Tues-P041	Jörg Maser	The Hard X-ray Nanoprobe at the Advanced Photon Source
Tues-P042	Marcel Mayer	A New Method for Manufacturing Fresnel Zone Plates
Tues-P043	Evgueni Nazaretski	Development of the Sub-nm Spatial Resolution Fiber Optic Interferometer for the Hard X-ray Microscope for the Nanoprobe Beamline at NSLS-II*
Tues-P044	Daniel Nilsson	Zone Plates for Hard X-ray FEL Radiation
Tues-P045	Thomas Nisius	Development of a Versatile End Station for Space- and Time-Resolved Experiments at FLASH and PETRA III
Tues-P046	Takuji Ohigashi	Development of a Computer Tomography System for the Soft X-ray Microscopy at Ritsumeikan University
Tues-P047	Bart Pauwels	Development of a Small-Animal Phase-Contrast MicroCT Scanner
Tues-P048	Eva Pereiro	MISTRAL Beamline Status at ALBA and Scientific applications
Tues-P049	Piero Pianetta	Advanced in Nanoscale Chemical Imaging Techniques Using Full-Field Hard X-ray Microscopy at SSRL
Tues-P050	Keith Powell	The Development of a Tabletop Soft X-ray in vitro Microscope
Tues-P051	Christoph Rau	The Imaging and Coherence Beamline I13L at Diamond
Tues-P052	Julia Reinspach	15-nm Efficiency-Enhanced Soft X-ray Zone Plates
Tues-P053	Elena Reznikova	25-keV Transmission X-ray Microscope Based on X-ray Refractive Lenses
Tues-P054	Elena Reznikova	30-keV Transmission X-ray Microscope Based on X-ray Refractive Planar Crossed Parabolic SU-8 Lenses
Tues-P055	Mark Rivers	4,000 Spectra or 4,000,000 ROIs per Second: EPICS Support for High-Speed Digital X-ray Spectroscopy with the XIA xMap

Facilities

Tues-P056	Juana Rudati	A Condenser Scanner for Large Field of View Full-field X-ray Microscopy at Synchrotrons
Tues-P057	Anne Sakdinawat	X-ray Microscopy with Second Order Optimized Zone Plates
Tues-P058	Alexander Sasov	New Lens-Free X-ray Source for Laboratory Nano-CT with 50-nm Spatial Resolution
Tues-P059	Deming Shu	Development of an Advanced Sample Scanning Stage System Prototype for an MLL-Based Hard X-ray Nanoprobe
Tues-P060	Nikolaos Simos	Achieving Desired Vibration Stability of the NSLS-II Hard X-ray Nanoprobe Beamline Endstation
Tues-P061	Peter Skoglund	Electron-Impact Water-Jet Microfocus Source for Water-Window Microscopy
Tues-P062	Yoshio Suzuki	Hard X-ray Microbeam by Combination of Spherical Mirrors
Tues-P063	Yoshio Suzuki	Hollow Cone Illumination for Hard X-ray Imaging Microscopy by Rotating Grating Condenser Optics
Tues-P064	Sufal Swaraj	HERMES: A Soft X-ray Microscopy Beamline
Tues-P065	J. Szlachetko	Wavelength-Dispersive Spectrometer for X-ray Micro-fluorescence Analysis at the ESRF ID21 Beamline
Tues-P066	Renzhong Tai	Scanning Transmission X-ray Microscope at SSRF
Tues-P067	Kenichiro Takaba	Development of Laboratory-Scale Coaxial Fluorescence and Soft X-ray Microsopy for Biological Observation
Tues-P068	Yasuko Terada	Nano-XAFS Measurements for Single-Particle Analysis Using High-Resolution X-ray Microprobe
Tues-P069	Juergen Thieme	The Submicron Resolution X-ray Spectroscopy Beamline at the Electron Storage Ring NSLS-II
Tues-P070	Andrei Tkachuk	Laboratory 3D 8-keV X-ray Imaging System with Automated Tomography at 50-nm Resolution
Tues-P071	Mitsunori Toyoda	Novel Multilayer-Mirror Optics for a Whole Tissue Imaging
Tues-P072	Kouichi Tsuji	Development of Micro- and 3D-XRF Instruments in the Laboratory
Tues-P073	Takuya Tsuji	Development of a Reflection Zone Plate for Hard X-ray Nanofocusing
Tues-P074	Toshihide Tsuru	Three-Dimensionally Controlled Ion Milling for Reflection Phase Manipulation of EUV Multilayer Mirrors
Tues-P075	Tolek Tyliszczak	New Ambient Pressure Scanning Photoelectron Microscope at the ALS
Tues-P076	Stephen Urquhart	Electron Yield Detection in Scanning Transmission X-ray Microscopy: Improving Surface Sensitivity
Tues-P077	Denis Van Loo	A Flexible Modular Laboratory X-ray Nano-CT Scanner
Tues-P078	Gavin Vaughan	High Energy Nanoscale Resolution X-ray Microscopy Based on Refractive Optics on a Long Beamline
Tues-P079	Joan Vila-Comamala	World Record Resolution in Scanning Transmission X-ray Microscopy
Tues-P080	Benjamin Watts	Novel Imaging at the PolLux STXM
Tues-P081	Samuel Webb	Hard X-ray Fluorescence Imaging Facilities at SSRL
Tues-P082	Samuel Webb	The Microanalysis Toolkit: X-ray Fluorescence Image Processing Software

List of Tuesday's Posters – Chicago Ballroom VI and VII

Facilities	Tues-P083	Markus Weigand	MAXYMUS--Features and Commissioning Results of a New UHV STXM at HZB/Bessy II, Berlin
	Tues-P084	Urs Wiesemann	X-ray Microscopy with Compact Sources
	Tues-P085	Urs Wiesemann	Table-Top XUV/EUV Setup for Imaging and Spectroscopy
	Tues-P086	Garth Williams	The Coherent Imaging and Diffraction Instrument at the Linac Coherent Light Source
	Tues-P087	Robert Winarski	Development of X-ray Nanotomography with the Hard X-ray Nanoprobe
	Tues-P088	Tiqiao Xiao	Microtomography for Material and Biomedical Science at SSRF
	Tues-P089	Gung-Chian Yin	A Temperature-Controlled Liquid Cell in Transmission X-ray Microscope
	Tues-P090	Qingxi Yuan	Current Status of the Transmission X-ray Microscopy in BSRF
	Tues-P091	Hirokatsu Yumoto	Long Working Distance Kirkpatrick-Baez Mirrors for Hard X-ray Beamlines at Spring-8
	Tues-P092	Xianghui Zeng	Capillary Wolter Mirrors as Condensers for X-ray Microscopy
	Tues-P093	Jingtao Zhu	Development of X-ray Microscopy in IPOE
Emerging	Tues-P094	John Corlett	Plans for a Soft X-ray FEL for Dynamic Imaging
	Tues-P095	Kamel Fezzaa	High-Speed X-ray Full-Field Imaging Applications at the APS
	Tues-P096	Daryl Howard	Scanning X-ray Fluorescence Elemental Mapping of Paintings with Sychrotron Radiation
	Tues-P097	Volker Rose	Nanoscale Chemical Imaging Using Synchrotron X-ray Enhanced Scanning Tunneling Microscopy (SXSTM)
Magnetism	Tues-P098	X.M. Cheng	Magnetic Vortex Core Dynamics and Reversal Studied Using X-ray Microscopy
	Tues-P099	Adam Hitchcock	X-Ray Magnetic Circular Dichroism of Individual 30-nm Magnetosomes in Magnetotactic Bacteria by STXM
	Tues-P100	M.-Y. Im	Magnetic Soft X-ray Microscopy of Stochastic Behavior in Nanoscale Magnetism
	Tues-P101	Hendrik Ohldag	Can Carbon Be Ferromagnetic?
	Tues-P102	Hendrik Ohldag	X-ray Microscopy and Magnetism – A Perfect Match
	Tues-P103	Thomas Schwarze	Sample Preparation of Epitaxially Grown Magnetic Materials for X-Ray Transmission Microscopy
Environmental	Tues-P104	Mareike Brettholle	Spatially Resolved Sulfur Speciation in Urban Soils
	Tues-P105	George Flynn	STXM Imaging of Organic Coatings on Interplanetary Dust
	Tues-P106	Sophie-Charlotte Gleber	Hard X-ray Fluorescence Microscopy to Determine the Element Distribution of Soil Colloids in Aqueous Environment
	Tues-P107	Volker Rose	Hard X-ray Nanoprobe Characterization of Geopolymers
	Tues-P108	Julia Sedlmair	C1s - X-ray Spectromicroscopy of Biomolecular Matter
	Tues-P109	Yen-Fang Song	Study on Smectite Flocculation Structure Modified by Al13 Macromolecules by Transmission X-ray Microscopy
	Tues-P110	Kuniko Takemoto	X-ray Imaging of Mucilaginous Sheath of Phytoplankton in Lake Biwa by Soft X-ray Microscopy
	Tues-P111	Ryan Tappero	Evidence of High Metal Tolerance in Seeds of Ni Hyperaccumulators Revealed by Fluorescence Computed Microtomography (F-CMT)

List of Thursday's Posters – Chicago Ballroom VI and VII

Methods

PAPER ID	1ST AUTHOR'S NAME	TITLE
Thurs-P001	Matthieu Boone	Improved Visualization Using Phase Retrieval Algorithms in Laboratory X-ray MicroCT
Thurs-P002	Loes Brabant	Latest Developments in 3D Analysis of CT Data by Morpho+
Thurs-P003	Sergio Carbajo	Stop-Action Extreme Ultraviolet Imaging
Thurs-P004	Marine Cotte	Micro-spectroscopies at ID21: Towards a Multi-modal Strategy
Thurs-P005	Marine Cotte	How to Deal with Complex X-ray Fluorescence Spectra?
Thurs-P006	Martin de Jonge	Recent Progress in Quantitative Fast Fluorescence Tomography with a Hard X-ray Sscanning Fluorescence Microprobe
Thurs-P007	Yoni De Witte	Phase Contract in Laboratory-Based X-ray Micro/Nano-CT
Thurs-P008	Yoni De Witte	Advanced Tomography Reconstruction Algorithms on the Graphical Processing Unit
Thurs-P009	Takeo Ejima	"Super-Hierarchical" Microscope in EUV Region
Thurs-P010	Xin Ge	Coherent Diffractive Imaging Using Hollow Cone Illumination
Thurs-P011	Natasa Grlj	Element-Selective Microscopy with Confocal mu-PIXE Arrangement
Thurs-P012	Levon Haroutunyan	Phase-Contrast X-ray Imaging by Means of Zone-Plate Interferometer
Thurs-P013	Christian Holzner	Scanning Zernike Phase Contrast Implemented in a Hard X-ray Fluorescence Microprobe
Thurs-P014	Christian Holzner	Comparison and Unification of Quantitative Scanning Phase Contrast Reconstruction Methods
Thurs-P015	Christian Holzner	Reconstruction of Zernike Phase Contrast for Tomography
Thurs-P016	Youli Hong	Quantitative Analysis of Absorption and Phase Difference Images in Differential Interference Contrast Microscopy
Thurs-P017	Masato Hoshino	Development of X-ray Laminography System at SPring-8
Thurs-P018	Wanxia Huang	Phase Tomography Based on the New Method to Extract the Refraction Angle Image
Thurs-P019	Xiaojing Huang	Incorrect Suppoart and Missing Center Tolerances of Phasing Algorithms
Thurs-P020	Konstantin Ignatyev	Phase-Contract Imaging with Coded Apertures Using Laboratory-Based X-ray Sources
Thurs-P021	Cameron Kewish	Reconstruction of an Astigmatic Hard X-ray Beam and Alignment of K-B Mirrors from Coherent Diffraction Measurements
Thurs-P022	Sunam Kim	Application of Micro Aperture for Coherent x-ray Diffraction Imaging
Thurs-P023	Peter Krüger	Improved Scanning Geometry to Collect 3D-Geometry Data in Flat Samples
Thurs-P024	Armen Kuyumchyan	X-ray Microscopy Based on Asymmetric Diffraction
Thurs-P025	Sang Joon Lee	Quantitative Visualization of Various Biofluid Flow Phenomena Using the Synchrotron X-ray Micro-Imaging Technique
Thurs-P026	Wenjie Li	The Best of Both Worlds: 3D X-ray Microscopy with Ultra-High-Resolution and a Large Field of View
Thurs-P027	Jae-Hong Lim	Implementation of Phase-Contrast Imaging Using a Polychromatic Beam from a Bending magnet Source

Methods

Thurs-P028	Yijin Liu	Quantitative Information Extraction from Zernike-Type X-ray Phase-Contrast Imaging System
Thurs-P029	Adrian Mancuso	Progress in Coherent Diffractive Imaging of Biological Samples with Synchrotron and Free Electron Laser Sources
Thurs-P030	Aleksey Maryasov	EUV Dark-Field Microscopy for Defect Inspection
Thurs-P031	Florian Meirer	Advancements in Hard X-ray TXM: XANES Mapping and Large Volume Tomography at Sub-100-nm Resolution
Thurs-P032	Alan Michette	Microstructured Optical Arrays for Cell and Tissue Probing
Thurs-P033	Peter Modregger	Artifacts in Dark-Field Tomography
Thurs-P034	Graeme Morrison	The Measurement of MTFs in X-ray Microscopy Using Diffractograms
Thurs-P035	Kenji Nomura	X-ray Fourier Transform Holography with a Separate Illumination Mask
Thurs-P036	Michael Pierce	Coherent Surface Diffraction, Reciprocal-Space and Real-Space Possibilities
Thurs-P037	Jonathan Potier	Enhanced High-Speed Coherent Diffraction Imaging
Thurs-P038	Corey Putkunz	Fresnel Coherent Diffraction Tomography
Thurs-P039	Leili Rad	Algorithmic Reconstructin Methods in Diffraction Microscopy Using a Priori Information
Thurs-P040	Jörg Schwenke	Digital In-line Holography on Amplitude and Phase Objects Prepared with Electron Beam Lithography
Thurs-P041	David Shapiro	Limited-View Ptychography of Isolated Objects
Thurs-P042	David Shapiro	Optimization of the Coherent Intensity from Multi-segment Undulators by Phase Matching
Thurs-P043	Anatoly Snigirev	X-ray Interferometers Based on Refractive Optics
Thurs-P044	Irina Snigireva	High-Resolution X-ray Microscopy on Mesoscopic Structures
Thurs-P045	Xiangxia Song	Simulation of NanoXCT System Based on Zone Plate Object
Thurs-P046	Motohiro Suzuki	Hard X-ray Fourier Transform Holography Using a Reference Scatter Fabricated by Electron-Beam-Assisted Chemical-Vapor Deposition
Thurs-P047	Hidekazu Takano	New Nanoscale Imaging with a Simple hard X-ray "Nano-Slit"
Thurs-P048	Akihisa Takeuchi	Efficiency Improvement of Imaging X-ray Microscopy by Using Double-Condenser Illuminating System
Thurs-P049	Ashish Tripathi	Effects of Missing Data and Limited Signal to Noise on Scanning Coherent X-ray Diffraction Microscopy
Thurs-P050	Kentaro Uesugi	High Spatial Resolution X-ray Phase Imaging with a Talbot Interferometer
Thurs-P051	Olov von Hofsten	Image Quality Limitations Due to Stray Light in High-NA X-ray Microscopy
Thurs-P052	Zhili Wang	Efficiency of the Novem Phase Extraction Algorithm in Grating-Based X-ray Phase-Contrast Imaging
Thurs-P053	Norio Watanabe	Cryo-Tomography with a Common-Path Interference Microscope
Thurs-P054	Norio Watanabe	Observation of Phase Objects by Using an X-ray Microscope with a Foucault Knife-Edge
Thurs-P055	Wataru Yashiro	X-ray Phase Imaging Using a Fresnel Zone Plate and a Phase Grating

Methods	Thurs-P056	Wataru Yashiro	Analysis of Microstructure Using Visibility Contrast in the X-ray Talbot Interferometry
	Thurs-P057	Irene Zanette	X-ray Imaging with a Grating Interferometer at ESRF-ID19
	Thurs-P058	Diling Zhu	Phasing Coherent Diffraction Patterns by Wavelength and Polarization Tuning
	Thurs-P059	Pei-Ping Zhu	Generalization of DEI Methods into Grating-Interferometer-Based Phase-Contrast Imaging
Biological	Thurs-P060	Hans Arora	Conjugation of Fe3O4@TiO2 Core-Shell Nanoparticles to Doxorubicin improves Localization and Cytotoxicity in Drug-Resistant Ovarian Carcinoma
	Thurs-P061	Chia-Chi Chien	Nanoparticle Uptake Study by Transmission X-ray Microscopy
	Thurs-P062	Tanja Dučić	X-ray Microscopy of Primary Dopaminergic Neurons: Trace Elements Distribution and Oxidative State
	Thurs-P063	Peter Fischer	Switchable Cell Trapping Using Superparamagnetic Beads
	Thurs-P064	Annelies Genbrugge	Comparative Cranial Osteology of Darwin's Finches Based on Micro-CT Scanning: Preliminary Results
	Thurs-P065	Huaidong Jiang	3D Imaging of Whole, Unstained Cells by Using X-ray Diffraction Microscopy
	Thurs-P066	Shiping Jiang	Cellular Imaging with SR-Based Soft X-ray Microscopy
	Thurs-P067	Masataka Kado	Observation of Organelles in Leydig Cells by Contact Soft X-ray Microscopy with a Laser Plasma X-ray Source
	Thurs-P068	Minna Krejci	Investigating Selectivity in Algal Biomineralization of Barium and Strontium with X-ray Fluorescence Microscopy
	Thurs-P069	Armen Kuyumchyan	Nanotechnology and X-ray Optics for Reproduction of the Three-Dimensional Structure of a Damaged Rat Spinal Chord after Gene Therapy
	Thurs-P070	Stefano Lagomarsino	Combined X-ray Microfluorescence and Atomic Force Microscopy Studies of Mg Distribution in Cells
	Thurs-P071	Jyotsana Lal	In situ Cohereht Diffraction Imaging of Cellulose Crystals
	Thurs-P072	Ulf Lundström	In-line Phase Contrast for High-Resolution Laboratory X-ray Imaging in Thick Tissue
	Thurs-P073	Haruo Mizutani	Nano-resolution X-ray Tomography for Deciphering a Wiring Diagram of the Mammalian Brain
	Thurs-P074	Ryuta Mizutani	Microtomographic Analysis of Human Brain Circuits
	Thurs-P075	Junichi Moriya	Micro-CT of Porous Apatite Fiber Scaffolds Studied by Projection X-ray Microscopy
	Thurs-P076	Bernd Pinzer	Differential Phase-Contrast Tomography of Amyloid Plaques in Alzheimer Mouse Models
	Thurs-P077	Var St. Jeor	Nitrogen Detection in Foods via Energy Dispersive Spectroscopy
	Thurs-P078	Var St. Jeor	Micro-X-ray Fluorescence in Food Forensics
	Thurs-P079	Anthony Stead	Ultrastructure of Frozen Hydrated Chlamydomonas Cells as Revealed by X-ray Tomography Using XM-2
	Thurs-P080	Kuniko Takemoto	Feasibility Study of X-ray Imaging with Near Carbon K-shell Edges on Deinococcus radiodurans

Biological	Thurs-P081	Kuniko Takemoto	Observations of Biological Specimens at Cryo-Temperatures with Soft X-ray Microscopy at the SR Center of Ritsumeikan University
	Thurs-P082	Arne Tapfer	Phase-Contrast Micro-CT for Studying Small-Animal Tumor Models
	Thurs-P083	Maho Uchida	Structural and Quantificational Analysis of Eukaryotic Cells Using Soft X-ray Tomography
	Thurs-P084	Maho Uchida	Soft X-ray Tomography: A High-Resolution Modality for 3-D Biological Imaging
	Thurs-P085	Jesse Ward	X-Ray Fluorescence Imaging of Chelator-Treated Erythrocytes Infected with the Malaria Parasite Plasmodium falciparum
	Thurs-P086	Yanling Xue	Application of X-ray Phase Contrast Microscopy to Xylem Cavitation and Water-Refilling in Plants
	Thurs-P087	Ye Yuan	Uptake Mechanisms of EGFR-Targeted nanoparticles
	Thurs-P088	Kai Zhang	3D Visualization of the Microstructure of Amphizoa davidi Lucas Using Micro-CT
Materials	Thurs-P089	Tohru Araki	Soft X-ray Spectromicroscopy to Study of Rubbery Polymer Nanocomposites
	Thurs-P090	Rozaliya Barabash	3D Laue Microscopy of Local Dislocation Densities and Elastic Strain Gradients in the Two-Phase Composites
	Thurs-P091	Markus Benk	Soft X-ray Microscopic Investigation on Self-assembling Nanocrystals
	Thurs-P092	Wonsuk Cha	Internal Strain Mapping of Zeolite Microcrystals by Coherent X-ray Diffraction Imaging
	Thurs-P093	Yu-chen Karen Chen	Three-Dimensional High-Resolution Imaging of Nanoporous Gold Using Fresnel and Bragg Coherent X-Ray Diffraction Imaging
	Thurs-P094	Francesco De Carlo	In situ Dynamics at the Advanced Photon Source X-ray Imaging Beamlines
	Thurs-P095	Yong Guan	Study the Relationship between Microstructure and Performance of Solid-Oxide Fuel-Cell Anode Using Nano-CT
	Thurs-P096	Peter Guttmann	X-ray Microscopy of TiO2-Based Nanostructures
	Thurs-P097	Christian Hub	STXM Investigations of in situ-Operated OFETs
	Thurs-P098	Kyuwook Ihm	Selective Adsorption of Bbenzoic Acid Species on Patterned OH/Si(100) Surface
	Thurs-P099	Sangsoo Kim	Three-Dimensional Mapping of Pore Structure in Nanoporous Gold by Fresnel Coherent Diffractive Imaging
	Thurs-P100	Wenjie Li	A Powerful Tool for Nano Materials Structure Characterization
	Thurs-P101	Ebrahim Najafi	X-ray Linear Dichroism in Single-Walled Carbon Nanotube Bundles
	Thurs-P102	Tatjana Rack	Coherent Synchrotron-Based Micro-Imaging Employed for Quantitative Studies of Micro-Gap Formation in Dental Implants
	Thurs-P103	Juan Angel Sans	Effect of Temperature on the Stability of Ga in ZnO
	Thurs-P104	Juan Angel Sans	Interfacial Diffusion in ZnO Grown on Sapphire
	Thurs-P105	Iris Schmid	Seeing and "Feeling" Polymer Blends in a Nano-Scale
	Thurs-P106	Matthew Shand	Characterization of Microstructured Optical Arrays (MOAs)
	Thurs-P107	Var St. Jeor	Specific Stainless Identification Using Micro-X-ray Fluorescence

Materials

Thurs-P108	Alberto Tagliaferri	Elastic Strain Relief in a Single Lithographic SiGe Nanostructure by Nanobeam X-ray Diffraction
Thurs-P109	Jun Wang	In situ Study of Energy Materials and Microelectronics by Transmission X-ray Microscopy (TXM)
Thurs-P110	Zhi Xie	Elemental Mapping of Ancient Glass Eye-Bead Using SRXRF

Conference Exhibitor Information

Booth #		
7	**attocube systems AG** http://www.attocube.com Koeniginstr. 11a, Rgb. Munich, Germany 80539 tel: +49-89-2877809-0 fax: +49-89-2877809-19	attocube systems AG manufactures and distributes a complete line of easy-to-use scanning probe microscopes and nanopositioning systems for temperatures in the range from 300 K down to 10 mK! The innovative nanopositioners are also compatible with high vacuum and ultra high vacuum environments as well as with high magnetic fields up to 31 Tesla. Central to our proven suite of low-temperature microscopes is our powerful combination of fully automated and absolute reliable low temperature positioning devices with modular and flexible scanning probe sensors, designed specially to meet the needs of today's low temperature research. Our instruments give users the ability to analyze samples down to the atomic level, even at milli-Kelvin temperatures.
10	**Bruker Advanced Supercon GmbH** http://www.bruker-asc.com Friedrich-Ebert-Str. 1 Bergisch Gladbachm, Germany 51429 tel: +49-2204-84-5000 fax: +49-2204-84-5001	Bruker ASC, a former ACCEL Instruments business, provides a complete spectrum of X-ray microscopes with scanning and full-field microscopes for synchrotron and laboratory sources. Within the Bruker group, Bruker ASC is specializing in synchrotron instrumentation and superconducting magnet devices. We are a leading supplier of complete beamlines, insertion devices, beamline components (monochromators, mirror systems, slit systems, etc.) and end stations, e.g. for microscopy or crystallography. We can support your project during all stages from ray tracing and FEM studies, design, manufacturing, installation, to commissioning at the synchrotron. With the recent integration of AIXUV, a leading manufacturer of soft X-ray plasma sources, we offer brilliant soft X-ray laboratory sources and integrated standalone systems to make available synchrotron techniques in your home lab.
8	**Energetiq Technology, Inc.** http://www.energetiq.com 7 Constitution Way Woburn, MA 01801 USA tel: +1-781-939-0763 fax: +1-781-939-0769	Energetiq Technology, Inc. is a developer and manufacturer of short wavelength light sources. The Energetiq EQ-10SX is a compact, easy-to-use, reliable and cost-effective soft x-ray (SXR) light source system, based on Energetiq's™ unique Electrodeless Z-pinch™ technology using nitrogen gas. The high brightness, reliable, low-cost source of SXR photons allows researchers to perform their studies in the area of water-window microscopy and microbeam irradiation of biological samples without a synchrotron.
11	**Huber Diffraktionstechnik GmbH & Co. KG** http://www.xhuber.com Sommerstr. 4 Rimsting, Germany 83253 tel: +498051-68780	Huber Diffraction is a manufacturer of precise positioning and diffraction equipment for laboratory and synchrotron applications. We present a new beam conditioning unit for protein crystallography in addition to our well-known precision motion systems. Together with AXO Dresden, we will present the latest developments in x-ray multilayer optics both for 1-D and 2-D diffraction applications (5keV < E < 30keV) and soft x-ray polarization (E ≤ 1keV).

Booth #		
13	**Luxel Corporation** http://www.luxel.com 515 Tucker Ave. P.O. Box 1879 Friday Harbor, WA 98250 USA tel: +1-360-378-4137 fax: +1-360-378-4266	For over 35 years, Luxel Corporation has been the preeminent supplier of ultrathin freestanding films used in soft x-ray and EUV regions. Researchers using microscopy beamlines at the nation's synchrotron light sources require specimen holders that can control the sample environment in order to investigate materials in their natural state or under controlled experimental conditions. Many samples such as soil, cement, or biological specimens, are best studied in a wet or hydrated state. However, there exist no standard sample holders for the in situ study of hydrated materials optimized for these techniques. Luxel has developed a standardized wet sample holder for x-ray microscopy optimized for three-dimensional imaging. Ultra thin polymer windows are held apart by a micrometer-scale support structure forming a chamber that enables x-ray microscopy of the sample, retains hydration over several hours, limits extraneous background scattering effects, and affords free rotation of the sample in the x-ray beam.
4	**Nano-UV** http://www.nanouv.com 16-18 Avenue de Quebec Bat Neflier Courtaboeuf, Paris, France 91961 tel: +0033169072414 fax: +0033169072850	Nano-UV sas, based near Paris, France, specializes in extreme ultra-violet product development and solutions for semiconductor lithography and for the life science sector. We have designed and perfected a breakthrough compact light source for applications in industries such as EUV HVM lithography and metrology. Nano-UV works in exclusive partnership with EPPRA a well-established R&D company that has been active in the field of pulsed power and plasma applications for many years. Nano-UV is introducing the first stand alone soft x-ray microscope for in vitro label-free imaging of living tissue on a table size compact platform.
2	**North Star Imaging, Inc.** http://www.4nsi.com 19875 S. Diamond Lake Road Suite 10 Rogers, MN 55374 tel: +1-763-463-5650 fax: +1-763-463-5651	North Star Imaging (est. 1986) offers a complete line of digital x-ray and computed tomography (CT) systems, designed and built at NSI's corporate facility in Rogers, Minnesota. The X-View series of real-time digital radiography (DR) systems are designed for conventional inspections, plus NSI covers the gamut offering custom systems to solve even the most complex radiographic applications. NSI's X-View CT series integrates the most powerful CT reconstruction and visualization software available, including modules for calibration, measurement, real-time density segmentation and surface extraction (point cloud and CAD capabilities). Through the use of NSI's industry leading efX-CT software, CT system speed and ease of use is unmatched in the industry. This software offers a simple 5-step, start-to-finish CT process, plus the ability to upgrade existing systems from DR to CT. NSI's Inspection Services Group (ISG) utilizes the most advanced x-ray/CT inspection lab in the country. ISG specializes in computed tomography and real-time digital radiography to help with any and all inspection needs. North Star Imaging ranks among the nation's most sophisticated resources for real-time digital radiography and x-ray computed tomography systems, non-destructive testing (NDT) equipment, services, training, supplies, and accessories.

Booth #		
6	**Scanco USA, Inc.** http://www.microCT.com P. O. Box 646 Southeastern, PA 19399 USA tel: +1-610-688-1440 fax: +1-610-688-4976	Scanco Medical is the leading global provider of x-ray micro-CT scanners and contract based scanning services for non-destructive scanning applications. The range of scanners offers capabilities of obtaining 3-dimensional images ~1 micron resolution capability with very short scan times and high-throughput. All Scanco scanners are bundled with high-performance hp integrity servers. The systems, together with standardized analysis and visualization software provide for comprehensive 3D analysis. Scanco Medical customers include the world's leading academic as well as industrial research laboratories. Worldwide support and service provided from Switzerland or the USA.
5	**Silson Ltd.** http://www.silson.com JBJ Business Park Northampton Road Blisworth Northampton, England NN7 3DW tel: +44-1604-859-996 fax: +44-1604-859-991	Silson Ltd. is a manufacturer of membrane substrates, filters, and optical components for x-ray microscopy.
3	**SkyScan** http://www.skyscan.be Kartuizersweg 3 Kontich, Belgium 2550 tel: +32-38775705 fax: +32-38775769	SkyScan is a fast growing company and one of the world's leading producers of micro-CT systems for a wide range of applications. Our research and development of 3D x-ray microscopy started in the early 1980s. This led to the first micro-CT imaging results being obtained in 1983-1987 and published in scientific journals and international conferences proceedings. Building on this early work, SkyScan was founded in 1996, and within a year we were manufacturing a commercially available micro-CT scanner with spatial resolution in the micron range. In 2001 we produced the first high-resolution in-vivo micro-CT scanner for small animal imaging. And in 2005 SkyScan became the world's first supplier of a laboratory nano-CT scanner with submicron spatial resolution. Responding to demand from the growing community of micro-CT users, we are continually active in research and development into new methods for non-destructive 3D microscopy.
12	**Spectral Instruments** http://www.specinst.com 420 N. Bonita Ave. Tucson, AZ 85745 USA tel: +1-520-884-8821 fax: +1-520-884-8803	Spectral Instruments specializes in the development and manufacture of cooled CCD cameras for demanding low-light applications. We provide the finest low noise <3e-, high sensitivity, -110C cooling, 16-bit CCD cameras that current technology can offer. Optical inputs can include windows with custom coatings through fiber optic tapers or faceplates for x-ray or other high-energy particle imaging. Readout options are designed to be flexible and customized to the application. SI is also beginning production of the Direct Detector, which can directly image high-energy particles impacting the sensor with little damage to the sensor. Lens-coupled designs to keep the camera and other electronics out of the way of the beam are available as well. Custom CCD designs and OEM camera production are available.

Booth #		
9	**VSG - Visualization Sciences Group** http://www.vsg3d.com 15 New England Executive Office Park Burlington, MA 01803 tel: +1-781-685-4855 fax: +1-781-685-4601	VSG - Visualization Sciences Group is the leading provider of high-performance 3D visualization software for engineers, scientists, and application developers. VSG's software technologies range from Avizo® 3D visualization and analysis software for scientists and engineers, to Open Inventor® 3D toolkits for application developers. VSG brings more than 20 years of innovation to the highly complex visualization challenges in engineering, materials science, oil & gas, earth and life sciences, and medical industry.
1	**Xradia, Inc.** http://www.xradia.com 5052 Commercial Circle Concord, CA 94520 USA tel: +1-925-771-8000 fax: +1-925-288-0310	Xradia designs and manufacturers a family of high resolution 3D X-ray computed tomography (CT) systems for non-destructive imaging of complex internal structures. The company enables innovation and productivity through 3D insight for industrial and research applications in advanced materials, life sciences, microstructure modeling for oil and gas drilling, nanotechnology and semiconductor package failure analysis.

SKYSCAN

WWW.SKYSCAN.BE

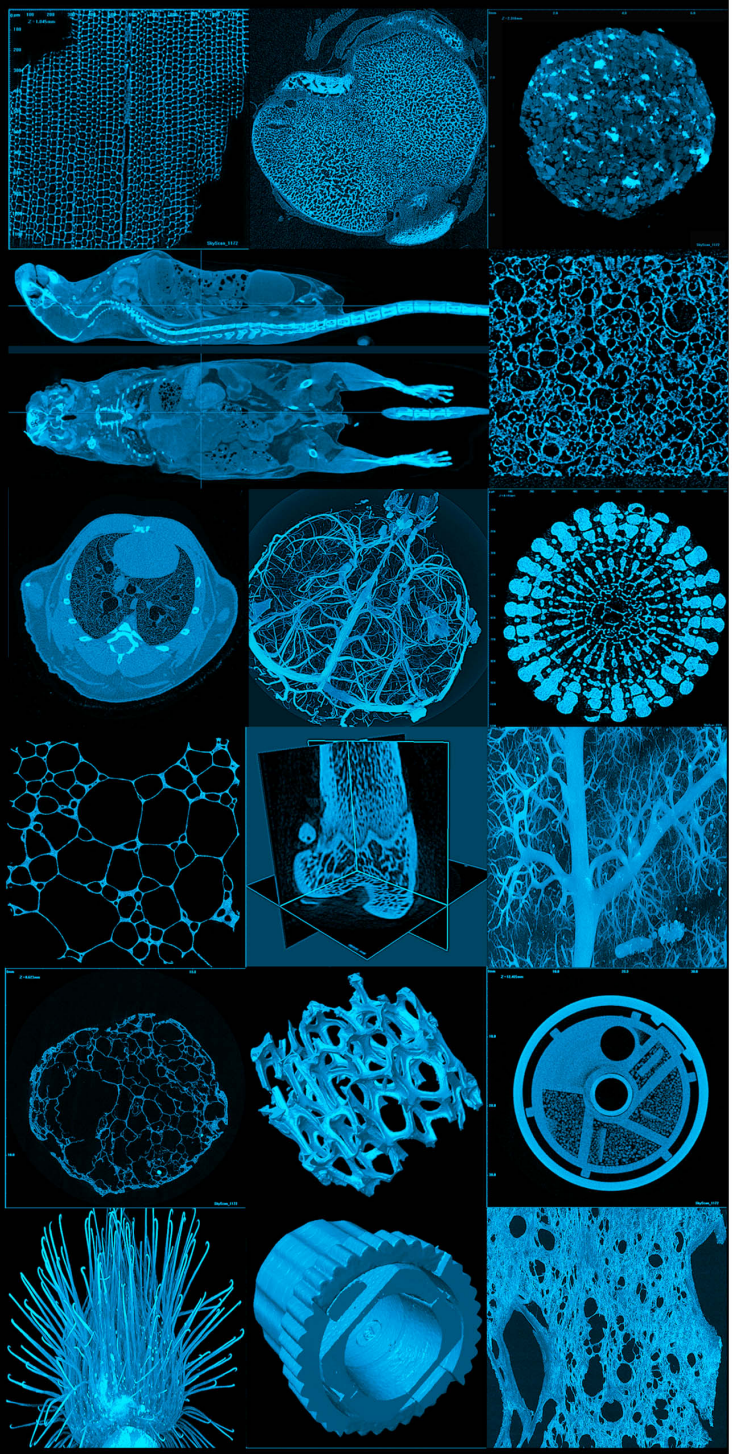

X-RAY MICROTOMOGRAPHY
X-RAY NANOTOMOGRAPHY
NON-INVASIVE 3D IMAGING
IN-VIVO SMALL ANIMAL SCANNING
2D / 3D IMAGE ANALYSIS

SkyScan1172: World's first 11Megapixel micro-CT

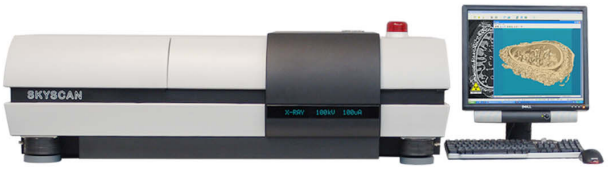

- fully distortion corrected 11Mp detector, up to 8Kx8K pixels in every slice,
- 600nm isotropic detail detectability, dynamically variable geometry,
- software for 2D / 3D image analysis and realistic visualization,
- scanning during compression, tension, cooling, heating

SkyScan 1173: World's first spiral micro-CT

- 140mm max. object size,
- 130kV X-ray source,
- flat panel detector,
- <5µm 3D resolution,
- 2D/3D image analysis
- no ring artifacts,
- no partial scan connections,
- integrated positioning stage.

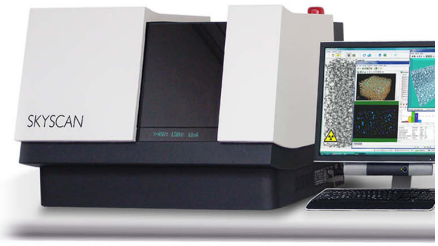

SkyScan 1174: World's most compact micro-CT

At a fraction of the price
of competitive systems,
with a small footprint,
this system provides fast,
high resolution 3D imaging
with superior quality.

SkyScan 2011: World's first lens-free Nano-CT

- compact laboratory system,
- 200nm detail detectability,
- integrated anti-vibration,
- no x-ray optics: all parts of object always in focus,
- single computer or cluster 3D reconstruction,
- 2D/3D image analysis, and realistic visualization.

SkyScan 1176: World's first spiral *in-vivo* micro-CT

- no ring artifacts,
- no partial scan connections,
- maintenance-free 90kV source,
- fully distortion corrected, dual-tap 11Mp X-ray camera,
- scanning cycle less than 1 minute,
- up to 8Kx8K pixels in every slice,
- 9µm 3D spatial resolution,
- full body mouse/rat scanning and distal limb scanning for big animals, such as rabbits,
- integrated physiological monitoring: breathing, movement detection, ECG,
- 4D time-resolved micro-CT

NORTH STAR IMAGING, INC.

INDUSTRIAL COMPUTED TOMOGRAPHY

High Resolution and High Power in One System

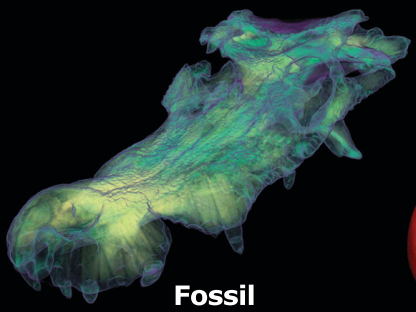

Fossil

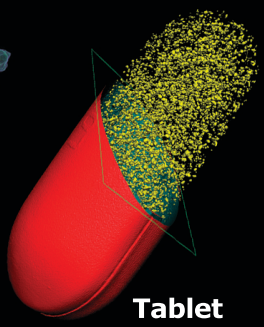

Tablet

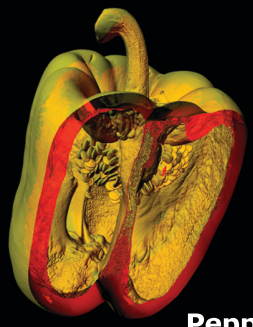

Pepper

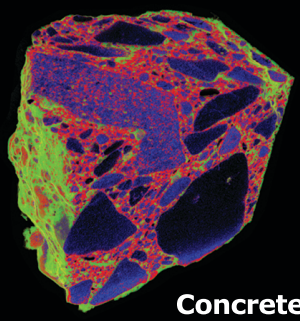

Concrete

North Star Imaging's **Industrial Computed Tomography X-ray Systems** are a complete solution for almost any **High Resolution** inspection application. NSI's CT systems lead the industry in flexibility and ease of use. Features include:

Multi-scale Capabilities

Submicron Resolution

Systems up to 450kV

In Situ Experiments

High Speed (record 2 sec.)

Upgradable

Current users include: University of Florida, South Dakota State University, U.S. Department of Energy, Battelle National Lab, John Hopkins University, Royal Institute of Sweden and many other research institutions.

19875 S DIAMOND LK RD • SUITE 10 • ROGERS, MN 55374 • 763-463-5650 • WWW.XVIEWCT.COM

Silicon Nitride Membrane Windows

Since 1994, Silson Ltd has supplied ultra-thin silicon nitride membrane windows to customers throughout the world. Membranes are now available to cover a wide range of x-ray applications. In addition to the standard range of membranes, Silson produces many bespoke windows for specific customer requirements.

Membrane Array

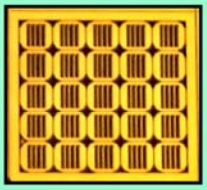

Multi-frame TEM Array

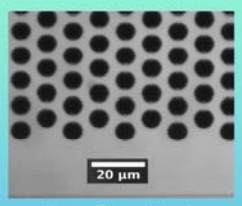

Perforated Membrane

Membranes Inspected 100%

Silson Standard Membrane Matrix

Frame Size (mm)

Membrane Size (mm)	TEM	5.0	7.5	10.0	12.5	14.0	17.5	23.5
0.25								
0.50								
0.75								
1.0								
1.5								
2.0					Available as Standard			
2.5								
3.0								
4.0								
5.0								
6.0								
7.0								
8.0								
9.0						X	X	X
10.0						X	X	X
11.0							XX	XX
12.0							XX	XX
13.0							XXX	XXX
14.0							XXX	XXX
15.0								XXX

Membranes are available on Silicon substrate thicknesses of 200 µm, 381 µm and 525 µm

Membranes are available in the following Silicon Nitride thicknesses:-
30 nm, 50 nm, 75 nm, 100 nm, 200 nm, 500 nm, and 1000 nm except where indicated.

75 nm not available:- X
50 nm not available:- X
30 nm not available:- X
20 nm by special request

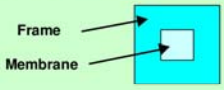

Differential pressure membrane selection guide

Membrane thickness (nm)	Membrane size (mm) 0.25	0.50	1.0	1.5	2.0	2.5	3.0	3.5	4.0	4.5	5.0	5.5	6.0	7.0	8.0	9.0	10.0
1000																	
500																	
200																	
100																	
50																	
30																	

> 2.0 bar	
1.0 bar - 2 bar	
0.5 bar - 1.0 bar	
200 mbar - 500 mbar	
100 mbar - 200 mbar	
30 mbar - 100 mbar	

Etched Finder Grids

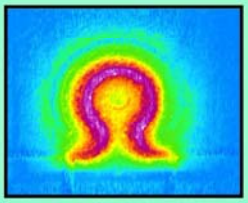

Heated Membrane

Mounted Vacuum Window

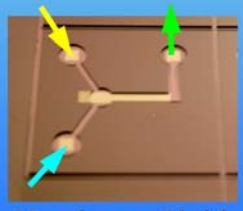

Membrane Fluid Mixing Channel

Silson Ltd • JBJ Business Park • Northampton Road • Blisworth • Northampton NN7 3DW • England
Tel: (+44) (0)1604 859996 • Fax: (+44) (0)1604 859991• Email: sales@silson.com • Web: www.silson.com

Oral Presentation Abstracts

Sub-10-nm Focusing of Hard X-rays Using Mirror Optics

K. Yamauchi[1,2], H. Mimura[1], T. Kimura[1], S. Handa[1], H. Yumoto[3], S. Matsuyama[1], Y. Sano[1], Y. Nishino[4], K. Tamasaku[5], M. Yabashi[5], T. Ishikawa[5]

[1]*Department of Precision Science & Technology, Faculty of Engineering, Osaka University, 2-1Yamada-oka, Suita, Osaka 565-0871, Japan*
[2]*Center of Ultraprecision Science & Technology, Faculty of Engineering, Osaka University, 2-1Yamada-oka, Suita, Osaka 565-0871, Japan*
[3]*JASRI, SPring-8, 1-1-1 Kouto, Sayo-cho, Sayo-gun, Hyogo 679-5148, Japan*
[4]*Research Institute for Electronic Science, Hokkaido University, Kita 21 Nishi 10 Kita-ku, Sapporo 001-0021, Japan*
[5]*RIKEN, SPring-8, 1-1-1 Kouto, Sayo-cho, Sayo-gun, Hyogo 679-5148, Japan*

This research was partially supported by Grant-in-Aid for the Specially Promoted Research (No. 18002009), "Promotion of X-ray Free Electron Laser Research," and the Global COE Program "Center of Excellence for Atomically Controlled Fabrication Technology" from the Ministry of Education, Culture, Sports, Science and Technology (MEXT).

Abstract:

We developed precision fabrication and measurement methods to realize nano-focusing mirror devices for synchrotron radiation hard X-rays [1-5]. The fabricated KB mirrors were tested at the 1-km-long beamline (BL29-XUL) of SPring-8, and confirmed to realize nearly diffraction-limited focusing with the spot size less than 30 nm at 15-keV X-ray [6].

In recent research project, we achieved 7-nm focusing of 20-keV X-ray by using Pt/C multilayer mirrors with an on-site wavefront phase measurement and correction method [7-11]. The on-site phase-error measurement is based on a phase retrieval method using precisely measured intensity-profiles near the beam waist. A bendable mirror is placed upstream of the focusing mirror to compensate the wavefront error due to the imperfection of focusing devices. Details of the method [12] will be presented with the latest results.

References:

[1] K. Yamauchi et al., J. Synchrotron Rad. **9**, 313 (2002).
[2] Y. Mori et al., Rev. Sci. Instrum. **71**, 4627 (2000).
[3] K. Yamauchi et al., Rev. Sci. Instrum. **73**, 4028 (2002).
[4] K. Yamauchi et al., Rev. Sci. Instrum. **74**, 2894 (2003).
[5] H. Mimura et al., Rev. Sci. Instrum. **76**, 045102 (2005).
[6] H. Mimura et al., Appl. Phys. Lett., **90**, 051903 (2007).
[7] K. Yumoto et al., Rev. Sci. Instrum. **77** (2006), 093107.
[8] H. Mimura et al., Phys. Rev. A, **77**, 015812 (2008).
[9] T. Kimura et al., Jpn. J. Appl. Phys. **48**, 072503 (2009).
[10] S. Handa et al., Jpn. J. Appl. Phys. **48**, 096507 (2009).
[11] H. Mimura et al., Nature Phys **6**, 122 (2010).
[12] S. Handa et al., Nucl. Instrum. Methods A (2010) to be published.

Towards 10-nm Zone-Plate Fabrication

A. Holmberg, J. Reinspach, M. Lindblom, E. Chubarova, M. Bertilson, O. von Hofsten,
D. Nilsson, P. Skoglund, U. Lundström, P. Takman, U. Vogt, H. M. Hertz

Biomedical and X-Ray Physics, Department of Applied Physics, Royal Institute of Technology, SE-10691 Stockholm, Sweden

Abstract:
We present our process improvements for fabricating high-resolution zone plates used for soft x-ray microscopy and our initial efforts on fabricating zone plates for hard x-ray free-electron-laser applications. In addition to the fabrication, recent activities in laboratory soft x-ray microscopy are reviewed.

High-quality zone plates with very narrow outermost zones are key components to improve the resolution in soft x-ray microscopy. Here we present the nanofabrication process allowing us to reach 13-nm outermost-zone-width, 35-nm high, soft x-ray nickel zone plates [1]. To increase their diffraction efficiency, we have extended the fabrication process to make so-called nickel-germanium zone plates [2]. We show a 50% enhancement in efficiency for 15-nm outermost-zone-width zone plates and discuss the possibility to reach higher resolution with this process.

Zone plates have the potential to provide diffraction-limited focusing for the forthcoming hard x-ray free-electron lasers. The impact of the high heat load and rapid temperature fluctuations of the intense and pulsed beam on zone plates has been analyzed [3]. We presently investigate fabrication limitations of several optical materials such as gold, platinum, tungsten, and diamond and show the first results for gold and platinum zone plates with down to 50-nm outermost zone width and with up to 7% diffraction efficiency measured at 8 keV.

Our in-house laboratory soft x-ray microscope is used for microscopy applications and testing of new optics [4-6]. The laser-plasma source is presently upgraded with a new 280 W Nd:YAG laser with the goal to reach bending-magnet water-window brightness. A new Cr/V normal-incidence multilayer-mirror condenser for $\lambda = 2.48$ nm has been installed in combination with a high-tilt cryo sample stage. This has made cryo-fixated-sample computed tomography possible. The potential improvement offered by these upgrades will be discussed also taking our recent zone plate development into consideration.

References:

[1] J. Reinspach, M. Lindblom, O. von Hofsten et al., J. Vac. Sci. Technol. B. **27**, 2593 (2009).
[2] M. Lindblom, J. Reinspach, O. v. Hofsten et al., J. Vac. Sci. Technol. B. **27**, L5 (2009).
[3] D. Nilsson, A. Holmberg, H. Sinn, U. Vogt (accepted to Nuclear Instruments and Methods A).
[4] O. von Hofsten, M. Bertilson, J. Reinspach et al., Opt. Lett. **34**, 2631 (2009).
[5] M. Bertilson, O. v. Hofsten, U. Vogt et al., Opt. Express. **17**, 11057 (2009).
[6] O. von Hofsten, M. Bertilson, M. Lindblom et al., Opt. Lett. **33**, 932 (2008).

Development of Multilayer Laue Lenses; (1) Linear Type

T. Koyama[1], H. Takenaka[2], S. Ichimaru[2], T. Ohchi[2], T. Tsuji[1], H. Takano[1], Y. Kagoshima[1]

[1]Graduate School of Material Science, University of Hyogo, 3-2-1 Kouto, Kamigori, Ako, Hyogo 678-1297, Japan

[2]NTT-AT Nanofabrication Corporation, 3-1 Wakamiya, Morinosato, Atsugi, Kanagawa, 243-0124, Japan

Abstract:

Multilayer Laue Lens (MLL) has been explored by the APS [1,2]. We have also developed the MLL as collaboration between Univ. of Hyogo and NTT-ATN [3]. In this paper, we report the fabrication and the performance test of the linear type MLL.

The multilayer of 1000 alternating $MoSi_2$ and Si layers with layer-thickness gradually increasing from 5 nm to 316 nm according to the Fresnel lens structure has been fabricated using DC magnetron sputtering. $MoSi_2$/Si material combination is good for MLL because Mo-silicide/Si multilayers have sharper interfaces, heat resistance, and high diffraction efficiency [4]. The depth structure of the multilayer has been measured by SEM as shown in Figure 1. The multilayer total thickness is about 10 □m. The $MoSi_2$/Si MLL has been obtained by cutting out a cross-sectioned piece and thinning it to the desired depth, several 10 □m.

The focusing test was performed at the SPring-8 beamline BL24XU by using 20 keV x-rays. By observing the far-field diffraction image of the MLL with various incident angles using a CCD detector, obtained intensity distributions showed similar structure to the calculated diffraction efficiency, so that dynamical diffraction effect was confirmed. In addition, obtained beam size was 13.1 nm as shown in Figure 2. Ten measurements were performed in order to confirm the reproducibility. This value was close to the diffraction limit. Maximum local diffraction efficiency measured was 62%. Further, two pieces of linear MLL were arranged in the KB configuration and applied to scanning microscopy. 2D image of a test chart as fine as 200-nm-L&S pattern was successfully obtained. This development was supported by SENTAN, JST.

References:

[1] J. Maser et al., Proc. SPIE **5539**, 185 (2004).
[2] C. Liu et al., Thin Solid Films **515**, 654 (2006).
[3] T. Koyama et al., Appl. Phys. Express **1**, 117003 (2008).
[4] H. Takenaka et al., Appl. Phys. **78**, 5227 (1995).

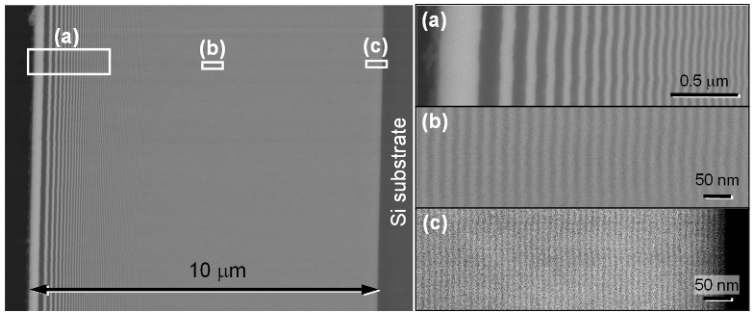

Figure 1: A Cross-sectional SEM image of the $MoSi_2$/Si multilayer Laue lens.

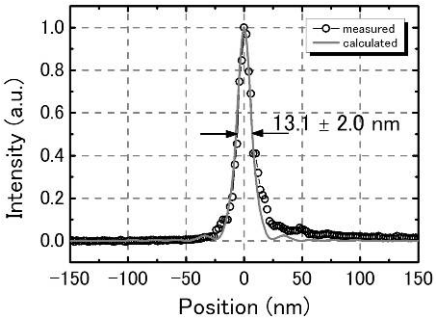

Figure 2: The result of beam size measurement.

Toward One-Nanometer Hard X-Ray Microscopy Using Multilayer Laue Lenses

H. Yan[1,3], H. C. Kang[4], V. Rose[2], D. Shu[2], E. Lima[3], R. Conley[2,3], C. Liu[2], N. Jahedi[2], A. T. Macrander[2], G. B. Stephenson[1], Y. S. Chu[3], J. Maser[1,2]

[1]Center for Nanoscale Materials, Argonne National Laboratory, Argonne, Illinois 60439, USA
[2]Advanced Photon Source, Argonne National Laboratory, Argonne, Illinois 60439, USA
[3]National Synchrotron Light Source II, Brookhaven National Laboratory, Upton, NY 11973, USA
[4]Department of Advanced Materials Engineering and BK21 Education Center of Mould Technology for Advanced Materials and Parts, Chosun University, Gwangju 501-759, Republic of Korea

* This work is supported by the U. S. Department of Energy, under Contract No. DE-AC02-06CH11357 for University of Chicago and Argonne, LLC., and under Contract No. DE-AC02-98CH10886 for Brookhaven Science Associates, LLC.

Abstract:

The difficulty of making x-ray focusing optics with high numerical aperture is the major obstacle of advancing x-ray microscopy into the nanometer regime. In the last decade there has been great progress in the fabrication of mirror, refractive and diffractive lenses to push the frontier of x-ray focusing well below 50 nm. Multilayer Laue lens (MLL) [1], a novel diffractive optic, have been shown to have a theoretical performance of below 1 nm focusing with very high efficiency in the hard x-ray regime [2]. To date, a 16 nm line focus with over 30% efficiency has been achieved by MLL optics at an x-ray energy 19.5 keV [3]. Because of its prospect for superior performance, the NSLS-II project has initiated an aggressive R&D program to explore the technical limit toward one nanometer focusing.

We will discuss the properties of MLLs from a theoretical perspective, including the effect of imperfections for realistic structures. The advantages and disadvantages of an MLL-based microscope will be discussed. Lastly, we will show the present status of the development of the MLL-based microscope [4].

References:

[1] H.C. Kang et al., Phys. Rev. Lett. **96**, 127401 (2006).
[2] H.F. Yan et al., Phys. Rev. B **76**, 115438 (2007).
[3] H.C. Kang et al., Appl. Phys. Lett. **92**, 221114 (2008).
[4] H.F. Yan et al., "Hard x-ray microscopy at the nanoscale," in preparation.

Instruments for Soft X-ray Tomography and Correlated Light Microscopy of Biological Specimens at the National Center for X-ray Tomography

C. Knoechel[1,2], M. LeGros[2,3], D. Parkinson[1,2], M. Uchida[1,2], G. McDermott[1,2], C. Larabell[1,2,3]

[1]*Department of Anatomy, University of California San Francisco, San Francisco, CA, USA*
[2]*National Center for X-ray Tomography, Advanced Light Source, Berkeley, CA, USA*
[3]*Physical Biosciences Division, Lawrence Berkeley National Laboratory, Berkeley, CA, USA*

Abstract:

XM-2 is a recently commissioned soft x-ray microscope at the Advanced Light Source, Berkeley. The new instrument was specifically designed and optimized for imaging biological specimens in 3-dimensions, close to their native state, and at high spatial resolution [1]. We will present the technical and optical design of the new instrument, including a description of a multi-function cryo-rotation stage. The primary function of this instrument is to both maintain radiation sensitive specimens at low temperature and allow them to be rotated around an axis during tomographic data collection. In modern biology it is rare that a single imaging technique can unambiguously provide all of the information required. Therefore we have designed the cryo-rotation stage to allow ready incorporation of other imaging modalities. In particular, we will present our latest results demonstrating the correlation of high numerical aperture fluorescence data with soft x-ray tomographic data. The combination of modalities allows the localization of fluorescently tagged molecules in the context of a high-resolution reconstruction of a cell [2]. This multi-modal approach will have a significant impact on research in areas such as fundamental cell biology, phenotypic switching and drug discovery, as well as the development of biofuels. Additionally, ongoing work on optimization of sample preparation and data analysis procedures will be presented.

References:

[1] G. McDermott, M.A. Le Gros, C.G. Knoechel et al., Trends Cell Biol. **19**, 587 (2009).
[2] M.A. Le Gros, G. McDermott, M. Uchida et al., J. Microsc. **235**, 1 (2009).

Fabrication of Diffractive Optics for Present and Future X-ray Sources

C. David, J. Vila-Comamala, S. Gorelick, V. A. Guzenko

Paul Scherrer Institut, 5232 Villigen-PSI, Switzerland

Abstract:

Diffractive x-ray optics play a key role in the progress of x-ray microscopy. Diffractive lenses, i.e. Fresnel zone plates (FZPs), are widely used to create nanometer-sized probes for scanning transmission x-ray microscopy (STXM), or as condenser and objective lenses in full-field type instruments. Besides their very high resolution power, diffractive x-ray optics have the advantage of providing an excellent control over the wavefront even for large apertures. This is important when used as optics in coherent diffraction imaging experiments and it allows for the realization of complex functionalities such as beam shaping or phase contrast imaging.

The performance of diffractive x-ray optics depends to a large extent on nanofabrication techniques. We have recently upgraded our nanolithography capabilities and developed new strategies for the development of high performance x-ray optical devices. This has led to a new generation of FZPs with unprecedented performance [1]. We were able to resolve 9 nm lines/spaces in STXM mode at 1.2 keV, and 15 nm lines/spaces at 6.2-keV photon energy. In addition, we have developed efficient techniques for the fabrication of very high aspect ratio gold FZPs [2]. These are used for various microscopy experiments such as the high resolution tomographic imaging in Zernike phase contrast with a beam shaping condenser or analysis of nanoscale polycrystalline samples by scanning diffraction.

The rapid progress in the performance of x-ray sources opens the path to new scientific experiments; however, it in turn raises demands on x-ray optics development. The dramatic increase in transverse coherence length will require wavefront preserving optics with sizes approaching the millimeter range. In addition, radiation damage will be a critical issue at x-ray sources based on the free electron laser (X-FEL) principle. We have started to investigate the relevant mechanisms of radiation damage and to develop radiation hard focusing devices for X-FEL radiation based on diamond.

References:

[1] J. Vila-Comamala, K. Jefimovs, J. Raabe et al., Ultramicroscopy **109**(11), 1360 (2009).

[2] S. Gorelick, V.A. Guzenko, J. Vila-Comamala et al., submitted to: Nanotechnology (2010).

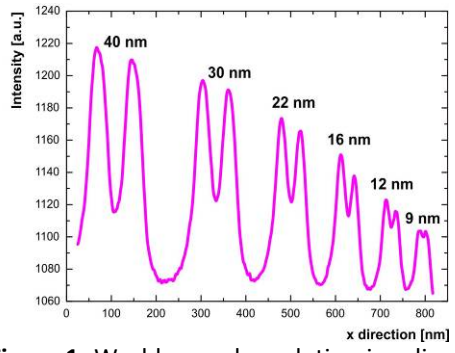

Figure 1: World record resolution in a line scan across a test object showing 9-nm-wide resolved lines.

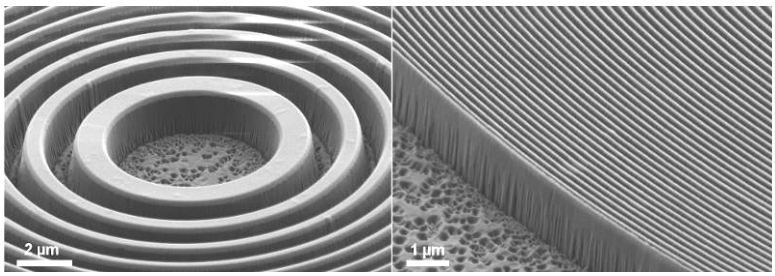

Figure 2: Diamond Fresnel zone plate for high heat load applications at free electron laser sources. The outermost zones are 100 nm wide and 1400 nm high.

X-ray Talbot Interferometry at ESRF: Applications and Recent Technical Developments

T. Weitkamp[1], I. Zanette[1], S. Lang[2], G. Schulz[2], H. Deyhle[2], B. Müller[2], M. Bech[3], A. Tapfer[3], F. Pfeiffer[3], E. Reznikova[4], J. Kenntner[4], J. Mohr[4], S. Rutishauser[5], T. Donath[5], C. David[5]

[1]*European Synchrotron Radiation Facility, 38043 Grenoble, France*
[2]*Biomaterials Science Center, University of Basel, 4031 Basel, Switzerland*
[3]*Technische Universität München, 85748 München, Germany*
[4]*Institut für Mikrostrukturtechnik, Karlsruher Institut für Technologie, 76021 Karlsruhe, Germany*
[5]*Labor für Mikro- und Nanotechnologie, 5232 Villigen PSI, Switzerland*

Abstract:
X-ray Talbot interferometry [1,2], a method yielding high-sensitivity phase-contrast images as well as scattering contrast ("dark-field" images), has recently been implemented and is under continuing development at several synchrotron radiation facilities. At the imaging beamline ID19 at ESRF, the high spatial coherence, relatively large beam, and wide energy range of the beamline offer unique possibilities for the exploitation of this technique in the life sciences, paleontology, and materials science. Recent instrumental improvements, such as a high-energy variant and a 2D interferometer (Fig. 1) and applications (Fig. 2 and ref. [3]) will be presented.

References:
[1] A. Momose, Jpn. J. Appl. Phys. **42**, L866 (2003).
[2] T. Weitkamp, A. Diaz, C. David et al., Opt. Express **13**, 6296 (2005).
[3] G. Schulz, T. Weitkamp, I. Zanette, F. Pfeiffer, F. Beckmann, C. David, S. Rutishauser, B. Müller, submitted.

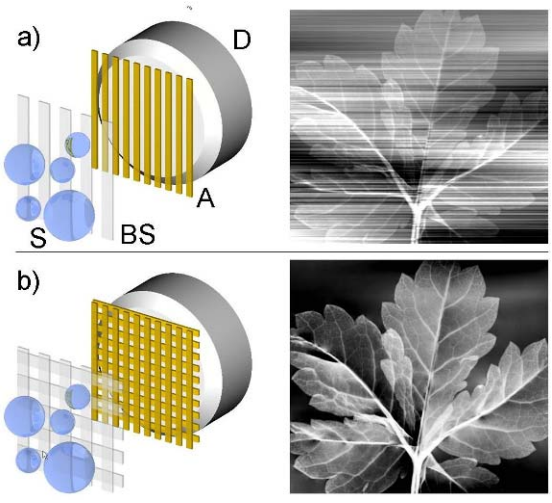

Figure 1: An X-ray grating interferometer (a), in which two line gratings BS and A and a detector D are used to image sample S, can be improved by using two-dimensional gratings (b), as the comparison of retrieved phase images (right) shows.

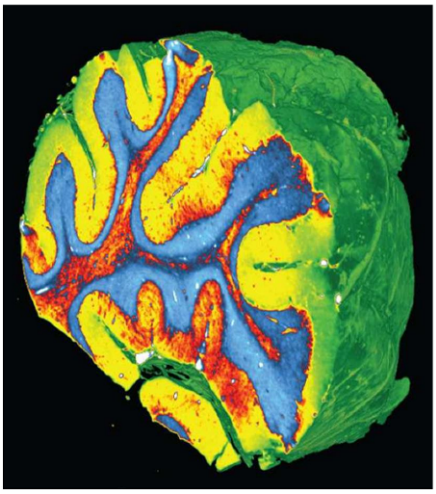

Figure 2: 3D color rendering of a human cerebellum from tomography data taken with a grating interferometer at the ESRF beamline ID19. The full study is reported in ref. [3], from which this picture is taken.

Zone Plate Development at the Helmholtz-Zentrum Berlin: Current Status and Future Possibilities with the New 100-keV e-Beam Writer

S. Rehbein, S. Werner, P. Guttmann, S. Heim, G. Schneider

Helmholtz-Zentrum Berlin für Materialien und Energie GmbH, Wilhelm-Conrad-Röntgen-Campus, BESSY II, Albert-Einstein-Str. 15, 12489 Berlin, Germany

Abstract:

We report on x-ray optical methods to improve the spatial resolution for imaging with zone plates towards 10 nm. At the Helmholtz-Zentrum Berlin, we work on two different approaches. The first approach is the traditional way to improve the resolution by decreasing the outermost zone width. For this purpose, a new state-of-the-art 100 keV e-beam system from VISTEC was recently installed at the Helmholtz-Zentrum Berlin. With this system, it becomes possible to expose zone plates with an outermost zone width significantly below 20 nm with high placement accuracy. However, the fabrication of zone plates with very narrow zones and high aspect ratios is still very challenging due to nanotechnology difficulties in the subsequent structuring processes. The second approach overcomes the problem to manufacture increasingly smaller zone widths by applying high orders of diffraction for imaging [1]. This significantly improves the numerical aperture of the zone plate objective since the numerical aperture scales with the order of diffraction. Nevertheless, also this approach requires advanced nanotechnology approaches for enhancing the high order efficiency. Both approaches are discussed and the achieved spatial resolution of the BESSY full-field x-ray microscope will be presented.

References:

[1] S. Rehbein, S. Heim, P. Guttmann et al., Phys. Rev. Lett. **103**, 110801 (2009).

Following Dynamic Processes by X-ray Tomographic Microscopy with Sub-second Temporal Resolution

R. Mokso[1], U. Kaydok [1,2], F. Marone[1], G. Mikuljan[1], A. Isenegger[1], M. Stampanoni[1,2]

[1]*Swiss Light Source, Paul Scherrer Institut, 5232 Villigen, Switzerland*
[2]*Institute for Biomedical Engineering, University and ETH Zurich, Zurich, Switzerland*

Abstract:

Several imaging techniques offer the possibility to observe rapid phenomena in real time. Yet most of these techniques fail when it comes to bulky samples and micrometer precision in three dimensions. The penetrating power of X-rays, coupled with the high flux of third-generation synchrotron sources, makes X-ray tomographic microscopy excel among fast imaging methods. Exploiting this asset of synchrotron sources was the motivation for setting up an ultra-fast tomography end station at the TOMCAT beamline [1]. The state-of-the-art instruments at synchrotron sources routinely offer a temporal resolution of tens to hundreds of seconds in tomography. For a number of processes of interest in biological or material science studies (breathing, heartbeat, foam expansion) the relevant time scales are rather in the range of 0.5-2 seconds.

To overcome motion artifacts when imaging such systems, a new ultra-fast tomographic data acquisition scheme needed to be developed. Our effort is directed towards achieving sub-second temporal resolution in 3D while keeping a high image quality. A full tomographic set of several hundred projections may be acquired in 50-500 ms in white-beam or monochromatic configuration, respectively. The ultimate goal is to develop acquisition schemes that allow quasi-real-time visualization of the tomographic reconstruction of the sample. We discuss the limitations and present our approach [2] to using various phase- and absorption-based contrast regimes. We will show the first biomedical and material science applications (Figure 1) that benefit from this new development in ultra-fast three-dimensional imaging.

References:

[1] M. Stampanoni et al., Proc. SPIE **6318**, 63180C, Developments in X-Ray Tomography V; U. Bonse, Ed., Aug. 2006.

[2] R. Mokso, F. Marone, M. Stampanoni, Proc. of SRI2009, AIP Conf. Proc. (in press).

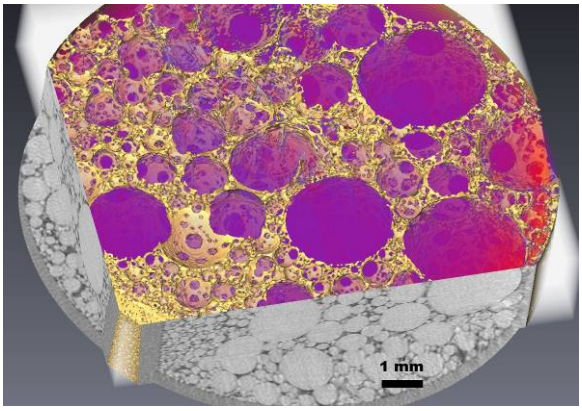

Figure 1: 3D image of a rapidly collapsing beer foam. Total tomographic acquisition time was 0.5 s with voxel size of 11 µm and X-ray energy of 20 keV.

Coherence Measurements and Coherent Diffractive Imaging Experiments at FLASH

I.A. Vartaniants, A.P. Mancuso, A. Singer, O.M. Yefanov, J. Gulden

Deutsches Electronen-Synchrotron DESY, Notkestraße 85, D-22607 Hamburg, Germany

Abstract:

FLASH (the Free-electron LASer in Hamburg) at DESY was the first operating free-electron laser (FEL) in the XUV energy range [1]. In this presentation an overview [2] of recent experiments focused on coherence measurements [3] and coherent x-ray diffractive imaging (CXDI) on a periodic [4] and non-periodic biological samples [5] at FLASH will be given.

Coherence is one of the most prominent features of laser sources. The measurement of the coherence properties of existing FELs is of vital importance for understanding the physical properties that lie behind the self amplified spontaneous emission (SASE) generation of coherent beams, for optimization of the parameters of these sources, and for the construction of the beamlines. Young's double slit experiment was perfomed at FLASH [3] to measure its coherence properties. Our analysis has shown that the coherence length 20 m downstream from the source is 300 μm (horizontal) and 250 μm (vertical).

CXDI for the reconstruction of a two-dimensional (2D) finite crystal structure with a single pulse train of FLASH radiation at 7.97 nm wavelength was demonstrated [4]. This measurement shows an advance on traditional CXDI techniques by applying it to a periodic structure. It is also significant that this approach paves the way for the imaging of the class of specimens which readily form 2D, but not three-dimensional crystals. We show that the structure is reconstructed to the detected resolution, given an adequate signal to noise ratio.

In our next experiment [5] we employ CXDI using FLASH in a *non-destructive* regime to compare images of a biological sample reconstructed using different, single, femtosecond pulses of FEL radiation. We demonstrated that images obtained from statistically different FEL pulses contain the same amount of structural information up to the measured resolution. This result is especially important for the success of a single molecule imaging approach [6]. Furthermore, for the first time, we demonstrate CXDI, in-line holography and Fourier Transform Holography (FTH) of the same unicellular marine organism using an FEL and present diffraction data collected using the third harmonic of FLASH, reaching into the water window. We provide quantitative results for the resolution of the CXDI images as a function of pulse intensity, and compare this with the resolutions achieved with in-line holography and FTH.

References:

[1] W. Ackermann et al., Nature Photonics **1**, 336 (2007).
[2] I.A. Vartanyants et al., J. Phys. B (2010) Topical issue: Intense X-ray science: The 8 years of FLASH (submitted).
[3] A. Singer et al., Phys.Rev. Lett. **101**, 254801 (2008).
[4] A. P. Mancuso et al., Phys. Rev Lett. **102**, 035502 (2009).
[5] A. P. Mancuso et al., New J. Phys. (2010) Focus issue: X-ray beams with high coherence (in print).
[6] K.J. Gaffney et al., Science **316**, 1444 (2007).

Multilayer-Based Optics for High-Brightness X-ray Sources

S. Bajt

Deutsches Elektronen-Synchrotron, Notkestrasse 85, 22607 Hamburg, Germany

Abstract:
High brightness X-ray sources, such as next-generation synchrotrons and free electron lasers (FELs), pose unique challenges for the development of x-ray optics. The peak intensities of x-ray pulsed sources, such as FLASH in Hamburg and LCLS at Stanford, can be high enough to covert any material placed in the focused beam into a plasma. Not only the samples but also the x-ray optics close to the focal spot experience partial or complete damage. Thus, one either tries to avoid direct interaction with the primary focused beam or has to accept limited optics lifetime or even complete destruction after each shot. In this talk I will discuss different types of multilayer-based optics successfully used in FLASH experiments with special emphasis on their performance and lifetime. They were used for reflecting, focusing and filtering of short pulsed x-rays in a variety of novel science applications.

Full-Field Microscope for EUVL Mask Characterization*

F. Brizuela[1], S. Carbajo[1], D. Alessi[1], Y. Wang[1], D. Martz[1], A. Sakdinawat[2], K. Goldberg[2], D. Attwood[2], M. Marconi[1], J. Rocca[1], C. Menoni[1]

National Science Foundation ERC for Extreme Ultraviolet Science and Technology
[1]Electrical and Computer Engineering, Colorado State University, Fort Collins, CO 80526
[2]Center for X-Ray Optics, Berkeley National Laboratory, Berkeley, CA 94720

* Work supported by the Engineering Research Centers Program of the National Science Foundation under NSF Award Number EEC-0310717.

Abstract:

As the semiconductor industry prepares to print the next generation of semiconductor chips using Extreme Ultraviolet Lithography (EUVL), the availability of compact inspection and metrology tools for Mo/Si multilayer-coated EUVL masks is crucial.

Aerial mask inspection microscopes require illumination from a source operating within the ~ 1 nm bandwidth reflectivity band of Mo/Si multilayers centered at 13.5 nm. Furthermore, these microscopes are required to provide the same illumination conditions encountered in an EUVL lithography stepper to allow evaluation of pattern and defect printability independently of resist response. We have developed a full-field microscope for EUVL aerial mask inspection that uses as illumination the high brightness output from on a table-top laser emitting at 13.2 nm wavelength [1, 2]. The microscope acquires high quality images of absorption patterns in EUVL exposures of tens of seconds in which 55 nm critical dimension features are fully resolved. The high uniformity of the illumination permits a detailed analysis of these printed features. These results open the path for the development of a practical and compact metrology tools for EUVL mask inspection.

References:

[1] F. Brizuela et al., Opt. Lett. **34**, 271 (2009).
[2] J. J. Rocca et al., Opt. Lett. **30**, 2581 (2005).

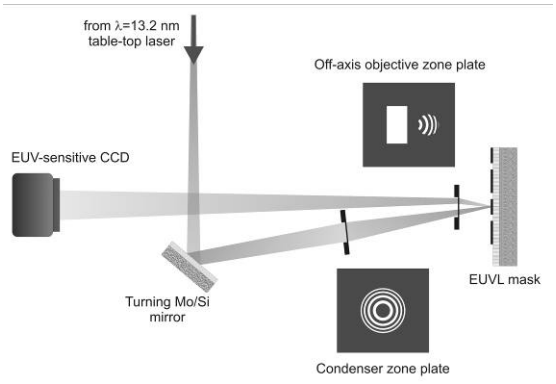

Figure 1: Schematic setup of the microscope.

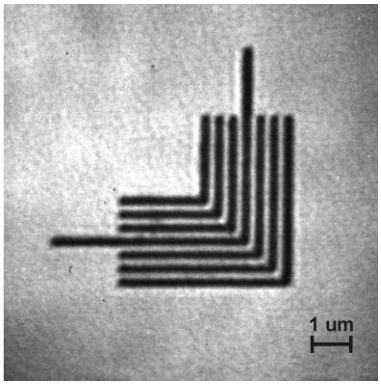

Figure 2: EUV image of a 180 nm half-pitch elbow structure.

Laboratory Soft X-ray Tomography of Cryo-Fixated Cells

M. Bertilson[1], O. von Hofsten, M. Lindblom, J. Reinspach, A. Holmberg, U. Vogt, H. M. Hertz

Biomedical and X-Ray Physics, Department of Applied Physics, Royal Institute of Technology/Albanova, SE-10691, Stockholm, Sweden
[1]michael.bertilson@biox,kth.se

Abstract:

High-resolution soft x-ray microscopy utilizes the high resolving power of zone plates and the natural contrast provided by the water window (λ = 2.4 - 4.4 nm). The technique is capable of imaging several-microns-thick cryo-fixated biological samples at sub-visible-microscopic resolution. Low-numerical-aperture optics and negligible scattering of x-rays make computed-tomography (CT) 3D imaging possible. Presently this is performed at synchrotron sources such as ALS and BESSY [1]. Many researchers would however benefit from having the microscope in their own laboratory. For this reason we developed the first laboratory soft x-ray microscope based on a liquid-jet laser-plasma x-ray source [2] and extended it to 3D imaging [3]. The microscope has so far been capable of imaging non-frozen samples at λ = 3.37 nm or λ = 2.48 nm. The shorter wavelength penetrates deeper, gives a longer depth of focus, and provides a longer working distance, all important for CT 3D imaging.

In this contribution we demonstrate 2D and 3D imaging of cryo-fixated biological specimens using a laboratory soft x-ray microscope operated at λ = 2.48 nm. The microscope is based on a liquid-nitrogen-jet laser-plasma source [4], a new Cr/V normal-incidence multilayer-mirror condenser, a long-working-distance in-house fabricated 30-nm-outer-zone-width zone plate, and a CCD. The sample stage is a modified FEI Compustage, compatible with standard TEM sample holders. A high-tilt cryo-holder enables acquisition of tilt series of cryo-frozen biological samples on TEM grids. Images of plunge frozen cells and parasites will be presented.

References:

[1] See, e.g., M. Uchida, G. McDermott, M. Wetzler et al., PNAS **109**, 46 19375 (2009).
[2] M. Berglund, L. Rymell, M. Peuker et al., J. Microsc. **197**, 268 (2000).
[3] M. Bertilson, O. von Hofsten, U. Vogt et al., Opt. Expr. **17**, 11057 (2009).
[4] P. Jansson, U. Vogt, H. M. Hertz, Rev. Sci. Instrum. **76**, 043503 (2005).

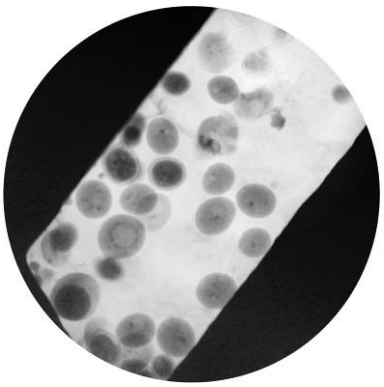

Figure 1: Cryo-fixated yeast cells. Field of view 37 µm.

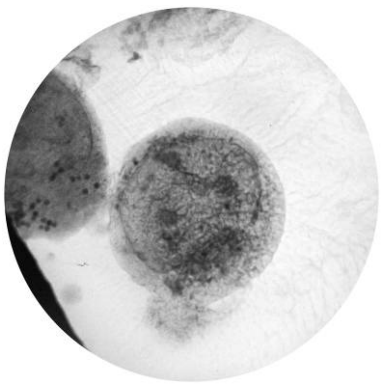

Figure 2: Cryo-fixated human immune system B-cells (721.221/HLA-Cw6). Field of view 37 µm.

The Application of Electron Microscopy to Nanomaterials*

A.K. Petford-Long[1,3], Y. Liu[2], C. Phatak[2]

[1]*Center for Nanoscale Materials, Argonne National Laboratory, Argonne, IL, USA*
[2]*Materials Science Division, Argonne National Laboratory, Argonne, IL, USA*
[3]*Materials Science & Engineering Dept., Northwestern University, Evanston, IL, USA*

* Work carried out at UChicago Argonne, LLC, Operator of Argonne National Lab, a U.S. DOE Office of Science Laboratory operated under Contract No. DE-AC02-06CH11357. Use of the Center for Nanoscale Materials and the Electron Microscopy Center at Argonne is acknowledged.

Abstract:

Nanomaterials display a very exciting range of novel properties that come about as a result of confinement and proximity effects. In order to understand this novel behavior and to harness it for potential applications in nanotechnology requires techniques that can be used to probe the microstructure, composition distribution and indeed the properties themselves with a spatial resolution that is appropriate. One such technique is transmission electron microscopy (TEM) (see e.g. [1]). As an example, Figure 1 shows FePt nanoparticles. The nanoparticle indicated by the solid arrow shows an ordered crystal structure, whereas the nanoparticle indicated with the dashed arrow shows a disordered fcc crystal structure. Although TEM is traditionally associated with high spatial resolution studies of microstructure and composition, it can also be used to carry out in-situ studies of the response of a nanomaterial to an external stimulus such as temperature, magnetic or electric field, or environment and since these can studies be carried out simultaneously with imaging structure/composition at high spatial resolution, TEM has become a widely used nanomaterials characterization tool. As an example Figure 2 shows the magnetic structure of an array of NiFe nanodots. The magnetization in each dot is arranged in a vortex state, and white or black dot in the center indicates the chirality of the vortex. Further developments in electron tomography are enabling the three-dimensional structure and magnetic/electric fields associated with nanostructures to be probed, and results will be presented illustrating a number of examples of the application of TEM to nanomaterials.

References:

[1] A.K. Petford-Long and A.N. Chiaramonti, Annu Rev. Mater. Res. **38**, 559 (2008).

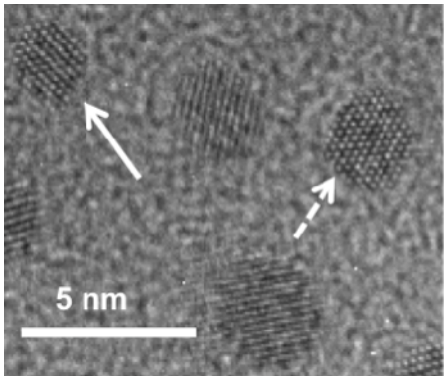

Figure 1: FePt nanocrystals synthesized by sol-gel technique.

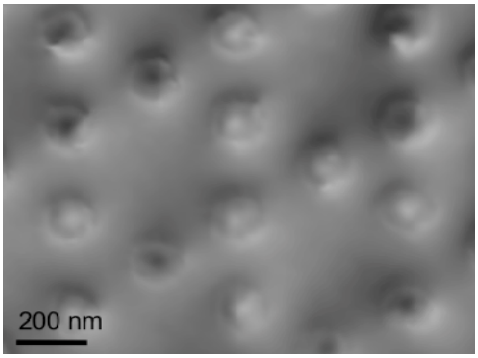

Figure 2: Lorentz TEM phase image of array of NiFe disks showing centered magnetic vortices. Black/white vortex contrast indicates chirality of magnetization

3D Chemical and Elemental Imaging by STXM Spectrotomography

J. Wang[1], A.P. Hitchcock[2], M. Obst[3], C. Karunakaran[1], A. Prange[4], T. Harkness[5]

[1]*Canadian Light Source Inc., U. Saskatchewan, Saskatoon, SK, Canada*
[2]*BIMR, McMaster University, Hamilton, ON, Canada*
[3]*Center for Applied Geoscience, Tuebingen University, Tuebingen, Germany*
[4]*Microbiology and Food Hygiene, Niederrhein University of Applied Sciences, Mönchengladbach, Germany*
[5]*College of Medicine, University of Saskatchewan, Saskatoon, SK, Canada*

Abstract:

The scanning transmission X-ray microscope (STXM) at the Canadian Light Source (covering 130 - 2500 eV) images the structure and quantitative distributions (maps) of chemical components for a wide range of samples at high spatial resolution (~30 nm). We have recently developed STXM spectrotomography [1-3] to enable morphological visualization and quantitative chemical mapping in 3D. Sample mounting, data acquisition, and 3D tomographic reconstruction strategies will be discussed. The method and its current capabilities will be illustrated with selected biological examples. Spatial distributions of calcite, protein, and polysaccharide in sulfur-metabolizing bacteria (*A. vinosum*) cultured in sulfide solution were determined by STXM spectro-tomography at the C 1s and Ca 2p edges. The 3D chemical mapping shows that the sulfur globules are located inside the bacteria with a strong spatial correlation with calcite and polysaccharide, suggesting an influence of the organic components onto the formation of the sulfur and calcite deposits. A second study determined copper accumulating in yeast cells (*Saccharomyces cerevisiae*) after cultivation in copper sulfate solution. STXM spectrotomography at the Cu 2p edge shows that Cu(II) is reduced to Cu(I) on the yeast cell wall. A novel needle-like wet cell, currently under development by Luxel for both X-ray and electron microscopy, was used for tomography studies of fully hydrated samples.

We thank Travis Ayers (Luxel Corporation) for providing developmental wet cell tomo-holders. Research funded by NSERC, Canada Research Chairs. CLS supported by NSERC, U. Saskatchewan.

References:

[1] G.A. Johansson et al., J. Synchrotron Radiat. **14**, 395 (2007).
[2] A.P. Hitchcock, et al., Appl. Phys. A **92**, 447 (2008).
[3] M. Obst, J. Wang and A.P. Hitchcock, Geobiology **7**, 577 (2009).

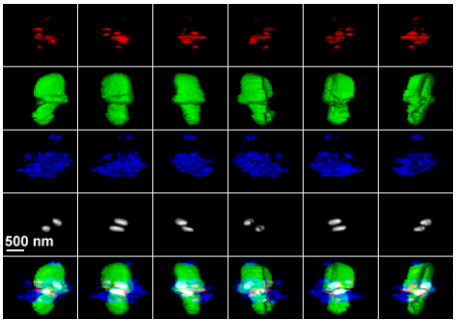

Figure 1: 3D chemical imaging of a sulfur bacterium at C 1s and Ca 2p edges. Red: calcite, green: protein, blue: polysaccharide, grey: sulfur globules.

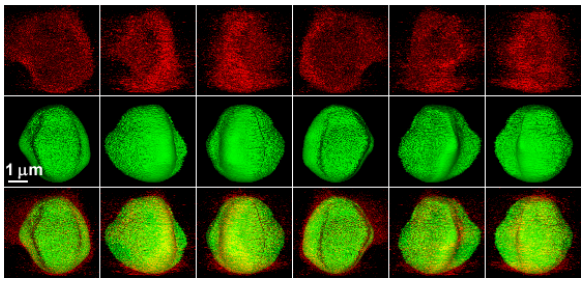

Figure 2: STXM spectro-tomography of a $CuSO_4$ treated yeast cell at Cu 2p edge. Red: Cu (I), green: yeast cell morphology.

Ultrafast X-ray Fluorescence Microscopy: What Does It Enable?

D. Paterson[1], M. D. de Jonge[1], D. L. Howard[1] C. G. Ryan[2], R. Kirkham[2], G. Moorhead[2], D. P. Siddons[3], B. E. Etschmann[4]

[1]*Australian Synchrotron, Clayton VIC, Australia*
[2]*CSIRO, Clayton VIC, Australia*
[3]*National Synchrotron Light Source, Brookhaven National Laboratory, NY, USA*
[4]*Department of Geology, University of Adelaide SA, Australia*

Abstract:
A hard X-ray micro-nanoprobe [1] has commenced operation at the Australian Synchrotron providing versatile X-ray fluorescence microscopy across an incident energy range from 4 to 25 keV. Two X-ray probes are used to collect µ-XRF and µ-XANES for elemental and chemical microanalysis: a Kirkpatrick-Baez mirror microprobe for micron resolution studies; and a Fresnel zone plate nanoprobe with laser interferometer position encoding capable of 60 nm resolution. Some unique aspects of the X-ray fluorescence microscopy beamline design, including a horizontal bounce DCM, will be discussed.

The beamline is commissioning an advanced energy dispersive x-ray fluorescence detection scheme named Maia developed by BNL [2] and CSIRO Australia [3]. The Maia detector employs an annular geometry of 384-element planar silicon array to create a large acceptance solid-angle and handle count rates greater than 10^7/s. On-the-fly scanning combined with event mode data acquisition enables sub-ms per virtual pixel dwell with real-time elemental deconvolution and image projection [4]. A 96-element Maia prototype has created high definition elemental maps with over 100 megapixels on a range of geological, materials and biological samples in practical time frames. Ultrafast X-ray fluorescence acquisition enables high definition elemental mapping [5,6], and creates the opportunity for fluorescence tomography [7] and XANES imaging [8] within practical time frames. Some examples of fluorescence XANES imaging using the Maia detector at will be presented.

References:

[1] D. J. Paterson et al., AIP Conf. Proc. **879**, 864-7 (2007).
[2] D. P. Siddons et al., AIP Conf. Proc. **705**, 953 (2004).
[3] R. Kirkham et al., Proc. of SRI 2009, AIP Conf. Proc., in press.
[4] C. G. Ryan, Int. J. Imag. Syst. Tech. **11**, 219 (2000).
[5] C. G. Ryan et al., these Proceedings.
[6] D. L. Howard et al., these Proceedings.
[7] M. D. de Jonge et al., these Proceedings.
[8] B.E. Etschmann et al., American Mineralogist, in press.

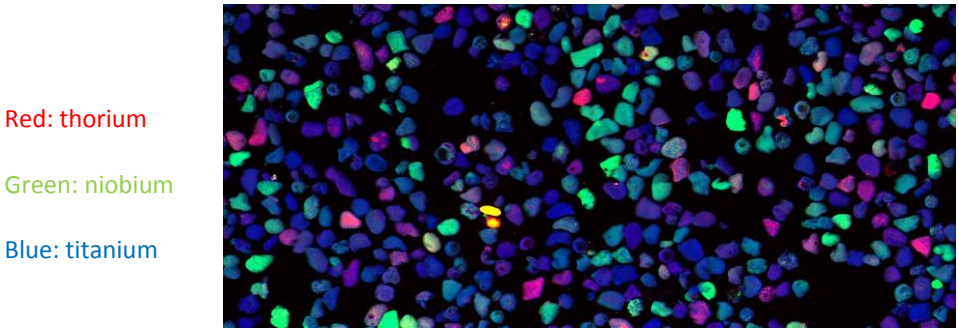

Figure 1: Elemental map of ilmenite sand, 8000×3600 1.25 µm pixels collected in 6 hours.

MAD Holography*

A. Scherz[1], D. Zhu[1,2], B. Wu[1,2], T. Wang[1,2], R. Rick[1,2], W. F. Schlotter[3],
J. Lüning[4], S. Roy[5], J. Stöhr[1,3]

[1]*Stanford Institute for Material & Energy Science, SLAC National Accelerator Laboratory, 2575 Sand Hill Road, Menlo Park, California 94025, USA*
[2]*Department of Applied Physics, Stanford University, Via Pueblo Mall, Stanford, California 94305, USA*
[3]*Linac Coherent Light Source, SLAC National Accelerator Laboratory, 2575 Sand Hill Road, Menlo Park, California 94025, USA*
[4]*Laboratoire de Chimie Physique, Université Pierre et Marie Curie, UMR du CNRS (7614), 11 Rue Pierre et Marie Curie, 75005 Paris, France, and Synchrotron SOLEIL, BP 48 91192, Gif-sur-Yvette, France*
[5]*Advanced Light Source, Lawrence Berkeley National Laboratory, Berkeley, California 94720, USA*

* The work is supported by the U.S. Department of Energy, Office of Basic Energy Sciences.

Abstract:

Multiple-wavelength anomalous diffraction (MAD) has revolutionized macromolecular structure determination on atomic length scales and has become a well-established technique in x-ray crystallography with dedicated synchrotron beamlines. An important prerequisite for conventional MAD is the periodicity of the sample for which it is required to assemble the macromolecules into a crystal.

In this work, the methodology of MAD is extended to non-periodic structures using the concept of coherent x-ray imaging [1]. The solution of the phase problem is demonstrated in a proof of principle experiment by a combination of two resonantly recorded scattering or speckle patterns at the carbon K edge. This new approach merges iterative phase retrieval and x-ray holography approaches and facilitates unique and rapid reconstructions [2].

MAD holography can be viewed as an in-line x-ray holography technique that eliminates the need for fabricating small reference structures compared with x-ray Fourier Transform Holography. Its inherent resonant aspect provides sensitivity to the elemental, chemical and magnetic state that further renders MAD holography widely applicable to a variety of inhomogeneous systems, representing regions with different atomic constituents, chemical composition such as organic functional groups, and magnetic behavior such as changes in moments and their orientations via polarization-dependent MAD imaging [3].

References:

[1] A. Scherz, D. Zhu, R. Rick et al., Phys. Rev. Lett. **101**, 076101 (2008).
[2] D. Zhu, B. Wu, R. Rick et al., Optics Lett. **34**, 2604 (2009).
[3] T. Wang et al., in preparation.

Coherent X-ray Diffraction Microscopy of Frozen-Hydrated Yeast Cells

J. Nelson[1], J. Steinbrener[1], X. Huang[1], J. Kirz[2], J. J. Turner[1], A. M. Neiman[3], C. Jacobsen[1,4,5]

[1]*Dept. Physics & Astronomy, Stony Brook University, Stony Brook, NY 11794-3800, USA*
[2]*Advanced Light Source, Lawrence Berkeley National Laboratory, Berkeley, CA 94720, USA*
[3]*Dept. Biochem. & Cell Biology, Stony Brook University, Stony Brook, NY 11794-5215, USA*
[4]*Dept. Physics & Astronomy, Northwestern University, Evanston, IL 60208, USA*
[5]*Advanced Photon Source, Argonne National Laboratory, Argonne, IL 60439, USA*

Abstract:
Coherent x-ray diffraction microscopy promises to be an attractive technique for 3D soft x-ray imaging of radiation-sensitive samples because it makes use of every photon interacting with the specimen by eliminating optic-induced inefficiencies such as transfer function losses and unfocused light [1]. In addition, by working in the far-field geometry one removes the geometric challenges of a sub-millimeter focal length and a depth-of-focus that would otherwise approach half a micron, a specimen thickness compatible with energy-filtered cryo electron microscopy.

We will report on progress in developing x-ray diffraction microcopy methods and analysis software and show applications of whole cell imaging of the yeast *S. cervisiae*. Using silver-enhanced immunogold labels, we have investigated the distribution of the α–mannan sugar in the cell wall of freeze-dried yeast; achieving a spatial resolution of 13 nm with some limited ability to distinguish the depth of specific labels [2]. We have also imaged frozen-hydrated yeast to high resolution [3]; such specimens are preserved without dehydration and are radiation hardy. We will describe current efforts to improve image fidelity through the recording of low-angle scattering data and better cryo specimen conditions. Finally, we will discuss recent work in scanning 2D as well as 3D x-ray diffraction microscopy on frozen-hydrated yeast.

References:
[1] X. Huang, H. Miao, J. Steinbrener et al., Opt. Express **17**, 13541 (2009).
[2] J. Nelson et al., (accepted to Proceedings of the National Academy of Sciences).
[3] X. Huang, J. Nelson, J. Kirz et al., Phys. Rev. Lett. **103**, 198101 (2009).

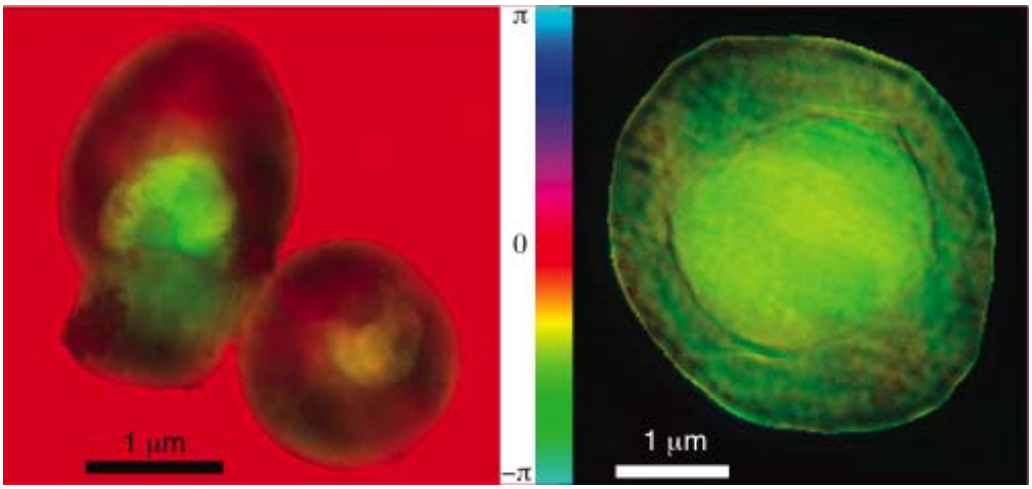

Figure 1: X-ray diffraction microscopy images of freeze-dried (*right*) and frozen-hydrated (*left*) yeast.

Lensless Biological Imaging with Waveguides: Holographic, Iterative and Ptychographic Reconstruction

K. Giewekemeyer, S.P. Krüger, S. Kalbfleisch, H. Neubauer, M. Bartels, T. Salditt

Institut für Röntgenphysik, Georg-August-Universität Göttingen,
Friedrich-Hund-Platz 1, 37077 Göttingen, Germany

Abstract:

Recent advances in the fabrication of two-dimensional X-ray waveguides (WGs) have allowed for beam confinement well below 20 nm [1] and provide a coherent quasi-point source which can be used for lensless imaging in the geometry of inline holography at multi-keV photon energies. Building upon and extending recent advances in algorithmic reconstruction of holographic images [2] it was possible to obtain reconstructions with quantifiable errors from unstained biological cells, which act as pure phase objects at 17.5 keV (see Fig. 1). Measured at around three times the photon energy used in a previous ptychographic diffraction experiment on unstained biological material using a pinhole for definition of the illumination function [3] a very similar ratio of resolution to the invested dose was obtained. At the same time, we have also applied the ptychographic technique to waveguide illumination, leading to a resolution of around 35 nm in one direction (see Fig. 2) for a lithographically fabricated test object [4]. Simulations show that resolutions on the order of the waveguide beam confinement are readily possible, profiting from the divergent WG exit wave, which allows for an easy adjustment of the needed fluence on the sample. Together with a dedicated WG-based imaging setup presently commissioned at the new PETRA III storage ring these advances lay the foundation for a standard application of WG-based imaging to quantitative biological imaging at the nm-range.

References:

[1] S.P. Krüger et al., submitted.
[2] T.E. Gureyev, Opt. Commun. **220**, 49 (2003).
[3] K. Giewekemeyer et al. PNAS **107**, 529 (2010).
[4] K. Giewekemeyer et al., New J. Phys. (in press).
[5] K. Giewekemeyer et al., unpublished.

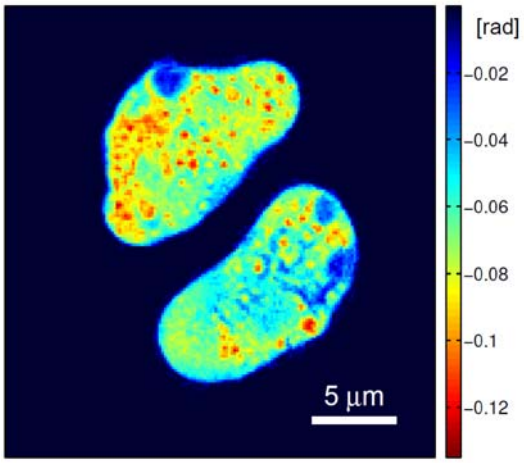

Figure 1: Freeze-dried *Dictyostelium* cells in a WG beam. Iterative phase reconstruction based on a modified HIO scheme [5].

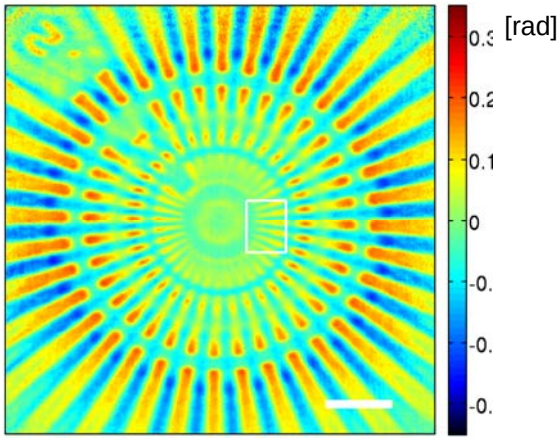

Figure 2: Ptychographic phase reconstruction from a tantalum test object. Line pairs within the white rectangle show a smallest half-period of 50 nm [4].

Wavefront Modulation Coherent Diffractive Imaging

F. Zhang and J. M. Rodenburg

Department of Electronic & Electrical Engineering, University of Sheffield, Sir Frederick Mappin Building, Sheffield, UK

Abstract:

Lens-based imaging is able to directly provide an image of objects, however, the high quality lenses required are not readily available for radiations including x-ray. *Coherent Diffraction Imaging (CDI)* bypasses this difficulty by numerically inverting the diffraction process undertaken by an object wave. The current CDI techniques still face several fundamental drawbacks: the extremely demanding experimental requirements in data collection, and the sample-dependent, unreliable convergence of phasing algorithm, as well as the sample damage. Here an approach, termed as wavefront modulation CDI (WMCDI), is presented, which overcomes or alleviates the above mentioned drawbacks without using devices that are difficult to fabricate.

In WMCDI, an modulator is used in data collection. Unlike lens-based imaging, there is no particularly strict requirement on the form of modulator. The use of a modulator greatly reduces the dynamic range requirement of detectors, the high brilliance requirement of radiation source, and in turn the sample damage. Importantly, the dataset so recorded also greatly facilitates the image recovery. The WMCDI idea has been implemented in two different ways that require different number of diffraction patterns and distinct phasing algorithms. The variant using multiple recordings [1] is related to Ptychography [2], but avoids all its difficulties in data collection; in practice, it is also much easier to know the modulator's transmission than a probe function. In the single-shot variant, the involved magnitude and support constraints are implemented in a completely innovative way [3]. As a result, it disposes the small and isolated sample requirement and exhibits computational robustness comparable to that of the multiple-shot CDI methods.

The principle of WMCDI and the experimental results with x-ray and visible light will be presented. Simulation results will also be given regarding to the algorithmic performance under various experimental nonideals and different modulator design. The implication of oversampling requirement in CDI will also be addressed.

References:

[1] F. Zhang, G. Pedrini, W. Osten, Phys. Rev. A, **75**, 043805 (2007).
[2] H.M.L. Faulkner and J. M. Rodenburg, Phys. Rev. Lett. **93**, 023903-4 (2004).
[3] F. Zhang and J.M. Rodenburg, "Wavefront Modulation Single-shot Coherent Diffractive Imaging," submitted to PRL.

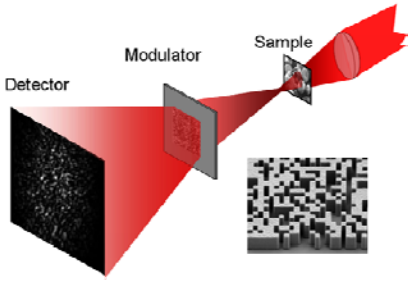

Figure 1: Experimental setup of WMCDI, inset is x-ray phase plate fabricated by e-beam lithography.

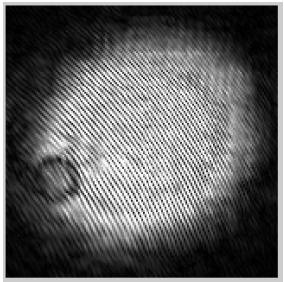

Figure 2: Reconstruction of part of x-ray zone plate by multiple-shot WMCDI method.

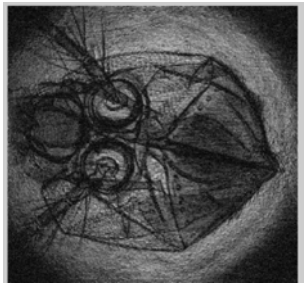

Figure 3: Reconstruction of a fly mouth sample by single-shot WMCDI method.

Scanning Small-Angle X-ray Scattering Microscopy of Biological Tissues

A. Menzel[1], F. Pfeiffer[2], M.J. Farquharson[3], D.A. Bradley[4], O. Bunk[1]

[1]*Paul Scherrer Institut, 5232 Villigen PSI, Switzerland*
[2]*Department Physik (E17), Technische Universität München, James-Franck-Str., 85748 Garching, Germany*
[3]*Department of Medical Physics and Applied Radiation Sciences, McMaster University, Hamilton ON, Canada*
[4]*Centre for Nuclear and Radiation Physics, Department of Physics, University of Surrey, Guildford GU2 7XH, UK*

Abstract:
Small-angle X-ray scattering (SAXS) is an invaluable tool for the characterization of nanometer-sized structures averaged over the illuminated volume of the specimen. Spatial resolution can be gained by raster scanning the specimen through a focused X-ray beam. The advent of highly brilliant light sources at 3rd-generation synchrotrons and rapid-readout area detectors has made possible the fast and efficient collection of tens of thousands SAXS data sets per hour, allowing macroscopic objects to be scanned with microscopic resolution [1]. Whereas dark-field imaging is sensitive merely to the presence of density fluctuations, which cause scattering, the more detailed SAXS analysis reveals dimension, shape, and orientation of structures far smaller than the spatial resolving power of this microscopy technique. Scanning SAXS proves particularly useful in life sciences [2], where tissues are structured over a wide range of length scales, making them quite challenging to be imaged with sufficient detail without losing sight of "the big picture." As any scanning-probe technique, scanning SAXS can easily be complemented by other microscopy techniques, such as fluorescence mapping.

References:
[1] O. Bunk et al., New J. Phys. **11**, 123016 (2009).
[2] D.A. Bradley et al., Radiat. Phys. Chem. **79**(2), 162 (2010).

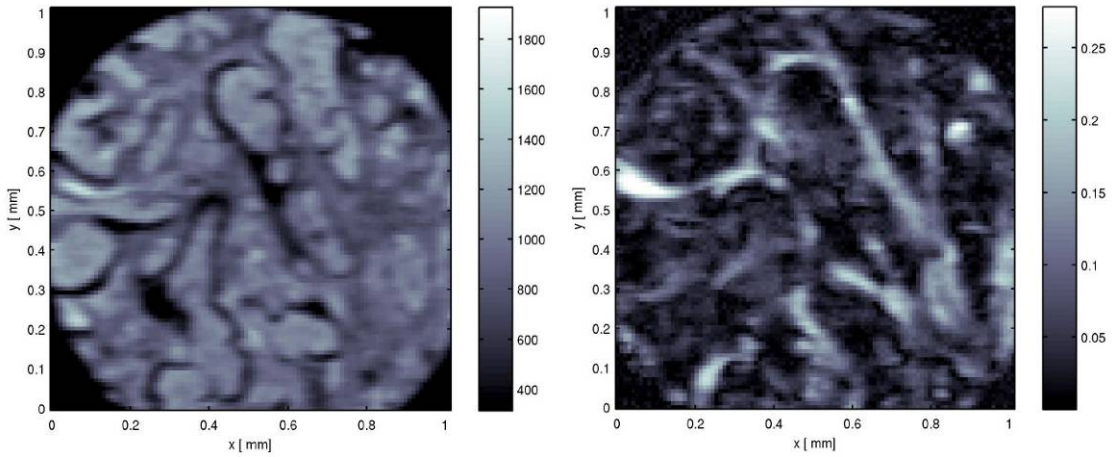

Figure: Breast cancer tissue imaged by scanning SAXS. The signals shown are from the 6–70nm range. Other wave vectors are sampled in parallel, and higher specificity can easily be chosen when processing. Left: the scattering intensity, similar to dark-field imaging; right: the anisotropy of the scattering signal indicating the degree of orientation.

Hard X-Ray Scanning Microscopy with Coherent Diffraction Contrast

C. G. Schroer[1], A. Schropp[1], P. Boye[1], J. M. Feldkamp[1], R. Hoppe[1], J. Patommel[1], D. Samberg[1], S. Stephan[1], K. Giewekemeyer[2], R. N. Wilke[2], T. Salditt[2], J. Gulden[3], A. P. Mancuso[3], I. Vartaniants[3], E. Weckert[3], S. Schöder[4], M. Burghammer[4]

[1]*Institute of Structural Physics, Technische Universität Dresden, D-01062 Dresden, Germany*
[2]*Institute of X-Ray Physics, Universität Göttingen, D-37077 Göttingen, Germany*
[3]*Deutsches Elektronensynchrotron DESY, Notkestr. 85, D-22607 Hamburg, Germany*
[4]*European Synchrotron Radiation Facility ESRF, B. P. 220, F-38043 Grenoble Cedex, France*

Abstract:
We report on the development of hard x-ray scanning microscopy based on nanofocusing refractive x-ray lenses [1]. Besides the large penetration depth of hard x-rays in matter, the key strength of this type of microscope is the use of x-ray analytical techniques as contrast mechanisms, such as fluorescence, absorption, and diffraction [2]. This opens a wide field of application, from physics, chemistry, materials, earth and environmental science to biomedicine and nanotechnology. The spatial resolution for conventional scanning microscopy is limited by the lateral size of the nanobeam that lies well below 100 nm for our microscope [1,3]. By using the nanofocused beam for coherent x-ray diffraction imaging (CXDI), we improved the spatial resolution for the imaging of small particles to about 5 nm [4]. Recently, CXDI was extended to image larger objects by combining a scanning technique with CXDI [5]. We have implemented this ptychographic scanning technique in our microscope to obtain transmission micrographs with a spatial resolution well below 50 nm [3]. At the same time, this technique gives access to the wave field in the focused beam with unprecedented accuracy and dynamic range. Figures 1 and 2 show the ptychographic reconstruction of an optical test pattern and the complex wave field in the focus, respectively. This new technique is illustrated with several examples, and its future application at the hard x-ray nanoprobe station P06 at PETRA III is discussed.

References:

[1] C. G. Schroer, et al., Appl. Phys. Lett. **87**. 124103 (2005).
[2] M. Hanke, et al., Appl. Phys. Lett. **92**, 193109 (2008).
[3] A. Schropp, et al., Appl. Phys. Lett. **96**, 091102 (2010).
[4] C. G. Schroer, et al., Phys. Rev. Lett. **101**, 090801 (2008).
[5] J. M. Rodenburg, H. M. L. Faulkner, Appl. Phys. Lett. **85**, 4795 (2004); P. Thibault et al., Science **321**, 379 (2008).

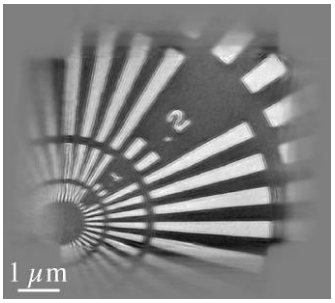

Figure 1: Reconstructed phase of an optical test pattern (NTT-AT). The smallest features are 50 nm lines and space.

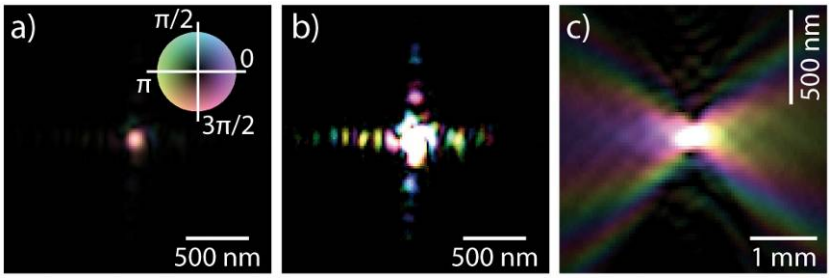

Figure 2: a) Reconstructed complex wave field in the focus, b) with enhanced contrast. c) Reconstructed horizontal beam profile on the optical axis. The intensity profile is nearly Gaussian with a size of 78 x 86 nm^2.

Ptychographic Coherent Diffractive Imaging: Weak-Object Studies and Artifact Suppression

M. Dierolf[1], P. Thibault[1], A. Menzel[2], C. M. Kewish[2], K. Jefimovs[3], I. Schlichting[4], K. von König[4], O. Bunk[2], F. Pfeiffer[1]

[1]*Department of Physics, Technische Universität München, DE-85748 Garching, Germany*
[2]*Swiss Light Source, Paul Scherrer Institut, CH-5232 Villigen PSI, Switzerland*
[3]*Swiss Federal Laboratories for Materials Testing and Research, CH-8600 Dübendorf, Switzerland*
[4]*Max Planck Institute for Medical Research, DE-69120 Heidelberg, Germany*

Abstract:
Applying iterative phase retrieval schemes to ptychographic data, i.e., diffraction patterns collected with a localized illumination probe from overlapping regions of a specimen, has enabled the investigation of extended specimens previously inaccessible by other coherent X-ray diffractive imaging methods [1]. While the technique had initially been limited by the requirement of precise knowledge of the illumination function, recent algorithmic developments allow now the simultaneous reconstruction of both probe and object [2–5]. However, these new approaches suffer from an inherent ambiguity, which especially affects the case of weakly scattering specimens.

We present new schemes to circumvent this problem and introduce new tools for obtaining information about the scattering behavior of weak phase objects already during data collection. The new techniques are experimentally demonstrated for a data set taken on *Magnetospirillum gryphiswaldense* [6].

References:

[1] J.M. Rodenburg, A.C. Hurst, A.G. Cullis et al., Phys. Rev. Lett. **98**, 034801 (2007).
[2] P. Thibault, M. Dierolf, A. Menzel et al., Science **321**, 379 (2008).
[3] M. Guizar-Sicairos, J. R. Fienup, Opt. Express **16**, 7264 (2008).
[4] A. M. Maiden, J. M. Rodenburg, Ultramicroscopy **109**, 1256 (2009).
[5] K. Giewekemeyer, P. Thibault, S. Kalbfleisch et al., PNAS **107**, 529 (2009).
[6] M. Dierolf, P. Thibault, A. Menzel et al., (accepted to New Journal of Physics).

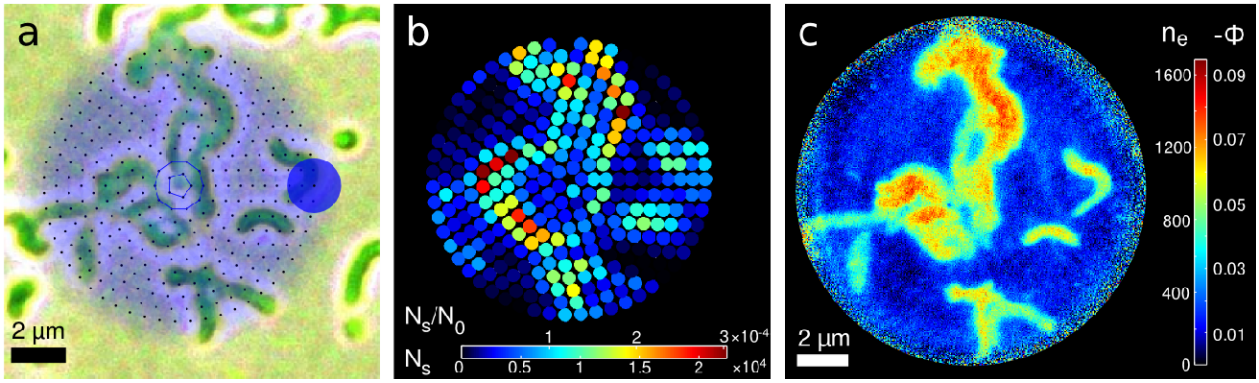

Figure 1: (a) Visible light micrograph of specimen (*Magnetospirillum gryphiswaldense*) overlayed with scan positions of ptychographic scan. (b) Online analysis, showing the amount of photons scattered by the specimen at each scan position. (c) Reconstruction of phase shift / electron density n_e (in $Å^{-2}$).

Fresnel Coherent Diffractive Imaging

A. G. Peele

The ARC Centre of Excellence for Coherent X-ray Science, Department of Physics, La Trobe University, Australia

Abstract:
In recent years the Australian Research Council Centre of Excellence for Coherent X-ray Science has been pursuing programs dedicated towards high resolution imaging of biological samples. The use of coherent diffractive imaging (CDI) with x-rays is a way to obtain both high resolution and intensity contrast for such samples, which often exhibit poor x-ray absorption contrast at higher energies.

The use of illumination with, typically, spherical phase curvature so as to produce a Fresnel diffraction pattern brings with it certain advantages as well as challenges, some of which are common across CDI methods and some of which are particular to Fresnel CDI. I will discuss advances that we have made in three areas that improve the outcomes of CDI – experiment design, equipment, and algorithms.

Experiment design includes the use of new approaches to data collection based on insights gained from an understanding of the reconstruction process. In particular, we have found that a generalized application of the ideas of phase-diversity [1] greatly improves the reconstructed image quality. We have recently applied this approach to the adhesive produced by the so-called sandcastle worm and results will be presented [2].

Our equipment development program has recently reached a point where the instrumentation used produces data that improves the quality of reconstructed images. For Fresnel CDI this largely centers on the stability of the sample with respect to the incident illumination. We will present our latest results.

Algorithmic advances include an approach based on a modal expansion of the diffraction pattern. For a broadband source, that expansion would be based on energy bands; for a partially coherent source, on coherent modes; for the case of movement, relative sample positions could be used and varying illumination can be used when phase diversity methods are applied. The appropriate summation of the various modes allows an estimate for the total diffraction pattern to be obtained, which can then be used as a constraint in the reconstruction process. We have demonstrated significant reconstruction improvements using these ideas [3,4].

References:

[1] R. A. Gonsalves, Opt. Eng. **21**, 829 (1982).
[2] C. T. Putkunz et al., (submitted).
[3] L.W. Whitehead, G.J. Williams, H.M. Quiney et al., Phys. Rev. Lett. **103**, 243902 (2009).
[4] R. A. Dilanian, B. Chen, G. J. Williams et al., J. Appl. Phys. **106**, 023110 (2009).

Development and Application of High-Resolution Diffraction Microscopy Using Focused Hard X-ray Beam

Y. Takahashi[1], Y. Nishino[2], E. Matsubara[3], T. Ishikawa[2], K. Yamauchi[1]

[1]*Osaka University, 2-1 Yamada-oka, Suita, Osaka 565-0871, Japan*
[2]*RIKEN SPring-8 Center, Kouto, Sayo, Sayo, Hyogo 679-5148, Japan*
[3]*Kyoto University, Yoshida, Sakyo, Kyoto 606-8501, Japan*

Abstract:

X-ray waves in the center of the beam waist of nearly diffraction limited focused x-ray beams can be considered to have amplitude and phase that are both almost uniform, i.e., they are x-ray plane waves. Here we report on the development and its application of high-resolution diffraction microscopy using the x-ray plane wave of the synchrotron x-ray beam focused using Kirkpatrick-Baez(KB) mirrors.

We designed the mirrors using a wave optical simulation [1], and purchased the mirrors, which were accurately fabricated by the elastic emission machining technique, from JTEC corporation. We developed the diffraction microscope with the KB mirror focusing system at SPring-8 [2].

We measured high-contrast diffraction patterns of an Ag nanocube and an Au/Ag nanobox using the diffraction microscope. An image of the nanocube with 3 nm resolution was successfully reconstructed by an iterative phasing method [3]. The hollow interior was clearly visible in the reconstructed image of the nanobox [4]. The present technique is a key technology for realizing single-pulse diffractive imaging using x-ray free-electron lasers.

References:

[1] Y. Takahashi et al., J. Appl.Phys. **105**, 083106 (2009).
[2] Y. Takahashi et al., Proc. SRI2009 (submitted).
[3] Y. Takahashi et al., Phys. Rev. B **80**, 054103 (2009).
[4] Y. Takahashi et al., (submitted).

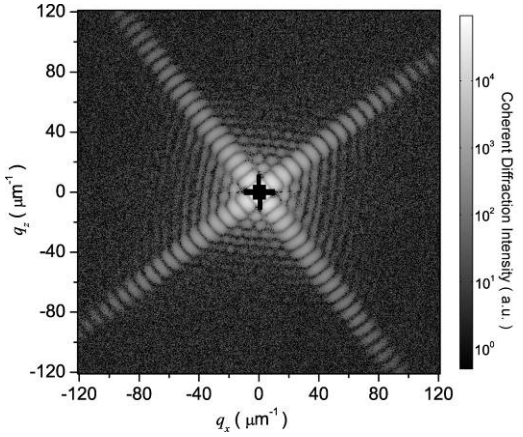

Figure 1: Coherent diffraction pattern of Ag nanocube.

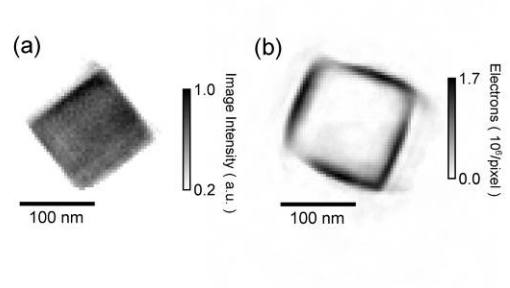

Figure 2: Reconstructed images of nanoparticles. (a) Ag nanocube, (b) Au/Ag nanobox.

Bragg Coherent Diffraction Imaging Using <100 nm Focused Hard X-rays*

S. O. Hruszkewycz[1], M. V. Holt[2], M. J. Highland[1], J. Maser[2], J. A. Eastman[1], D. L. Proffit[1,3], G. R. Bai[1], D. D. Fong[1], P. H. Fuoss[1]

[1]*Argonne National Laboratory, Materials Science Division, Argonne IL, 60439 USA*
[2]*Argonne National Laboratory, Center for Nanoscale Materials, Argonne IL, 60439 USA*
[3]*Northwestern Univ. Dept of Materials Science & Engineering, Evanston IL, 60308 USA*

*This work, including use of the Advanced Photon Source and the Center for Nanoscale Materials, was supported by the U.S. Department of Energy, Office of Science, Office of Basic Energy Sciences, under Contract No. DE-AC02-06CH11357

Abstract:

We will present data collection and computational approaches for nanofocused Bragg coherent diffraction imaging (CXDI) - a technique that can extend the resolution of x-ray nanoprobes and isolate individual nanostructures for study. Nanofocused Bragg CXDI uses hard x-rays focused to <100 nm to measure volumetric diffraction peaks from a set of spatially overlapping beam footprints with curved phase illumination. The set of diffraction data collected from all incident angles and beam positions (if sampled properly) must be consistent with a single compact nanocrystal and an incident beam profile.

Lensless coherent x-ray diffraction imaging (CXDI) techniques have been developed that generate two-dimensional complex image reconstructions of diffracting planar samples [1,2] and that yield 3D internal strain fields of isolated nanocrystals from volumetric Bragg diffraction [3]. However, the sample requirements of these CXDI methods make studying densely populated epitaxial three dimensional nanostructures difficult. While nanofocusing can isolate individual structures and avoid those difficulties, modeling and inverting the resulting large and complex data set requires a departure from the typical single processor fast Fourier transform based algorithms. We are developing parallel algorithms that compute kinematic focused diffraction patterns from finely sampled model nanocrystals and are integrating those algorithms into iterative phasing routines that will find unique solutions to data from nanofocused Bragg CXDI experiments.

We have used the CNM/APS Hard X-Ray Nanoprobe to test our approaches on samples of δ-Bi_2O_3 nanostructures grown on single crystal oxide substrates. This material is the focus of our research because it is an extremely good oxygen conductor that in the bulk is stable only at high temperature. We recently succeeded in stabilizing this phase at room temperature via strained, epitaxial growth [4]. We will present ptychographic Bragg CXDI data from 200-nm diameter particles and discuss our preliminary strategies and attempts to model and invert coherent nanobeam diffraction from these crystals. Our results indicate that nanofocused Bragg CXDI promises to advance the current state of the art in coherent diffractive imaging towards three dimensional focused beam reconstructions of epitaxial nanocrystals.

References:

[1] P. Thibault, M. Dierolf, O. Bunk et al., Ultramicroscopy **109**(4), 338 (2009).
[2] B. Abbey, K.A. Nugent, G. J. Williams et al., Nature Physics **4**(5), 394 (2008).
[3] I. Robinson and R. Harder, Nature Materials **8**(4), 291 (2009).
[4] D.L. Proffit, G.-R. Bai, D.D. Fong et al., Appl. Phys. Lett. **96**(2), 021905 (2010).

Latest Development of Ultra-high Resolution Soft X-ray Zone Plate Microscopy*

W. Chao[1], T. Tyliszczak[2], J. Kim[3], P. Fischer[1], S. Rekawa[1], E. H. Anderson[1],

[1]Center for X-ray Optics, Lawrence Berkeley National Laboratory, Berkeley, CA 94720 USA
[2]Advanced Light Source, Lawrence Berkeley National Laboratory, Berkeley, CA 94720 USA
[3]University of California, Berkeley, CA 94720 USA. Presently at NanoStructures Laboratory, Department of Electrical Engineering, Princeton University, Princeton, NJ 08544 USA

* This work was supported by the Director, Office of Science, Office of Basic Energy Sciences, of the U.S. Department of Energy under Contract No. DE-AC02-05CH11231, and the Engineering Research Centers Program of the National Science Foundation under NSF Award Number EEC-0310717.

Abstract:

Reaching single-digit spatial resolution with soft x-ray microscopy (SXRM) has been the focus of recent studies. With the increasing need to study materials at the nanometer scale, achieving such a resolution will extend the powerful capabilities of SXRM such as in-situ application of electric/magnetic fields and ultra-high chemical sensitivity to many scientific fields. For zone plate microscopy, the resolution performance of the zone plate lenses is the main limitation to its resolution. To this end, we successfully fabricated micro zone plates of 12 nm outer zone width (Δr = 12 nm) using a new double patterning nanofabrication processes [1]. Imaging resolution of 12 nm was achieved with the zone plate in first diffraction order at the XM-1 full-field transmission microscope in Berkeley [2] [Fig. 1]. Separately, using a high quality 20 nm zone plate, a test pattern of 12 nm half-period was clearly resolved with the scanning transmission x-ray microscope (STXM) at the Advanced Light Source (BL 11.0.2). Furthermore, third diffraction order imaging with the STXM has been successfully demonstrated using a 39 nm (Δr = 39 nm) zone plates optimized for third order. Preliminary results indicate that a resolution of 15 nm was achieved. In the presentation, I will detail zone plate design and fabrication, experimental setup and challenges, and the latest results.

References:

[1] W. Chao, J. Kim, S. Rekawa et al., J. Vac. Sci. Tech. B **27**, 2606 (2009).
[2] W. Chao, J. Kim, S. Rekawa et al., Opt. Exp. **17**, 17669 (2009).

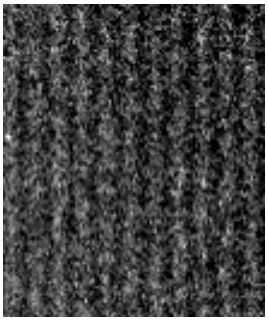

Figure 1: A soft x-ray image of a 12 nm half-period Mo/Si test pattern obtained with a 12 nm micro zone plate at 1.75 nm wavelength (707eV) using the XM-1 full-field transmission x-ray microscope.

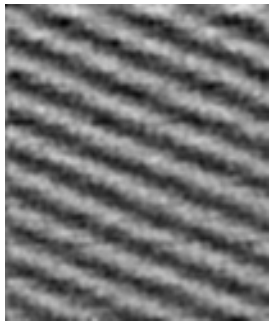

Figure 2: A soft x-ray image of a 12 nm half-period Mo/Si test pattern obtained with a 20 nm zone plate at 1.75 nm wavelength (707eV) using the scanning transmission x-ray microscope at ALS BL 11.0.2.

X-ray Microscopy Beamlines at the SSRF: Present Status and Future Plan

H. Xu, R. Tai, X. Yu

Shanghai Synchrotron Radiation Facility, Shanghai Institute of Applied Physics, Chinese Academy of Sciences, Zhangheng Rd. 239, Pudong Dist., Shanghai 201204, China

Abstract:
Shanghai Synchrotron Radiation Facility (SSRF) is a 3.5 GeV third-generation light source. This high brightness x-ray source is an ideal platform for the development of x-ray microscopy and its applications. Presently, SSRF has two scanning x-ray microprobe beamlines, namely Soft X-ray Spectromicroscopy Beamline (STXM) and Hard X-ray Microfocusing Beamline (HXMF). The STXM beamline is used for 2D/3D mapping with high spatial resolution, chemical sensitivity (NEXAFS) and magnetic contrast (XMD). The characteristic parameters of this beamline are: energy range 200-2000eV, energy resolution ($E/\Delta E$) ~18000 @ 244eV and spatial resolution < 30nm. The HXMF beamline is devoted to hard x-ray microanalysis with various techniques include 2D μ-XRF mapping, μ-XANES and μ-XRD. One-micron spatial resolution and sub-ppm elemental sensitivity have been achieved at the HXMF beamline presently, and sub-100 nm resolution using Fresnel zone plate optics will be available later. These two microscopy beamlines have accommodated more than 100 user experiments after opening to user operation, with a diverse range of environmental, biological and materials science applications.

The construction of SSRF phase II beamlines will be carried out during 2011-2016. Quite a few x-ray microscopy beamlines have been planned with emphasis on better spatial, temporal resolution and wider applications. The planned x-ray microscopy beamlines include: A hard x-ray nanoprobe beamline with 20-30nm focal spot sizes, full field soft x-ray and hard x-ray nano imaging and nano-CT beamlines with sub-30nm spatial resolution, a fast x-ray imaging beamline with sub-um spatial resolution and sub-ns time resolution, a beamline for the development of coherent diffraction microscopy and new imaging techniques.

The Nanoscopium Scanning Nanoprobe Beamline at Synchrotron Soleil

A. Somogyi, F. Polack, T. Moreno, A. Zozulya

Synchrotron Soleil, L'Orme des Merisiers, Saint-Aubin - BP 48, 91192 Gif-sur-Yvette Cedex, France

Abstract:

Nanoscopium is the single scanning hard X-ray nano-probe beamline planned at SOLEIL. This ~155 m long beamline will fully exploit the high brilliance and coherence characteristics of the X-ray beam both for diffraction limited focusing and for contrast formation. It will offer the most advanced imaging techniques in multimodal mode. The different scanning techniques offered by the beamline will permit elemental mapping at trace (ppm) levels (scanning XRF), speciation mapping (XANES), phase gradient mapping (differential phase contrast), and density-contrast based imaging of internal structures (coherent diffraction imaging) down to 30 nm spatial resolution range.

The beamline will share the SDL13 source straight section with the future tomography beamline by using canted undulators. The U20 in-vacuum undulator (min. magnetic gap: 5.5 mm) of the Nansocopium beamline will cover the 5-20 keV energy range without energy gaps. The stability of the nanobeam will be ensured by the horizontally reflecting beamline optics. A secondary source will be created by the sagitally and by the tangentially pre-focusing mirrors in front of the overfilled secondary slits. Trade-off between high energy resolution ($\Delta E/E \sim 10^{-4}$) and high flux (10^{11} ph/s with $\Delta E/E \sim 10^{-2}$) will be achieved by two interchangeable horizontally reflecting monochromators (a double crystal and a double multilayer one). KB mirror and Fresnel Zone Plates will be used as focusing devices.

The beamline is in the design and construction phase. It is foreseen to be open for users in 2013.

Nano and Life Sciences with the TwinMic Soft X-ray Transmission and Emission X-ray Spectromicroscope at Elettra

B. Kaulich, A. Gianoncelli, M. Kiskinova

Elettra – Sincrotrone Trieste, S. S. 14, km 163.5 in Area Science Park, I-34149 Trieste-Basovizza, Italy

Abstract:
Exploring the biochemistry and functionality of complex biological systems at sub-cellular length scales continues to be a challenge. It requires interdisciplinary approaches for discriminating qualitatively and quantitatively the constituent elements and correlating them to the sub-cellular morphology. In this respect high resolution X-ray imaging combined with its chemical sensitivity and complemented by other microanalytical techniques is attractive since it provides specific information not achievable by a single method. The contribution will present the most recent achievements demonstrating the capabilities of the TwinMic soft X-ray spectromicroscope at the Elettra synchrotron radiation facility (Trieste, Italy) in tissue, cellular or subcellular analysis based on imaging with low-energy X-ray fluorescence spectroscopy and micro-spot X-ray absorption spectroscopy. Selected results will represent research fields including biotechnology, biomaterials, food science and nanotoxicology, neuroscience and clinical medicine. They will illustrate new insights into the morphology and compositional enrichment, distribution and correlation of the elements resulting from growth of plants under altered environmental or toxic conditions, concentration dependence of penetration of engineered nanoparticles in different cell organelles and changes in the nanoparticle chemistry inside the cells, chemical reaction of lung tissue in the presence of inhaled asbestos species, among others. The importance of complementing the X-ray imaging and spectromicroscopy by PIXE, synchrotron-based FTIR spectromicroscopy, other microscopies and conventional lab-based techniques as well as future developments will be outlined.

Pushing the Resolution Limit of Visible Light Microscopy*

B. Huang

Department of Pharmaceutical Chemistry, Department of Biochemistry and Biophysics
University of California, San Francisco, San Francisco, CA 94158, USA

* This work is partially supported by NIH, HHMI and UCSF Programs in Breakthrough of Biomedical Research.

Abstract:

The ability of fluorescence microscopy to perform noninvasive imaging of live samples with molecular specificity has made it one of the most powerful imaging techniques to study cellular processes. However, the diffraction of light limits the spatial resolution of conventional visible light microscopy, leaving many biological structures too small to be observed in detail. To overcome this limit, we have developed the Stochastic Optical Reconstruction Microscopy (STORM) technique [1,2]. It utilizes the photoswitching of fluorophores to isolate their spatially overlapped images, and single-molecule localization to reconstruct the sample structure with the position of labeled fluorescent probes. We have achieved a 20-30 nm lateral resolution in cellular samples, which is an improvement by more than an order of magnitude over conventional fluorescence microscopy. The incorporation of three-dimensional (3D) single molecule localization further enables 3D STORM of a whole cell with 50-60 nm axial resolution [3,4]. We have also created photoswitchable fluorophores for multicolor imaging by combinatorial pairing of various activator dyes and reporter dyes [5]. We have demonstrated the ability of STORM to visualize structures not resolvable by conventional fluorescence microscopy, including in vitro reconstituted clathrin-mediated endocytic machinery and synapses in the olfactory system.

References:

[1] M. Rust, M. Bates, X. Zhuang, Nat. Methods **3**, 793 (2006).
[2] B. Huang, M. Bates, X. Zhuang, Ann. Rev. Biochem. **17**, 993 (2009).
[3] B. Huang, W. Wang, M. Bates et al., Science **319**, 810 (2008).
[4] B. Huang, S. A. Jones, B. Brandenburg et al., Nat. Methods **5**, 1047 (2008).
[4] M. Bates, B. Huang, G. T. Dempsey et al., Science **317**, 1749 (2007).

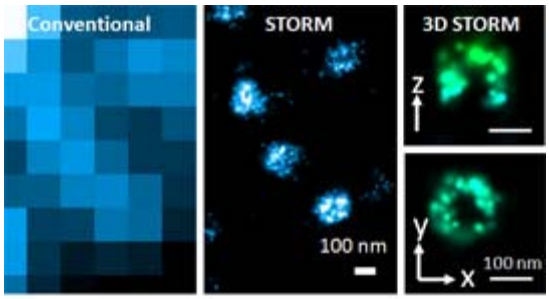

Figure 1: STORM is not only able to resolve individual clathrin-coated pits (~100 nm in diameter) from their blurred conventional fluorescence images but also their hemispherical-cage-like three-dimensional shape.

Combined Holographic and Fluorescence Laminography for Three-Dimensional Imaging of Flat Nanostructures

L. Helfen[1], F. Xu[1], T. Baumbach[1], P. Reischig[1], H. Suhonen[2], P. Cloetens[2]

[1]*ANKA/Institute for Synchrotron Radiation, Karlsruhe Institute of Technology, Germany*
[2]*European Synchrotron Radiation Facility (ESRF), Grenoble, France*

Abstract:

X-ray microscopy techniques are used in a variety of implementations for two-dimensional (2D) imaging with spatial resolutions on the nm scale. Imaging of regions of interest (ROIs) on laterally extended films and substrates is common practice. In combination with computed tomography (CT), cross sections and also 3D images can be reconstructed but then the lateral extensions of the substrates must be reduced significantly or the angular range of CT scanning has to be limited like usually done in transmission electron microscopy.

We propose a different scanning scheme for non-destructive three-dimensional (3D) imaging of ROIs from laterally extended specimens. Computed laminography (CL) using hard synchrotron radiation (SR) has already been developed [1] and successfully applied for imaging on the µm scale [2,3]. The principal difference towards computed tomography is the inclination between rotation axis and the transmitted x-ray beam smaller than 90° which enables acquisition of reliable projection data and 3D reconstruction of the ROIs of such flat specimens.

In this paper we will present the physical principles and experimental implementation of nano-laminography. X-ray focusing to focal spot sizes in the order of 100 nm is performed by a Kirkpatrick-Baez multilayer mirror arrangement at ESRF beamline ID22NI [4]. High spatial resolutions on the nm scale (see Fig. 1) via x-ray focusing and chemical sensitivity via fluorescence scanning can be achieved, as demonstrated in material and life science applications.

References:

[1] L. Helfen et al., App. Phys. Lett. **86**, 071915 (2005).
[2] L. Helfen et al., App. Phys. Lett. **94**, 104103 (2009).
[3] F. Xu et al., J. Synchrotron Radiat. **17**, 222 (2010) and references therein.
[4] P. Bleuet et al., Rev. Sci. Instrum. **80**, 056101 (2009).

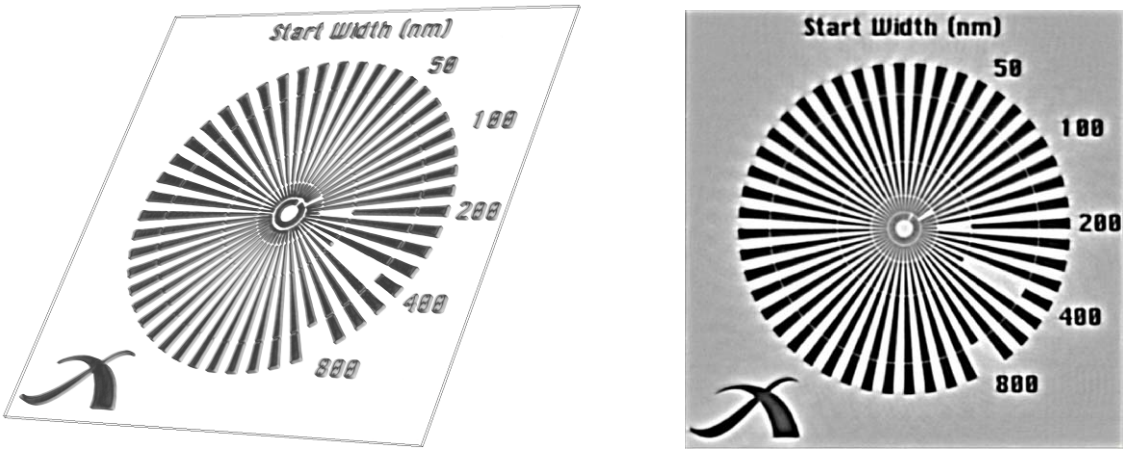

Figure 1: 3D rendition (left) and reconstructed cross section (right) of a test pattern (Xradia Inc. CA, type X50) with nm-sized structures reconstructed by nano-laminography (E=17.5 keV).

Chemical Imaging of Nanodevices with Zone Plate-Based SPEM

L. Gregoratti, M. Amati, M. Kazemian

Sincrotrone Trieste SCpA, SS14-km163.5 in Area Science Park, 34149 Trieste, Italy

Abstract:

A scanning photoemission microscope (SPEM) uses the most direct approach to obtain spatial resolution i.e., the focalization of the incoming x-ray beam. The x-ray SPEM at the Elettra synchrotron light source located at Trieste, Italy [1] de-magnifies the photon beam by means of a Fresnel zone plate. Recently, thanks to the improvement in the quality of the focusing optics, nanostructures as wide as 45 nm have been imaged and characterized. The available range of photon energies (400-800 eV) covers the most intense core levels of the majority of the atomic species making the SPEM an ideal tool for the chemical characterization at the meso- and nanoscale regime. The overall energy resolution achievable in working conditions at room temperature is around 200 meV. In-situ samples can be heated, cooled and biased.

Investigations on of the electronic, physical and chemical properties of nanostructures are key topics of the research addressed by the SPEM. An overview of the most recent results obtained will be offered. It will include the following issues: (i) metal interfaces, gas interaction and mass transport on the multiwall CNT by probing an individual nanotube [2]; (ii) compositional and electronic studies of TCO nanostructures based on ITO, InN, SnO_2, etc. compounds [3,4]; (iii) chemical and electronic behavior of e-noses and nanosensors under working conditions [5]; (iv) size and surface chemistry effects on the conductivity of MBE-grown GaAs nanowires [6].

Finally an overview of the limits in the applications of the x-ray photoelectron microscopy imposed by the operation principles will be given together with the future developments allowing the investigation of materials at mbar and even ambient pressure.

References:

[1] http://www.elettra.trieste.it
[2] A. Barinov, L. Gregoratti, P. Dudin et al., Adv. Mater. **21**(19), 1916 (2009).
[3] D. Maestre, A. Cremades, L. Gregoratti et al., J. Phys. Chem. C **114**(8), 3411 (2010).
[4] D. Maestre, A. Cremades, L. Gregoratti et al., J. Nanosc. and Nanotech. **9**(3), 1772 (2009).
[5] A. Kolmakov, A. Potluri, A. Barinov et al., ACS Nano **2**(10), 1993 (2008).
[6] S. Rubini et al., article in preparation.

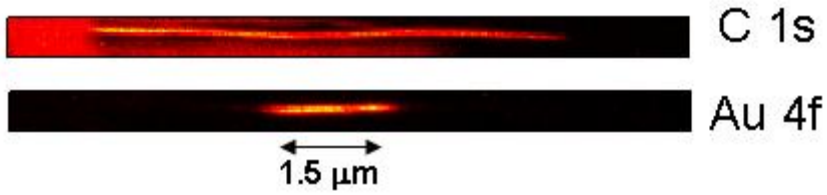

Figure 1: Photoemission images of an individual MWCNT grown on an Si substrate partially covered by an Au patch. The diameter of the MWCNT is approximately 90 nm. As is clearly visible in the Au map, the gold patch is about 1.5 µm long.

Polarized X-ray Excited Optical Luminescence Imaging of Nano-LEDs

G. Martínez-Criado[1], J. A. Sans[1], R. Tucoulou[1], P. Cloetens[1], J. Susini[1], A. Homs[1], B. Alén[2], L. González[2], J. Yoo[3], G.-C. Yi[3]

[1]*European Synchrotron Radiation Facility, 38043 – Grenoble, France*
[2]*Microelectronics Institute Madrid, CNM-CSIC, 28760 – Tres Cantos, Spain*
[3]*Seoul National University, Seoul 151-747, Republic of Korea*

Abstract:

A compact and mobile X-ray Excited Optical Luminescence (XEOL) apparatus has been developed and well adapted on the beamline ID22 of the European Synchrotron Radiation Facility. Linked by multimode optical fibers, its special modular design provides precise scanning capabilities, allowing easy access for multiple detection modes: XRF, XAS and XEOL [1,2]. With excellent mechanical stability, its suitable setup on the UV/VIS and IR wavelength ranges was assembled for both nanoprobe and microprobe experimental hutches [3]. Details of the optical equipments, spectral calibration and typical results are described in details. The excellent performance of the XEOL approach has been illustrated by the study of the excitonic lines of coaxial GaN/ZnO quantum nanotubes. At the nanoimaging station, spatially and spectrally resolved XEOL microscopy was applied to correlate the optical failures, structure and composition of the nano-LEDs. Data collections from InGaN quantum nanotubes support sharp sidewalls with regular separation among the hexagonal nanorods. Information on stress of a single GaN nanorod was deduced from the relative position of the luminescence lines (see Figures 1 and 2). The spatial intensity and energy variations of the ZnO emission lines were attributed to both local composition changes and strain-induced modifications. Polarization-sensitive measurements reveal a striking XEOL anisotropy recorded with the beam parallel and perpendicular to the long axis of a nanowire.

References:

[1] G. Martinez-Criado, B. Alen, A. Homs et al., Appl. Phys. Lett. **89**, 221913 (2006).
[2] G. Martinez-Criado, R. Steinmann, B. Alen et al., Rev. Sci. Instrum. **78**, 025106 (2007).
[3] P. Gundel, G. Martinez-Criado, M. C. Schubert et al., Phys. Status Solidi RRL **3**(9), 275 (2009).

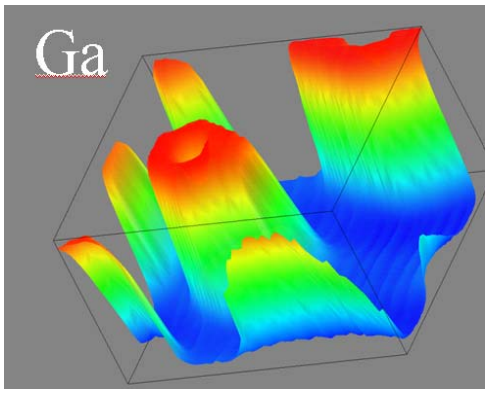

Figure 1: 2D color map of Ga Kα XRF intensity over a single nanorod (4 x 4 μm^2). Red represents high intensity, blue low one.

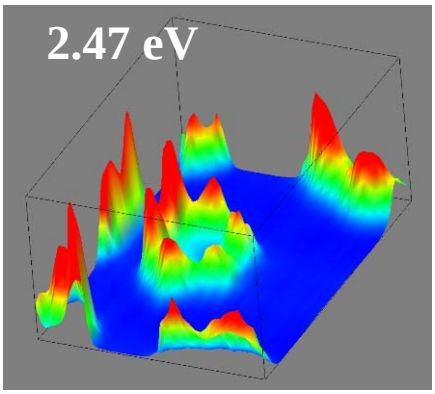

Figure 2: Spatial variation of the intensity of the emission line located at 2.47 eV. Red represents high signal, blue low one.

Imaging Interfacial Topography and Reactivity with X-ray Reflection Interface Microscopy (XRIM) *

P. Fenter*[1], S. S. Lee[1], C. Park[2], J. Catalano[3], Z. Zhang[4], N. C. Sturchio[5]

[1] *Chemical Sciences and Engineering, Argonne National Laboratory, Argonne IL USA*
[2] *HP-CAT, Geophysical Laboratory, Carnegie Institution of Washington, Argonne, IL USA*
[3] *Dept. of Earth and Planetary Sciences, Washington Univ. at St. Louis, St. Louis, MO, USA*
[4] *Advanced Photon Source, Argonne National Laboratory, Argonne IL USA*
[5] *Dept of Earth and Environmental Sciences, University of Illinois at Chicago, Chicago IL USA*

* This work supported by the Geoscience Research Program of the US Department of Energy, Office of Basic Energy Sciences.

Abstract:

A fundamental understanding of interfacial reactivity is essential for fields ranging from geochemistry to materials science. X-ray reflection interface microscopy (XRIM) is a powerful new tool for interfacial studies. XRIM is a full field microscope that uses the weak *interface-reflected* X-ray beam to image a surface. It therefore incorporates all of the sensitivities of X-ray reflectivity (XR), including sensitivity to interfacial topography, structure and composition, along with the ability to spatially resolve heterogeneous systems and processes. This presentation will present recent applications of XRIM. Initial studies ex-situ observations performed on the orthoclase $KAlSi_3O_8$ (001) surface have demonstrated: the ability to see elementary surface topography (6.5 Å-high steps) with ~100 nm spatial resolution [1]; demonstrated the basis for XRIM image contrast [2]; and demonstrated the first use of XRIM to image interfacial reactivity [3]. Ongoing success in the use of XRIM as an in situ probe of the mineral-water interfaces will also be presented along with the specific challenges of in-situ studies, including an intrinsically reduced signal strength and avoiding radiation damage. Future improvements in the XRIM instrument and its use as an in-situ real-time probe of interfacial processes will be discussed.

References:

[1] P. Fenter et al., Nat. Phys. **2**(10), 700 (2006).
[2] P. Fenter et al., J. Synchrotron Radiat. **15,** 558 (2008).
[3] P. Fenter et al., Geochim. Cosmochim. Acta, in review (2010).

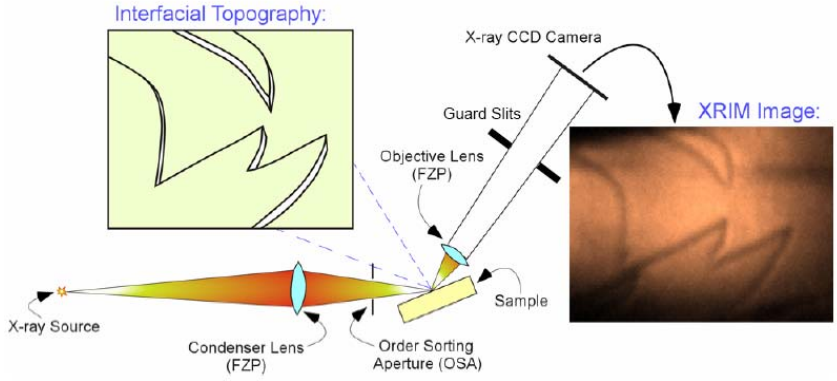

Figure 1: Schematic of the XRIM system.

Hard X-ray Phase-Contrast Tomographic Nanoimaging

M. Stampanoni[1,2], R. Mokso[1], F. Marone[1], J. Vila-Comamala[1], S. Gorelick[1], C. David[1], P. Trtik[3], K. Jefimovs[3]

[1] *Paul Scherrer Institut, 5232 Villigen, Switzerland*
[2] *Institute for Biomedical Engineering, University and ETH Zurich, 8092 Zurich, Switzerland*
[3] *EMPA, Materials Science and Technology, 8600 Dübendorf, Switzerland*

Abstract:

Synchrotron-based full-field tomographic microscopy established itself as a tool for non-invasive investigations. Many beamlines worldwide routinely achieve micrometer spatial resolution while the isotropic 100 nm barrier is reached and trespassed only by few instruments, mainly in the soft X-ray regime. We present an X-ray, full field microscope with tomographic capabilities operating at 10 keV and with a 3D isotropic resolution of 144 nm recently installed at the TOMCAT beamline of the Swiss Light Source [1]. Custom optical components including a beam-shaping condenser and phase-shifting dot arrays were used to obtain an ideal, aperture-matched sample illumination and very sensitive phase contrast imaging. Due to the use of broad-band radiation, tomographic investigations can be performed within few minutes. This presentation describes the novel optical components and the setup which can be quickly installed on-top of the microtomography endstation. We present simulations of the illumination and imaging process and we show that, in practice, the instrument has been successfully used for the non-destructive, volumetric investigation of single, non-fixed, unstained cells.

References:

[1] M. Stampanoni et al., Proceedings of SPIE, Developments in X-ray Tomography **6318**, doi:10.1117/12.679497 (2006).

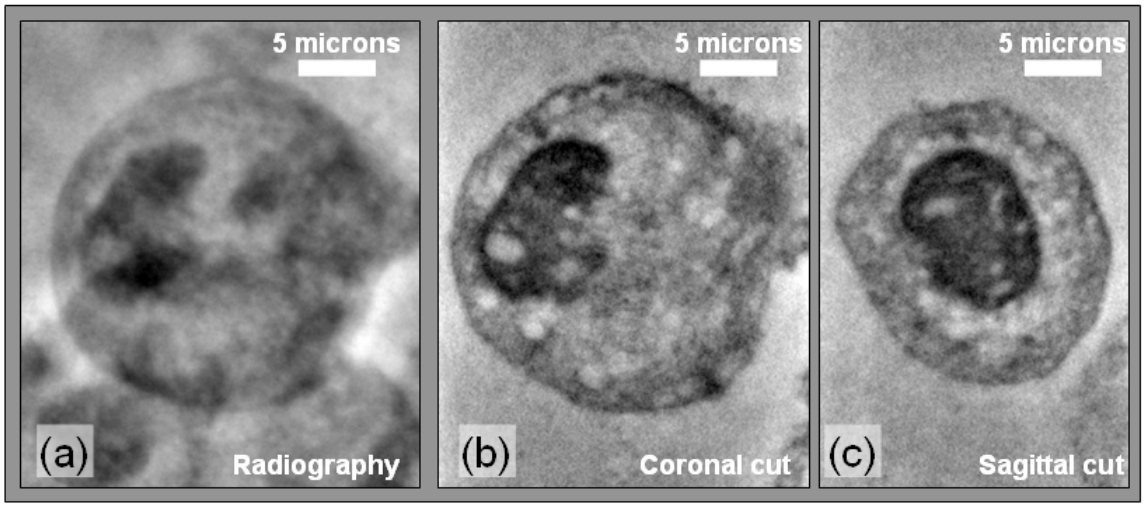

Figure 1: Zernike phase contrast nanotomography of an unstained MC3 preosteoblast cell. (a) shows a nano-radiographic projection of the MC3 cell together with other cells which happened to be in the beam path during the snapshot. (b) and (c) show coronal and sagittal cut of the MC3 cell respectively. A total of 251 angular projections over 180° have been collected within 10 minutes. Clearly visible are the nucleus (dark) with several intracellular structures.

The Maia X-ray Detector Array at the Australian Synchrotron: High-Definition SXRF Trace Element Imaging

C.G. Ryan[1,6,7], R. Kirkham[2], D.P. Siddons[3], P.A. Dunn[2], A. Kuczewski[3], G. Moorhead[2,6], G. De Geronimo[4], D. Paterson[5], M.D. de Jonge[5], D.L. Howard[5], B.E. Etschmann[8], S. Borg[1,7], R.M. Hough[1], J. Cleverley[1], M.J. Lintern[1], S.J. Barnes[1], P. Davey[2], M. Jensen[2]

[1]CSIRO Earth Science and Resource Engineering, Clayton VIC, Australia; [2]CSIRO Materials Science and Engineering, Clayton VIC, Australia; [3]National Synchrotron Light Source, Brookhaven National Laboratory, NY, USA; [4]Instrumentation Division, Brookhaven National Laboratory, Brookhaven NY, USA; [5]Australian Synchrotron, Clayton VIC, Australia; [6]School of Physics, University of Melbourne, Parkville VIC, Australia; [7]CODES Centre of Excellence, University of Tasmania, Hobart TAS, Australia; [8]Department of Geology, University of Adelaide SA, Australia

Abstract:
Motivated by the need for megapixel high definition trace element imaging of natural material, faster acquisition and improved counting statistics, using a scanned sample and a microfocused X-ray probe, a large energy-dispersive detector array with dedicated processor called Maia has been developed by CSIRO and BNL for SXRF elemental imaging. Following a year using a 96 detector prototype for a wide range of applications at the X-ray Fluorescence Microscopy (XFM) beamline at the Australian Synchrotron, construction of the Maia annular 384 detector array [1,2] has been completed and tests are underway. This paper provides an update on the Maia concept, reports on developments in methods for real-time processing of event data, methods for spectral deconvolution and quantitative imaging using a large detector array with extended solid-angle, a software approach to cope with large data-sets and illustrates Maia performance using applications involving rare fine-scale features in complex geological samples.

Maia combines a 96 or 384 silicon detector array and a high speed, FPGA based, pipelined, parallel processor that enables real-time processing of each detected X-ray event tagged by detector number and XY position in the image scan. Using an embedded spectral deconvolution algorithm based on the Dynamic Analysis (DA) method [3], the processor accumulates deconvoluted element images in real-time. The real-time processing pipeline includes: (i) event correction for linearization, (ii) gain trimming to match spectra from individual detector channels, (iii) pile-up rejection, (iv) DA image accumulation, (v) monitor spectra accumulation, (vi) intelligent sub-sampling to conserve disk space, and (vii) logging of raw and accumulated data to disk. The detector systems may drive the XY sample stage directly, or read back stage encoder or laser interferometer values to sample position and focusing zone-plate location.

Real-time event processing enables transit times per pixel as short as 50 µs and scanning up to ~10000 lines to collect high definition SXRF images up to ~100M pixels (or 3D fluorescence tomography [4] and XANES imaging data-sets [5]). The result at XFM is spatial detail spanning 4 orders of magnitude from ~1 µm to ~10 mm that can detect rare µm scale features (e.g. sub-µm gold grains at depth in a section) and place them within a broad and detailed spatial context.

References:

[1] D.P. Siddons et al., AIP Conference Proceedings **705**, 953 (2004).
[2] R. Kirkham et al., Proc. of SRI 2009, AIP Conference Proceedings, in press.
[3] C.G. Ryan, Int. J. of Imaging Systems and Technology **11**, 219 (2000).
[4] M.D. de Jonge et al., these Proceedings.
[5] B.E. Etschmann et al., American Mineralogist, in press.

An Innovative Low-Dose Single-Step Method for Grating-Based X-ray Phase-Contrast Imaging

Z. Wu[1,2]

[1]*National Synchrotron Radiation Laboratory, University of Science and Technology of China, Hefei 230026, China*

[2]*Beijing Synchrotron Radiation Facility, Institute of High Energy Physics, Chinese Academy of Sciences, Beijing 100049, China*

Abstract:

In the last year phase contrast X-ray imaging methods based on grating interferometry have been widely used. The method utilizes Moiré fringes to extract quantitative phase information from multiple images [1,2]. The phase-stepping method has been usually considered to acquire phase information from multiple radiographic images in each projection for 3D imaging. We present here an original X-ray tomographic phase contrast imaging approach based on grating interferometry, which requires only a single-step and a "reverse projection" to extract phase information [3]. Compared to the already know phase-stepping approach, our method is fast and significantly reduces the total radiation dose delivered to the sample without image quality degradation. The method is particularly suitable for X-ray phase contrast imaging applications such as biological in-vivo studies and clinical application, for which the radiation dose is the main parameter to control.

References:

[1] A. Momose et al. , Jpn J Appl Phys. **42**, L866 (2003).
[2] T. Weitkamp et al., Opt. Express **13**, 6296 (2005).
[3] P.P. Zhu, K. Zhan, Z. Wang et al., PNAS, under review.

Femtosecond X-ray Imaging Using Free Electron Lasers

A. Barty

Center for Free Electron Laser Science, Notkestraße 85, 22607 Hamburg, Germany

Abstract:
The ultrafast pulses from X-ray free-electron lasers enable X-ray imaging beyond conventional radiation damage limits. Although sufficient dose is deposited in a single pulse to completely destroy the sample, it is nevertheless possible to collect meaningful diffraction patterns from the undamaged sample before it is destroyed using ultra-short X-ray pulses that terminate pulse before the effects of sample damage are manifested.

The ability to collect images using ultrafast, extremely intense single X-ray pulses that outrun sample damage whilst simultaneously destroying the sample has been demonstrated at the FLASH free electron laser at DESY in Hamburg. Single-pulse X-ray imaging has been used to study the time evolution of non-cyclic phenomena such as laser-induced ablation with nanoscale resolution and a shutter speed measured in femtoseconds. Meanwhile the ability of single-pulse imaging to freeze motion has been used to image nanoscale objects in free flight not supported on any membrane, including cells viruses and nanoscale aerosols. Time-resolved measurements of X-ray sample damage rates using holographic pump-probe techniques show agreement with numerical models of the X-ray induced damage processes as well as imaging the process of sample explosion induced by the X-ray beam.

Recent results obtained using the Linac Coherent Light Source (LCLS) free electron laser at SLAC National Accelerator Laboratory have demonstrated femtosecond diffraction from sub-micron nanocrystals embedded in a continuous liquid jet stream intersecting the pulsed LCLS X-ray beam. Clear diffraction is seen to the measured resolution limits and little evidence of X-ray damage is observed at sub-nanometer spatial resolution using individual 2 keV X-ray pulses of only a few femtoseconds and with more than 1012 photons per pulse. Extending the same techniques using harder X-rays may enable atomic resolution imaging of proteins that cannot be crystallized.

This work was carried out as part of a large collaboration consisting of CFEL DESY, Arizona State University, SLAC, Uppsala University, LLNL, The University of Melbourne, LBNL, the Max Planck Institute for Medical Research, and the Max Planck Advanced Study Group (ASG) at the CFEL. The names and addresses of all do not fit on one page. The experiments were carried out using the CAMP apparatus, which was designed and built by the Max Planck ASG at CFEL. The LCLS is operated by Stanford University on behalf of the U.S. Department of Energy, Office of Basic Energy Sciences.

Cultural Heritage Science at the ESRF

M. Cotte[1,2], J. Susini[1], S. Lahlil[2], I. Biron[2]

[1]*European Synchrotron Radiation Facility, Polygone Scientifique Louis Néel - 6, rue Jules Horowitz – F-38000 Grenoble, France*

[2]*Centre of Research and Restoration of French Museums (LC2RMF), CNRS UMR 171, Palais du Louvre, Porte des Lions, 14, Quai François Mitterrand, F-75001 Paris, France*

Abstract:

Within the last decades, synchrotron-based micro-imaging techniques have been used to an increasing extent in the field of Cultural Heritage Science. These methods offer a combination of attributes particularly well suited for the chemical analysis of works of art. Their non-invasive character, low detection limit, high lateral resolution and high chemical sensitivity are highly relevant properties for the morphological and chemical characterizations of precious, heterogeneous and complex materials.

On one hand, some analyses try to unlock artists' and craftsmen's secrets, by revealing the chemical signature trapped inside the matter. On the other hand, some works try to better understand the alteration processes that can affect works of art, as well as to assess conservation treatments.

Analyses can be performed directly on entire objects or more specifically on small fragments. Within the large range of SR-based analytical techniques, micro X-ray fluorescence, micro-X-ray diffraction, micro-X-ray absorption spectroscopy as well as micro-FTIR are increasingly applied for such micro-chemical characterization. As an example, figure 1 shows the evolution of the number of publications reporting XAS analyses on works of art, over the last ten years [1].

In addition to recent examples (e.g. evolution of glass opacification processes across centuries [2]), some methodological developments fostered by the analyses of such complex materials will be addressed and illustrated.

References:

[1] M. Cotte, J. Susini, J. Dik et al., Acc. Chem. Res., in press (2010).

[2] S. Lahlil, I. Biron, M. Cotte et al., Appl. Phys. A **98**, 1 (2010).

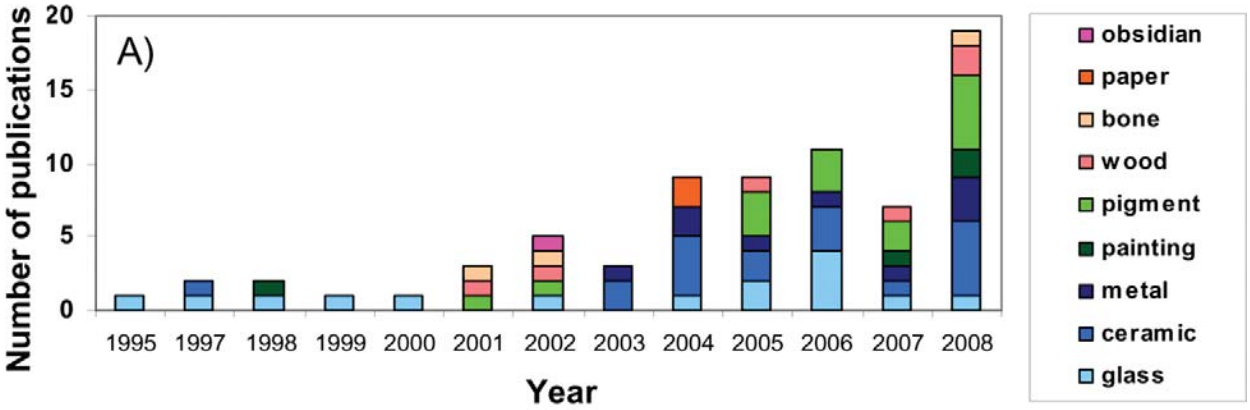

Figure 1: Evolution of the publications reporting XAS analyses on Cultural Heritage Science items over the last decade. Statistics are sorted by type of material versus time [1].

One-Nanometer-Scale Elemental Analysis by SR-Based Scanning Tunneling Microscopy

A. Saito[1,2,3], T. Tanaka[1], Y. Takagi[4], H. Notsu[1], G. Ohzeki[1], Y. Tanaka[2], Y. Kohmura[2], M. Akai-Kasaya[1], T. Ishikawa[2], Y. Kuwahara[1], M. Aono[5]

[1]*Dept. of Precision Sci. and Technology, Osaka Univ., 2-1Yamada-oka, Osaka 565-0871, Japan*
[2]*RIKEN SPring-8 Center, 1-1-1 Kouto, Sayo-cho, Hyogo 679-5148, Japan*
[3]*JST, PRESTO, 4-1-8 Honcho, Kawaguchi, Saitama 332-0012, Japan*
[4]*Institute for Molecular Science, Myodaiji-cho, Okazaki 444-8585, Japan*
[5]*WPI center, National Institute for Materials Science, Tsukuba 305-0003, Japan*

Abstract:
Scanning Tunneling Microscopy (STM) combined with synchrotron radiation (SR) enabled the elemental analysis on solid surfaces at a nanometer scale. The principle of the analysis is based on the inner-shell excitation of a specific energy level under STM observation. A key to accomplish successful results is to effectively increase the signal to noise (S/N) ratio and to extract the element-specific modulation of the tunneling current giving local information. On this purpose, we developed a special SR-STM system [1,2] and STM tip that can eliminate the noisy electrons coming from a wide area [3].

After first demonstrative results on a semiconductor hetero-interface (Si(111)7x7-Ge) [1], a second trial of the nanoscale elemental analysis was accomplished for Ge(111)-Cu nano-domains [4]. For both cases, the surface domains had a thickness of less than one atomic layer, and the spatial resolution of the analysis was estimated to be 1~4 nm.

By controlling precisely the incident beam and STM conditions, we have recently succeeded in obtaining successive STM images at a same area without drift or sample damages. Thus, we could obtain a dependence of the element contrast on the incident photon density as shown in Fig.1 (right), whereas no change was observed in conventional STM topographic images (left). Such information gives us an important clue to approach the mechanism to obtain a higher resolution. It is notable that the right images in Fig. 1 give the contrast based on the chemical difference, which is not affected by the surface step height.

Also we have recently achieved a direct observation of X-ray induced atomic motion with atomic scale using the SR-STM system under the incident photon density of ~2×10^{15} photon/sec/mm^2 [5].

These results will allow us to investigate the chemical analysis and control of the local reaction with the spatial resolution of STM, giving hope of wide application.

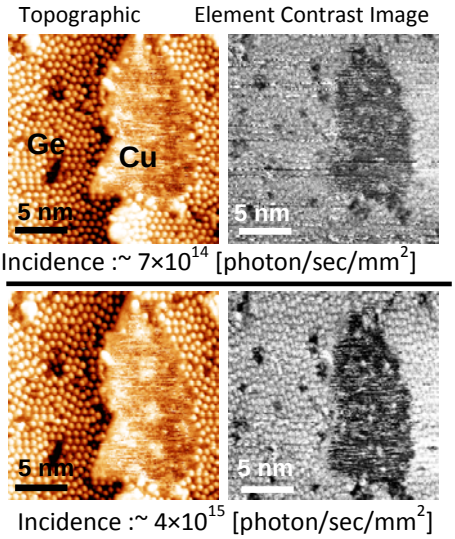

Figure 1: STM images of Ge(111)-Cu nano-domain and dependence of the element contrast on the incident X-ray photon density: (left) topographic and (right) element contrast image under Cu-excitation condition.

References:

[1] A. Saito et al., J. Synch. Rad. **13**, 216 (2006).
[2] A. Saito et al., Jpn. J. Appl. Phys. **45**, 1913 (2006).
[3] A. Saito et al., Surf. Sci. **601**, 5294 (2007).
[4] A. Saito et al., Surf. Interface Anal. **40**, 1033 (2008).
[5] A .Saito et al., J. Nanosci. and Nanotech., to be published (2010).

Imaging of Spin Phenomena in Magnetic Nanostructures Using Magnetic Soft X-ray Microscopy *

M.-Y. Im[1], P. Fischer[1], L. Bocklage[2], G. Meier[2], S. Kasai[3]

[1]*Center for X-ray Optics, Lawrence Berkeley National Lab, Berkeley, CA 94720, USA*
[2]*Institute of Applied Physics and Center for Microstructure Research, University of Hamburg, 20355 Hamburg, Germany*
[3]*Institute for Chemical Research, Kyoto University, Uji 611-0011, Japan*

* This work is supported by the Director, Office of Science, Office of Basic Energy Sciences, Materials Sciences and Engineering Division, of the U.S. Department of Energy under Contract No. DE-AC02-05-CH1123, Deutsche Forschungsgemeinschaft via SFB 668 "Magnetism from the Single Atom to the Nanostructure" and via Graduiertenkolleg 1286 "Functional Metal-Semiconductor Hybrid Systems."

Abstract:

The study of spin phenomena in nanoscale magnetic structures is scientifically interesting and technologically of the highest relevance. Magnetic transmission soft X-ray microscopy (MTXM) with a high spatial resolution down to 15 nm provided by Fresnel zone plate optics [1] allows the study of statistical behavior and fast dynamics of magnetic processes on a nanoscale in confined ferromagnetic structures.

The reproducibility of magnetic processes such as magnetic domain-wall motion along magnetic nanowires and generation of magnetic vortex structures is a key issue in current technological developments of novel classes of storage and memory devices [2]. A statistical analysis of high-resolution magnetic soft X-ray microscopy images revealed the stochastic behavior of the domain-wall depinning field in notch-patterned $Ni_{80}Fe_{20}$ (permalloy) nanowires [3] and the vortex state creation process in permalloy nanodot arrays [4]. A stochastic component has been identified in those systems, which could be traced back to geometrical and multiplicity effects for the DW depinning in the nanowires and a Dzyaloshinsky-Moriya coupling effect for the generation of magnetic vortex structures.

X-ray pulses from synchrotron sources have an inherent time structure with less than 100-ps length at typically MHz frequencies. This perfectly matches magnetization dynamics such as precession and relaxation time of domain wall and magnetic vortex core motions. Direct observation of dynamics behavior of a constricted domain wall [5] and magnetic vortex core [6] utilizing MTXM, but also quantitative analysis of the mass of a single domain wall and the spin polarization of currents has been performed.

Based on the experimental studies, we provide new and fundamental insight into magnetic processes, and thus open the path to further technological developments in practical applications of nanomagnetism.

References:

[1] W. Chao, B.H. Harteneck, J.A. Liddle et al., Nature **435**, 1210 (2005).
[2] M.-Y. Im, S.-H. Lee, D.-H. Kim et al., Phys. Rev. Lett. **100**, 167204 (2008).
[3] M.-Y. Im, L. Bocklage, P. Fischer et al., Phys. Rev. Lett. **102**, 147204 (2009).
[4] M.-Y. Im et al., to be submitted (2010).
[5] L. Bocklage, B. Krüger, R. Eiselt et al., Phys. Rev. B **78**, 180405 (2008).
[6] S. Kasai, P. Fischer, M.-Y. Im et al., Phys. Rev. Lett. **101**, 237203 (2008).

Probing Magnetic Domain Structure via Coherent X-ray Diffractive Imaging

O. G. Shpyrko[1], A. Tripathi[1,3], J. Mohanty[1], S. Dietze[1], E. Shipton[2], E. E. Fullerton[2], S.S. Kim[3], I. McNulty[3]

[1]*Department of Physics, University of California, San Diego, La Jolla, CA 92093, USA*
[2]*Department of Electrical and Computer Engineering, University of California, San Diego, La Jolla, CA 92093, USA*
[3]*Advanced Photon Source, Argonne National Laboratory, Argonne, IL 60439, USA*

Abstract:
Polarized x-rays are an appealing choice for magnetic imaging due to their penetrating power and elemental specificity. The spatial resolution of traditional microscopy is limited by the precision required to fabricate x-ray focusing optics. I will present a novel approach for lensless imaging of extended magnetic nanostructures, in which a scanned series of coherent diffraction patterns are recorded across the sample and numerically inverted to map the magnetic domain configuration. We demonstrate this approach by imaging labyrinthine domains in a perpendicular anisotropy Gd/Fe multilayer, and follow the evolution of the domain structure through part of the magnetization hysteresis loop (see Figure 1). This approach is scalable to imaging with diffraction-limited resolution, a prospect that is rapidly becoming a reality in view of the new generation of x-ray sources.

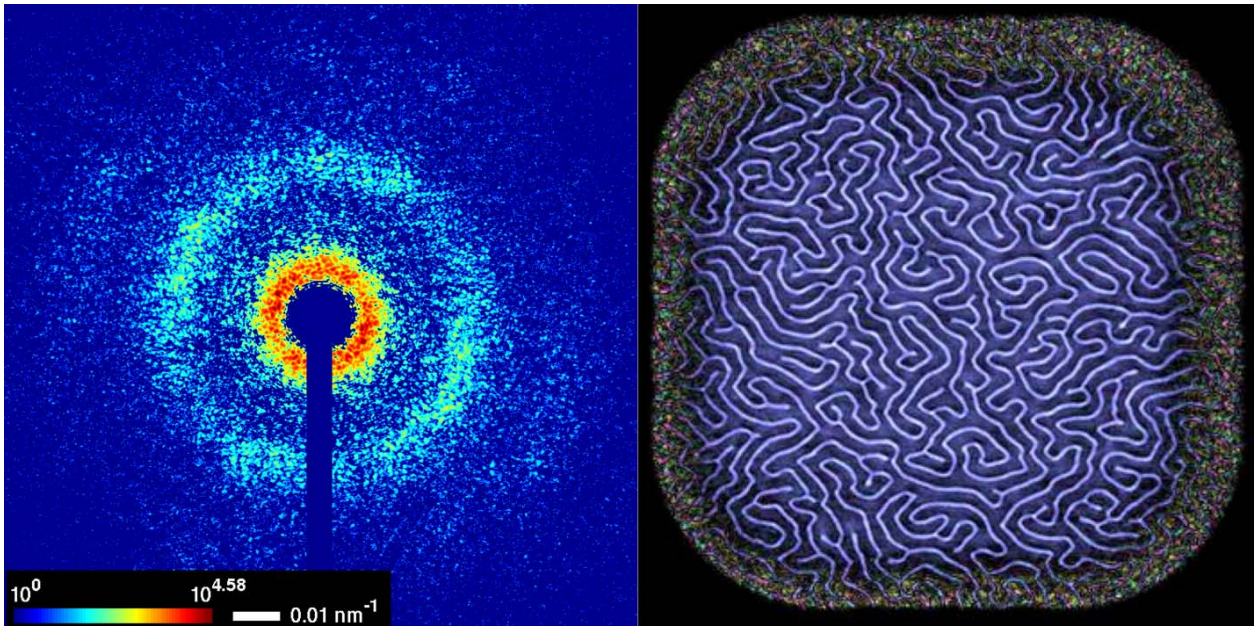

Figure 1: Left panel shows the resonant coherent x-ray diffraction pattern collected from GdFe labyrinthine domains. Right panel shows the results of ptychographic reconstruction of magnetic domain structure from diffraction patterns using phase-retrieval algorithm.

Spins and Twins: Correlation Between Crystallographic and Magnetic Domains at Co/NiO(001) Interfaces

H. Ohldag[1], G. van der Laan[2], E. Arenholz[3]

[1]*Stanford Synchrotron Radiation Lightsource, Menlo Park, CA, USA*
[2]*Diamond Light Source, Chilton, UK*
[3]*Advanced Light Source, Berkeley, CA, USA*

Abstract:

Elucidating the mechanisms behind the magnetic ordering and coupling at interfaces is crucial for the understanding of complex magnetic systems, such as nanomagnet assemblies and magnetic heterostructures. One particular area of interest concerns antiferromagnetic (AF) surfaces and their interfaces to ferromagnetic (FM) layers. Since AF systems are not sensitive to external fields they can induce an uniaxial anisotropy in an FM layer through AF/FM exchange coupling. Using soft x-ray spectromicroscopy we show that NiO(001) exhibits a crystallographic and magnetic domain structure near the surface identical to that of the bulk. Using linear dichroism in soft x-ray absorption it is possible to separate magnetic and crystallographic domains in complex magnetic oxides – an approach that is applicable to a wide range of multifunctional oxide interfaces and surfaces.

Upon Co deposition a perpendicular coupling between the Ni and Co moments is observed that persists even after formation of uncompensated Ni spins at the interface through annealing. The chemical composition at the interface alters its crystallographic structure and leads to a reorientation of the Ni moments from the <112> to the <110> direction. We show that this reorientation is driven by changes in the magnetocrystalline anisotropy rather than exchange coupling mediated by residual uncompensated spins.

References:

[1] H. Ohldag, G.v.d. Laan and E. Arenholz, Phys Rev. B **79**, 052403 (2009).

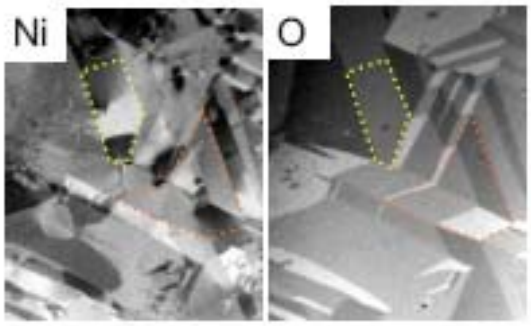

Figure 1: Using magnetic linear dichroism at the Ni L –edge (left and linear dichroism at the O K-edge (right) magnetic and crystallographic domains can be distinguished.

Vortex and Vortex Core Dynamics Imaged by Time-Resolved X-ray Microscopy

B. Van Waeyenberge[1], H. Stoll[2], M. Curcic[2], M. Weigand[2], A. Vansteenkiste[1], M. Kammerer[2], M. Noske[2], A. Bissig[2], K.W. Chou[3] T. Tyliszczak[3], G. Woltersdorf[4], C.H. Back[4], G. Schütz[2]

[1]*Department of Solid State Science, Ghent University, Krijgslaan 281, S1, 9000 Ghent, Belgium*
[2]*Max Planck Institute for Metals Research, Heisenbergstr. 3, 70569 Stuttgart, Germany*
[3]*Advanced Light Source, Lawrence Berkeley National Laboratory, MS 6-2100, Berkeley, CA 94720, USA*
[4]*University of Regensburg, Universitätsstraße 31, 93040 Regensburg, Germany*

Abstract:

The simplest, non-trivial magnetic ground state configuration of soft magnetic thin film platelets is a vortex state. The nanometer sized, out-of-plane magnetized vortex core plays a key role in the dynamics of these structures. We have studied the vortex dynamics in micron and submicron Permalloy thin film elements by means of time-resolved magnetic X-ray microscopy. The dynamic response was recorded with high spatial (30 nm) and temporal (70 ps) resolution after the application of different excitations: magnetic field pulses, alternating magnetic fields and rotating magnetic fields and spin polarized currents.

These studies have revealed a new reversal mechanism for the out-of-plane vortex core. By excitation with short bursts of an in-plane alternating field as low as 1.5 mT, the vortex core could be toggled from its up to down state and vice versa [1]. Vortex core switching after different types of excitation has now also been investigated. Experimental data will be presented on vortex core switching resulting from linear, RF magnetic fields, rotating magnetic fields, short magnetic field pulses and spin polarized currents.

The dynamics of the vortex core were directly studied by direct imaging of the out-of-plane magnetization of the vortex core [2] under different excitations. We could evaluate the critical vortex velocity for switching [2-5] and detect the deformation of the vortex core profile as the first step in the core reversal mechanism [5]. An advanced pump-and-probe approach at the Scanning Transmission X-ray Microscope enabled us to image the switching transients during the core reversal process.

References:

[1] B. Van Waeyenberge et al., Nature **444**, 461 (2006).
[2] K.W. Chou et al., Appl. Phys. Lett. **90**, 202505 (2007).
[3] M. Curcic et al., Phys. Rev. Lett. **101**, 197204 (2008).
[4] M. Weigand et al., Phys. Rev. Lett. **102**, 077201 (2009).
[5] A. Vansteenkiste et al., Nature Physics **5**, 332 (2009).

STXM Analysis of Impact Tracks in the Stardust Interstellar Dust Collector Aerogel

A. L. Butterworth[1], T. Tyliczszak[2], A. J. Westphal[1] D. Frank[3], Z. Gainsforth[1], R. C. Ogliore[1], Stardust Interstellar Preliminary Examination Team

[1]*Space Sciences Laboratory, U. C. Berkeley, Berkeley, California, USA*
[2]*Advanced Light Source, Lawrence Berkeley Laboratory, Berkeley, California, USA*
[3]*KT NASA Johnson Space Center, Houston, Texas, USA*

The ALS is supported by the Director, Office of Science, Office of Basic Energy Sciences, of the U.S. DOE under Contract No. DE-AC02-05CH11231.

Abstract:

NASA's Stardust Mission undertook the first sampling of contemporary interstellar dust. The Stardust Interstellar Dust Collector was a ~0.1 m^2 array of low-density aerogel and aluminum foils, exposed to the interstellar dust stream for a total exposure factor of 20 m^2·day [1]. The Stardust Interstellar Preliminary Examination is a consortium effort using non-destructive techniques to characterize the contents of the Interstellar Dust Collector returned in 2006 [2].

Several complementary synchrotron techniques are being used to analyze impact tracks directly in small volumes of the aerogel [3]. We use Scanning Transmission X-ray Microscopy (STXM) at the Advanced Light Source, Beamline 11.0.2. This beamline uses a Fresnel zone plate to focus soft x-rays, 200 to 2000 eV, for 15 nm spatial resolution. We image tracks <2 µm in diameter by mapping variations in aerogel density. We first verify that a particle, typically <1 µm, is associated with an impact track, then characterize it using high resolution element mapping, and constrain its mineralogy with Mg, Al or Si K-edge XANES where appropriate. Elements with edges above 700 eV (e.g. Fe L_{23}) have sufficient x-ray transmission through 70-µm thick 20 mg/cm^3 silica aerogel for detection.

We have found several tracks to be secondary ejecta from impacts on the Stardust spacecraft, because they contain Al metal consistent with spacecraft composition, or Ce from the solar panel glass coating. One track, named Orion, is a possible candidate to be interstellar dust [4].

References:

[1] P. Tsou et al., J. Geophys. Res. **108**, 8113 (2003).
[2] A. J. Westphal et al., 39th Lunar and Planetary Science Conference, p. 1855 (2008).
[3] A. J. Westphal et al., 20th Int. Conf. on X-ray Optics and Microanalysis (in press).
[4] A. J. Westphal et al., 41st Lunar and Planetary Science Conference, p. 2050 (2010).

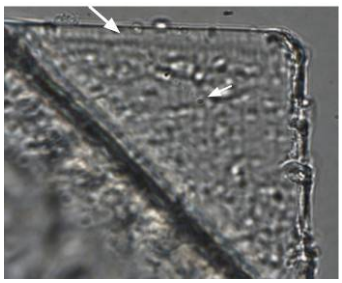

Figure 1: 50x optical image of aerogel with 70-µm long track "Orion". Top arrow shows entry direction, lower arrow points to the terminal particle.

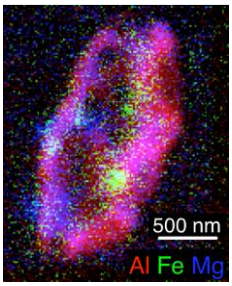

Figure 2: Three element RGB map of particle "Orion" shows major Al with heterogeneous ~100 nm Fe and Mg components.

High-Resolution Imaging of Green Construction Materials

P.J.M. Monteiro[1], M. Mancio[1], R. Chae[1], P. Fischer[2]

[1]*Department of Civil and Environmental Engineering, University of California, Berkeley, CA, USA*
[2]*Center for X-ray Optics, Lawrence Berkeley National Laboratory, Berkeley CA USA*

Abstract:
The present status of the cement and concrete industry is not sustainable. Concrete typically contains about 12 percent cement, 8 percent mixing water, and 80 percent aggregate by mass. This means that, world-wide, in addition to 1.5 billion tons of cement, the concrete industry is consuming annually 9 billion tons of sand and rock together, with one billion tons of mixing water [1]. This rate of consumption of materials by the world's population is only exceeded by our use of water. The production of Portland cement is now responsible for 7 percent of the CO2 emissions world-wide. The change in the existing technology requires new developments in the understanding of nanostructure of the hydration products and of the complex deterioration reactions. We are performing an elaborate research program to push the exiting cement and concrete science by optimizing the structure of calcium silicate hydrates by producing organic/inorganic nanohybrids. A new generation of green cements is being studied using x-ray spectroscopy at a nano-level. The complex nature of the calcium silicate hydrates and of the geopolymers will be studied in-situ full view microscopy and with high-resolution nanotomography.

Figure 1 shows the hydration process for a Portland cement obtained by soft x-ray microscopy. The cement hydration reaction is characterized by a brief period of dissolution and reaction during which a thin layer of hydration products forms around the cement grain. After one hour and thirteen minutes, few needle-like hydration products on the surfaces of the grains are observed. After the fast dissolution, an "induction period" of very slow reaction follows. Soft x-ray microscopy is able to capture the massive precipitation of the hydration products at the end of the induction period.

Reference:

[1] P. K. Mehta and P.J.M. Monteiro, *Concrete: Microstructure, Properties, and Materials*, McGraw-Hill, third edition (2006).

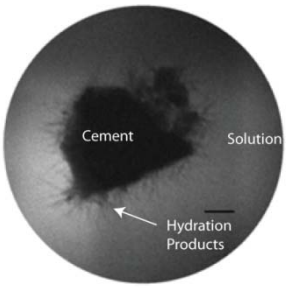

a) 1 h 13 min

Figure 1a: In situ soft x-ray images of hydrating Type II cement particles in a saturated calcium hydroxide-calcium sulfate solution. Hydration time is indicated.

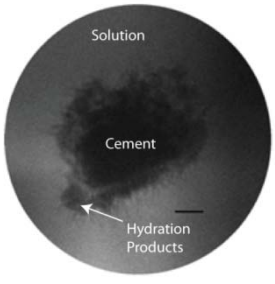

b) 2 h 49 min

Figure 1b: Scale bar corresponds to 1 µm. Images taken at 516 eV.

Hard X-ray Imaging of Mercury Accumulation in Plants

J. C. Andrews[1,2], S. Carrasco-Gil[3,4], D. LeDuc[2], L. E. Hernández[3], R. Millán[4], Y. Liu[1], F. Meirer[1], S. Webb[1], P. Pianetta[1]

[1]*Stanford Synchrotron Radiation Lightsource, SLAC National Accelerator Laboratory, Menlo Park CA, USA*
[2]*Dept of Chemistry and Biochemistry, California State University, East Bay, Hayward CA USA*
[3]*Faculty of Sciences, Universidad Autónoma de Madrid, Madrid, Spain*
[4]*Centro de Investigaciones Energéticas, Medioambientales y Técnológicas, Madrid, Spain*

Abstract:
Both hard X-ray full field imaging at 30 nm resolution and X-ray fluorescence mapping at 2 micron resolution have been used to determine mercury distribution throughout the vascular system of several plants, and to examine chemical speciation of the metal. This can be relevant both for phyotoremediation, which is the study of remediation of environmental contaminants with plants, and to understanding metal transformations that can increase or decrease metal toxicity within the environment. In particular, the transformation of mercury to methylmercury results in biomagnification up the food web such that fish advisories must be implemented in areas contaminated with mercury to limit consumption of fish higher in the food chain. In imaging studies of alfalfa grown hydroponically in Hg, Hg was found to accumulate in various portions of the vascular system of roots, stems and shoots, often collocating with sulfur. Micro-XANES confirmed that most of the Hg was bound to cysteine, a sulfur-containing amino acid that is a key component of phytochelatins, which are synthesized by plants to aid in metal sequestration to minimize harm to the plant. In roots of cordgrass, Hg was found within the root vascular system and also in microorganisms within the root zone thought to be sulfate-reducing bacteria that convert Hg to methylmercury. Speciation with micro-XANES confirmed mainly Hg-S ligation but also some methylation. The results found using these two complementary X-ray methods increase understanding of the fate and transformation of Hg within the environment which is of ultimate use in controlling its accumulation and toxicity within the food web.

Synchrotron X-ray Fluorescence Microtomography in Geo-, Cosmo-, and Biochemistry*

A. Lanzirotti[1], S. Sutton[1], M. Rivers[1], M Newville[1], R. Tappero[2]

[1]*Center for Advanced Radiation Sources, The University of Chicago, 5640 S. Ellis Avenue, Chicago, IL 60637*

[2]*The National Synchrotron Light Source, Brookhaven National Laboratory, Upton, NY 11973*

* This work is supported by Department of Energy (DOE) - Geosciences (DE-FG02-92ER14244 to The University of Chicago - CARS) and by DOE under Contract No. DE-AC02-98CH10886.

Abstract:

Synchrotron-based X-ray fluorescence computed microtomography is a unique method for imaging major and trace element distributions within natural materials nondestructively and with high spatial resolution. The technique is particularly useful in imaging and quantifying elemental abundance in small objects that may be too precious or too difficult to section, or in the analysis of materials in which sectioning may potentially alter elemental distributions. This presentation will highlight how this technique is being applied at beamlines X26A and X27A at the National Synchrotron Light Source (Brookhaven National Laboratory) and at 13-ID at the Advanced Photon Source (Argonne National Laboratory). These instruments utilize 1-10 μm diameter focused, monochromatic X-ray beams to non-destructively measure x-ray fluorescence from a sample as it is translated and rotated within the beam. The resultant fluorescence intensities are then reconstructed as either two-dimensional cross sectional or three-dimensional elemental distribution using a fast-Fourier-transform-based computational reconstruction algorithm. Reconstruction of multi-elemental distributions at concentrations down to approximately 1 μg g^{-1} (element dependent) can be obtained. By collecting and storing full energy dispersive spectra from a multi-channel analyzer for every pixel (rather than regions of interest), it is possible to evaluate a reconstructed spectrum within the object for more robust elemental analysis. For high density matrices in particular, corrections are necessary to account for x-ray absorption by the object of both incoming X-rays and outgoing fluorescent X-rays. These effects limit the size of objects and elements that can be imaged; however reasonable corrections can be made if an estimate of linear absorption coefficient through the material is made. It is also possible to couple fluorescence tomography with microbeam x-ray absorption and diffraction analysis. When coupled to absorption spectroscopy, the fluorescence tomography analysis is conducted at multiple incident x-ray energies that preferentially target a given oxidation state of an element. This allows for three-dimensional visualization of an element's speciation. Coupled with simultaneous x-ray scattering studies utilizing a CCD area detector, individual mineral reflections can be reconstructed in three dimensions simultaneously with the x-ray fluorescence data. Examples of materials analyzed by this technique at X26A, X27A and 13-ID include interplanetary dust particles, fluid inclusions, plant materials, and heavy metals sorbed to mineral grains.

Tomographic Analysis by X-ray and Electron Microscopy of Vaccinia Virus Structure and Assembly: A.

J.L. Carrascosa[1], F.J. Chichón[1], E. Pereiro[2], M.J. Rodríguez[1],
S. Heim[3], P. Guttmann[3], G. Schneider[3]

[1] Centro Nacional de Biotecnología, CSIC, Campus Cantoblanco, 28049 Madrid, Spain
[2]ALBA Synchrotron Light Source, 08194 Bellaterra, Barcelona, Spain
[3]Helmholtz-Zentrum Berlin für Materialen und Energie GmbH, Electronenspeichrring BESSY II, 12489 Berlin, Germany

Abstract:
Vaccinia virus is one of the largest and more complex viruses, and it is assembled in infected cells following a process that involves the interaction of cellular and viral components. We have used a combination of electron and x-ray tomography to get insights into the suitability of tomographic methods to get a high resolution topological description of a complex assembly process at the cellular level.

Assembly of Vaccinia involves modification of specific cellular membranes, local disorganizations, and membrane remodeling and internalization [1], but the study of the general topology of the process has been limited by the thickness of the sections suitable for electron microscopy. To overcome this limitation we have explored the possibility to use x-ray cryo-tomography to reconstruct the whole cell volume of infected cells.

Whole infected cells were frozen without any additional fixative or contrasting reagent. Tomograms of frozen samples 6-12 µm thick were obtained in the full-field x-ray microscope at U41 in BESSY II electron storage ring (Berlin). The comparison of these tomographic reconstructions with the corresponding electron microscopy images obtained from thin sections of plastic embedded samples of the same infected cells, reveals that it is possible to detect viral factories and different cellular changes associated to the viral infection in the cryo-x-ray tomograms of infected cells.

To make a quantitative assessment of the resolution attained in cryo-x-ray tomography, we made cryo tomograms of purified vaccinia virus particles. These x-ray tomograms showed the presence of envelopes and internal components in the virus particle. The resolution was estimated using the $FSC_{e/o}$ criterion to be 25.7 nm half pitch. The corresponding cryo-electron tomograms of the same viral particles showed a value around 6.7 nm half pitch, yielding an electron/ x-ray resolution ratio of around 3.5 [2].

References:

[1] F.J. Chichon, M.J. Rodríguez, J.J. Fernández et al., Biol. Cell **101**, 401-414 (2009).
[2] J.L. Carrascosa, F.J. Chichon, M.J. Rodríguez et al., Struct. Biol. **168**, 234-239 (2009).

Use of X-ray Fluorescence Microscopy for Elemental Mapping of Samples Treated with Contrast Agents for Medical Imaging*

G. E. Woloschak[1], T. Paunesku[1], A. G. Wu[2], S. Vogt[3], S. A. Jansen[4], G. S. Karczmar[4]

[1]*Northwestern University, Chicago, IL, USA*
[2]*Ningbo University, Ningbo, Zhejiang, China*
[3]*Advanced Photon Source, Argonne National Laboratory, Argonne, IL, USA*
[4]*University of Chicago, Chicago, IL, USA*

* This work was supported by NIH grants CA107467, EB002100, P50 CA89018, U54CA119341. Use of the Advanced Photon Source was supported by the U.S. Department of Energy, Basic Energy Sciences, Office of Science, under Contract number DE-AC02-06CH11357.

Abstract:
Efficiency and toxicity of newly developed contrast agents for medical imaging requires testing in vivo and in vitro. In most cases, these agents are not accessible by optical microscopy in vitro or ex vivo, and one of the best ways to detect them directly is to map and quantify them using X-ray fluorescence imaging. Moreover, even in those cases when the nanoparticles are optically fluorescent, X-ray fluorescence provides essential and unique complementary information. Among possible contrast agents for magnetic resonance imaging are many different nanoparticle and nanocomposites formulations; these agents can be prepared to target tumors or other targets of medical interest either passively or "actively". We have shown this concept in practice with several nanocomposites and nanoconjugates. For in vitro testing we used cultured cells, for in vivo work we used a mouse model for breast and prostate cancer. With mice injected intravenously with MRI capable nanoparticles we performed several extended experiments with non-invasive MRI imaging at different timepoints. At the completion of these studies targeted and control tissues were harvested and tissue investigated by different microscopy techniques. Elements detected by X-ray fluorescence were those naturally present in cells and tissues, such as P, S, Cl, K, Ca, Mn, Cu, and Zn, while elements comprising nanocomposites included Ti, Co, Fe and Au. Accumulation of nanoparticles in tumors, targeted in these experiments, was detected as well as in several healthy control tissues.

Investigating the Subcellular 3D Structures of the Oldest Found Embryo Fossils Using Synchrotron Hard X-ray Phase Contrast Microtomography*

G. Li [1], J.-Y. Chen [2], P. Tafforeau[3], D.-C. Xian[1], E.H. Davidson[4], D.J. Bottjer[5], M.G. Hadfield[6]

[1]*Beijing Synchrotron Radiation Facility, IHEP, CAS, Beijing, China*
[2]*LPS of Nanjing Institute of Geology and Paleontology, CAS, Nanjing, China*
[3]*European Synchrotron Radiation Facility, Grenoble, France*
[4]*Division of Biology, California Institute of Technology, Pasadena, California, USA*
[5]*Department of Earth Sciences, University of Southern California, Los Angeles, California, USA*
[6]*Kewalo Marine Laboratory, University of Hawaii at Manoa, Honolulu, Hawaii, USA*

* This work was supported by National Science Foundation of China Grants 60972116 and 10675140. Synchrotron imaging was performed at ID19, ESRF (proposal ec-138 and ec-609).

Abstract:

3D preserved embryos from the Precambrian Ediacaran Doushantuo Formation, Weng'an, Guizhou, China, have attracted great attention as the oldest fossil evidence yet found for multicellular animal life on Earth. However, the potential of the Weng'an Fauna has not been fully realized because of the scarcity of the non-destructive high-resolution 3D method. We already demonstrated [1-3] that the synchrotron hard x-ray microtomography (SR-μCT) approach is the most powerful way to investigate their 3D inner subcellular structures with submicron resolution and high-density resolution (using phase contrast).

Several interesting results based on SR-μCT images will be presented, such as the discovery of lobe-forming embryos [1] and the discovery of remarkable embryos that display a complex organization similar to that found in modern bilaterian embryos [2,3]. These embryos provide further evidence for the presence of bilaterian animals in the Weng'an Fauna, indicating that the last common ancestor of the bilaterians lived much earlier than is usually thought. Several kinds of the organelles found in these embryo fossils also will be presented.

References:

[1] J-Y. Chen, D.J. Bottjer, E.H. Davidson et al., Science **312**, 1644 (2006).
[2] J-Y. Chen, D.J. Bottjer, G. Li et al., PNAS, **106**(45), 19056 (2009).
[3] J-Y. Chen, D.J. Bottjer, E.H. Davidson et al., Precambrian Res. **173**, 191 (2009).

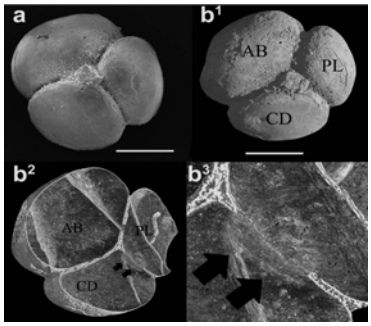

Figure 1: The narrow cytoplasmic channel between polar lobe (PL) and CD cell is revealed from SR-μCT images (Fig. 1b). It is one of the key evidences that the polar lobe embryo is already extant in the Precambrian. Scale: 250 microns.

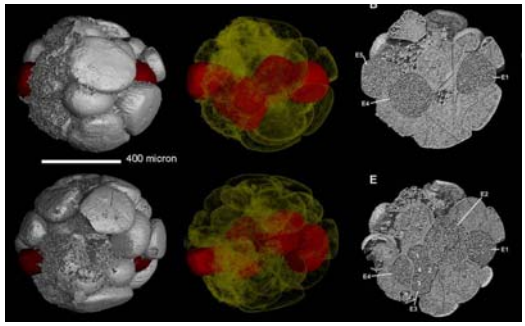

Figure 2: From SR-μCT images we can reveal the post-gastrular embryos displaying a complex bilaterian character, including: anterior-posterior, dorso-ventral, right-left polarities, cell differentiation. Scale: 400 microns.

High-Resolution Phase-Contrast Imaging of Sub-micron Particles in Unstained Lung Parenchyma*

J. C. Schittny[1], S. F. Barré[1], D. Haberthür[1], M. Semmler-Behnke[2], S. Takenaka[2], W. G. Kreyling[2], A. Tsuda[3], M. Stampanoni[4,5]

[1]*Institute of Anatomy, University of Bern, Bern, Switzerland*
[2]*Institute of Lung Biology, Helmholtz Center Munich, Munich, Germany*
[3]*Molecular and Integrative Physiological Sciences, Dept. of Environmental Health, Harvard School of Public Health, Boston, MA, USA*
[4]*Swiss Light Source, Paul Scherrer Institut, Villigen, Switzerland*
[5]*Institute for Biomedical Engineering, University and ETH Zürich, Zürich, Switzerland*

* Supported in part by NIH HL070542, HL074022 and HL054885, Swiss National Science Foundation 3100A0-109874 and 310030-125397

Abstract:

RATIONALE – In order to judge the risks and chances of the deposition of sub-micron particles in the lung parenchyma a precise three-dimensional (3D) localization of the sites of deposition is very important - especially because an inhomogeneous deposition and local hot spots of very high particle concentrations are expected in the acinar tree as well as in individual alveoli.

OBJECTIVES – The aim of this study is to combine different synchrotron radiation X-ray tomographic microscopy (SRXTM) imaging modes for the 3D localization of sub-micron particles.

METHOD – 200 nm gold particles were administered to young adult rats by intratracheal instillation. Thirty minutes after instillation the lungs were fixed by vascular perfusion and embedded in paraffin. 3D-imaging was done using high resolution SRXTM at the TOMCAT beamline [1] of the Swiss Light Source in Villigen, Switzerland.

RESULTS – We used phase contrast [2] for the imaging of unstained lung tissue and absorption contrast for the detection of 200nm gold particles. The uptake of the gold particles into the alveolar septa occurred so fast that 30 minutes after the exposure basically all of the particles were observed inside the tissue.

CONCLUSIONS – The combination of phase and absorption contrast SRXTM imaging was necessary because none of the two kinds of contrast allowed us to image both, the tissue and the gold particles. The smallest image of the particles possessed a size of 1-2 voxels of 370 nm side length. Most likely these images represent single particles, even if we were not able to distinguish unquestionably between small clusters of 1-3 particles and single particles. We would like to apply this method to study the distribution of ultrafine particles in the lung parenchyma.

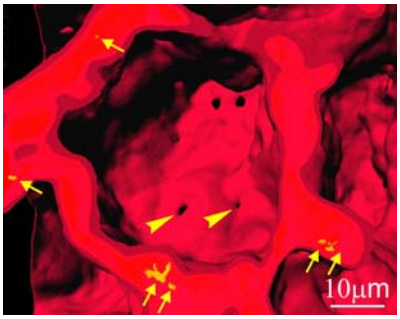

Figure 1: SRXTM 3D-image of alveolar septa containing 200 nm gold particles. The alveolar septa of one alveolus were cut in order to see the gold particles at their cut surface. Arrows, gold particles; arrow head, interalveolar pores (pores of Kohn).

References:

[1] M. Stampanoni, A. Groso, A. Isenegger et al., AIP Conf. Proc. **879**(1), 848 (2007).
[2] A. Groso, M. Stampanoni, R. Abela et al., Appl. Phys. Lett. **88**(21), 214104 (2006).

3-D Cellular Fine Structure Resolved by a Partially Coherent X-ray Microscope

J.G. McNally[1], P. Guttmann[2], W.G. Müller[1], G. Schneider[2], S. Heim[2], S. Rehbein[2], F. Mueller[1], K. Nagashima[1], J.B. Heymann[3]

[1]*Laboratory of Receptor Biology and Gene Expression, National Cancer Institute, National Institutes of Health, 41 Library Drive, Bethesda MD USA 20892*

[2]*Helmholtz-Zentrum Berlin fur Materialien und Energie GmbH, Elektronenspeicherring BESSY II, Albert-Einstein-Str. 15 12489 Berlin, Germany*

[3]*Laboratory of Structural Biology, National Institute of Arthritis, Musculoskeletal and Skin Diseases, National Institutes of Health, 50 South Drive, Bethesda, MD USA 20892*

Abstract:

We have built a novel x-ray microscope to image adherent mammalian cells in 3-D. The microscope uses partially-coherent object illumination instead of the quasi-incoherent illumination used in earlier setups. For partially coherent imaging, the x-ray source produces a more collimated photon beam which contains ~100x more coherent light than previously achieved. An increase in coherence is also obtained because the coherent beam diameter is now a substantial fraction of the condenser diameter. Finally, the numerical aperture of the objective is more than twice that of the condenser, enabling simultaneous capture of more positive and negative diffractive orders of the object. This partially-coherent design has significant advantages, as theory predicts it should achieve markedly better contrast at higher spatial frequencies, enabling detection of many more ultrastructural cell details.

An added advantage of the design is that space is available to insert a commercial tilt stage enabling x-ray tomography of adherent mammalian cells. The extra space arises because the optical design does not require a pinhole in front of the specimen to obtain monochromaticity. Instead we use a beamline with a focusing spherical grating monochromator. The monochromatic light produced is collected by an elliptically shaped single bounce glass capillary which serves as the condenser.

We have used this x-ray microscope to image mouse adenocarcinoma cells. The partially-coherent x-ray images of these cells show many of the features visible by conventional transmission electron-microscopy (TEM) of thin sections of the same cell type. By either modality, mitochondria, lysosomes, ER and vesicles predominated in the cytoplasm, while the nuclei contained prominent nucleoli but lacked heterochromatin, even at the nuclear periphery. Very few Golgi structures are present in these cells as detected by either TEM or x-ray microscopy. Measurement of the 3-D distribution of cytoplasmic organelles revealed a packing density close to theoretical limits, providing direct demonstration of cytoplasmic crowding. Strikingly, the x-ray images frequently revealed nuclear channels that partially traversed the nuclear interior, even though comparable channels were not detected by TEM. Similar nuclear channels have been reported in interphase nuclei of many cell types, but they are rarely detected by TEM presumably because the channels usually intersect the section plane at glancing angles. Such tubular structures are ideally detected and tracked by a 3-D modality like partially coherent x-ray microscopy.

Cryo Transmission X-ray Imaging of the Malaria Parasite *P. falciparum* *

K. Nugent[1,4], E. Hanssen[1,2], C. Knoechel[3], S. Deed[1,2], T. Abu-Bakar[1,2], M. LeGros[3], C. Larabell[3], L. Tilley[1,2]

[1]*ARC Centre of Excellence for Coherent X-ray Science*
[2]*La Trobe Institute for Molecular Science, La Trobe University, Melbourne 3086, VIC, Australia*
[3]*National Center for X-ray Tomography, Lawrence Berkeley Laboratory, Berkeley, CA 94720, USA*
[4]*School of Physics, The University of Melbourne, Vic., 3010, Australia*

*This work was funded by the the Australian Research Council through its Centre of Excellence program and the NIH National Center for Research Resources Grant RR019664 and the Department of Energy Office of Biological and Environmental Research Grant DE-AC02-05CH11231

Abstract:

During its intra-erythrocytic development, the human malaria parasite, *Plasmodium falciparum*, develops it digests its host cell from the inside, consuming ~75% of the host hemoglobin. This process is of interest as it targeted by antimalarial drugs however there is currently some debate regarding the mechanisms involved in the endocytic process.

An X-ray microscope (XM-2) capable of performing cryo-tomography on thick samples (several microns) at high resolution (~50 nm) has been developed at the Advanced Light Source, Lawrence Berkeley National Laboratory, CA, USA. Cryo transmission x-ray microscopy in the “water window” of photon energies exploits the natural contrast of biological samples. Due to the shorter wavelength of x-rays this technique can achieve higher resolution than optical microscopy and can be performed on whole hydrated cells. The cryo-sample handling limits x-ray damage during imaging and the tomographic capability of XM2 and the improved optics, permits good image quality with a correspondingly high information content.

We have used tomographic x-ray imaging of different stages of growth of the intraerythrocytic malaria parasite, *Plasmodium falciparum,* to examine the cellular architecture of this important human pathogen. The cells are unstained and the contrast relies on the natural differences in absorption arising from different chemical composition of different regions of the cell. The host cell membrane, the parasite surface and the nucleus and rhoptries are readily identified. The digestive vacuole (DV), with accumulated hemozoin crystals, is also readily distinguished. We also observed large invaginations of the parasite surface that appear to be involved in haemoglobin uptake. These are of particular interest as they have not been observed previously in hydrated cells. The data provide insights into the mechanism of uptake of hemoglobin. Quantitative analysis of changes in the density of material in the parasite cytoplasm during intraerythrocytic development reveals a previously unrecognized change in ribosome packing density. We have used immunospecific labelling with gold/silver aggregates to confirm the identity of compartments in the host cell cytoplasm.

Cryogenic X-ray Diffraction Microscopy for Biological Samples

E. Lima[1], L. Wiegart[1], P. Pernot[2], M. Howells[2], J. Timmins[2], F. Zontone[2], A. Madsen[2]

[1]*Brookhaven National Laboratory, Upton, New York 11973 USA*
[2]*European Synchrotron Radiation Facility, B.P. 220, F-38043 Grenoble, France*

Abstract:

Imaging of biological material, such as a whole cell, in three dimensions (3D) will deepen our understanding of cellular biology [1]. As we look into cellular organization with high-resolution towards 10 nanometers or below, we begin to see how sub-cellular organelles and macromolecules mutually interact, thus explicating cellular functions. However, as we push the resolution in biological imaging, the challenge becomes how do we preserve samples close to their natural state, especially with thick samples that are not easily accessible by electron microscopy without sectioning them into thin slices.

X-ray diffraction microscopy (XDM) utilizes the high penetration power of x-rays to probe thick samples, avoiding needless sample preparation such as plastic embedding and sectioning. It uses a computational algorithm to reach high resolution by phasing a diffraction pattern to a real space image. Thus, it bypasses many hurdles in optics-based imaging such as short depth-of-field and the resolution set by optics. However, XDM is an indirect imaging method that requires high-quality diffraction data to reach a solution. Its previous low success rate with biological samples, especially in the frozen-hydrated state, reflected this problem. However, two groups have recently shown the feasibility of frozen-hydrated imaging using soft and hard x-rays at resolutions reaching 25 nm and 30 nm respectively [2,3]. This paper will present this recent development in cryogenic (cryo-) XDM with hard x-rays. We have developed non-vacuum cryo-XDM using x-rays at 8 keV with a cryogenic gas-jet environment and imaged a frozen-hydrated bacterium *D. radiodurans* in natural contrast with a resolution of 30 nm to 50 nm. The recent upgrade of the end station allows 3D data collection in semi-automatic mode to minimize sample degradation during data collection. These developments in cryo-XDM toward high-resolution 3D imaging can provide a method to probe whole-cell architecture in a spatio-temporal investigation of cellular processes.

References:

[1] A. Leis, B. Rockel, L. Andrees et al., Trends. Biochem. Sci. **34**, 60 (2009).
[2] X. Huang et al., Phys. Rev. Lett. **103**, 198101 (2009).
[3] E. Lima et al., Phys. Rev. Lett. **103**, 198102 (2009).

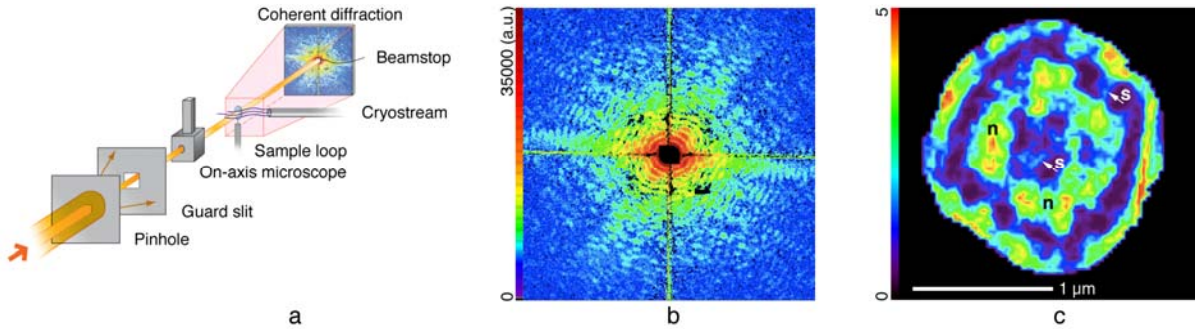

Figure 1: Cryo-XDM with hard x-rays. (a) experimental setup (b) diffraction pattern from a frozen-hydrated *D. radiodurans* (c) reconstructed image denoting "n" for nucleoid regions and "s" for septa.

Application of XRM to Human Disease and Therapies*

P. A. Lay[1], J. B. Aitken,[1] H. H. Harris,[1,2] A. Levina,[1] Z. J. Lim,[1] M. Liu,[1] A. I. McLeod,[1] S. Tarr,[1]
L. E. Wu,[1] S. V. Kunnamkumarath,[2] C. J. Glover,[3] M. D. de Jonge,[3] B. Johannessen,[3]
D. J. Paterson,[3] L. Finney,[4] B. Lai,[4] S. Vogt[4]

[1]School of Chemistry, The University of Sydney, NSW, 2006, Australia
[2]School of Chemistry and Physics, The University of Adelaide, SA 5005, Australia
[3]Australian Synchrotron, 800 Blackburn Rd, Clayton, VIC 3168, Australia
[4]X-ray Science and Biosciences Divisions, Advanced Argonne National Laboratory, 9700 S Cass Ave, Argonne, IL 60349, USA

* We are grateful for support from the Australian Research Council (ARC) for Discovery Grants, Australian Professorial Fellowships to PAL and a QEII Fellowship to HHH and to the Australian Synchrotron and Australian Synchrotron Research Program for travel grants. This work was also supported by the DOE Office of Science under contract DE-AC02-06CH11357

Abstract:

The combined use of X-ray microprobe techniques: synchrotron-radiation-induced X-ray emission (SRIXE); differential-phase contrast; and micro-X-ray absorption near-edge structure (μ-XANES) spectroscopy, with other microspectroscopies, enables enhanced insights into disease processes and their potential treatment [1]. With respect to studies with individual mammalian cells, the cells can be grown and differentiated directly on a silicon nitride substrate in order to perform studies on the cell in its normal morphology [2]. SRIXE and μ-XANES spectroscopy can also be conducted on protein gels in order to speciate the biotransformations of pro-drugs and toxins in blood and cell lysates [3].

Examples will be discussed on the effects of chromium and vanadium anti-diabetic prodrugs on adipocytes (fat cells) and their speciation in blood and cells and also on ruthenium anti-cancer prodrugs. In particular, maps of protein gels will be used to understand the speciation of the metal that is delivered by the prodrug in blood and, in the case of the anti-diabetic drugs, the biodistributions and biotransformations in target cells. The use of the information gained from these techniques, combined with other biospectroscopies and biological assays, will be discussed in terms of understanding the mechanisms that lead to both efficacy and to potential toxicities. Such an understanding can lead to more rapid and targeted design of new drugs, as well as assisting in the development of existing drugs [4].

References:

[1] J.B. Aitken, E.A. Carter, H. Eastgate et al., Radiat. Phys. Chem. **90**, 176(2010).
[2] E.A. Carter, B.S. Rayner, A.I. McLeod, L.E. Wu, C.P. Marshall, A. Levina, J.B. Aitken, P.K. Witting, B. Lai, Z. Cai, S. Vogt, Y.-C. Lee, C.-I. Chen, M.J. Tobin, H.H. Harris, P.A. Lay (accepted to Mol. Biosyst.)
[3] L. Finney, Y. Chishti, T. Khare, C. Giometti, A. Levina, P.A. Lay, S. Vogt, (accepted to ACS Chem. Biol.)
[4] J. B. Aitken, A. Levina, P. A. Lay (accepted to Curr. Topics Med. Chem).

Subcellular X-ray Fluorescence Imaging as a Tool to Better Understand Metal-Induced Pathologies

M. Ralle[1], S. Vogt[2], B. Lai[2], A. Capps[1], J. Burkhead[3], R. Woltjer[1], C. Harris[1], T. Wadsworth[1], J. Quinn[1], S. Lutsenko[4]

[1]*Oregon Health & Science University, 3181 SW Sam Jackson Park Rd, Portland OR, USA*
[2]*Advanced Photon Source, Argonne National Laboratory, 9700 S Cass Ave, Argonne, IL, USA*
[3]*University of Alaska, Anchorage, 3211 Providence Dr., Anchorage AK, USA*
[4]*Johns Hopkins University, 725 N. Wolfe Street 203 Hunterian, Baltimore, MD 21205, USA*

Abstract:
Mechanisms of human pathologies that are caused by or associated with metal misbalances remain poorly understood. This is in part due to the inherent difficulties of analyzing metal distributions and concentrations in biological tissue. We have optimized an X-ray imaging technique, synchrotron-based X-ray fluorescence (SXRF), to be used with biological tissue material to better understand the role of metals in these diseases. Here, we are showing how SXRF in combination with other biochemical techniques was utilized to better understand the multifaceted role of copper in Wilson disease (WD). We will furthermore present how SXRF can be used to elucidate a possible involvement of copper in Alzheimer's disease (AD).

Specifically, we have found that copper is markedly increased in hepatic nuclei (7.2 mM) early in WD, suggesting that it regulates remodeling of the liver transcriptome observed in WD, while Atox1 or metallothionein are not elevated in the nucleus. Further pathology development is associated with copper re-distribution between nuclei, cytosol, and concentrated (>25 mM) deposits, rather than a simple copper elevation. Analysis of individual cells revealed that copper accumulation in hepatocytes has an apparent limit of 90-300 femtomoles. The lack of further accumulation is associated with the loss of the copper transporter Ctr1 from the plasma membrane and the appearance of extracellular copper deposits and copper-loaded lymphocytes.

Mounting evidence also suggests a pivotal role of altered metal metabolism in AD and utilized SXRF to determine copper concentrations and distributions in brains of control and Tg2576 mice, a commonly used mouse model for AD. Our current results suggest that the copper levels in different areas of the brains are not uniformly altered. Localized differences in copper concentrations were found in a limited number of scans. We furthermore imaged ex-vivo human tissue from diseased AD patients and will present those results.

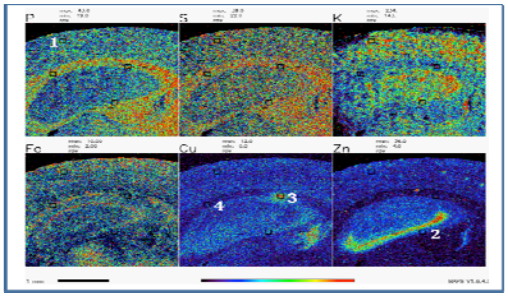

Figure 1: 3 x 3 mm overview scan of the hippocampus in a symptomatic Tg2576 mouse brain section. High resolution scans (marked 1 -4) were subsequently taken and the elemental concentrations determined.

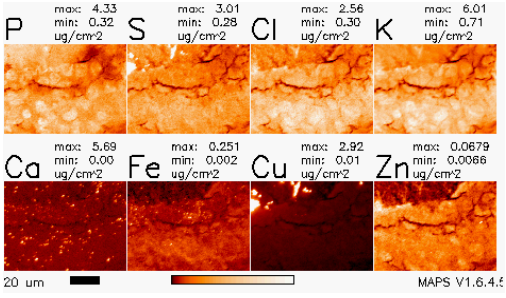

Figure 2: 2-D elemental maps around at the lateral ventricle in a control mouse brain. Copper is highly elevated in the ependymal cell layer around the lateral ventricle. Copper concentration of ~300mM were observed.

Visualizing a Role for Zinc in Stem Cell Differentiation through X-ray Fluorescence Mapping

L. Finney[1], J. Wolford[1], Y. Chishti[1], J. Ward[2], Q. Jin[1], L. Chen[1], S. Vogt[2]

[1]*Biosciences Division, Argonne National Laboratory, 9700 S. Cass Ave, Argonne, IL USA*
[2]*X-ray Science Division, Advanced Photon Source, Argonne National Laboratory, Argonne, IL USA*

Abstract:
Human embryonic stem cells (hESC) are pluripotent, or able to differentiate into any cell type in the body. Mastering their directed differentiation promises to vastly reduce the costs of many diseases to society. But, the factors controlling differentiation are not well understood.

Through mapping the distribution of elements in hESCs at high resolution, using hard x-ray microscopy at 2-ID-E of the Advanced Photon Source, we find evidence that the loss of pluripotency is directly correlated with an increase in nuclear zinc.

Zinc elevation not only redefines our understanding of the mechanisms that support pluripotency, but also may act as a biomarker and an intervention point for stem cell differentiation. The development of complementary x-ray fluorescence techniques may further aid in identifying the molecular partners of zinc during differentiation.

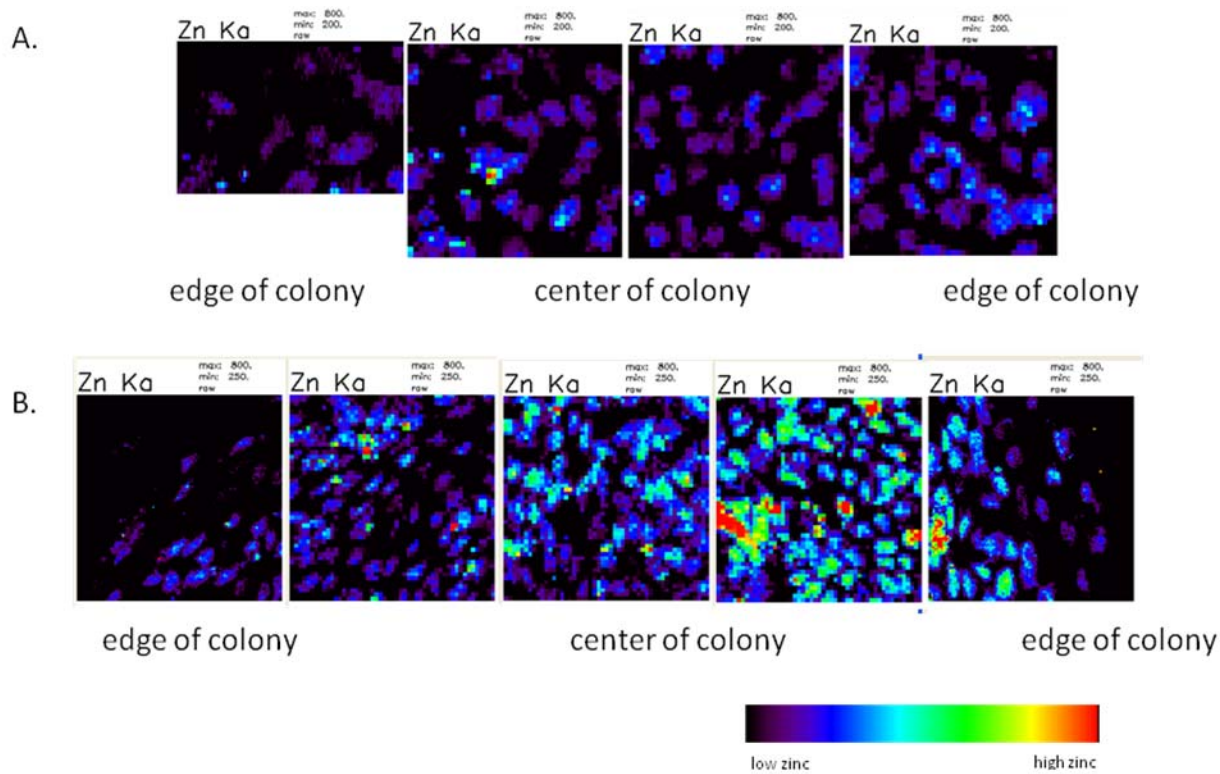

Figure 1: Images of zinc in the cells of stem cell colonies. In panel A, a series of images are taken across a control colony of pluripotent stem cells. In panel B, a similar series of images display the cellular zinc contained in cells of a stem cell colony that has been induced to differentiate. Zinc levels remain constant across a section of a control colony (A), but increase at the middle of a differentiating colony (B).

In situ Nanoscale Chemical Imaging of Catalysts

E. de Smit, M.M. van Schooneveld, L.R. Aramburo, B.M. Weckhuysen, F.M.F. de Groot

Inorganic Chemistry and Catalysis, Debye Institute for Nanomaterials Research, Utrecht University, Sorbonnelaan 16, 3584 CA, Utrecht, The Netherlands

Abstract:

Microscopy is a widely applied tool in the characterization of heterogeneous catalysts. From infrared light to electron beams, the full wavelength spectrum is utilized to image catalytic materials on different microscopic scales. Modern microscopes often integrate spectroscopy with imaging techniques to simultaneously obtain morphological and quantitative chemical information from the sample (e.g., Scanning Transmission Electron Microscopy – Electron Energy Loss Spectroscopy (STEM-EELS), Infrared Microscopy and Fluorescence Microscopy). In order to get a better fundamental understanding of the active sites responsible for catalytic activity, there is a continuous drive to increasing the spatial resolution of microscopes while maximizing the chemical information content under relevant (i.e., *in situ/operando*) conditions.

Recently, we have illustrated the potential of Scanning Transmission X-ray Microscopy (STXM) as a high resolution/high chemical speciation probe under catalytic reaction conditions [1,2]. The main experimental challenge to overcome when studying catalysts *in situ*, is the strong attenuation of soft X-rays in gaseous atmospheres, making it difficult to apply typical catalytic reaction conditions (~1-20 bar, 200-500^{o}C). In addition, the design of any type of *in situ* reactor in STXM is restricted by the typical small distances between the sample plane and order sorting aperture of the X-ray Microscope.

Here, we illustrate the use of a specially designed nanoreactor to overcome these challenges and focus on two examples where we have applied *in situ* STXM to study the distribution and chemical identity of catalyst species in an iron based Fischer-Tropsch Synthesis (FTS) catalyst [1,3] and a Cu/ZnO methanol synthesis catalyst.

References:

[1] E. de Smit, I. Swart, J.F. Creemer et al., Nature **456**, 222 (2008).
[2] F.M.F. de Groot, E. de Smit, M.M. van Schooneveld et al., Chem. Phys. Chem. **11**, 951 (2010).
[3] E. de Smit, I. Swart, J.F. Creemer et al., Angew. Chem. Int. Ed. **48**, 3632 (2009).

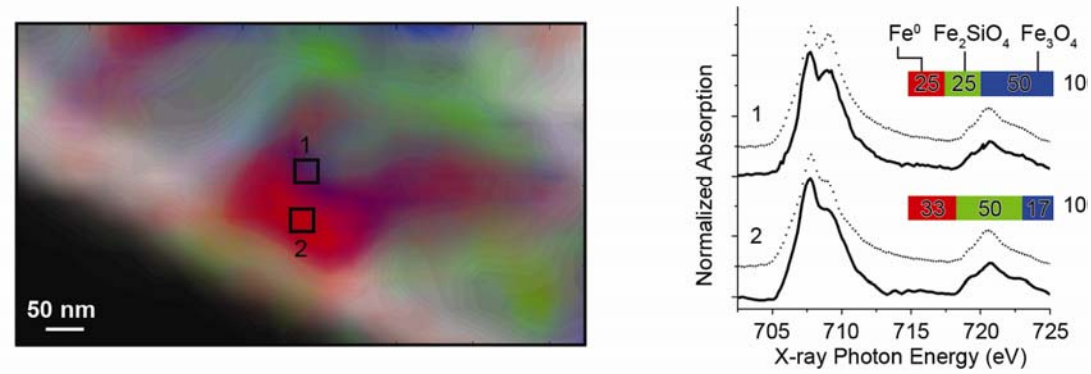

Figure 1: Spatial distribution map of iron species over the SiO_2 support (white) and Fe $L_{2,3}$-edge XAS spectra of a $Fe_2O_3/CuO/K_2O/SiO_2$ catalyst after reduction in H_2 at 350^{o}C for 2 h.

Elemental Mapping and Analysis of Solid Oxide Fuel Cells by Transmission X-ray Microscopy

W.K.S. Chiu[1†], K.N. Grew[1], Y.S. Chu[3], J. Yi[2], J.R. Izzo, Jr.[1],
A.A. Peracchio[1], Y. Hwu[4], F. De Carlo[2]

[1]*Department of Mechanical Engineering, University of Connecticut, Storrs, CT 06269-3139*
[2]*Advanced Photon Source, Argonne National Laboratory, Argonne, IL 60439*
[3]*National Synchrotron Light Source II, Brookhaven National Laboratory, NY, 11973*
[4]*Institute of Physics, Academia Sinica, Taipei 115, Taiwan*
[†]*E-mail: wchiu@engr.uconn.edu*

This work is supported by an Energy Frontier Research Center on Science Based Nano-Structure Design and Synthesis of Heterogeneous Functional Materials for Energy Systems (HeteroFoaM Center) funded by the U.S. Department of Energy, Office of Science, Office of Basic Energy Sciences (Award DE-SC000106).

Abstract:

There is a critical need to understand the role of a solid oxide fuel cell's (SOFC's) structure, morphology, and composition on system performance [1]. We present a non-destructive approach to image and characterize SOFCs using a transmission x-ray microscope at the Advanced Photon Source 32-ID-C [2]. Taking advantage of elemental sensitivity of synchrotron x-rays, three-dimensional structures within the sample volume are tomographically reconstructed with unprecedented contrast. Statistically meaningful descriptions of 3D pore structures are obtained using segmentation analysis. Multicomponent lattice Boltzmann methods are used to analyze mass transfer, heat transfer, ionic/electronic charge transfer, and chemical/electrochemical reaction rates [3]. Chemical elements, chemical bonding, and phase- and pore-network structures in a solid oxide fuel cell are examined to provide fundamental insight into the origins of transport-related losses during operation.

References:

[1] J.R. Izzo, Jr., A.S. Joshi, A.A. Peracchio et al., J. Electrochem. Soc.**155**, B504 (2008).
[2] K.N. Grew, Y.S. Chu, J. Yi et al., accepted to J. Electrochem. Soc. (2010).
[3] K.N. Grew, A.S. Joshi, A.A. Peracchio et al., J. Power Sources **195**, 2331 (2010).

Time-Dependent Dealloying and Coarsening Studies of Nanoporous Gold Using Transmission X-ray Microscopy

Y. K. Chen[1, 2], S. Wang[2], J. Yi[2], W. Lee[2], P. W. Voorhees[1], I. McNulty[2], D. C .Dunand[1]

[1]*Department of Materials Science and Engineering, Northwestern University, Evanston, Illinois, USA*

[2] *Advanced Photon Source, Argonne National Laboratory, Argonne, Illinois, USA*

Abstract:

Nanoporous gold, with its large specific area and bio-compatibility, has attracted a great deal of attention for its numerous potential applications in catalysis, sensing, and medicine [1]. Nanoporous gold can be created by a dealloying method, in which the silver from a silver-gold alloy is dissolved in nitric acid. The resulting sponge-like nanoporous gold consists of a network of gold ligaments that are 5-20 nm in size [2]. The mechanical properties of the bulk material can be varied by structural coarsening of the ligament and pore size through heat treatment [3].

To better understand the structural evolution and mechanisms governing the dealloying and coarsening behaviors of nanoporous gold, we studied samples during the dealloying process and after a series of heat treatments at various temperatures by high resolution x-ray microscopy using the transmission x-ray microscope at the Advanced Photon Source [4]. This instrument provides the capability to image thick (>20 μm) samples at high (<40 nm) resolution within the reaction environment in real time. The structural evolution of this material as a function of time, during both dealloying and coarsening, will be discussed.

References:

[1] Y. Ding and M. Chen, MRS Bull. **34**, 8 (2009).
[2] J. Erlebacher, M. J. Aziz, A. Karma et al., Nature **410**, 450 (2001).
[3] A.M. Hodge, J. Biener, J.R. Hayes et al., Acta Materialia **55**, 1343 (2007).
[4] Y.K. Chen, Y.S. Chu, J. Yi et al., Appl. Phys. Lett. **96**, 043122 (2010).

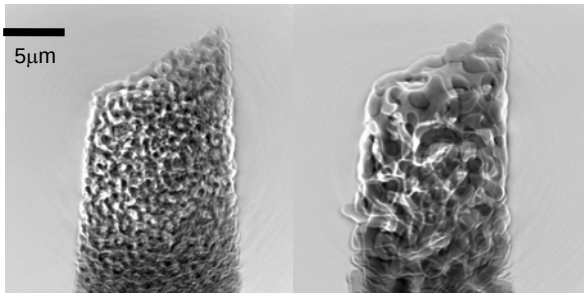

Figure 1: TXM radiographs showing the structural coarsening of nanoporous gold at 650°C after 5 min (left) and 160 min (right).

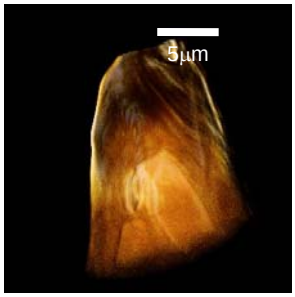

Figure 2: A 3D reconstruction of a nanoporous gold sample in its early dealloying stage (90 sec. dealloying in nitric acid). A sharp dealloying front between the nanoporous gold and the alloy is visible.

Coherent X-ray Diffraction Imaging of Strain on the Nanoscale

R. Harder[1], M. Newton[3], L. Beitra[2], S.J. Leake[4], I.K. Robinson[2]

[1]*Argonne National Laboratory, 9700 S Cass Ave, Argonne, IL, USA*
[2]*University College London, London, UK*
[3]*Surrey University, Surrey, UK*
[4]*Paul Scherrer Institut, Villigen, Switzerland*

Abstract:

In nanoscience, the bulk concepts of lattices and crystal defects must be reconsidered in order to explain why nanomaterials have new and exciting properties. To study these properties, we have developed the method of coherent x-ray diffraction (CXD) imaging to obtain quantitative three-dimensional maps of the deformation of a crystal from its equilibrium lattice spacing. By measuring the coherently scattered photons in the vicinity of Bragg peaks of the samples, and computationally inverting the intensities to an image, we gain this powerful capability.

Very recently we have developed instrumentation and methods that allow us to image, in three dimensions, the total lattice deformation field of micron- and sub-micron-size crystals with high spatial resolution. Using this data, the entire strain tensor of the sample can be determined in three dimensions.

The technique of coherent x-ray diffraction imaging in the Bragg geometry will be explained and recent results from micron size zinc oxide crystals and sub-micron gold crystals will be discussed.

References:

[1] M.C. Newton, S.J. Leake, R. Harder et al., Nature Materials **9**(2), 120 (2010).

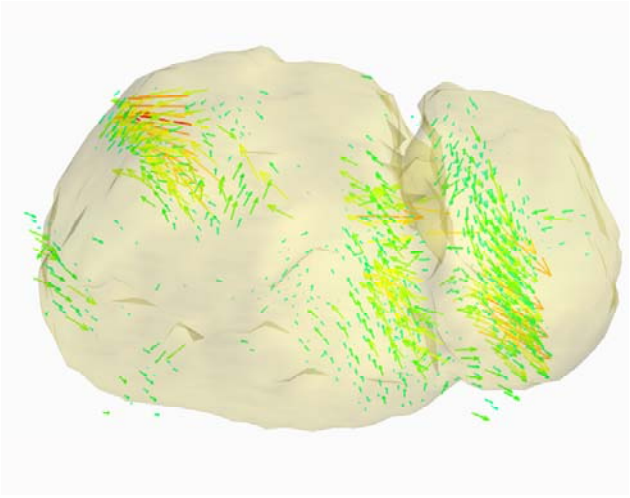

Figure 1: An isosurface shown in the amplitude of the density of a 200-nm gold crystal measured with CXD. The vector field (colored arrows) shows the distortion of the lattice from ideal crystallographic positions.

Submicron-Resolution Three-Dimensional Polychromatic X-ray Microdiffraction*

J.Z. Tischler[1], G.E. Ice[1,2], B.C. Larson[1], J.D. Budai[1], W. Liu[2]

[1]*Oak Ridge National Laboratory, Oak Ridge, TN, USA*
[2]*Argonne National Laboratory, Argonne, IL, USA*

*Research sponsored by the Division of Materials Sciences and Engineering, Office of Basic Energy Sciences, U.S. Department of Energy; the Advanced Photon Source is supported by the Facilities Division of the U.S. DOE.

Abstract:
Submicron resolution polychromatic microbeams provide the capability to investigate a wide range of microstructure and evolution problems in two-dimensional single- and poly-crystalline samples. With the inclusion of submicron depth resolution, three-dimensional mesoscale materials science and condensed matter physics issues involving the local crystal structure, orientation, grain morphology, elastic strain, and plastic deformation can be examined. We will present a brief description of our technique for performing submicron-resolution 3D microdiffraction as implemented on sector 34 at the Advanced Photon Source (APS), followed by some specific illustrations of our work. Examples will include polychromatic microbeam measurements of thermal grain growth in polycrystalline aluminum and investigations of local plastic deformation under spherical-indentations in single crystal copper.

Imaging and Structural Analysis of Ferroelectric Domains Written by Piezoresponse Force Microscopy*

P. Chen[1], R.T. Smith[1], R.J. Sichel[1], J.Y. Jo[1], C.-B. Eom[1], M.V. Holt[2], N. Balke[3], S.V. Kalinin[3], P.G. Evans[1]

[1]*University of Wisconsin-Madison, Madison, Wisconsin USA*
[2]*Center for Nanoscale Materials, Argonne National Laboratory, Argonne, Illinois USA*
[3]*Oak Ridge National Laboratory, Oak Ridge, Tennessee USA*

* Supported by the U. S. Department of Energy, Office of Science through contract DE-FG02-04ER46147, and by the U. S. National Science Foundation contract DMR-0705370. Use of the Center for Nanoscale Materials was supported by the U. S. Department of Energy, Office of Science, Office of Basic Energy Sciences, under contract No. DE-AC02-06CH11357.

Abstract:

Piezoresponse Force Microscopy (PFM) is widely used to image the nanoscale local piezoelectric distortion of ferroelectric materials, and to modify the local domain population by applying a large voltage to the scanned tip. These processes are the defining tools of nanoscale domain dynamics in ferroelectrics, but have to date lacked structural precision.[1] Here we complement PFM with x-ray nanobeam analysis, which provides the structural sensitivity to study the structural and mechanical phenomena associated with PFM.

Domain patterns written by PFM in an 80 nm thin film of the ferroelectric $PbZr_{0.45}Ti_{0.55}O_3$ (PZT) were imaged by x-ray nanodiffraction. The intensity of diffraction from domains with opposite polarization differs by 25% [2], allowing us to image the domain pattern (Figure 1). Contrast in the x-ray nanodiffraction images, however, arises from both domains and purely structural effects. Detailed structural information can be deduced from the diffraction patterns acquired at different positions across the domains (Figure 2a). Fringes in the domain pattern carry the imprint of the nanoscale domain pattern (Figure 2b), as observed previously with large beams.[3]

References:

[1] S. V. Kalinin and D. A. Bonnell, Phys. Rev. B **65**, 125408 (2002).
[2] D. H. Do, P. G. Evans, E. D. Isaacs et al., Nature Mater. **3**, 365 (2004).
[3] C. Thompson, A. Munkholm, S. K. Streiffer et al., Appl. Phys. Lett. **78**, 3511 (2001).

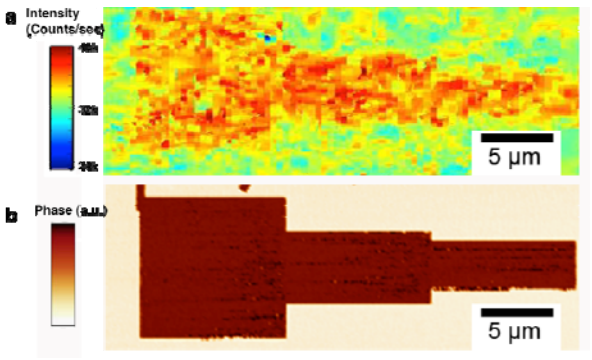

Figure 1: (a) PZT domain image using the intensity of (002) Bragg reflection. (b) PZT domain image using the out of plane phase PFM signals.

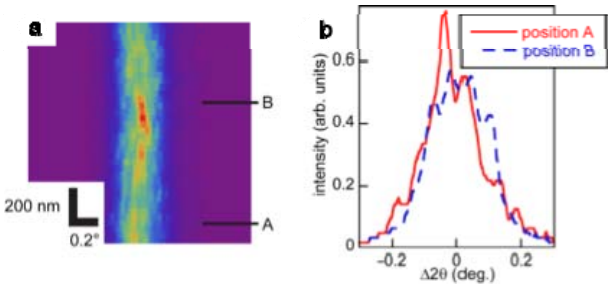

Figure 2: (a) PZT (002) Bragg reflection as a function of 2ϑ (horizontal axis) acquired at positions across a domain wall (vertical axis). (b) Intensity vs. 2θ at position A and B.

Poster Presentation Abstracts

Tuesday, August 17

Session:	Poster #:
Facilities, Instruments, & Optics	Tues-P001 – Tues-P093
Emerging Fields	Tues-P094 – Tues-P097
Magnetism & Magnetic Materials	Tues-P098 – Tues-P103
Environmental, Earth, & Space Sciences	Tues-P104 – Tues-P111

A High-Efficiency Dynamically Figured KB System for High-Energy Nanofocusing at the ESRF*

R. Barrett, R. Baker, P. Cloetens, Y. Dabin, C. Morawe, A. Rommeveaux, L. Zhang

European Synchrotron Radiation Facility, BP220, 38043 Grenoble Cedex 09, France

* The research leading to these results has received funding from the European Community's Seventh Framework Programme (FP7/2007-2013) under grant agreement nº 226716.

Abstract:

We describe an in-house designed Kirkpatrick-Baez mirror system for high-throughput nanofocusing down to 50 nm beam sizes at the ID22-NI end station. In order to maximize the system aperture, multilayer coated optics are used in conjunction with two dynamically figured mirror benders. This approach, which has been developed at the ESRF for many years, allows the focusing performance to be optimized when operating the system in the 13–25 keV photon energy range [1]. This latest system has driven many aspects of our dynamical bending approach to their currently feasible limits.

We will discuss the key technologies that are required for the production of mirror bending systems with dynamic figuring behavior close to the theoretical performance. These include system optimization via finite element analysis (FEA) modelling of the mechanical behavior of the bender-mirror combination [2], manufacturing techniques for precisely shaped multilayer substrates, multilayer deposition with steep lateral gradients, and stitching metrology techniques developed for the characterization and figure optimization of the strongly aspherical surfaces. We will subsequently describe how the mirror benders (Figure 1) have been integrated into a compact and stable assembly (Figure 2) designed for routine beamline operation, and finally we will report upon the initial performance of the system.

References:

[1] O. Hignette, P. Cloetens, C. Morawe et al., AIP Conf. Proc. **879**, 792 (2007).

[2] L. Zhang, R. Baker, R. Barrett et al., to appear in Synchrotron Radiation Instrumentation: Tenth International Conference, AIP Conference Proceedings.

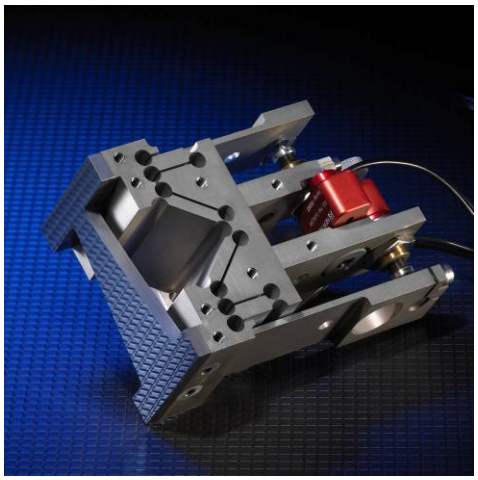

Figure 1: ESRF monolithic dynamic X-ray mirror bender for nanofocusing applications.

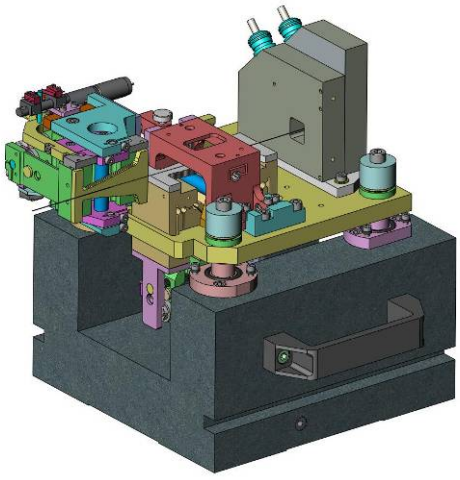

Figure 2: ESRF ID22NI integrated KB assembly.

Gas Discharge Source and Collector Module for Soft X-ray Microscopy in the Water Window Spectral Range*

M. Benk[1], K. Bergmann[1], D. Schaefer[2], T. Wilhein[2]

[1]*Fraunhofer Institute for Laser Technology, Aachen, Germany*
[2]*Institute for X-Optics (IXO), RheinAhrCampus, Remagen, Germany*

* This work is supported by the German Federal Ministry of Education and Research under contract 13N8914.

Abstract:

Laboratory based soft x-ray microscopy is a strongly advancing field [1]. Activities aim at bringing the performance of synchrotron based systems into a compact commercial microscope. Fraunhofer ILT has developed a source collector module for the water window spectral range, based on a hollow cathode triggered pinch plasma source [2].

At this stage work is focused on characterization, advance and integration of the setup. The current status of the module is presented. Spectral bandwidth of the 2.88 nm nitrogen emission line is measured applying an off-axis reflection zone plate. Influence of the specific spectral properties of the source to image formation is discussed.

Condenser optics are designed and geometries are reviewed by means of ray tracing. Photon flux, angular distribution and spot size of different condenser optics are investigated. At present a grazing incidence condenser with a numerical aperture matched to the imaging optics is being machined. The optics is designed to deliver a photon flux of 1×10^7 photons / (μm^2 s) for the 2.88 nm emission in the present state of the gas discharge source. The source size enables homogeneous illumination of the object plane with this condenser.

Microscopic imaging of test samples and biological specimen is performed with a microscope demonstrator to investigate overall performance of the module.

References:

[1] M. Bertilson, O. von Hofsten, U. Vogt et al., Opt. Express **17**(13), 1157 (2009).
[2] M. Benk, K. Bergmann, D. Schäfer et al., Opt. Express **33**(20), 2359 (2008).

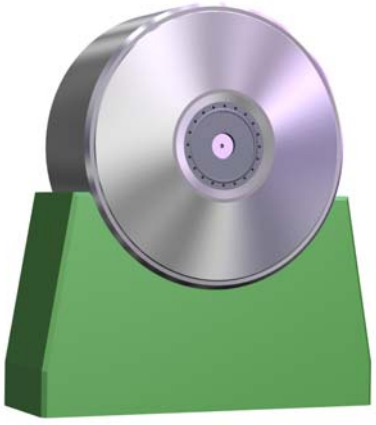

Figure 1: Next generation source head design.

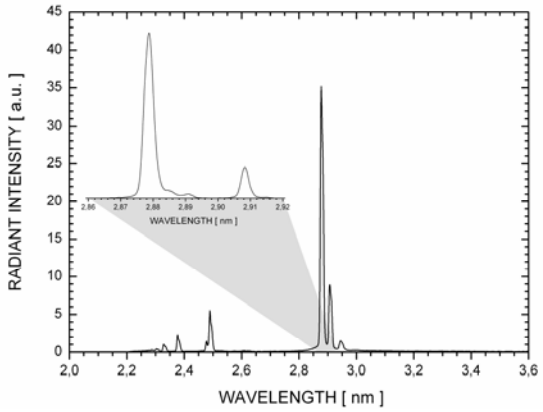

Figure 2: Emission spectrum exhibiting a spectral linewidth $\lambda/\Delta\lambda$=840.

Preliminary Results of a Combined Laboratory Micro-CT and XRF System

M.N. Boone[1], M.A. Boone[2], J. Dewanckele[2], D. Van Loo[1], M. Dierick[1], V. Cnudde[2], L. Van Hoorebeke[1]

[1]UGCT, Dept. Physics and Astronomy, Ghent University, Proeftuinstraat 86, 9000 Ghent, Belgium
[2] UGCT, Dept. Geology and Soil Science, Ghent University, Krijgslaan 281 – S8, 9000 Ghent, Belgium

Abstract:
In recent years, X-ray micro-tomography (µCT) has become an established tool for 3D microscopy, with many applications in various fields such as geology, pharmacy, biology and many others. The technique allows researchers to visualize their sample non-destructively in 3D. The non-destructive character of µCT makes it an ideal tool for visualization and analysis of precious and rare objects, or to study the same sample under different circumstances.

The resulting images show the linear attenuation coefficient in each voxel. This coefficient is influenced by both the atomic composition and density of the material in that voxel. However, due to this combined influence, no exact information on the atomic composition of the sample can be derived from the µCT data.

To overcome this problem, a combination of different techniques can be used. µCT has been combined with synchrotron X-ray fluorescence (XRF) in multiple studies, amongst others to characterize a sandstone crust [1] and to study tissue-specific metal distributions in a *Daphnia Magna* [2]. XRF in laboratory has also been combined with µCT, amongst others to identify the different phases in an igneous rock sample in 3D [3]

The disadvantage of this combination is that it requires two different measurement techniques, which can be time-consuming and pose misalignment problems. An alternative is to measure XRF radiation during the CT scan. However less accurate, it allows for *a priori* knowledge about the sample, facilitating the identification of the gray values visualized in the CT scan [4].

For this reason, a dedicated scanner capable of measuring XRF spectra directly associated with the µCT scan is developed at UGCT. Design features of the scanner, as well as some preliminary results are shown in this work

References:

[1] V. Cnudde, G. Silversmit, M. Boone et al., Sci. Total Environ. **407**(20), 5417 (2009).
[2] B. De Samber, R. Evens, K. De Schamphelaere et al., J. Anal. At. Spectrom. **23**(6), 829 (2008).
[3] M.N. Boone et al. (submitted to Geosphere).
[4] J. Dewanckele, V. Cnudde, M. Boone et al., J. Physics - Conference Series **186**, 012082 (2009).

Reactive Ion Etching of WSi_2/Si Structures for Multilayer Laue Lens Fabrication *

N. Bouet[1], R. Conley[1,3], R. Divan[2], J. Biancarosa[1], A.T. Macrander[3]

[1]*National Synchrotron Light Source II, Brookhaven National Laboratory, Upton, New York USA*
[2]*Center for Nanoscale Materials, Argonne National Laboratory, Argonne, Illinois USA*
[3]*X-ray Science Division, Advanced Photon Source, Argonne National Laboratory, Argonne, Illinois USA*

* Research supported by U.S. Department of Energy, Office of Basic Energy Sciences, under Contract No. DE-AC02-98CH10886 for BNL and DE-AC02-06CH11357 for ANL.

Abstract:

To allow x-ray focusing at the nanometer scale, one promising candidate is the multilayers Laue lens (MLL), which is used in transmission mode [1,2]. Such lenses need to present a very large aspect ratio and optimal mechanical stability. Preparation of MLLs involves deposition of multilayers with a depth-graded period and sectioning to the appropriate thickness for operation at specific photon energy.

The current technique to section the multilayers [3] is based on TEM cross-section-like preparation. Despite the good results provided by this method, it has the disadvantage of being highly time and material consumptive, as well as imparting mechanical stress on the MLLs being sectioned. Reactive ion etching appears to be the technique of choice to achieve a high-quality sectioning of the multilayers while preserving the as-grown qualities of the samples. In addition, this preparation technique would allow access to more exotic shapes, looking for optimal mechanical stability of the MLL for use in synchrotron applications.

Here we report on reactive ion etching and inductively coupled plasma reactive ion etching of WSi_2/Si multilayered films grown by DC magnetron sputter deposition on Si(100) substrates. A variety of reactive SF_6, CF_4, and O_2 mixtures were studied. Our results show that etch rate and profile can be controlled through appropriate variations in O_2 and fluorinated gas flow, choice of temperature, and plasma conditions. Etching profiles were characterized by *ex situ* SEM (Figure 1) and stylus profilometry. The deepest (6.4 μm) anisotropic etching of multilayer stacking reported to date has been achieved. These results contribute to the research of an alternative process to TEM-like sectioning for fabricating multilayer Laue lenses.

References:

[1] H. Yan, Phys. Rev. B **79**, 165410 (2009).
[2] H.C. Kang, J. Maser, G.B. Stephenson et al., Phys. Rev. Lett. **96**, 127401 (2006).
[3] H.C. Kang, G.B. Stephenson, C. Liu et al., Rev. Sci. Instrum. **78**, 046103 (2007).

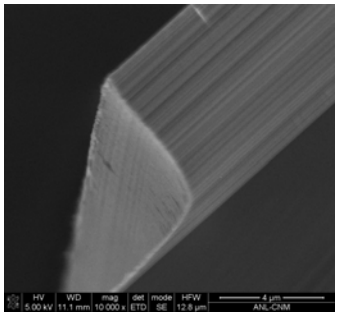

Figure 1: SEM image of WSi_2/Si multilayers etched by SF_6/O_2.

Laboratory 3D Micro XRF - Micro CT Imaging System

P. Bruyndonckx, A. Sasov, X. Liu

SkyScan, Kartuizersweg 3B, 2550 Kontich, Belgium

Abstract:
X-ray fluorescence (XRF) imaging is an imaging modality to visualize the chemical composition of a specimen. Currently the dissemination of 3D volumetric XRF imaging using standard techniques is hampered by the requirement to access a synchrotron facility. To overcome this hurdle we developed a combined micro-CR/micro-XRF laboratory system that can produce 3D chemical maps.

The system employs pin-hole x-ray optics combined with a Deep Depleted (DD) CCD operating in energy-sensitive photon counting mode. The latter allows the detected fluorescence photons to be recorded in list mode format, storing the CCD pixel and the measured energy. Keeping all the x-ray information for each event gives us maximum flexibility in creating XRF images afterwards. The low statistics in the XRF scans imply that an iterative expectation-maximization (EM) algorithm has to be used to reconstruct 3D chemical maps. To facilitate the image analysis, a CT imaging modality was integrated in the system such that morphological coefficients obtained by the CT part is also used to partially correct self absorption of the fluorescence x-rays in the sample.

The use of a DD-CCD ensures a good detection efficiency for high energy fluorescence x-rays but it also necessitates that special care is taken to correct for the signal spreading in the sensitive layer of the CCD in order to obtain a good energy spectrum needed to identify the chemical elements.

The system dead time due to CCD read-out is minimized by optimizing the exposure times dynamically as a function of the x-ray flux distribution on the CCD, such that the probability of having more than one x-ray per pixel per exposure is negligible. This requirement is mandatory to properly measure the energy of the fluorescence x-rays. Because an XRF scan typically requires a long scan time, a procedure to compensate for a possible shift of the energy zero-point has been implemented.

The prototype system has a spatial resolution around 50-60 micron and an energy resolution of 180 eV for 5.9 keV photons. Figure 1 shows a 3D volume rendered CT image of a geological sample. The corresponding 3D volume rendered XRF image is shown in Figure 2.

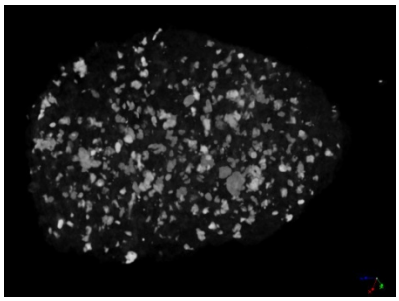

Figure 1: 3D volume rendered CT image of a geological sample

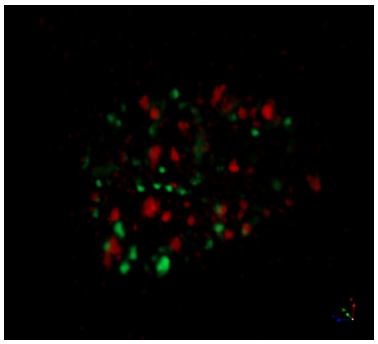

Figure 2: 3D volume rendered XRF image showing pockets or Fe (green) and Ti (red)

Coherent Diffraction and Projection Imaging at FERMI@ELETTRA

F. Capotondi[1], E. Pedersoli[1], B. Kaulich[1], R. Menk[1], A. Locatelli[1], O. Mentes[1], D. Cocco[1], M. Zangrando[1], M. Kiskinova[1], S. Bajt[2], A. Barty[2], H. Chapman[2], L. Gumprecht[2], M. Frank[3], A. Nelson[3], M. Pivovaroff[3], B. Woods[3], M. Bogan[4]

[1]*Sincrotrone Trieste, Area Science Park, 34012 Trieste, Italy*
[2]*CFEL, DESY, Notkestraße 85, D-22607 Hamburg, Germany*
[3]*Lawrence Livermore National Laboratory, Livermore CA 94550, USA*
[4]*PULSE Institute, SLAC, Menlo Park, CA 94025*

Abstract:
The experimental station for coherent DIffraction and PROjection Imaging (DIPROI), which will be operated using soft x-rays in the 1-32 nm range at the FEL facility FERMI@ELETTRA, has passed the design and assembling phases and is now undergoing a series of commissioning tests on the Nanospectroscopy beamline at Elettra.

The DIPROI station (Figures 1 and 2) has a flexible and modular construction adaptable for different experimental set-ups. It will work under high vacuum conditions (10^{-6} - 10^{-8} mbar) using two different detection systems: for wavelengths between 32 nm and 10 nm, the main beam will pass through a hole in a 45° multilayer mirror (MML) that will reflect the diffracted light to a CCD; the shorter wavelength range will instead be covered by a set of two in-line CCDs (see Figure 1) to collect photons scattered at large and small angles, respectively. The station has several adaptable ports for sample introduction and additional detectors, such as (a) TOF-MS providing ion spectrum and the fragmentation pattern during the exposure, (b) UV-VIS light emission from the sample as it turns into plasma, (c) photodiodes. The design is based on the transferred know-how accumulated by our partners in fixed target, time-delay holography, and particle injection imaging at FLASH.

To meet the requirements for performing static and stroboscopic imaging experiments, the microscopy beamline at FERMI@ELETTRA includes KB optics to demagnify the beam to 3×5 μm^2 and a split-delay correlation system for stroboscopic imaging, as well as shot-to-shot diagnostics for intensity fluctuations, spectral profiles, pulse shapes, and pulse lengths.

With the tunability and multiple polarization of FERMI, different measurement modes will allow access to the structure of non-periodic inorganic and organic targets of different complexities and sizes and to dynamic phenomena, such as structural deformation, magnetic domain dynamics, phase separation/nucleation, and complex rearrangements of constituents in cells.

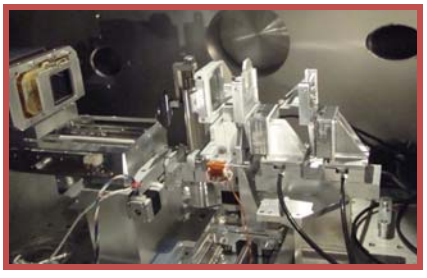

Figure1: Cleaning apertures, sample and detector stage inside DIPROI chamber.

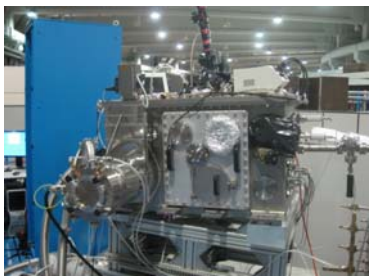

Figure 2: The experimental station at nanospectroscopy beamline at Elettra

Developments in the Fabrication of Zone Plates and Other Nanostructures

P. Charalambous

ZonePlates.com, 8 South Way, Claverings Industrial Estate, London N9 0AB, UK

Abstract:

We have been involved in all aspects of nanofabrication for many years. This includes zone plates, calibration test objects, gratings, Young's slits, and a variety of arrays of nanoholes both ordered and random [1].

Most of the nanostructures are fabricated in tungsten, a material very well suited for a wide range of X-ray energies, with the added advantage that it is the closest thermally matched material to the usual Si_3N_4 substrate. When necessary, we do fabricate in other materials that offer better performance at the intended operating energy. A good example is shown in Figure 1 and Figure 2, a zone plate made in molybdenum, which gives 30% diffraction efficiency at around 100 eV.

Recently we have been working on the optimization of the deposition parameters for various materials, particularly niobium and tungsten. Niobium is another good alternative to molybdenum for operation at ~13 nm. In the case of tungsten, we have been able to deposit smooth stable films thicker than 3 µm and use these to produce both zone plates and calibration structures with aspect ratios >10, for operation at energies up to 30 keV, examples of which will be presented at the conference.

References:

[1] G.R. Morrison, P.S. Charalambous, A. Gianoncelli, B. Kaulich (this conference).

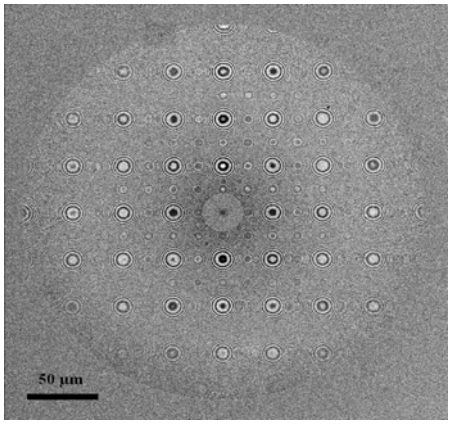

Figure 1: Molybdenum ZP, Diameter=278 m, drn=50 nm, E=30% at 13 nm.

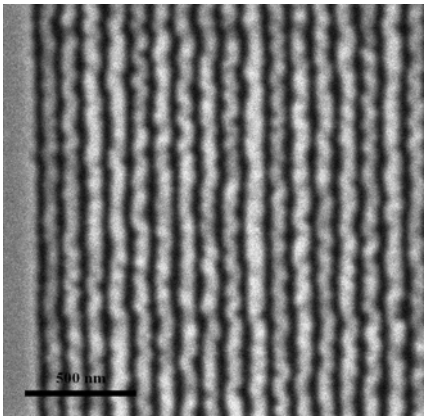

Figure 2: Close up on 50 nm outermost Zones Molybdenum thickness, 90 nm

X-ray Imaging Using Characteristic X-rays Generated from a Conventional X-ray Tube

K. S, Chon[1], K.-H. Yoon[2]

[1]*Department of Radiological Science, Catholic University of Daegu, 330 Kumrak, Hayang, Korea*
[2]*Center for Radiation Imaging Technology, Jeonbuk Technopark, 723-1 Pallbk, Jeonbuk, Korea*

Abstract:

X-rays generated from a conventional x-ray tube have a polychromatic property, i.e., white beam. In medical applications, the generated x-rays do not contribute to making the x-ray image but give a radiation dose to an object. Monochromatic x-rays can be one solution to solve radiation dose, contrast, and background noise problems in x-ray imaging [1].

Monochromatic x-rays can be obtained from combining a conventional x-ray tube and a multilayer mirror, which plays the role of a monochromator, and any mono-energy can be chosen by controlling the Bragg angle. However, the photon flux of the monochromatic x-ray with a mono-energy is not enough to make an x-ray image. This means that a long exposure time is required to obtain a monochromatic x-ray image. The exposure time can be reduced by using the characteristic x-ray.

The characteristic x-ray of the target material in the x-ray tube shows the highest intensity in the x-ray spectrum and monochromatic property. The characteristic x-ray of the molybdenum target was applied to x-ray imaging [2].

The characteristic x-ray had a fan-beam shape, i.e., narrow beam width. A characteristic x-ray image could be obtained by sample scanning and combining each fan-beam image. The contrast of the characteristic x-ray image was better than that of a conventional polychromatic x-ray image.

References:

[1] J.M. Boone and J.A. Seibert, J. X. Sci. Tech. **4**, 334 (1994).
[2] K.S. Chon, S.K. Juhng, K.H. Yoon, J. Korean Phys. Soc. **54**, 23 (2009).

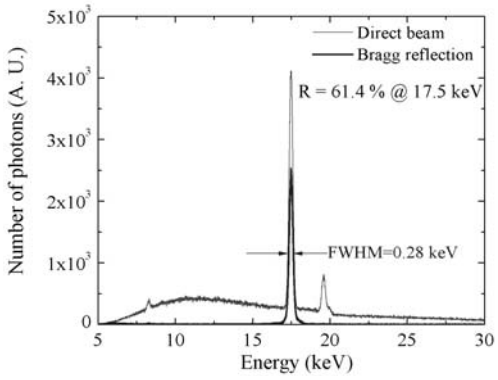

Figure 1: Characteristic x-ray spectrum obtained from a polychromatic x-ray generated by a conventional x-ray tube.

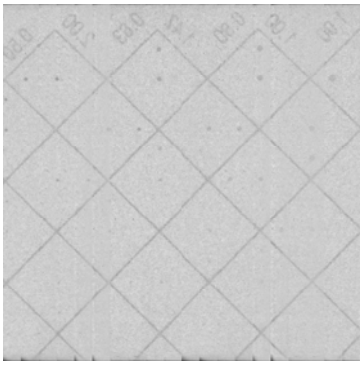

Figure 2: Characteristic x-ray image for a CDMAM phantom.

Capabilities of the Hard X-ray Nanoprobe at the NSLS-II*

Y. S. Chu, L. Margulies, K. Evans-Lutterodt, H. Yan, E. Lima, R. Conley, N. Bouet,
J. Biancarosa, E. Nazaretski, N. Simos, S. O'Hara, D. Kuhne, A. Broadbent, Q. Shen

Brookhaven National Laboratory, Upton, NY 11973, U.S.A.

* This work was supported by the Brookhaven Science Associates, LLC under Contract No. DE-AC02-98CH10886 with the U.S. Department of Energy.

Abstract:
The Hard X-ray Nanoprobe (HXN) beamline at the NSLS-II aims to explore the new frontiers of hard x-ray microscopy by achieving unprecedented spatial resolution and measurement sensitivity. The initial goal of the HXN is to achieve scanning fluorescence and diffraction/scattering at a spatial resolution of 10-30 nm using multilayer Laue lenses and a Fresnel zone plate over the energy range of 6-25 keV. Achieving a resolution below 10 nm will be explored as a longer-term goal. In order to achieve this ambitious goal, we are employing novel approaches for x-ray optics, nanopositioning, and beamline design. The presentation will focus on the current progress of the optics and nanopositioning R&D programs and conceptual design of the HXN beamline.

Multilayer Laue Lens Growth at NSLS-II*

R. Conley, N. Bouet, K. Lauer, J. Biancarosa

NSLS-II, Brookhaven National Laboratory, Upton New York, USA

*Research at Brookhaven National Laboratory is sponsored by the U.S. Department of Energy under Contract No. DE-AC02-98CH10886.

Abstract:

The new NSLS-II deposition laboratory has been commissioned to include a variety of thin-film characterization equipment and a next-generation deposition system [1]. The primary goal for this effort is R&D on wedged multilayer Laue lens (MLL) [2,3] (see Figure 1), which is a new type of x-ray optic with the potential for an unprecedented level of x-ray nanofocusing. This unique deposition system (a side-view is shown in Figure 2) contains many design features in order to facilitate growth of combined depth-graded and laterally graded multilayers with precise thickness control over many thousands of layers, providing total film growth in one run of up to 100-µm thickness or greater. A precision in-vacuum linear motor servo system raster scans a substrate over an array of magnetrons with shaped apertures at well-defined velocities to affect a multilayer coating. The design, commissioning, and performance metrics of the NSLS-II deposition system will be discussed. The latest growth results of both MLL and reflective multilayers in this machine will be presented.

References:

[1] R. Conley, N. Bouet, J. Biancarosa et al., Proc. SPIE **7448**, 74480U (2009).
[2] H.C. Kang, J. Maser, G.B. Stephenson et al., Phys. Rev. Lett. **96**, 127401 (2006).
[3] R. Conley, C. Liu, J. Qian et al., Rev. Sci. Instrum. **79**, 053104 (2008).

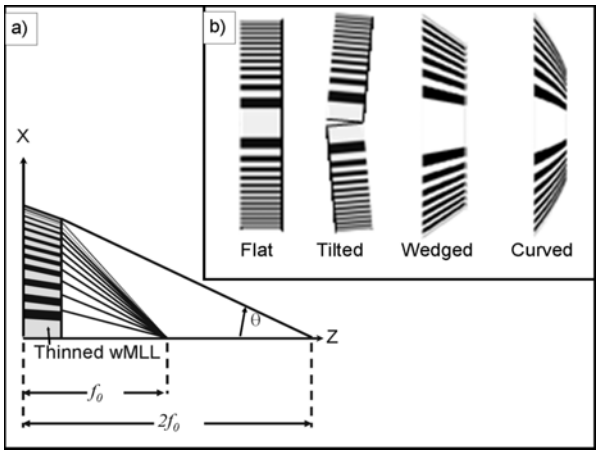

Figure 1: Different types of multilayer Laue lenses; flat, tilted, wedged, and curved. At the lower left is a detailed schematic representation of the wedged MLL.

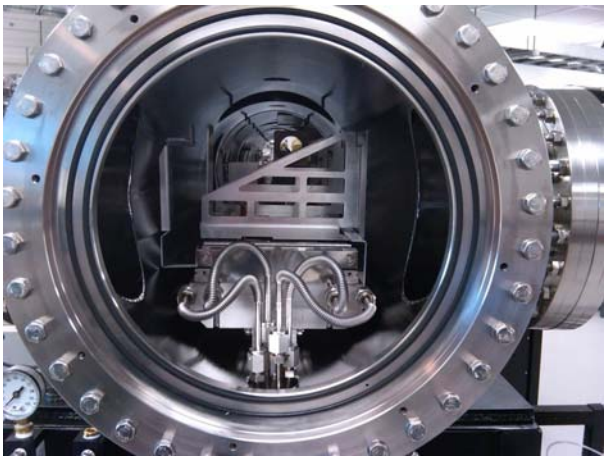

Figure 2: Side-view of the 6.4-meter-long deposition system showing the in-vacuum liquid-cooling rail lines and the linear-motor-driven substrate transport.

Scanning X-ray Fluorescence Microscopy at CHESS

D.S. Dale, A.R. Woll, D.H. Bilderback

Cornell High Energy Synchrotron Source, Cornell University, Wilson Lab, Ithaca, N.Y., USA

Abstract:

The scanning x-ray fluorescence microscopy capability at the Cornell High Energy Synchrotron Source (CHESS) has been improved in a number of ways in recent years. The F3 bending magnet beamline has been overhauled to include bendable, meridional white beam and monochromatic x-ray mirrors to provide vertical focusing. The double-bounce monochromator has been rebuilt to accommodate multilayers or crystals, to extend the range of obtainable incident energies, and to allow the beamline to operate with or without the x-ray mirrors. The in-house glass capillary pulling facility provides the single-bounce capillary condenser optics [1] and can provide optics optimized for a given experiment on short notice. The scanning x-ray microscope itself has also been completely rebuilt, and is routinely used to scan samples requiring spatial resolution on the order of 10-20 microns and surface areas as large as 280 mm x 280 mm. Some notable experiments include studies attempting to reveal lost or hidden information, such as ancient inscriptions [2] or confocal studies of paintings [3], and studies of samples that archive environmental information, such as cross sections of ancient trees that have been dated using dendrochronology [4], or studies of fish otoliths [5].

We have also been developing software that builds on existing open-source resources to provide real-time data acquisition and analysis. The current implementation is written primarily in Python. It uses the SpecClient library [6] to communicate with the Spec instrument control program using the latter's client-server interface. The software uses the PyMca library [7] for advanced x-ray fluorescence peak fitting and quantitative analysis, which can generally handle complicated multi-channel analyzer spectra with many overlapping fluorescence peaks. The software also makes use of Python's emerging distributed computing capabilities to process data in parallel. CHESS users are able to interact with false-color images of element distributions while data acquisition is ongoing. In many cases, users leave the facility with the data already processed, but users can install the software at home for further analysis. This software is freely available, but will be rewritten to provide a plug-in framework to support many different kinds of experiments and analyses. Some advantages and limitations of this framework and its relationship with other acquisition and analysis frameworks will be discussed.

References:

[1] D.H. Bilderback, A. Kazimirov, R. Gillilan et al., AIP Conf. Proc. **879**, 758 (2007).
[2] J. Powers, N. Dimitrova, R. Huanget al., Zeitschrift für Papyrologie und Epigraphik **152**, 221 (2005).
[3] A.R. Woll, J. Mass, C. Bisulca et al., Stud. Conserv. **53**(2), 93 (2008).
[4] C.L Pearson, D.S. Dale, P.W. Brewer et al., J. Geophys. Res. **114**, G01023 (2009).
[5] K. Limburg, R. Huang, D. Bilderback, X-ray Spectrometry **36**, 336 (2007).
[6] M. Guijarro, http://forge.epn-campus.eu/projects/show/specclient
[7] V.A. Solé, E. Papillon, M. Cotte et al., Spectrochim. Acta Part B **62**, 63 (2007).

Large-Area Zone-Plate Fabrication with Optical Lithography

G. Denbeaux

College of Nanoscale Science and Engineering, University at Albany, Albany, New York, USA

Abstract:

Zone plates as condenser optics for x-ray microscopes offer simple optical designs for both the illumination and spectral resolution when used as a linear monochromator. However, due to the long write times for electron beam lithography, both the availability and the size of zone plates for condensers have been limited. Since the resolution provided by the linear monochromator scales almost linearly with the diameter of the zone plate, the full potential for zone plate monochromators as illumination systems for x-ray microscopes has not been achieved. For example, the 10-mm-diameter zone plate has demonstrated a spectral resolution of $E/\Delta E = 700$ [1], but with a 26-mm-diameter zone plate, the calculated spectral resolution is higher than $E/\Delta E = 3000$.

These large-area zone plates are possible to fabricate with the leading edge semiconductor lithography tools available at the College of Nanoscale Science and Engineering. Two of the lithography tools available are the ASML TWINSCAN XT:1700i with 45-nm resolution and the ASML TWINSCAN XT:1950i with 37-nm resolution. Since the multiple layer overlay for these tools is about 2 nm, multilevel processing for efficiency improvements are possible. Both tools use 300-mm wafers with over 60 fields per wafer so they could print the pattern for 60 large-area condenser zone plates on a single wafer in about a minute.

This presentation will focus on the process flow and challenges in the development of large-area zone plate optics. It will also cover the calculated optical performance of the optics and the design of a full field x-ray microscope using these optics.

References:

[1] G. Denbeaux, L. Johnson, W. Meyer-Ilse, AIP Conf. Proc. **507**, 478 (2000).

Performance of Multilayer Monochromators for Hard X-ray Imaging with Coherent Synchrotron Radiation

R. Dietsch[1], A. Rack[2], T. Weitkamp[2], M. Riotte[3], D. Grigoriev[3], T. Rack[3], L. Helfen[3], T. Baumbach[3], T. Holz[1], M. Krämer[1], D. Weissbach[1], F. Siewert[4], M. Meduna[5], P. Cloetens[2], E. Ziegler[2]

[1]*AXO Dresden GmbH, Siegfried-Raedel-Str. 31, 01809 Heidenau, Germany*
[2]*European Synchrotron Radiation Facility (ESRF), 38043 Grenoble, France*
[3]*Forschungszentrum Karlsruhe / K.I.T. (ANKA), 76021 Karlsruhe, Germany*
[4]*Helmholtz Zentrum Berlin / BESSY-II, 12489 Berlin, Germany*
[5]*Masaryk University, 61137 Brno, Czech Republic*

Abstract:

We present a study [1] in which multilayers of different composition (W/Si, Mo/Si, Pd/B_4C), periodicity (from 2.5 to 5.5 nm), and numbers of layers have been characterized. Particularly, we investigated the intrinsic quality (roughness and reflectivity) and the performance (flatness and coherence of the outgoing beam) of the samples as monochromators in synchrotron microradiography. The results indicate that material composition is the dominating factor for the performance. This is important for synchrotron-based hard X-ray imaging methods. In these techniques, multilayer monochromators are popular because of their good tradeoff between spectral bandwidth and photon flux density of the outgoing beam, but sufficient homogeneity and preservation of the coherent properties of the reflected beam are major concerns. The experimental results we collected may help scientists and engineers specify multilayer monochromators, and can contribute to better exploitation of the advantages of multilayer monochromators in microtomography and other full-field imaging techniques.

References:

[1] A. Rack, T. Weitkamp, M. Riotte, D. Grigoriev, T. Rack, L. Helfen, T. Baumbach, R. Dietsch, T. Holz, M. Krämer, F. Siewert, M. Meduna, P. Cloetens, E. Ziegler (accepted to J. Synchrotron Radiat.).

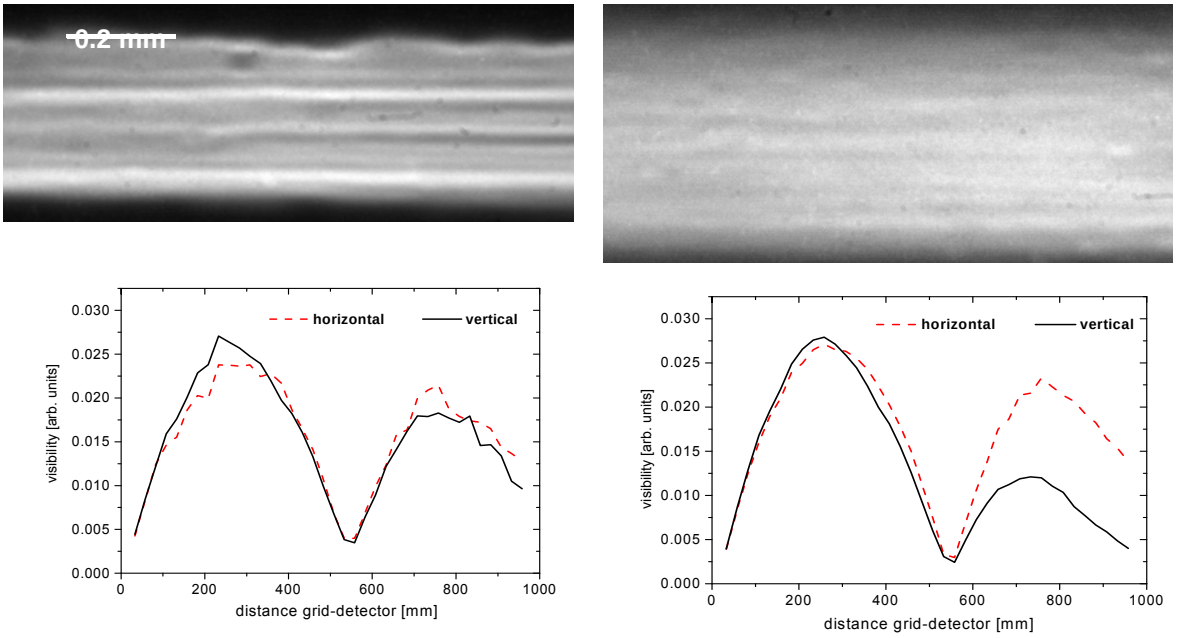

Figure 1: Beam profile after reflection on a Mo/Si (top, left) and on a Pd/B_4C (top, right) multilayer; bottom: coherence measurements (visibility of a phase grating in dependence on its distance to the detector).

Biological Imaging at Diamond: The Cryo-Transmission X-ray Microscope Beamline

E.M.H. Duke[1], L. Alianelli[1], M.R. Howells[1,2]

[1]*Diamond Light Source, Harwell Science and Innovation Campus, Didcot, Oxon. OX11 0DE UK*
[2]*Permanent Address: Lawrence Berkeley National Lab, Berkeley, CA 94720 USA*

Abstract:
A transmission X-ray microscope dedicated to biology is currently being designed on Diamond, the UK's 3rd generation synchrotron source.

The beamline will operate from 200 eV to 2.6 keV, using absorption contrast in the water window regime (~500eV) and phase contrast at higher energies. The X-ray microscope end station will be designed taking into account that the prime focus of the beamline is the imaging of biological samples and cells in particular. Because of this and the consequent requirement to reduce the effects of radiation damage as much as possible, a cryogenic sample stage will be vital for the success of the beamline. Laboratory facilities both at the beamline and close by will be well equipped for sample preparation. Preliminary plans for the beamline and the facility as a whole will be presented.

This Cryo-TXM beamline forms a part of Diamond's plans to establish multi-technique biological imaging on the Harwell Science and Innovation Campus as a whole. The aim and aspirations of this project will be presented, including progress to date.

Our ultimate scientific aim is to bridge the gap between the atomic level detail obtained from macromolecular crystallography and that obtained at the cellular level via microscopy. A program of research in various aspects of cell biology is underway and the most recent results in this will be presented.

Source Size Characterization of a Nanofocus X-ray Tube used for In-Line Phase Contrast Imaging

J. Ewald, T. Wilhein

RheinAhrCampus Remagen, University of Applied Sciences, Suedallee 2, D-53424 Remagen, Germany

Abstract:

We describe a high resolution point projection X-ray imaging system using in-line phase contrast to image weakly absorbing specimens. By employing a nanofocus X-ray tube, features down to 1 µm and less can be resolved using both phase and absorption contrast.

A front-illuminated deep-depleted CCD with a Be-window was used as an imaging sensor for the 8-keV radiation emitted from the Cu transmission target in the X-ray tube. Exposure times ranging from a few minutes down to ten seconds were possible, depending on the specimen and target power.

Periodic gold gratings on a custom-made resolution object were used to evaluate the X-ray source size at the target plane, which directly affects the overall resolution of the system [1]. By comparing horizontal and vertical lines in one image, source size variations in two directions could be recorded in the same image. Furthermore, samples including other resolution targets, plastic structures, and various insects were imaged with up to 100x magnification.

References:

[1] J. Reinspach, Master's thesis, Royal Institute of Technology Stockholm, 2007.

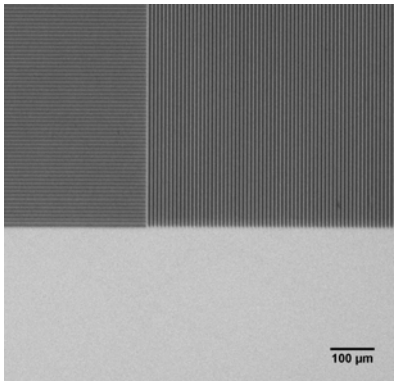

Figure 1: Clearly resolved vertical and blurry horizontal gold lines due to focus-broadening in one direction (5 µm lines, M = 30, T = 30 s, U = 25 kV, I = 170 µA).

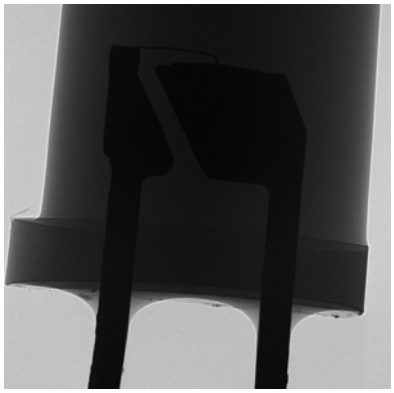

Figure 2: Image of a 5-mm LED showing edge effects on the epoxy case and dust particles due to phase-contrast (T = 60 s, U = 25 kV, I = 140 µA).

The Hard X-ray Micro/Nanoprobe Beamline P06 at PETRA III

G. Falkenberg, G. Wellenreuther, N. Reimers

Deutsches Elektronen-Synchrotron (DESY), Notkestr. 85, D-22603 Hamburg, Germany

Abstract:

Two years after the shutdown of PETRA II and a complete rebuilding and refurbishment of the ring, PETRA III has seen the first stored beam as a dedicated synchrotron radiation source in April 2009. With 1 nmrad horizontal emittance at 6-GeV positron energy, PETRA III is one of the most brilliant (high-energy) X-ray sources worldwide. The new experimental hall will accommodate a total of 14 undulator beamlines with up to 30 experimental stations. At present the installation of the beamlines and experimental hutches is underway and the first 3 beamlines are under commissioning.

The Hard X-Ray Microprobe/Nanoprobe-beamline P06 will enable advanced visualization using different contrast mechanisms, namely X-ray fluorescence (XRF), X-ray absorption spectroscopy (XAS), X-ray diffraction (XRD), phase and absorption contrast imaging, and coherent X-ray diffraction imaging (CXDI). In the microprobe experiment, KB mirrors will be applied for focusing down to the sub-micrometer range and will enable spectroscopy (achromatic optic), fast scanning (high flux), and work in environments (200-mm working distance) in the energy range 5-23 keV. For high energies up to 80 keV, Be and Al compound refractive lenses will be employed. The Nanoprobe-experiment, build by Prof. Chr. Schroer's group (TU Dresden, BMBF funding), is optimized for the smallest practical beam size in the nanometer range (~30 nm) and is based on refractive nanofocusing X-ray lenses (NFL) [1]. The NFL can be easily replaced by Fresnel zone plates for applications at lower energies. The commissioning phase of the P06 beamline will begin in the summer of 2010.

References:

[1] C.G. Schroer, P. Boye, J.M. Feldkamp et al., Nucl. Instrum. Methods A, (2010) in press, available online at doi:10.1016/j.nima.2009.10.094.

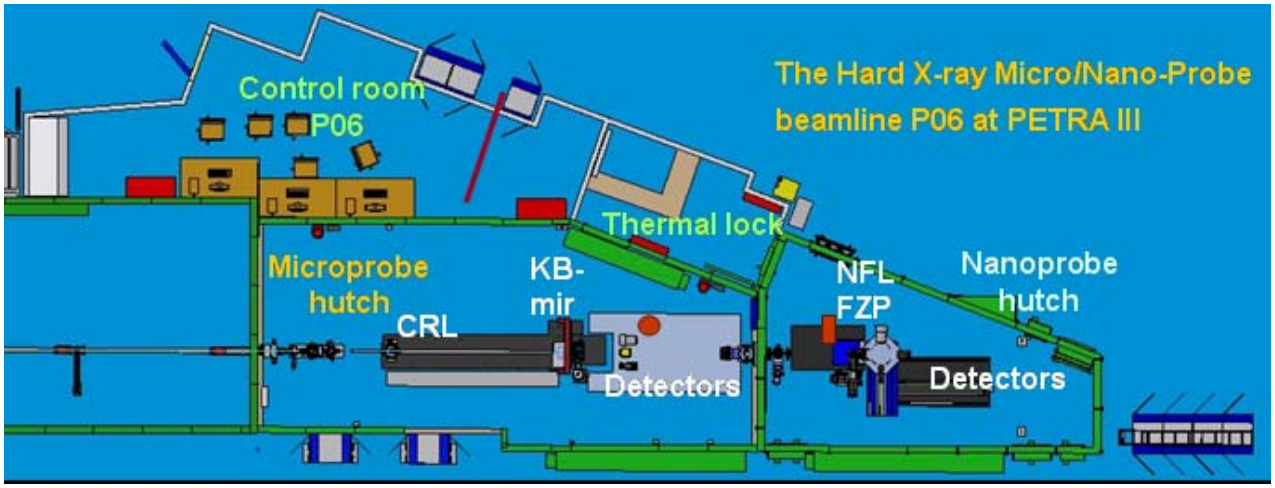

Figure 1: Experimental area of the Hard X-ray Micro/Nano-Probe beamline at PETRA III. The focusing elements in both experiments are indicated.

Germanium-Based Circular Zone Plates for Soft and Hard X-rays

A. Firsov[1], R. Belkhou[1], M. Idir[1], A. Svintsov[2], S. Zaitsev[2]

[1]*Synchrotron SOLEIL, L'Orme des Merisiers Saint-Aubin - BP 48, 91192 GIF-sur-Yvette Cedex, France*
[2]*Institute of Microelectronics Technology RAS, 142432, Chernogolovka, Moscow distr., Russia*

Abstract:
Since April, 2009 the works on organization of technological base for the fabrication of required diffraction optical elements are conducted at Synchrotron SOLEIL. These diffraction focusing elements are: zone plates and condenser lenses for "soft" x-rays (80 eV - 2500 eV,), focusing zone plates for "hard" x-rays (4 keV - 24 keV,), diffraction elements working under complete external reflection conditions with elliptical diffraction zones and a topology appropriate to operate at glancing incidence to fulfill the conditions of total external reflection (energy range 100 eV - 1500 eV).

In this work the results of fabrication of a circular germanium-based zone plates are submitted. The results of numerical calculations of a behavior of a zone plates with real topology in real experimental conditions are submitted as well. The software used for calculations allows taking into account the undercut of zones that occur after plasmachemical etching and also variations of the height of zones. Such variations could be used to correct or improve zone plate efficiency after electroplating or plasmachemical etching and can be performed by a focused ion beam (FIB) etching [1] (direct or with active gas assistance). Data preparation and ion beam control for these corrections were carried out by Nanomaker software (Interface Ltd).

References:

[1] A. Svintsov, S. Zaitsev, G. Lalev et al., Microelectron. Eng. **86**, 544 (2009).

Diamond Fresnel Zone Plates for High-Power X-ray Beams

S. Gorelick[1], J. Vila-Comamala[1], V. Guzenko[1], R. Barrett[2], B. Patterson[1], C. David[1]

[1]*Paul Scherrer Institut, CH-5232 Villigen, Switzerland*
[2]*ESRF, 6 rue Jules Horowitz, BP220, F-38043 Grenoble Cedex, France*

Abstract:

Focusing of intense beams from X-ray free electron lasers (XFELs) by Fresnel zone plates (FZPs) is attractive because they can provide very high spatial resolution and, at the same time, accept a full millimeter-sized XFEL beam. In addition, the wave-front can be preserved or manipulated using FZPs. However, since FZPs consist of nanostructures on thin support membranes, they are prone to suffer from radiation damage, and they may even be destroyed after a single XFEL pulse [1]. Unique properties of diamond, such as extremely high thermal conductivity, low thermal expansion, in addition to its low X-ray absorption make diamond the most thermally stable material that is likely to survive intense XFEL beams. Making zone plates of diamond is, therefore, an excellent solution for wave-front preserving focusing of intense X-rays with a high spatial resolution. Efficient focusing of hard X-rays by diamond FZPs is difficult because the zones must be sufficiently tall (>>1 μm) to provide a phase-shift as close to π as possible for the best diffraction efficiency. Diamond can be structured by oxygen plasma etching; however, because of the very slow etching rates of diamond, erosion of the etch-mask becomes an issue, and achieving sufficiently tall structures in diamond is challenging. By using 100-keV electron beam lithography, we were able to fabricate thick etch-masks that were more resistant to the erosion processes. Using these thick masks and an optimized reactive ion etching (RIE) process in inductively coupled plasma (ICP) allowed us to etch deeper (down to 2 μm) into the diamond layers. In this paper we present the first ever fabricated FZPs made entirely of diamond, discuss the fabrication details, and present first resolution and efficiency tests.

References:

[1] V. Ayvazyan et al., Eur. Phys. J. D **37**, 297 (2006).

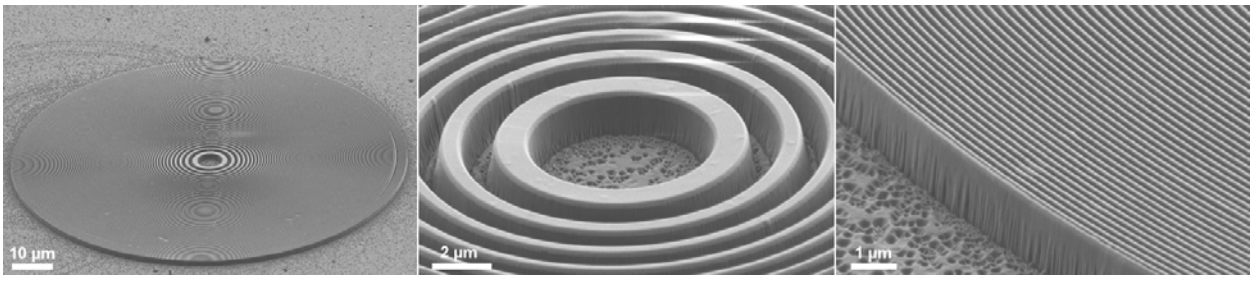

Figure 1: Fresnel zone plate with a 100-nm outermost zone etched 1.4 μm deep into a CVD diamond layer. (from left to right) Overview of the zone plate, central zones, and outermost zones.

High Efficiency Au Zone Plates for Multi-keV X-rays

S. Gorelick[1], J. Vila-Comamala[1], V. Guzenko[1], R. Barrett[2], M. Salomé[2], C. David[1]

[1]*Paul Scherrer Institut, CH-5232 Villigen, Switzerland*
[2]*ESRF, 6 rue Jules Horowitz, BP220, F-38043 Grenoble Cedex, France*

Abstract:
We report a direct e-beam writing process of Fresnel zone plates (FZPs) in thick layers of PMMA to produce a plating mold used to transfer the pattern into Au. Previously, the fabrication process of FZPs was based on a three-level process in which PMMA patterned with low keV electrons was used as an etch mask to transfer the pattern into an intermediate metal mask used to etch into a hard polymer (e.g., polyimide) to produce a plating mold. This method involved many subsequent steps which were often hard to optimize. Compared to the previous method, the deeper penetration of 100-keV electrons into the resist with reduced forward scattering allows exposures of thick PMMA layers which can be directly used as plating mold without the need of intermediate etching steps. High quality 500-nm and 1-µm thick gold zone plates with down to 50-nm and 70-nm outermost zones, respectively, and with diameters in the range of 20–600 µm were fabricated using this method. In this paper we present the details of the optimized fabrication process, such as development times, developer, dose tables, and line shrinkages required to obtain the desired zone widths and the gaps between the zones. The diffraction efficiencies of some of the fabricated FZPs were measured for a wide range of X-ray energies showing excellent diffraction efficiencies which are 65-75% of the theoretical maximum, reflecting the good quality of the zone plates.

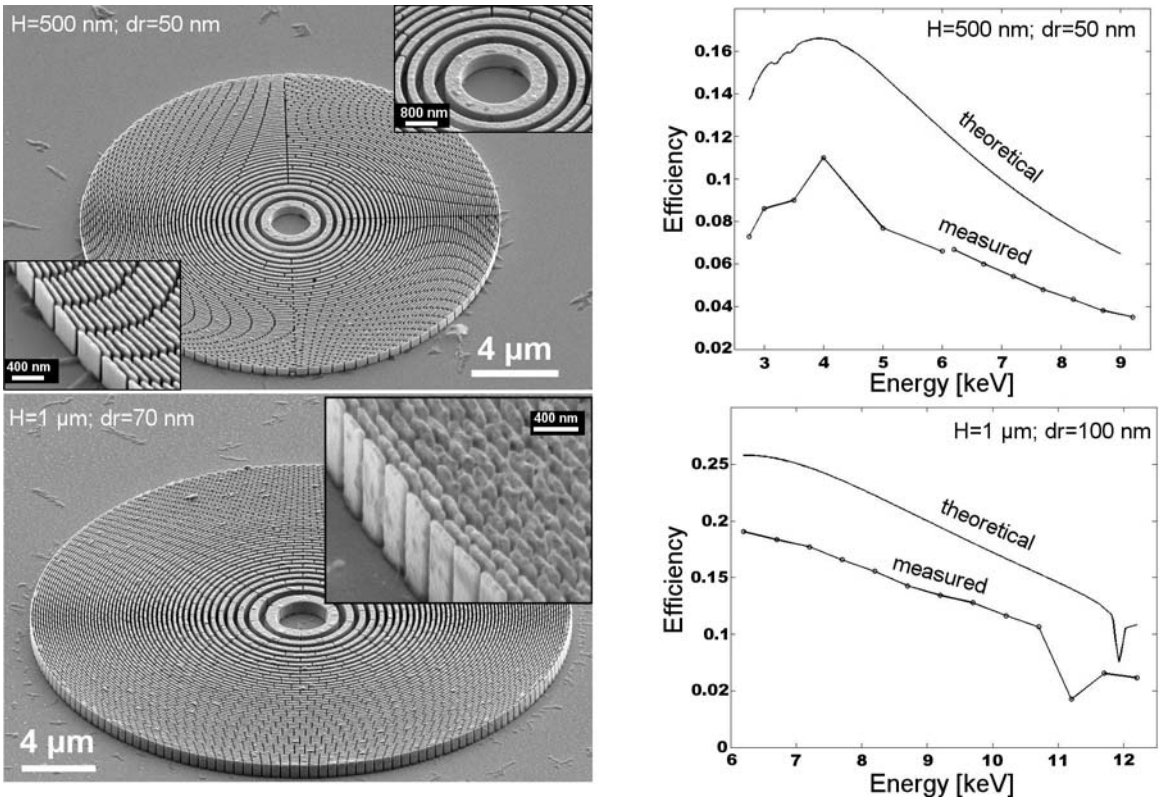

Figure 1: (left) Au Fresnel zone plates fabricated by electroplating into PMMA molds produced in a direct e-beam writing process. (right) Diffraction efficiencies of corresponding zone plates.

Investigation of Damage in Diffractive Optics Induced by High Intensity X-ray Beams

S. Gorelick, K. Nygård, J. Vila-Comamala, V. Guzenko, B. Patterson, A. Bergamaschi, C. David

Paul Scherrer Institut, CH-5232 Villigen, Switzerland

Abstract:

Fresnel zone plates (FZP) are used successfully for X-ray focusing as they provide spatial resolution values down to th 10 nm range [1]. In addition, they are capable of controlling the X-ray wave front within a fraction of a wavelength. However, since FZPs are made of nanostructures on thin support membranes, they are less robust in terms of radiation damage compared to, e.g., refractive lenses or mirrors. Severe radiation damage effects are observed at modern insertion device beam lines, which severely limit the lifetime of FZP optics. This topic will become even more important at future X-ray sources. In order to estimate the applicability of FZPs, fabrication processes, and materials in terms of radiation damage, the relevant damage causes (thermal, environmental, crack formation, etc.) and damage thresholds (radiation dose and dose rate) need to be characterized quantitatively. The possible damage mechanisms are complex and need to be determined experimentally.

In this study we used an intense pink wiggler beam (effective X-ray energy: 10.5 keV, incident power on the sample: 1 W mm^{-2}) of the Powder Diffraction beamline (4S) of the Swiss Light Source (SLS) [2] to induce damage in linear diffraction gratings made of Au, Ir/Si, and Au embedded in polyimide. We recorded the changes of diffraction efficiency, which allowed us to sense even small structural changes in the gratings, and which also allowed us to develop a suitable criterion for the degree of damage in the gratings by analyzing how the diffraction efficiency evolved with the dose. As expected, the Au gratings embedded in polymer matrix were damaged by the beam when the gratings were in the air (Figure 1). However, these gratings were damaged even if they were irradiated in vacuum or in He atmosphere, albeit at a significantly slower rate. The Au gratings that did not have polymer between the Au lines, as well as Ir/Si gratings, were considerably more radiation-hard and suffered only limited radiation damage even after prolonged irradiations in air. Although only long time scales (minutes-hours) were addressed in this study, this preliminary investigation represents a first step toward the understanding of radiation-induced damage mechanism in FZPs, which will contribute to the development of optics for high intensity X-ray sources.

References:

[1] J. Vila-Comamala et al., Ultramicroscopy **109**, 1360 (2009).

[2] http://sls.web.psi.ch/view.php/beamlines/ms/index.htm

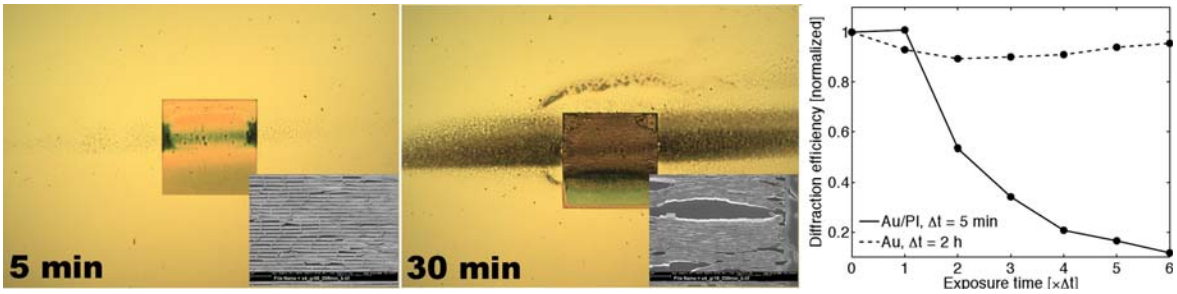

Figure 1: (left and center) Optical microscope images of 200 × 200 µm Au gratings embedded in a polymer matrix with a period of 200 nm that were exposed with a high power focused pink beam for different periods of time (5-30 min). Magnified scanning electron microscope images of selected damaged regions are presented in the inserts. (right) Normalized diffraction efficiencies of the gratings as a function of irradiation time in the air for Au gratings with and without the polymer.

X-ray Zone Plate in Combination with Diffraction Reflections

A.H. Grigoryan[1], A.H. Toneyan[2], M.K. Balyan[3]

[1]*Center for the Advancement of Natural Discoveries using Light Emission (CANDLE), Research Institute at YSU, Acharyan 31, Yerevan 0040, Armenia*
[2]*Web AM LLC, Yerevan, Armenia*
[3]*Yerevan State University, Faculty of Physics, Department of Solid State Physics, Solid State Physics Research Laboratory, Alex Manoogyan 1, Yerevan 0025, Armenia*

Abstract:

As was shown in [1,2], successive asymmetric Bragg reflection can significantly reduce the focal length of the lens if the lens is placed in the gap between the two asymmetric *(+n,–n)*reflecting plates (Figure 1). Then the focal length F_0 of the lens becomes equal to $F = F_0 b^2$, where $b = \gamma_0/\gamma_h$ is the factor of asymmetry, $\gamma_0 = \sin(\vartheta - \alpha)$, and $\gamma_h = \sin(\vartheta + \alpha)$If $b << 1$, then $F << F_0$. F_0 decreases 400 times at $b = 0.05$, and the resulting system would be equivalent to a compound lens consisting of 400 lenses [3]. In this work we investigate the influence of asymmetric double diffraction on the focusing parameters of zone plates (Figure 2). Based on the Huygens-Fresnel principle both in the reflecting plates [4] and in the vacuum, it is shown that $F = F_0 b^2$, where F_0 is the focal distance of the zone plate and F is the focal distance in the double-diffracted beam of the system.

References:

[1] A.H. Grigoryan, M.K. Balyan, L.G. Proc. Natl. Acad. Sci. Armenia, Physics **39**(4), 262 (2004).
[2] A.H. Grigoryan, M.K. Balyan, A.H. Toneyan**,** J. Synchrotron Radiat. **17**(3) (2010); doi:10.1107/ S0909049510003754.
[3] B. Lengeler, C. Schroer, J. Tümmler et J. Synchrotron Radiat. **6,** 1153 (1999).
[4] T. J. Phys. Soc. Jpn. **27**(1), 147 (1969).

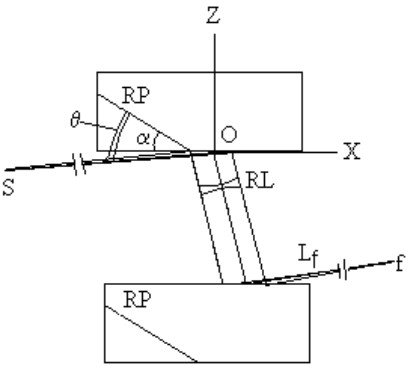

Figure 1: *S*: point source; *RP*: reflecting plane; θ: angle-incident beam-reflecting plane; α: angle-reflecting plane, crystal surface; *RL*: parabolic lens; L_f:focusing distance; *f*: focus.

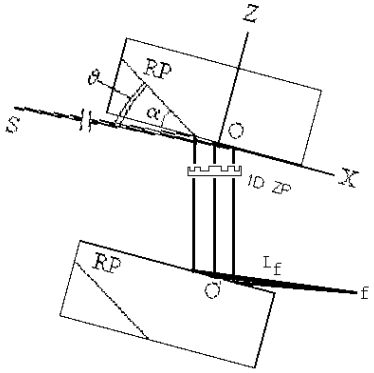

Figure 2: Scheme of the zone plate in combination with a double-diffraction reflection. *1D ZP* is the one-dimensional zone plate; the remaining notations are as in Figure 1.

X-Ray Diffractive Optics Simulation Using a GPU, Web Service, and Graphical User Interface

R. F. Gunion[1], I.-H. Byun[2], Y. Liu[2,3], S. Marchesini[3], A. Sakdinawat[2,3]

[1]*Center for X-Ray Optics, Lawrence Berkeley National Laboratory, Berkeley, CA, USA*
[2]*University of California, Berkeley, CA, USA*
[3]*Advanced Light Source, Lawrence Berkeley National Laboratory, Berkeley, CA, USA*

Abstract:
A new diffractive optics simulation engine and user interface has been designed for use with Nvidia Tesla graphics processing unit (GPU)-based parallel computation architecture. The diffractive optics simulation engine is capable of simulating various types of imaging configurations with zone plates, apertures, and other optical elements. It can simulate different degrees of partial coherence and effects of spectral bandwidth. This engine has been used to accelerate some preliminary calculations at up to 17 times the CPU-only based calculations using equivalent hardware. The engine leverages Matlab for its familiarity to scientists and built-in GPU-accelerated Fourier Transform, custom C code for additional GPU-based parallel code, and Java for communicating with a back-end database.

In addition, an easy-to-use graphical user interface (GUI) has been designed and written to make the calculation engine more accessible and to provide quicker turnaround times for novel calculations. The GUI can make recommendations to the user, based on the input geometry, for the optimal sampling and algorithm, further increasing the potential accuracy of the calculation results. This user interface, which is based on the Eclipse rich client platform, communicates with the calculation engine with the help of a Restlet-based Web Service and a MySQL database. The use of the web service as an intermediary between the user interface and the calculation engine provides the additional benefit of monitoring the progress of calculations through an ordinary web browser.

We believe this architecture, using modern software tools combined with rigorous Matlab-based calculations familiar to scientists, will provide a platform for uniquely flexible and highly available diffractive optics simulations.

References:

[1] J. W. Goodman, *Introduction to Fourier Optics*, (New York: McGraw-Hill Book Company, Inc., 1968).

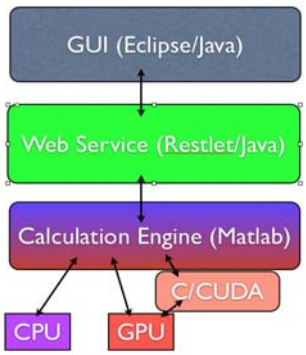

Figure 1: Block diagram illustrating the major components of the optics simulation application.

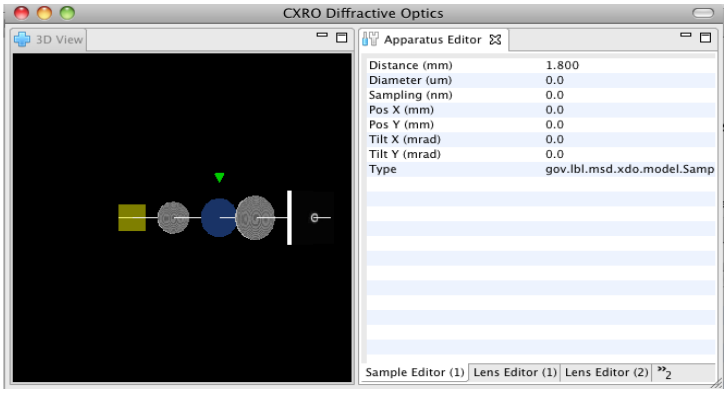

Figure 2: Eclipse-based graphical user interface to the Matlab-based diffractive optics simulation engine.

Efficient EBL Exposure Strategies for Diffractive X-ray Optics

V.A. Guzenko[1], H. Romijn[2], J. Vila-Comamala[1], S. Gorelick[1], C. David[1]

[1]*Paul Scherrer Institut, 5232 Villigen PSI, Switzerland*
[2]*Vistec Lithography BV, 5684 PS Best, Netherlands*

Abstract:
Electron beam direct writers are designed and widely utilized for the fabrication of micro- and nanostructures, e.g., electronic circuits. These are defined in Cartesian coordinates and fit well into the addressing grid of the tool. Unfortunately, they are not well suited for exposing the structures with rotational symmetry, like Fresnel zone plates (FZPs).

In this work, the exposure of Fresnel zone plates was performed using a Vistec EBPG5000Plus e-beam writer operated at 100 keV. The deflection system of this e-beam tool is capable of a resolution well below 1 nm and beam stepping frequencies up to 50 MHz. One important issue is the optimization of the exposure strategies in order to reduce the exposure times without loss of resolution. The exposure data are pre-processed (fractured) in order to reduce the amount of data that has to be processed during the exposure. For example, an FZP with a diameter of 500 µm and an outermost zone of 30 nm is built of more then 2000 rings consisting of about 20 millions of trapeziums. An inefficient fracturing can lead to a dramatic increase of data flow during the exposure and, consequently, to a significant overhead. In some cases the exposure time can increase by a factor of two or more. We have applied an improved fracturing strategy based on the symmetry considerations and the optimized control of the deflection system. Further optimization has been applied to the stage movement during the exposure of the FZPs that are bigger than one write field.

These optimized FZP patterns were transferred into thick layers of positive tone (PMMA) or negative tone (HSQ) resist, serving as a mold for the fabrication of high aspect ratio FZPs. This is a challenging task, which the in case of diffractive elements can be relaxed by introducing supporting elements (zone interruptions for positive tone resists and bridges between the zones for negative tone resists) preventing the collapse of the outer zones. In this way we fabricated FZPs with the high aspect ratio features (more then 10) that have been successfully utilized in the scanning transmission X-ray microscopes at the Swiss Light Source (Villigen, Switzerland).

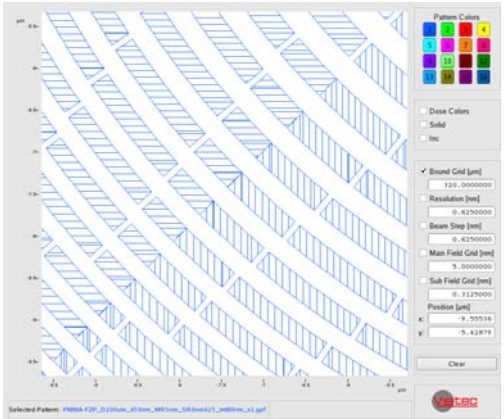

Figure 1: Fragment of an optimized Fresnel zone plate pattern designed to be exposed in positive tone resists, e.g. PMMA. Periodic interruptions of the zones increase the stability of the structures.

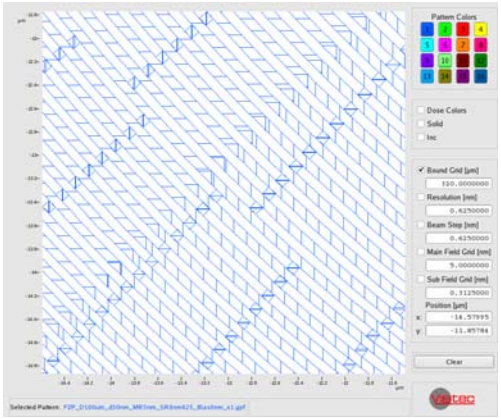

Figure 2: Fragment of an optimized FZP pattern to be exposed in negative tone resists, e.g. HSQ. The supporting bridges prevent the collapse of the zones during the drying step.

Scanning Probe Diffraction Microscopy at the CNM/APS Hard X-ray Nanoprobe Beamline

M. Holt[1], R. Winarski[1], V. Rose[1,2], G. B. Stephenson[1,3], J. Maser[1,2]

[1]*Center for Nanoscale Materials, Argonne National Laboratory, Argonne IL 64039 USA*
[2]*Advanced Photon Source, Argonne National Laboratory, Argonne IL64039 USA*
[3]*Materials Science Division, Argonne National Laboratory, Argonne IL64039 USA*

* Use of the Center for Nanoscale Materials was supported by the U. S. Department of Energy, Office of Science, Office of Basic Energy Sciences, under Contract No. DE-AC02-06CH11357.

Abstract:
The recent completion of the Hard X-ray Nanoprobe Beamline at the Advanced Photon Source as part of the Center for Nanoscale Materials provides a dedicated facility for nanomaterials characterization utilizing hard x-ray microscopy at a landmark ~40 nm spatial resolution [1]. The unique capabilities of hard x-ray microscopy techniques such as large penetration depths, experimental sensitivity to elemental composition, crystallographic phase, and strain when applied at this length scale offer unique opportunities for many fields of science.

Current research will be presented based on the use of nanoscale Bragg diffraction microscopy at the Hard X-ray Nanoprobe Beamline (HXN) as a probe of local structural physics of materials. This is associated with three key areas: 1) unique material behavior of nanoscale objects, 2) nanoscale phase phenomena of active materials, and 3) frontier imaging of nanoscale disorder via coherent Bragg diffraction.

References:

[1] J. Maser, R. Winarski, M. Holt et al., Proc. 8th International Conference on X-ray Microscopy, IPAP Conference Series **7,** 26 (2005).

Cryogenic Transmission X-ray Nano-Tomography in the Water Window with a Z-Pinch Plasma Source*

B. Hornberger[1], M. Feser[1], M. Freed[1], D. Gustafson[2], J. Harroun[1], W. Holber[2], S. Horne[2], G. Hsu[1], D. Hunt[1], W. Li[3], R. Pastrick[1], J. Silterra[2], I. Spink[1], A. Tkachuk[1], D. Trapp[1]

[1]*Xradia Inc., 5052 Commercial Circle, Concord, CA 94520, USA*
[2]*Energetiq Technology Inc., 7 Constitution Way, Woburn, MA 01801, USA*
[3]*National Synchrotron Radiation Laboratory, University of Science and Technology of China, Hefei, Anhui 230029, P. R. China*

* Supported by NIH grants 5R44RR022488-03 and 5R44RR023753-03

Abstract:
Transmission X-ray Microscopes (TXMs) operating in the water-window region of the electromagnetic spectrum have been established at synchrotron light sources since the 1970s [1]. More recently, various extensions of the technique have been reported, in particular the use of laboratory-based x-ray sources [2], tomographic imaging [3] and cryogenic tomography [4].

We present here results from a TXM coupled to a table-top Z-pinch plasma source operating at 430-eV photon energy. The microscope is designed for tomographic data acquisition at cryogenic temperatures utilizing a cartridge-based sample handling system. It comprises a glass capillary condenser [5,6] and a Fresnel zone plate with 25 or 40 nm outermost zone width to produce images of magnification ~800 on a direct x-ray detection CCD camera. The x-ray source is based on the Energetiq EQ-10 platform [7] originally developed for EUV lithography, modified for operation in Nitrogen VI [8].

References:

[1] B. Niemann, D. Rudolph, and G. Schmahl. Appl. Optics **15**, 1883 (1976).
[2] M. Berglund, L. Rymell, M. Peuker et al., J. Microsc. **197**, 268 (2000).
[3] J. Lehr, Optik **104**(4), 166 (1997).
[4] D. Weiß et al., Ultramicroscopy **84**, 185 (2000).
[5] X. Zeng et al., Appl. Optics **47**(13), 2376 (2008).
[6] J. L. Carrascosa et al., J. Struct. Biol. **168**(2), 234 (2009).
[7] S. F. Horne et al, Proc. SPIE **6151**, 61510P (2006).
[8] S. F. Horne et al, J. Radiat. Res. **166**, BioOne, 652 (2006).

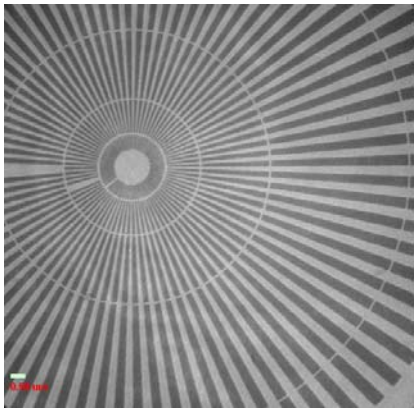

Figure 1: Image of a Siemens star pattern with 30 nm finest features, recorded with a 40 nm zone plate. Features of about 45 nm size are resolved.

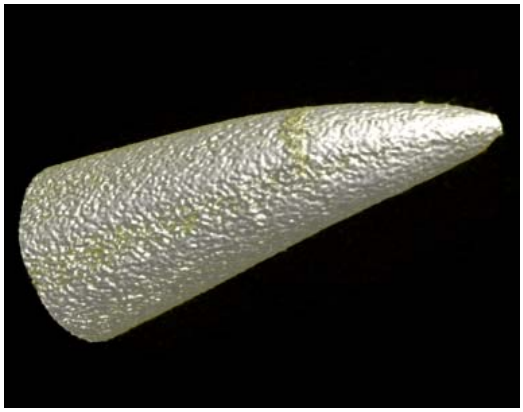

Figure 2: Tomographic reconstruction of a Tungsten STM tip.

Development of the Electrode-less Z-pinch Soft X-ray Source for Water-Window Microscopy*

S. Horne, B. Holber, J. Silterra, D. Smith

Energetiq Technology Inc., 7 Constitution Way, Woburn, MA 01801, USA

* Supported by NIH grants 5R44RR022488-03 and 5R44RR023753-03

Abstract:

Using the commercially successful EQ-10 EUV source as a starting point [1], we have developed a source of x-rays at 430 eV suitable for use as an illumination system for water-window x-ray microscopy [2]. The source relies on a unique, inductively driven Z-pinch plasma topology. Source operating characteristics will be detailed, and our experience with a prototype microscope will be described.

References:

[1] S.F. Horne et al, Proc. SPIE **6151**, 61510P (2006).

[2] S.F. Horne, J. Silterra, W. Holber, J. Phys.: Conf. Series **186**(1), 012028 (2009).

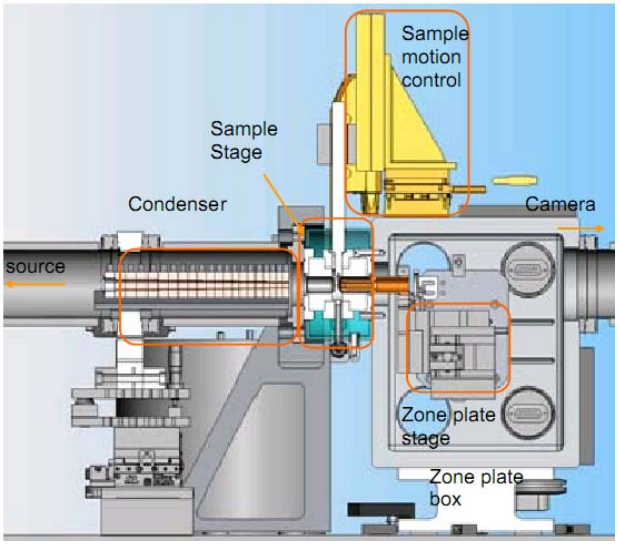

Figure 1: Layout of sample area of a demonstration microscope.

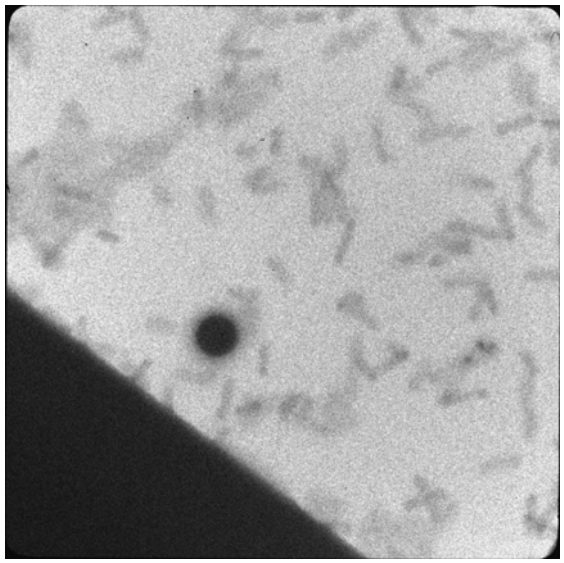

Figure 2: Image of biologically fixed *E coli*, with 2.1-micron sphere.

Normal-Incident Multilayer Optics with LPP Light Source

F. Ishida[1], T. Ejima[1], M. Toyoda[1], T. Tsuru[1], T. Hatano[1], M. Yanagihara[1], H. Mizutani[2]

[1]*IMRAM, Tohoku Univ., 2-1-1, Katahira, Aoba-ku, Sendai, 980-8577, Japan*
[2]*Dept. of Fron. Sci. & Sci. Int., Organ. Inter. Res. Projects, Univ. of Tokyo, 5-1-5, Kashiwa-no-ha, Kashiwa, Chiba, 277-8568, Japan*

Abstract:
Living organisms have an internal structural hierarchy. The structures within each hierarchy have characteristic shapes and functions related to their shape. Some small structures within a hierarchy combine interactively and make new structures by which a new characteristic function is achieved in the upper hierarchy. It is therefore important to understand the functions of a structure to simultaneously observe component structures and clarify their specific role [1]. One example of the hierarchy structures is a brain, which is composed of complex neural networks that include millions of neurons connected with billions of synapses. Detail maps of synaptic connectivity will be needed to clarify the functions of brains [2]. The size of a neuronal connection called a "synapse" is from several tens to several hundreds nm; therefore X-ray microscopes will observe synapses with neuronal fibriform structures (axons and dendrites), which are larger than synapses.

A microscope that can observe living organisms across several hierarchies, which can be called "super-hierarchical", has features that include a wide field of view where multi-hierarchical observation can be achieved, and high spatial resolution by which the smallest organelle can be observed [3]. We present and demonstrate the use of an extreme ultraviolet (EUV) microscope that was developed in-house [4]. Images are acquired using Bragg reflection multilayer optics and a laser-produced plasma light source. The upper-limit spatial resolution of the EUV microscope is 130 nm with a 10-ns exposure time and a 250 x 250 μm^2 field of view in 13.4-nm wavelengths. The EUV image of the cerebral cortex of a mouse is demonstrated as a “super hierarchy” observation [5]. The details of the microscope and the quality of the obtained image will be presented.

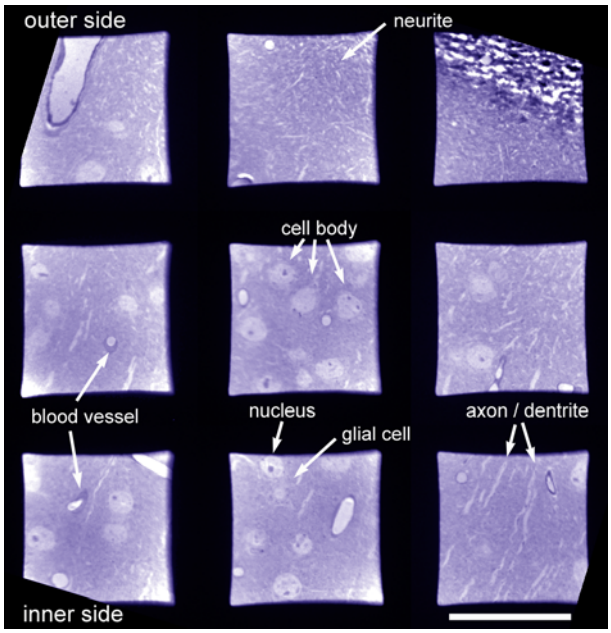

Figure 1: EUV image of the cerebral cortex of a mouse. Scale bar is 50 μm [4].

References:

[1] For example, B. Alberts, A. Johnson, J. Lewis et al., *Molecular Biology of the Cell*, (New York: Garland Science, Taylor & Francis Group, 2007).
[2] J. W. Lichtman, J. Livet, J. R. Sanes, Nature Rev. Neurosci. **9**(6), 417 (2008).
[3] T. Ejima et al., *ibid*.
[4] T. Ejima, F. Ishida, H. Murata et al., Opt. Express **18**(7), 7203 (2010).
[5] H. Mizutani et al., *ibid*.

Preparation and Characterization of Thin Film Elemental Standards for X-ray Fluorescence Microscopy

S. A. James[1], M. D. de Jonge[2], S. Vogt[3], G. F. Moorhead[1], B. Sexton[1], P. Hoobin[1], D. Paterson[2], D. L. Howard[2], C. G. Ryan[1]

[1]CSIRO, Clayton VIC, Australia
[2]Australian Synchrotron, Clayton, Australia
[3]Argonne National Laboratory, Argonne, Illinois, USA

Abstract:
The X-ray fluorescence microprobe (XFM) is finding application in biomedical sciences to investigate the exquisite sensitivity of biological systems to changes in elemental content or distribution. XFM is unique as a method for visualizing the detailed spatial organization of elements in cells and tissues, combining high spatial resolution with high sensitivity to a large number of elements. In general, such systems are overwhelmingly composed of low-Z elements (H,C,N, & O) but heavier 'P-block' elements (P, S, and Cl), alkali and alkali earth metals (Na, Mg, K, and Ca), and transition metals (Fe, Cu, and Zn) all play important roles in fundamental biological processes. Other elements (As, Pb, and Hg) are of interest due to their potent toxicity and still more (Au, U) can be used for selective labeling of particular cellular substructures.

XFM studies can provide quantitative elemental analysis by calibrating x-ray fluorescence count rates to elemental density. This can be derived from a detailed forward-model of the interaction process; however, this approach is prone to model errors, and so we prefer instead to scan a standard reference material (SRM). National Institute of Standards and Technology SRMs 1832 and 1833 [1], consisting of a silica-based glass film containing known mass fractions of the oxides of selected elements, have been widely used for this purpose. However, the Certificates of Analyses of these standards specifically state that they are not recommended for use at the size scales probed by XFM experiments. Furthermore, these standards are no longer produced and the need for new, stable, and well-characterized XFM standards is growing along with the recent global proliferation of synchrotron sources.

Here we report the production and characterization of an initial thin film standard consisting of ca. 15-nm layers of Cr, Fe, Ni and Ti. The films were prepared from focused ion spluttering of a pure target onto 1-µm-thick silicon nitride membranes. The SiN windows were positioned on a silicon wafer during coating and this substrate was analyzed using ICP-OES to establish the areal density of each element. The coated SiN windows were then scanned at the XFM beamline at the Australian Synchrotron and at 2-ID-E at the Advanced Photon Source for comparison. Current status and future goals of the project will be reported.

References:

[1] http://ts.nist.gov/MeasurementServices/ReferenceMaterials/

The Holographic Imaging Setup at the P10 Beamline of PETRA III

S. Kalbfleisch[1], B. Hartmann[1], K. Giewekemeyer[1], S. Krüger[1], H. Neubauer[1], M. Osterhoff[1], M. Bartels[1], O. Leupold[2], M. Sprung[2], T. Salditt[1]

[1] *Institut für Röntgenphysik, Universität Göttingen, Göttingen, Germany*
[2] *Hasylab, DESY, Hamburg, Germany*

Abstract:
The upcoming x-ray source PETRA III at DESY/Hamburg (Germany) will provide outstanding coherence properties. This source will enable a novel quality of hard x-ray coherent imaging based on iterative and holographic object reconstruction.

We are commissioning a dedicated setup for biological imaging at PETRA III with an optional cryogenic environment for biological samples, and *in situ* optical microscopy. The beam path is based on a non-dispersive coherent focusing scheme, compatible with monochromatic and pink beam operations, and a wide range of coherent imaging modalities. A fixed curvature Kirkpatrick-Baez (KB) mirror system with EEM polished mirrors [1] will provide a focal spot of about 200 nm diameter. For further beam reduction and cleanup as well as for additional coherence filtering, an x-ray waveguide stage with a set of 2nd-generation x-ray waveguides can be inserted in the focal plane [2]. Fresnel-type coherent diffraction imaging (FCDI) [3] as well as cone-beam holographic imaging based on an in-line (single beam) or off-axis (dual beam) configuration can be carried out [4]. All modalities can be extended by scanning [5] and tomography options, enabling large field of view in 3D.

References:

[1] H. Mimura et al., Appl. Phys. Lett. **90**, 051903 (2007).
[2] T. Salditt et al., Phys. Rev. Lett. **100**, 184801 (2008).
[3] B. Abbey et al., Nature Physics **4**, 394 (2008).
[4] C. Fuhse et al., Phys. Rev. Lett. **97**, 254801 (2006).
[5] K. Giewekemeyer et al., PNAS **107**, 529 (2010).

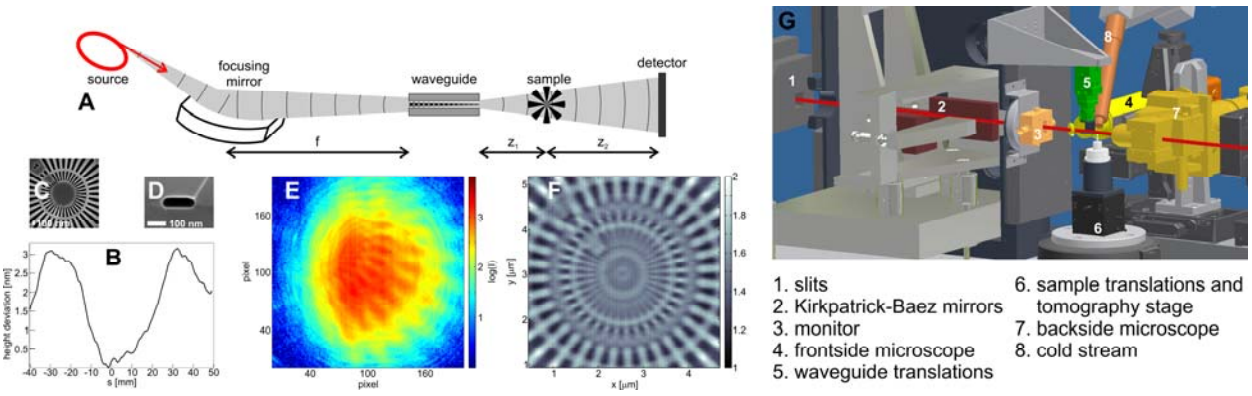

Figure 1: A Principle experimental scheme for waveguide based holographic imaging. **B** Measured deviation of the polished mirror from its ideal (elliptical) figure shape. **C** SEM image of a Siemens star. **D** SEM image of the entrance of a bonded waveguide. **E** Hologram of the Siemens star recorded by the pixel detector. **F** Combined reconstruction of several holograms, 50-nm lines and spaces are visible. **G** Schematic arrangement of the beamline and instrument components.

A New Scanning Transmission X-ray Microscope at the Advanced Light Source for Operation from 280 eV to 2500 eV *

D.A.L. Kilcoyne[1], A. Warwick[1], T. Tyliszczak[1], S. Rekawa[2], P. McKean[1], P. Monteiro[3]

[1]SSG, ESG, Advanced Light Source, LBNL, One Cyclotron Road, Berkeley, USA
[2]Center for X-Ray Optics, LBNL, One Cyclotron Road, Berkeley, USA
[2]Department of Civil and Environmental Engineering, University of Berkeley, Berkeley, California, USA

* This work was supported by the U.S. Department of Energy under contract number DE- AC02-05CH11231.

Abstract:

We report on the design and construction of a higher energy scanning transmission x-ray microscope on a new bend magnet beam line [1] at the Advanced Light Source. Previously we have operated such an instrument on a bend magnet for C, N, and O 1s NEXAFS spectroscopy [2]. The new instrument will have similar performance at higher energies up to and including the S 1s edge at 2472 eV.

A new microscope configuration is planned. A more open geometry will allow a fluorescence detector to count emitted photons from the front surface of the sample. There will be a capability for zone plate scanning in addition to the more conventional sample scanning mode. This will add the capability for imaging a massive sample at high resolution over a limited field of view, so that heavy reaction cells may be used to study processes *in situ*, exploiting the longer photon attenuation length and the longer zone plate working distances available at higher photon energy. The energy range will extend down to include the C 1s edge at 300 eV, to allow high energy NEXAFS microscopic studies to correlate with the imaging of organics in the same sample region of interest.

References:

[1] T. Warwick, H. Ade, D. Kilcoyne et al., J. Synchrotron Radiat. **9**, 254 (2002).
[2] A.L. Kilcoyne, T. Tyliszczak, W.F. Steele et al., J. Synchrotron Radiat. **10**, 125 (2003).

Development of Multilayer Laue Lenses; (2) Circular Type

T. Koyama[1*], T. Tsuji[1], H. Takano[1], Y. Kagoshima[1], S. Ichimaru[2], T. Ohchi[2], H. Takenaka[2]

[1]*Graduate School of Material Science, University of Hyogo, 3-2-1 Kouto, Kamigori, Ako, Hyogo 678-1297, Japan*

[2]*NTT-AT Nanofabrication Corporation, 3-1 Wakamiya, Morinosato, Atsugi, Kanagawa, 243-0124, Japan*

**present address: JASRI/SPring-8, 1-1-1, Kouto, Sayo-cho, Hyogo 679-5198, Japan*

Abstract:

Multilayer Laue Lens (MLL) which consists of thin film structure was pioneered and has been developed by the APS group [1]. It introduces Bragg diffraction effect for improving the spatial resolution and the diffraction efficiency. We have also developed MLL's as collaboration between Univ. of Hyogo and NTT-ATN [2]. In this paper, we report the fabrication and the performance test of the circular type MLL for producing a point focus.

The circular type MLL is fabricated by depositing a multilayer with DC magnetron sputtering on a graded wire core with the each boundary according to Fresnel zone configuration. Then sectioning and thinning was done to appropriate thickness for optimal diffraction efficiency. We adopted $MoSi_2$/Si as the multilayer materials. The $MoSi_2$/Si material combination having diffusion-less interfaces, heat resistance, and high diffraction efficiency is available for multilayer system [3]. The minimum (maximum) layer thickness, total multilayer thickness, and the number of layers is designed to be 13.2 (14.0) nm, 1.9 μm, and 140, respectively. The thickness along to the optical axis (optical depth) is set to be 50 μm. SEM micrographs of the circular type MLL were shown in Figure 1.

The focusing test was performed at Hyogo-ID (BL24XU) of SPring-8. A scanning transmission microscope was constructed using this circular type MLL. A Si(111) monochromator was used to select an X-ray energy of 20 keV. The obtained scanning transmission image of a test chart is shown in Figure 2. The measurement conditions were set to be 80 (460) pixels with 100 (10) nm step scan in horizontal (vertical) direction respectively, and the exposure time was set to be 0.1 s/pix. The finest structure of 50 nm line & space was resolved in vertical direction. The 1st order diffraction efficiency of the multilayer part was measured to be ~50%. This development was supported by SENTAN, JST.

References:

[1] H. C. Kang *et al*., Phys. Rev. Lett. **96**, 127401 (2006).

[2] T. Koyama *et al*., Appl. Phys. Express **1,** 117003 (2008).

[3] H. Takenaka *et al*., J. Appl. Phys. **78**, 5227 (1995).

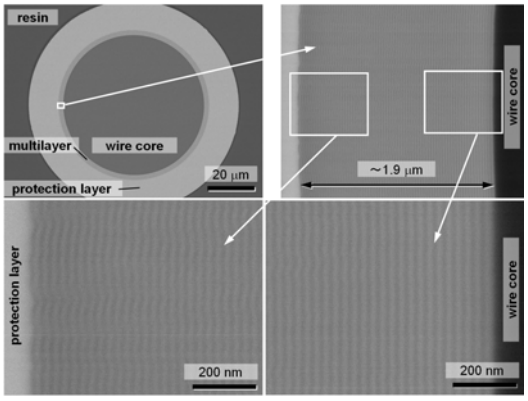

Figure 1: SEM micrographs of a $MoSi_2$/Si multilayer on a wire core.

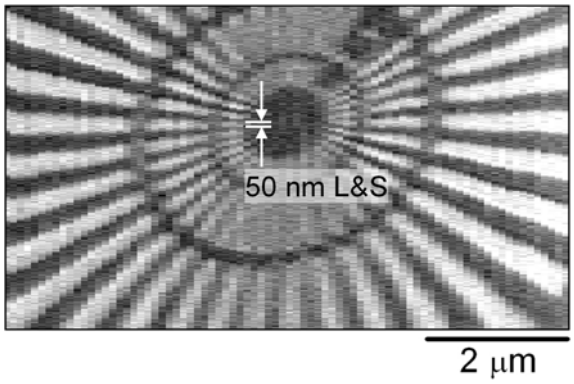

Figure 2: Scanning transmission intensity distribution of a Siemens-star test pattern.

Copper Speciation Studies of Biological Samples Using a Compact, Short Focal Distance Bent Crystal Laue Analyzer*

N. Kujala[1], C. Karanfil[2], D. Chen[3], Q. P. Dou[3], T. C. Irving[1], R. Barrea[1]

[1]*The Biophysics Collaborative Access Team (BioCAT), Dept of Biological Chemical, and Physical Sciences, Illinois Institute of Technology, Chicago, IL, USA*
[2]*Physics Department, Faculty of Arts & Sciences, Muðla University, Kötekli-Muðla 48187, Turkey*
[3]*The Prevention Program, Barbara Ann Karmanos Cancer Institute, and Department of Pathology, School of Medicine, Wayne State University, Detroit, Michigan, USA*

* This work was supported by National Cancer Institute, National Institutes of Health, and DOE.

Abstract:
Tumor growth and metastasis depend upon angiogenesis that, in turn, requires growth factors, proteases, and other cofactors including copper (Cu). Although the Cu oxidation state has not been directly implicated as being a characteristic of the tumor growth process, this can not be completely excluded as a potential role of Cu in tumor growth. Cu is also considered as a target for novel cancer therapies that offer a lower level of toxicity compared to current available chemotherapies.

An emerging technique that could potentially answer such questions is micro-X-ray fluorescence spectroscopy. Micro X-ray fluorescence spectroscopy can detect very low metal concentrations with high efficiency and identify oxidation states and coordination chemistry using spectral lines that are normally unresolved by other techniques. There are, however, some technical roadblocks to realizing the potential of this technique, mainly having to do with the detection/energy discrimination schemes used. Firstly, it is very difficult to analyze a system where the sample contains a dilute mixture of different Cu species with very similar spectral features. The mixture could be composed of Cu(I) and a relatively low concentration of Cu(II) species, which can be easily masked by the Cu(I) component, making their identification very difficult.

To overcome these limitations a high-energy-resolution and high-efficiency detection system has been developed for copper speciation in biological samples. The compact-short focal distance Bent Crystal Laue Analyzer (BCLA) with energy resolution of ~18 eV @ Cu Kα line has notable advantages to resolve the Cu Kα1, Kα2, and Kβ fluorescence lines, offering a very low background signal. The design involves a selection of the proper silicon crystal's thickness and bending curve to achieve an optimized energy resolution and sample-to-analyzer distance (~50 mm) with a detection limit ~10 ppm. This paper reports the performance results of the new BCLA with representative microXAS results from model compound samples.

Nanofabrication of Optical Elements for SXR- and EUV Applications: Ion Beam Lithography as New Approach

J. Lenz[1,2], T. Wilhein[1], S. Irsen[2]

[1]University of Applied Sciences Koblenz, RheinAhrCampus, Suedallee 2, 53424 Remagen, Germany
[2]Center of Advanced European Studies and Research (CAESAR), Ludwig-Erhard-Allee 2, 53175 Bonn, Germany

Abstract:
Diffractive optical elements are important components for applications in soft x-ray and extreme ultraviolet radiation. At present, the standard fabrication method for such optics is based on electron beam lithography followed by nanostructuring. This requires a series of complex processes including exposure, reactive ion-etching and electro-plating [1].

We report on experiments showing the single-step fabrication of such elements using ion beam lithography. Both, transmission and reflection gratings were fabricated (see Figures 1 and 2) and successfully implemented as spectrometers at laboratory soft x-ray sources. Structure sizes of 70 nm (reflection), 180 nm (transmission) and recently 40 nm in resolution test samples were achieved using a focused ion beam system [2]. In addition, first efforts towards zone plate pattern recording with FIB will be described.

Due to shorter process paths and higher flexibility regarding material choice, ion beam lithography is a promising alternative to existing fabrication methods.

References:

[1] M. Lindblom, J. Reinspach, O. v. Hofsten et al., J. Vac. Sci. Technol. B **27**(3), L5 (2009)
[2] J. Lenz, T. Wilhein and S. Irsen, Appl. Phys. Lett. **95**, 191118 (2009)

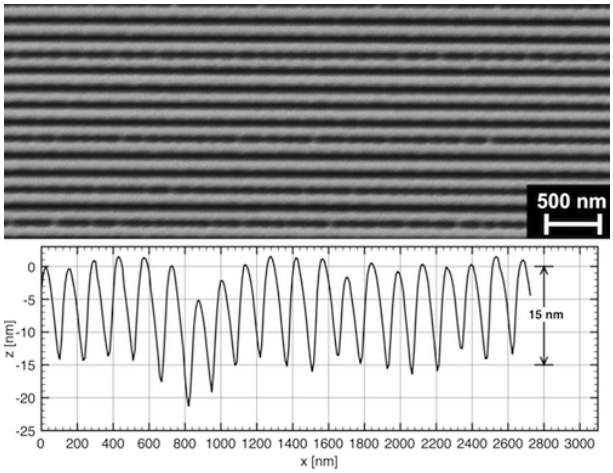

Figure 1: SEM-micrograph and AFM-profile of a grating (g = 140 nm, 153 periods) milled in 15 nm Cr on Si-substrate.

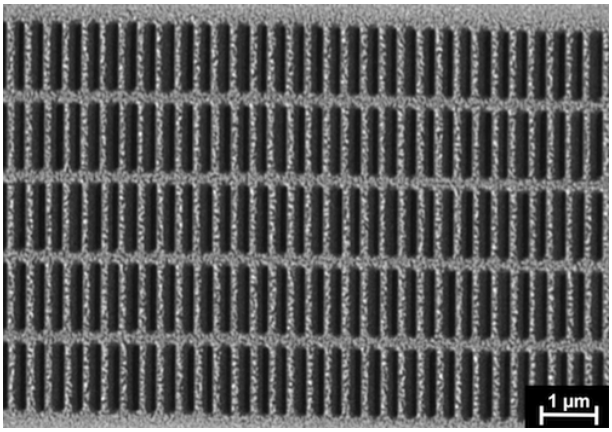

Figure 2: SEM-micrograph showing a freestanding grating (g = 363 nm, 256 periods, four horizontal support stripes) in 100 nm Si_3N_4 membrane (5 nm Au-coating).

Approaching Diffraction-Limited Resolution in Zone Plate-Based Soft X-ray Lithography

A. F. G. Leontowich, A. P. Hitchcock

McMaster University, Department of Chemistry, 1280 Main St. W., Hamilton, Ontario, Canada, L8S 4M1

Abstract:

The scanning transmission X-ray microscope (STXM) at Advanced Light Source beamline 5.3.2 (Berkeley, California, U.S.A.) routinely focuses monochromatic soft X-rays (250 - 700 eV) to a 30 nm spot under diffraction limited focusing conditions. We use this fine X-ray beam to pattern polymers in a manner analogous to lithography with a focused electron beam. Under optimized conditions <50 nm wide developed lines in poly(methylmethacrylate) (Figure 1) have been produced, which is approaching the diameter of the beam.

When high doses are administered radiation damage is observed well outside the position of the beam on the sample. This can extend more than 1 µm beyond the well defined exposure area (Figure 2) [1,2]. A multi-technique approach combining near edge X-ray absorption fine structure spectromicroscopy, chemical development, atomic force microscopy and scanning electron microscopy is being used to investigate processes of radiation damage and damage migration in polymers. The ultimate outcome is expected to be a much improved understanding of radiation chemistry and physics of resist materials.

References:

[1] J. Wang, H.D.H. Stöver, A.P. Hitchcock, T.J. Tyliszczak, Synchrotron Rad. **14**, 181-190 (2007).

[2] J. Wang, H.D.H. Stöver, A.P.J. Hitchcock, Phys. Chem. C **111**, 16330-16338 (2007).

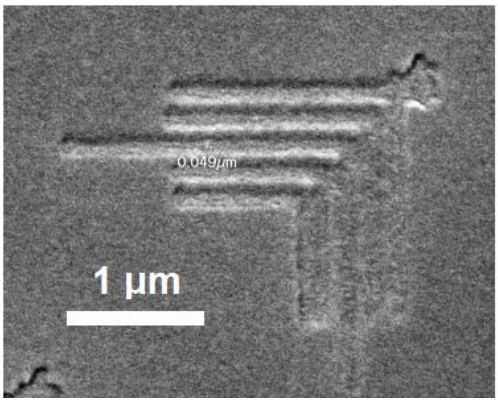

Figure 1: 1:1 elbow pattern in 50 nm PMMA on 75 nm Si_3N_4 demonstrating developed 40 nm lines. Dose: 0.7 MGy @ 300 eV

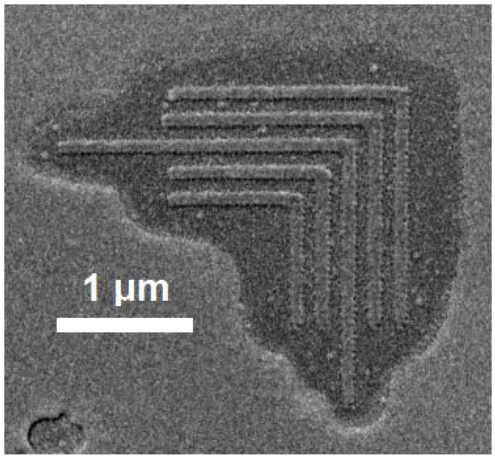

Figure 2: Dose: 170 MGy @ 300 eV, otherwise identical to Figure 1. The dose in the written elbow areas exceeds the threshold for cross-linking and thus these regions are converted from positive to negative resist.

The Commissioning Results and User Opening of the Hard X-Ray Micro-focus Beamline BL15U1 at SSRF

A. Li, K. Yang, H. Wang, F. Yan, X. Yu

Shanghai Synchrotron Radiation Facility, Shanghai Institute of Applied Physics, Chinese Academy of Science, Shanghai 201204, China

Abstract:

The commissioning results and condition of user opening at BL15U1 were introduced. BL15U1 is a hard x-ray micro-focus beamline for the energy range 3.5–22 keV combined with micro-X-ray fluorescence (μ-XRF), micro-X-ray absorption (μ-XAS), and micro-X-ray diffraction (μ-XRD). The first beam was observed on February 6, 2009. On April 18, important parameters of the beamline were tested and a beam size of 1.6 (H) × 1.8(V) μm^2 was achieved. The beamline was open for users on May 6, 2009. Up to December 31, 2009, 50 projects were performed and 253 shifts (8 hours/shift) were provided to users. In the future, 100 nm will be achieved at BL15U1 by using zone plate.

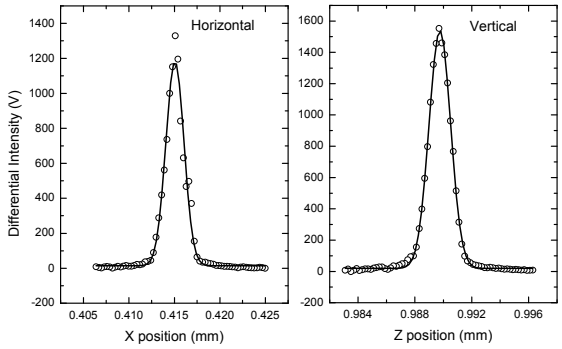

Figure 1: A beam size of 1.6 × 1.8 μm^2 was achieved.

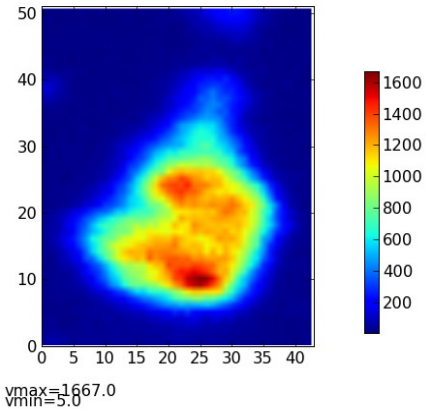

Figure 2: Ti distribution in the TiO_2-exposed A549 cell.

A Compact Sample-in-Air Soft-X-ray Microscope at PLS

J. Lim[1,2], H. J. Shin[1,2], C. K. Hong[2]

[1]*Pohang Accelerator Laboratory, POSTECH, San31, Pohang, Korea*
[2]*Department of physics, POSTECH, San31, Pohang, Korea*

Abstract:
Lens-based soft x-ray microscope [1-3] has become a promising probe for in-depth studies on nanostructures. A compact *in-situ*-experiment-capable full-field transmission soft-x-ray microscope (TXM) has been developed at Pohang Light Source (PLS). The TXM consists of a condenser zone plate with 2 mm-diameter for illumination and an objective zone plate with 40 nm-wide outermost zone for imaging scattered x-rays from a sample to an image plane. The measured spatial resolution was below 50 nm at photon energy of 500 eV (wavelength ~ 2.49 nm). The TXM is pinhole free and has been designed such that sample can be positioned in-air (with He flow) by using Si_3N_4 windows for separation of vacuum and air. This feature enables the total design compact and allows the use of commercial kinematic mounts for the optical elements, providing easy and fast alignment for focus. The air-gap around the sample is ~3 mm, within which various kinds of *in-situ* experimental setups can be implemented.

References:
[1] W.L. Chao, B.D. Harteneck, J.A. Liddle et al., Nature **435**, 1210 (2005).
[2] W.L. Chao, J. Kim, S. Rekawa et al., Opt. Express **17**, 17669 (2009).
[3] S. Rehbein, S. Heim, P. Guttmann et al., Phys. Rev. Lett. **103**, 110801 (2009).

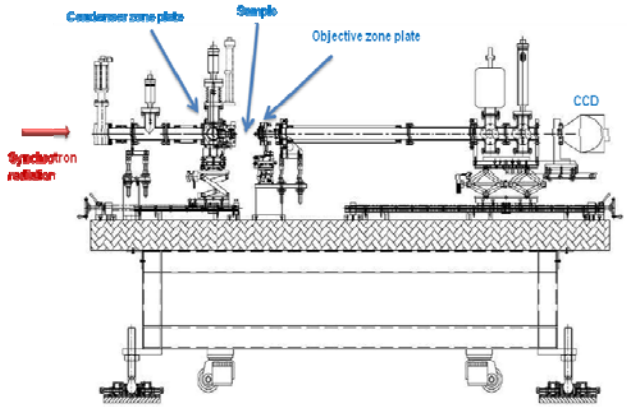

Figure 1: Optical configuration of a TXM at PLS.

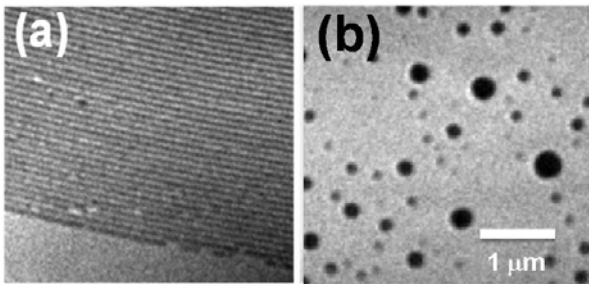

Figure 2: TXM images on (a) 50 nm lines and spaces and (b) Au nanoparticles.

Investigation on High Diffraction Orders of a Fresnel Zone Plate

E. Lima[1], S. Kim[2], A. Tripathi[2], Y. S. Chu[1], D. Legnini[2], M. Lu[1], D. J. Vine[2], H. Yan[1], I. McNulty[2]

[1]Brookhaven National Laboratory, Upton, New York 11973 USA
[2]Advanced Photon Source, Argonne National Laboratory, Argonne, Illinois 60439 USA

* This work is supported by the U. S. Department of Energy, under Contract No. DE-AC02-06CH11357 for the University of Chicago and Argonne, LLC., and under Contract No. DE-AC02-98CH10886 for the Brookhaven Science Associates, LLC.

Abstract:

X-ray microscopy provides a unique method for non-invasive, high-resolution imaging of thick samples such as biological cells or buried material structures. The advantages of the high-penetration power of x-rays combined with high-resolution optics have motivated numerous innovative approaches to x-ray optic development, bridging the gap between electron microscopy and optical microscopy [1-4].

Fabricating high-resolution x-ray optics, however, is intrinsically challenging since x rays interact with matters weakly and the resolution is ordinarily limited by the precision with which the smallest features can be made. In effort to overcome this limitation, several groups have shown that the high diffraction orders of a zone plate lens can be used for x-ray imaging, reaching a resolution beyond that of the first diffraction order [5,6]. However, zone plate performance with higher orders has not been fully investigated, especially the even orders, which have zero efficiency in the ideal case. In this paper, we report on the wavefield characterization of the first several diffraction orders (first through fourth) of a zone plate with a 50-nm outermost zone width using the method by Quiney et al. [7]. Distinct aberrations were observed in the higher orders as shown in Figure 1. We expect that future experiments combined with deconvolution after wavefield recovery can improve image quality in achieving ultra-high resolution utilizing the higher diffraction orders of x-ray zone plates.

References:

[1] W. Chao, et al., Nature **435**, 1210-1213 (2005).
[2] C.G. Schroer et al., Appl. Phys. Lett. **87**, 124103 (2005).
[3] H. C. Kang et al., Phys. Rev. Lett. **96**, 127401 (2006).
[4] K. Evans-Lutterodt et al., Phys. Rev. Lett. **99**, 134801 (2007).
[5] G. Yin et al., Appl. Phys. Lett. **89**, 221122 (2006).
[6] S. Rehbein et al., Phys. Rev. Lett. **103**, 110801 (2009).
[7] H. M. Quiney et al., Nat. Phys. **2**, 101 (2006).

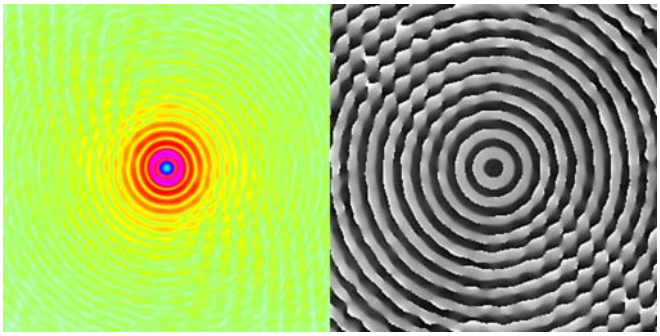

FIG. 1: The retrieved wavefield of 2nd diffraction-order at the focal plane, showing two-dimensional image of magnitude (left) and phase (right): aberrations in the side lobes are observed while the diffraction-limited focal size is obtained.

X-ray Laue Diffraction 3D Microscopy at the 34-ID Beamline of the Advanced Photon Source*

W. Liu[1,†], P. Zschack[1], J. Tischler[2], G. Ice[2], B. Larson[2]

[1]*Advanced Photon Source, Argonne National Laboratory, 9700 S Cass Ave, Argonne, IL 60439, USA*
[2]*Oak Ridge National Laboratory, 1 Bethel Valley Rd, Oak Ridge, TN 37831, USA*
[†]*Contact: wjliu@anl.gov*

* Work at the Advanced Photon Source is supported by the U.S. Department of Energy, Office of Science, Office of Basic Energy Sciences, under Contract No. DE-AC02-06CH11357.

Abstract:
Studies of materials on mesoscopic-length scales require a penetrating structural probe with submicron point-to-point spatial resolution. The principle research activities at beamline 34-ID-E of the Advanced Photon Source (APS) involve development of exciting new micro-/nano-diffraction techniques for characterization and microscopy in support of both applied engineering and fundamental materials research. Taking advantage of the high brightness of the source, advanced focusing mirrors [1], the depth-profiling technique [2], and high-speed area detectors, three-dimensional scanning polychromatic and monochromatic diffraction microscopy provides detailed local structural information of crystalline materials, such as crystallographic orientation, orientation gradients, and strain tensors (Figure 1). It is general and applicable to single-crystal, polycrystalline, composite, deformed, and functionally graded materials.

Applications include 3D diffraction investigations to a diverse and growing user community with interests in materials deformation [3], electro-migration, recrystallization, fatigue, solid-solution precipitation, high-pressure environments [4], and condensed matter physics.

References:

[1] B.C. Larson et al., Nature **415**, 887 (2002).
[2] W. Liu et al., Rev. Sci. Instrum. **76**, 113701 (2005).
[3] W. Liu et al., Ultramicroscopy **103**, 199 (2005).
[4] L. Wang et al, Proc. Natl. Acad. Sci. USA **107**, 6140 (2010).

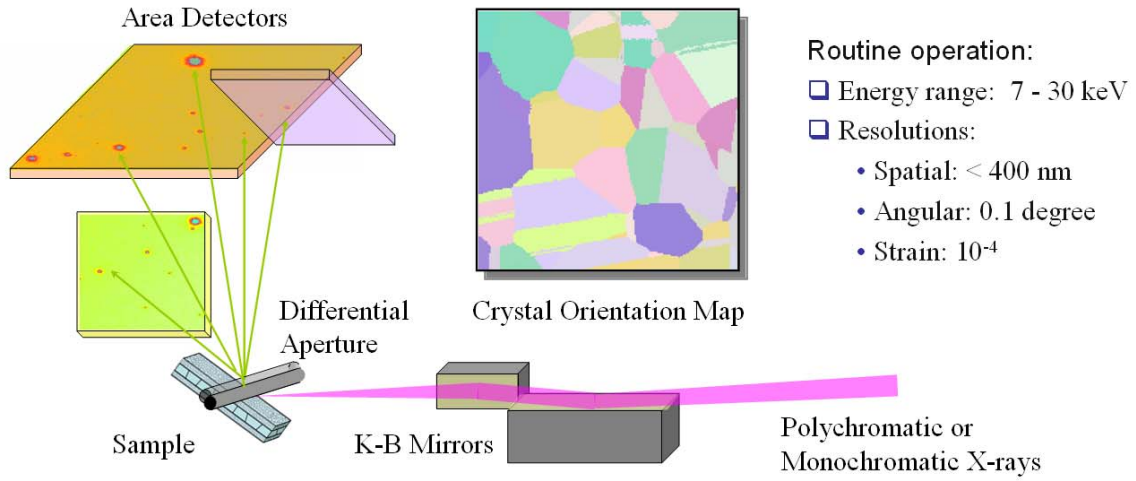

Figure 1: X-ray Laue diffraction 3D microscope at the 34-ID-E beamline, Advanced Photon Source.

Hard X-ray Zone Plates Using Ultrananocrystalline Diamond Molds*

D. C. Mancini, M. J. Wojcik, V. Joshi, A. V. Sumant, R. Divan, L. E. Ocola

Center for Nanoscale Materials, Argonne National Laboratory, Argonne IL 60439, USA

* Use of the Center for Nanoscale Materials was supported by the U. S. Department of Energy, Office of Science, Office of Basic Energy Sciences, under Contract No. DE-AC02-06CH11357.

Abstract:

To fabricate hard x-ray zone plates in high-density metals such as Au, the final zone plate structure is formed by electroforming Au in a high-aspect-ratio nanofabricated mold of a dielectric [1]. This mold structure must maintain its mechanical stability during subsequent processing. Current commercially produced zone plates are made by either direct patterning in organic resist by electron-beam lithography (EBL), or by pattern transfer into an organic layer by oxygen reactive ion etching (RIE) [2]. Recently, we have used HSQ as a resist material for the mold structure [3]. All of these materials are limited in their mechanical stability. Moreover, the mold must be removed prior to using the zone plates with intense x-rays because of radiation-induced damage. Diamond, however, is a dielectric with superior mechanical properties and radiation hardness: thus it is an ideal mold material for zone plate fabrication. Ultrananocrystalline diamond (UNCD), in particular, can be grown in thin films with the controlled stress and small grain size necessary to allow fabrication of molds for hard x-ray zone plates. Here, we describe our progress in the fabrication zone plates with Au electroformed in a UNCD mold.

UNCD is deposited by microwave plasma chemical vapor deposition to provide uniform layers on silicon substrates or window materials [4]. A thin film of metal, such as W or Ti, provides a surface that allows high-density seeding to enhance nucleation for the growth of the UNCD film, as well as to act as the plating base for subsequent electroforming. The pattern is transferred into the UNCD using an oxygen RIE etch that provides high anisotropy with good selectivity for UNCD over HSQ. The outermost zones can easily obtain aspect ratios greater than 8 with good adhesion and mechanical stability. Au is deposited into the UNCD mold structures by electroplating from solution. The resulting gold structures demonstrate the ability to produce hard x-ray zone plates. Application of these structures to hard x-ray nanofocusing optics is discussed.

References:

[1] R. Divan et al., Proc. SPIE **4783**, 82 (2002).
[2] W. Yun et al., Proc. SPIE **5539**, 133 (2004).
[3] M. Lu et al., Proc. SPIE **7039**, 70390V (2008).
[4] J.E. Butler and A. Sumant, Chem. Vapor Depos. **14**(7-8), 145 (2008).

Present and Future X-ray Tomographic Microscopy at TOMCAT

F. Marone[1], R. Mokso[1], P. Modregger[1,2], J. Fife[1,3], B. Pinzer[1,2], T. Thüring[1,2], K. Mader[1,2], G. Mikuljan[1], A. Isenegger[1], M. Stampanoni[1,2]

[1]*Swiss Light Source, Paul Scherrer Institut, Villigen, Switzerland*
[2]*Institute for Biomedical Engineering, University and ETH Zurich, Zurich, Switzerland*
[3]*Computational Materials Laboratory, EPFL, Lausanne, Switzerland*

Abstract:
During its first four years of life, the TOMCAT beamline [1] at the Swiss Light Source has established itself as a state-of-the art hard X-ray tomographic microscopy endstation for experiments on a large variety of samples, ranging from the field of biology to materials science. It routinely performs absorption as well as phase contrast imaging with an isotropic voxel size ranging from 0.360 up to 14.8 microns. Phase contrast is obtained either with simple edge-enhancement, a modified transport of intensity approach [2] or grating interferometry [3]. Typical acquisition times are in the order of few minutes, depending on energy and resolution. An automatic sample exchanger is available for high throughput studies [4].

In addition to further developments of phase contrast imaging, current scientific activities at the beamline focus on pushing spatial and temporal resolution by few orders of magnitude, aiming at nano- [5] and "real time" [6] tomography.

In addition to an overview of the hardware and techniques available at TOMCAT, we present here a palette of recent results.

References:

[1] M. Stampanoni et al., Proceedings of SPIE, Developments in X-ray Tomography **6318**; doi:10.1117/12.679497 (2006).
[2] A. Groso et al., Optics Express **14**, 8103-8110 (2006)
[3] S. McDonald et al., J. Synchrotron Radiat. **16**, 562-572 (2009)
[4] K. Mader et al., in preparation.
[5] M. Stampanoni et al., submitted (2010).
[6] R. Mokso et al., Proceedings of SRI09, to be published as an AIP Conference Proceedings.
[7] E.M. Friis et al., Int. J. Plant. Sci. **170**, 1086-1101 (2009).

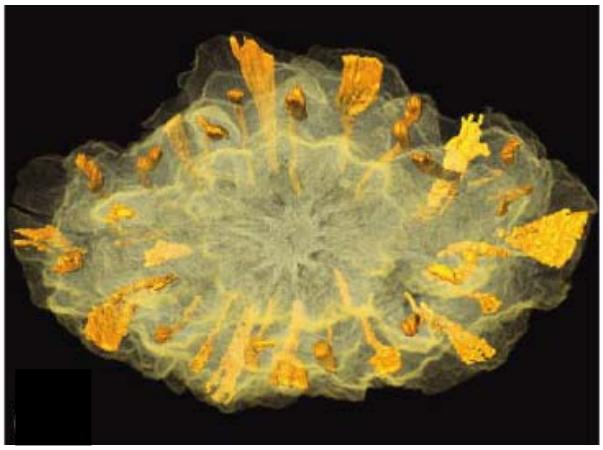

Figure 1: Early Cretaceous fossil flower of Portugal [7]: Vasculature embedded in a semitransparent reconstruction of the whole flower. Scale bar: 500 microns.

The Hard X-ray Nanoprobe at the Advanced Photon Source*

J. Maser, M. V. Holt, R. P. Winarski, V. Rose, G. B. Stephenson, P. Fuesz

Argonne National Laboratory, Argonne, Illinois 60439, USA

* Work supported by the U.S. Department of Energy, Office of Science, Office of Basic Energy Sciences, under Contract No. DE-AC02-06CH11357.

Abstract:

The Hard X-ray Nanoprobe (HXN) beamline at the Advanced Photon Source is designed to characterize composition and structure of nanoscale materials and devices with high spatial resolution [1]. Operating in the range of photon energies between 3 keV and 30 keV, the HXN takes advantage of the good penetration of hard X-rays to study buried structures and interfaces. Using a beam chopper, the HXN takes advantage of the pulsed nature of synchrotron radiation to study dynamic processes. X-ray fluorescence is used to identify and map trace constituents with high elemental sensitivity. X-ray diffraction and Bragg coherent diffraction are used to identify crystallographic phase, strain, and structure in novel materials and devices. In addition, the HXN integrates a tomographic full-field transmission mode that is used to characterize the 3-dimensional structure of complex systems and devices. All operation modes can be changed *in situ*. The HXN takes advantage of the good penetration of hard X-rays to study buried structures and interfaces

The HXN is optimized for the study of novel materials, such as ferroelectrics, complex oxides, thin films with novel structural and electronic/magnetic properties, and devices that utilize these properties. Typical applications include Si-based materials and devices, and novel materials and materials systems for potential use in energy applications, actuation, and switching. The high trace element sensitivity is also useful for characterizing metal distributions in biological systems such as cells and tissues. We will present the performance of the HXN and show initial nanoscience and materials science applications.

References:

[1] J. Maser, G.B. Stephenson, D. Shu et al., AIP Conf. Proc. **705**, 470 (2004).

A New Method for Manufacturing Fresnel Zone Plates

M. Mayer[1], C. Grévent[1], A. Szeghalmi[2], M. Weigand[1], S. Rehbein[3], M. Knez[2],
B. Baretzky[1], G. Schneider[3], G. Schütz[1]

[1]*Max-Planck-Institute for Metals Research, Heisenbergstr. 3, Stuttgart, Germany*
[2]*Max-Planck-Institute of Microstructure Physics, Weinberg 2, Halle (Saale), Germany*
[3]*HZB for Materials and Energy, BESSY II, Albert-Einstein-Str. 15, Berlin, Germany*

Abstract:
The most popular focusing device for x-ray microscopes is the Fresnel zone plate (FZP). Driven by the desire for higher resolution, several approaches have been taken to push the resolution towards 10nm and beyond [1-3].

For the first time, a new method to manufacture FZPs circumventing the drawbacks related to electron beam lithography is presented. This approach is based on the deposition of concentric thin films of x-ray absorbing and transmitting material on a rotational symmetric substrate via atomic layer deposition (ALD). Subsequent thinning and polishing of the FZPs to thicknesses suitable for the soft x-ray regime are performed with focused ion beam (FIB) milling in an FEI DualBeam™ (FIB/SEM) instrument [4]. This technique offers great potential for the fabrication of fine outermost zones thus enhancing resolution and enabling the production of FZPs suitable for both the soft and hard x-ray regime.

First measurements with these new FZPs as focusing element in the recently introduced SXM at BESSYII, MAXYMUS, allowed us to resolve features down to 47nm in size, in the soft x-ray regime [5].

References:
[1] W. Chao et al., Nature **435**, 1210 (2005).
[2] J. Vila-Comamala et al., Ultramicroscopy **109**, 1360 (2009).
[3] S. Rehbein et al., Phys. Rev. Lett. **103**, 110801 (2009).
[4] M. Mayer, C. Grévent, B. Baretzky, G. Schütz, German patent application Nr. 10 2009 050 688.8, (2009).
[5] M. Mayer et al., manuscript in preparation

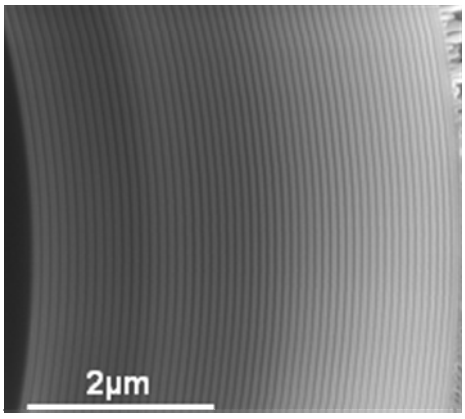

Figure 1: SEM micrograph of the Zone-structure of a FZP obtained with ALD in close-up view.

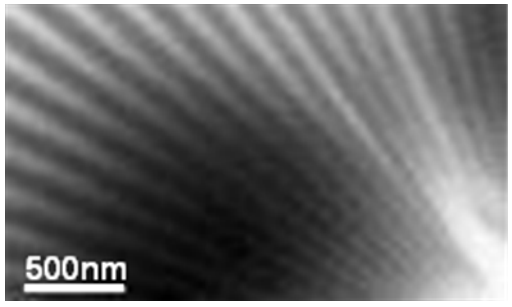

Figure 2: SXM image of a Ni Siemensstar test pattern obtained with the new FZP.

Development of the Sub-nm Spatial Resolution Fiber Optic Interferometer for the Hard X-ray Microscope for the Nanoprobe Beamline at NSLS-II*

E. Nazaretski[1], S. O'Hara[1], D. Shu[2], H. Yan[1], J. Maser[2], Q. Shen[1], Y. S. Chu[1]

[1]*Brookhaven National Laboratory, Upton, NY 11973, USA*
[2]*Argonne National Laboratory, Argonne, IL 60439, USA*

* This work was supported by the Brookhaven Science Associates, LLC under Contract No. DE-AC02-98CH10886 with the U.S. Department of Energy.

Abstract:
We present a recently developed fiber-optic-based interferometer to be used in the hard X-ray microscope at the Nanoprobe beamline at NSLS-II. The interferometric system developed in collaboration with Attocube AG has a compact design (enabling active feedback on a measurement point very close to the sample or the x-ray optics, thereby minimizing the drift due to temperature gradients), sub-nanometer spatial resolution, and a working distance of up to 100 millimeters. In this presentation we discuss details of the design and evaluate the performance of the system. We discuss two sets of experiments that allow us to characterize the long-term stability and the spatial resolution of the instrument. For stability measurements the cryogenically cooled interferometric cavity has a well-defined length and enables characterization of the drifts associated with the stability of the laser source and control electronics. Mounting of the reflector on a PI scanner and direct comparison of the interferometric read-outs with the built-in capacitive sensors of a PI PicoCube scanning stage operated in a closed-loop mode allows us to determine the spatial resolution/bandwidth of the interferometer. The compact design and high spatial resolution of the instrument reduce the linear dimensions of a hard X-ray microscope at NSLS-II.

Zone Plates for Hard X-ray FEL Radiation

D. Nilsson[1], A. Holmberg[1], H. Sinn[2], U. Vogt[1]

[1]Biomedical and X-Ray Physics, Department of Applied Physics, Royal Institute of Technology, SE-106 91 Stockholm, Sweden

[2]European XFEL – Notkestrasse 85, D-22607 Hamburg, Germany

Abstract:

Zone plates are high-quality optics that have the potential to provide diffraction-limited nano-focusing of hard x-ray free electron laser radiation. We theoretically investigate the temperature behavior of metal zone plates on a diamond substrate irradiated by 0.1-nm x-rays from the European X-ray Free Electron Laser [1]. The proposed design has the advantage of being compatible with current nanofabrication techniques. Two different zone plate designs are considered, one smaller zone plate placed in the direct beam and one larger zone plate after a monochromator. Using finite element software, we simulate the temperature in the optic during a full pulse train of 3000 pulses. The simulations show that the proposed cooling scheme is efficient enough to keep the zone plate well below melting temperature throughout the pulse train. However, zone plates in the direct beam will experience large and rapid temperature fluctuations of several hundred Kelvin that might prove fatal to the optic. The situation is much improved behind the monochromator where the fluctuations are in the 20 K range. The simulation results give valuable indications on the temperature behavior to expect and are a basis for future experimental investigations of fabricated nanostructures. We also present our first results from fabrication of hard x-ray zone plates in gold and platinum.

References:

[1] D. Nilsson, A. Holmberg, H. Sinn, U. Vogt, Nucl. Instrum. Methods A, in press; doi: 10.1016/j.nima. 2010.03.115

Development of a Versatile End Station for Space- and Time-Resolved Experiments at FLASH and PETRA III*

T. Nisius[1], M. Wieland[2], M. Schlie[2], M. Drescher[2], T. Wilhein[1]

[1]*Institute for X-Optics (IXO), RheinAhrCampus, Remagen, Germany*
[2]*Institute for Experimental Physics, Hamburg University, Hamburg, Germany*

* This work is supported by the German Federal Ministry of Education and Research under contract 05 KS7GU4 and 05 KS7UL1.

Abstract:
A versatile end station for FLASH and PETRA III is presented. This end station offers the possibility to perform a wide variety of experiments like high-intensity x-ray matter interaction, high-resolution microspectroscopy, and x-ray microscopy.

The setup consists of three separate cylindrical vacuum chambers dedicated to beam forming, x-ray-matter interaction, and detection. Each chamber is equipped with a rail-guide system to support different optical modules and allows their movement along the beam direction. Transversal movement is provided by compact piezomotor stages.

The modular concept of the vacuum chambers (Figure 1) in conjunction with exchangeable motorized stages makes it possible to easily adapt the measurement setup to the experimental requirements. The detector section can be equipped with different space- and time-resolving detectors like CCD cameras as well as ion and electron spectrometers.

One of the main applications is nanofocusing in order to achieve ultra-high x-ray intensities up to 10^{18} W/cm^2 at FLASH. When configured for imaging applications, it is possible to perform microspectroscopy or x-ray microscopy experiments.

Furthermore, a wavelength-tunable femtosecond laser capable of the high repetition rate of PETRA III can be synchronized to the x-ray pulses for performing time-resolved pump-probe experiments.

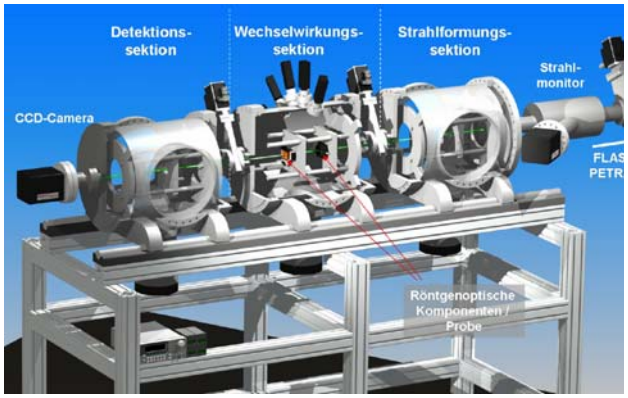

Figure 1: The modular concept of the proposed end station consisting of three dedicated modules.

Development of a Computer Tomography System for the Soft X-ray Microscope at Ritsumeikan University

T. Ohigashi[1], H. Fujii[2], K. Usui[2], H. Namba[2], H. Mizutani[3], K. Takemoto[4], H. Kihara[4]

[1]*Research Organization of Science & Engineering, Ritsumeikan University, 1-1-1 Noji Higashi, Kusatsu, Shiga, Japan*
[2]*Department of Physics, Ritsumeikan University, 1-1-1 Noji Higashi, Kusatsu, Shiga, Japan*
[3]*Science Integration Program, Organization for Interdisciplinary Research Projects, University of Tokyo, 5-1-5 Kashiwanoha, Kashiwa, Chiba, Japan*
[4]*Department of Physics, Kansai Medical University, 18-89 Uyamahigashi, Hirakata, Osaka, Japan*

Abstract:
The soft x-ray microscopy system at the SR Center in Ritsumeikan University (575 MeV, 300 mA) was designed for the observation of biological samples by using the water window region, and an x-ray transmission image of ~50 nm resolution can be acquired [1,2]. This system is still in development for performing further applications [3,4]. Recently, a set of sample stages were also installed and the optical system was optimized for performing computed tomography (CT). In case of the observation of a thick sample with complex structures, the overlapped structures along the optical axis are imaged as one integrated image so that the image is resolved less. Then, the 3-dimensional imaging by CT solves this problem and provides structural information of line absorption coefficients. In this study, the performance of our system is evaluated and some examples of the 3D observations are shown.

In Figure 1, the volume rendering image of the bacteria is shown. The bacteria were dried and held on the tip of a glass capillary tube. Fifty projected images were acquired every 3.6 degrees using an x-ray wavelength of 1.9 nm. Then the image was magnified 1000 times, and the each exposure time was 150 s. The images were aligned manually and reconstructed by the filtered back-projection method. Figure 2 shows a cross sectional image, whose position is indicated in Figure 1.

References:

[1] A. Hirai, K. Takemoto, K. Nishino et al., J. Synchrotron Radiat. **5**, 1102 (1998).
[2] A. Hirai, K. Takemoto, K. Nishino et al., Jpn. J. Appl. Phys. **38**, 274 (1999).
[3] K. Takemoto, H. Namba, M. Mukai et al., J. Phys.: Conf. Ser. **186**, 012019 (2009).
[4] M. Kimura, K. Takemoto, Y. Ohashi et al., Jpn. J. Appl. Phys., submitted.

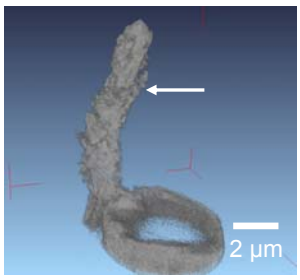

Figure 1: Volume rendering image of the bacteria.

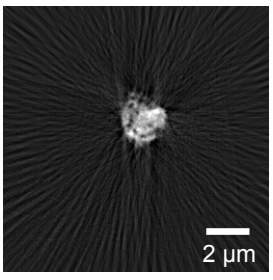

Figure 2: Cross sectional image of the bacteria.

Development of a Small-Animal Phase-Contrast MicroCT Scanner

B. Pauwels[1], A. Sasov[1], K. Sorgeloos[1], P. Bruyndonckx[1], J. Kenntner[2], J. Schulz[2], J. Mohr[2], A. Tapfer[3], M. Bech[3], K. Achterhold[3], F. Pfeiffer[3]

[1]*SkyScan, Kartuizersweg 3B, 2550 Kontich, Belgium*
[2]*Karlsruhe Institute of Technology, 76344 Eggenstein-Leopoldshafen, Germany*
[3]*Technische Universität München, 85748 Garching, Germany*

Abstract:

During the last years, a number of different phase-contrast and reconstruction techniques for X-ray imaging have been explored. Most of them can be easily implemented when using synchrotron radiation; however, adapting the same techniques for lab-based x-ray sources is more challenging. Grating interferometry may overcome some of these challenges, and has proven its potential for lab-based X-ray phase-contrast imaging in several recent proof-of-principle experiments using lab-sources [1-5].

With this contribution, we present the concept and first experimental commissioning results concerning the ongoing developments of a first phase-contrast microCT scanner dedicated to future in-vivo small-animal imaging applications. The initial experimental test set-up consists of an x-ray source with an Ag target, a rotation stage connected with a plexiglas sample holder and a camera assembly. The camera assembly consists of a scintillator and a 1.3 megapixel cooled 14-bit CCD camera with a fixed focus lens in front. The source-to-object and the object-to-detector distances are taken in such a way that the field of view at the position of the object is 35 mm, sufficient to visualize a mouse.

Quantitative phase-contrast, absorption, and dark-field images are obtained using the three-grating method [1-5]: a grating G0 is positioned just in the front of the source to divide the large x-ray spot into multiple smaller x-ray sources, a phase grating G1 is placed approx. 50 mm behind the sample stage and an analyzer grating G2 just before the scintillator of the camera assembly. The total setup length is compact enough to fit into rotating gantry, with a total length of 45 cm. After the initial commissioning experiments with a non-rotating static gantry and a rotating sample, the setup will be mounted onto rotating gantry with the immobile small animal sample in the center.

References:

[1] F. Pfeiffer et al., Nature Physics **2**, 258 (2006).
[2] F. Pfeiffer et al., Phys. Rev. Lett. **98**, 108105 (2007).
[3] F. Pfeiffer et al., Nature Materials **7**, 134 (2008).
[4] M. Bech et al., Phys. Med. Biol. **54**, 2747 (2009).
[5] J. Herzen et al., Opt. Express **17**, 10010 (2009).

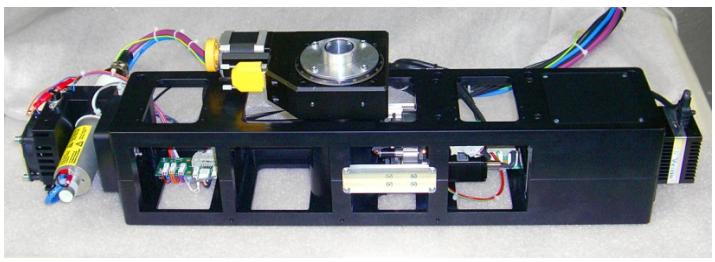

Figure 1: Photograph of the assembled gantry for the small-animal phase-contrast microCT system.

MISTRAL Beamline Status at ALBA and Scientific Applications

E. Pereiro, M. Brzhezinskaya, D. Bacescu, R. Valcárcel, A. Milán

ALBA Synchrotron Light Source, Carretera BP 1413 de Cerdanyola del Vallès a Sant Cugat del Vallès km 3.3, 08290 Cerdanyola del Vallès, Barcelona, Spain

Abstract:
The ALBA synchrotron radiation facility will be opened for users in 2011. It is a 3 GeV, low-emittance storage ring able to run in top-up mode. The storage ring is planned to be operated at a nominal current of 250 mA, although in the future it is foreseen to operate at a maximum of 400 mA.

One of the beamlines in first construction phase is the Transmission X-ray Microscopy (TXM) beamline, MISTRAL (MIcroscopy and Spectroscopy in TRansmission at ALba), which is located at a bending magnet port. This project is driven by the needs of a biological community for a TXM with capabilities for cryo-tomography in the water window and multi-keV spectral regions. X-ray microscopy has been shown to provide insight into the internal structure of whole cells [1,2], and its aim, in combination with other techniques, is to be able to locate subcellular structures during key cellular events.

In what follows, we report the status of the MISTRAL beamline which installation was achieved in spring 2010. A Variable-Line-Spacing Plane Grating Monochromator with an entrance slit delivers monochromatic light in the range of 270 - 2600 eV to a single-reflection elliptical hollow glass capillary, which will in turn, focus the light on to the sample. The transmitted signal will be collected by an objective Fresnel zone plate and a magnified image will be delivered to a CCD detector. The Transmission X-ray Microscope will be installed at the beginning of September 2010.

Scientific applications have already started with the group of Prof. Carrascosa (CNB CSIC, Madrid, Spain) using the TXM of the Helmholtz Zentrum Berlin (Bessy II) [3]. After revealing inner structure compartments of isolated vaccinia virus particles with a spatial resolution of 51 nm [4], we have acquired x-ray tomograms at cryogenic temperature of Ptk2 cells infected with vaccinia virus at different post-infection times so to investigate the morphogenesis of the virus and compare the results with the standard electron microscopy methodologies, which are limited by the fact that only cellular sections on the order of half of the virus particle size can be investigated.

References:

[1] G. Schneider, Ultramicroscopy **75**, 85 (1998).
[2] C.A. Larabell and M. A. Le Gros, Mol. Biol. Cell **15**, 957 (2004).
[3] G. Schneider, P. Guttmann, S. Heim et al., AIP Conf. Proc. **879**, 1241 (2007).
[4] J.L. Carrascosa, F.J. Chichón, E. Pereiro et al., J. Struct. Biol. **168**, 234 (2009).

Advances in Nanoscale Chemical Imaging Techniques Using Full-Field Hard X-ray Microscopy at SSRL*

P. Pianetta, J. C. Andrews, F. Meirer, Y. Liu

Stanford Synchrotron Radiation Lightsource, SLAC National Accelerator Laboratory, Menlo Park CA, USA

*This work has been supported by the National Institutes of Health (NIH)/ National Institute of Biomedical Imaging and Bioengineering (NIBIB) grant number 5R01EB004321. SSRL is supported by the Department of Energy, Office of Basic Energy Sciences.

Abstract:
The full-field hard x-ray transmission microscope on BL 6-2 at SSRL is capable of imaging from 5-14 keV, with up to 30 nm resolution. It has been used to image biological samples including mineralized tissue used for studies of dental regeneration and of osteoporosis in bones, environmental studies of heavy metal transformation and distribution in plants useful in phytoremediation, and in studies of energy materials including nanowires and recharging of battery electrodes. Recent advances have been in determination of attenuation coefficients from 3D tomography to quantify absorption by elements within a sample, and in X-ray absorption near edge structure (XANES) determination by imaging as the monochromator is tuned. Applications of these advances to samples from several fields will be highlighted.

The Development of a Tabletop Soft X-ray *in vitro* Microscope

K. Powell[1], G. Duffy[1], P. Choi[1], R. Aliaga-Rossel[1], C. Zaepffel[2], A. Michette[3]

[1] *NANO-UV sas, 16-18 av du Québec, SILIC 705, Villebon/Yvette 91140, France*
[2] *EPPRA sas, 16 av du Québec, SILIC 706, Villebon/Yvette 91140, France*
[3] *Kings College London, Strand, London, WC2R 2LS, UK*

Abstract:
The use of X-ray microscopy has become well established, particularly at wavelengths in the region of the so-called 'water window', where good contrasts at high resolution can be achieved naturally in hydrated samples. Soft X-ray microscopy is thus an attractive option for the study of biologically derived samples *in vitro*. The penetrating nature of X-rays removes the necessity for such samples to be specially prepared, by thin sectioning for example, or by the need to make them compatible with the high vacuum requirements of electron microscopy. Staining or otherwise denaturing the sample to provide enhanced contrast levels, as is often required with other microscopy techniques, can also be avoided.

Traditionally, the only suitable sources of soft X-rays for microscopy are provided by dedicated synchrotron beam lines, creating a roadblock to the commercialization and rollout of smaller laboratory scale X-ray microscopes for use in the wider community. A number of laboratories have worked to develop a soft X-ray microscope using laser-generated plasma radiation sources, but there are as yet no commercial products available for routine operation. To overcome this roadblock, NANO-UV has engaged in a product development program to introduce the first affordable standalone compact soft X-ray microscope for *in vitro* studies, known as McXI (Microscope X In-vitro).

This is made possible by a compact, impulse-discharge, plasma-based soft X-ray source that combines the properties of high brightness, high flux, and small beam divergence. The initial specification of McXI is to provide 100-nm resolution on *in vitro* specimens, with a unique wavelength selection mechanism in the 2.3-4.4 nm region. This source is coupled to a set of diffractive optics to provide a first magnification between x50 to x100, depending on the wavelength. The sample is imaged onto a scintillator screen to provide a visible light image. This image contains details at the nanometer scale and is further magnified by a conventional optical microscope, yielding a maximum total magnification of x20,000 to x40,000. Design consideration and operation data of McXI will be presented.

In parallel with this development, a Eurostars Project McXI E!4885 has been initiated with partners Delong Instrument from the Czech Republic and Silson Ltd in the UK. The project goal is to extend the resolution of McXI down to 20 nm, with improved sample handling and man-machine interface design to broaden the application range of this standalone microscope. An outline of this project will be presented.

The Imaging and Coherence Beamline I13L at Diamond

C. Rau[1], U. Wagner[1], Z. Pesic[1], I.K. Robinson[2], B. Singh[1]

[1]Diamond Light Source Ltd., Harwell Science and Innovation Campus, Didcot, OX 11 0DE, United Kingdom
[2]University College London, London Centre for Nanotechnology, 17-19 Gordon Street, London WC1H 0AH, United Kingdom

Abstract:
The coherence and imaging beamline I13L is dedicated to hard X-ray microscopy either in direct or reciprocal space. For both lens and lensless imaging, two independent stations will be operated at a distance of 250 m from the source. The coherence length can be adjusted over a large range by a modification of the electron beam in the storage ring and slits in the front end. The imaging branch will perform In-line phase contrast imaging and tomography over a large field of view in the 6-30 keV energy range. In addition it will be possible to switch to full-field microscopy with 50-nm spatial resolution. Projection microscopy will be developed, as it is dose efficient and therefore particularly suitable for radiation-sensitive samples.

Resolution beyond the limitations given by the detector and X-ray optics may be achieved with techniques working in the far field. For crystalline samples, coherent x-ray diffraction allows us not only to reconstruct the shape of nano-crystals but also to provide 3D information about parameters such as internal stress. Other coherent diffraction imaging techniques such as ptychography will be also implemented on the same 'coherence' branch. The stations will be operational in 2011.

The different microscopy methods available at I13L and the optical layout of the beamline will be discussed. Typical applications from the scientific program will be presented.

References:

[1] C. Rau, U. Wagner, A. Peach et al., "The Diamond Beamline I13L for Imaging and Coherence", Proc. SRI 2009, to be published.
[2] C. Rau, U. Wagner, "Optical Design in Phase-Space for the I13L X-Ray Imaging and Coherence Beamline at Diamond using PHASY," Proc. SRI 2009, to be published.
[3] B. Singh, R. Bartolini, R. Fielder, E.C. Longhi, I.P. Martin, U.H. Wagner, C. Rau, PAC09 proceedings to be published.

15-nm Efficiency-Enhanced Soft X-ray Zone Plates

J. Reinspach, M. Lindblom, O. von Hofsten, M. Bertilson, H. M. Hertz, A. Holmberg

Biomedical and X-Ray Physics, Department of Applied Physics, Royal Institute of Technology, SE-10691 Stockholm, Sweden

Abstract:

The development of zone plates is essential for the progress of high-resolution soft x-ray microscopy. A narrow outermost zone width must be combined with a high-aspect ratio zone profile to attain both high resolving power and high diffraction efficiency.

In this contribution we present our recent advances in soft x-ray zone plate fabrication at the Royal Institute of Technology (KTH), Stockholm. The resolution in our trilayer-resist-based process [1] has been improved by introducing cold development of the electron-beam-patterned resist ZEP 7000 in hexyl acetate at -50 °C [2]. With this process, nickel zone plates with 13 nm outermost zone width and 35 nm nickel height were fabricated (see Fig. 1). To increase the diffraction efficiency of these high-resolution nickel zone plates, a process for fabricating so-called nickel-germanium zone plates has been developed [3]. In this process a nickel zone plate is used as hardmask for a CHF_3 dry etch into an underlying germanium film, resulting in a higher efficiency nickel-germanium zone plate. By a direct measurement of the diffraction efficiency of zone plates with 15 nm outermost zone width we demonstrate an efficiency enhancement of 50% compared to the corresponding nickel zone plate [4].

References:

[1] A. Holmberg, S. Rehbein, and H. M. Hertz, Microelectron. Eng. **73–74**, 639 (2004).
[2] J. Reinspach, M. Lindblom, O. v. Hofsten et al., J. Vac. Sci. Technol. B **27**, 2593 (2009).
[3] M. Lindblom, J. Reinspach, O. v. Hofsten et al., J. Vac. Sci. Technol. B **27**, L5 (2009).
[4] J. Reinspach et al., in preparation.

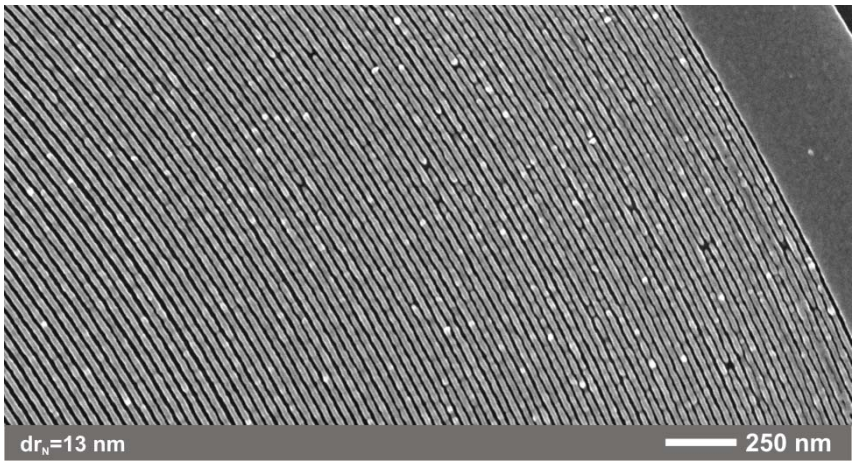

Figure 1: SEM image of the outer part of a nickel zone plate with 13 nm outermost zone width. The nickel thickness is 35 nm.

25-keV Transmission X-ray Microscope Based on X-ray Refractive Lenses

E. Reznikova[1], R. Simon[2], V. Nazmov[1], M. Simon[1], J. Mohr[1], V. Saile[1]

[1]*Institute for Microstructure Technology, Karlsruhe Institute of Technology, Germany*
[2]*Institute for Synchrotron Radiation, Karlsruhe Institute of Technology, Germany*

Abstract:

The optical scheme of the 25-keV transmission X-ray microscope (TXM) assembled at the ANKA FLUO beamline was the following: monochromatic synchrotron radiation → slits → laminar horizontal grating → condenser lens → test object → objective lens → digital X-ray imaging detector (Fig. 1). The crossed linear concave-concave elements of the planar lenses focused in vertical (V) and horizontal (H) directions due to the lens fabrication by tilted deep X-ray lithography [1] (Fig. 2a). The VHVH sequence of the objective lens elements provided an equivalent magnification factor for 2D imaging due to identical object and image focal lengths for the lens elements that focused in vertical and horizontal directions, respectively. Test objects were placed in the object focal plane of the image lens and in the image focal plane of the VVHH type condenser with 280×280 μm^2 aperture. The horizontal gold grating with a period of 2.4-μm spread the condenser focal spot to the 60×60 μm^2 area corresponding to the objective lens aperture; this resulted in a gain factor of ~ 4 for the object illumination. Phase contrast images of different test nano structures were obtained for an X-ray magnification factor of 41 with the detector scale of 12 nm/pixel and exposure time of 5 sec (Fig. 2b). Special test star nanostructures with a low phase shift of 0.03 radians were imaged; ~ 200-nm lines were resolved in the level of the image intensity noise for the exposure time limit of 65 sec (Fig. 2c). The calculated resolution of the images by means of Modulation Transfer Functions is about 60 nm.

The result demonstrates in principle the possibility to use the 25-keV TXM for imaging of living biological cells having a low phase contrast but close-to-zero X-ray absorption and radiation damage. In order to improve visibility of the objects and to observe them in a real time we tend to increase the photon flux of their illumination using new types of rolled condensers with large apertures and to modulate the low phase contrast by means of additional diffractive optics with a nano periodical phase shift.

Reference:

[1] E. Reznikova, T. Weitkamp, V. Nazmov et al., J. Phys.: Conf. Ser. **186**, 012070 (2009); online open-access.

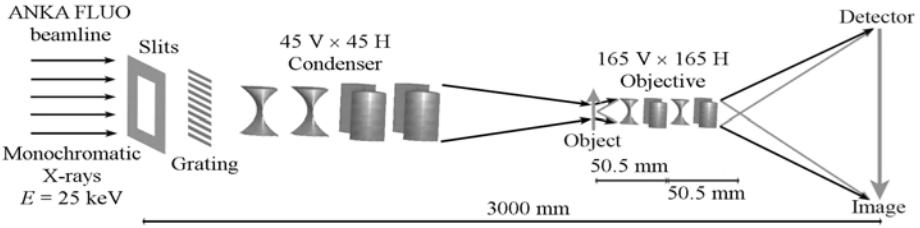

Figure 1: Optical scheme of the 25-keV TXM.

(a) 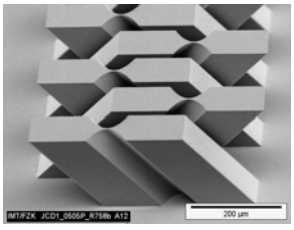 (b) 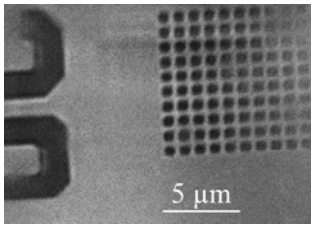 (c) 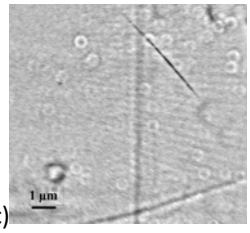

Figure 2: (a): SEM view of the objective lens elements. (b) and (c): 25-keV TXM images of test objects.

30-keV Transmission X-ray Microscope Based on X-ray Refractive Planar Crossed Parabolic SU-8 Lenses

E. Reznikova[1], M. Radtke[2], H. Riesemeier[2], V. Nazmov[1], J. Mohr[1], V. Saile[1]

[1]*Institute for Microstructure Technology, Karlsruhe Institute of Technology, Germany*
[2]*BAM Bundesanstalt für Materialforschung und -prüfung, Division I.3 Structure Analysis; Polymer Analysis, Germany*

Abstract:

A transmission X-ray microscope (TXM) was set up in an air environment at the BESSY 7T-WLS/1-BAMline-KMC [1]. The TXM was tested with 30-keV X-ray photons and refractive crossed parabolic lenses made out of SU-8 polymer by a ±45° tilted deep X-ray lithography [2]. The objective and condenser planar lenses with apertures of 45 x 45 μm^2 and 216 x 216 μm^2, radii of curvatures 4 µm and 27 µm, number of elements in vertical (V) and horizontal (H) directions of 187VH and 57VH with sequences of VHVH and VVHH, respectively, were fixed at the optical table under 45° on towers motorized for the lens alignment with 3D-translations and V&H rotations. Different test gold nano-objects with X-ray phase shifts from 1 to 0.05 radians were placed in the object focal plane of the objective lens and illuminated by the divergent beam behind the image focus of the condenser lens. The distances from the objects to the centers of the lenses were 46 mm and 990 mm, respectively. The TXM field of view was 36 x 36 μm^2 with a measured illumination gain factor of ~40. The digital X-ray imaging detector based on a 30-µm-thin $CdWO_4$ crystal scintillator was arranged near the experimental hutch wall resulting in an X-ray magnification factor of 70 for detector image scales of 62 nm or 12.5 nm per 2 x 2 binning pixels. The TXM images were observed within a square image of the objective lens aperture itself (Fig. 1) using slit openings for the condenser aperture. The resolution of the TXM phase contrast images of the objects was studied for different exposures from 6 sec to 10 min and object position variation within ± 8 mm with a 100-µm step along the optical axis. The resolution of the TXM images, calculated by means of modulation transfer functions, is better than 50 nm. To demonstrate the principle possibility to image living biological cells without radiation damage by the 30-keV TXM set-up, movable soil protozoa were placed in a water microcapillary layer and illuminated by the output monochromatic beam with an absorbed dose of ~140 J/cm^3. A reduction of the cell number was not observed by optical microscope control. Further developments of optical elements for the 30-keV TXM to image such objects in real time are discussed.

References:

[1] H. Riesemeier, http://www.bessy.de/upload/bitpdfs/ID_02_2.pdf
[2] E. Reznikova, T. Weitkamp, V. Nazmov et al., Phys. Status Solidi A **204**, 2811 (2007).

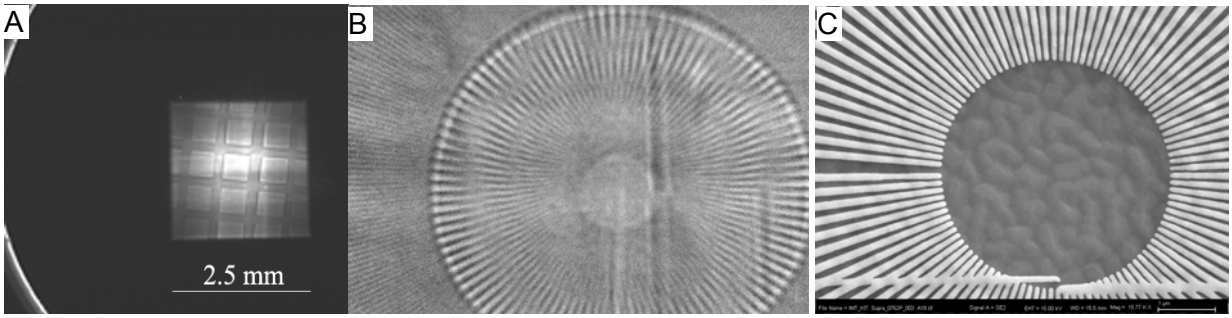

Figure 1: 30-keV TXM images of (A) a mesh with 10-µm period, without flat-field corrections, exposure is 10 sec, scintillator screen diameter is 10 mm; (B) 105 lines and spaces between rings of 4-µm and 20-µm diameters with X-ray phase shift of 0.05 radian, 1 min exposure; (C) SEM view of the nanostructures.

4,000 Spectra or 4,000,000 ROIs per Second: EPICS Support for High-Speed Digital X-ray Spectroscopy with the XIA xMap

M.L. Rivers

Center for Advanced Radiation Sources, University of Chicago, 9700 South Cass Avenue, Building 434A, Argonne National Laboratory, Argonne, IL, USA

Abstract:
The xMAP is a high-performance DSP-based x-ray spectroscopy system from XIA. It contains on a single PXI card the functional equivalent of the shaping amplifiers, ADCs, and MCAs of a conventional pulse-height analysis system for four detectors. It also contains 4 MB of on-board double-buffered memory that can be used to rapidly buffer complete x-ray spectra or the counts in up to 16 regions of interest (ROIs). Such a system allows very high-performance x-ray fluorescence mapping to be performed.

In order to incorporate the xMAP in a synchrotron beamline, it is necessary to make it communicate with the beamline control system. Many synchrotron beamlines use the EPICS control system, and I have developed an EPICS module that provides control of the xMAP, as well as other XIA spectroscopy modules, including the single-channel Saturn (USB or parallel port interface), 4-channel DXP2X (CAMAC interface), and soon the 4-channel Mercury (USB interface). The EPICS software runs on Windows (xMAP and Saturn), Linux (Saturn), and vxWorks (DXP2X). The software allows control of all spectroscopy parameters (e.g., peaking time, gain) as well as control of data acquisition.

Data from the xMAP can be acquired either a single spectrum at a time, in high-speed spectra mapping mode, or in high-speed ROI mapping mode. In the mapping modes acquisition is advanced to the next pixel on receipt of a software or hardware trigger. The data are streamed to disk as the buffers fill up, and because the system is double-buffered, continuous data acquisition with no pauses is supported. In the spectra mapping mode the throughput is determined by the rate with which data can read from the buffers over the PXI bus. Over 4,000 spectra, each 2048 channels, can be collected per second. On a 4-detector system this is 1,000 pixels per second, while on a 16-detector system over 250 pixels per second can be collected. In the ROI mapping mode the throughput is determined by the overhead in the xMAP itself, which is about 100 microseconds. Thus, 10,000 pixels per second can be collected, each with up to 16 ROIs per detector. On a 30-element detector this would be over 4 million ROIs per second.

The EPICS software streams the data to disk using any of the file formats supported by the EPICS areaDetector package. These include netCDF, NeXus/HDF, and TIFF. There are IDL and Python routines available to return the pixel data from these files.

This new software is now in use on the x-ray microprobe at GSECARS (APS sector 13), where it is used for high-speed fluorescence maps and fluorescence microtomography. We use a Newport XPS motor control to provide the hardware pixel triggers for the xMAP as the stage is driven. Other signals such as ion chambers with V/F converters are collected simultaneously in an SIS 3801 multi-channel scaler using the same trigger signal from the XPS.

The software is freely available, at http://cars.uchicago.edu/software/epics/dxp. Note that although the software is based on EPICS, it can be used on non-EPICS beamlines as long as the control system has a way to talk to EPICS. It is being used, for example, at a number of beamlines that primarily use the SPEC control system.

A Condenser Scanner for Large Field-of-View Full-field X-ray Microscopy at Synchrotrons

J. Rudati[1], J. Irwin[1], A. Tkachuk[1], J. C. Andrews[2], P. Pianetta[2], M. Feser[1]

[1]*Xradia Inc., Concord, CA 94520, USA*
[2]*Stanford Synchrotron Radiation Lightsource, SLAC, Menlo Park, CA 94025, USA*

Abstract:
Most full-field microscopes at synchrotrons exhibit a highly peaked illumination in the center of the field of view. Although the illumination pattern is typically reference corrected by division with an image without the sample, and the final images don't show the uneven illumination, the correction cannot affect key factors such as the signal-to-noise ratio and image quality that vary across the field of view due to photon statistics and uneven illumination. This causes uniformity problems for imaging strategies needed for large samples, which stitch several fields of view together. The center of the field of view has much higher photon counts (and hence higher signal-to-noise ratio) while the edges are very noisy. Of course, there are ways to solve this—e.g., by using longer exposures so that the darkest area has enough photons, and by overlapping tiles so that every part of the image has the same count—but they require much longer data acquisition times.

We have developed a condenser scanner for spreading the illumination evenly over large fields of view in beamlines where the incoming illumination is too collimated and exhibits a large degree of coherence. The scanner physically translates the condenser parallel to the beam axis vertically and horizontally in a predetermined Lissajou pattern. Since there is no absorbing material included in the beam path (as in a rotating diffuser, used frequently), there is no attenuation of the beam. The full incoming beam is used to illuminate the sample, and coherence artifacts in images are eliminated by time-space averaging.

We will present the current implementation of the condenser scanner, experimental results, and signal-to-noise comparisons.

X-ray Microscopy with Second-Order Optimized Zone Plates

A. Sakdinawat[1], Y. Liu[1], B.D. Harteneck[2], D. Attwood[1]

[1]*University of California, Berkeley, Berkeley, California 94720, USA*
[2]*Molecular Foundry, Lawrence Berkeley National Laboratory, Berkeley, California 94720, USA*

Abstract:

Zone plate imaging can be performed using higher-order diffraction in order to achieve higher spatial resolution than with first order [1-3]. Using second-order diffraction from a zone plate provides a good tradeoff between improved resolution and decreased efficiency. Here we report tests conducted with a zone plate optimized for use in second order. The zone plate was fabricated with asymmetric open and closed zones in a 1:3 duty cycle, as seen in Figures 1 and 2. The gold zone plate was fabricated with a 29-nm outermost zone width, 224 zones, and a 1:3 duty cycle. Images of a URA test pattern were obtained in second order using 1.05-keV radiation at the ALS soft x-ray microscope XM-1. An image is shown in Figure 3. Efforts to extend these studies to smaller outermost zone widths are presently underway. For higher-resolution zone plates, where fabrication limitations typically result in a duty cycle that is not 1:1 in the outermost zones, optimization for second-order diffraction may provide additional opportunities.

References:

[1] G.-C. Yin, Y.-F. Song, M.-T. Tang et al., Appl. Phys. Lett. **89**, 221122 (2006).
[2] S. Rehbein, S. Heim, P. Guttmann et al., Phys. Rev. Lett. **103**, 4 (2009).
[3] O. von Hofsten, M. Bertilson, J. Reinspach et al., Opt. Lett. **34**, 2631 (2009).

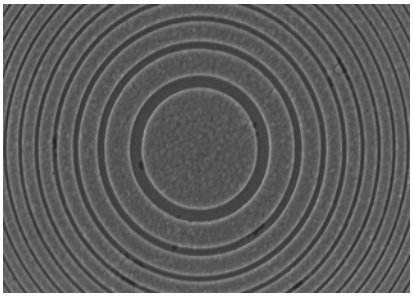

Figure 1: SEM image of inner zones from second-order optimized zone plate.

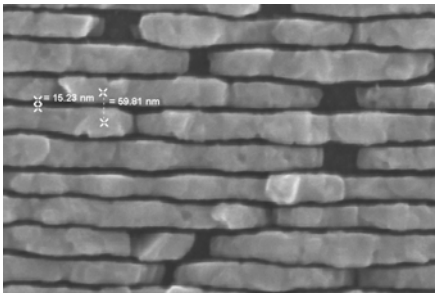

Figure 2: SEM image of the outer zones of the zone plate.

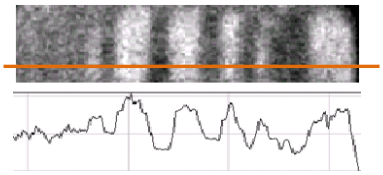

Figure 3: 1-keV image of a URA pattern and a line profile. While the features are larger, edge structures in the range of 12-15 nm are observed.

New Lens-Free X-ray Source for Laboratory Nano-CT with 50-nm Spatial Resolution

A. Sasov, B. Pauwels, P. Bruyndonckx, X. Liu

SkyScan, Kontich 2550, Belgium

Abstract:

X-ray optics such as zone plates are often used to obtain a spatial resolution better than 100 nm in x-ray projection images [1]. Such type of optics is not always suited for tomographic imaging due to its limited depth of focus, which restricts the size of a specimen to a few microns [2]. To overcome this limitation, a new lens-free set-up for a nano-CT system is developed.

A scanning electron microscope was used as an electron beam source. The interaction between the electron beam and a metal target generated an x-ray beam. The x-rays, which penetrated through the sample, were acquired by a fully depleted cooled CCD (Hamamatsu S10747). A specimen holder, with the sample, was mounted on a rotation stage to acquire a number of angular views for tomographic reconstruction.

Spatial resolution of an x-ray source depends on the target shape and the focusing of the electron beam. A typical way to improve spatial resolution is based on the replacement of a bulk metal target by a thin film. A submicron spot size can be obtained that way, but with a significantly reduced x-ray flux. To overcome this flux limitation without compromising spatial resolution we applied a new type of target, shaped as a rod or needle, pointing toward the camera. 50-nm resolution can be reached with a reasonable flux. An ATN/XRESO-50HC (NTT-AT, Japan) resolution pattern is used for resolution tests (Fig. 1). Small random mechanical movements during tomographic imaging were compensated in the image reconstruction process by iterative fitting by forward/backward projection [3].

References:

[1] Y.S. Chu, J.M. Yi, F. De Carlo et al., Appl. Phys. Lett. **92**, 103119 (2008).
[2] Y. Suzuki, SPring-8 summer school (2008).
[3] A. Sasov, X. Liu, P. Salmon, Proc. of SPIE **7078**, 70781C.1-9 (2008).

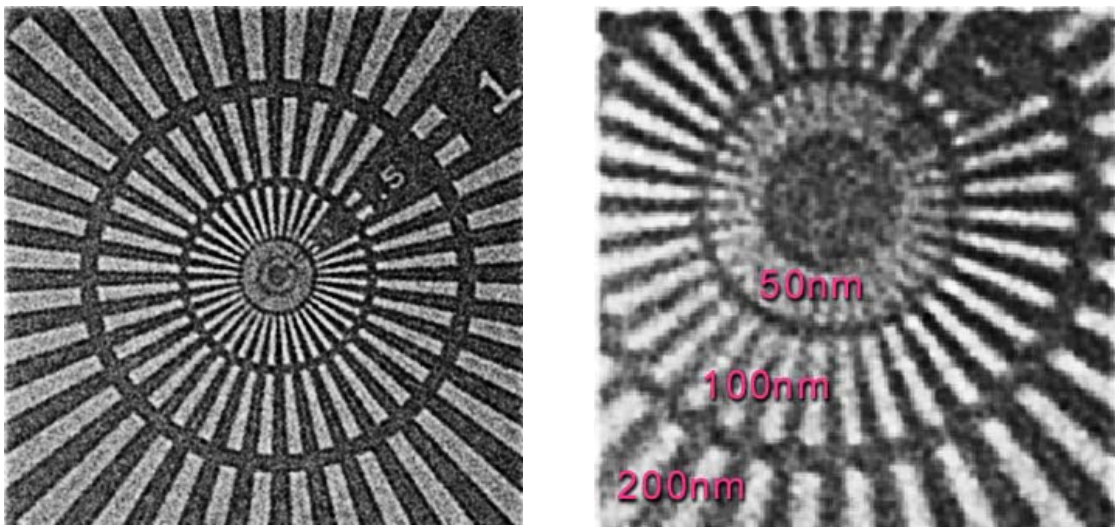

Figure 1: X-ray projection image of the resolution chart (left) and close up of the central part (right) with 200-, 100-, and 50-nm structures.

Development of an Advanced Sample Scanning Stage System Prototype for an MLL-Based Hard X-ray Nanoprobe*

D. Shu[1], J. Maser[1], Y. Chu[2], H. Yan[2], E. Nazaretski[2], S. O'Hara[2], J. Quintana[1], Q. Shen[2],

[1]*Argonne National Laboratory, Argonne, IL 60439, USA*
[2]*Brookhaven National Laboratory, Upton, NY 11973, USA*

* This work is supported by the U.S. Department of Energy, Office of Science, Office of Basic Energy Sciences under Contract No. DE-AC02-06CH11357.

Abstract:

Based on the experiences gained from Argonne's nanopositioning system designed for the CNM/APS linear multilayer Laue lenses (MLL)-based hard x-ray nanoprobe project [1-4], a new nanopositioning system will be designed for the NSLS-II Hard X-ray Nanoprobe (HXN) prototype through a Brookhaven/Argonne joint work project. The joint work project was started in September 2009, and is expected to last for three years. The scientists and engineers at Argonne AES, CNM, XSD, and Brookhaven NSLS-II will collaborate on the following important nanopositioning tasks:

- Identifying and solving engineering and technical tasks with the HXN prototype.
- Developing flexure-based linear and rotary stages.
- Developing a laser encoding scheme to ensure stability between the sample and the MLL optics.
- Developing a sample holder to allow easy fiducialization of the sample with ancillary pre-alignment microscopes.
- Developing an HXN with adequate vibration properties.
- Solving various engineering challenges that will be encountered during prototype development.

In this paper we present the design and development of an advanced sample scanning stage system prototype for an MLL-based hard x-ray nanoprobe. The design and prototyping activities for the NSLS-II nanopositioning system will also benefit the ongoing CNM/APS MLL-based hard x-ray nanoprobe development with hard x-ray focusing in the nanometer scale.

References:

[1] J. Maser, R. Winarski, M. Holt et al., Proc. 8th Int. Conf. X-ray Microscopy, IPAP Conf. Series **7**, 26 (2006).
[2] H.C. Kang, J. Maser, G.B. Stephenson et al., Phys. Rev. Lett. **96**, 127401 (2006).
[3] D. Shu and J. Maser, Proc. 23rd ASPE Annual Meeting, Portland, OR, Oct. 19-24, 2008, 23-26 (2008).
[4] U.S. Patent granted No. 7,597,475, D. Shu, H. Yan, and J. Maser, Oct. 2009.

Achieving Desired Vibration Stability of the NSLS-II Hard X-ray Nanoprobe Beamline Endstation*

N. Simos, Y. S. Chu, L. Margulies, E. Nazaretski, S. O'Hara, A. Broadbent, O. Dyling, M. Fallier, Q. Shen

Brookhaven National Laboratory, NSLS-II Project, Upton, NY 11973, USA

* This work was supported by the Brookhaven Science Associates, LLC under Contract No. DE-AC02-98CH10886 with the U.S. Department of Energy

Abstract:

In an effort to achieve stringent vibration stability levels at the Hard X-ray Nanoprobe (HXN) beamline station floor of the NSLS-II accelerator, a comprehensive approach was adopted to identify the controlling parameters and thus influence the design of both the vibration-sensitive probe support floor and its interface with the enveloping nanoprobe structure as well as the rest of the accelerator. The ground vibration environment in the vicinity of the nanoprobe endstation, expected to influence the response of its floor and subsequently the probe itself supported on the floor, is a combination of a number of modes, both stationary and transient, each of which is accompanied with wave types, amplitude, and spectral content. These modes include the natural ground vibration measured at the nanoprobe endstation location, cultural noise stemming from mechanical sources that support the operation of the NSLS II accelerator, traffic-borne vibration in the vicinity of the HXN endstation, wind-induced ground vibration by its enveloping structure, as well as the overall superstructure of NSLS-II.

Driven by the desire to meet wide-band and narrow-band vibration criteria established for the probe support floor, the location of the beamline station in reference to the overall accelerator as well as the structural characteristics of the vibration-sensitive floor and its isolation from the surrounding structures were optimized and adopted into the design of the facility. The optimization of the nanoprobe endstation was achieved through the integration of (a) site-specific field measurements of natural ground vibration and of cultural sources such as heavy traffic in the proximity of the endstation; (b) quantification of the effect of accelerator-related operations and their potential impact on the nanoprobe station; and (c) the utilization of a large-scale, high-fidelity computational models/analyses that provided the means of vibration generation at the identified sources, propagation to and filtering by the nanoprobe structure. The effectiveness of the concept schemes explored in minimizing the ambient vibration of the substrate resulting from stationary and transient effects was assessed and feedback to the design of the integrated structure was rendered.

This paper summarizes all the elements of the multi-faceted effort that led to the adopted design of the NSLS-II HXN beamline. In particular, it discusses the rationale that led to adoption of the HXN-specific stability criteria, the selection of key structural (such as the geometric dimensions of the probe-supporting floor slab) and isolating features, and the quantification of the expected vibration on the floor location where the sensitive probe will be supported both in terms of amplitude and spectral content. An overview of the complex analyses that enabled the latter is also presented. Finally, the coupling of the anticipated nanoprobe floor vibration to the dynamic response of the sensitive probe supported on it and the influence on the probe infrastructure are discussed.

Electron-Impact Water-Jet Microfocus Source for Water-Window Microscopy

P. Skoglund, U. Lundström, U. Vogt, P. Takman, H.M. Hertz

Biomedical and X-Ray Physics, Department of Applied Physics, Royal Institute of Technology, SE-10691 Stockholm, Sweden

Abstract:

Laboratory water-window (2.3-4.4 nm, 539-282 eV) x-ray microscopy requires high-brightness table-top soft x-ray radiation sources. The liquid-jet laser plasma [1], with a brightness of up to 2-4×10^{10} ph/(s×µm^2×sr×line), enabled the first high-resolution water-window compact x-ray microscopy [2]. Unfortunately, high-brightness laser-plasma sources currently have to rely on delicate and expensive lasers.

Recent progress on electron-impact microfocus sources with liquid-metal-jet anodes has paved the way for high-brightness high-power hard x-ray sources by increasing the brightness and power of microfocus sources by 2-3 orders of magnitude [3].

We now demonstrate stable high-brightness operation of an electron-impact water-jet-anode soft x-ray source [4]. A 30-kV, 7.8-W electron beam is focused onto a 20-µm-diameter jet resulting in water-window oxygen line emission at 525 eV/2.36 nm with a brightness of 3.0×10^9 ph/(s×µm^2×sr×line). The source has potential to increase the x-ray power and brightness another 1-2 orders of magnitude, making it an attractive alternative for table-top x-ray microscopy.

References:

[1] P.A.C. Jansson, U. Vogt, and H.M. Hertz, Rev. Sci. Instrum. **76**, 43503 (2005).
[2] M. Berglund, L. Rymell, M. Peuker et al., J. Microsc. **197**, 268 (2000).
[3] O. Hemberg, M. Otendal, and H.M. Hertz, Appl. Phys. Lett. **83**, 1483 (2003).
[4] P. Skoglund, U. Lundström, U. Vogt et al., Appl. Phys. Lett. **96**, 084103 (2010).

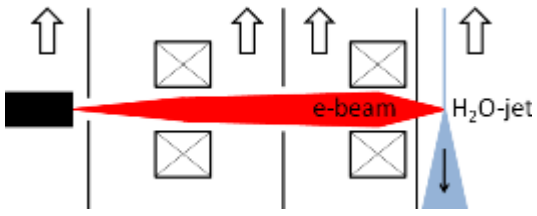

Figure 1: Schematic view of electron-beam focusing system and water jet with arrows and apertures indicating differential vacuum pumping.

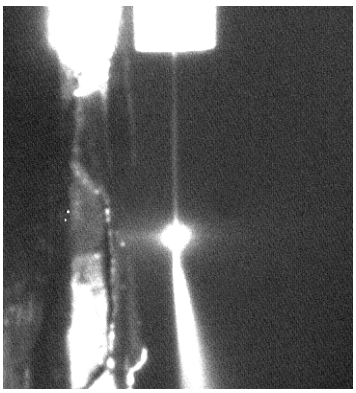

Figure 2: A 7.8-W electron beam impinging on a 60-m/s, 20-µm-diameter water jet, resulting in 525-eV x-ray generation.

Hard X-ray Microbeam by Combination of Spherical Mirrors

Y. Suzuki, A. Takeuchi

Japan Synchrotron Radiation Research Institute (JASRI), SPring-8, Hyogo, Japan

Abstract:

In the grazing incidence optics with spherical mirrors, spherical aberration and astigmatism are most serous aberrations. The astigmatism can be eliminated by a crossed spherical mirror configuration introduced by Kirkpatrick and Baez (KB) [1]. The spherical aberrations in the KB optics can be also eliminated by aspherical (plane ellipse or plane parabola) mirror [2]. These aspherical KB optics are widely used for generation of hard x-ray microbeams.

However, there is another method of spherical aberration reduction. The spherical aberrations can be reduced by combination of two concave spherical mirrors in tandem configuration as shown in Fig. 1. This optical system is based on a tandem toroidal mirror x-ray microscope optics by Sakayanagi [3]. The spherical aberration at the second mirror has inversed direction to the first mirror. By choosing appropriate parameters, radiuses of mirrors, glancing angles and distance between two mirrors, the total spherical aberration term can be perfectly eliminated. The higher order aberrations are still remaining, but they are usually much smaller. Therefore, a submicrometer resolution is possible in hard x-ray region even by the spherical concave mirrors.

A preliminary experiment on hard x-ray microbeam has been performed at beamline 20XU of SPring-8. Platinum-coated concave spherical mirrors with a radius of 26.5 m and a length of 30 mm were used. The glancing angles were 6 mrad for the first mirror and 6.9 mrad for the second mirror, respectively. The focus is at about 18 mm from the near edge of second mirror. The focused beam profile at 8 keV measured by knife-edge scan method is less than 200 nm, as shown in Fig. 2. Although the result shown in the figure is one-dimensional focusing, it is apparent that two-dimensional focusing is possible by analogue of KB optics. A hard x-ray imaging microscope would be also possible by the combination of spherical mirrors, because the tandem mirror optics naturally satisfies Abbe's sine condition.

References:

[1] P. Kirkpatrick and A. V. Baez, J. Opt. Soc. Am. **38**, 766 (1948).
[2] Y. Suzuki and F. Uchida, Rev. Sci. Instrum. **63**, 578 (1992).
[3] Y. Sakayanagi, Optica Acta **23**, 217 (1976).

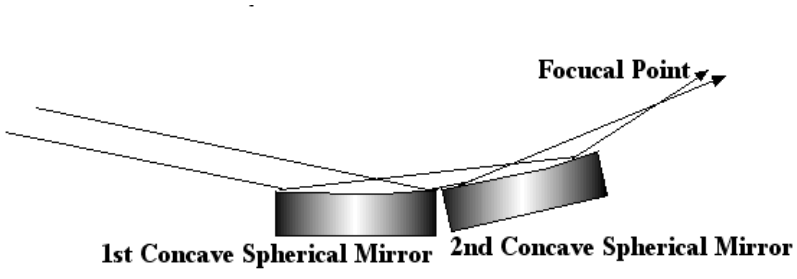

Figure 1: Schematic diagram of optical system.

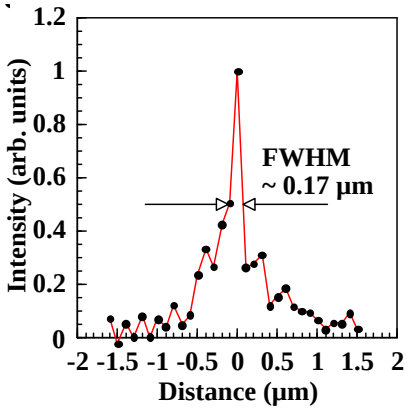

Figure 2: Focused beam profile at 8 keV.

Hollow Cone Illumination for Hard X-ray Imaging Microscopy by Rotating Grating Condenser Optics

Y. Suzuki, A. Takeuchi, K. Uesugi, M. Hoshino

Japan Synchrotron Radiation Research Institute (JASRI), SPring-8, Hyogo, Japan

Abstract:

Critical illumination, forming a demagnified image of light source, is widely used in x-ray imaging microscopy. However, this method is not suitable for low emittance synchrotron radiation x-ray sources, because the imaging field becomes very narrow for small source size. The hollow cone illumination (a kind of Köhler illumination) is the best method that was realized in soft x-ray microscopy using a rotating double total-reflection-mirror optics [1]. However, alignment of the rotating mirror optics is not an easy task, and application to hard x-ray microscopy is difficult because much longer mirrors are needed for hard x-rays.

We had already developed a quasi-Köhler type illumination by sector condenser zone plate optics that is routinely used for hard x-ray imaging microscopy experiment at beamline 47XU of SPring-8 [2]. The sector condenser is a combination of constant pitch grating as shown in Fig. 1. The sector condenser zone plate gives fairly flat and wide field of view. However, there is another problem on illuminating optics with high brilliance synchrotron light sources, which is speckle noises. Although a diffuser (random phase plate) is generally used for speckle reduction, disadvantages of diffuser are loss of flux and increase of stray light. In order to achieve an ideal hollow cone illumination, we have developed a rotating grating system (rotation of sector condenser zone plate) for illumination optics of hard x-ray microscopy, as shown in Fig. 1.

The sector zone plate used in the experiment is octagon configuration with 400 nm grating period. The inscribed circle diameter of octagon is 1 mm. The objective zone plate has an outermost zone width of 100 nm, and focal length of 100 mm at 8 keV. The microscopy image in Fig. 2 is taken at a magnification, b/a, of 67. An extremely uniform, speckle-free and stable field is achieved by the synchronized rotation of sector condenser zone plate, for example one turn within an exposure time of 1s.

References:

[1] B. Niemann, P. Guttmann, D. Hambach et al., AIP Conf. Proc. **507**, 440 (2000).

[2] A. Takeuchi, K. Uesugi, Y. Suzuki, J. Phys. CS **186**, 012020 (2009).

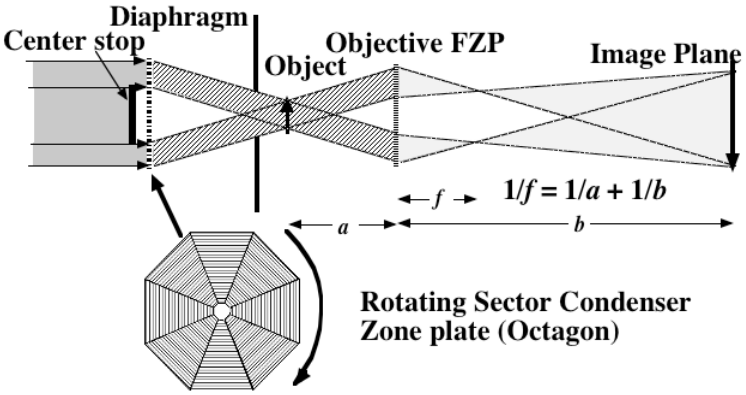

Figure 1: Schematic diagram of optical system.

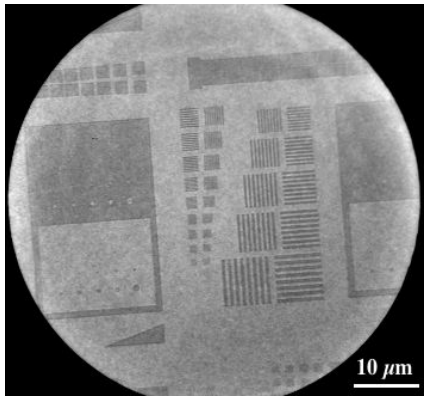

Figure 2: Image of test patterns.

HERMES: A Soft X-ray Microscopy Beamline

S. Swaraj, R. Belkhou, A. Bendounan, A. Besson, D. Dallé, K. Benzerara,
B. Lagarde, F. Polack

Synchrotron SOLEIL, L'Orme des Merisiers, Saiint-Aubin - BP 48, F-91192 Gif-sur-Yvette cedex, France

Abstract:
A new soft X-ray microscopy beamline, HERMES (High Efficiency and Resolution beamline dedicated to X-ray Microscopy and Electron Spectroscopy) is under construction at synchrotron SOLEIL. The beamline will be equipped with two complementary microscopy techniques namely STXM (scanning transmission x-ray microscopy) and X-PEEM (x-ray photoemitted electron microscopy). X-PEEM is a photon-in-electron-out technique and hence this branch will provide mainly a surface-interface microscopy and spectroscopy with an ultrahigh vacuum sample environment. On the other hand STXM, being a photon-in-photon-out microscopy technique, will allow the investigation of "bulk" properties of natural and synthetic materials. The source for this beamline would be a set of two undulators covering an energy range of 70 eV to 2.5 keV between them. Both branches will offer a spatial resolution of better than 25 nm along with a number of detection techniques. The beamline design is optimized for high photon flux, low spectral contamination, and high stability. Many different fields, including those related to life and medical science, earth and environmental science, magnetism, nanomaterials, and soft condensed matter will benefit from this beamline. A prototype cryo stage suitable for biological samples is also planned and will be implemented at the STXM branch of the beamline.

Wavelength-Dispersive Spectrometer for X-ray Micro-fluorescence Analysis at the ESRF ID21 Beamline

J. Szlachetko[1,2], M. Cotte[1,5], J. Morse[1], M. Salomé[1], J. Susini[1], P. Jagodzinski[2], J. Cl. Dousse[4], J. Hoszowska[4], Y. Kayser[4]

[1]*European Synchrotron Radiation Facility, Grenoble, France*
[2]*Institute of Physics, Jan Kochanowski University, Kielce, Poland*
[3]*Department of Physics, University of Technology, Kielce, Poland*
[4]*Department of Physics, University of Fribourg, Fribourg, Switzerland*
[5]*C2RMF, CNRS UMR 171, Palais du Louvre, 14, Quai F. Mitterrand, F-75001 Paris, France*

Abstract:
The attainable energy resolution (120~180 eV) of energy dispersive detectors (EDS) is inadequate in many applications in order to enable elemental and chemical specification. For this reason a wavelength dispersive spectrometer of higher resolution (a few tens of eV) was developed for micro-fluorescence analysis at the ID21 beamline.

The new spectrometer employs a polycapillary that gives a large ($3x10^{-2}$ srad) collection solid angle for the sample X-ray fluorescence. This collimating polycapillary optic outputs a quasi-parallel beam which is directed onto a plane Si(111) or Ge(220) crystal analyzer, and the diffracted X-rays are detected by a gas proportional counter, all these operated under vacuum. The simple design results in a compact spectrometer, which is compatible with the limited space around the immediate sample environment of the scanning X-ray microscope of ID21.

We present the construction details, operational characteristics, and the performance achieved with the new spectrometer. We show examples from applications in research fields requiring energy resolution combined with two dimensional imaging. Further possibilities for improving the energy resolution, down to the ~1 eV level, will be discussed and preliminary results presented.

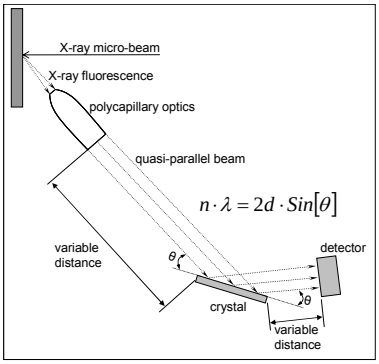

Figure 1: Schematic drawing of the parallel beam wavelength-dispersive arrangement employing polycapillary optics for x-ray fluorescence collection.

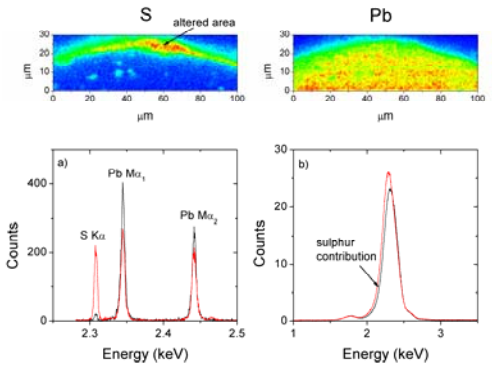

Figure 2: The x-ray fluorescence map of S and Pb in the painting cross-section containing the altered area. a) the WDS spectrum recorded in the altered (red) and safe (black) areas, b) the same as a) but acquired with a SDD detector.

Scanning Transmission X-ray Microscope at SSRF

R. Tai[1], Y. Wang[1], Z. Guo[1], Y. Wu[1], M. Chen[1], W. Yun[2]

[1]*Shanghai Synchrotron Radiation Facility, Shanghai Institute of Applied Physics, Chinese Academy of Sciences, Zhangheng Rd 239, Pudong Distr, Shanghai 201204, China*
[2]*Xradia, Inc. 5052 Commercial Circle, Concord, CA94520*

Abstract:

SSRF has developed a transimission soft x-ray spectromicroscope facility consisting of a commercial scaning x-ray microscope, an elliptically polarized undulator, and an optimized beamline. It is one of major beamlines in the 1st-phase construction project. The operating photon energy covers from 250 to 2000 eV, covering the K-edge of C, N, O, F, Na, Mg, Al, Si, and L edges of P, S, Cl, K, Ca, Fe, Cu, Zn, etc.. Studies on these elements are important in a wide range of scietific disciplines, including biological science, environmental science, polymer, and material science. In addition, the elliptical polarized undulator source offers more capabilties to study x-ray-polarization-dependent properties.

The scanning transmission x-ray microscopy (STXM) can produce a small beam spot down to 30 nm and get the transmitted 2D NEXAFS spectra. In addition, the 3D function will be realized in the future.

The commissioning of the Soft X-ray Spectromicroscope at SSRF was formally started from the end of December, 2008. The beamline performances have reached or surpassed the designing goals according to the measurements by domestic experts. Since its first operation to users from May 6, 2009 until the end of 2009, 42 research groups had conducted their experiments with beam time of 2100 hours. Following shows several examples.

Figure 1 demonstrates that the STXM has a spatial resolution of 30 nm. Figure 2 shows the oxygen dual energy (532eV, 533.5 eV) contrast image at in the pre-oxidized PAN fibre [1]. Figure 3 shows the STXM image of automobile particles of Gol and Satana 3000 [2].

References:

[1] X. Z. Zhang, R. Z. Tai, Z. J. Xu, X.J. Zhen, Z. Guo, R. Yan, R. Chang, R. R. Zhou, Acta Phys. Sin. (in press).
[2] C. J. Yang, Z. Guo, X. Z. Zhang, R. Z. Tai L. M. Bao, X. L. Li, G. L. Zhang, Y. Li, Acta Phys. Sin. (in press).

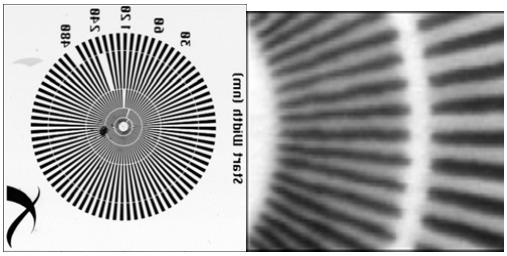

Figure 1: STXM image of a standard sample, the finest line in the right figure is 30 nm.

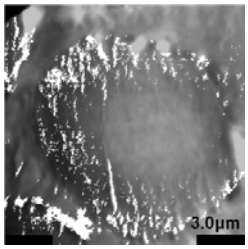

Figure 2: Oxygen distribution in a pre-oxidized PAN fiber cross-section.

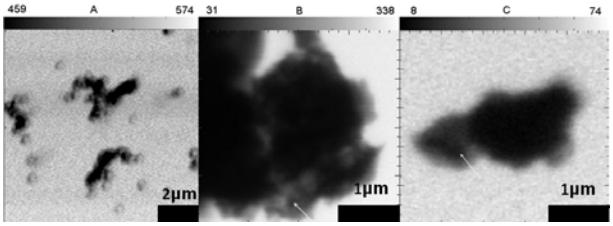

Figure 3: STXM image of Automobile exhaust particles of Santana3000 (A, B) and Gol (C) at 410 eV.

Development of Laboratory Scale Coaxial Fluorescence and Soft X- ray Microscopy for Biological Observation

K. Takaba, S. Aoki

Graduate School of Pure and Applied Sciences, University of Tsukuba,
1-1-1 Tennohdai, Tsukuba, Ibaraki 305-8573, Japan

Abstract:
Our understanding of cell structures and functions can be more informative by combining inner structural images with localization data of interest within the specimen. For this purpose, in recent years multi-modal images, which can be more informative than a single image alone, have been obtained around the world [1,2]. Here we report the development of a laboratory-scale coaxial fluorescence and soft X-ray microscope for biological observation. The characteristic features of a fluorescence microscope were introduced to the conventional soft X-ray microscope where the specimens can be set in air [3]. One of the technical difficulties in detecting visible fluorescence is the chromatic aberration. This was overcome by applying a reflective optics—a Wolter mirror—to the coaxial optical system. The coaxial optical system offers experimental simplicity, and it is possible to obtain soft X-ray images and fluorescence images of identical specimens without technical difficulties. Therefore, the newly developed coaxial optical system offers high-quality structural and morphological details of biological specimens with the ability to localize specific cells and other important subcellular targets. Soft X-ray images and fluorescence images of an identical DNA, which were derived from redfish testes and stained with DAPI (4',6-diamidino-2-phenylindole), were obtained by the newly developed coaxial optical system.

References:

[1] R. McRae, B. Lai, S. Vogt et al., J. Struct. Biol. **155**, 22 (2006).
[2] G. McDermott, M.A.L. Gros, C.G. Knoechel et al., Trends Cell Biol. **19**(11), 587 (2009).
[3] M. Hoshino and S. Aoki, Jpn. J. Appl. Phys. **45**, 989 (2006).

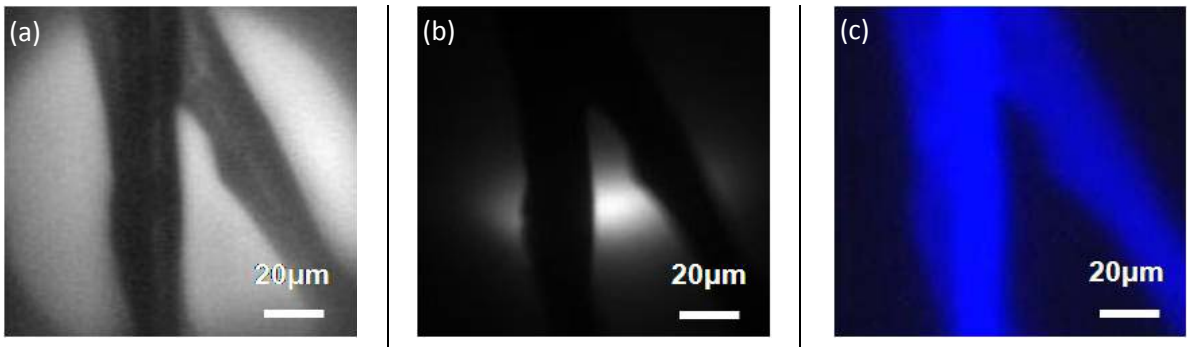

Figure 1: Comparative images of an identical DNA, which were derived from redfish testes and stained with DAPI, using the newly developed coaxial optical system. (a) Visible image, (b) soft X-ray image, (c) fluorescence image.

Nano-XAFS Measurements for Single-Particle Analysis Using High-Resolution X-ray Microprobe

Y. Terada, H. Tanida, T. Uruga, A. Takeuchi, Y. Suzuki, S. Goto

JASRI/SPring-8, 1-1-1 Koto, Sayo, Hyogo 679-5198, Japan

Abstract:

A scanning X-ray microprobe has been developed at BL37XU of SPring-8 using total-reflection mirror optics [1]. As a typical example, it was reported that micro spectroscopy of cloud droplets was carried out using the X-ray microprobe [2]. Recently X-ray absorption fine structure (XAFS) analysis required the use of a nano-order probe for measurement of single particles such as electrode material and catalyst. In this study, we developed a nano-probe by using a spatial filter to investigate chemical state analysis of nano particles.

Figure 1 shows the experimental setup for the X-ray microprobe at BL37XU of SPring-8. Parabolic mirrors were fabricated by Cannon Co. Ltd., Japan. The focal length is 90 mm for the vertical focusing mirror and 40 mm for the horizontal focusing mirror. The reflective surface is coated with rhodium, and the average glancing angle is 4 mrad. Typical beam size is 1 μm (V) × 1.2 μm (H) at an X-ray energy of 10 keV, and a total photon flux of the focused beam is about 5×10^{10} photons/s. A horizontal slit is located downstream of the monochromator, and its width is variable by pulse motor control. The slit is used as a spatial filter for the horizontal focusing mirror. Applying the slit width of 40 μm, a focused beam size in the horizontal direction was achieved to be around 700 nm.

We have successfully measured micro XAFS spectra with fluorescence mode using the X-ray microprobe. Tantalum L_{III}-edge XANES spectrum of a test dot (500 nmϕ) is shown in Figure 2. Although the spectrum seems to show poor statistics because of too short a correction time, it clearly indicates tantalum oxide (Ta_2O_5). Experimental results of XAFS analysis for a single particle in the catalyst will be presented.

References:

[1] S. Hayakawa, N. Ikuta, M. Suzuki et al., J. Synchrotron Radiat. **8**, 328 (2001).

[2] C.-J. Ma, S. Tohno, M. Kasahara et al., Nucl. Instrum. Methods B **217**, 657 (2004).

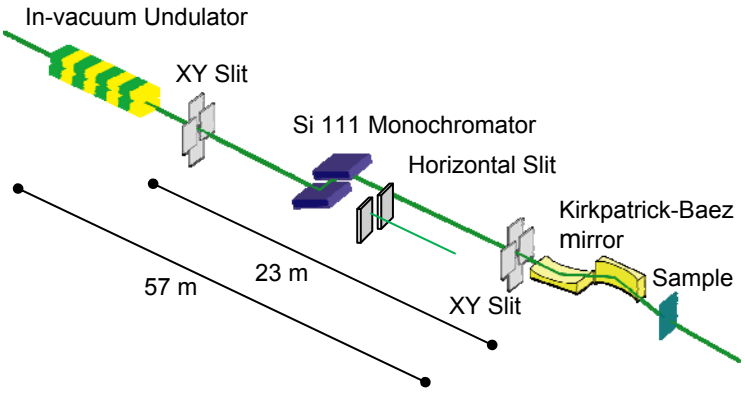

Figure 1: Schematic diagram of experimental setup at BL37XU of SPring-8.

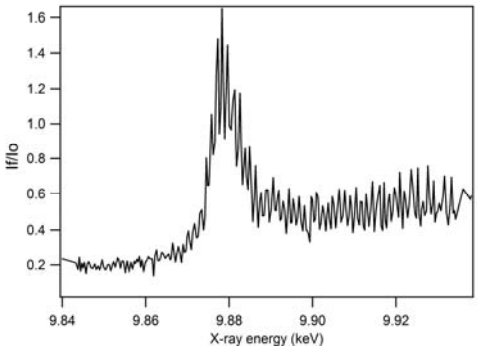

Figure 2: Ta L_{III}-edge nano XANES spectrum of a test dot.

The Submicron Resolution X-ray Spectroscopy Beamline at the Electron Storage Ring NSLS-II

J. Thieme[1], V. de Andrade[1], P. Northrup[1], A. Lanzirotti[2], Q. Shen[1]

[1]*Brookhaven National Laboratory, NSLS-II Project, Building 817, Upton, NY 11973, USA*
[2]*Consortium for Advanced Radiation Sources, The University of Chicago, 5640 South Ellis Avenue, Chicago, Illinois 60637, USA*

Abstract:
Analytical resources have to be developed to advance our understanding of complex natural and engineered systems that are heterogeneous on the micron to submicron scale. They should support scientists in their efforts to understand better the chemical and physical properties of such systems. This is true for many research areas such as life, environmental, or material sciences as well as in energy research. The new National Synchrotron Light Source II at Brookhaven National Laboratory will be a source of synchrotron radiation with a very low emittance, horizontally down to 0.5 nm-rad, vertically diffraction-limited at 8 pm-rad (for 12 keV), supporting a high current of 500 mA at the same time. Therefore, this facility will be very well suited for hosting experiments in need of coherent radiation.

One of the six project beamlines that will be constructed first at NSLS-II will be a sub-micrometer-resolution spectroscopy beamline, dedicated especially as an analytical tool to study complex systems on a submicron length scale. When fully equipped, this beamline will have two branch lines, the first of which is planned to address the energy range from 4.65 keV to 23 keV, using Kirkpatrick-Baez mirrors to focus the beam, targeting at a spot size of 100 x 100 μm^2. A horizontally deflecting double-crystal monochromator with maximum stability will ensure the possibility of spectroscopy with simultaneously very high spectral and spatial resolution. The energy range will allow for XANES experiments starting at the K-absorption edge of titanium, reaching up to the K-edge of rhodium. Ultimately, EXAFS studies with sub-micrometer spatial resolution will be possible for samples with reasonable concentrations of the studied element. A 1.5 m long in-vacuum undulator with 21 mm period length will serve as a light source. The expected photon flux in the focal spot will be in the range of up to 7 x 10^{13} photons/s. This flux in a submicron spot, combined with the use of new energy-dispersive detectors like the MAIA, will open new possibilities for imaging and spectroscopy of trace elements.

Using a canted setup, a second undulator will serve as an independent light source for the other branch of this beamline. This branch is planned for experiments with lower X-ray energies, addressing the range of 2 keV up to 15 keV. Using Fresnel zone plates as focusing optics, the spatial resolution aimed for is in the range of 30 nm. It is expected that this branch would be attractive for many biological applications from life and environmental science due to elements of interest like phosphorus, sulfur, chlorine, or calcium within that energy range. In both experimental stations X-ray fluorescence will be used for imaging, spectroscopy, and tomography experiments. Diffraction-imaging experiments will be possible as well. Commissioning of this beamline will start in early 2014; therefore a detailed design description will be presented here.

Laboratory 3D 8-keV X-ray Imaging System with Automated Tomography at 50-nm Resolution

A. Tkachuk, I. Spink, M. Freed, R. Pastrick, X. Zeng, S. Chen, Y. Feng,
M. Feser, B. Hornberger, D. Hunt, W. Yun

Xradia Inc., 5052 Commercial Circle, Concord, CA 94520, USA

Abstract:
We present here the novel capabilities of a high-resolution hard x-ray microscope based on a previously reported laboratory system [1]. The key feature is fully automated tomography capability down to 50 nm resolution, which means that for the tomographic reconstruction no image alignment of the 2-D projections is necessary. Automated tomography is achieved by employing a high stability rotation stage with an integrated capacitor sensor metrology system that measures the remaining wobble/runout, and software that aligns individual tomographic projections automatically without relying on any fiducial or alignment markers (see Figure 1). The system operates at 8 keV x-ray energy in absorption and Zernike phase contrast modes employing a high-flux commercial laboratory (or synchrotron) x-ray source, a ~90% efficient capillary reflective condenser [2], a 35 nm outermost zone width high efficiency zone plate objective lens [3], and a high-resolution detector system. In addition, motorized objective zone plates allow switching between different magnifications with 60 x 60 or 16 x 16 µm field of view with 150-nm and 50-nm resolution, respectively. An additional integrated visible microscope allows aligning the sample region of interest to the field of view inside of the microscope.

References:

[1] A. Tkachuk, F. Duewer, H. Cui et al., Z. Kristallogr. **222**, 650 (2007).
[2] X. Zeng et al., Appl. Optics **47**(13), 2376 (2008).
[3] Y. Feng, M. Feser, A. Lyon et al., J. Vac. Sci. Technol. B. **25**, 2004 (2007).

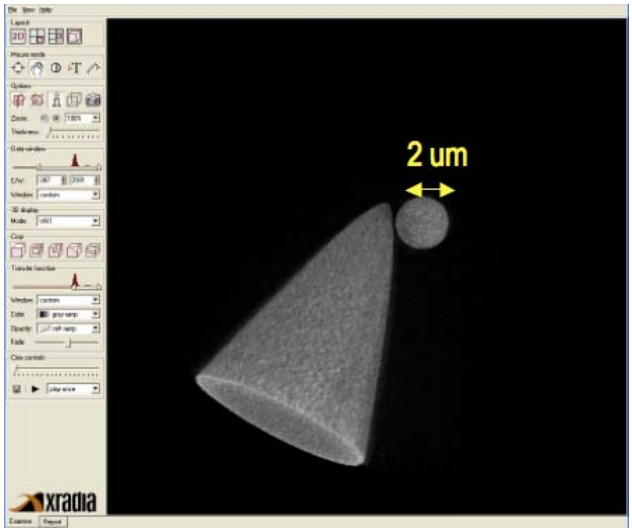

Figure 1: Demonstration of automated tomography reconstruction with fully automated image alignment of a 1 micron tungsten tip and attached to it a 2 micron gold ball. Tomographic projections were automatically aligned using a metrology sensor system without relying on any fiducial or alignment markers. The voxel size of the reconstructed 1k x 1k x 1k volume is 16 x 16 x 16 nm. The outermost zone width of the zone plate used is 35 nm.

Novel Multilayer-Mirror Optics for a Whole Tissue Imaging

M. Toyoda, T. Jinno, T. Harada, T. Hatano, M. Yanagihara

Institute of Multidisciplinary Research for Advanced Materials, Tohoku University, 2-1-1 Katahira, Aoba-ku, Sendai, 981-8577 Japan

Abstract:

As compared with historical zone plate microscopes, Schwarzschild microscopes corrected for off-axis aberrations, coma and astigmatism [1], could be designed to have a wider field of view, which allows us to observe a high definition soft-X-ray image of a whole living tissue in a few hundred micron scale with a diffraction-limited resolution better than 30 nm. Several investigators have reported Schwarzschild microscopes with soft-X-ray multilayer mirrors for a full-field imaging [2,3]. In these studies, a magnification *m* of the microscope was configured below *m*=100, and X-ray films with sub-μm spatial resolution should be required as the 2D detector for a diffraction-limited imaging. Therefore, observation has been restricted to a still image.

In this study, we develop a novel multilayer-mirror optics with a magnification over *m*=1000, where movies of a living sample could be observed with an X-ray CCD of a moderate spatial resolution. A configuration of the mirror system was designed based on a third-order aberration theory [4] to satisfy both the high magnification and the low off-axis aberrations, which results in a novel system consisting of three spherical mirrors, as shown in Fig. 1. A full-field transmission microscope was developed by combining the novel optics with a Mo/Si multilayer coating and a laser-produced plasma light source operating at a wavelength of 13.5 nm. We report the first observation to confirm the high magnification and the wide field of view.

References:

[1] P. Erdos, J. Opt. Soc. Am. **49**, 877 (1959).
[2] K. Murakami, T. Oshino, H. Nakamura et al., Appl. Optics **32**, 7057 (1993).
[3] I.A. Artyukov, A.I. Fedorenko, V.V. Kondratenko et al., Opt. Commun. **102**, 401 (1993).
[4] M. Toyoda and M. Yamamoto, Opt. Rev. **13**, 149 (2006).

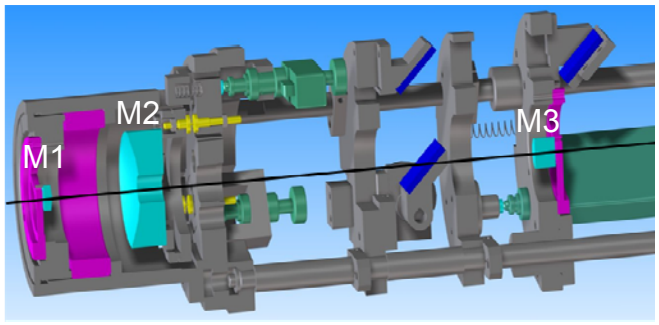

Figure 1: The novel optics consisting of three spherical mirrors, M1 to M3. The optics was designed to have magnification m=1037, a numerical aperture NA=0.25, and an object-image distance t=1 m.

Development of Micro- and 3D-XRF Instruments in the Laboratory

K. Tsuji and K. Nakano

Department of Applied Chemistry & Bioengineering, Graduate School of Engineering, Osaka City University, 3-3-138 Sugimoto, Sumiyoshi, Osaka, Japan

Abstract:

This poster reports on the recently developed 3D-XRF in our laboratory. The first 3D-XRF setup consisted of two x-ray beams of different x-ray tubes [1]. The spatial resolution of the first setup was about 90 micrometers. The spatial resolution was improved in the second 3D-XRF setup to be about 45 micrometers [2]. To investigate the depth sensitivity of the confocal 3D-XRF analysis, the multilayered plastic reference samples were prepared by using a spin coating method. It was confirmed that these plastic-layered reference materials were useful for evaluating the analytical performance of confocal 3D-XRF. Nondestructive 3D elemental maps of K, Ca, Cl, S, and Zn were successfully taken for a young sardine [2]. In addition, many applications of 3D-XRF to industrial plastics, chemical microchips, and biological samples were demonstrated taken under the confocal XRF configuration [2]. Recently, we developed the third setup of 3D-XRF. The spatial resolution was about 14 micrometers at Au La. Some results obtained for layered materials will be shown in the poster.

We will also report on a transportable micro XRF instrument [3]. This instrument consisted of a small x-ray tube and a Si-PIN detector with a polycapillary half x-ray lens. The lateral resolution was about 100 micrometers. Therefore, this instrument can easily be applied to x-ray analysis of contamination particles that can be seen by eye. Besides scanning x-ray chemical imaging, a projection mode imaging has been studied [4,5]. This result will also be reported.

References:

[1] K. Tsuji, K. Nakano, X-Ray Spectrom. **36**, 145 (2007).
[2] K. Nakano, K. Tsuji, J. Anal. At. Spectrom. **25**, 562 (2010).
[3] T. Yonehara, D. Orita, K. Nakano et al., X-Ray Spectrom. **39**, 78 (2010).
[4] K. Tsuji, K. Nakano, M. Yamaguchi et al. Proc. SPIE, **7077**, 70770W-1 (2008).
[5] T. Yonehara, M. Yamaguchi, K. Tsuji, Proc. TXRF2009, Spectrochim. Acta Part B, (2010) in press.

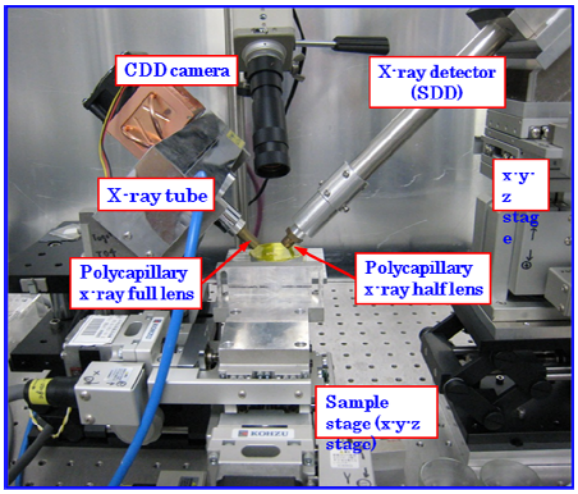

Figure 1: 3D-XRF instrument (second setup in our laboratory) [2].

Development of a Reflection Zone Plate for Hard X-ray Nanofocusing

T. Tsuji, H. Takano, T. Hashimoto, S. Konishi, M. Morikawa,
T. Koyama, Y. Tsusaka, Y. Kagoshima

Graduate School of Material Science, University of Hyogo, 3-2-1 Kouto, Kamigori, Ako, Hyogo 679-1297, Japan

Abstract:

High-resolution X-ray imaging has been performed following the development of focusing devices and high-spatial-coherence X-ray sources. A focusing beam with a size of 7~30 nm can be obtained using a Fresnel zone plate and an elliptical mirror, a multilayer Laue lens, and a multilayer elliptical mirror. However, they require high fabrication accuracy to achieve such beam size. We have developed a total reflection zone plate (TRZP) [1] THAT does not require high fabrication accuracy comparatively and has a high potential as a nanofocusing device.

The TRZP consists of Pt zone plate patterns drawn on a flat Si substrate. The reflection only from the zone pattern can be extracted by operating the TRZP with a grazing incident angle between critical angles of Pt and Si. The schematic drawing of the TRZP and the arrangement for X-ray focusing are shown in Figure 1. The reflection ratio between Pt and Si is 136 with a grazing incident angle of 6 mrad. Also the effective zone size is fully reduced to the drawn zone width with a small reduction ratio of 1/167. A part of the zone plate pattern is drawn in order to prevent the desired focal point from being overlapped by the undesired direct reflection of the substrate. Parameters of the fabricated TRZP are designed for 10 keV X-rays, as the number of zones, and the focal lengths of 1000 and 4.16 mm, respectively. Then the geometrical diffraction limit with grazing incident angle of 6 mrad is estimated to be 14.7 nm.

A focusing test was performed at the "Hyogo-ID" beamline (BL24XU) of SPring-8. The obtained intensity distribution profile is shown in Figure 2. The ideal profile is calculated by the Fresnel-Kirchhoff diffraction formula. The obtained beam size was 14.4 ± 1.7 nm in the full-width at half-maximum. Forty-one measurements were performed in order to confirm the reproducibility. This value was close to the diffraction limit.

References:

[1] T. Tsuji, H. Takano, T. Koyama et al., Jpn. J. Appl. Phys. **49**, 030207 (2010).

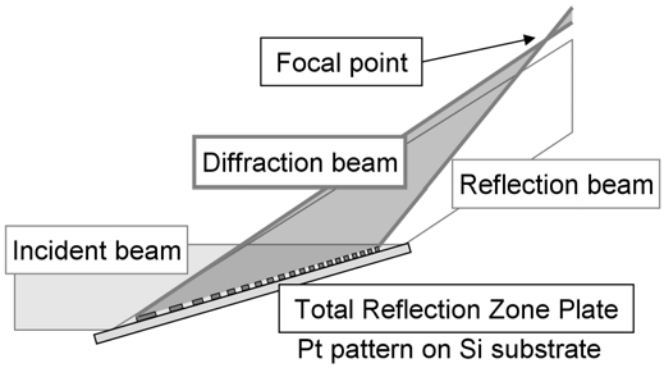

Figure 1: Schematic drawing of the TRZP and arrangement for hard X-ray.

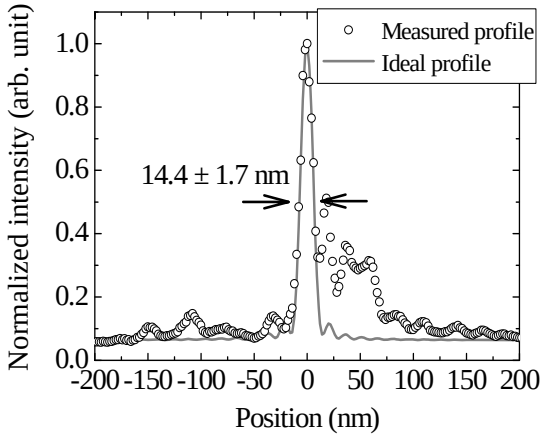

Figure 2: Intensity distribution profile of focused beam at the focal plane.

Three-Dimensionally Controlled Ion Milling for Reflection Phase Manipulation of EUV Multilayer Mirrors

T. Tsuru, T. Hatano, M. Yamamoto

IMRAM, Tohoku University, 2-1-1 Katahira, Aoba-ku, Sendai 980-8577, Japan

Abstract:

In the extreme ultraviolet (EUV) wavelength region, reflection phase-corrected EUV multilayer mirrors are required for high-definition imaging. For the diffraction-limited imaging needed for microscopy, the reflection wavefront error should be reduced to within a sub-nm level due to the short wavelength in this region. As a possible and practical technique to achieve the high precise wavefront, we developed an ion milling system with a wide-area ion beam enabling period-by-period milling of multilayer mirrors [1]. For the demonstration of nm-figure error correction by a stepwise, 0.1-nm-per-period [2] milling, area-, depth-, and boundary structure-controlled ion milling [3] and reflection phase measurement by EUV interferometry were carried out in this study.

Forty periods of Mo/Si multilayer surface were locally milled for 10 periods by a homogenizer mask. Although the optical pass difference between milled and untreated surfaces corresponds to 10 wavelengths, 2/3π reflection phase-change would be expected by the refractive index contrast between the vacuum and multilayer. Since the EUV reflectance of a few-μm-thick photoresist is low enough, a double slit aperture made of photoresist was patterned on a locally milled multilayer for the phase measurement by a Young-type interferometer in the reflection configuration. Figure 1 shows a schematic drawing of a milled multilayer with contact double slit. The slit width and distance are 30 μm and 80 μm, respectively. The sharp milled boundary between slits was made by a photoresist mask. To avoid the fringe jump, the graded area was formed within a slit pattern by a Mo mask set 3 mm apart from a multilayer. Referring to the interference fringe pattern generated by reflections at untreated areas, the reflection phase at the milled area can be measured as a shift of fringe pattern. The fringe observation was performed at BL-12A, the Photon Factory. Figure 2 shows the fringe pattern observed at 14.15 nm. Ten periods removal by surface milling showed a small phase change, as we predicted.

References:

[1] T. Tsuru, A. Tosaka, Y. Sakai et al., J. Phys.: Conf. Ser. **186**, 012077 (2009).
[2] M. Yamamoto, Nucl. Instrum. Methods A **467-468**, 1282 (2001).
[3] T. Tsuru, Y. Sakai, T. Hatano et al., accepted to AIP Conf. Proc.

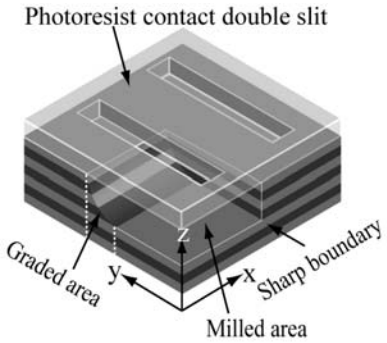

Figure 1: Schematic drawing of a locally milled Mo/Si multilayer with photoresist contact double slit for EUV interferometry.

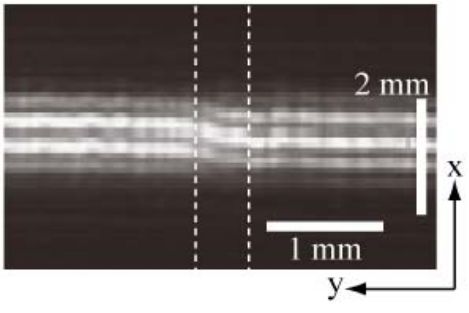

Figure 2: Fringe pattern observed by a Young-type interferometer in the reflection configuration at 14.15 nm. Dotted lines correspond to graded area.

New Ambient Pressure Scanning Photoelectron Microscope at the ALS

T. Tyliszczak, Z. Hussain, H. Bluhm

Lawrence Berkeley National Laboratory, 1 Cyclotron Rd., Berkeley, USA

Abstract:

We have designed and constructed a scanning ambient pressure scanning photoemission microscope with a spatial resolution of better than 100 nm for the investigation of heterogeneous chemical reactions at solid/vapor interfaces under conditions relevant to atmospheric/environmental science, energy research, and heterogeneous catalysis.

Synchrotron-based ambient pressure photoemission spectroscopy (APPES), which was developed at LBNL 10 years ago [1], has shown its utility for the investigation of solid/vapor and liquid/vapor interfaces at pressures up to 5 torr (the equilibrium water vapor pressure at 0 °C is 4.6 torr). In particular, in the fields of heterogeneous catalysis and atmospheric/environmental science the investigation of surfaces under realistic conditions of temperature, gas composition, and pressure is essential for a fundamental understanding of the molecular processes at liquid/vapor and solid/vapor interfaces that govern interfacial chemistry. Many of the most relevant solid/vapor interfaces are spatially and chemically inhomogeneous. In current APPES experiments this aspect cannot be adequately evaluated since the measurements average over the whole sample area that is illuminated by the incident X-ray beam, which is usually 100 μm in diameter or larger.

We implemented the scanning ambient pressure spectromicroscope in the new APPES end station at beamline 11.0.2. This end station features a third-generation differentially pumped electrostatic lens system with an acceptance half angle of better than 20 deg. Custom-designed sample cells can easily be attached and exchanged, which will greatly simplify the design and test of the instrument. The main challenges in the design and operation of a zone-plate-based APPES instrument are due to: the close proximity of the zone plate and order sorting aperture (OSA) to the conical entrance aperture of the differential pumping system and the sample; the requirement for very precise alignment and motion of zone plate, OSA, and sample; and the limit on the relative vibration of zone plate and sample to less than about 20 nm.

The zone plate and sample motion control is based on an interferometer feedback design first introduced in the ALS STXM end station [2].

References:

[1] D.F. Ogletree, H. Bluhm, G. Lebedev et al., Rev. Sci. Instrum. **73**, 3872 (2002).

[2] A.L.D. Kilcoyne, T. Tyliszczak, W.F. Steele et al., J. Synchrotron Radiat. **10**, 125 (2003).

Electron Yield Detection in Scanning Transmission X-ray Microscopy: Improving Surface Sensitivity*

S.G. Urquhart[3], S. Behyan[1], B. Haines[1], C. Karunakaran[2], J. Wang[2], M. Obst[2], T. Tyliszczak[3]

[1]*Department of Chemistry, University of Saskatchewan, Saskatoon, SK, Canada*
[2]*Canadian Light Source, University of Saskatchewan, Saskatoon, SK, Canada*
[3]*Advanced Light Source, Lawrence Berkeley National Laboratory, Berkeley, CA, USA*

* Supported by NSERC (Canada). Experiments performed at the Canadian Light Source and the Advanced Light Source.

Abstract:

We have modified Scanning Transmission X-ray Microscopes (STXM) at the Canadian Light Source and the Advanced Light Source to enhance their surface sensitivity. A channeltron, mounted behind the sample, detects secondary electrons that escape from the sample surface. This surface-sensitive signal can be recorded in parallel with transmission detection. This method provides for improved surface sensitive imaging of ultrathin films such as phase-separated Langmuir-Blodgett monolayer films, as well as differentiation of surface and bulk oxides of patterned metallic thin films. Figure 1 presents the transmission (left) and the total electron yield STXM image (right), recorded at the Cr 2p → 3d transition energy (576 eV), of a patterned metal sample. Dark regions in the transmission image indicate the decreased transmission from photon absorption by Cr. The contrast is reversed in the TEY image; the Cr surface film leads to increased photoemission at the Cr 2p → 3d transition energy. Fe 2p and Cr 2p NEXAFS spectra, recorded in total electron yield, are presented in Figure 2. As expected and demonstrating preferential surface sensitivity, Cr 2p features are only observed from the sample region where the Cr layer is present. Fe 2p features are observed over the entire sample surface; however, the Fe 2p edge jump is smaller and the pre-edge absorption is higher in the sample regions where the Cr overlayer is present. We will outline the experimental challenges of this new method and the opportunities for correlative surface and bulk measurements of complex samples [1].

References:

[1] B.M. Haines, S. Behyan, S.L. Christensen et al., Canadian Light Source, Activity Report No. 2008, 154 (2008).

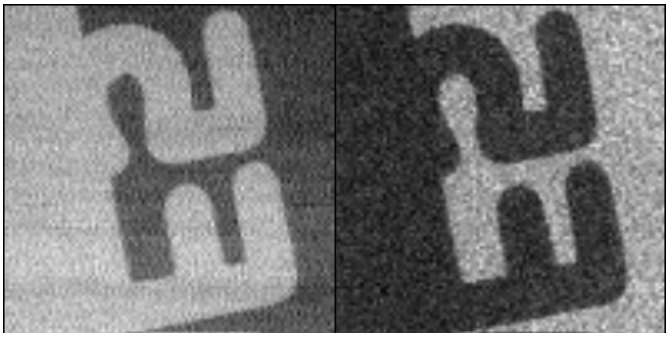

Figure 1: Scanning X-ray Microscopy images of a patterned 5 Å Cr pattern evaporated onto a 20 Å Fe film, recorded at the energy of the Cr 2p → 3d transition, recorded in transmission (left) and surface sensitive total electron yield (right).

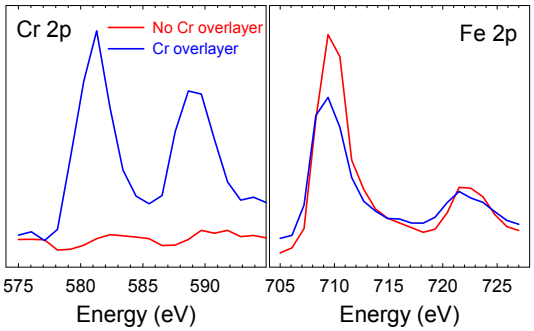

Figure 2: Cr 2p (left) and Fe 2p (right) NEXAFS spectra of a patterned sample (Cr on Fe). The blue trace is from regions with the Cr overlayer and the red trace from regions without the Cr overlayer.

A Flexible Modular Laboratory X-ray Nano-CT Scanner*

D. Van Loo[1], B. Masschaele[1], M. Dierick[1], M.N. Boone[1], J. Van den Bulcke[2], D. Vansteenkiste[2], L. Van Hoorebeke[1], J. Van Acker[2], P. Jacobs[3]

[1]*UGCT, Dept. Physics and Astronomy, Ghent Univ., Proeftuinstraat 86, 9000 Ghent, Belgium*
[2]*UGCT, Laboratory of Wood Technology, Ghent Univ., Coupure Links 653, 9000 Ghent, Belgium*
[3]*UGCT, Dept. of Geology and Soil Science, Ghent Univ., Krijgslaan 281/S8, B-9000 Ghent, Belgium*

*The authors gratefully acknowledge IWT Flanders for its financial support for this project (Strategic Basic Research SBO 060032).

Abstract:
X-ray micro/nano-CT (μCT) has recently become a very powerful and common tool for non-destructive 3D visualization and analysis of small objects. Many systems are commercially available, but they are typically limited in terms of resolution and/or sample size range, and come in closed cabinets, thus limiting the experimental freedom. The Centre for X-ray Tomography of the Ghent University (UGCT, Belgium: www.ugct.ugent.be) has designed and built a state-of-the-art modular micro/nano-CT scanner. Its dual source / dual detector design attains resolutions down to 400 nm for small samples, but also allows scanning samples up to 30 cm in diameter at lower resolution. The performance of the system will be characterized in detail. Specific design elements built-in to achieve the very high resolution will be presented, as well as the wide range of acquisition modes (helix scanning, tiled acquisition, continuous rotation, etc). A picture of the new scanner is shown in Figure 1. The scanner has already been used in multiple research applications. One of the results can be found in Figure 2, where a very small piece of wood is shown at a voxel size of approx. 500 nm.

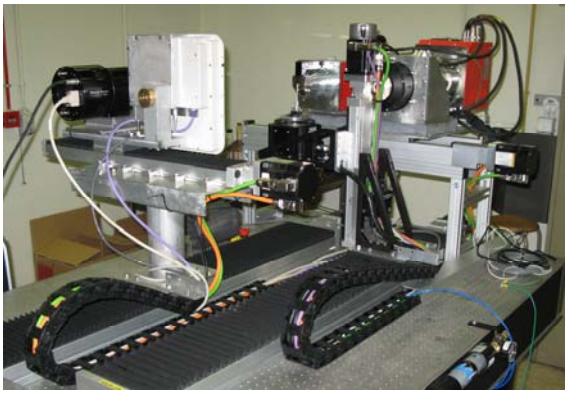

Figure 1: The nano-CT scanner, with two X-ray sources and two X-ray detectors.

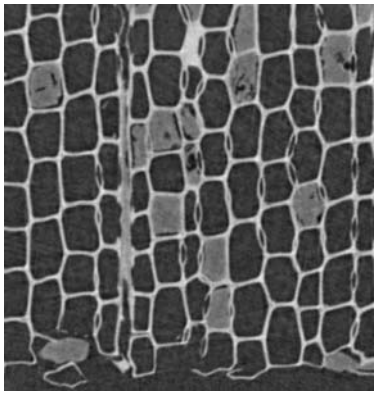

Figure 2: A reconstructed CT slice of a wood sample. Voxel size is approximately 500 nm.

High Energy Nanoscale Resolution X-ray Microscopy Based on Refractive Optics on a Long Beamline

G.B.M. Vaughan, I. Snigireva, A. Snigirev

European Synchrotron Radiation Facility (ESRF), 38043 Grenoble, France

Abstract:

The long length and good coherence properties of ID11 at the ESRF has led to the development of X-ray microscopy applications. For the highest resolution full-field microscopy, the sample is placed at ~40 m from the source, which can be micro-focused by a transfocator [1,2]. Due to the long length of the beamline and consequent long sample-detector distance, an objective (Be lenses) can be placed up to a meter behind the sample and still allow for magnification of 60x on a detector located at 99 m—enough to achieve easily 100-nm resolution with a typical high-resolution detector. Even higher magnifications could be achieved with a shorter objective distance, but resolution will likely be limited by other factors. The long focal length and relatively high energy allow the use of complex sample environments and highly absorbing samples. Furthermore, the long focal length means that there is a reasonable depth-of-focus, often a limitation in such experiments.

In order to validate the microscopy performance, test objects have been measured in this configuration at 29.2 keV, using 66 50-µm-radius Be lenses as an objection. With this prototypical configuration, we can clearly see 200-nm features on test objects, and further tests on optical benches have shown that the optics themselves are high enough quality to produce sub-100-nm resolution once an appropriate mounting has been constructed. All of the optics used in these experiments are in-line, allowing rapid switching between the imaging mode described here and micro- or nano-diffraction applications. The near-simultaneous combination of full-field X-ray microscopy with high-resolution diffraction is straightforward and can be applied to the study of multi-length scale materials such as inverted photonic crystals [3] and other high-Z materials.

References:

[1] A. Snigirev et al, J. Phys.: Conf. Ser. **186**, 012073 (2009).
[2] G. Vaughan et al., to be published.
[3] A. Bosak, I. Snigireva, K. Napolskii et al., Adv. Mater. (2010), accepted.

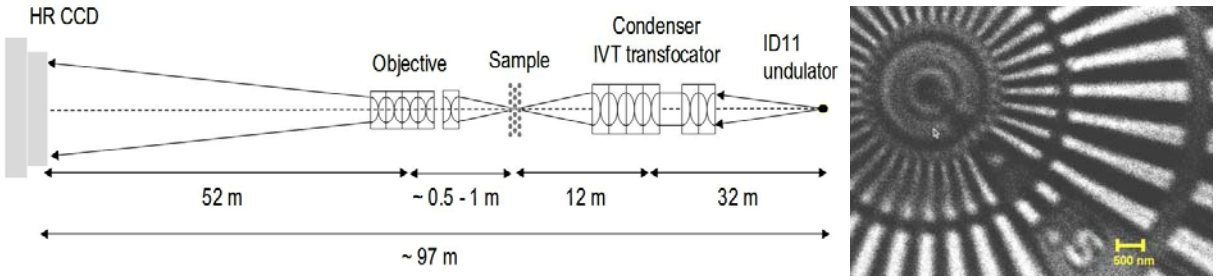

Figure 1: HE X-ray microscopy setup at ID11 beamline (left) and X-ray image of a Siemens' Star test object (500-nm-thick Ta) taken at 29.2 keV (right).

World-Record Resolution in Scanning Transmission X-ray Microscopy

J. Vila-Comamala[1], S. Gorelick[1], V. A. Guzenko[1], E. Färm[2], C. M. Kewish[1], A. Diaz[1], J. Raabe[1], M. Ritala[2], A. Menzel[1], O. Bunk[1], C. David[1]

[1]*Paul Scherrer Institut, CH-5232 Villigen, Switzerland*
[2]*Department of Chemistry, FI-00014 University of Helsinki, Finland*

Abstract:

We demonstrate the highest spatial resolution ever reported in scanning transmission X-ray microscopy (STXM) to date. For the first time in X-ray microscopy, features below 10 nm in width were resolved in the soft X-ray regime (1.2 keV) and 15 nm lines and spaces were visible at multi-keV photon energies (6.2 keV). These achievements were accomplished by using line-double Fresnel zone plates (FZP). The lenses were fabricated by combining electron-beam lithography with atomic layer deposition [1]. In the soft X-ray regime, the spatial resolution tests were performed by acquiring transmission images of line pair structures of a GaAs/AlGaAs heterostructure. A zone-doubled Fresnel zone plate with 100 µm diameter and outermost zone width of 12.5 nm was used. Figure 1 shows the STXM image of the sample containing line widths ranging from 40 to 9 nm. The set of three lines of 9 nm is resolved [2]. During the STXM experiments at multi-keV photon energies, the full divergent radiation cone was sequentially recorded by a pixel fast framing detector at each scanning position. These data were processed to obtain the transmission, dark-field, differential phase contrast, and the integrated phase signals for every sample. A zone-doubled Fresnel zone plate with 100 µm diameter and outermost zone width of 15 nm was used. The STXM image of test structures shown in Figure 2 demonstrates the extreme resolving power. In addition, high spatial resolution STXM images of several biological specimens have been acquired in transmission, dark-field, and differential phase contrast modes.

References:

[1] K. Jefimovs, J. Vila-Comamala, T. Pilvi et al., Phys. Rev. Lett. **99**, 264801 (2007).
[2] J. Vila-Comamala, K. Jefimovs, J. Raabe et al., Ultramicroscopy **109**(11), 1360 (2009).

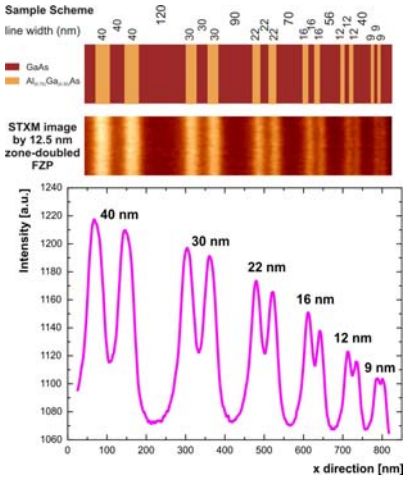

Figure 1: STXM image of GaAs/AlGaAs hetero-structure acquired at 1.2-keV photon energy by zone-doubled FZP with 12.5-nm outermost zone width. The set of three lines of 9 nm is resolved.

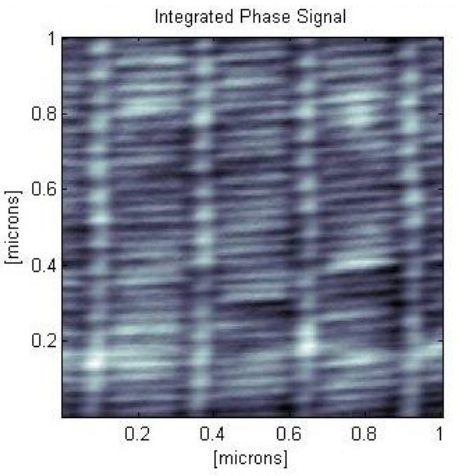

Figure 2: STXM image of 15-nm lines and spaces resolved at 6.2-keV photon energy. The data were acquired by a zone-doubled FZP outermost zone width of 15 nm.

Novel Imaging at the PolLux STXM*

B. Watts[1], C. R. McNeill[2], J. Raabe[1]

[1]*Paul Scherrer Institut, 5232 Villigen PSI, Switzerland*
[2]*Cavendish Laboratory, University of Cambridge, J J Thomson Ave, Cambridge, CB3 0HE, United Kingdom*

*PolLux is funded by the BMBF (Project No. 05KS7WE1). This work was supported by the Engineering and Physical Sciences Research Council, U.K. (Advanced Research Fellowship EP/E051804/1).

Abstract:

Thin polymer films are of increasing technological importance in optoelectronic devices such as LEDs, lasers, FETs, and solar cells [1]. However, the morphology of such films is complex, often displaying three-dimensional composition structure or molecular alignment effects. The structure of the polymer film incorporated into a device can strongly affect its performance characteristics, e.g., via the connectedness between polymer domains and to the device electrodes, or due to anisotropic material properties due to molecular alignment [2].

Recent work at the PolLux STXM has demonstrated two new developments in the imaging of thin polymer films. Firstly, simultaneous imaging of the sample bulk and surface regions has been enabled by the installation of a channeltron detector (operated in TEY mode) next to the standard phosphor-coated PMT detector. Secondly, mapping of the molecular orientation within an annealed F8BT polymer film has been achieved via imaging at the energy of an anisotropic resonance combined with rotation of the sample. Details of the measurements, analysis, and scientific interest will be presented.

References:

[1] C.R. McNeill, N.C. Greenham, Adv. Mater. **21**, 3840 (2009).
[2] M. Redecker, D.D.C. Bradley, M. Inbasekaran et al., Appl. Phys. Lett. **74**, 1400 (1999).

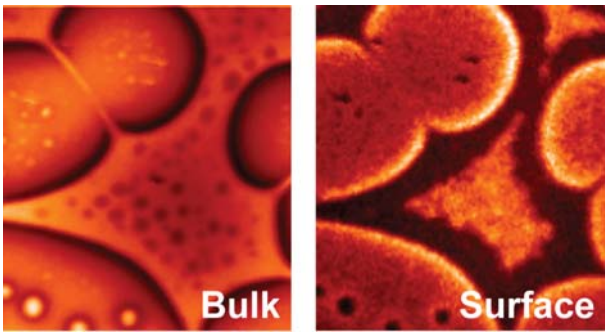

Figure 1: 7x7 µm bulk and topside surface images of a 1:1 PFB:F8BT polymer blend film spincast from xylene, measured at the 285 eV PFB π* resonance.

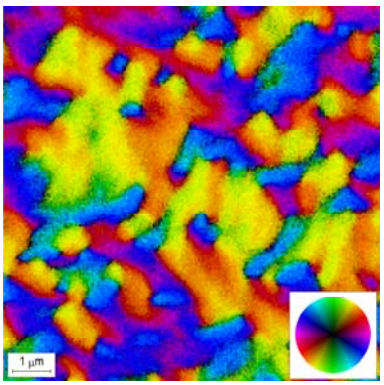

Figure 2: False color plot showing the molecular orientation (colors) and degree of alignment (brightness) in an annealed F8BT film.

Hard X-ray Fluorescence Imaging Facilities at SSRL*

S.M. Webb

Stanford Synchrotron Radiation Lightsource, SLAC National Accelerator Laboratory, 2575 Sand Hill Road, Menlo Park, California, USA

* Portions of this research were carried out at the Stanford Synchrotron Radiation Lightsource, a national user facility operated by Stanford University on behalf of the U.S. Department of Energy, Office of Basic Energy Sciences. The SSRL Structural Molecular Biology Program is supported by the Department of Energy, Office of Biological and Environmental Research, and by the National Institutes of Health, National Center for Research Resources, Biomedical Technology Program.

Abstract:

The Stanford Synchrotron Radiation Lightsource has developed several hard x-ray imaging stations across several beam lines. These stations form a facility that covers a wide range of x-ray spot sizes (from 2 to 250 microns), x-ray energies (from 2 to 23 keV), and variety of sample sizes (up to 300 x 600 mm). Techniques such as μ-XRF mapping, μ-XAS, μ-XRD, and pencil-beam-based μ-fluorescence tomography are routinely performed. The characteristics of each of the beam line stations and exciting recent scientific results will be presented.

The Microanalysis Toolkit: X-ray Fluorescence Image Processing Software*

S.M. Webb

Stanford Synchrotron Radiation Lightsource, SLAC National Accelerator Laboratory, 2575 Sand Hill Road, Menlo Park, California, USA

* Portions of this research were carried out at the Stanford Synchrotron Radiation Lightsource, a national user facility operated by Stanford University on behalf of the U.S. Department of Energy, Office of Basic Energy Sciences. The SSRL Structural Molecular Biology Program is supported by the Department of Energy, Office of Biological and Environmental Research, and by the National Institutes of Health, National Center for Research Resources, Biomedical Technology Program.

Abstract:

The Microanalysis Toolkit is an analysis suite designed for the processing of x-ray fluorescence microprobe data. The program contains a wide variety of analysis tools, including image maps, correlation plots, simple image math, image filtering, XAS image fitting, semi-quantitative elemental analysis, x-ray fluorescence spectrum analysis, PCA analysis, and tomographic reconstructions. To be a widely useful as possible, data formats from many synchrotron sources can be read by the program with more formats available by request. An overview of the most common features will be presented.

MAXYMUS – Features and Commissioning Results of a New UHV STXM at HZB/Bessy II, Berlin

M. Weigand[1], M. Bechtel[1], C. Wolter[1], E. Goering[1], B. Van Waeyenberge[2], B. Baretzky[3]

[1]*Max-Planck-Institute for Metals Research, Heisenbergstr. 3, 70569 Stuttgart, Germany*
[2]*Ghent University, Sint-Pietersnieuwstraat 25, 9000 Ghent, Belgium*
[3]*Karlsruher Institut für Technologie, Institut für Nanotechnologie, Hermann-von-Helmholtz-Platz 1, 76344 Eggenstein-Leopoldshafen, Germany*

Abstract:
In 2009, a new UHV-compatible and interferometer-controlled scanning x-ray transmission microscope (STXM) manufactured by Bruker ASC (former ACCEL) and based on the design of the ALS STXM [1] was installed at a helical undulator beamline at Bessy, Berlin.

Fundamental advances implemented are a fully UHV-adapted design with bake temperatures up to 110°C, the inclusion of zone-plate scanning in addition to the scanning of the sample, and a complete UHV preparation system for bulk sample investigations performed in total electron yield mode.

The microscope itself features sample holders for *in situ* sample rotation, a permanent magnet system allowing full field strength and directional control and multiple detectors: phosphor-coupled photomultiplier tubes and fast CCDs, as well as avalanche photodiodes with lock-in amplification of single photon counts.

The microscope infrastructure includes a newly build hutch with high-stability air conditioning, and user workspace for sample preparation including Flowbox, optical microscopy, and sample storage. In addition signal generation and processing equipment for multi-GHz pump-and-probe experiments is available.

Some of the major milestones during the commissioning process were dynamic pump and probe measurements of in- and out-of-plane magnetization dynamics with 50-ps resolution and total electron yield measurements on magnetic samples. In addition, we could achieve hydrocarbon partial pressures better than 10^{-10} mbar.

We will present those milestones, results of first beam times of friendly users, as well as research possibilities available at the microscope for future external users.

References:

[1] A.L.D. Kilcoyne, T. Tyliszczak, W.F. Steele et al., J. Synchrotron Radiat. **10,** 125 (2003).

X-Ray Microscopy with Compact Sources

U. Wiesemann[1], W. Diete[1], M. Benk[2], K. Bergmann[2], H. Legall[3], H. Stiel[3]

[1]*Bruker ASC GmbH, Friedrich-Ebert-Str. 1, 51429 Bergisch Gladbach, Germany*
[2]*Fraunhofer Institute for Laser Technology, Steinbachstraße, Aachen, Germany*
[3]*Max-Born-Institut, Max-Born-Straße 2A, 12489 Berlin, Germany*

Abstract:
In a publicly funded research network, a number of partner institutes and companies led by Bruker ASC (formerly ACCEL Instruments) have built a laboratory transmission X-ray microscope (LTXM) to demonstrate the practicability of standalone soft X-ray microscopy. The development focus is on high brilliance sources, efficient optics, and the overall system integration.

Building upon the developments for EUV lithography, a high brilliance gas discharge source has been built allowing exposure times of about 30 s and below even for biological samples [1,2]. Using a high power laser, the smaller jet target laser plasma source provides brilliance reserves e.g., for higher tomography throughput or for working at very high resolutions.

To efficiently transfer the light of each source to the sample, different condenser concepts are employed. A normal incidence spherical multilayer condenser or a zone plate condenser is used with the laser plasma source (λ=2.48 nm). For operation with the gas discharge source at 2.88 nm, a grazing incidence ellipsoidal condenser has been developed.

The sample environment including vacuum load lock, goniometer for tomography, and sample holder is based on the existing developments for transmission electron microscopy. Using a cryogenic sample holder, images of frozen hydrated samples can be acquired.

In this paper we will report on the performance of the LTXM components and show recent results obtained with the microscope [3].

References:

[1] K. Bergmann, F. Küpper, M. Benk, J. Appl. Phy. **103**(12), 123304 (2008).
[2] M. Benk, K. Bergmann, D. Schaefer, and T. Wilhein, this conference.
[3] M. Benk, K. Bergmann, A. Querejeta, S. Srivastava, N.A. Kotov, D. Schaefer, and T. Wilhein, this conference.

Figure 1: The LTXM demonstrator.

Figure 2: Ellipsoidal grazing incidence condenser.

Table-Top XUV/EUV Setup for Imaging and Spectroscopy

U. Wiesemann[1], W. Diete[1], D.D. Mai[2], T. Salditt[2], F. Barkusky[3], K. Mann[3]

[1]*Bruker ASC GmbH, Bergisch Gladbach, Germany*
[2]*Institute for X-Ray Physics and Courant Research Centre for Nano Spectroscopy and X-Ray Imaging, University of Goettingen, Goettingen, Germany*
[3]*Laser-Laboratorium Goettingen e.V., Goettingen, Germany*

Abstract:
Compared to light microscopy, X-ray imaging techniques are still in an early stage of development. Current dedicated diffractometry and imaging instruments are limited to few specific optical arrangements. In this poster, we present a new experimental setup making possible a wide range of experimental concepts. The compact experimental chamber can be operated both at a home laboratory source and as a synchrotron end station. This allows users to start to study new methods and procedures at the laboratory source and then to continue the experiments with higher resolution at the synchrotron. Building upon the optical bench and breadboard principles established in light optics, the setup allows one to arrange optical elements almost arbitrarily. The optical elements are mounted on standardized in-vacuum compact linear and rotational stages.

In the home laboratory, a compact gas target laser plasma source is used [1]. By choosing the gas target, different EUV/XUV wavelengths can be generated. The modular principle of the whole setup also allows the implementation of alternative targets, lasers, or sources.

Commissioning is planned to start in autumn 2010. Proposed experiments include:

- X-ray imaging (coherent diffractive imaging or zone plate based)
- Scanning techniques (ptychography [2], STXM, etc.)
- Waveguide optics [3]
- In-line X-ray holography [3]
- NEXAFS spectroscopy [4]
- XRD and reflectometry

References:

[1] S. Kranzusch et al., Rev. Sci. Instrum. **74**, 969 (2003).
[2] K. Giewekemeyer et al., PNAS **107**(2), 529 (2010).
[3] C. Fuhse et al., Phys. Rev. Lett. **97**, 254801 (2006).
[4] C. Peth et al., J. Phys. D : Appl. Phys. **41**, 105202 (2008).

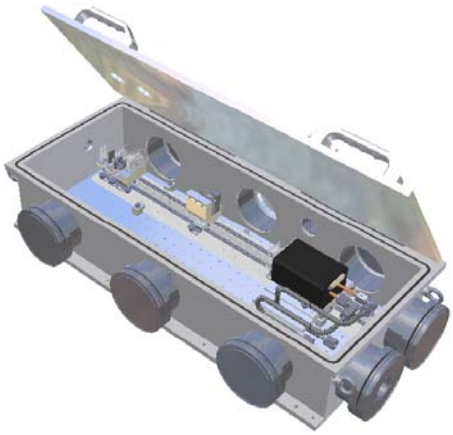

Figure 1: Experimental chamber.

The Coherent Imaging and Diffraction Instrument at the Linac Coherent Light Source*

G. J. Williams, S. Boutet

SLAC National Accelerator Laboratory, 2575 Sand Hill Rd, Menlo Park, CA, USA

Abstract:
Coherent imaging techniques that utilize the diffraction pattern formed by the interaction of an illuminating beam and a sample of interest have garnered much interest at synchrotron X-ray facilities over the past decade. The primary characteristic required of the source is its coherence properties and so third generation rings have been regarded as prime real estate for the development of these methods, whose advantage lies in the lensless imaging of micron-sized samples at a resolution of a few times the X-ray wavelength.

The Linac Coherent Light Source (LCLS), at SLAC is the world's first hard X-ray free electron laser (XFEL) user facility, providing extraordinarily brilliant flux in a pulse, which is variable from 10 to 300 femtoseconds. We will discuss one of the six instruments available to general users: the coherent X-ray imaging (CXI) instrument.

The CXI instrument supports structure determination in sub-micron samples, whether the method be coherent imaging or diffraction studies. The instrument will be commissioned during the third run of user experiments in 2010-2011 and available to general users starting in the spring of 2011. Here, we will present a summary of the instrument capabilities and preliminary commissioning results, including those related to the large 2D pixel array detector.

Development of X-ray Nanotomography with the Hard X-ray Nanoprobe*

R. P. Winarski[1], M. V. Holt[2], V. Rose[1], F. De Carlo[1], J. Maser[1]

[1]*Center for Nanoscale Materials, Argonne National Laboratory, 9700 South Cass Avenue, Argonne, Illinois 60439, USA*

[1]*Advanced Photon Source, Argonne National Laboratory, 9700 South Cass Avenue, Argonne, Illinois 60439, USA*

* Use of the Center for Nanoscale Materials was supported by the U. S. Department of Energy, Office of Science, Office of Basic Energy Sciences, under Contract No. DE-AC02-06CH11357.

Abstract:

The Hard X-ray Nanoprobe beamline is one of the featured instruments of the new Center for Nanoscale Materials at Argonne National Laboratory [1]. Located at sector 26 of the Advanced Photon Source, the Nanoprobe will explore nanoscale objects with an initial spatial resolution of 30 nanometers, using x-ray fluorescence spectroscopy, transmission imaging, diffraction, and scattering. X-ray fluorescence measurements will provide element-specific imaging of individual nanoparticles inside of samples. Transmission imaging and precisely controlled sample positioning will display detailed three-dimensional mappings of thick specimens and devices. X-ray diffraction and scattering capabilities will examine strain states and ordering in nanoscale systems. We are developing a nanotomography program to characterize samples using the unique capabilities of the Nanoprobe [2].

References:

[1] J. Maser, G.B. Stephenson, R.P. Winarski et al., Microsc. Microanal. **11**(2), 680 (2005).

[2] For more information: http://www.cnm.anl.gov/research/xray.html

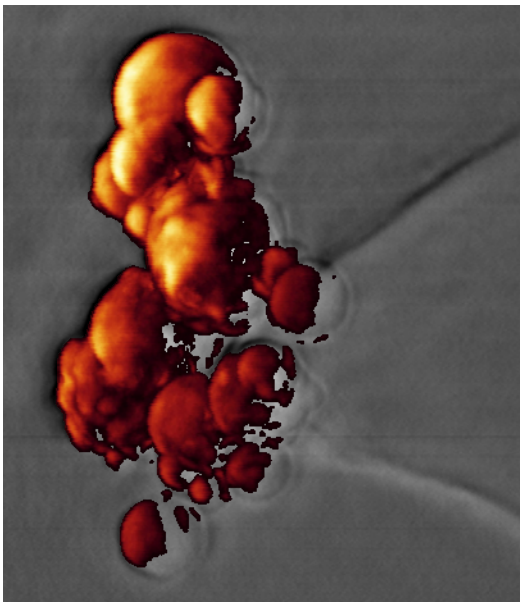

Figure 1: Gold particles on the edge of an aerogel sample. Features as small as 200 nm are well defined in the reconstruction.

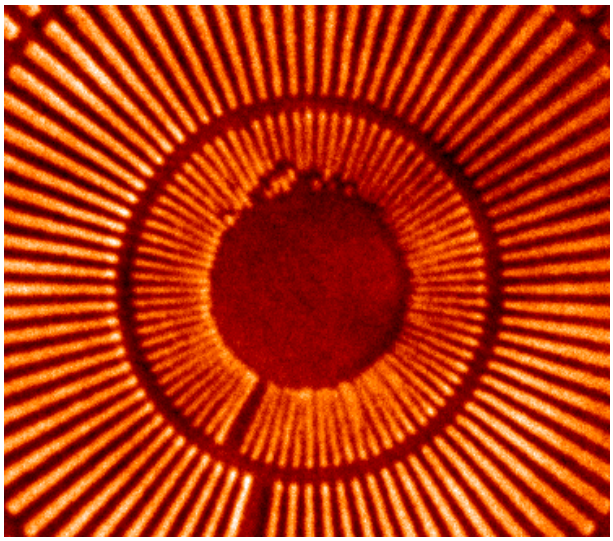

Figure 2: Seimen star pattern with 24-nm smallest spokes imaged in transmission mode.

Microtomography for Material and Biomedical Science at SSRF

T. Xiao*, G. Du, H. Xie, B. Deng, R. Chen, Y. Wang, F. Shen, H. Liu

Shanghai Synchrotron Radiation Facility, SINAP, CAS, Zhangheng Road 239, Shanghai 201204, China
** Corresponding author: tqxiao@sinap.ac.cn*

Abstract:
Micro-computed tomography, in phase or absorption contrast, was established in late 2008 at the X-ray imaging beamline of the Shanghai Synchrotron Radiation Facility (SSRF). A nano-stage on a high precision translation and rotation stage was employed to position the sample accurately and quickly. Sample-to-detector distance could be adjusted remotely from a few millimeters to several meters. For biomedical samples, X-ray CCD integrated with optical fiber is usually employed to improve the efficiency. For material samples or sample with higher resolution requirements, another detector system is used, which includes a piece of scintillator, a CCD, and a set of interchangeable objectives with the field of view varing from 0.38 x 0.38 mm^2 to 12.1 x 12.1 mm^2, while pixel sizes ranging from 0.19 x 0.19 μm^2 to 5.9 x 5.9 μm^2. Spatial resolution of 0.8 µm could be achieved, which is evaluated by a resolution chart. CT reconstruction software has been developed, with phase retrieval and spiral CT function included. In order to improve the reconstructing efficiency greatly, program running in GPU is underway. Examples of micro-CT by users, such as blood vessels in mouse kidney, polymer material, and paleontological embryo fossils and nonwoven fibers etc., will be introduced.

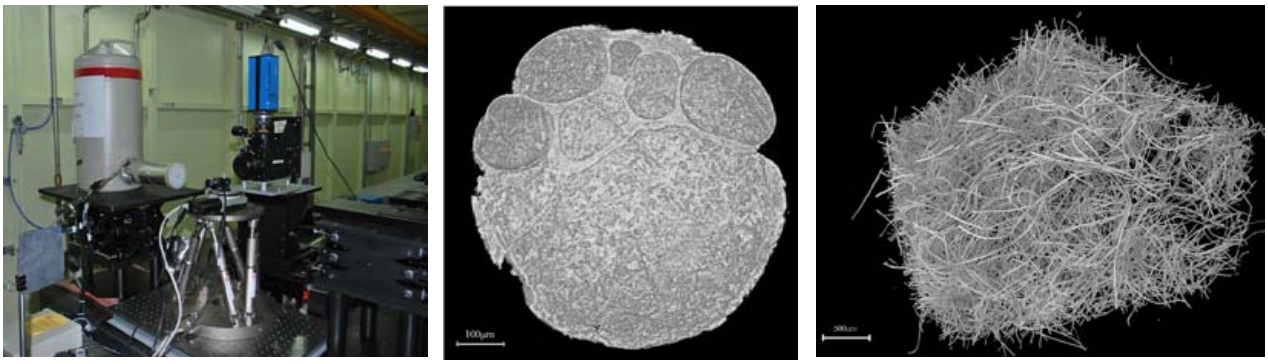

Figure 1: Setup for X-ray microtomography (left) and reconstructed slices for Precambrian animal embryo fossil (by Maoyan Zhu et al.) with space bar 100 micron (middle) and fiber in nonwoven cloth(by Hong Wang et al., fiber size: around 15 micron, right).

A Temperature-Controlled Liquid Cell in Transmission X-ray Microscope

G.-C. Yin[1], T.-W. Huang[2], D. J. Wang[1], S.-Y. Peng[1], F.-R. Chen[1,2], Y. Hwu[1,3], K. S. Liang[1]

[1]*National Synchrotron Radiation Research Center, 101 Hsin-Ann Road, Hsinchu, Taiwan*
[2]*Department of Engineering and System Science, National Tsing Hua University, Taiwan*
[3]*Institute of Physics, Academia Sinica, Taiwan*

Abstract:
In this report, we will present full-field transmission x-ray microscope studies of samples that are confined in a liquid cell. The transmission x-ray microscope (TXM) has 60-nm resolution with both absorption and phase contrast with hard x-rays [1-3]. A temperature-controlled liquid cell (environmental cell, Fig. 1) is specially designed and fabricated for the microscope to operate with 8-keV x-rays to provide a focus depth of about 100 μm and penetration depth larger than 100 μm. The temperature of the cell can be varied from -5 to 98 °Celsius. The results of studies using biological HeLa cell, macro-phage and *E coli* in the water, which demonstrates the potential of visualizing the biological cell in hard x-ray TXM, will be presented. An image of the *E coli* in the frozen state is shown in Figure 2.

The dynamic images can also be obtained with liquid cell. The images of the nano-particles are captured 2 frames per second. Their trajectories between each frame can be traced and analyzed. Applications using this capability will be presented.

References:
[1] G. Yin, M. Tang, Y. Song et al., Appl. Phys. Lett. **88**, 241115 (2006).
[2] G. Yin, F.W. Duewer, M. Feser et al., Appl. Phys. Lett. **89**, 221122 (2006).
[3] G.C. Yin, F.R. Chen, Y. Hwu et al., Appl. Phys. Lett. **90**, 181118 (2007).

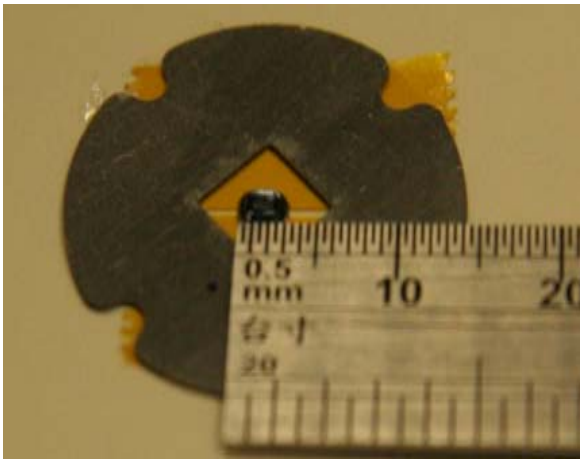

Figure 1: The image of the wet cell.

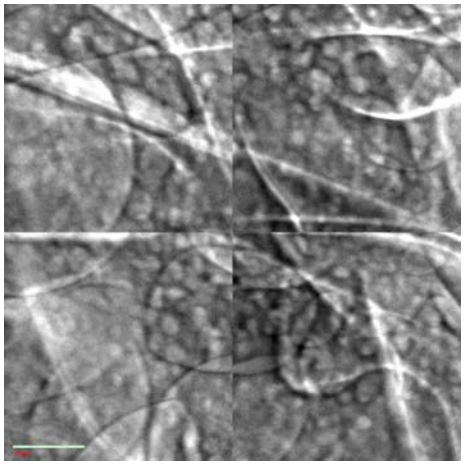

Figure 2: The frozen *E coli* imaged by TXM. The scale bar is 5 μm.

Current Status of the Transmission X-ray Microscopy in BSRF *

Q. Yuan[1], W. Huang[1], Y. Hong[1], K. Zhang[1], P. Zhu[1], Z. Wu[1,2],
J. Gelb[3], A. Tkachuk[3], W. Yun[3]

[1]*Institute of High Energy physics, Chinese Academy of Science, Beijing 100049, China*
[2]*National Synchrotron Radiation Laboratory, University of Science and Technology of China, Hefei 230026, China*
[3]*Xradia Inc., 4075A Sprig Drive, Concord, CA 94520, USA,*

Abstract:
Transmission X-ray microscope is a powerful nondestructive 3D imaging technique, which enables the visualization of three dimensional structures of complex, optically opaque samples [1,2]. High resolution X-ray microscope exploiting the light source generated from a wavelength shifter and a commercially available laboratory x-ray source was installed in December 2008at the 4W1A beamline at BSRF. It was designed to provide 2D imaging and 3D tomography in the energy range 5-11 keV with a spatial resolution in the range 30-150 nm and with a Zernike-phase contrast capability to investigate light materials. This contribution presents the design concept of the microscope, the installation and commissioning, and the description of a sub-50 nm resolution X-ray microscope system operating at 8 keV in absorption. A Zernike phase contrast mode based on a commercially available laboratory x-ray source is also described. The system utilizes high-efficiency Fresnel zone plates with an outermost zone width of 40 nm and 700 nm structure height resulting in a current spatial resolution better than 50 nm. In addition to the description of the system and its specifications, we present the recent commissioning results of this X-ray microscopy now available for experiments at BSRF.

References:

[1] P. Withers, Mater. Today **10**, 26 (2007).
[2] W. Chao, J. Kim, S. Rekawa et al., Opt. Express **17**, 17669 (2009).

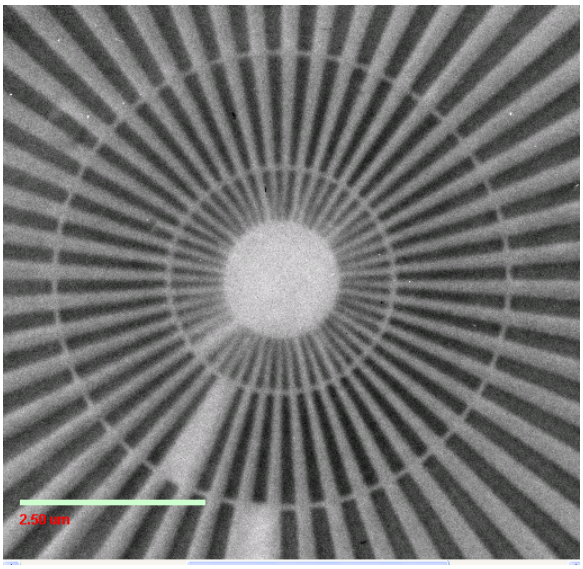

Figure 1: The electroplated gold spoke pattern with a 50 nm finest line width that was adapted to test the resolution of the microscope.

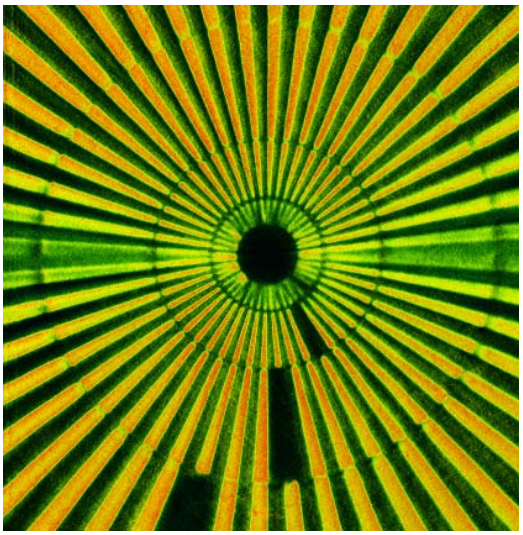

Figure 2: 3D reconstruction of the test pattern.

Long Working Distance Kirkpatrick-Baez Mirrors for Hard X-ray Beamlines at SPring-8

H. Yumoto[1], H. Ohashi [1,2], M. Yamamoto[2], S. Goto [1,2]

[1]SPring-8/Japan Synchrotron Radiation Research Institute (JASRI), 1-1-1, Kouto, Sayo-cho, Sayo-gun, Hyogo 679-5198, Japan
[2]SPring-8/RIKEN, 1-1-1, Kouto, Sayo-cho, Sayo-gun, Hyogo 679-5148, Japan

Abstract:
We designed and installed long working distance Kirkpatrick-Baez (KB) mirrors and corresponding manipulators, which were customized into hard X-ray beamlines at SPring-8. Microbeams with a long working distance are required frequently in analyses that need to set devices around sample positions, such as an intensity monitor and/or an X-ray coaxial camera. In other cases, for example, analyses under extreme environmental conditions, such as intense magnetic fields, low temperatures, and/or high pressures, use large instruments [1].

Here, we describe KB mirrors for the BL32XU RIKEN Targeted Proteins beamline. 400-mm and 400-mm-long KB mirrors for 1-μm focusing beam with a 730-mm-long working distance were designed for carrying out the structural analysis of microcrystal proteins. In 2009, we installed the KB mirrors focusing system and evaluated focusing properties. We realized focusing beam size of 0.9 × 0.9 μm^2 (FWHM) and focusing intensity of 6 × 10^{10} (photons/sec) at an X-ray energy of 12.4 keV. Conditioning process of this beamline for user operation in 2010 is currently underway.

References:

[1] H. Yumoto et al., Proc. of SPIE **7448**, 74480Z (2009).

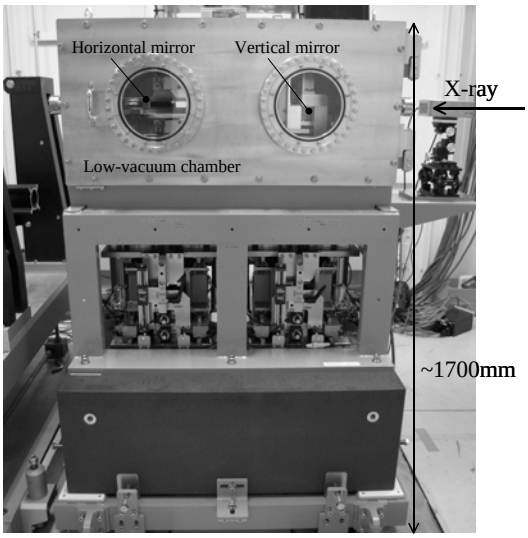

Figure 1: Developed manipulator for KB mirrors with a 730-mm-long working distance.

Capillary Wolter Mirrors as Condensers for X-ray Microscopy

X. Zeng, M. Feser, E. Huang, A. Lyon, W. Yun

Xradia Inc., 4075B Sprig Drive, Concord, CA 94520, USA

Abstract:

In the practical applications of full-field x-ray microscopy with laboratory x-ray sources, a high brightness illumination within the field of view is preferred for high throughput. The rotating anode x-ray sources have large spot sizes and can provide a large area (~100um) illumination, but their brightness is still not enough for high throughput; while the transmission sources can have much higher brightness than the rotating anode sources, but their spot sizes are too small (<5um) for a reasonable field of view (~15um). The combination of a magnifying Wolter mirror with a transmission source may solve the problem [1], in which the Wolter mirror can magnify the source spot size and reserve its brightness at the same time.

Glass capillary Wolter mirrors with short focal length were chosen to have compact microscopes. In the condenser design, the numerical aperture (NA) match with the objective zone plate and the x-ray critical angle were taken into account. Wolter mirrors with magnifications 2x, 4x and 6x were designed for fabrication.

The glass capillary Wolter mirrors were shaped in a computer controlled electrical oven. The fabrication technique was reported in our previous paper [2]. In this paper, we report on the Wolter mirror condenser design, fabrication and results of figure errors and x-ray test. We also discuss total slope error tolerance and the challenges in the fabrication.

References:

[1] W. Yun, Y. Wang, M. Feser e, “X-ray Microscope with Microfocus Source and Wolter Condenser,” U.S. Patent 7406151 (2008).

[2] X. Zeng, F. Duewer, M. Feser et al., Appl. Optics **47**(13), 2376 (2008).

Development of X-ray Microscopy in IPOE*

J. Zhu, B. Mu, Q. Huang, C. Huang, S. Yi, Z. Zhang, F. Wang, Z. Wang*, L. Chen

Institute of Precision Optical Engineering (IPOE), Physics Department,
Tongji University, Shanghai 200092, China
**Corresponding author: wangzs@tongji.edu.cn*

Abstract:

In order to meet the different requirements of synchrotron radiation sources and plasma diagnosis in China, focusing and imaging optics based on advanced Kirkpatrick-Baez mirrors (KBA), compound refractive lenses (CRL), and multilayer Laue lenses (MLL) were researched in the Institute of Precision Optical Engineering (IPOE), Tongji University, China.

To diagnose the high-temperature plasma, a one-dimensional KBA structure using a mirror coating of double periodic multilayers was developed. The multilayer mirror can work both at 4.75 keV (Ti K-line) and 8.05 keV (Cu K-line) simultaneously, which made the alignment and assemblage convenient. The 1D-KBA microscope achieves 2-3 μm resolution in a 250-μm field of view at an energy of 8.05 keV.

For hard x-ray microscopy, the spherical and planar compound refractive lens was researched. A spherical CRL with 123 biconcave micro-lenses reaches a focusing spot (FWHM) of 33.3 × 65.9 μm^2 and an imaging resolution of 5.5 μm at the energy of 8.05 keV (Cu K-line). With a SU-8 resist planar parabolic refractive lens, a focal line of 27.2 μm width was also measured.

To focus hard x-rays into nanometer-level efficiently, the multilayer Laue lens was fabricated using a WSi_2/Si multilayer. The multilayer structure consisted of 324 alternating WSi_2 and Si layers with a total thickness of 7.9 μm. After deposition, the sample was sliced and polished into an ideal aspect ratio, while the measured results showed an intact structure remained and a surface roughness of only 0.5 nm after these preparation processes. The diffraction measurements of “local gratings” also showed consistent efficiency compared to the design.

References:

[1] A. Snigirev, I. Snigireva, M. Michiel et al. Proc. SPIE **5539,** 244 (2004).
[2] H.C. Kang, H. Yan, R.P. Winarski et al., Appl. Phys. Lett. **92**, 221114 (2008).
[3] G.R. Bennett, J.A. Folta, Appl. Opt. **40**(25), 4588 (2001).

Plans for a Soft X-ray FEL for Dynamic Imaging*

J. Corlett, P. Denes, R. Falcone, J. Kirz, R. Schoenlein

Lawrence Berkeley National Laboratory, Berkeley, CA, USA

* Supported by the Office of Basic Energy Sciences, U.S. Department of Energy.

Abstract:

Microscopy experiments at FLASH and at LCLS have amply demonstrated the power of free electron lasers to perform imaging experiments using ultrashort pulses. The coherence of the source, the ability to capture an image before radiation damage manifests itself, and to observe phenomena on the femtosecond time scale has opened up a broad array of microscopy applications

The sample is usually destroyed by a single FEL pulse in these experiments. In order to do systematic dynamical studies on the same sample, one needs a gentler probe, and one that operates at high repetition rates. At Lawrence Berkeley Laboratory an array of high rate soft X-ray FEL-s is being designed [1] that will be ideally suited for the study of dynamics on time scales from a fraction of a femtosecond to milliseconds. The transform-limited coherent beams will be fully tunable up to 1.2 KeV in the fundamental, and up to 6 KeV (at reduced fluence) in the higher harmonics. The pulse-rate will be user-selectable with complete flexibility up to 100 KHz or even higher.

References:

[1] J. Corlett et al., Synchrotron Radiation News **22**(5), 25 (2009).

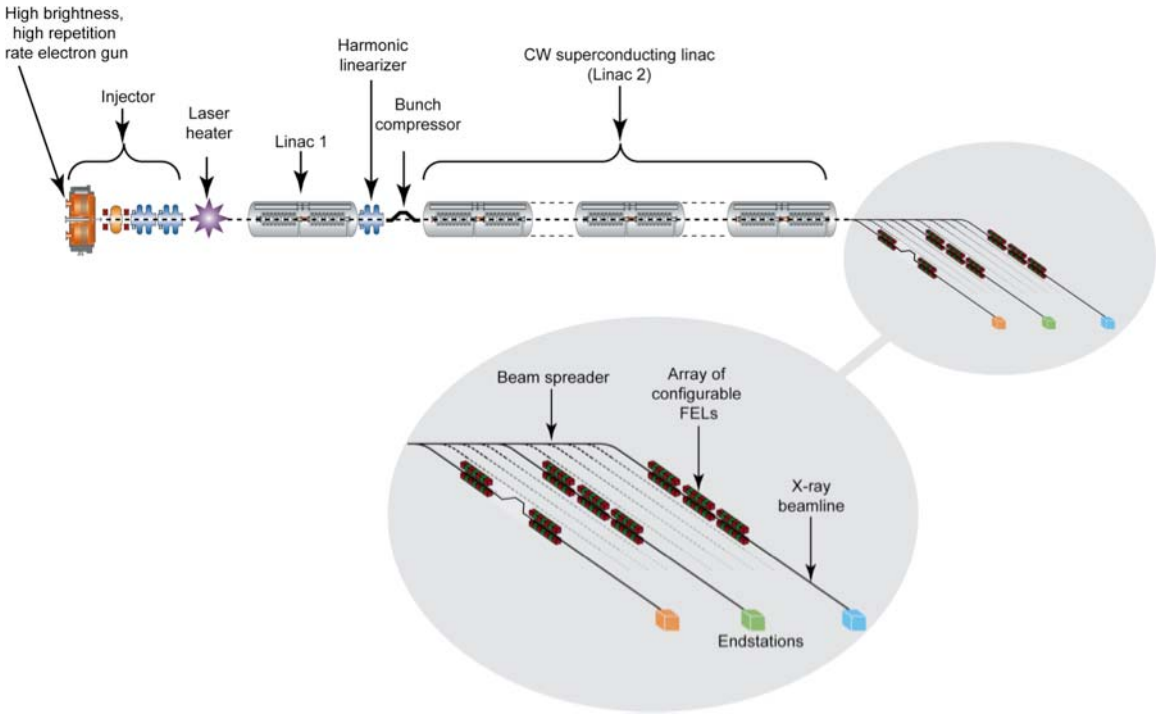

Figure 1: Schematic diagram of the proposed FEL array.

High-Speed X-ray Full-Field Imaging Applications at the APS

K. Fezzaa

X-ray Imaging Group, Advanced Photon Source, Argonne National Laboratory, Argonne, IL 60439, USA

* Use of the Advanced Photon Source was supported by the U. S. Department of Energy, Office of Science, Office of Basic Energy Sciences, under Contract No. DE-AC02-06CH11357.

Abstract:

The availability of x-ray sources such as the Advanced Photon Source (APS), with very bright beam, wide energy tenability, and flexible storage ring filling structure, allows us to push the limits on the speed of the traditional full-field phase-contrast imaging in terms of exposure time and repetition rate. We are limited by the current state of the art of high-speed digital camera technology. We will present some examples of studies done with exposure time down to 100 ps and repetition rate up to ~ 0.5 million fps. These include fluid dynamics singularities [1,2], fuel injector inner dynamics [3], and rapid gasless reactions propagation [4].

References:

[1] Y. Wang, K.-S. Im, K. Fezzaa, Phys. Rev. Lett. **100**, 154502 (2008).
[2] K. Fezzaa and Y. Wang, Phys. Rev. Lett. **100**, 104501 (2008).
[3] Y. Wang, X. Liu, K.-S. Im et al. Nature Physics **4**, 305 (2008).
[4] R.V. Reeves, J.D.E. White, E.M. Dufresne et al., Phys. Rev. B **80**, 224103 (2009).

Scanning X-ray Fluorescence Elemental Mapping of Paintings with Synchrotron Radiation

D.L. Howard[1], D. Lau[2], D. Hay[2], C.G. Ryan[2], R. Kirkham[2], G. Moorhead[2], M. Varcoe-Cocks[3], J. Payne[3], C. Villis[3], M.D. de Jonge[1], D.J. Paterson[1], D. Thurrowgood[3]

[1]*Australian Synchrotron, 800 Blackburn Road, Clayton, VIC, Australia*
[2]*CSIRO, Clayton, VIC, Australia*
[3]*National Gallery of Victoria, Melbourne, VIC, Australia*

Abstract:
Scanning x-ray fluorescence mapping using synchrotron radiation is a powerful non-destructive technique for the imaging of cultural heritage items such as paintings. One of its unique strengths is the potential to reveal metal distributions in the pigments of underlying brushstrokes, thus providing information critical to the interpretation of a painting. The mapping technique utilized Kirkpatrick-Baez focusing optics and the prototype event-mode Maia x-ray fluorescence detector [1] at the XFM beamline of the Australian Synchrotron [2].

Test canvases, some with an overlayer of ubiquitous lead white pigment, were used for a pilot study towards our goal of recording high definition scans of whole artworks. The underlying brushstrokes were successfully revealed, and tri-tonal colour images were constructed based on metal to pigment associations. The fluorescence mapping technique and the analysis of the test images will be discussed.

References:

[1] C. G. Ryan et al., Nucl. Instrum. Methods B **260**, 1 (2007).
[2] D. J. Paterson et al., AIP Conf. Proc. **879**, 864 (2007).

Nanoscale Chemical Imaging Using Synchrotron X-ray Enhanced Scanning Tunneling Microscopy (SXSTM)*

V. Rose[1], C. Preissner[1], M.L. Cummings[2,3], S. Vogt,[1] V. Madhavan[2,4], M. Bode[2], J.W. Freeland[1]

[1]*Advanced Photon Source, Argonne National Laboratory, Argonne, IL 60439, USA*
[2]*Center for Nanoscale Materials, Argonne National Laboratory, Argonne, IL 60439, USA*
[3]*Mechanical Engineering & Materials Science Department, Rice University, Houston, TX 77005, USA*
[4]*Department of Physics, Boston College, Chestnut Hill, MA 02467, USA*

*This work was supported by the U. S. Department of Energy, Office of Science, Office of Basic Energy Sciences, under contract DE-AC02-06CH11357.

Abstract:

Nanoscale structures are at the forefront of fundamental research as well as the keystone for whole new classes of potential applications. Proper understanding of these systems requires tools with the ability to resolve the nanometer scale as well as provide detailed information about chemical, electronic, and magnetic structure. Scanning probe microscopies achieve the requisite high spatial resolution; however, direct elemental determination is not easily accomplished. X-ray microscopies, on the other hand, provide elemental selectivity, but currently have spatial resolution only of tens of nanometers. We present a radically different concept that employs detection of local x-ray interactions utilizing a scanning probe that provides spatial resolution and x-ray absorption, which directly yields chemical, electronic, and magnetic sensitivity [1,2]. If during electron tunneling the sample is illuminated with monochromatic x-rays, characteristic absorption will arise, and core electrons are excited into unoccupied states above the Fermi energy. Those electrons may modulate the conventional tunnel current and facilitate chemical imaging at the nanoscale. In this talk, we will summarize the latest progress in the development of this approach at the Advanced Photon Source.

References:

[1] V. Rose, J.W. Freeland, S.K. Streiffer, "New capabilities on the interface of X-ray and scanning tunneling microscopy," in *Scanning Probe Microscopy of Functional Materials: Nanoscale Imaging and Spectroscopy*, to be published by Springer (2010).

[2] V. Rose, J.W. Freeland, K.E. Gray et al., Appl. Phys. Lett. **92**, 193510 (2008).

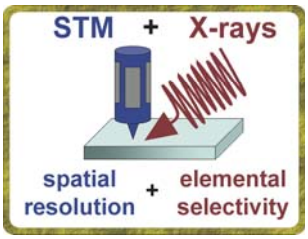

Figure 1: SXSTM combines the exceptional spatial resolution of scanning tunneling microscopy and the chemical sensitivity of synchrotron radiation.

Magnetic Vortex Core Dynamics and Reversal Studied Using X-ray Microscopy*

X.M. Cheng[1] and D.J. Keavney[2]

[1]*Bryn Mawr College, Bryn Mawr, PA USA*
[2]*Advanced Photon Source, Argonne National Laboratory, Argonne, IL USA*

* Work at Argonne National Laboratory is supported by the U. S. Department of Energy, Office of Science, Office of Basic Energy Sciences, under Contract No. DE-AC02-06CH11357.

Abstract:
The dynamics of nanoscale magnetic structures are of fundamental interest and have importance for devices that incorporate nanomagnets into high-speed electronics. One of the principal questions is the behavior of magnetic vortices. We use time-resolved x-ray photoemission electron microscopy to image the response of micron-scale patterned $Ni_{80}Fe_{20}$ disks to fast magnetic field pulses. We have imaged the relaxation of a displaced magnetic vortex core in 6-μm disks after a field pulse. We find a strong dependence of the core relaxation behavior on the excitation amplitude, and a link to core polarity reversals. Below the critical field amplitude of ~2.5 mT, the core follows the expected spiral motion towards the center of the disk with an oscillation frequency in agreement with theoretical predictions. However, above the critical field the trajectory of the core is dependent on the excitation amplitude, with elliptical trajectories appearing as the field is increased. The observed elliptical trajectories turn out to be associated with transient magnetic domain states that appear in the first 300 ps of the core relaxation. In Figure 1, we show selected PEEM images of the initial core evolution (top row) along with micromagnetic simulations at the corresponding times (bottom row) These arise as a result of nonlinear effects that become significant when the core is displaced more than 20% of the disk radius [1]. These states are associated with distortions of the core and vortex anti-vortex pairs that promote multiple core polarity reversals [2], and profoundly influence the core motion.

References:
1. X.M. Cheng et al., Phys. Rev. B **79**, 172411 (2009).
2. D.J. Keavney, X.M. Cheng, and K.S. Buchanan, Appl. Phys. Lett. **94**, 172506 (2009).

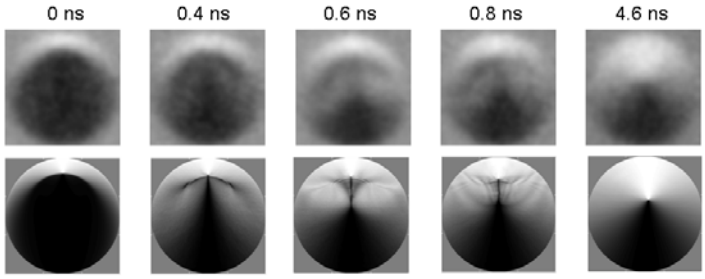

Figure 1: PEEM images (top row) and simulations (bottom row) of a 6-μm NiFe disk immediately following the removal of a 4-mT field.

X-Ray Magnetic Circular Dichroism of Individual 30-nm Magnetosomes in Magnetotactic Bacteria by STXM*

A.P. Hitchcock[1], K.P. Lam[1], J. Wang[2], M. Obst[3], U. Lins[4], D.A. Bazylinski[5]

[1]*Chemistry & Chemical Biology, McMaster University, Hamilton, ON, Canada*
[2]*Canadian Light Source Inc., U. Saskatchewan, Saskatoon, SK, Canada*
[3]*Center for Applied Geoscience, Tuebingen University, Tuebingen, Germany*
[4]*Microbiology, Universidade Federal do Rio de Janeiro, 21941-590, Rio de Janeiro, RJ, Brazil*
[5]*School of Life Sciences, U. Nada at Las Vegas, Las Vegas, NV, 89154-4004, USA*

* Research supported by NSERC. CLS is supported by Canada Foundation for Innovation (CFI), NSERC, Canadian Institutes of Health Research (CIHR), National Research Council (NRC) and U. Saskatchewan.

Abstract:

Magnetotactic bacteria (MTB) use chains of single crystal magnets, known as magnetosomes, to align themselves with respect to the earth's magnetic field, which helps them migrate to their preferred habitat at the oxic-anoxic transition zone. The biomineralization mechanism whereby MTBs produce these single-domain nano-crystals of magnetite (Fe_3O_4) or greigite (Fe_3S_4) (typically 30-60 nm in size) is of great interest since their quality and uniformity is superior to those made by inorganic synthesis. Soft X-ray scanning transmission X-ray microscopy (STXM) at the Canadian Light Source was used to measure the Fe $L_{2,3}$ X-ray magnetic circular dichroism (XMCD) signal from magnetosomes in individual MTB [1]. Relative to that published work, recent improvements to the STXM data acquisition have allowed measurement of much higher quality XMCD data, by measuring left and right circularly polarized signals alternately at each photon energy in a stack. Results from a marine vibrio, strain MV-1 are indicated in Figures 1 and 2. The presentation will also report STXM-XMCD studies of an unusual MTB from Pettaquamscutt River estuary that produces both magnetite and greigite magnetosomes in the same cells. Fe 2p spectro-microscopy studies also reveal the presence of Fe outside of magnetosomes in both strains of MTB, with a spectral signature significantly richer in Fe(II) than that of magnetite. Such results give insight into the bio-mediated crystallization which helps us to understand and possibly duplicate in biomimetic structures.

References:

[1] K.P. Lam et al., Chemical Geology **270**, 110 (2010).

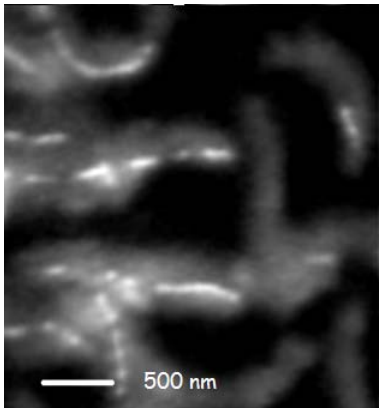

Figure 1: STXM image at 709.8 eV (Fe $2p_{3/2}$) showing magnetosomes in MV1 MTB cells.

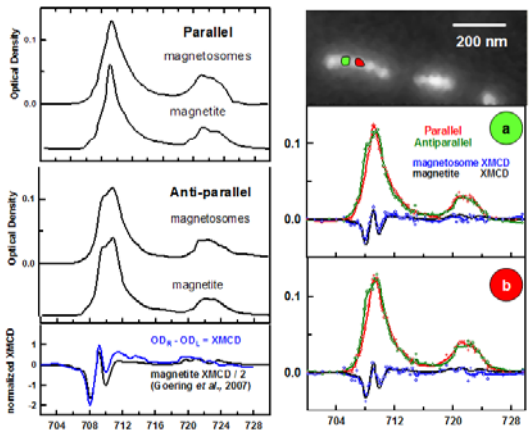

Figure 2: Fe 2p absorption and XMCD of (left) all in one cell, (2) individual 30-nm-diameter magnetosomes, compared to the XMCD of magnetite.

Magnetic Soft X-ray Microscopy of Stochastic Behavior in Nanoscale Magnetism*

M.-Y. Im[1], P. Fischer[1], L. Bocklage[2], G. Meier[2], D.-H. Kim[3], S.-C. Shin[4]

[1]*Center for X-ray Optics, Lawrence Berkeley Nat. Lab., Berkeley, CA 94720, USA*
[2]*Inst. of Appl. Phys. and Center for Microstructure Res., U. Hamburg, 20355 Hamburg, Germany*
[3]*Department of Physics, Chungbuk National University, Cheongju 361-763, Korea*
[4]*Department of Physics and Center for Nanospinics of Spintronic Materials, Korea Advanced Institute of Science and Technology, Daejeon 305-701, Korea*

* This work is supported by the Director, Office of Science, Office of Basic Energy Sciences, Materials Sciences and Engineering Division, of the U.S. Department of Energy under Contract No. DE-AC02-05-CH1123, the Deutsche Forschungsgemeinschaft via the Collaborative Research Center 668, and the City of Hamburg via the Cluster of Excellence Nano-Spintronics.

Abstract:

The question, as to whether magnetic processes on a nanoscale are fully deterministic or exhibit a certain degree of stochasticity is both of fundamental scientific interest and of technological relevance. We address this issue utilizing magnetic transmission soft X-ray microscopy (MTXM), where Fresnel zone plate optics provide a spatial resolution down to better than 12 nm [1] and inherent elemental specificity is achieved due to X-ray circular magnetic dichroism.

We have studied a large variety of ferromagnetic systems with respect to their stochastic behavior. Our experiments show that e.g. for domain nucleation in thin CoCrPt films with a pronounced perpendicular magnetic anisotropy thermal fluctuations have a strong impact [2]. Studies of Barkhausen avalanches in these films show a sudden increase in the scaling exponent of the power law distribution function, which is driven by a proximity effect occurring in the vicinity to the coercive field [3].

While earlier experiments with MTXM on current induced domain wall motion in 1dim magnetic nanowires indicated a stochastic behavior [4], more recently we performed a detailed study of field driven depinning and pinning processes in permalloy nanowires with artificial notch structures. Again a strong stochastic component is observed. The multiplicity of domain walls occurring around the notches is largely responsible for this behavior. However, by choosing the right geometry, such as notch depth, wire width and thickness the degree of stochasticity can be significantly reduced [5].

Magnetic vortices, which occur e.g. in permalloy disks have attracted recently increased interest, in particular since the switching of the vortex core is considered as an energetically stable binary concept for novel magnetic storage devices. Core reversal has been observed upon applying single magnetic field pulses, rotating fields or injection of spin currents. We have studied the degree of stochasticity in an array of vortex structures with varying disk diameter and thickness and we observe that below 800 nm diameter the chirality creation process is completely deterministic. An interpretation of the findings is based on a surface induced Dzyaloshinsky-Moriya coupling [6].

References:

[1] W. Chao, J. Kim, S. Rekawa et al., Optics Express **17**(20) 17669 (2009).
[2] M.-Y. Im, D.-H. Kim, K.-D. Lee et al., Adv. Mater. **20**, 1750 (2008).
[3] M.-Y. Im, P. Fischer, D.-H. Kim et al., Appl. Phys. Lett. **95**, 182504 (2009).
[4] G. Meier, M. Bolte, R. Eiselt et al., Phys. Rev. Lett. **98**, 187202 (2007).
[5] M.-Y. Im, L. Bocklage, P. Fischer et al., Phys. Rev. Lett. **102**, 147204 (2009).
[6] M.-Y. Im et al. to be submitted (2010).

X-ray Microscopy and Magnetism – A Perfect Match

H. Ohldag

Stanford Synchrotron Radiation Lightsource, Menlo Park CA, USA

Abstract:
Today's fundamental and applied magnetism research is particularly focused on magnetic materials that are suitable as magnetic sensors, spin valves, spin transistors, or magnetic media consisting of complex magnetic multilayer structures. Scientific investigations in this area are concerned with the origin of magnetic coupling, spin transport across interfaces, magnetic properties of magnetic oxides, and the complex magnetic structures that evolve when different kind of magnets—for example, antiferromagnets (AF) and ferromagnets (FM)—are brought into contact. Dichroism x-ray absorption spectroscopy (XAS) using synchrotron radiation represents a unique tool to understand complex nanomagnetic samples. The power of XAS is that it provides a possibility to address individual magnetic properties of different elements in a sample and a way to distinguish between different magnetic orders, like AF and FM, at the same time. It can furthermore be used to study the magnetism of buried interfaces, diluted magnetic systems like FM semiconductors, or other exotic new magnets. The pulsed nature of the synchrotron as x-ray source allows for studying the time-dependent behavior of a sample with a temporal resolution of a few tens of picoseconds. Dichroism soft x-ray absorption spectroscopy can furthermore be used to obtain spatially resolved information with less than 50-nm lateral resolution in a modern full field or scanning x-ray microscopes.

Can Carbon Be Ferromagnetic?

H. Ohldag[1], P. Esquinazi[2], E. Arenholz[3], D. Spemann[2], M. Rothermel[2], A. Setzer[2], T. Butz[2]

[1]*Stanford Synchrotron Radiation Lightsource, Menlo Park CA, USA*
[2]*University of Leipzig, Leipzig, Germany*
[3]*Advanced Light Source, Berkeley CA, USA*

Abstract:

The existence of long-range magnetic order at ambient temperatures in carbon-based structures without magnetic elements is unexpected and therefore has attracted the attention of the solid state community over the past years. Theoretical results from different groups suggest that the existence of long-range magnetic order in a graphite structure is possible if one takes the effects of defects and/or the incorporation of hydrogen atoms on the electronic properties into account. SQUID results provided first systematic hints for the existence of magnetic order at room temperature in virgin as well as proton- or carbon-irradiated [1] highly oriented pyrolytic graphite (HOPG) samples.

We present an x-ray dichroism microscopy study of graphite surfaces [2] that addresses the origin and magnitude of ferromagnetism in metal-free carbon. Using element-specific x-ray microscopy, we can show that metallic impurities do not play a role in the ferromagnetism of carbon and that carbon can be ferromagnetic without ferromagnetic impurities. A detailed spectroscopic study of proton-irradiated areas in carbon shows that in addition to carbon *pi*-states, also hydrogen-mediated electronic states exhibit a net magnetization with significant magnetic remanence at room temperature. The observed magnetism is restricted to the top ~10 nm of the sample, whereas the actual magnetization reaches ~15 emu/g at room temperature, a value similar to classic ferromagnetic materials like Nickel.

References:

[1] H.H. Xia, W.F. Li, Y. Song et al., Adv. Mater. **20**(24), 4679 (2008).
[2] H. Ohldag et al., Phys. Rev. Lett. **98,** 187204 (2007) and submitted to NJP (2010).

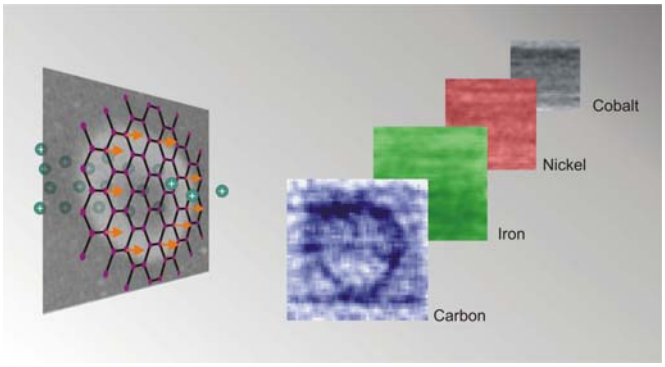

Figure 1: Proton irradiation leads to formation of ferromagnetic area in thin carbon films and surfaces. Element-specific x-ray microscopy reveals that the macroscopically observed magnetism originates from carbon sites only.

Sample Preparation of Epitaxially Grown Magnetic Materials for X-Ray Transmission Microscopy

T. Schwarze[1], B.L. Mesler[2], M. Im[3], A. Sakdinawat[2]

[1]*University of Applied Sciences Koblenz, RheinAhrCampus Remagen, D-53424 Remagen, Germany*
[2]*University of California, Berkeley, Berkeley, California 94720, USA*
[3]*Center for X-ray Optics, Lawrence Berkeley National Laboratory, Berkeley, California 94720, USA*

Abstract:
Imaging epitaxially grown magnetic materials, e.g., magnetic oxides at high spatial resolution, is of great interest both fundamentally as well as technologically. Soft x-ray transmission microscopies, both lens-based and lensless, have become an important tool in studying magnetic materials with high spatial resolution [1], elemental specificity, and in some cases, high temporal resolution. Currently, however, studies have been limited mainly to samples that can be fabricated on amorphous silicon nitride membranes. Since many materials of interest require growth on single-crystalline substrates, e.g., strontium titanate (STO) [2] or magnesium oxide (MgO) [3], they have not been studied using soft x-ray transmission microscopy. We have designed and built a jet-etcher, shown in Figure 1, which is used to backside-thin epitaxially grown magnetic samples, and we have also developed several specific sample fabrication and etching procedures. The complex oxide material $LaSrMnO_3$, grown on a single crystalline STO/silicon substrate as well as MgO, has been thinned using this method. Using x-ray transmission microscopy at the Advanced Light Source (ALS) in Berkeley we were able to obtain significant XMCD contrast for the $LaSrMnO_3$/STO test sample as shown in Figure 2. Patterned samples of $LaSrMnO_3$ are currently being thinned for future imaging. We continue to investigate the possibility of fabricating membranes from other commonly used substrates, which will expand the range of materials that can be imaged using transmission x-ray microscopy.

References:

[1] J. Vila-Comamala, K. Jefimovs, J. Raabe et al., Ultramicroscopy. **109**(11):1360 (2009).
[2] Y. Takamura, R. V. Chopdekar, A. Scholl et al., Nano Letters **6**, 1287 (2006).
[3] T. Kubota, K. Kodama, T. Nakamura et al., Appl. Phys. Lett. **95**, 222503 (2009).

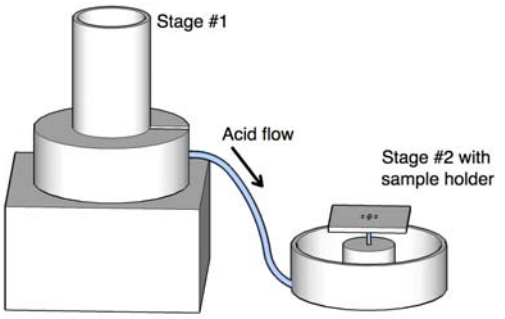

Figure 1: Jet etcher setup, where a small acid fountain is created at stage #2 in order to controllably backside-thin magnetic samples.

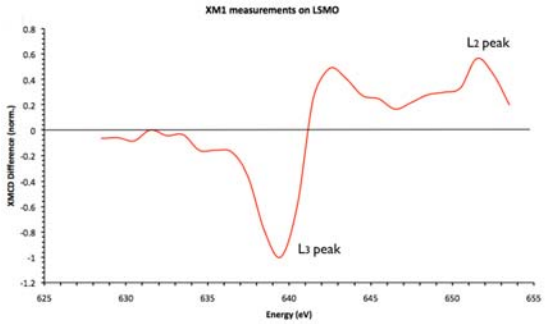

Figure 2: X-ray transmission microscope measurement on LSMO showing significant XMCD contrast (Mn $L_{3,2}$ peaks are indicated).

Spatially Resolved Sulfur Speciation in Urban Soils

M. Brettholle[1], S.-C. Gleber[1,4], B. Mekiffer[3], D. Legnini[4], I. McNulty[4], G. Wessolek[3], J. Thieme[2]

[1]*Institute for X-Ray Physics, Georg-August-University Goettingen, Friedrich-Hund-Platz 1, 37077 Goettingen, Germany*

[2]*Brookhaven National Laboratory, NSLS-II Project, Building 817, Upton, NY 11973, USA*

[3]*Institue for Ecology, TU Berlin, Am Salzufer 11, 10587 Berlin, Germany*

[4]*Argonne National Laboratory, Building 401, 9700 S. Cass Avenue, Argonne, IL 60439, USA*

Abstract:

X-ray microscopy is an ideal method to resolve structures at a wide range of length scales. It is non-invasive, non-destructive for many substances, requires minimal sample preparation and is therefore well suited for the investigation of environmental samples and soil samples in particular.

Synchrotron-based x-ray absorption near edge fine structure spectroscopy (XANES) at the K-absorption edge of sulfur (E = 2472 eV) has emerged as a powerful tool for determining the speciation of sulfur in soil extracts [1] and in soils [2,3].

A combination of both methods, x-ray spectromicroscopy and elemental mapping, was used to analyze the path of sulfur from war debris into urban soils from Berlin, Germany. This sulfur release is a contemporary and exigent issue, as it has a crucial impact on urban water quality. Samples were taken from different debris-loaded sites in Berlin. These soils are well aerated and the samples could be investigated without further treatment.

The interface of debris particles and surrounding soil was explored and differences in the sulfur speciation were quantified on small length scales, leading to a better understanding of the sulfur release processes.

References:

[1] M.J. Morra, S.C. Fendorf, P.D. Brown, Geochim. Cosmochim. Acta **61**, 683 (1997).

[2] J. Prietzel, J. Thieme, U. Neuhäusler et al., Eur. J. Soil Sci. **54**, 423 (2003).

[3] J. Thieme, J. Prietzel, N. Tyufekchieva et al., IPAP Conf. Series **7**, 318 (2006).

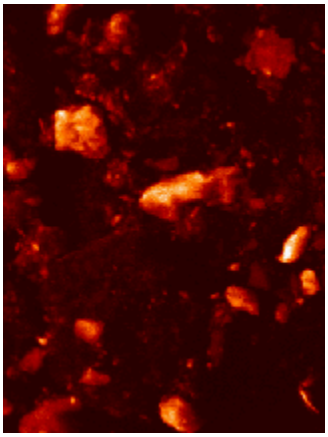

Figure 1: Si-map of ROI.

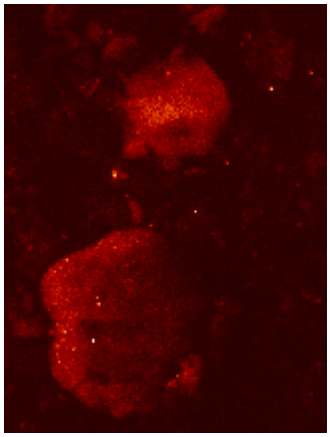

Figure 2: S-map of ROI.

STXM Imaging of Organic Coatings on Interplanetary Dust

G. J. Flynn[1], S. Wirick[2], L. P. Keller[3], S. A. Sandford[4]

[1]*Dept. of Physics, SUNY-Plattsburgh, Plattsburgh NY 12901 USA*
[2]*Dept. of Physics and Astronomy, SUNY- Stony Brook, Stony Brook, NY 11794 USA*
[3]*NASA Johnson Space Center, Houston TX 77058 USA*
[4]*NASA Ames Research Center, Moffett Field, CA 94035 USA*

Abstract:

Chondritic, porous interplanetary dust particles (CP IDPs) are the most primitive samples of extraterrestrial material available for laboratory analysis [1]. These CP IDPs are unequilibrated aggregates of mostly submicron, anhydrous grains of a diverse variety, including olivine, pyroxene, glass, and sulfide. They contain organic matter not produced by parent body aqueous processing [2], some carrying H and N isotopic anomalies consistent with molecular cloud or outer Solar System material [3]. Scanning Transmission X-Ray Microscope (STXM) imaging at the C K-edge shows the individual grains in ~10 micron CP IDPs are coated by a layer of carbonaceous material ~100 nm thick. This structure implies a three-step formation sequence for the dust from the Solar Nebula. First, individual grains condensed from the cooling nebular gas. Then complex, refractory organic molecules covered the surfaces of the grains either by deposition, formation in-situ, or a combination of both processes. Finally, the grains collided and stuck together forming the first dust-size material in the Solar System, these CP IDPs.

Ultramicrotome sections, ~100 nm thick, were cut from several CP IDPs, embedded in elemental S to avoid exposure to C-based embedding media, and X-ray Absorption Near Edge Structure (XANES) spectra were derived from image stacks obtained using the STXM on Beamline X1A of the National Synchrotron Light Source. We compared C-XANES spectra from each of the pixels in an image stack and identified groups exhibiting similar spectra using "cluster analysis," which identified most carbonaceous grain coatings in each CP IDP as material having similar C-XANES spectra.

Two processes are commonly suggested in the literature for production of organic grain coatings. The similarity in thickness and C-XANES spectra of the coatings on different minerals in the same IDP indicates the first, mineral specific catalysis (e.g., the Fischer-Tropsch process), was not the process that produced these organic rims. Our results are consistent with this primitive organic matter being produced by the alternative process of condensation of C-bearing ices onto the grain surfaces and production of refractory organic matter by UV or other ionizing radiation bombarding the ices [4].

The processes by which primitive grains aggregate to form the first dust of our Solar System are not well understood. Collision experiments indicate that bare rocky grains bounce apart at collision speeds less than 30 to 50 m/s and shatter each other at larger speeds [5]. However, collision experiments indicate grains coated with organic matter stick quite easily, even at collision speeds up to 5 m/s – an order of magnitude higher than the speed at which silicate- or ice-based grains accrete [6]. Thus the organic grain coatings we have identified probably played a critical role in dust aggregation in the early Solar System.

References:

[1] H. Ishii et al., Science **319**, 447 (2008).
[2] G.J. Flynn et al., Geochim. Cosmochim. Acta **67**, 4791 (2003).
[3] L.P. Keller et al., Geochim. Cosmochim. Acta **68**, 2577 (2004).
[4] M.P. Bernstein et al., Astrophys. J. **454**, 327 (1995).
[5] W.K. Hartmann, Icarus **33**, 50 (1978).
[6] T. Kudo et al., Meteoritics & Planet. Sci. **37**, 1975 (2002).

Hard X-ray Fluorescence Microscopy to Determine the Element Distribution of Soil Colloids in Aqueous Environment

S.-C. Gleber[1,2], S. Vogt[2], J. Niemeyer[3], L. Finney[2], I. McNulty[2], J .Thieme[4]

[1]*Institut für Röntgenphysik, Georg-August-Universität Göttingen, Friedrich-Hund-Platz 1, 37077 Göttingen, Germany*
[2]*Advanced Photon Source, Argonne National Laboratory, 9700 S Cass Avenue, Argonne, IL 60439, USA*
[3]*Department für Nutzpflanzenwissenschaften, Georg-August-Universität Göttingen, Carl-Sprengel-Weg 1, 37075 Göttingen, Germany*
[4]*National Synchrotron Light Source II Project, Brookhaven National Laboratory, Building 817, Upton, NY 11973, USA*

Abstract:

A prominent feature of oil colloids is their huge specific surface. It determines colloidal properties such as adsorption capacity or diffusion. The colloidal interactions differ significantly from the behavior of the same materials in a bulk system. There is still a need for better-suited analytical resources when studying interactions in the colloidal regime, as these are crucial, e.g., for the transport and release of nutrients and toxicants in soils, which then influences directly the growth of plants.

To reveal the correlation of the particular trace elements and their distribution in correlation to colloidal interactions as well as changing pH values, experiments at the hard x-ray fluorescence nanoprobe at beamline 2-ID-E, APS, were performed with colloidal clay and soil samples in an aqueous environment as naturally relevant. To obtain further spatial information, stereo imaging has been used. To study the dynamical behavior of these colloidal suspensions at changing pH, a wet sample chamber allowing *in situ* manipulation was developed and utilized.

References:

[1] S. Vogt, J. Phys. IV France **104**, 635 (2003).

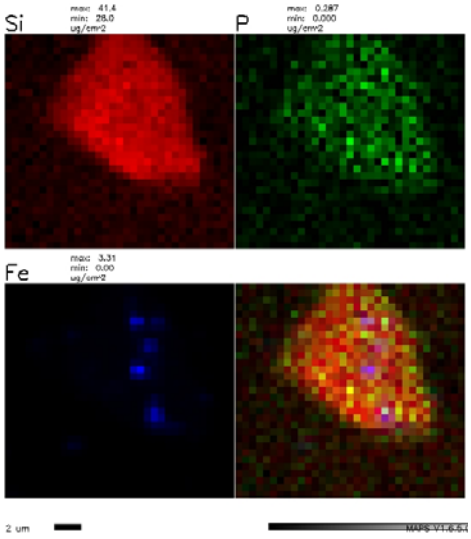

Figure 1: Colocalization of Si, P, and Fe within a soil particle in water, showing adsorbed Fe containing colloids. Scale bar 2 µm. MAPS data analysis [1].

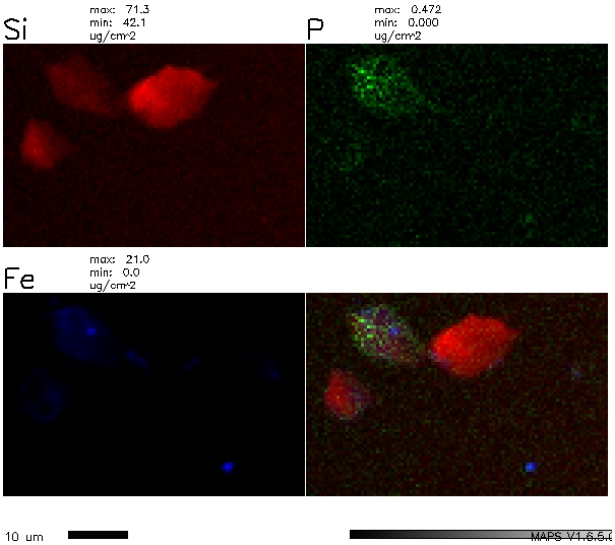

Figure 2: Colocalization of Si, P, and Fe within three colloids of different composition in water. Scale bar 10 µm. MAPS data analysis [1].

Hard X-ray Nanoprobe Characterization of Geopolymers*

V. Rose[1], J.L. Provis[2], S.A. Bernal[2,3], J. Maser[4], M.V. Holt[4], R.P. Winarski[4], J.S.J. van Deventer[2]

[1]*Advanced Photon Source, Argonne National Laboratory, Argonne, Illinois 60439, USA*
[2]*Department of Chemical and Biomolecular Engineering, University of Melbourne, Victoria 3010, Australia*
[3]*Materials Engineering Department, Composite Materials Group, Universidad del Valle, Cali, Colombia*
[4]*Center for Nanoscale Materials, Argonne National Laboratory, Argonne, Illinois 60439, USA*

*This work was supported by the U. S. Department of Energy, Office of Science, Office of Basic Energy Sciences, under contract DE-AC02-06CH11357; the Australian Research Council (ARC); Colciencias; and the Walter Mangold Trust.

Abstract:

We have utilized the hard x-ray nanoprobe (HXN) at ID-26 of the Advanced Photon Source to obtain fluorescence maps of a hydroxide-activated geopolymer (fly ash + KOH solution). Geopolymers are currently being developed as an environmentally beneficial replacement to Portland cement for concrete production, offering comparable performance and cost while reducing greenhouse emissions by approximately a factor of 5. Given that cement production is responsible for up to 8% of global anthropogenic CO_2 emissions, this equates to the opportunity to reduce CO_2 by at least tens of millions of tons per annum worldwide. The exceptional spatial resolution and penetration power of the HXN enables the study of the poorly understood heterogeneity in order to tailor geopolymer formulations to ensure optimal performance for materials based on the available precursor materials. This study provides for the first time direct evidence of the formation of discrete high-calcium particles within the binder structure of a geopolymer synthesized from a low-calcium (2.6 wt.% as oxides) fly ash.

References:

[1] J.L. Provis, V. Rose, S.A. Bernal et al., Langmuir **25**, 11897 (2009).

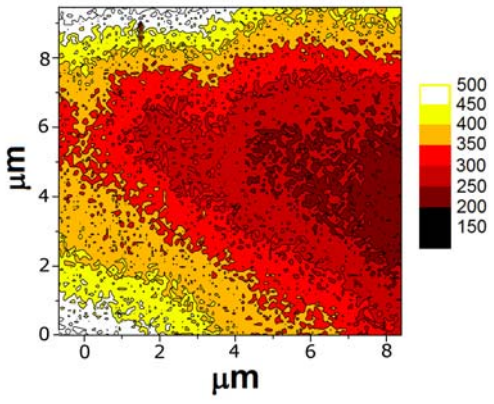

Figure 1: Calcium distribution in a fly ash/potassium silicate sample [1].

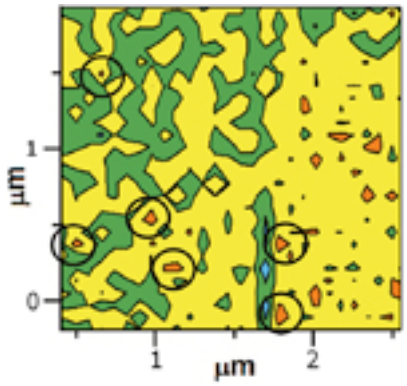

Figure 2: The geopolymer binder region exhibits localized regions of high Ca concentration.

C1s – X-Ray Spectromicroscopy of Biomolecular Matter

J. Sedlmair[1], S.-C. Gleber[1], M. Bertilson[2], O. von Hofsten[2], T. Pfohl[3], H. Zänker[4], J. Thieme[5]

[1]Institute for X-Ray Physics, Georg-August-University, Friedrich-Hund-Pl. 1, D-37077 Goettingen, Germany
[2] Biomedical and X-Ray Physics, Royal Institute of Technology (KTH), SE-10691 Stockholm, Sweden
[3]Biophysical Chemistry, Basel University, Klingelbergstr. 80, CH-4056 Basel, Switzerland
[4]Forschungszentrum Dresden-Rossendorf e. V., Bautzner Landstraße 400, D-01328 Dresden, Germany
[5]NSLS II, Brookhaven National Lab, Bld. 817, Upon, NY 11973, USA

Abstract:
Combining X-ray microscopy with NEXAFS spectroscopy, X-ray spectromicroscopy is a powerful tool for investigating key questions in many scientific areas. Using this technique, structures in the environment or from biological samples can be studied showing dimensions on the nanoscale while concurrently gaining insight into chemical interactions. The spectral range around the C K-edge, located in the so-called water window (285-523eV), is especially well suited for the examples mentioned above, since it allows for working under aqueous and natural conditions [1,2].

We have explored the potential of x-ray spectromicroscopy on biological and environmental specimens in a sequence of experiments, going from simple to more complex structured samples. To evaluate the obtained NEXAFS spectra, we used an approach associating absorption edge and resonance for every peak [3]. The influence of radiation damage on the quality of the results has been assessed, too.

Additionally, we compared the results from synchrotron-based instruments with table-top setups using laser-driven sources [3,4]. Recently, more and more of these laboratory devices are available for experiments. Due to their constant improvement, they certainly could serve as a complementary technique in the future, if not as a quick alternative for some experiments.

References:
[1] J. Thieme, J. Sedlmair, S.-C. Gleber et al., J Synchrotron Rad. **17**, 149 (2010).
[2] J. Sedlmair, S.-C. Gleber, S. Öztürk, T. Pfohl, J. Thieme (in preparation).
[3] J. Sedlmair, S.-C. Gleber, C. Peth, K. Mann, J. Thieme (submitted).
[4] J. Thieme, J. Sedlmair, S.-C. Gleber et al., J. Phys.: Conf. Ser. **186**, 012107 (2009).

Study on Smectite Flocculation Structure Modified by Al_{13} Macromolecules by Transmission X-ray Microscopy

Y.-F. Song[1], M. S. Zbik[2], Y.-M. Chen[1]

[1]*National Synchrotron Radiation Research Center , 101 Hsin-Ann Road, Hsinchu Science Park, Hsinchu 30076, Taiwan, R.O.C.*
[2]*Faculty of Sciences and Technology, Queensland University of Technology, 2 George Street, GPO box 2434, Brisbane Old 4001, Australia*

Abstract:
The aggregate structure which occurs in aqueous smectite suspensions is responsible for poor water clarification, difficulties in sludge dewatering and the unusual rheological behavior of smectite rich soils. These macroscopic properties are dominated by its 3-D structural arrangement of smectite finest fraction within flocculated aggregates. We utilize transmission x-ray microscopy (TXM) to investigate the natural structure and 3-D tomographic reconstruction of the smectite clay aggregates modified by Al_{13} Keggin macromolecule $[Al_{13}(O)_4(OH)_{24}(H_2O)_{12}]^{7+}$ in an aqueous environment. The X-ray microscope with 60 nm tomographic resolution at energy 8-11 keV and Zernike-phase capability is installed at the BL01B1 end-station [1,2] at the National Synchrotron Radiation Research Center (NSRRC). This technique provides peculiar accurate images to study clay mineral particles and aggregates in the natural aqueous environment and in three dimensions [3-5].

Three different treatment methods were shown that resulted in three different micro-structural environments of the resulting flocculation. In method 1, smectite was previously intercalated by Al_{13} and dried. A gel sample in method 2 was prepared by the addition of a Keggin-diluted solution to a smectite suspension. Method 3 was based on the addition of dried smectite into a dilute Keggin solution. In the cases of smectite prepared in methods 1 and 3, particles fell into the primary minimum where Van der Waals forces acted between FF-oriented smectite flakes and aggregates approached irreversible flocculation. In the case of the sample prepared using method 2, particles contacting by edges (EE) and edge to face (EF) orientation fell into secondary minimum, and weak flocculation resulted in severe gelatin and formation of the micelle-like texture in the fringe superstructure, which was the first time this was observed in smectite-based gel.

References:

[1] Y.F. Song, C.H. Chang, C.Y. Liu et al., J. Synchrotron Radiat. **14**, 320 (2007).
[2] G.C. Yin, Y.F. Song, M.T. Tang et al., Appl. Phys. Lett. **89**, 221122 (2006).
[3] M.S. Zbik, R.L. Frost, Y.F. Song, J. Colloid Interf. Sci. **319**, 169 (2008).
[4] M.S. Zbik, R.L. Frost, Y.F. Song et al., J. Colloid Interf. Sci. **319**, 457 (2008).
[5] M. Zbik, W. Martens, R. Frost et al., Langmuir **24**, 8954 (2008).

X-ray Imaging of Mucilaginous Sheath of Phytoplankton in Lake Biwa by Soft X-ray Microscopy

K. Takemoto[1], S. Ichise[2], T. Ohigashi[3], H. Namba[4], H. Kihara[1]

[1]*Department of Physics, Kansai Medical University, Osaka, Japan*
[2]*Lake Biwa Environmental Research Institute, Shiga, Japan*
[3]*Ritsumeikan University Research Organization of Science and Engineering, Shiga, Japan*
[4]*Department of Physical Science, Ritsumeikan University, Shiga, Japan*

Abstract:
Lake Biwa is the largest lake in Japan. It is the source of tap water for about 14 million people in the Kyoto-Osaka-Kobe region. It also supplies water for industry and agriculture. Because the deterioration of water quality affects water supply, various programs to monitor the water quality of Lake Biwa have been implemented. Recently, its chemical oxygen demand (COD) index is increasing in spite of a decrease in the values of the biochemical oxygen demand (BOD) index. In order to elucidate the mechanism, the X-ray images of a microstructure of picophytoplankton inhabiting Lake Biwa were taken.

Picophytoplankton is the fraction of the plankton performing photosynthesis composed by cells between 0.2 and 2 μm. Picophytoplankton is considered as an important source of dissolved organic matter. We are advancing the quantification of the organic matter from an X-ray image of a mucilaginous sheath around the picophytoplankton *Synechococcus*. Laboratory-cultured *Synechococcus* cells have been observed by soft X-ray microscope (BL-12) at the SR Center of Ritsumeikan University [1]. After centrifugation and chemical fixation, air-dried cells were observed at 2.3 nm. Each cell showed a high absorption from a sub-micron core and a low absorption from a region around the core. The low absorption region was interpreted as the mucilaginous sheath. The cells were estimated 0.7 μm in diameter, and mucilaginous sheaths were estimated as 1.2 μm in diameter. However, it was impossible to quantify the organic matter because the data of the X-ray images of the mucilaginous sheaths under natural ambient was insufficient. In order to obtain the natural ambient X-ray images of the mucilaginous sheath, other phytoplankton with the sheath, *Microcystis wesenbergii* and *Phormidium tenue*, were also observed by the X-ray microscope.

References:

[1] K. Takemoto, S. Ichise, M. Ichikawa et al., J. Phys.: Conf. Ser. **186**, 012097 (2009).

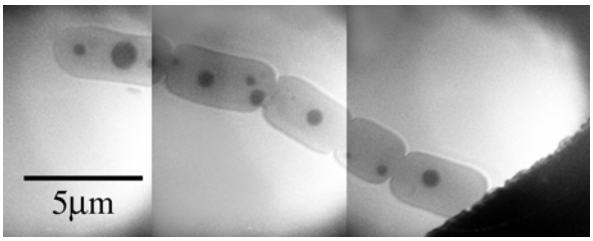

Figure 1: X-ray image of *Phormidium tenue*. Wavelength : 1.9 nm.

Evidence of High Metal Tolerance in Seeds of Ni Hyperaccumulators Revealed by Fluorescence Computed Microtomography (F-CMT)

R. Tappero[1], A. Lanzirotti[2], L. Miller[1], R.L. Chaney[3]

[1] *National Synchrotron Light Source, Brookhaven National Laboratory, Upton, NY, USA*
[2] *The University of Chicago, Center for Advanced Radiation Sources, Chicago, IL, USA*
[3] *USDA-Agricultural Research Service, Environmental Management, Beltsville, MD, USA*

Abstract:
Hyperaccumulator plants are used in commercial phytoremediation and phytomining operations to recover metals from enriched soils or sediment. Seeds of hyperaccumulator plants contain elevated levels of accumulated metals that could be bioavaiable and toxic to non-tolerant organisms and perhaps the embryo itself. Information regarding the distribution of metals at the micron scale is needed to locate the phenomena of hyperaccumulation in tissues, cells, and organelles in order to understand (hyper)tolerance mechanisms and ultimately improve phytoextraction efficiency.

Metal (hyper)tolerance in mature plants occurs via chemical binding of metals (e.g., chelation) coupled with intracellular compartmentalization to detoxify metals. Hard X-ray microprobe (HXM) was used to investigate metal localization and speciation *in situ* because standard sample preparation methods (e.g., embedding) cause redistribution of metals or alter their speciation.

Nickel in whole seeds was localized exclusively in embryonic tissue with greatest enrichment in the cotyledons, hypocotyl, and radicle; nickel was nearly absent from the testa (seed coat). Computed microtomography (F-CMT) revealed compartmentalization of Ni in epidermal tissue of seed embryos of Ni hyperaccumulator plants *Alyssum murale* and *Thlaspi goesingense*, and high-resolution X-ray fluorescence imaging (XRF) of seed tissue cryosections verified Ni was preferentially localized within epidermal cells. Nickel speciation in seeds was a near equal mixture of Ni-citrate and Ni-histidine species, consistent with Ni speciation in mature plants. Thus, the tolerance mechanism appears to be the same in the seed embryo as the mature plant.

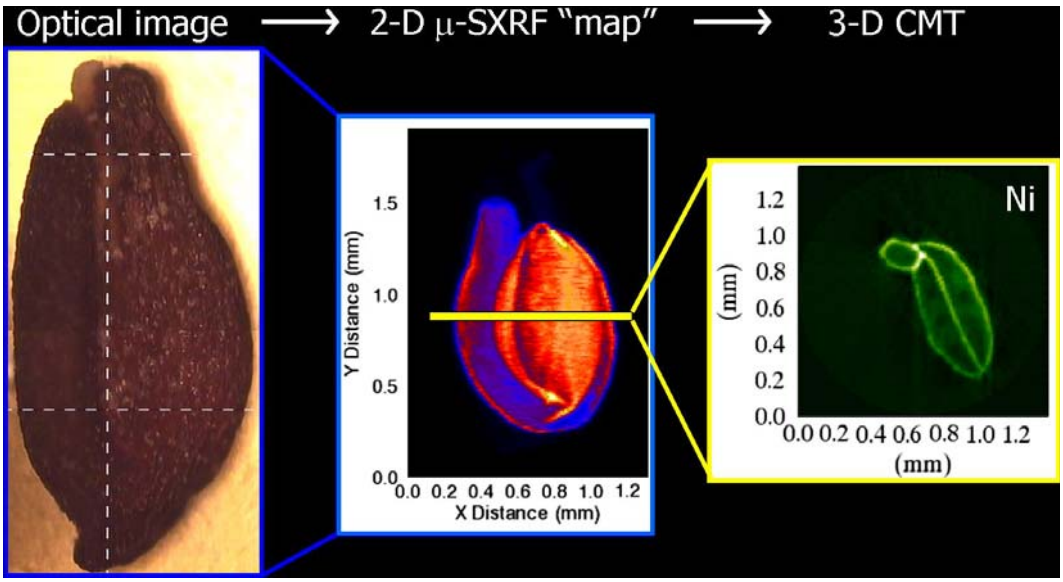

Figure 1. *T. goesingense* seed: Optical image (left), XRF image of Ni in T.g. seed (center), and F-CMT image of Ni in virtual cross section of T.g. seed embryo (right).

Poster Presentation Abstracts

Thursday, August 19

Session:	Poster #:
X-ray Microscopy Methods	Thurs-P001 – Thurs-P059
Biological & Biomedical Science	Thurs-P060 – Thurs-P088
Materials and Condensed Matter	Thurs-P089 – Thurs-P110

Improved Visualization Using Phase Retrieval Algorithms in Laboratory X-ray µCT

M.N. Boone[1], Y. De Witte[1], M. Dierick[1], A. Almeida[2], J. Van den Bulcke[3], L. Van Hoorebeke[1]

[1]*UGCT, Dept. Physics and Astronomy, Ghent Univ., Proeftuinstraat 86, 9000 Ghent, Belgium*
[2]*Dept. Pharmaceutical Sciences, Ghent Univ., Harelbekestraat 72, 9000 Ghent, Belgium*
[3]*Dept. Forest and Water Management, Ghent Univ., Coupure Links 653, 9000 Ghent, Belgium*

Abstract:

In recent years, X-ray microtomography (µCT) has become a very powerful tool for non destructive visualization and analysis in many fields. Due to the quickly increasing achievable resolution, it has become possible to scan very small samples with high accuracy. However, X-ray attenuation can become very small in these samples, especially in organic material.

Besides X-ray attenuation, X-ray refraction becomes visible at the edges of the samples. This effect, called phase contrast, results in a typical edge-enhancement profile on the projection data. This gives rise to artifacts in the reconstructed data if "uncorrected" projection data are being used.

Several methods exist to exploit this phase contrast effect. For laboratory setups with X-ray tubes, the most important are the use of phase gratings [1] and phase retrieval [2,3] or removal [4] based on image processing.

A particular effect of the phase retrieval algorithm is an improvement of the visibility of very small density fluctuations in a matrix. This effect will be demonstrated in this work based on two different samples. A fungus inside a wood sample (Figure 1) is hardly visible in the normal reconstruction, but phase retrieval reveals the fungus filling up some cells. Figure 2 shows a pharmaceutical sample where regions with fewer micropores become visible in phase retrieval reconstruction.

References:

[1] F. Pfeiffer, M. Bech, O. Bunk et al., Nature Materials **7**(2), 134 (2008).
[2] A. Groso, R. Abela, M. Stampanoni, Opt. Express **14**(18), 8103 (2006).
[3] M. Boone, Y. De Witte, M. Dierick et al., Nucl. Instrum. Methods B **267**, 1182 (2009).
[4] Y. De Witte, M. Boone, J. Vlassenbroeck et al., J. Opt. Soc. Am. A **26**(4), 890 (2009).

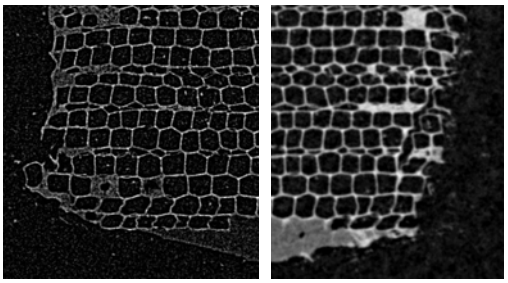

Figure 1: A wood sample with fungus inside. Regular reconstruction on left half, phase retrieval on right half.

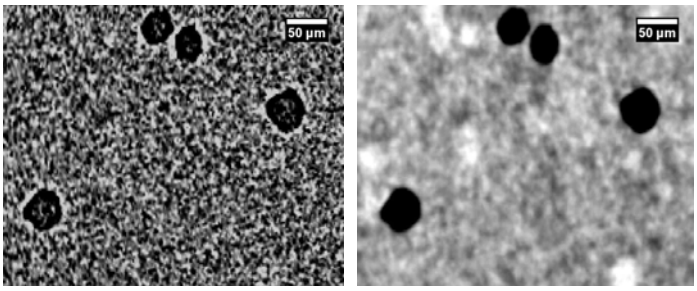

Figure 2: Pharmaceutical sample with higher density regions, invisible in regular reconstruction (left) but visible in phase retrieval reconstruction (right).

Latest Developments in 3D Analysis of CT Data by Morpho+

L. Brabant[1], J. Vlassenbroeck[2], V. Cnudde[3], Y. De Witte[1], L. Van Hoorebeke[1], P. Jacobs[3]

[1]*Department of Physics and Astronomy, Ghent University, Proeftuinstraat 86, B-9000 Ghent, Belgium*
[2]*inCT,IIC UGent, Technologiepark 3, B-9052 Ghent, Belgium*
[3]*Department of Geology and Soil Science, Ghent University, Krijgslaan 281/S8, B-9000 Ghent, Belgium*

Abstract:

At the Centre for X-ray Tomography of the Ghent University (Belgium) (www.ugct.ugent.be), a lot of progress is being made in hardware development for high-resolution X-ray CT scanners as well as in the field of software for data reconstruction and 3D analysis. We present the latest developments in the in-house developed package Morpho+ [1], a flexible 3D analysis software program which provides several structural 3D parameters of a scanned sample.

Morpho+ is able to calculate several geometrical parameters for both the complete sample as for specific components of the sample, such as grains or pores. These parameters include the surface, diameter of the maximum inscribed sphere, diameter of the minimum circumscribed sphere, equivalent diameter, orientation and a measure for the sphericity (shape parameter). In addition, total sample porosity (or volume fraction) and partial porosity (radial and longitudinal) can be determined. To measure the connectivity of the sample, a skeletonization algorithm and calculation of parameters such as the Euler Number and the size of bottlenecks of a network are included in the program.

Morpho+ produces a quantitative output, but it is also possible to visualize the different steps of the analysis, enabling easy interpretation of the results. For example different elements in a 3D volume can be colour-labelled based on their size. Additionally, the surfaces of the analysed components can be saved an STL-file for easy visualisation or further analysis.

References:

[1] J. Vlassenbroeck, M. Dierick, B. Masschaele et al., Nucl. Instrum. Methods A **580**(1), 442 (2007).

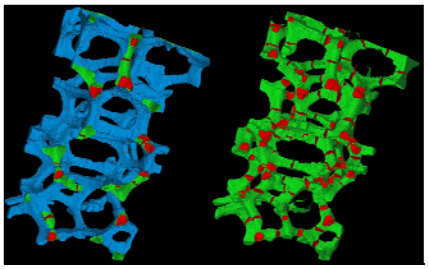

Figure 1: Isosurfaces (front=blue, back=green) of an aluminum foam with bottlenecks (red)

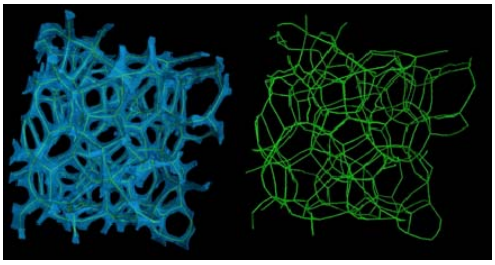

Figure 2: Skeleton (green) of an aluminum foam (blue)

Stop-Action Extreme Ultraviolet Imaging*

S. Carbajo[1†], F. Brizuela[1], O. Buccafusca[2], E.H. Anderson[3], W. Chao[3], D.T. Attwood[3], J.J. Rocca[1], C.S. Menoni[1]

[1]*Electrical and Computer Engineering, Colorado State University, Fort Collins, CO 80523, USA*
[2]*Avago Technologies, Fort Collins, CO 80525, USA*
[3]*Center for X-ray Optics, Lawrence Berkeley National Laboratory, Berkeley, CA 94720, USA*

*Work supported by the National Science Foundation through Award EEC-0310717.
[†]S.C acknowledges the support from Programa de Formación de Personal Investigador del Departamento de Educación, Universidades e Investigación, Gobierno Vasco.

Abstract:
We report on the first demonstration of stop-action imaging with nanoscale spatial resolution using a compact full-field microscope based on a desktop-size λ=46.9 nm extreme ultraviolet (EUV) laser [1]. In the transmission configuration used in this application, the microscope captures full-field images with a single nanosecond laser pulse and with a measured spatial resolution of 54 nm [2]. Single-shot images of a micro-electro-mechanical system (MEMS) cantilever were obtained using an objective zone plate with 0.12 NA. The device was driven by a sinusoidal signal of amplitude 5 V at its resonant frequency 136 kHz, during acquisition. Displacements of the cantilever as small as 130 nm can be measured from a set of images acquired by synchronizing the laser with respect to the sinusoidal driving signal. On a full cycle, the MEMS device displaces ~2.8 μm. This proof-of-principle stop-action extreme ultraviolet imaging demonstration opens up opportunities for assessing the linear and nonlinear dynamics of nanoscale devices with nanometer spatial resolution.

References:
[1] S. Heinbuch, M. Grisham, D. Martz et al., Opt. Express **13**(11), 4050 (2005).
[2] C.A. Brewer, F. Brizuela, P. Wachulak et al., Opt. Lett. **33**, 518 (2008).

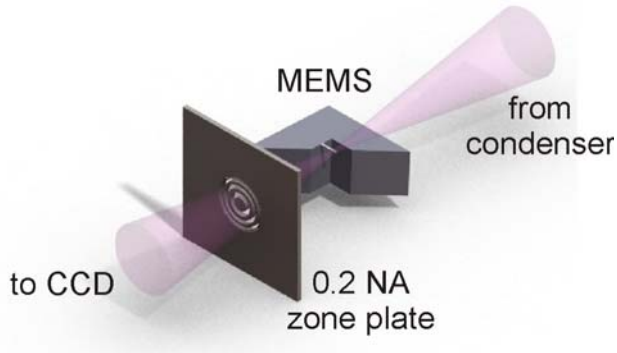

Figure 1: Schematics of the EUV microscope configuration used for single-shot imaging of MEMS dynamics.

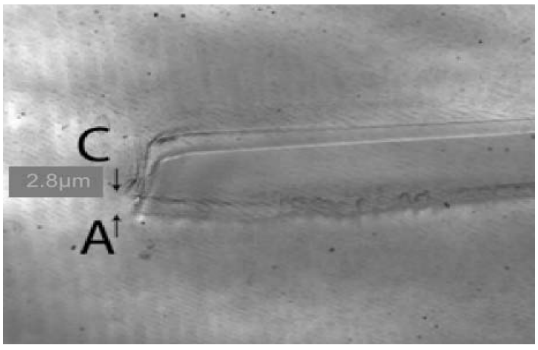

Figure 2: Superposition of two single-shot images of the cantilever at maximum (A) and minimum (C) of deflection.

How to Deal with Complex X-ray Fluorescence Spectra?

M. Cotte[1,2], J. Szlachetko[1,3], V. A. Solé[1], M. Salomé[1], J. Susini[1]

[1]*European Synchrotron Radiation Facility, Polygone Scientifique Louis Néel, 6, rue Jules Horowitz, F-8000 Grenoble, France*

[2]*Centre of Research and Restoration of French Museums (LC2RMF), CNRS UMR 171, Palais du Louvre, Porte des Lions, 14, Quai François Mitterrand, F-75001 Paris, France*

[3]*Institute of Physics, Jan Kochanowski University, Kielce, Poland*

Abstract:

ID21 is an ESRF beamline dedicated to micro-spectroscopy in the tender X-ray domain (2-7keV). Acquisition of X-ray fluorescence (XRF) spectra in this range of energy leads to several technical challenges (operation under vacuum, lower detection efficiency) as well as physical limits (limited penetration depth and reabsorption phenomena). In addition, high Z elements can highly interfere with the detection of K lines of low Z elements, by the emission of numerous M or L lines, with a overlap smaller than the energy resolution of classical solid state energy dispersive detectors. To tackle this last issue, two parallel strategies have been developed at ID21.

At the software level, an effort was made to develop a user friendly program for X-ray fluorescence spectra fitting and semi-quantitative analysis, PyMca. Complete description of the M shell is possible, which is particularly helpful for analysis of data collected at low energy and for the decomposition of overlapping peaks (Fig. 1). This program allows interactive as well as batch processing of large data sets [1].

At the hardware level, a high resolution and compact wavelength-dispersive spectrometer has been designed. It is based on a polycapillary optic for XRF collection and is operated in a flat-crystal geometry. Energy resolutions of tens of eV can easily be achieved. This detector enables a very good separation of M, L and K-lines, hence a more reliable and more sensitive elemental identification (Fig. 2). Line selectivity is also an asset for background free absorption spectroscopy [2].

Applications of these two approaches to complex materials will be exemplified.

References:

[1] V.A. Solé, E. Papillon, M. Cotte et al., Spectrochim. Acta B **62**, 63 (2007).

[2] J. Szlachetko, M. Cotte, J. Morse et al., submitted to J. Synchrotron Radiat., submitted.

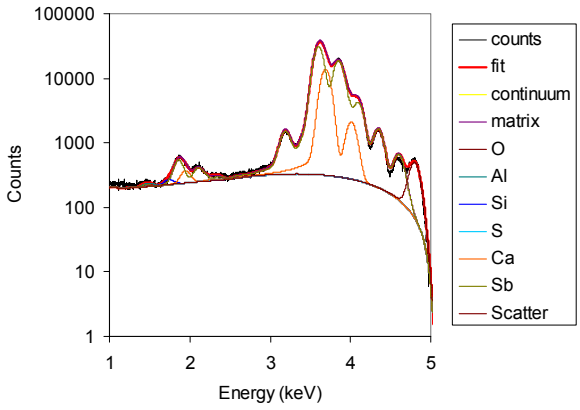

Figure 1: XRF spectra of $CaSb_2O_6$, acquired with an EDS and fitted with PyMCA [1].

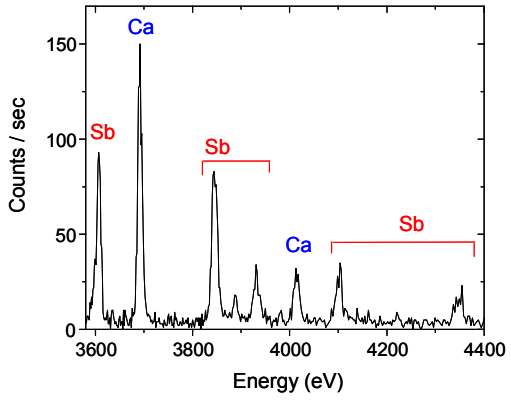

Figure 2: XRF spectra of $CaSb_2O_6$, acquired with the WDS [2].

Micro-spectroscopies at ID21: Towards a Multi-modal Strategy

M. Cotte[1,2], M. Salomé[1], J. Szlachetko[1,3], B. Fayard[1], M. Rak[1], F. Di Chiaro[1], V. de Andrade[1], E. Gagliardini[1], G. Berruyer[1], V. A. Sole[1], J. Morse[1], J. Susini[1]

[1]*European Synchrotron Radiation Facility, BP220 – F-38000 Grenoble, France*
[2] *C2RMF, CNRS UMR 171, Palais du Louvre, 14, Quai F. Mitterrand, F-75001 Paris, France*
[3]*Institute of Physics, Jan Kochanowski University, Kielce, Poland*

Abstract:
The ID21 ESRF beamline is primarily dedicated to micro-X-ray fluorescence (µXRF) and micro X-ray absorption spectroscopy (µ-XANES) in the tender X-ray domain (2-7keV). Typical scientific questions concern the co-localization and/or speciation of trace elements in heterogeneous matrices at the submicron scale, with applications in the fields of Environmental Sciences, Earth and Planetary Sciences, Life Sciences and Cultural Heritage. Several developments have been recently undertaken to enlarge the functionalities of the beamline.

The scanning X-ray microscope (SXM) itself has been completely refurbished in 2008. It now offers a very high versatility in terms of focusing optics, detection and sample environment [1]. The X-ray beam spot size ranges from ~20 µm (with a polycapillary focusing optics) to ~500 nm (either using focusing zone plates, or using a Kirk-Patrick Baez mirror system). A large panel of complementary detectors is available and provides: high sensitivity (with a 7-element Ge detector), high throughput (with a 100mm² SDD detector) or high spectral resolution (with a compact wavelength dispersive spectrometer [2]), which enables the collection of µ-XRF and µ-XANES spectra on a large variety of samples. The samples can be studied in various conditions (room temperature, cryo, wet cells). In parallel to this well-established micro-scanning configuration, a new set-up based on XANES full-field parallel beam imaging has also been recently implemented [3].

The ID21 SR-based FTIR end-station can provide complementary molecular mapping, with a ~5µm lateral resolution. Besides, various ancillary equipments, such as visible and electron microscopes, are available for additional observation and characterization of the samples. Simultaneously to instruments developments, efforts are continuously made to provide users with friendly integrated graphical user interface (GUI) for data acquisition, and with as friendly software (e.g., PyMca) for data treatment.

References:

[1] M. Salome, P. Bleuet, S. Bohic et al., Proc. of XRM2008, J. Physics: Conference Series **186**, 012014 (2009).
[2] J. Szlachetko, M. Cotte, J. Morse et al., submitted to J. Synchrotron Radiat.
[3] V. De Andrade, J. Susini, M. Salome et al., submitted to Anal. Chem.

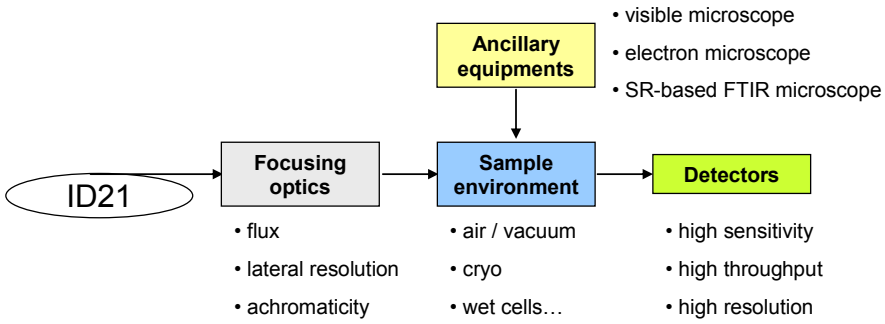

Figure 1: Versatility strategy of the new Scanning X-ray Microscope at ID21, ESRF.

Recent Progress in Quantitative Fast Fluorescence Tomography with a Hard X-ray Scanning Fluorescence Microprobe

M. D. de Jonge[1], C. Holzner[2], D. L. Howard[2], D. Paterson[2], C. G. Ryan[3], R. Kirkham[3], G. Moorhead[3], S. Baines[2], K. Ignatyev[4], C. Jacobsen[2], S. Vogt[5]

[1]*Australian Synchrotron, 800 Blackburn Road, Clayton, Australia*
[2]*Stony Brook University, Stony Brook, NY, USA*
[3]*CSIRO, Clayton VIC, Australia*
[4]*Medical Physics and Bioengineering, University College London, London, UK*
[5]*Argonne National Laboratory, Argonne, IL, USA*

Abstract:

The hard x-ray scanning fluorescence microprobe is ideally suited to map trace metal quantities within whole biological specimens. The elemental sensitivity of the fluorescence probe provides information valuable for investigations in a variety of biological applications, and the highly penetrating nature of hard x-rays enables measurement of whole cells. While 3D information is greatly desired, practice has largely been restricted to 2D or low-definition applications by a number of experimental factors including (i) the time required to measure each pixel (generally greater than 0.1 sec) and (ii) measurement time scales as the number of pixels in the reconstructed volume due to the serial nature of the scanning measurement. Based on these figures, ~1.2 days are required to measure a 10-µm object at 100-nm resolution.

We have performed fluorescence tomography of the whole 10-µm diatom *Cyclotella* with a reconstruction resolution of around 400 nm using a zone-plate microprobe at the 2-ID-E beamline of the Advanced Photon Source. A new event-mode fluorescence detector known as Maia [1] has been used with a KB mirror system at the XFM beamline of the Australian Synchrotron [2] to record a 180-projection tomographic series at modest definition (192 by 600 pixels FoV) in less than 12 hours, representing an average data rate of 1.7 Mpix/hour. We present an overview of the progress to date.

References:

[1] C.G. Ryan, D.P. Siddons, G. Moorhead et al., Nucl. Instrum. Methods B **260**, 1 (2007).
[2] D.J. Paterson, J.W. Boldeman, D.D. Cohen et al., AIP Conf. Proc. **879**, 864 (2007).

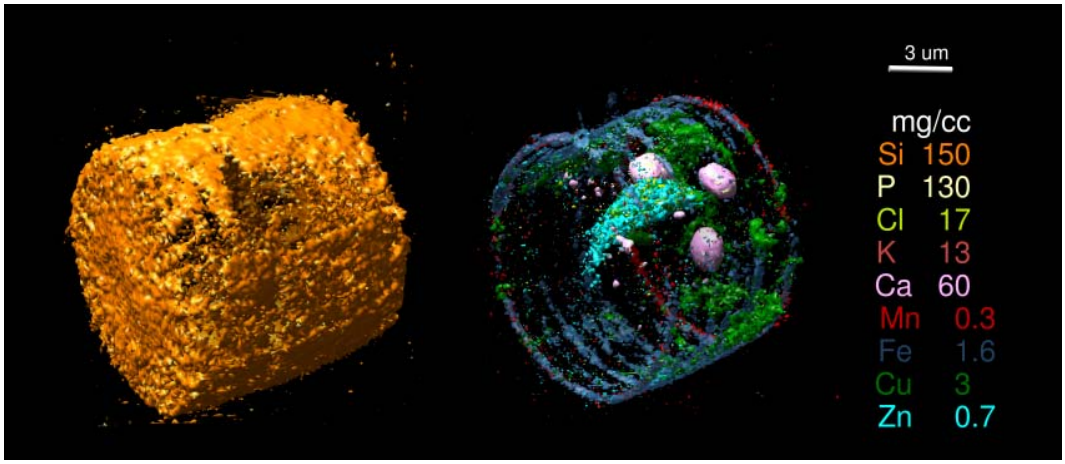

Figure 1: Elemental distributions in *Cyclotella meneghiniana*, showing very clearly the silicon frustule (left) and internal structure (right). Quantitative elemental concentrations of the isosurface values are provided in the key.

Phase Contrast in Laboratory-Based X-ray Micro/Nano-CT

Y. De Witte, M.N. Boone, M. Dierick, L. Van Hoorebeke

UGCT, Dept. Physics and Astronomy, Ghent Univ., Proeftuinstraat 86, 9000 Gent, Belgium

Abstract:

X-ray micro/nano-CT has evolved into an extremely valuable tool for various research fields. The current state-of-the-art laboratory-based systems can scan samples with a resolution below 1 micrometer. Achieving such high resolution usually means scanning very small and thus low absorbing samples, which is done using an X-ray tube with a very small focal spot size. Under these conditions, the acquired projections not only contain absorption contrast, but also phase contrast due to refraction of the X-rays. This phase contrast results in edge enhancement, which can be beneficial to detect very small features in radiography. In tomography however, the reconstruction of such mixed projections using a conventional algorithm yields cross-sections that are severely distorted by so-called phase contrast artifacts.

These artifacts can be prevented by applying a phase retrieval method like the *Modified Bronnikov Algorithm* (MBA) [1], or the similar *simultaneous phase and amplitude extraction* [2], which allows reconstructing the object's refraction function instead of its attenuation function. Alternatively, one can use the *Bronnikov-Aided Correction* (BAC) [3] to reduce the phase contrast signal in the projections, which can then be reconstructed without introducing phase artifacts in the reconstructed attenuation function.

At the Centre for X-ray Tomography of the Ghent University (UGCT), these two complementary methods MBA and BAC are commonly applied in every-day practice, thereby improving the reconstruction quality of high-resolution CT scans significantly [3,4] (illustrated in figures 1 and 2). Since neither method requires changes in the scanner hardware or the acquisition, they can be readily applied to projection data from any high-resolution scanner. In addition to results from the scanners of UGCT, results will also be presented for the successful application of both methods on data acquired using other high-end X-ray micro/nano CT systems.

References:

[1] A. Groso et al., Opt. Express **14**(18), 8103 (2006).
[2] D. Paganin et al., J. Microscopy **206**(1), 33 (2002).
[3] Y. De Witte et al., J. Opt. Soc. Am. A **26**(4), 890 (2009).
[4] M. Boone et al., Nucl. Instrum. Methods B **267**, 1182 (2009).

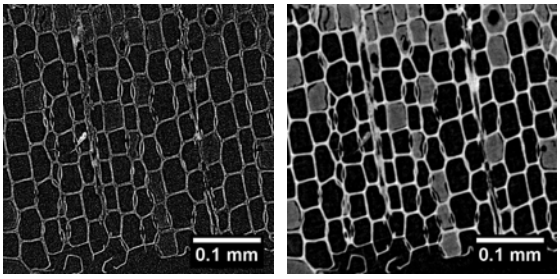

Figure 1: The MBA (right) applied on a piece of wood, revealing fungus inside the vessels, as compared to the conventional reconstruction (left).

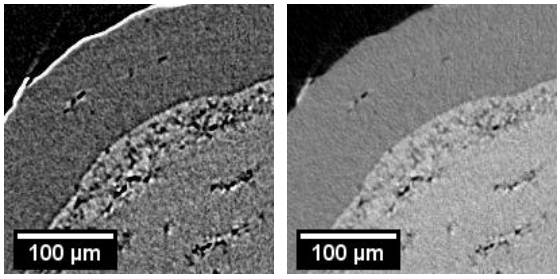

Figure 2: Phase artifact reduction using the BAC (right) on a pharmaceutical bead, as compared to the conventional reconstruction (left).

Advanced Tomography Reconstruction Algorithms on the Graphical Processing Unit

Y. De Witte[1], J. Vlassenbroeck[2], M. Dierick[1], L. Van Hoorebeke[1]

[1]UGCT, Dept. Physics and Astronomy, Ghent Univ., Proeftuinstraat 86, B-9000 Ghent, Belgium
[2]inCT, IIC UGent, Technologiepark 3, 9052 Zwijnaarde, Belgium

Abstract:

For many years the FDK algorithm has been the standard algorithm for the reconstruction of projection data acquired in cone beam geometry, which is the standard geometry in high resolution X-ray tomography. Iterative reconstruction algorithms such as SART [1] can however provide superior image quality. Additionally, artifacts associated with the cone beam geometry can be overcome by using alternative scanning trajectories such as the helical cone beam geometry, of which the data can for instance be reconstructed using the Katsevich algorithm [2]. However, the advanced algorithms for iterative reconstruction and helical cone beam reconstruction are far more complex than the FDK algorithm. The combination of this computational complexity and the large datasets encountered in high resolution X-ray tomography has prevented their application in this field.

The recent breakthrough of 'manycore' computing devices such as the Graphical Processing Units now allows the practical use of both helical cone beam geometry and iterative reconstruction methods in high resolution X-ray tomography. Here we present the implementation of these algorithms on the NVDIA CUDA architecture in the Octopus reconstruction package [3]. The performance of the algorithms is illustrated by means of timing results for typical data volumes. Additionally, the advantages with respect to image quality and the reduction of cone artifacts are illustrated by presenting reconstruction results for several applications (e.g. figures 1 and 2).

References:

[1] A. Andersen, Ultrason. Imaging **6**, 81 (1984).
[2] A. Katsevich, Phys. Med. Biol. **47**, 2583 (2002).
[3] J. Vlassenbroeck et al., Nucl. Instrum. Methods A **580**(1), 442 (2007).

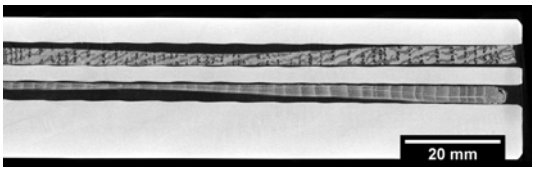

Figure 1: Helical cone beam reconstruction of several drill cores used for wood densitometry.

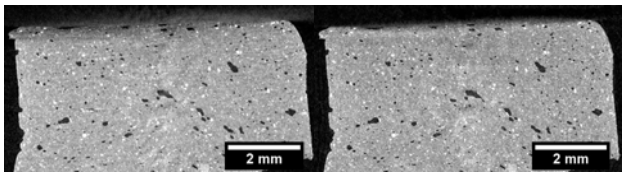

Figure 2: Comparison of the FDK (left) and SART (right) reconstruction of a low-cost, local building material.

"Super-Hierarchical" Microscope in EUV Region

T. Ejima, M. Toyoda, T. Tsuru, T. Hatano, M. Yanagihara

IMRAM, Tohoku University, 2-1-1 Katahira, Aoba-ku, Sendai, Japan

Abstract:

Living organisms and a part of high molecular compounds or self-assembly materials have an internal structural hierarchy. The structures within each hierarchy have characteristic shapes and functions related to their shape. Some small structures within a hierarchy combine interactively and make new structures by which a new characteristic function is achieved in the upper hierarchy. It is therefore important to understand the functions of a structure to simultaneously observe component structures and clarify their specific role [1]. A microscope that can observe hierarchical objects across several hierarchies can be called "super-hierarchical"; these features include a wide field of view where multi-hierarchical observation can be achieved and high spatial resolution by which the smallest structure can be observed.

For an example of hierarchical objects, the hierarchy of living organisms is designated according to the scale of the objects in Figure 1. When we observe a hierarchical object of active living organisms, the details of the structure will be blurred by Brownian motion [2]. The degree of blurriness depends on the exposure time and the spatial resolution of the observation tool; the structure will be indistinct when the motion is greater than the radii of the structure. The boundary of blurriness, which is calculated on the basis of the thermal diffusion, is also designated in the figure [2].

Spatial resolutions, fields of view, and minimum exposure time of standard microscopes are designated as the sides of boxes in the figure. The box represents the observation ability of space-time in the structural hierarchy of active living organisms. The largest box represents the estimated ability of a new microscope that includes our reflection multilayer objective with a laser-produced plasma light source [3]. The observation range of the space-time will be larger than any other microscope. In the presentation, we will discuss the reliability of this "super-hierarchical" microscope in the EUV region.

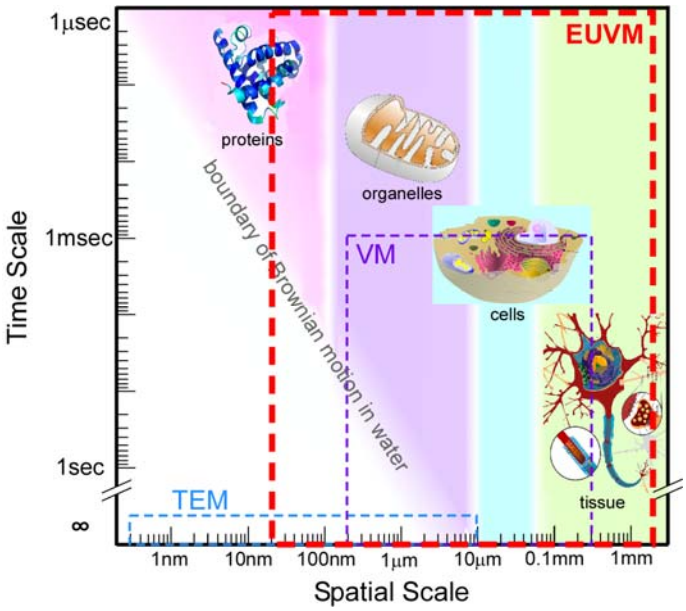

Figure 1: Hierarchy of living organisms with a boundary of Brownian motion. Broken boxes represent the abilities of microscopes. The left side of the boxes represents spatial resolution; right side, field of view, respectively. Upper side is minimum exposure time.

References:

[1] For example, B. Alberts, A. Johnson, J. Lewis et al., *Molecular Biology of the Cell*, (New York: Garland Science, Taylor & Francis Group, 2007).

[2] A. Ito and K. Shinohara, Cell Struct. Funct., **17**(4), 209 (1992).

[3] M. Toyoda et al. *ibid*, T. Tsuru et al., *ibid*., F. Ishida et al., *ibid*.

Coherent Diffractive Imaging Using Hollow Cone Illumination

X. Ge[1], K. Gao[1], Y. Hong[2], K. Zhang[2], Z. Wu[1,2]

[1] *National Synchrotron Radiation Laboratory, University of Science and Technology of China, Hefei 230026, China*

[2] *Beijing Synchrotron Radiation Facility, Institute of High Energy Physics, Chinese Academy of Sciences, Beijing 100049, China*

Abstract:

Coherent diffractive imaging (CDI) has been known as an efficient lensless imaging method in X-ray microscopy [1,2]. Conventional CDI schemes with planar wave or spherical wave illumination have a simple configuration [1], but also require light sources of high coherency. We propose a CDI scheme with hollow cone illumination, which is typical in transmission X-ray microscopes [3]. Compared to planar wave and spherical wave illumination in conventional CDI schemes, the new scheme is expected to have a higher signal-to-noise ratio for high spatial frequency and thus easier retrieval of more information. The corresponding reconstruction algorithm is also presented to demonstrate a simulated sample. The idea of adapting hollow cone illumination into a CDI scheme does not only bring higher efficiency and better resolution, but also leads to potential CDI applications for less-coherent sources [4].

References:

[1] G.J. Williams, H.M. Quiney, B.B. Dhal et al., Phys. Rev. Lett. **97**, 025506 (2006).
[2] H.M. Quiney, A.G. Peele, Z. Cai et al., Nat. Lett. **2**, 101 (2006).
[3] www.xradia.com
[4] L.W. Whitehead, G.J. Williams, H.M. Quiney et al., Phys. Rev. Lett. **103**, 101 (2006).

Element-Selective Microscopy with Confocal µ-PIXE Arrangement

N. Grlj[1]*, M. Žitnik[1], P. Pelicon[1], D. Sokaras[2], A.G. Karydas[2], B. Kanngiesser[3]

[1]*Jožef Stefan Institute, Jamova 39, SI-1000 Ljubljana, Slovenia*
**Presenting author: natasa.grlj@ijs.si*
[2]*Institute of Nuclear Physics, NCSR "Demokritos", GR-15310 Athens, Greece*
[3]*Institute of Optics and Atomic Physics, Technical University of Berlin, D-10623 Berlin, Germany*

Abstract:
Confocal µ-PIXE set-up combines excellent scanning possibilities of a proton microprobe with the spatially restricted solid angle of emission detection channel in order to obtain depth-resolved and eventually three-dimensional elemental images of the target without any sample rotation [1,2]. The so called confocal X-ray microscopy (CXM) [3] makes use of X-ray optics, usually polycapillary lenses, mounted in front of the X-ray spectrometer. Results of preliminary measurements and reconstruction analysis will be demonstrated for several cases together with the initial alignment and lens characterization procedure. A special emphasis will be given on the new developments of the confocal µ-PIXE set-up at Jožef Stefan Institute.

In order to achieve adequate depth resolution of the confocal µ-PIXE method, new approaches to the X-ray optics in the detection channel have to be introduced. Possible further developments of the method will be discussed.

References:

[1] M. Žitnik, P. Pelicon, N. Grlj et al., Appl. Phys. Lett. **93**, 094104 (2008).
[2] M. Žitnik, N. Grlj, P. Vaupetič et al., J. Anal. At. Spectrom. **25**, 28 (2010).
[3] D. Sokaras, A.G. Karydas, W. Malzer et al., J. Anal. At. Spectrom. **24**, 611 (2009).

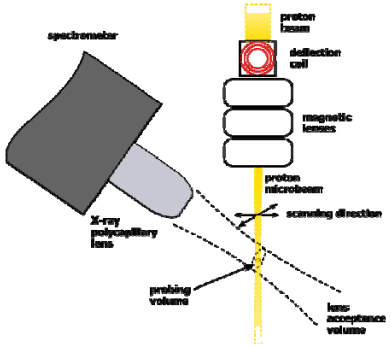

Figure 1: The principle of confocal set-up. The focal points of both proton microbeam and X-ray lens field of view are brought together to create a probing volume for target investigation.

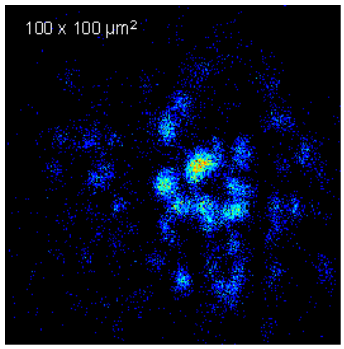

Figure 2: Aerosols particles in quartz filter – shown is the iron map – from the sequence of such measurements at different sample positions, a three-dimensional particle distribution and concentration can be reconstructed.

Phase Contrast X-ray Imaging by Means of Zone Plate Interferometer

L. A. Haroutunyan[1], K. G. Trouni[2], A. V. Kuyumchyan[3,4]

[1]*Yerevan State University, Alex Manoogian St. 1, Yerevan 375025, Armenia*
[2]*Institute of Applied Problems of Physics NAS RA, Hr. Nersisyan St. 25, Yerevan 375014, Armenia*
[3]*Institute of Microelectronics Technology, RAS, 142432, Chernogolovka, Russia*
[4]*American NanoScience and Advanced Medical Equipment, Inc., CA 91206, USA*

Abstract:
In the present work a new technique of X-ray phase imaging with increased scale has been considered based on the so-called three-block zone plate (ZP) interferometer composed of three identical crystal ZP [1] with common lens axis that are separated from each other by a constant step equal to double the focus length of the ZP (see Figure 1). The interference pattern on the exit surface of the third ZP has been considered. Channels of interfering beams are shown in Figure 1 with large and fine dotted lines and the different diffraction orders in each ZP are presented in Figure 2. The phase object (PO) to be investigated is located on the lens axis a small distance from the focus point of the second beam channel. As a result the phase distribution in the second channel beams is modulated along the entire cross section according to the inhomogeneities of PO. Meanwhile, the phase distribution in the first channel beams remains practically unchanged because of the significantly small size of the PO compared with the beam width.

For the phase reconstruction of the interference pattern, the third ZP must be slightly shifted along the lens axis (defocused interferometer). This causes the second channel beam behind the third block to converge or diverge, depending on the shifting direction. As a result, an interference pattern in the shape of concentric rings forms, which in turn can serve as the basis for phase retrieval with well-known methods of Fourier transform [1] and fringe scanning [2]. The phase shifter necessary for the second method can be placed across the reference beam, near the focal spot, as shown in Figure 1.

References:

[1] A. Kuyumchyan, V. Arvanian, D. Kuyumchyan et al., Proc. of SPIE **7442**, 74420J-1 (2009).
[2] M. Takeda, H. Ina, S. Kobayashi, J. Opt. Soc. Am. **72**, 156 (1982).
[3] J. Bruning, D. Herriott, J. Gallagher et al., J. Appl. Opt. **13**, 2693 (1974).

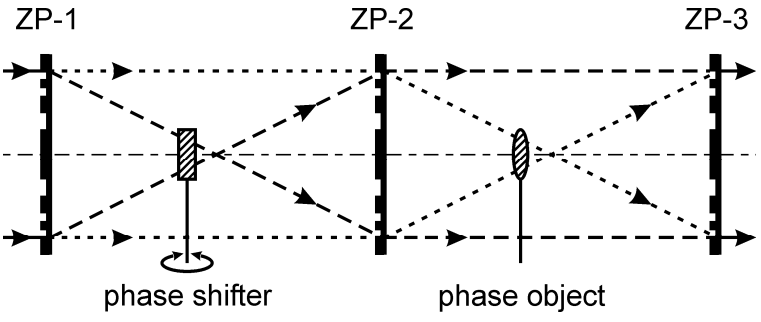

Figure 1: Three-block zone plate interferometer and beam paths. Large dotted lines: first beam channel, fine dotted lines: second beam channel.

	ZP-1	ZP-2	ZP-3
channel 1	+1	-1	0
channel 2	0	+1	-1

Figure 2: Interfering beam diffraction orders for each ZP.

Scanning Zernike Phase Contrast Implemented in a Hard X-ray Fluorescence Microprobe

C. Holzner[1], M. Feser[2], S. Vogt[3], B. Hornberger[2], S. B. Baines[4], C. Jacobsen[1]

[1]*Department of Physics and Astronomy, Stony Brook University, Stony Brook, NY 11794, USA*
[2]*Xradia Inc., 5052 Commercial Circle, Concord, CA 94520, USA*
[3]*Advanced Photon Source, Argonne National Laboratory, Argonne, IL 60439-4856, USA*
[4]*Department of Ecology and Evolution, Stony Brook University, Stony Brook, NY 11794, USA*

Abstract:
Scanned imaging, such as hard x-ray fluorescence microscopy, is widely utilized to reveal information beyond the absorption and phase contrast provided by full-field microscopy. Yet scanning does not often readily deliver the sample's structural information. While absorption is easy to realize in a scanning microscope, phase contrast, which dominates in particular for biological samples, is more difficult to achieve.

Zernike phase contrast [1] is an established and well-suited technique for directly visualizing weakly absorbing specimens in full-field microscopy with visible light, electrons and X-rays. The contrast is formed by an annular illumination and a phase shifting ring in the Fourier plane of the imaging system, translating phase variations into intensity modulations in the detector plane.

By employing the principle of reciprocity we have, for the first time, realized Zernike phase contrast in a scanning hard x-ray microscope [2], obtaining phase images in parallel with maps of trace elemental content—demonstrating unprecedented detail and structural sensitivity. We report on the implementation of this new technique, discuss its imaging properties, and further illustrate its application on biological examples.

Adding to the attractiveness of the method is the absence of any requirements for specialized detectors and analysis techniques, such as needed for differential phase contrast imaging and reconstruction. In principle, the approach can be extended to other scanning microscopy techniques.

References:

[1] F. Zernike, Phys. Zeitschr. **36**, 848 (1935).
[2] C. Holzner et al., submitted (2010).

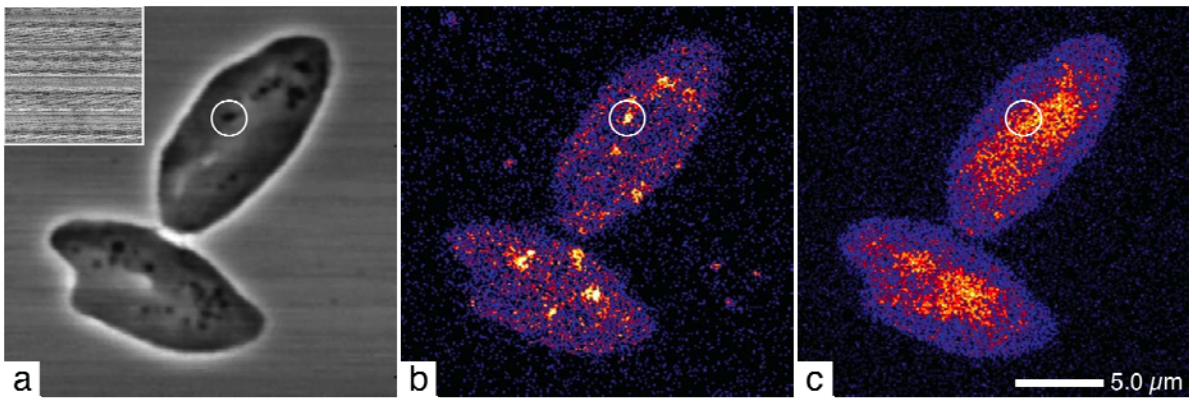

Figure: (a) Scanning Zernike with absorption image as inlay, (b) Mn and (c) Zn fluorescence. The Zernike image allows one to assign a localized elevation in Mn to an organelle; otherwise this Mn "hotspot" might have been interpreted as being part of a cytoplasmic column as given through the Zn fluorescence.

Comparison and Unification of Quantitative Scanning Phase Contrast Reconstruction Methods

C. Holzner[1], M. Feser[2], M. D. de Jonge[3], B. Hornberger[2], S. Vogt[4], C. Jacobsen[1,4]

[1]*Department of Physics and Astronomy, Stony Brook University, Stony Brook, NY 11794, USA*
[2]*Xradia Inc., 5052 Commercial Circle, Concord, CA 94520, USA*
[3]*Australian Synchrotron, 800 Blackburn Road, Clayton, VIC 3168, Australia*
[4]*Advanced Photon Source, Argonne National Laboratory, Argonne, IL 60439-4856, USA*

Abstract:
Phase contrast typically dominates over absorption contrast in transmission imaging with hard x-rays. In a scanning microscope, sensitivity to the object's phase can easily be achieved through differential phase contrast, resembling a gradient image of the phase distribution. Reconstruction of such differential phase images yields the true and quantitative phase representation of the sample.

Two procedures for the quantitative reconstruction of scanning x-ray phase contrast images have been reported in the past. The first is the filtering method [1], which is a deconvolution and a Wiener filtering approach in the limit of a weak specimen. It takes into account the imaging properties of the microscope and considers the inherent noise in the data. The second procedure, the integration method [2], applies a Fourier derivative technique [3] to integrate directional phase gradients, independent of optical imaging properties and image noise levels.

We compare both methods in their performance of quantitative reconstruction of scanning hard x-ray phase contrast data. It will be shown that both methods are very similar and can be reconciled in a unified formalism [4]. Subtle differences due to different assumptions and approximations employed in both approaches are discussed.

References:

[1] B. Hornberger et al., Ultramicroscopy **107**, 644 (2007).
[2] M.D. de Jonge et al., Phy. Rev. Lett. **100**, 163902 (2008).
[3] M.R. Arnison et al., J. Microsc. **214**, 7 (2004).
[4] C. Holzner et al., in preparation (2010).

Reconstruction of Zernike Phase Contrast for Tomography

C. Holzner[1], B. Hornberger[2], J. Gelb[2], M. Feser[2]

[1]*Department of Physics and Astronomy, Stony Brook University, Stony Brook, NY 11794, USA*
[2]*Xradia Inc., 5052 Commercial Circle, Concord, CA 94520, USA*

Abstract:

Zernike phase contrast images suffer from artifacts due to the nature of how the contrast is formed; typically through an annular shaped illumination and a phase shifting ring in the back-focal plane of the objective lens. A halo appearance around sample feature edges and a shade-off effect across extended uniform regions are common in Zernike images. These artifacts lead to a shell-like and flat impression of tomographic reconstructions from Zernike phase contrast data, making their interpretation and segmentation difficult.

By realizing the equivalence between scanning and full field imaging as a result of the principle of reciprocity, it is possible to apply a reconstruction technique from scanned imaging [1] to Zernike phase contrast data [2]. Through this reconstruction process artifacts in the Zernike image are removed for each projection and the results allow for a true volumetric reconstruction of the sample. We discuss the theoretical and practical details of the method and describe its application to experimental data.

References:

[1] B. Hornberger et al., Ultramicroscopy **107**, 644 (2007).
[2] B. Hornberger, M. Feser, Poster at the 9th International Conference on X-ray Microscopy (2008).

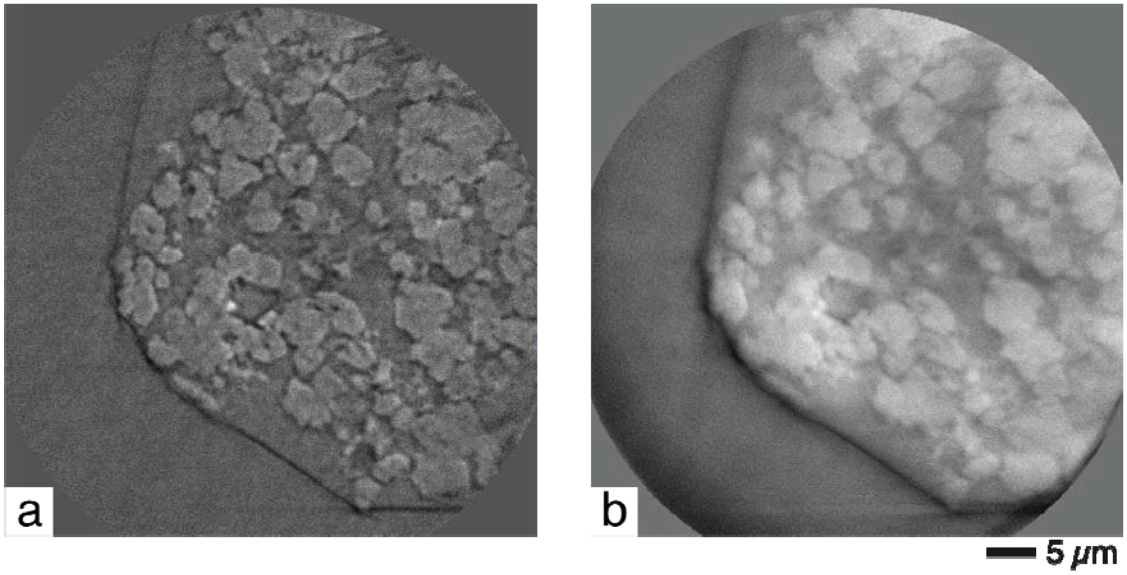

Figure: Slice through a tomographic reconstruction of rock imbedded in epoxy from (a) conventional and (b) reconstructed Zernike phase contrast data.

Quantitative Analysis of Absorption and Phase Difference Images in Differential Interference Contrast Microscopy

Y. Hong[1], P. Zhu[1], K. Zhang[1], X. Liu[1], Z. Wang[1], W. Huang[1], Q. Yuan[1], Z. Wu[2]

[1]*Beijing Synchrotron Radiation Facility, Institute of High Energy Physics, Chinese Academy of Sciences, Beijing 100049, China*
[2]*National Synchrotron Radiation Laboratory, University of Science and Technology of China, Hefei 230026, China*

Abstract:
As one of X-ray phase contrast imaging methods, diffraction enhanced imaging (DEI) is widely used to abstract absorption image and refraction angle image [1]. Here we utilize a similar method for quantitative analysis of absorption and phase difference images from two images at different shifts of the birefringent prism in differential interference contrast microscopy. We use interference curve to extract information of absorption and phase difference images, as in the diffraction enhanced imaging (DEI). Based on some kind of coherence illumination, theoretical analysis and preliminary quantitative experiment results of liquid paraffin are both presented. The results show that the image contrast is enhanced in a sense. We get better image contrast. At the same time, the quantitative information is extracted in a simple way compared to the methods proposed before [2]. In some conditions, we can also calculate the refractive index spatial variation or thickness of various cellular components.

References:
[1] P.P. Zhu, J.Y. Wang, Q.X. Yuan et al., Appl. Phys. Lett. **87**, 264101 (2005).
[2] M.R. Arnison, K.G. Larkin, C.J.R. Sheppard et al., J. Microsc. **214**, 7 (2004).

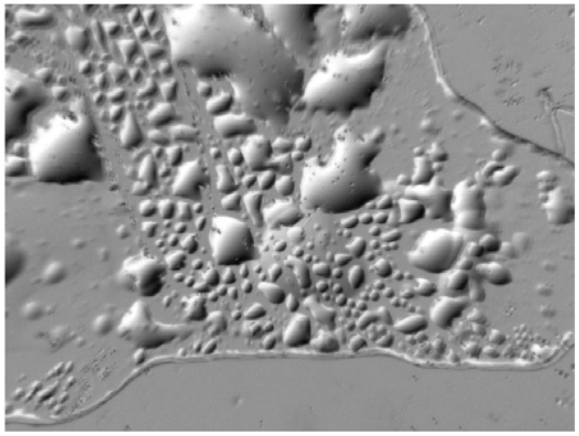

Figure 1: This is a phase difference image.

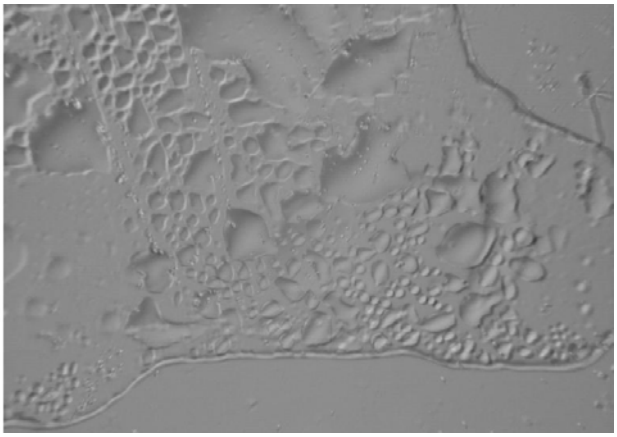

Figure 2: This is the absorption image.

Development of X-ray Laminography System at SPring-8

M. Hoshino, K. Uesugi, A. Takeuchi, Y. Suzuki, N. Yagi

Japan Synchrotron Radiation Research Institute, 1-1-1 Kouto, Sayo, Hyogo 679-5198, Japan

Abstract:

X-ray computed tomography (CT) is a powerful tool to measure the inner structures of opaque samples. However, it is hard to observe flat objects by conventional X-ray CT because adequate X-ray transmission cannot be obtained in the longitudinal direction. X-ray laminography is a promising candidate to overcome this problem [1]. It is possible for X-ray laminography to reconstruct the arbitrary layer as well as X-ray CT. Here, the X-ray laminography system developed at SPring-8 is described.

A schematic diagram of the optical setup for X-ray laminography is shown in Figure 1. It was constructed at BL20XU of SPring-8. Optical components of the system are the same as those of projection-type X-ray CT, whereas the rotational axis of a sample stage is inclined from the normal direction. By inclining the rotational axis, the transmission images at the region of interest of flat objects can be obtained even if they have much larger area size than the effective field of view of the detector. In this case, the inclination angle of the rotational axis is set to be 30 degrees. It can be also changed from 20 degrees to 40 degrees depending on the thickness and transmission of a sample.

A filtered-back projection method considering the inclination angle of the rotational axis is applied to the projection images acquired from 360 degrees rotation in the θ-direction to reconstruct the slice image, which is perpendicular to the rotational axis (θ-axis). A reconstructed image of a copper mesh pattern is shown in Figure 2. In this case, a mesh sheet was attached on the acryl pillar. The upper and lower images show the slice images in the parallel and vertical directions to the flat surface, respectively. The spatial resolution in the parallel direction almost corresponds to that of the detector. In this case, it is better than 2 μm, where the effective pixel size is 0.5 μm. In the vertical direction, however, the streak artifact generated by the inclined back projection process is observed. This artifact blurs the boundary surface between the high-density and low-density region in the sample. Fortunately, it was experimentally found that the effect of the streak artifact is effectively reduced in the complicated flat object such as a printed board. Therefore, X-ray laminography is adequately applied to the high-resolution non-destructive inspection of the flat objects that cannot be observed by X-ray CT.

References:

[1] L. Helfen, T. Baumbach, P. Mikulik et al., Appl. Phys. Lett. **86**, 071915 (2005).

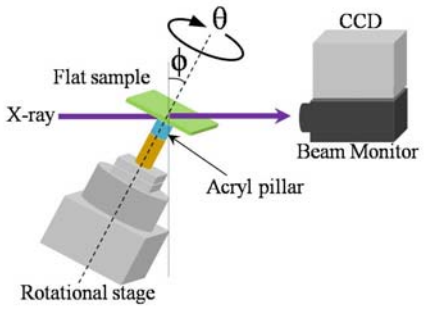

Figure 1: Schematic diagram of the optical setup for X-ray laminography developed at SPring-8.

Figure 2: Reconstructed images of copper mesh. Bar: 50 μm. X-ray energy: 25 keV.

Phase Tomography Based on the New Method to Extract the Refraction Angle Image

W. Huang[1], K. Zhang[1], P. Zhu[1]*, Q. Yuan[1], Y. Liu[1,2]
X. Liu[1], Z. Wang[1], Y. Hong[1], Z. Wu[1,2]

[1]*Institute of High Energy Physics, Chinese Academy of Science, Beijing 100049, China*
[2]*National Synchrotron Radiation Laboratory, University of Science and Technology of China, Hefei 230026, China*

Abstract:

Phase tomography based on the diffraction-enhanced imaging (DEI) is an attractive tool for observing weakly absorbing materials. This DEI imaging system required two images acquired with the analyzer crystal set on each side of the rocking curve to extract the refraction angle image, which is complicated and easy to increase the misalignment in tomography [1-3]. In this paper, we use an alternative method of obtaining the refraction angle of the object in which the analyzer is fixed and the object is rotated. Within this new theoretical framework the three components of the gradient of the refractive index can be reconstructed. And the recent commissioning results of this phase tomography now available for experiments at BSRF were presented. The resultant images verify the new analysis method and are compared with the images obtained by the original method of DEI. It can be concluded that this new method can make the procedure of phase tomography as simple as conventional tomography, and it is also useful in situations where it is important to keep the analyzer fixed in angle, which may improve the angular stability of the system.

References:

[1] D. Chapman, W. Thomlinson, R.E. Johnston et al., Phys. Med. Biol. **42**, 2015 (1997).
[2] M. Wang, P. Zhu, K. Zhang et al., J. Phys. D: Appl. Phys. **40**, 6917 (2007).
[3] K. Zhang, P. Zhu, W. Huang et al., Phys. Med. Biol. **53**, 5757 (2008).

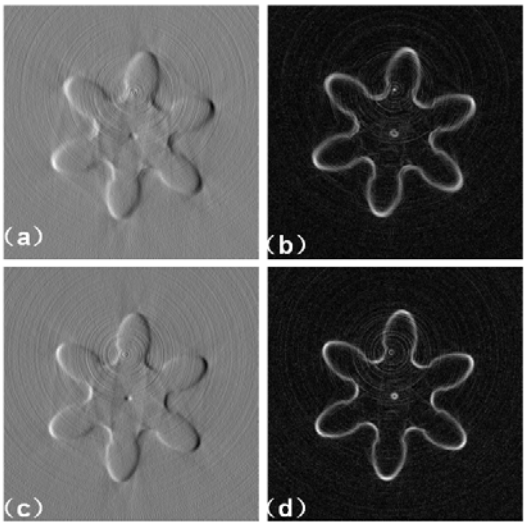

Figure 1: Reconstructed slice images of (a) $\partial n/\partial x$ and (b) $|\nabla n|$ of a gear using the Chapman method; (c) and (d) show the reconstructed images of the same gear obtained with the new method.

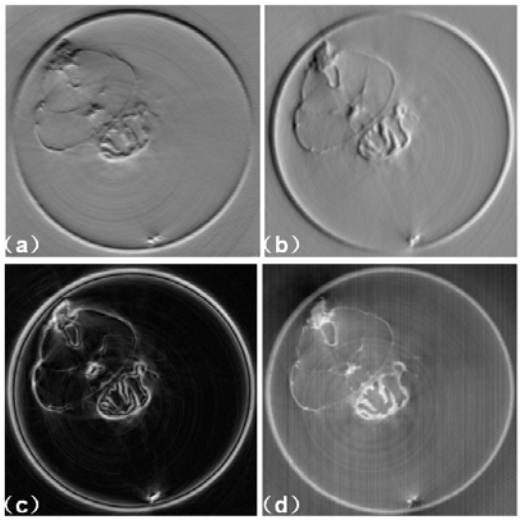

Figure 2: Reconstructed slice images of (a) $\partial n/\partial y$, (b) $\partial n/\partial x$, (c) $|\nabla n|$, and (d) $|n|$ of a fly using the new method.

Incorrect Support and Missing Center Tolerances of Phasing Algorithms

X. Huang[1,*], J. Nelson[1], J. Steinbrener[1], J. Turner[1], C. Jacobsen[1,2,3]

[1]*Department of Physics and Astronomy, Stony Brook University, Stony Brook, NY, USA*
[2]*Department of Physics and Astronomy, Northwestern University, Evanston, IL, USA*
[3]*Advanced Photon Source, Argonne National Laboratory, Argonne, IL, USA*
[*]*Now at: London Centre for Nanotechnology, University College London, London, UK*

Abstract:

The lost phase information in x-ray diffraction microscope (XDM) experiments is retrieved from oversampled far-field diffraction intensity measurements by iterative algorithms using *a priori* constraints [1].

The most commonly used constraints are the support constraint in real space, which localizes the object in a finite and isolated area, and the Fourier modulus constraint in reciprocal space, which replaces the Fourier magnitudes with the measured values. Algorithms using these constraints have been successfully applied on phasing diffraction patterns.

In some cases of experimental reality, either constraint is not perfectly determined. For soft matter objects or biological samples without sharp boundaries, dedicated effort is required to refine the estimated support, although the autocorrelation function and shrink-wrap procedure [2] can guide the way to some extent. Since the dynamic range of a diffraction pattern exceeds the dynamic range of a CCD detector, the center of diffraction patterns for low spatial frequency signal is usually blocked by a beam stop leaving an area with missing data. Flaws in both support and Fourier modulus constraints can affect the reconstruction quality and convergence speed of phase retrieval algorithms.

We compare the performance of three categories of algorithms [3]: ER (gradient descent to local minimum), HIO and DM (spiral convergence to local minimum), and RAAR (mixture between the other two), with incorrect supports and varying amount of missing low spatial frequency data through simulation. We conclude that HIO and DM give best reconstruction quality overall and over-tight supports or a missing speckle number greater than 14 can prevent algorithms from successful convergence.

References:

[1] D. Sayre, Acta Crystallogr. **5**, 843 (1952).
[2] S. Marchesini et al., Phys. Rev. B **68**(14), 140101 (2003).
[3] S. Marchesini, Rev. Sci. Instrum. **78**, 011301 (2007).

Phase-Contrast Imaging with Coded Apertures Using Laboratory-Based X-ray Sources

K. Ignatyev, P.R.T. Munro, R.D. Speller, A. Olivo

Department of Medical Physics and Bioengineering, University College London, London, UK

Abstract:

X-ray phase-contrast imaging is a powerful technique that allows detection of changes in the phase of an X-ray wavefront as it passes through the sample. As a result, details not visible in conventional X-ray absorption imaging can be detected. Until recently the majority of applications of phase contrast imaging were at synchrotron facilities due to the availability of their high flux and coherence [1]. However, a number of techniques have appeared recently that allow performing phase contrast imaging using laboratory sources.

Here we describe a phase-contrast imaging technique, developed at University College London [2], which uses a set of coded apertures. The X-ray beam is shaped by the pre-sample aperture and small deviations in the x-ray propagation direction are detected with the help of the detector aperture. In contrast with other methods it has a much more relaxed requirement for the source size (it works with source sizes up to 100 µm). A working prototype, coded-aperture system has been built. Coded apertures were manufactured from highly absorbing material with a detector grid period of 98 µm and a pre-sample grid period of 79 µm. The pre-sample aperture defines the sample field of view of 5 x 5 cm, which can easily be scaled up. Source – detector distance was 200 cm and the pre-sample aperture was positioned 160 cm from the source. An X-ray detector with directly deposited columnar CsI has been used to minimize signal spill-over into neighboring pixels. Phase-contrast images obtained with the system have demonstrated its effectiveness for imaging low absorption materials with exposure times compatible with typical absorption imaging in medical and other fields.

References:

[1] A. Snigirev, I. Snigireva, V. Kohn et al., Rev. Sci. Instrum. **66**, 5486 (1995).
[2] A. Olivo, R. Speller, Appl. Phys. Lett. **91**, 074106 (2007).

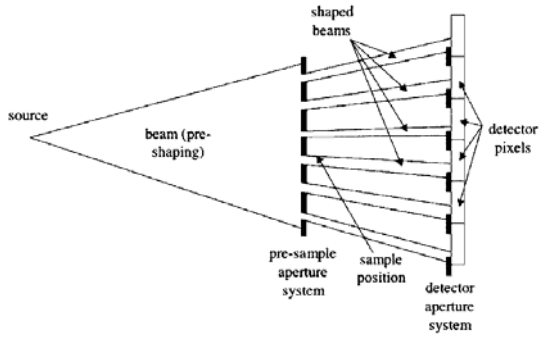

Figure 1: Schematic of the experimental setup.

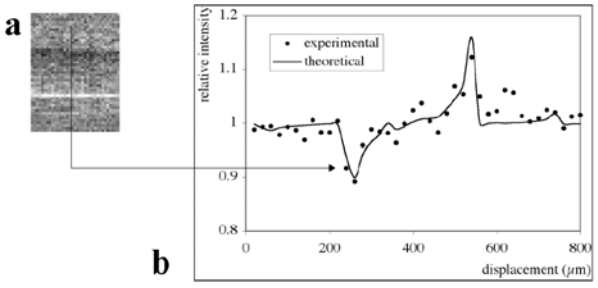

Figure 2: Phase contrast image of 300-µm polyethylene fiber obtained with conventional lab source (a) and its experimental and theoretical intensity profile (b).

Reconstruction of an Astigmatic Hard X-ray Beam and Alignment of K-B Mirrors from Coherent Diffraction Measurements

C. M. Kewish[1], M. Guizar-Sicairos[2], L. Assoufid[3], A. T. Macrander[3], J. Vila-Comamala[1], C. Liu[3], B. Shi[3], J. Qian[3], C. Benson[3], A. M. Khounsary[3], O. Bunk[1], J. R. Fienup[2]

[1]*Paul Scherrer Institut, CH-5232 Villigen PSI, Switzerland*
[2]*The Institute of Optics, University of Rochester, Rochester, New York, 14627, USA*
[3]*X-ray Science Division, Argonne National Laboratory, Argonne, Illinois, 60439, USA*

Abstract:

The ability to reconstruct a coherent focused X-ray beam [1-6] has important applications in X-ray optics fabrication. Because the aberrations in the wavefronts can be related to the optical quality of a focusing element [7,8], this provides useful feedback on how certain fabrication tolerances affect the focusing performance at the wavelength of interest. Numerically propagating the reconstructed complex field additionally reveals information about misalignments or larger-scale aberrations in the whole optical system.

We have used coherent X-ray diffraction experiments to characterize the 1-D and 2-D foci produced by profile-coated elliptical mirrors [9] in the Kirkpatrick-Baez (K-B) geometry. A nanofabricated phase structure was translated in the beam to provide a series of diffraction patterns with a known perturbation. The incident beam was then reconstructed using phase retrieval algorithms related to ptychography [1-6].

A 3-D reconstruction of the beam waist, using data measured when the mirrors were not optimally aligned, indicates that we could use this technique [2,4,6] as an alignment tool for the X-ray optics in a beamline. Considerable astigmatism was evident in the reconstructed beam. The location of the two foci allowed us to calculate the movements that would be required to bring them into coincidence. Comparing the reconstructed wavefield with a geometrical projection of the wavefront errors expected from optical metrology data allowed us to diagnose a 40-μrad misalignment of the mirror relative to the optical axis that had occurred during the experiment. This angle corresponds to a focal shift of –1.2 mm. Furthermore, there was good agreement between the metrology data and the reconstructed wavefront, illustrating the promise of this diffractive imaging method as a metrology tool for nanofocusing optics.

References:

[1] P. Thibault, M. Dierolf, A. Menzel et al, Science **321**, 379 (2008).
[2] P. Thibault, M. Dierolf, O. Bunk et al., Ultramicroscopy **109**, 338 (2009).
[3] A.M. Maiden, J.M. Rodenburg, Ultramicroscopy **109**, 1256 (2009).
[4] C.M. Kewish, P. Thibault, M. Dierolf et al., Ultramicroscopy **110**, 325 (2010).
[5] M. Guizar-Sicairos, J.R. Fienup, Opt. Express **16**, 7264 (2008).
[6] M. Guizar-Sicairos, J.R. Fienup, Opt. Express **17**, 2670 (2009).
[7] C.M. Kewish, L. Assoufid, J. Qian et al., Appl. Optics **46**, 2010 (2007).
[8] H. Mimura, H. Yumoto, S. Matsuyama et al., Phys. Rev. A **77**, 015812 (2008).
[9] C. Liu, L. Assoufid, R. Conley et al., Opt. Eng. **42**, 3622 (2003).

Application of Micro Aperture for Coherent X-ray Diffraction Imaging

S. Kim[1], C. Kim[1], S. Marathe[1], H. C. Kang[2], D. Y. Noh[1]

[1]*Department of Materials Science and Engineering, and Nanobio Materials and Electronics, Gwangju Institute of Science and Technology, Gwangju, Korea*
[2]*Department of Advanced Materials Engineering, Chosun University, Gwangju, Korea*

Abstract:
We demonstrated a coherent x-ray diffraction imaging (CXDI) that utilizes a specially prepared aperture for confining the illumination area at 5.5 keV. We found the rectangular aperture, an assembly of four elaborately polished metal pieces that produced an almost ideal far field diffraction pattern, and its exit wave field was successfully reconstructed through an iterative phase retrieval algorithm. Then, a weak phase object, periodic structure on a silicon substrate was applied and its optical properties were also deduced through phase reconstruction. Furthermore, we investigated the applicability of the aperture to CXDI for a truly extended specimen. Missing the central part and requirement of isolated objects [1,2], experimental barriers in the previously reported CXDI were greatly relaxed. In addition, a relatively weak phase object would be applicable due to negligible parasitic scattering, a deterministic factor of the signal-to-noise ratio from the aperture.

References:
[1] J. Miao et al., Nature **400**, 342 (1999).
[2] Y. Nishino et al., Phy. Rev. Lett **102**, 018101 (2009).

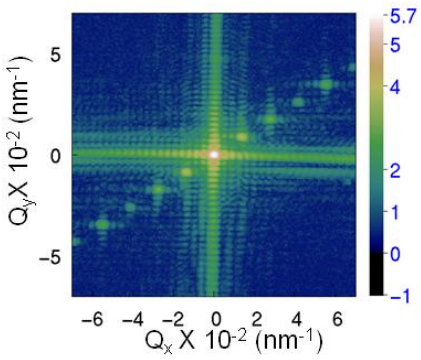

Figure 1: Diffraction pattern of a trench structure defined by a rectangular aperture.

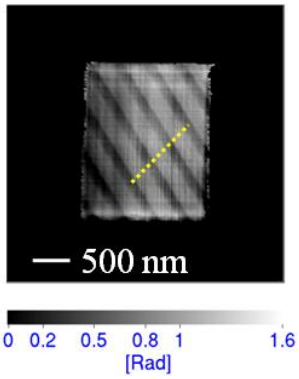

Figure 2: Reconstructed phase image of the trench structure.

Improved Scanning Geometry to Collect 3D-Geometry Data in Flat Samples

P. Krüger[1], E. Zschech[1], J. Gelb[2], M. Feser[2]

[1]*Fraunhofer IZFP-D, Maria-Reiche-Str. 2, 01109 Dresden, Germany*
[2]*Xradia Inc., 5052 Commercial Circle, Concord, CA 94520*

Abstract:
Three-dimensional-integration through silicon via technology of integrated circuits challenges nondestructive testing methods. Three-dimensional x-ray methods are the techniques of choice to localize defects in interconnects. The development of high power x-ray sources enabled the use of x-ray microscopy in laboratory tools. Those devices are able to resolve features down to 35 nm in an acceptable measuring time. However, the field of view is very limited to 35 µm in high-resolution mode and to 60 µm in large-field-of-view mode. To record tomography data, the size of the samples must not exceed the field of view to circumvent specific artifacts. Semiconductor samples usually do not fulfill the condition mentioned above since they have the shape of flat sheets. The usual way to do a 3D scan on those samples is limited angle tomography. The missing angles cause typical capping artifacts and poor signal to noise.

We present a modified scanning geometry that overcomes some of the artifacts and yields a better image quality. The geometry and potential applications are presented in comparison to the traditional limited-angle tomography.

X-ray Microscopy Based on Asymmetric Diffraction

A.V. Kuyumchyan[1,2,3], V.G. Kohn[4], A. Snigirev[5], I. Snigireva[5], M.V. Grigorev[1], E.V. Shulakov[1]

[1]*Institute of Microelectronics Technology, RAS, 142432, Chernogolovka, Russia*
[2] *American NanoScience and Advanced Medical Equipment, Inc., CA 91206, USA*
[3]*ORP Inc., Seattle, WA 98103, USA*
[4]*Russian Research Center "Kurchatov Institute", 123182, Moscow, Russia*
[5]*European Synchrotron Radiation Facility, B.P. 202, F - 38043 Grenoble, France*

Abstract:
We present results of focusing and imaging properties of a lens-crystal system for hard x-ray radiation using a parabolic refractive lens made from beryllium and an asymmetrically cut crystal made from silicon. As was shown in [1], such a refractive lens has advantages like small absorption, high efficiency, and high spatial resolution.

This work demonstrates, for the first time, imaging using focusing of x-rays by an asymmetrically cut crystal. Magnified images were recorded in x-ray phase contrast using a Si (220) asymmetric crystal [2] with an asymmetry factor of b=9, at an x-ray energy of 17 keV. The experimental investigations were conducted on station BM-5 at the ESRF, France. The peculiarities of redistribution of intensity are investigated both experimentally and theoretically when the focus of refractive lens is moved across the optical axis. The intensity distribution along the optical axis is also investigated.

We elaborate a computer program for theoretical study of image transmission system based on a lens–crystal system with asymmetric Bragg diffraction. The calculation is based on the use of Kirchhoff propagator in a paraxial approximation and fast Fourier procedure. The intensity map on the plane perpendicular across the optical axis is calculated for any parameters, including the phase shift of the test object.

References:

[1] A. Snigirev, V. Kohn, I. Snigireva et al., Nature, **384**, 49 (1996).
[2] V. Aristov, S. Kuznetsov, A. Kuyumchyan et al., Phys. Stat. Sol. (a) **125**, 57 (1991).

Quantitative Visualization of Various Biofluid Flow Phenomena Using the Synchrotron X-ray Micro-Imaging Technique

S. J. Lee, S. S. Ahn, B. H. Kim, H. K. Kim

Centre for Biofluid and Biomimic Research, School of Integrative Bioscience and Biotechnology, Pohang University of Science and Technology, Pohang, 790-784, Kyungbuk, Korea

Abstract:

The synchrotron X-ray micro-imaging technique was employed to investigate the biofluid flows in a wide range of biological organisms from small insects to plants [1]. Conventional optical imaging methods are not suitable to visualize bio-dynamic phenomena inside opaque bodies. In order to reveal some important bio-fluid flow phenomena using the advanced X-ray imaging technique, we developed bio-compatible nanoscale contrast material (CM) tracers suitable for the phase-contrast hard X-ray [2]. Using this imaging technique with CM tracers, we investigated the blood-sucking phenomena of female mosquitoes and transport of sap in rice leaves. As a result, the developed X-ray imaging technique was found to be a unique and powerful tool for observing biofluid flows in small insects such as mosquitoes. The dynamic motion of two pumps in the head of mosquitoes was consecutively visualized using a high-speed camera to reveal the blood-sucking mechanism of female mosquitoes [3]. For plant hydraulics studies, the understanding of flow dynamics inside xylem vessels is essential [4]. Various gold nanoparticles (AuNPs) were selected to track sap flow during the refilling process of embolized vessels in a rice leaf. The AuNPs interactions with xylem structure also revealed important properties of xylem cell walls. In addition, the X-ray micro-imaging technique was applied to measure blood flows in various micro-scale vessels. This X-ray imaging technique will play an important role in visualizing unknown biofluid flow phenomena.

References:

[1] M.W. Westneat, J.J. Socha, W.K. Lee, Annu. Rev. Physiol. **70**, 119 (2008).
[2] S.J. Lee, S.Y. Jung, S. Ahn, Biosens. Bioelectron. **25**, 1571 (2010).
[3] S.J. Lee, B.H. Kim, J.Y. Lee, J. Biomech. **42**, 857 (2009).
[4] S.J. Lee, Y. Kim, Ann. Bot. **101**, 595 (2008).

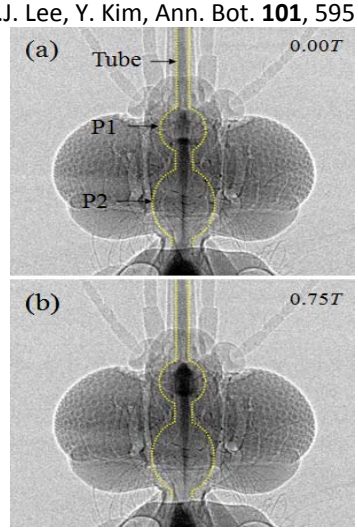

Figure 1: Systaltic motion of the two pumping organs of a female mosquito during sucking of diluted iodine solution.

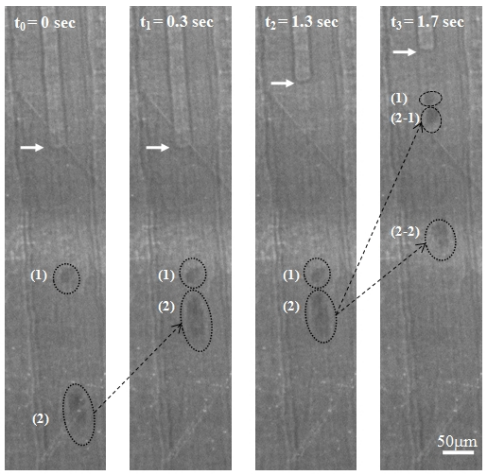

Figure 2: Four still cuts of continuous AuNPs uptake inside xylem vessels visualized by X-ray imaging of rice leaf sheath.

The Best of Both Worlds: 3D X-ray Microscopy with Ultra-High Resolution and a Large Field of View

W. Li[1], J. Gelb[2], Y. Yang[1], Y. Guan[1], W. Wu[1], X. Song[1], J. Chen[1], Z. Wu, Y. Tian[1]

[1]*National Synchrotron Radiation Laboratory, University of Science and Technology of China, Hefei, Anhui, 230029, P. R. China*
[2]*Xradia, Inc., 5052 Commercial Cir., Concord, CA, 94520, USA*
Email:ychtian@ustc.edu.cn

Abstract:
In 3D computed tomography (CT) imaging systems, such as x-ray microscopes, 3D visualizations of the complex structures within various samples have been achieved with high spatial resolution [1-3]. While high spatial resolution generally comes at the expense of field of view by stitching many 2D images together, a larger 2D image may be created with the same high resolution in each frame. This method may be extended to 3D imaging if each slice of the 3D tomographic images are carefully stitched together, significantly increasing the size of the field of view while preserving resolution. At National Synchrotron Radiation Laboratory (NSRL) in Hefei, China, we have successfully stitched two stacks of 3D virtual slices together into a single 3D volume. Combining this approach with a full-field transmission x-ray microscope utilizing Fresnel zone plate focusing optics, we have achieved sub-50 nm resolution with about a 20 μm field of view. This has enabled non-destructive 3D visualization of clustered yeast cells that were too large for a single field of view and shows high promise for imaging other large samples in the future.

References:

[1] Y. Tian, W. Li, J. Chen et al., Rev. Sci. Instrum. **79**, 103708 (2008).
[2] J. Chen, C. Wu, J. Tian et al., Appl. Phys. Lett. **92**, 233104 (2008).
[3] W. Li, N. Wang, J. Chen et al., Appl. Phys. Lett. **95**, 053108 (2009).

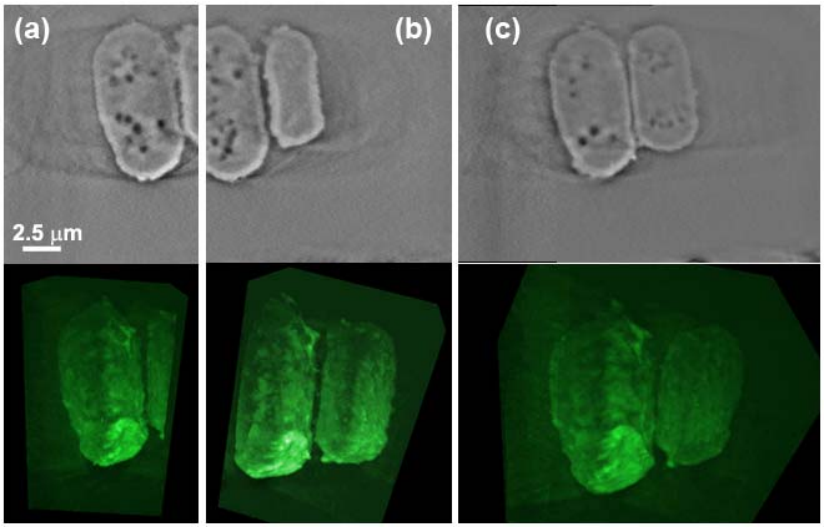

Figure 1: Three stacks of yeast cells. Upper image of each stack is a single slice of the 3D volume while lower image of each stack is the 3D rendering. The stack of (c) is created by stitching the two stacks of (a) and (b).

Implementation of Phase-Contrast Imaging Using a Polychromatic Beam from a Bending Magnet Source

J.-H. Lim[1], H. T. Kim[2], H. Y. Kim[1], J. Y. Huang[1], H. S. Youn[1], K. S. Jin[1], S. D. Jang[1], H.-J. Choi[1], K. H. Gil[1]

[1]*Pohang Accelerator Laboratory, POSTECH, San 31 Hyoja-Dong, Pohang 790-784, Korea*
[2]*Departments of Surgery, Anatomy, College of Medicine, Catholic University of Daegu, Daegu, Korea*

Abstract:
Phase contrast imaging is based on the coherent properties of a source. The technique is best implemented at synchrotron facilities by employing both a monochromator and an insertion device, the latter of which is to increase the flux of the beam which is essential for practical data acquisitions. Recently, Peele et al. demonstrated that an ordinary bending magnet source also has a potential to be a useful tool for phase contrast imaging. Notably, application of an extremely wide bandwidth-, polychromatic beam could yield the reconstructed images similar to those of the monochromatic cases while reducing the exposure times substantially [1]. The beamline 7B2 of Pohang Light Source at Pohang Accelerator Laboratory is specialized in hard x-ray tomography using a polychromatic beam from the bending magnet source. Due to absence of any X-ray optics, the beamline is much affordable and easy to maintain. We are currently exploring the utility of the beamline for phase contrast imaging, and the findings will be presented in this presentation. Since the radiation dose on samples is enormous with this beamline and often causes heat-associated deformation of biological specimens during tomographic scan we make use of sample cooling systems such as thermoelectric coolers or a cryostream generated from liquid nitrogen. The effects of set temperatures and ways of cooling on bio-specimens will also be discussed.

References:

[1] A. G. Peele, F. De Carlo, P. J. McMahon et al., Rev. Sci. Instrum. **76**, 083707 (2005).

Quantitative Information Extraction from Zernike-Type X-ray Phase-Contrast Imaging System

Y. Liu[1], F. Meirer[1,2], J. C. A. Hayter[1], J. Wang[3], P. Zhu[4], Z. Wu[4,5], P. Pianetta[1]

[1]*Stanford Synchrotron Radiation Lightsource, SLAC National Accelerator Laboratory, CA, USA*
[2]*Institute of Atomic and Subatomic Physics, Vienna University of Technology, Vienna, Austria*
[3]*Advanced Photon Source, Argonne National Laboratory, Argonne, Illinois, USA*
[4]*Beijing Synchrotron Radiation Facility, Institute of High Energy Physics, Beijing, China*
[5]*National Synchrotron Radiation Laboratory, University of Science and Technology of China, Hefei, China*

Abstract:
X-ray phase contrast imaging (XPCI) has been well recognized as a powerful method for structural investigation, especially in cases of weak sample absorption. One of the latest developments in XPCI is the implementation of Zernike-type phase contrast imaging [1] in the X-ray wavelength range, better known as Zernike-type transmission x-ray microscopy (TXM). A state-of-the-art Zernike-type TXM system with spatial resolution well below 50 nm is currently used at beamline 6-2 at the Stanford Synchrotron Radiation Lightsource (SSRL) [2]. The capability for inner structure investigation at a nanometer scale has made it a popular instrument for various applications.

However, images generated by Zernike-type phase contrast contain a mixture of contributions from different sample-beam interactions—such as absorption, refraction, and scattering—complicating a quantitative evaluation. This has become the main drawback of Zernike-type XPCI systems.

We propose a novel image acquisition strategy for a Zernike-type TXM system, which scans the phase ring plate while collecting a series of images with different offset value of the phase ring. The new method allows extraction of quantitative information regarding sample-beam interactions. Thus, quantitative phase retrieval from a Zernike-type XPCI system is achieved.

References:

[1] F. Zernike, Physica (Amsterdam) **9**, 686 (1942).
[2] J. C. Andrews, S. Brennan, Y. Liu et al., J. Phys.: Conf. Ser. **186**, 012081 (2009).

Progress in Coherent Diffractive Imaging of Biological Samples with Synchrotron and Free Electron Laser Sources

A. P. Mancuso, A. Singer, O. M. Yefanov, J. Gulden, I. A. Vartaniants

Deutsches Elektronen-Synchrotron DESY, Notkestraße 85, D-22607, Hamburg, Germany

Abstract:

Coherent x-ray diffractive imaging (CXDI) provides a relatively new imaging modality that exploits the bright, coherent beams available at synchrotron and free electron laser (FEL) sources. In particular, CXDI is a method that is limited in resolution only by the scattered signal from a given sample. The canonical example seeks to image whole, macromolecules with ultra-bright, ultra-short pulses of x-ray FEL radiation. These short pulses potentially allow radiation scattered from these samples to escape and be collected without the influence of the sample's inevitable destruction [1]. An injection of particles is the preferred delivery system for reproducible samples [2]. For non-reproducible samples (e.g., cells), fixed targets are a sample conserving alternative and in some cases present unique advantages.

In this work we will present CXDI measurements from fixed-target biological samples collected at synchrotron sources and FLASH, the Free electron LASer in Hamburg [3], and the corresponding reconstructed images produced from this data. We have investigated a variety of biological samples, including pollen grains with Fresnel coherent diffractive imaging (FCDI) [4] at the Advanced Photon Source (APS) and a *Navicula* diatom [5] with FLASH. We provide quantitative results for the resolution of the CXDI images of *Navicula* as a function of FEL pulse intensity.

We also consider using nano-beams from synchrotron sources in alternative CXDI modalities. Scanning coherent diffractive imaging, known as ptychography, has been demonstrated for biological specimens [6]. We discuss the implications and benefits of using nano-beams, characterized using ptychography [7], for high-resolution biological imaging.

References:

[1] R. Neutze et al, Nature **406**, 752 (2000).
[2] K. J. Gaffney, H. N. Chapman, Science **316**, 1444 (2007).
[3] W. Ackermann et al., Nature Photonics **1**, 336 (2007).
[4] G. J. Williams et al., Phys. Rev. B **75**, 104102 (2007).
[5] A. P. Mancuso et al., New J. Phys. (2010) (accepted).
[6] K. Giewekemeyer et al., PNAS, **107**, 529 (2010).
[7] A. Schropp et al., Appl. Phys. Lett., **96**, 091102 (2010).

EUV Dark-Field Microscopy for Defect Inspection

A. Maryasov[1], S. Herbert[1], L. Juschkin[1], K. Bergmann[2], R. Lebert[3], A. Aretz[4]

[1]*Chair for Technology of Optical Systems (TOS), RWTH Aachen University, Steinbachstr. 15, 52074 Aachen, Germany*
[2]*Fraunhofer Institute for Laser Technology, Steinbachstr. 15, 52074 Aachen, Germany*
[3]*Bruker Advanced Supercon GmbH, Friedrich-Ebert-Straße 1, 51429 Bergisch Gladbach, Germany*
[4]*Central Facility for Electron Microscopy (GFE), RWTH Aachen University, Ahornstraße 55 52074 Aachen, Germany*

Abstract:

Next-generation EUV lithography for 32 nm half pitch and beyond demands even higher quality—and defect cleanliness—levels of multilayer mask (ML) blanks during all fabrication steps. So-called phase defects hidden inside an ML could significantly affect final mask features at the working wavelength. These types of defects can only be detected at the same wavelength (actinic) [1]. The detection and mapping of critically sized defects on 6-inch mask blanks with a high throughput is a challenging task, as with increasing magnification one usually has losses in field of view (FOV) and signal intensity, which significantly increase the inspection time [2]. To overcome these limitations, an actinic EUV microscope for defect detection on mask blanks for operation in dark-field mode [3] using a table-top discharge-produced plasma (DPP) source has been developed. Several test structures (pits and bumps) and natural defects on multilayer mirrors were characterized with an atomic force microscope (AFM) and then investigated by our Schwarzschild objective (SO)-based EUV microscope at λ = 13.5 nm. Possible defect detection limits with large field of view (FOV = 650 µm) and moderate magnification (21x) will be discussed in terms of required source photon flux and detection camera performance.

References:

[1] T. Terasawa, T. Yamane, T. Tanaka et al., Jpn. J. Appl. Phys. 48, 06FA04 (2009).
[2] K.A. Goldberg et al., Proc. SPIE **6730**, 67305E (2007).
[3] L. Juschkin, R. Freiberger, K. Bergmann, J. Phys. - Conference Series **186**, 012030 (2009).

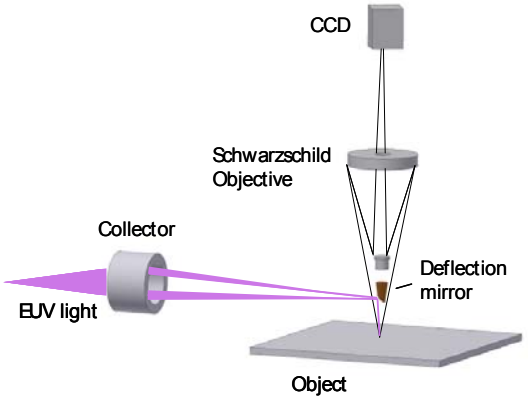

Figure 1: Scheme of the EUV dark-field microscope.

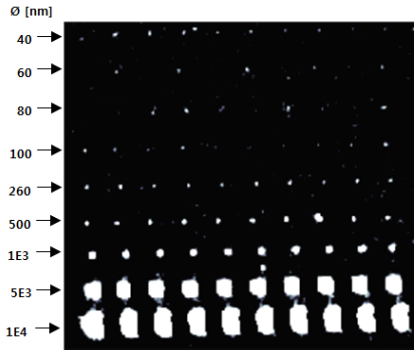

Figure 2: EUV image of programmed pit defects in a multilayer mirror of sizes from 10 µm to 40 nm.

Advancements in Hard X-ray TXM: XANES Mapping and Large Volume Tomography at Sub-100-nm Resolution

F. Meirer[1,2], J.C. Andrews[1], Y. Liu[1], A. Mehta[1], P. Pianetta[1]

[1]*Stanford Synchrotron Radiation Lightsource, SLAC National Accelerator Laboratory, CA, USA*
[2]*Institute of Atomic and Subatomic Physics, Vienna University of Technology, Vienna, Austria*

Abstract:

The full-field Xradia Transmission X-ray Microscope (TXM) installed at the Stanford Synchrotron Radiation Lightsource (SSRL) at beam line 6-2 (54-pole wiggler end station) is optimized to operate from 5-14 keV in absorption contrast and at 5 and 8 keV in Zernike phase contrast. The microscope provides a high-resolution (as high as 30-nm resolution) single flat field image of 15 x 15 µm² or 30 x 30 µm² area typically collected in a few seconds to a minute [1]. Many materials of interest today, such as electrodes for advanced batteries, and biological materials, are hierarchically heterogeneous. To fully understand functioning of these materials it is necessary to probe their structures from several hundreds of microns down to a few tens of nanometers. To accomplish this goal with the TXM multiple fields of view must be stitched together (mosaic mode) to reconstruct a large volume of the sample in three dimensions at ultra-high resolution. Furthermore, the use of synchrotron radiation can extend the range of applications to absorption spectroscopy in which the energy of incoming X–rays is tuned across the absorption edge of an element of interest within the sample. By combining the outstanding spatial resolution of the microscope with the brilliant, energy-tunable synchrotron source it is now feasible to obtain X-ray absorption near edge structure (XANES) spectra at every image pixel quickly. This makes it is possible to map structural phases and oxidation state variation at sub-100-nm resolution.

This paper will present recent developments at SSRL in sub-100-nm XANES imaging and large volume reconstructions from multiple 2D images via tomographic techniques. These advances will be illustrated from examples from a wide range of disciplines,S from archeometry to electrochemistry.

References:

[1] J. C. Andrews et al., “Nanoscale X-ray Microscopic Imaging of Mammalian Mineralized Tissue,” Microscopy and Microanalysis (2010), in press.

Microstructured Optical Arrays for Cell and Tissue Probing

A.G. Michette[1], S.J. Pfauntsch[1], G.R. Morrison[1], D. Hart[1], M. Shand[1], J.T.M. Stevenson[2], C. Dunare[2], W. Parkes[2], T.W. Button[3], D. Rodriguez-Sanmartin[3], D. Zhang[3], C. Meggs[3], R. Willingale[4], C.H. Feldman[4]

[1]King's College London, Department of Physics, Strand, London WC2R 2LS, UK
[2]Scottish Microelectronics Centre, University of Edinburgh, The King's Buildings, West Mains Road, Edinburgh EH9 3JF, UK
[3]University of Birmingham, School of Metallurgy and Materials, Edgbaston, Birmingham, B15 2TT, UK
[4]University of Leicester, Department of Physics and Astronomy, Leicester, LE1 7RH, UK

Abstract:
This presentation describes a case study in integrating a laboratory-scale x-ray source with appropriate optics for a particular application, namely the study of radiation-induced cancers. Previous work [1] using carbon K x-rays (284 eV), from a microfocus source, focused using zone plates onto individual biological cells, allowed studies of phenomena such as the bystander effect, whereby unirradiated cells in a collection in which only one is irradiated display signs of radiation damage. This may be related to another effect, low-dose hypersensitivity, in which more cells are damaged at very low doses than would be expected from extrapolations from high doses. However, to date it has only been possible to study cell death, rather than the much more important — for the understanding of cancers — effect of mutations. Additionally, it is also important to study effects in tissue samples, as these will be more relevant to living organisms. In order to achieve these aims, it is necessary to deliver higher dose rates (so that more material can be irradiated in a given time) at higher energies (to penetrate into tissue). The UK Smart X-Ray Optics (SXO) consortium [2] is, as one of its goals, developing a microfocus source that will provide chromium K_α x-rays (5.4 keV) focused to a sub-micrometer spot using custom-built microstructured optical arrays [3] that use two successive grazing-incidence reflections from channels etched in silicon. The arrays, which will deliver about two orders of magnitude more focused flux than a zone plate, may be flexed using piezo actuation to provide focal length control and reduction of aberrations. Progress in the design, construction, and characterization of the source and optics will be discussed.

References:

[1] M. Folkard, K.M. Prise, A.G. Michette et al., Nucl. Instrum. Methods A **580**, 446 (2007).
[2] In addition to the institutions listed, the other members of the SXO consortium are University College London (including the Mullard Space Science Laboratory) and STFC Daresbury Laboratory. Silson Ltd. and Diamond Light Source are associate members. SXO is supported by the UK Basic Technology Programme (EPSRC grant D04880X) and in part by the EU COST Action MP0601 *Short Wavelength Laboratory Sources*.
[3] A.G. Michette, S.J. Pfauntsch, S. Sahraei et al., Proc. SPIE **7360**, 736007 (2009).

Artifacts in Dark-Field Tomography

P. Modregger[1,3], T. Thüring[1,2], B. Pinzer[1], M. Stampanoni[1,2]

[1]*Swiss Light Source, Paul Scherrer Institut, 5232 Villigen PSI, Switzerland*
[2]*Institute for Biomedical Engineering, University and ETH Zurich, 8092 Zurich, Switzerland*
[3]*Department of Radiology, University of Lausanne Medical School, Lausanne, Switzerland*

Abstract:

Grating interferometry is a recently established phase-sensitive X-ray imaging method that provides a particular high sensitivity towards density variations in the sample [1,2]. In addition to the absorption and phase contrast the grating interferometer also delivers the complementary information of local scattering strength at the sample (i.e. the dark-field image) [3]. Since scattering may be regarded as unresolved local phase variations, the scattering signal provides information on a length scale smaller than the pixel size of the utilized detector.

Based on a theoretical description of small scattering contribution to the image formation process [4], Wang *et al.* established a first approach to quantitative dark-field tomography with the grating interferometer. However, this approach is based on several approximations and the extent of validity of these approximation as well as the artifacts that arise from violations of these approximation are still unknown. Therefore, we used numerical simulation of the dark-field tomography in order to determine the limitations of the previously proposed algorithm.

References:

[1] C. David, B. Noehammer, H.H. Solak et al., Appl. Phys. Lett. **91**, 3851 (2002).
[2] S.A. McDonald, F. Marone, C. Hintermüller et al., J. Synchrotron Radiat, **16**, 562 (2009).
[3] F. Pfeiffer, M. Bech, O. Bunk et al., Nature Materials **7**, 134 (2008).
[4] G. Khelashvili, J. Brankov, D. Chapman et al., Phys. Med. Biol. **51**, 221 (2006).
[5] Z. Wang, K. Kang, Z. Huang et al., Appl. Phys. Lett. **95**, 094105 (2009).

The Measurement of MTFs in X-ray Microscopy Using Diffractograms

G. R. Morrison[1], P. S. Charalambous[2], A. Gianoncelli[3], B. Kaulich[3]

[1]*King's College London, Dept. of Physics, Strand, London WC2R 2LS, UK*
[2]*ZonePlates Ltd, 8 South Way, Claverings Industrial Estate, London N9 0AB, UK*
[3]*Sincrotrone Trieste S.C.p.A., S.S. 14, km 163.5 in Area Science Park, 34149 Trieste, Italy*

Abstract:

In order to make a quantitative interpretation of image contrast, it is important to know the modulation transfer function (MTF) for the imaging system, as this gives information not only on the available resolution, but also on how different spatial frequency components transfer from object to image. The MTF is a measurement made in Fourier space; an equivalent characterization in real space is to measure the point spread function (PSF) of the optical system. Estimation of the MTF using test objects such as a Siemens star pattern (a set of radial spokes forming an isotropic grating-like structure with a continuously varying period), is well established [1] but can be rather time consuming. Some novel forms of ptychographic imaging in STXM [2,3] are able to reconstruct both the complex object transmittance and the form of the incident x-ray probe by iterative methods, but other methods of image analysis require an accurate knowledge of the probe for the reconstruction to be successful [4].

In this paper we describe a method that can be used to measure the MTF directly from x-ray image data. The method relies on the use of a test object with a power spectrum that is essentially constant over the spatial frequency range of interest. In this case, an x-ray diffractogram (obtained by calculating the power spectrum of the image data) then yields an intensity distribution that relates directly to the MTF of the imaging system. Such an approach was developed many years ago in transmission electron microscopy [5], where it was found that thin films of amorphous carbon were very suitable random phase objects. The challenge in x-ray microscopy has been to find an equivalent random object structure that would provide an essentially constant power spectrum in the spatial frequency range of relevance to high-resolution x-ray microscopy.

One form of object with the appropriate properties is an artificially generated random array of holes in a thin tungsten film. Such holes can be produced by electron-beam lithography with sizes significantly smaller than the spatial resolution available in a transmission x-ray microscope, analogous to the individual atoms in amorphous carbon films, whose size is below the resolution limit of most electron microscopes. By adding Siemens star test patterns to adjacent regions of the same tungsten film, it is possible to compare directly the results of x-ray diffractogram analysis of the probe shape with the more conventional analysis of Siemens star patterns imaged under equivalent conditions.

References:

[1] C. Jacobsen, J. Kirz, S. Williams, Ultramicroscopy **47**, 55 (1992)**.**
[2] P. Thibault, M. Dierolf, A. Menzel et al., Science **321**, 379 (2008).
[3] A. M. Maiden, J. M. Rodenburg, Ultramicroscopy **109**, 1256 (2009).
[4] J. M. Rodenburg, A.C. Hurst, A.G. Cullis et al., Phys. Rev. Lett. **98**, 034801 (2007).
[5] F. Thon, Z. Naturforsch. **21a**, 476 (1966).

X-ray Fourier Transform Holography with a Separate Illumination Mask

K. Nomura[1], S. Doi[1], N. Awaji[1], S. Isogami[2], K. Kodama[3], T. Nakamura[3], M. Suzuki[3], M. Tsunoda[2]

[1]*Fujitsu Ltd., 10-1 Morinosato-Wakamiya, Atsugi 243-0197, Japan*
[2]*Tohoku University, Aobayama 6-6-05, Sendai 980-8579, Japan*
[3]*SPring-8/JASRI, Kouto 1-1-1, Sayou-cho 679-5198, Japan*

Abstract:
The attention on coherent X-ray imaging has been growing due to the recent development of X-ray Free Electron Laser (XFEL) or the tabletop coherent x-ray sources. Among them, X-ray Fourier Transform Holography (XFTH) provides a simple and unambiguous image reconstruction for nanomaterials. While the technique has been successfully demonstrated to the magnetic materials [1], a difficulty exists in the sample preparation. To prepare the XFTH samples, we need to deposit an opaque film like Au on one side of SiN membrane as an absorber of X-ray, and fabricate the object window with the size of around 2micron in addition to the small through-hole around 0.1 μm size as a reference hole in the absorber by the focused ion beam (FIB). In addition, sample layer has to be formed on the other side of the membrane. In this sample structure, the size of object window limits the field of view for the imaging. To improve these problems, we tried to separate the illumination mask that contains an object window and a small reference hall, from the sample membrane. In this configuration, we can scan the sample with a high resolution stage or even changed the sample. The technique was successfully applied to the magnetic domain imaging of Co/Pt perpendicular magnetized film at soft x-ray beamline BL25SU in SPring-8, as shown in Figures 1 and 2. In addition, for the imaging of an embedded semiconductor structure, we tried to extend this technique to the hard x-ray region around 6 keV. As a result, we have succeeded to image the Cu wire of 240 nm width at hard X-ray beamline BL16XU in SPring-8.

The synchrotron radiation experiments were performed at the BL25SU and BL16XU in the SPring-8 with the approval of the Japan Synchrotron Radiation Research Institute (JASRI) (Proposal No. 2008A1513, 2009A1840, 2009B1844, and 2009B5110). This study was supported by the Promotion of XFEL Research of MEXT.

References:

[1] S. Eisebitt et al., Nature, **432**, 885 (2004).

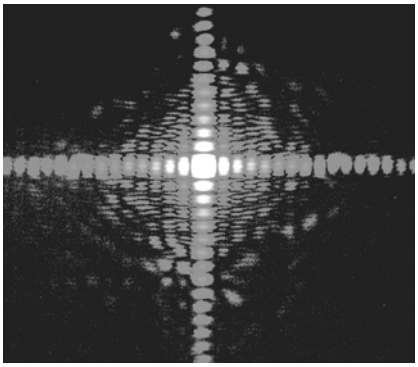

Figure 1: The hologram recorded at E=778.4 eV.

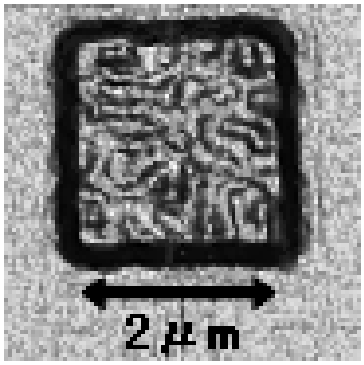

Figure 2: Reconstructed image of Fig. 1 where the separate mask was used.

Coherent Surface Diffraction, Reciprocal-Space and Real-Space Possibilities

M.S. Pierce[1], D. Hennessy[1], K.-C. Chang[1], A. Barbour[1], V. Komanicky[2], J. Strzalka[3], A. Sandy[3], H. You[1]

[1]*Materials Science Division, Argonne National Laboratory, Argonne IL, USA*
[2]*Faculty of Sciences, Safarik University, Košice, 04001, Slovakia*
[3]*Advanced Photon Source, Argonne National Laboratory, Argonne IL, USA*

* This work and use of the Advanced Photon Source were supported by the U.S. Department of Energy, Office of Science, Office of Basic Energy Sciences, under Contract No. DE-AC02-06CH11357

Abstract:

Using methods such as holography, phasing, and direct inversion algorithms, scientists have begun to open up the realm of complete 3D real-space structure from complex and interesting systems. However, at the current time, it is often too difficult to obtain the full real-space structure given the experimental constraints, or the information of interest can be obtained without inversion of the diffraction pattern. How difficult would it be to obtain nanoscale real-space structures from surfaces using coherent diffraction? What can we learn from the diffraction patterns even when reconstruction is not possible?

We present the extension of coherent diffraction to the surfaces of metal single crystals (see Figure 1) such as Au (001) [1] and Pt (001) [2]. The speckle patterns we obtained were not of sufficient quality to invert for the surface structure. However, we were able to record the changes in the speckle pattern to study the dynamics of the surface phase transitions. Using those speckle patterns we have been able to obtain quantitative measurements of dynamic temperature-dependent surface processes for these two systems.

We will also present some of our recent efforts to bridge the gulf between imaging and diffraction. We address the question of measuring correlation from speckle patterns and how that compares to correlations calculated from real-space images of the same systems, in particular for 2D systems in both reflection and transmission.

References:

[1] M.S. Pierce, K.C. Chang, D. Hennessy et al., Phys. Rev. Lett. **103**, 165501 (2009).
[2] M.S. Pierce, D. Hennessy, A. Barbour, K-C. Chang, V. Komanicky, J. Strzalka, A. Sandy, H. You, in preparation.

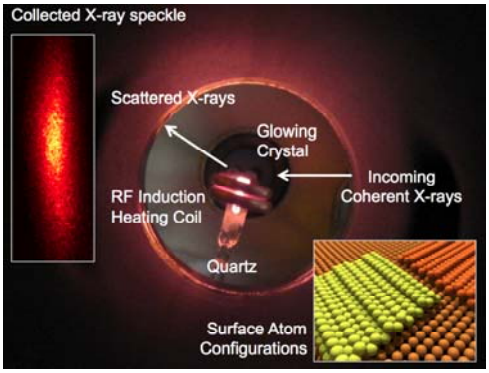

Figure 1: X-rays with a high degree of coherence scatter from the surface of a single crystal. The resulting scattering pattern is highly speckled and contains information about the reconstruction, surface morphology. Changes in the speckle can be used to determine properties of the dynamic evolution of the surface of interest.

Enhanced High-Speed Coherent Diffraction Imaging

J. Potier[1], S. Fricker[1], M. Idir[2]

[1]*PhaseView, 7 rue de la Croix Martre, 91120, Palaiseau, France*
[2]*Synchrotron SOLEIL, L'Orme des Merisiers, 91192, Saint-Aubin, France*

Abstract:

Due to recent advances in X-ray microscopy, we are now able to image objects with nanometer resolution thanks to synchrotron beamlines or free electron lasers (FEL). Phase contrast imaging (PCI) is a robust technique that can recover the wavefront from measurements of only two intensity pictures in the Fresnel field. With our fast straightforward calculus methods, we manage to provide the phase induced by a microscopic specimen in a few seconds. We can therefore obtain high contrast from transmittive materials at very small scales. To reach atomic-resolution imaging and thus make a transition from the near to the far field, the coherent diffraction imaging (CDI) technique finds its roots in the analysis of diffraction patterns to obtain the phase of the altered complex wave. Theoretical results about existence and uniqueness of this retrieved piece of information by both iterative and direct algorithms have already been released [1,2]. However, the performance of the algorithms remains limited by the coherence of the X-ray beam, the presence of random noise, and the saturation threshold of the detector.

We will therefore present reconstructions of samples using enhanced versions of the three different algorithms (HIO, RAAR, and Difference-Map) [2,3] improving the speed of convergence and its repeatability. Discussion will be provided about empirical strategies offering the best compromises between time processing and efficiency of the reconstruction.

The aim of this work is to overcome the diffraction imaging problem caused by the influence of the source's quality and the limitations of the detector in order to be compatible with a practical tabletop imaging system.

References:

[1] P. Thibault, Thesis at Cornell University (2007).
[2] H. H. Bauschke, P. L. Combettes, and D. R. Luke, J. Opt. Soc. Am. A **20**, 1025 (2003).
[3] J. R. Fienup, Appl. Optics **21**, 2758 (1982).

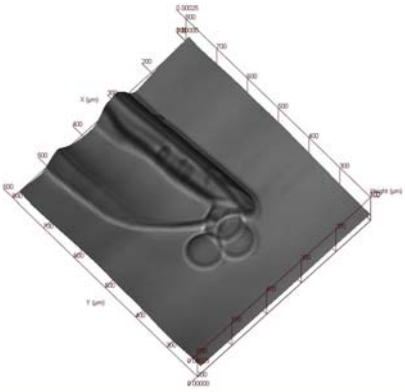

Figure 1: Reconstructed pipette with three carbon spheres (40 µm in diameter) with PCI technique.

Figure 2: Illustration of CDI using a buccal cell (50 µm in diameter).

Fresnel Coherent Diffraction Tomography

C. Putkunz[1,3], M. Pfeifer[1,3], B. Abbey[2,3], G. Williams[2,3], H. Quiney[2,3], K. Nugent[2,3], A. Peele[1,3]

[1]*Department of Physics, La Trobe University, Bundoora, Victoria 3086, Australia*
[2]*Department of Physics, University of Melbourne, Victoria 3052, Australia*
[3]*Centre of Excellence for Coherent X-ray Science, Victoria, 3010, Australia*

Abstract:
The ability to three-dimensionally image both crystalline and amorphous objects at near nanometer resolution is possible by either combining current techniques for two-dimensional Fresnel coherent diffractive imaging (FCDI) with traditional tomography, or by utilizing super computing clusters to perform image reconstruction on large three-dimensional data sets.

Two-dimensional CDI experiments have already shown the ability to resolve objects to a resolution of less than 20 nm. These experiments have been conducted at various synchrotron beamlines using coherent x-rays to illuminate samples and in-vacuum detectors to attain diffraction measurements. The introduction of phase curvature to the illuminating wave-fields (FCDI) has allowed for faster convergence and unique 2D image reconstructions using iterative algorithms.

Through measurements taken at optical wavelengths and with x-ray simulations, we demonstrate that it is possible to image with elemental sensitivity in three dimensions using techniques developed specifically for curved beam diffraction (FCDI). These algorithms take diffraction data recorded from a multitude of projections, and, using supercomputing clusters to overcome memory and processor constraints, recover information about the three-dimensional refractive index of compound (multi-element) samples. This work opens up a wide range of opportunities for use in x-ray imaging of micron-scale objects, with particular applications to buried and ``thick'' three-dimensional samples.

Algorithmic Reconstruction Methods in Diffraction Microscopy Using *a priori* Information

L. B. Rad[1], J. Miao[2], P. Pianetta[1], R. F. W. Pease[1]

[1]*Department of Electrical Engineering, Stanford University, Stanford, California 94305, USA*
[2]*Department of Physics and Astronomy and California NanoSystems Institute, University of California, Los Angeles, CA 90095, USA*

Abstract:
There exists a clear need for an inspection microscope that features sub-optical resolution and high penetration but requires no ambient vacuum for the sample. The most prominent application of such a microscope is the non-destructive examination of fabricated integrated circuits. Current semiconductor fabrication processes would require resolution of approximately 10 nm to a penetration depth of 100 µm. These requirements are expected to increase over time due to process shrinks. The coherent X-ray diffraction microscope is a recent development where highly coherent X-ray sources are used without focusing optics. Instead, the diffraction pattern of the beam is recorded and reconstruction of the sample image is achieved by recovering the phase information using computational algorithms.

Phase retrieval is a central problem in coherent X-ray diffraction microscopy. Various methods have been proposed to solve the problem with the most successful being iterative methods such as Fienup's Hybrid Input Output algorithm and the generalized Difference Map algorithm [1,2]. These algorithms are constraint satisfaction problems where a solution satisfying two sets of constraints is sought. In the context of diffraction microscopy these are diffraction measurements in the Fourier domain and typically some form of finite support in the spatial domain. In the proposed approach the design specification and other constraints such as positivity, known indices of refraction, and smoothness are imposed and are compared to conventional algorithms as shown in Figure 1. These constraints enable reconstruction of an extended object with improved resolution and faster convergence. This is the first time that a successful reconstruction of such an object from a single exposure has been demonstrated.

References:

[1] V. Elser, J. Opt. Soc. Am. **20**(1), 40 (2003).
[2] J.R. Fienup, Appl. Optics **21**, 2758 (1982).

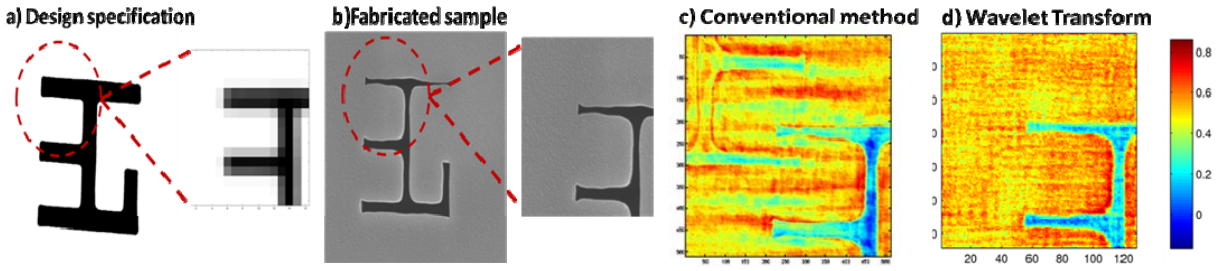

Figure 1: Iterative phase reconstruction where constraints are enforced in the Fourier domain and in the wavelet domain. (a) shows the original sample from which diffraction measurements are obtained and the low resolution approximation used for the wavelet constraint; (b) shows the fabricated sample; (c) shows a reconstruction using a basic finite support constraint (the support is not modified as the algorithm progresses, as such the phase ambiguity is not resolved); and (d) shows the reconstruction using constraints in wavelet space.

Digital In-line Holography on Amplitude and Phase Objects Prepared with Electron Beam Lithography

J. Schwenke[1,2], E. Lorek[1], R. Rakowski[1], X. He[1], A. Mikkelsen[1], I. Maximov[1], A. L'Huillier[1]

[1]*Department of Physics, Lund University, P.O. Box 118, 22100 Lund, Sweden*
[2]*MAX-Lab, Lund University, P.O. Box 118, 22100 Lund, Sweden*

Abstract:
At the Lund high-power laser facility, an intense XUV harmonic beam source is being developed for coherent imaging applications [1]. The high-order harmonic beam is generated by focusing femtosecond infrared pulses from a terawatt laser system into a cell filled with Argon gas. The generated XUV pulses are spectrally filtered and focused by a Schwarzschild objective to create a point source for digital in-line holography. Sample objects are imaged in transmission, and the holograms can be recorded by either a micro-channel plate (MCP) or a back-illuminated x-ray CCD camera. A numerical algorithm is applied to reconstruct the complex field in the object plane. Due to the high intensity of the source, a single pulse is sufficient for imaging in most applications.

The setup is characterized by investigating layers of gold and chromium of varying thicknesses and shapes as amplitude and phase objects. The sample structures are evaporated on extremely thin silicon nitride membranes, where the spatial distribution can be precisely controlled with electron beam lithography: The membrane is first covered with a polymer and then exposed to an electron beam in chosen regions. A developer solvent removes the polymer from the exposed parts and allows for the metal to stick to the membrane during evaporation. The remaining polymer is removed with acetone so that an effectively free-standing object remains.

This contribution will describe the experimental setup and results obtained with different types of targets. Its planned extension towards time-resolved measurements will also be presented.

References:

[1] J. Schwenke et al., J. Mod. Optic. **55**, 16, 2723 (2008).

Limited-View Ptychography of Isolated Objects

D. Shapiro

National Synchrotron Light Source-II, Brookhaven National Laboratory,
Upton, NY 11973-5000, USA

Abstract:
A new diffractive imaging scheme that combines standard full-view coherent x-ray diffraction microscopy (CXDM) with two-view x-ray ptychography is described. The addition of two ptychography views to CXDM provides for the ability to reconstruct complex-valued and soft-edged objects (the most difficult type of object) without precise knowledge of the object support function. This scheme, called limited-view ptychography, works only with isolated samples but significantly reduces the amount of data needed for imaging while still benefiting from the uniqueness of ptychographical reconstructions. The ability to reconstruct soft-edged, complex-valued objects without a precise support function and with limited illumination is a vital extension of diffraction microscopy that will find application in the study of biological cells and engineered organic nano-materials. The limited-view ptychography set-up and algorithm are described and a numerical simulation that proves the effectiveness of the algorithm is presented.

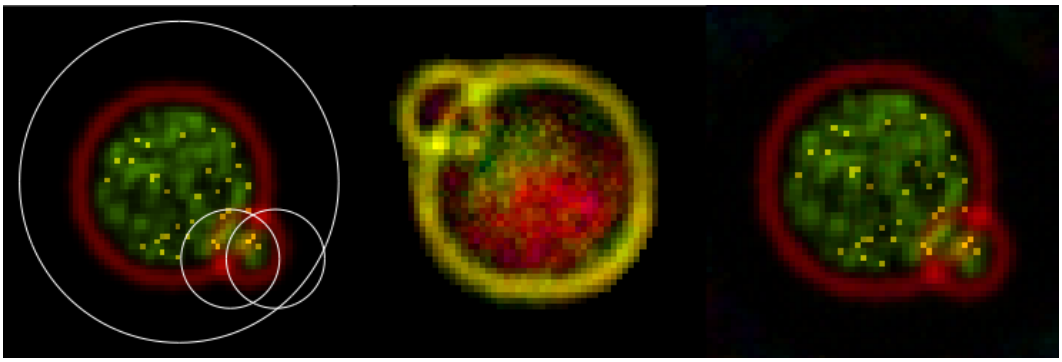

Figure 1: Left: Original object is complex valued (hue indicates phase and brightness indicates magnitude) and has soft edges (Gaussian filtered with a width of 3 pixels). The circles show the illumination pattern used to generate the diffraction data used for the reconstructions. Center: reconstruction using the standard HIO method and only the full diffraction pattern (large circle) with a loose support (the object enantiomorph is reconstructed). Right: Limited-view ptychography reconstruction using diffraction data from the full view and the two smaller ptychography views also using a loose support.

Optimization of the Coherent Intensity from Multi-segment Undulators by Phase Matching

D. Shapiro, O. Chubar, C. Sanchez-Hanke, R. Reininger

National Synchrotron Light Source-II, Brookhaven National Laboratory, Upton, NY 11973, USA

Abstract:

It has become common to place multiple insertion devices in a single storage-ring straight section so that they may be used either in a canted or inline geometry. The use of inline insertion devices at low emittance synchrotron sources results in interference between the emitted wavefronts, which can significantly alter the power distribution in the combined central radiation cone. The relative phase between the two wavefronts can actually reduce the on-axis brightness well below that of a single device and therefore reduce the performance of the beamline for brightness-limited experiments. We simulate the photon source generated by two inline APPLE-II type elliptically polarizing undulators (EPUs) in a low-β straight section of the planned NSLS-II storage ring. The relative phase between wavefronts emitted by the two devices is adjusted by an intermediate chicane section with variable field amplitude. Using the formalism of physical optics, we generate the monochromatic wavefront downstream of a focusing optic and investigate the phasing conditions that maximize the coherent flux intensity delivered to the sample area. We find that these differ from the phasing condition that maximizes on-axis emission from the compound undulator. Furthermore, by focusing the optical system to different longitudinal positions within the EPU pair we are able to localize the source position within the straight section. The values of wavelength and phase shift for which the EPU pair behave as a single long undulator are mapped, and the results are discussed within the context of the planned coherent soft x-ray beamline at the NSLS-II synchrotron source.

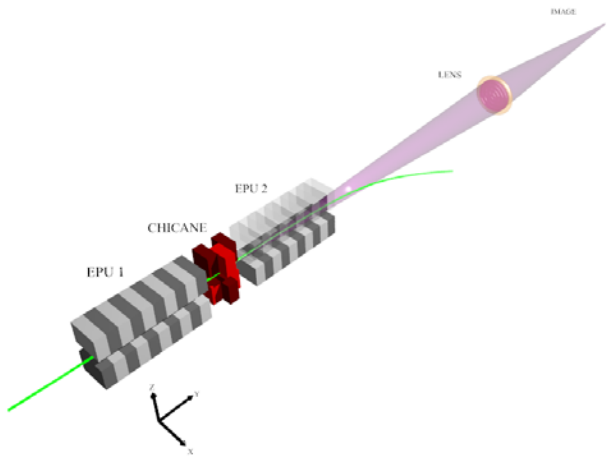

Figure 1: Layout showing the double EPU plus chicane. Brightness is measured downstream of the lens.

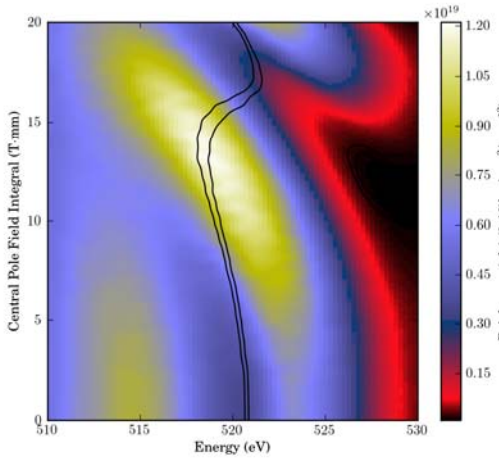

Figure 2: Brightness of the EPU pair depends strongly on energy and phasing condition (chicane field integral) for a given k-value. The bounded region indicates the values for a single 4-m-long device. The on-axis resonant energy is 520 eV.

X-ray Interferometers Based on Refractive Optics

A. Snigirev[1], I. Snigireva[1], V. Kohn[2], S. Kuznetsov[3], V. Yunkin[3]

[1]*European Synchrotron Radiation Facility (ESRF), 38043 Grenoble, France*
[2]*Russian Research Centre "Kurchatov Institute", Moscow, Russia*
[3]*Institute of Microelectronics Technology RAS, 142432 Chernogolovka, Russia*

Abstract:

Following successful development of refractive optics we propose a new type of interferometry for high energy X-rays. One such interferometer is similar to the model of the Billet split lens from classical optics [1]. It consists of two identical, parallel, planar compound refractive lenses separated transversally by a distance smaller than the spatial coherence length of the incoming beam. As a consequence each lens is illuminated coherently, and therefore it generates a coherent, diffraction-limited focal spot. At a certain distance the cones diverging from these secondary sources overlap, and interference occurs in the region of superposition. This interference pattern has a variable period ranging from tens of nanometers to tens of micrometers, depending on the distance. In order to extend the field of view the interferometer can be evolved into a multi-lens system where more than two parallel arrays can be used.

Such coherent spatially harmonic illumination can be used for new diffraction and imaging methods to study mesoscopic materials. A phase contrast imaging technique was performed where a sample is inserted into one of the beams, as in the case of a classical interferometer. Any interaction with that beam induces significant changes in the interference pattern, allowing the extraction of high resolution information on the sample from the new pattern produced. A second technique would be a moiré imaging whereby the sample is placed behind the bilens within the interference field. Standing wave techniques are evident: a sample could be scanned across the periodic interference field and secondary processes (fluorescence, secondary electrons, etc.) would be detected by a detector placed to side of the beam. In addition to imaging applications, the bilens interferometer could also be used for coherence diagnostics at existing synchrotrons and future free electron X-ray laser sources.

References:

[1] A. Snigirev et al, Phys. Rev. Lett. **103**, 064801 (2009).

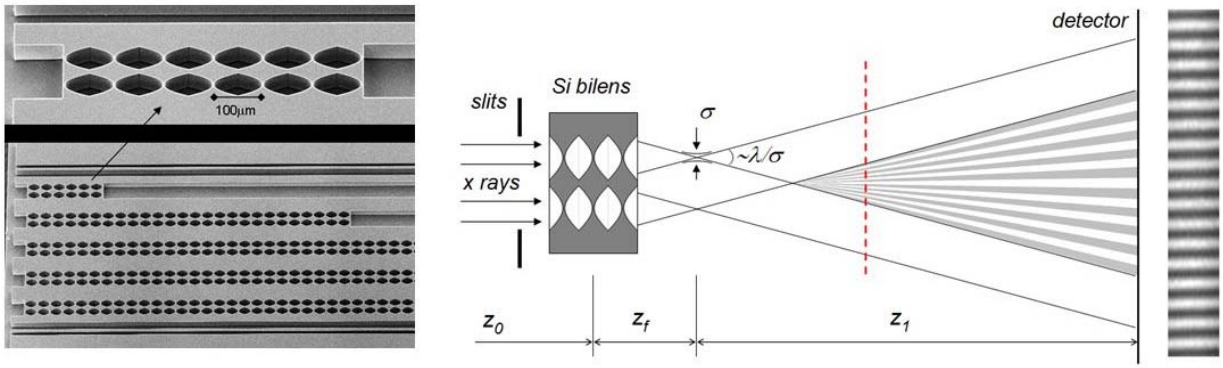

Figure 1: SEM image of the Si planar bilens chip and schematic view of the X-ray bilens interferometer.

High Resolution X-ray Microscopy on Mesoscopic Structures

I. Snigireva, A. Bosak, A. Snigirev

European Synchrotron Radiation Facility (ESRF), 38043 Grenoble, France

Abstract:

We developed a high-resolution transmission x-ray microscopy (HRTXM), combining full-field imaging with x-ray diffraction, which was applied for the volume-specific studies of periodic mesoscopic structures. This methodologically proposed approach is similar to the studies of "traditional" crystals by high-resolution transmission electron microscopy (HRTEM). HRTXM was realized by employing x-ray refractive optics. The immediate benefit of using compound parabolic refractive lenses is the possibility to retrieve the Fraunhofer diffraction pattern and real-space images in the same experimental setup.

The HRTXM was realized at the Micro-Optics Test Bench of ID06 BL with x-ray energy from 10 to 20 keV. It consists of two sets of condensers—used for sample illumination in imaging mode and as a Fourier transformer in diffraction mode—the objective lens and two (large area and high resolution) CCD detectors. The tunable objective lens provides magnification between 10 and 25. At maximum magnification the resolution of ~100 nm was achieved. The ~70 µm thick single domain grain of an Australian gem opal was used for the benchmark study. The obtained results demonstrate the abilities of the technique and shed some light on the opals genesis processes, i.e., the apparent reduction of symmetry of Australian opals to three-fold necessitates the action of shear forces on some stages of their formation [1].

The proposed approach provides the tools for the efficient studies of the real structure of mesoscopic materials. A number of TEM and HRTEM approaches can be directly transferred to the domain of x-rays. Among the immediate practical applications is the utility of real structure knowledge for photonic crystal growth technology.

References:

[1] A. Bosak, I. Snigireva, K. Napolskii, A. Snigirev, Adv. Mater. (2010); doi: 10.1002/adma.201000173.

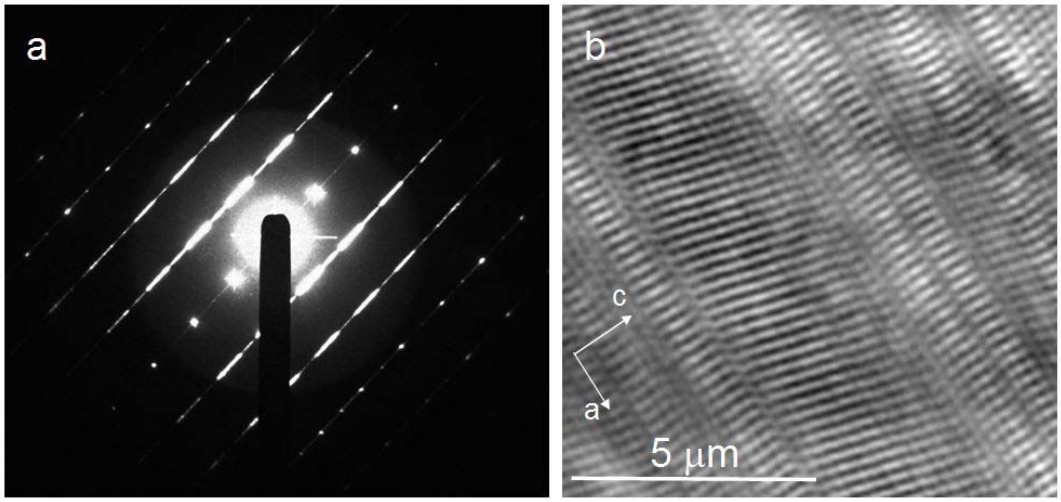

Figure 1: X-ray microscopy on natural opal (a) selected area diffraction pattern in (1-20) zone and (b) corresponding x-ray image.

Simulation of NanoXCT System Based on Zone Plate Object

X. Song, X. Zhang, G. Liu, X. Cheng, W. Li, Y. Guan, J. Chen, Y. Xiong, Y. Tian

National Synchrotron Radiation Laboratory, University of Science and Technology of China, Hefei, Anhui 230029, People's Republic of China

Email: ychtian@ustc.edu.cn

Abstract:

The Hefei nanoXCT layout is made up of a light source, monochromator, condenser, pinhole, sample, zone plate and CCD camera. NanoXCT is applied in many areas, such as biomedical, nanomaterials, and so on. The nanomaterials, with complex three-dimensional (3D) shapes and thick ordered structures, are a challenging area for imaging since the overlap of complex features in projections will complicate image analysis. Thus, high-resolution imaging techniques will be necessary for such investigations. To meet requests, the nanoCT system based on zone plates was developed. It is important to place components accurately and reasonably to optimize imaging. In fact, the optical instruments are so tiny that it is difficult to adjust them to the best position. Therefore we raised a new method for improving the quality of an image by using a simulation of the device to guide experiment operations. In this paper, we utilize ray-tracing formulas to simulate the propagation of light through the condenser and simulate zone plates with the Rayleigh-Sommerfeld diffraction theory. This algorithm, after computers' running, can draw different spot images when the condenser and zone plates are at any location. The comparison of simulation results and experimental results helps to instruct experimental specific operations. A simulation algorithm is used to calculate the best position and angle for each imaging device. When each imaging device position and angle is consistent with the calculation, we can get the best image quality. Some factors which affect the imaging quality, such as location change of components and spherical aberration, will also be discussed.

Hard X-ray Fourier Transform Holography Using a Reference Scatter Fabricated by Electron-Beam-Assisted Chemical-Vapor Deposition*

M. Suzuki[1], Y. Kondo[2], S. Isogami[3], M. Tsunoda[3], S. Takahashi[4], S. Ishio[4]

[1]*Japan Synchrotron Radiation Research Institute/Spring-8, Sayo, Hyogo 671-5198, Japan*
[2]*Akita Research and Development Center, Akita 010-1623, Japan*
[3]*Department of Electronic Engineering, Tohoku University, Sendai 980-8579, Japan*
[4]*Faculty of Engineering and Resource Science, Akita University, Akita 010-8502, Japan*

* This work was supported by Grant-in-Aid for Scientific Research (C) (20612023) and The Murata Science Foundation (A81130).

Abstract:

We present a fabrication method of a reference source efficient for lensless Fourier transform holography (FTH) [1]. This method gives a high spatial resolution and better statistics in a Fourier-transformed real-space image and is particularly useful for FTH experiments in the hard X-ray region [2].

The lateral size of a reference object determines the practical spatial resolution in an FTH measurement. A reference "pinhole" is often used for FTH in the soft X-ray region. Currently the spatial resolution is limited to a few tens of nanometers. Further reduction of the resolution requires fabrication of a reference pinhole with an extremely high aspect ratio (e.g., 10 nm in diameter and a few 100 nm in depth). For hard X-ray FTH, it is hopeless to prepare a 10-nm pinhole on a few-μm-thick film of heavy material that may be opaque for hard X-rays.

In this paper, we propose the use of a phase scatterer object as a reference source for hard X-ray FTH. We used a tungsten pillar with a high aspect ratio, fabricated by electron-beam-assisted chemical-vapor deposition (EB-CVD) [3]. The sample observed was a 5 x 5 array of 100 x 100 nm dots made of $[Co(0.4\ nm)/Pt(0.7\ nm)]_{40}$ multilayer on a SiN membrane. In a separate post-process, a reference W pillar of ϕ40 nm in diameter and 380 nm in height was fabricated at a distance 2.5 μm from the center of the sample dot array. This design of a small and tall reference object gave sufficient scattering amplitude and a clear hologram pattern, maintaining a high spatial resolution. A Fourier-transformed image with a resolution of 30 nm is shown to demonstrate the validity of our method. The spatial resolution and statistics of the image are compared with that obtained for a similar dot sample with a Co/Pt reference dot made by electron-beam lithography and Ar ion milling [4].

This method will extend the range of available samples for FTH experiments. A reference pillar by EB-CVD may be placed adjacent to several kinds of samples prepared by different preceding processes. Metal nanoparticles, magnetic dots, biomaterials, or inorganic samples may be applicable. The improved statistics would allow magnetic imaging by hard X-ray FTH, which has not yet been obtained using hard X-rays. Additionally, the method is useful for a single fs-pulse FTH imaging using an X-ray free electron laser.

References:

[1] S. Eisebitt, J. Lüning, W. F. Schlotter et al., Nature **432**, 885 (2004).
[2] L.-M. Stadler, C. Gutt, T. Autenrieth et al., Phys. Rev. Lett. **100**, 245503 (2008).
[3] S. Isogami, M. Tsunoda, M. Takahashi, IEEE Trans. Magn. **41**, 3607 (2005).
[4] Y. Kondo, T. Chiba, J. Ariake et al., J. Mag. Mag. Mat. **320**, 3157 (2008).

New Nanoscale Imaging with a Simple Hard X-ray "Nano-Slit"

H. Takano, Y. Nakayama, T. Hashimoto, T. Tsuji, T. Koyama, Y. Tsusaka, Y. Kagoshima

Graduate School of Material Science, Univ. of Hyogo, 3-2-1, Kouto, Hyogo 678-1297, Japan

Abstract:

A knife-edge scanning method has been widely applied to evaluation of focusing optics. A heavy metal wire is available as the knife-edge object in hard x-ray region because of the easiness of the handling. In the case of the knife-edge scan with transmission geometry, the edge response degrades by effect of transmission when the diameter of the wire is small. However, high-spatial response can be obtained with dark-field geometry [1,2]. This effect can be represented by contribution of total reflection as shown in Fig. 1. When parallel x-rays are incident to a wire with the radius *r*, total reflection occurs at a fraction of the wire surface satisfying total reflection condition with the critical angle of θ_c. Then an effective aperture size *d* to incident beam can be defined as $r\theta_c^2 / 2$, so that the wire object work as an equivalent single slit with a tiny aperture size. This simple device has been applied to point-like source generation with nano-meter scale [3]. The "nano-slit" can measure intensity distribution of not only focusing spot but coherent wave-front.

The spatial response of the "nano-slit" was experimentally investigated at BL24XU of SPring-8. As the "nano-slit", a platinum wire of *r* = 150 μm is set at 1.3 mm after a crossed-slit with the size of 5 μm (H) and 10 μm (V) being illuminated with coherent x-rays of 10 keV. The intensity distribution of Fresnel fringes generated by the crossed-slit can be measured by scanning the wire in vertical direction and detecting the only reflected x-rays. The measurement result is shown in Fig 2. Fresnel fringes with the finest pitch of about 30 nm were successfully resolved.

When the wire is scanned in every longitudinally direction across an optimal wave-front, the two-dimensional wave-front distribution can be reconstructed by using tomography reconstruction. In the presentation, the first results of high-resolution imaging with the nano-slit experiment will be presented.

References:

[1] Y. Suzuki, A. Takeuchi, H. Takano et al., Jpn. J. Appl. Phys. **44,** 1994 (2005).
[2] T. Koyama, S. Ichimaru, T. Tsuji et al., Appl. Phys. Express **1**, 117003 (2008).
[3] S. Aoki, N. Watanabe, T. Ohigashi et al., Jpn. J. Appl. Phys. **44**, 417 (2005).

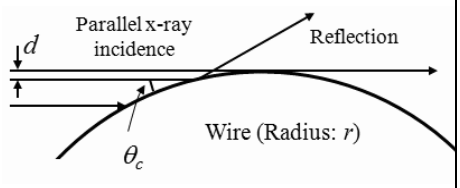

Figure 1: Schematic diagram of "nano-slit" effect of a wire object in hard x-ray region.

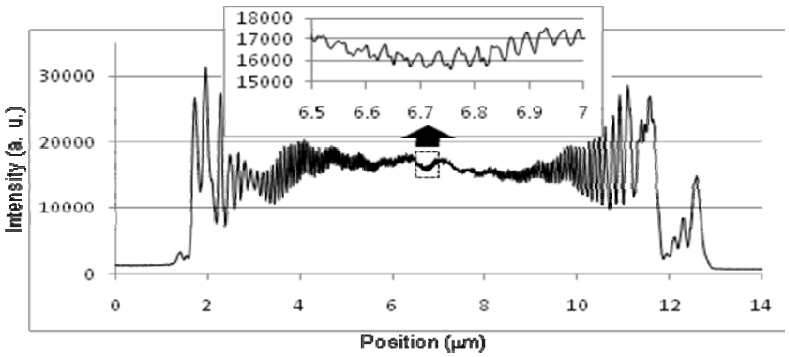

Figure 2: Intensity distribution of Fresnel fringes generated by a crossed slit (aperture: 10 μm in vertically) measured by the "nano-slit."

Efficiency Improvement of Imaging X-ray Microscope by Using a Double-Condenser Illuminating System

A. Takeuchi, Y. Suzuki, K. Uesugi

Japan Synchrotron Radiation Research Institute (JASRI), SPring-8, Hyogo, Japan

Abstract:

X-ray imaging microscope optics is now in widespread use for the nanometer order three-dimensional observation by combining tomographic imaging technique. Such an x-ray tomography system with close to 100 nm spatial resolution has been developed at beamline 47XU of SPring-8 (Figure 1) and is now routinely used for various fields. The x-ray energy range used is 6-12 keV. The system consists of two x-ray diffractive devices fabricated by the e-beam lithography technique; one is a Fresnel zone plate (FZP) as an objective, and the other is a condenser zone plate (CZP). The CZP has a constant grating pitch pattern for a quasi-Köhler type (hollow cone) illumination. This illuminating system gives a wide and flat field of view and makes it easy to introduce a Zernike phase-contrast imaging mode [1]. However, low efficiency of these devices is a serious problem especially for high spatial resolution. Since there is a technical restriction to the aspect ratio of the zone stricture, the relationship between spatial resolution (zone pitch) and the efficiency (zone thickness) is a trade-off at the hard x-ray region. One of the solutions is stacking plural devices. Snigireva et al. have succeeded in raising the efficiency by stacking two FZPs [2]. They are kept aligned with high accuracy and must be almost in contact due to their narrow depth of focus (100 μm order). In this presentation, instead of FZPs, we propose installing two CZPs. Because the hollow cone beam produced with the CZP has a very large depth of the circle of least confusion (100 mm order), alignment of two CZPs may be much easier. The longitudinal distance between two CZPs, however, must be carefully set. Since the used CZP is a kind of periodic phase grating, the phase modulation is changed periodically along the longitudinal distance from the CZP, based on the Talbot effect. Therefore, according to this phenomenon, total efficiency of a couple of CZPs will show periodic changes along the distance d between these two with a period of $2d^2/\lambda$, where λ is the x-ray wavelength.

A preliminary experiment on the double CZP has been performed at 20XU. Parameters of a couple of CZPs are as follows; diameter is 0.5 mm, grating pattern pitch is 400 nm, material is 1.65-μm-thick tantalum, and efficiency of the 1st diffraction at 9.85 keV x-ray is 0.19. The total efficiency of the 1st diffraction of the double-CZP system has been measured by changing the distance between the two CZPs. Figure 2 shows the experimental result and the theoretical calculation at 9.85 keV x-rays. Maximum values of more than 0.3 are obtained at the periodic distance of ~2.5 mm, which is in good agreement with the theoretical value of $2d^2/\lambda$ = 2.54 mm.

References:

[1] A. Takeuchi, K. Uesugi, Y. Suzuki, J. Phys.: Conf. Ser. **186**, 012020 (2009).

[2] I. Snigireva et al., AIP Conf. Proc. **879**, 998 (2007).

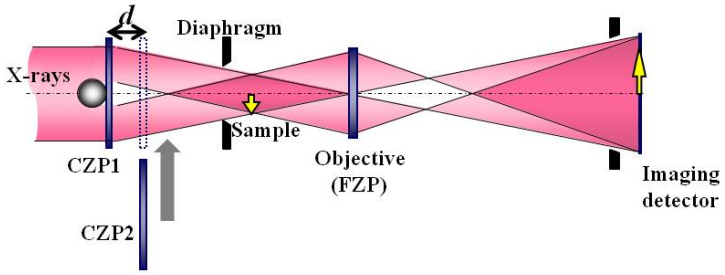

Figure 1: Schematic diagram of optical system.

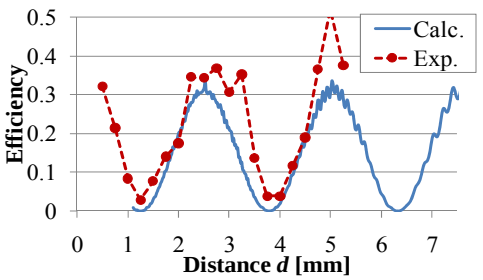

Figure 2: Efficiency of double-CZP system.

Effects of Missing Data and Limited Signal to Noise on Scanning Coherent X-ray Diffraction Microscopy

A. Tripathi[1,2], O. Shpyrko[1], I. McNulty[2]

[1]*University of California San Diego, 9500 Gilman Dr, La Jolla, USA*
[2]*Argonne National Laboratory, 9700 S. Cass Avenue, Argonne, USA*

* Use of the Advanced Photon Source is supported by the U.S. Department of Energy, Office of Science, Office of Basic Energy Sciences, under contract No. DE-AC02-06CH11357.

Abstract:

Learning to control emergent magnetic properties such as colossal magnetoresistance and phase separation is crucial for developing future spin-based data storage and computational technologies. Probes with the ability to map magnetically interacting materials beneath surfaces on the nanometer scale, ultimately on ultrafast time scales, would greatly enhance our understanding of these systems. scanning coherent x-ray diffraction microscopy (SXDM) is a promising new technique [1,2] for imaging magnetic nanostructure with potentially wavelength-limited resolution that can probe beneath surfaces. The essence of this technique is that, rather than using optics to image the nanostructure, we record a series of coherent diffraction patterns as the sample is scanned, then algorithmically invert them using known constraints on the sample (real space) and on the diffraction measurements (reciprocal space) to arrive at the sample structure.

Although preliminary experimental results using this technique are extremely promising [3], there are several unresolved questions regarding the effects of non-ideal diffraction quality on the reconstruction fidelity. Foremost of these are missing data regions in the recorded diffraction patterns, regions with poor signal to noise, and various experimental uncertainties that are in turn uncertainties on real space constraints upon which the algorithm depends. The questions we explore here are quantitative effects of degraded diffraction information on algorithm performance, additional constraints in real and reciprocal space to use in the algorithm and improve performance, and new algorithms that handle the constraints more intelligently and perform better with the same degraded diffraction information than existing SXDM algorithms.

References:

[1] J.M. Rodenburg et al., Phys. Rev. Lett. **98**, 034801 (2007).
[2] P. Thibault et al., Science **321** (5778), 379 (2008).
[3] O. Shpyrko et al., these proceedings.

High Spatial Resolution X-ray Phase Imaging with a Talbot Interferometer

K. Uesugi, A. Takeuchi, M. Hoshino, Y. Suzuki

JASRI / SPring-8, 1-1-1 Kouto, Sayo, Hyogo 679-5198, Japan

Abstract:

A high spatial resolution X-ray phase imaging system has been developed at SPring-8, which has used a full-field X-ray microscope with a Fresnel zone plate (FZP) as an objective and a condenser zone plate (CZP) for a pseudo-Kohler illuminating system [1-3]. The spatial resolution is around 200 nm in absorption contrast imaging with the field of view of 100 µm. The system is usually used between 6 keV and 12 keV of X-ray energy at BL47XU. The absorption contrast of small samples is often quite weak in the energy region. Therefore, a phase contrast imaging system with a grating interferometer (Talbot-type interferometer) has been developed to obtain better contrast (Figure 1).

The gratings were made by electron beam lithography at NTT-ATN. The grating pitch is 5 µm and the materials of the gratings are 0.96-µm-thick tantalum and 5-µm-thick tantalum, respectively. The former is a phase grating designed for 8 keV and the latter is an absorption grating inclined to increase the effective optical path length.

Visibility of the career fringe was measured for evaluation of the phase imaging system. The illuminating beam condition (variation of angular spread) to the sample was varied by changing the aperture size in front of CZP. The variation of the angle was 0 mrad, ±0.10 mrad, and ±0.19 mrad. Only the center of CZP was used in 0 mrad condition; ±0.19 mrad corresponds to full aperture of the CZP. The measured visibilities were 70.8%, 65.5%, and 60.2% for 0 mrad, ±0.10 mrad, and ±0.19 mrad conditions, respectively.

The measured visibility curves are shown in Figure 2. The figure shows that the beam illumination with small angular spread makes a triangle wave that contains a significant amount of harmonics, while the angled illuminations make sine waves. The procedure of quantitative phase retrieval requires a fringe scan with many steps. However the number of steps can be reduced when the career fringe has a sine wave. In addition the pseudo-Kohler illuminating system can adjust the magnitude of harmonics in the career fringe. Therefore the system is suitable for x-ray phase imaging with a grating interferometer.

References:

[1] A. Takeuchi, K. Uesugi, H. Takano et al., Rev. Sci. Instrum. **73**, 4246 (2002).
[2] K. Uesugi et al., Proc. of SPIE **6318**, 63181F (2006).
[3] A. Takeuchi et al., J. Phys.: Conf. Ser. **186**, 012020 (2009).

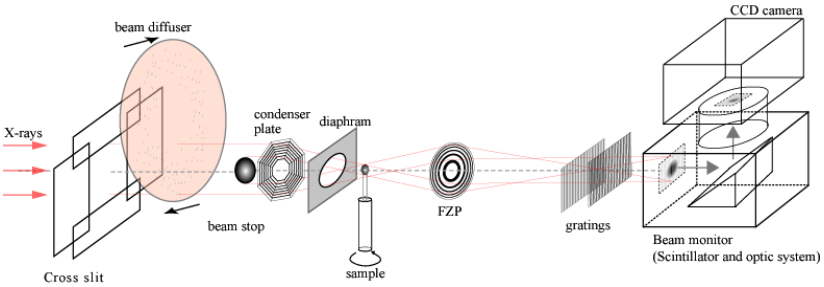

Figure 1: Schematic illustration of phase imaging system with grating interferometer at BL47XU.

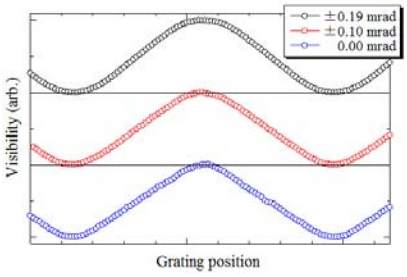

Figure 2: Visibility curve in different conditions.

Image Quality Limitations Due to Stray Light in High-NA X-ray Microscopy

O. von Hofsten, M. Bertilson, J. Reinspach, M. Lindblom, A. Holmberg, H. M. Hertz, U. Vogt

Biomedical & X-ray Physics, Department of Applied Physics, Royal Institute of Technology, Albanova, SE-10691 Stockholm, Sweden

Abstract:

The image quality in transmission x-ray microscopy has until now been primarily determined by the zone plate outermost zone width. As zone plate fabrication is now approaching 10 nm [1-3], other factors will grow in importance and may effectively limit the image quality, i.e., resolution and contrast. Off-axis aberrations and stray light were easily mitigated for low-numerical aperture optics but are substantial problems for high-NA 10-nm optics. In addition, low zone plate height impairs the efficiency of the optics and subsequently leads to extended exposure times. In the present paper we consider the influence of source-dependent stray light in transmission soft x-ray microscopes when using zone plates with high numerical aperture.

For monochromaticity and fabrication reasons, all high-resolution zone plates have short focal lengths compared to conventional zone plate optics. In soft x-ray microscopy, this leads to source-size-dependent stray light, which may greatly reduce image contrast and thus the achievable resolution. This background originates mainly from the -1st diffraction order and is best eliminated using an aperture in the object plane but can also be reduced by modifying the illumination conditions. Here we present detailed ray-trace simulations of image quality as a function of stray light for different experimental arrangements. In particular, we investigate the case of a compound zone plate used in a high-resolution laboratory x-ray microscope and show that high-angle illumination successfully reduces stray light to allow 25-nm resolution imaging. The simulations are confirmed by experiments.

References:

[1] W. Chao, B.H. Harteneck, J.A. Liddle et al., Nature **435**, 1210 (2005).
[2] J. Vila-Comamala, K. Jefimovs, J. Raabe et al., Ultramicroscopy **109**, 11 (2009).
[3] J. Reinspach, M. Lindblom, O.von Hofsten et al., Microelectron. Eng. **87**, 1583 (2010).
[4] O. von Hofsten, M. Bertilson, J. Reinspach et al., Opt. Lett. **34**, 17 (2009).

Efficiency of the Novel Phase Extraction Algorithm in Grating-Based X-ray Phase-Contrast Imaging

Z. Wang[1], P. Zhu[1], K. Zhang[1], X. Liu[1], Y. Hong[1], Q. Yuan[1], W. Huang[1], Z. Zhu[1], Z. Wu[2]

[1] Beijing Synchrotron Radiation Facility, Institute of High Energy Physics, Chinese Academy of Sciences, Beijing 100049
[2]National Synchrotron Radiation Laboratory, University of Science and Technology of China, Hefei 230026, China

Abstract:
We discuss here the concept of the shifting curve in the grating-based phase contrast imaging [1]. It describes the recorded intensity as a function of the transverse shift between the two gratings. A novel phase extraction algorithm, named "Reverse-Projection" (RP) technique, is also proposed, based on the linear approximation of the shifting curve. The RP technique has been validated by experimental results, in agreement with those obtained by the phase-stepping (PS) technique [2]. In this contribution, we assess the efficiency of the RP technique, in terms of the minimum detectable refraction angle with a sufficient signal-to-noise ratio as a function of the available photon flux. Indeed, the photon statistics affects the detected intensities and impose a limit to the refraction angle. We determine the relation between the incident photon number and the detection limit, and define a figure of merit for a monochromatic spherical wave illumination. The dependence of the figure of merit on the optical system parameters is also discussed. Numerical simulations provided also a quantitative insight of the efficiency of the RP technique.

References:

[1] Z. Wang, X. Liu, P. Zhu, K. Zhang, W. Huang, Q. Yuan, Y. Hong, X. Ge, Z. Wu, to be submitted to Optics Express.
[2] P. Zhu, K. Zhang, Z. Wang, Y. Liu, X. Liu, Z. Wu, S. A. McDonald, F. Marone, M. Stampanoni, to be submitted to PNAS.

Observation of Phase Objects by Using an X-ray Microscope with a Foucault Knife-edge

N. Watanabe, T. Sasaya, Y. Imai, S. Iwata, K. Zama, S. Aoki

Institute of Applied Physics, University of Tsukuba, Tsukuba, Ibaraki, 305-8573, Japan

Abstract:

The schlieren method using the Foucault knife-edge is a standard tool in visible light optics. This method is easily applicable for microscope optics of parallel beam illumination. When the edge covers half of the back focal plane of the objective lens, a phase-contrast image of a sample can be observed. We have been developing an x-ray phase-contrast microscope as shown in Figure 1 [1]. In this experiment, the Zernike $\pi/2$ phase plate was replaced with the Foucault knife-edge.

The synchrotron radiation from the Photon Factory BL3C was used. An objective zone plate has the outermost zone width of 50 nm and the diameter of 330 μm. Monochromatic parallel x-rays of 5.4 keV were incident onto a specimen and enlarged by the zone plate at a magnification ratio of about 50. A gold wire 250 μm in diameter was placed at the back focal plane of the zone plate.

Figure 2 shows x-ray images of balsa wood. Figure 2(a) and (b) show schlieren images when the gold wire was placed at the upper half and lower half of the back focal plane, respectively. Figure 3(c) shows the differential phase image calculated from (Fig.2(a) – Fig.2(b))/ (Fig.2(a) + Fig.2(b)) [2]. Figure 2(d) shows the bright field image without the knife-edge. The almost transparent specimen could be observed with good contrast. The application to tomography will be presented.

References:

[1] S. Aoki, M. Hoshino, N. Watanabe, J. X-ray Science and Technology **15**, 65 (2007).
[2] K. Nagayama, J. Phys. Soc. Jpn. **73**, 2725 (2004).

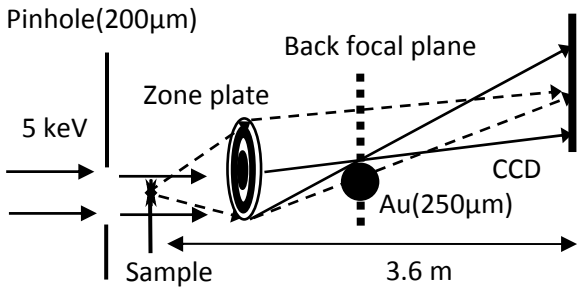

Figure 1: Optical system.

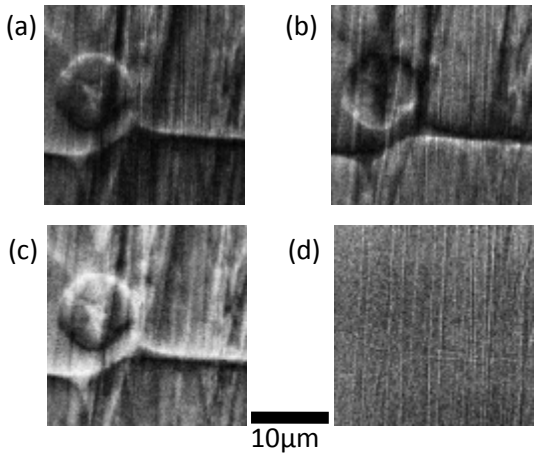

Figure 2: X-ray images of balsa wood: (a) the upper half knife-edge, (b) the lower half knife-edge, (c) the calculated differential phase image, (d) the bright field image.

Cryo-Tomography with a Common-Path Interference Microscope

N. Watanabe[1], T. Sasaya[1], S. Iwata[1], Y. Imai[1], S. Aoki[1], A. Takeuchi[2], Y. Suzuki[2]

[1]*Institute of Applied Physics, University of Tsukuba, Tsukuba, Ibaraki 305-8573, Japan*
[2]*SPring-8, JASRI, Mikazuki, Hyogo 679-5198, Japan*

Abstract:
A hard x-ray interference microscope can determine the absolute value of the phase change by a sample. Therefore, it is the optimal system for the phase micro-tomography of a biological sample, which is almost transparent for hard x-rays. We have been developing an x-ray common-path interference microscope with zone plates at the SPring-8 undulator beam line BL20XU [1]. In the application to tomography of a hydrated biological sample, it is advantageous to freeze a sample, because the position stability is increased and the radiation damage is decreased. We present the application to tomography of frozen biological samples, such as bovine cartilage at 8 keV.

The optical system is shown in Figure 1. The diameter and the outermost zone width were 330 μm and 50 nm, respectively. Two zone plates were placed twice the focal length apart from each other. The first-order x-rays of ZP1 were focused on a CCD camera. The minus first-order x-rays of ZP2 of the reference beam were overlapped with the image of a specimen. Then, the interference image was observed without any interference fringes. The phase of the reference beam could be changed by the phase shifter in front of ZP1. The phase images were obtained by a 4-step fringe-scanning method. A sample was frozen and cooled down to about 150 K by cryogenic nitrogen gas (Cryojet, Oxford).

Figure 2 shows a section image of frozen-hydrated bovine cartilage. It seems that the sample had been damaged by crystallization of ice because of the low freezing speed. However, the section image could be reconstructed with sub-micron resolution.

References:

[1] N. Watanabe, M. Hoshino, K. Yamamoto et al., J. Phys.: Conf. Ser. **186**, 012021 (2009).

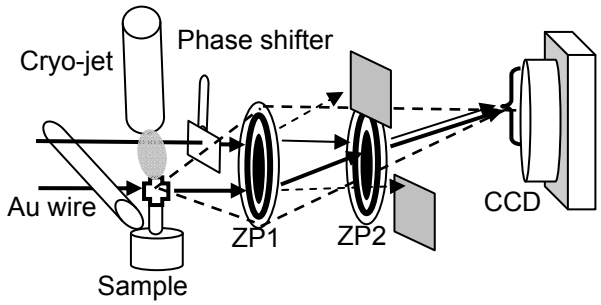

Figure 1: X-ray interference microscope.

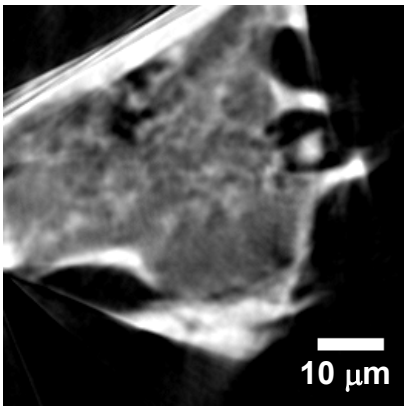

Figure 2: Section image of frozen-hydrated bovine cartilage.

X-ray Phase Imaging Using a Fresnel Zone Plate and a Phase Grating

W. Yashiro[1], H. Kuwabara[1], H. Mizutani[2], A. Takeuchi[3], Y. Suzuki[3], A. Momose[1]

[1]*Department of Advanced Materials Science, Graduate School of Frontier Sciences, University of Tokyo, 5-1-5 Kashiwanoha, Kashiwa, Chiba 277-8561, Japan*
[2]*Science Integration Program, Organization for Interdisciplinary Research Projects, University of Tokyo, 5-1-5 Kashiwanoha, Kashiwa, Chiba 277-8568, Japan*
[3]*Japan Synchrotron Radiation Research Institute (JASRI), 1-1-1 Kouto, Sayo-cho, Sayo-gun, Hyogo 679-5198, Japan*

This study was financially supported by Grants-in-Aid for Science Research (B) (19360027) from the Ministry of Education, Culture, Sports, Science, and Technology, and partly supported by Japan Science and Technology Agency (JST).

Abstract:

Non-destructive and quantitative nanometer-scale visualization of internal structures of materials consisting of light elements will bring dramatic progress in life and material sciences. We have proposed a hard X-ray phase imaging microscopy that consists of an objective and a transmission grating [1]. The simple optical system provides a quantitative phase image, and does not need a wave field mostly coherent on the objective, which is essential for most X-ray phase imaging microscopes proposed previously. The sensitivity and spatial resolution of our microscope were compared with those of the absorption contrast microscope that was attained by simply removing the grating; we showed that our method has a spatial resolution almost the same as that of the absorption contrast microscope, and a sensitivity of about two orders of magnitude higher than it for light elements. X-ray phase tomography was also performed by our microscopy. Our approach is attractive for easily appending a quantitative phase-sensitive mode to normal X-ray microscopes.

In this paper we show a result of the phase imaging microscopy, where a π/2-phase grating with a 0.7-μm pitch was used. Figure 1 shows the experimental setup of the X-ray phase imaging microscopy. Figure 2 shows a phase image of a 0.5-μm-thick Ta resolution test chart obtained by the microscopy. The experiment was carried out at BL20XU in SPring-8, Japan. Here the X-ray energy and magnification were set to be 9 keV and 24.9, respectively.

References:

[1] W. Yashiro, Y. Takeda, A. Takeuchi et al., Phys. Rev. Lett. **103**, 180801 (2009).

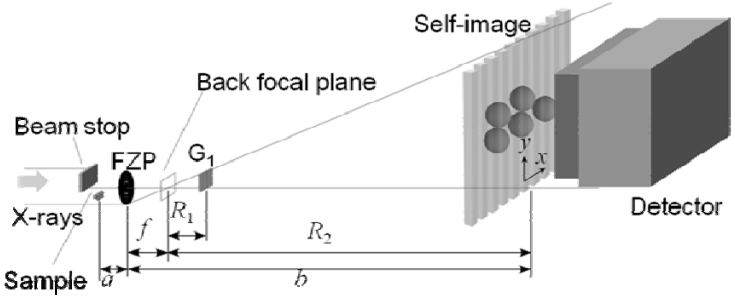

Figure 1: Experimental setup of our X-ray phase imaging microscopy with a phase grating.

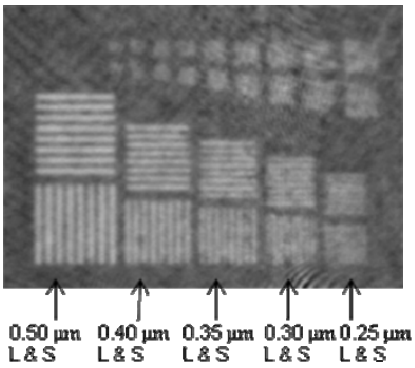

Figure 2: A phase image of a 0.5-μm-thick Ta resolution test chart.

Analysis of Microstructure Using Visibility Contrast in the X-ray Talbot Interferometry

W. Yashiro[1], Y. Terui[2], K. Kawabata[1], A. Momose[1]

[1]*Department of Advanced Materials Science, Graduate School of Frontier Sciences, University of Tokyo, 5-1-5 Kashiwanoha, Kashiwa, Chiba 277-8561, Japan*
[2]*Department of Applied Physics, School of Engineering, University of Tokyo, 7-3-1 Hongo, Bunkyo-ku, Tokyo 113-8656, Japan*

Abstract:
Recently X-ray phase imaging using transmission gratings (X-ray Talbot and Talbot-Lau interferometry) attracts increasing attention because it works with polychromatic and cone beam from a compact laboratory source [1]. In the X-ray Talbot(-Lau) interferometry, we can retrieve two quantitative images, i.e., absorption and differential-phase images, from a series of experimentally obtained moiré images. Recently F. Pfeiffer *et al*. has proposed another approach to form image contrast, where a relative decrease in the visibility of the moiré image is quantified by defining a normalized visibility [2]. They reported that the visibility contrast is formed through the mechanism of small angle X-ray scattering from microstructures with a scale much smaller than the spatial resolution of the imaging system. But so far no general formulation of the phenomenon, which is essential for quantitative structure analysis, has been provided.

In this paper we show that the visibility contrast can be generally formulated by an autocorrelation function describing spatial fluctuation of the wavefront due to the microstructure. Experimentally obtained visibility contrasts due to microspheres and melamine sponge were successfully explained by the formula. The autocorrelation function is characterized by the Hurst exponent and the correlation length; the Hurst exponent is relevant to the shape of the microstructure, while the correlation length is interpreted to the averaged size of it. Experimental results supported this interpretation.

The experiment was performed at Photon Factory (PF). This study was financially supported by Japan Science and Technology Agency (JST).

References:

[1] For example, A. Momose, W. Yashiro, and Y. Takeda, *Biomedical Mathematics: Promising Directions in Imaging, Therapy Planning and Inverse Problems*, Y. Censor, M. Jiang, and G. Wang, Eds., (Medical Physics Publishing, 2008, Madison, Wisconsin, USA).
[2] F. Pfeiffer et al., Nat. Mat. **7**, 134 (2008).

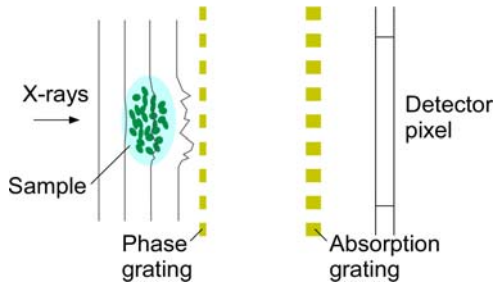

Figure 1: Experimental setup of the X-ray Talbot interferometer.

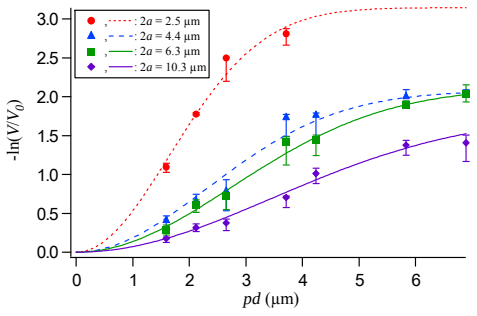

Figure 2: Dependence of the normalized visibility on the product of the Talbot order *p* and the pitch of grating *d*.

X-ray Imaging with a Grating Interferometer at ESRF-ID19

I. Zanette[1], C. David[2], T. Donath[2], S. Rutishauser[2], F. Pfeiffer[3], M. Bech[3], A. Tapfer[3], B. Müller[4], G. Schulz[4], S. Lang[4], H. Deyhle[4], J. Kenntner[5], E. Reznikova[5], J. Mohr[5], P. Tafforeau[1], T. Weitkamp[1]

[1]*European Synchrotron Radiation Facility, 38043 Grenoble, France*
[2]*LMN, Paul Scherrer Institut, 5232 Villigen PSI, Switzerland*
[3]*Physik-Department, Technische Universität München, 85748 Garching, Germany*
[4]*Biomaterials Science Center, University of Basel, 4031 Basel, Switzerland*
[5]*IMT, Karlsruhe Institute of Technology, 76344 Eggenstein-Leopoldshafen, Germany*

Abstract:
X-ray grating interferometry, also known as Talbot interferometry, is a recently developed imaging technique which gives access to various image modalities, among them differential phase contrast and scattering contrast ("dark-field imaging") [1,2].

The method performs best when used to obtain high-sensitivity phase images and directional scattering images [3] over a large field of view and with correspondingly moderate spatial resolution (down to a few µm); its potentials may be beneficial for different application areas, such as the life sciences, paleontology and materials science.

An X-ray grating interferometer has recently been installed at beamline ID19 of the European Synchrotron Radiation Facility (ESRF) where it is under constant improvement. The unique possibilities of the beamline offer an ideal environment for applications, tests of ultimate performance limits and implementation of new methodological concepts.

The presentation will address the latest developments in the instrumentation and new application results. These include the development of a two dimensional grating interferometer [4] and measurements at high photon energies above 80 keV (see Figure 1).

References:

[1] A. Momose et al., Jpn. J. Appl. Phys. **42**, L866 (2003).
[2] T. Weitkamp et al., Optics Express **13**, 6296 (2005).
[3] F. Pfeiffer et al., Nature Materials **7**, 134 (2008).
[4] I. Zanette et al., ICXOM20 proceedings, (2009) and manuscript in preparation.

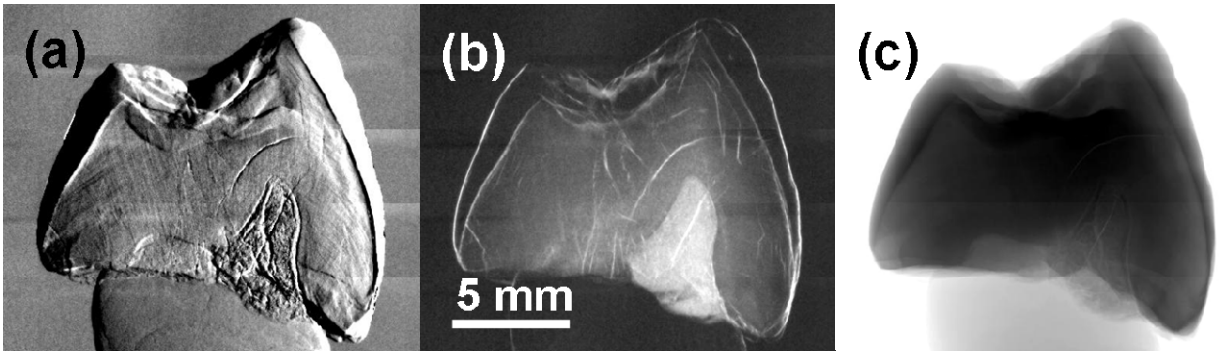

Figure 1: High energy (82 keV) grating interferometric radiographs of a fossilized orangutan tooth. Panels (a) to (c) show, respectively, the differential phase image, the dark-field image (scattering image) and the conventional absorption image.

Phasing Coherent Diffraction Patterns by Wavelength and Polarization Tuning*

D. Zhu[1, 2], T. Wang[3, 2], B. Wu[1, 2], R. Rick[1, 2], J. Stöhr[4], A. Scherz[2]

[1]*Department of Applied Physics, Via Pueblo Mall, Stanford University, Stanford, California, 94305, USA*
[2]*Stanford Institute for Materials and Energy Science, SLAC National Accelerator Laboratory, 2575 Sand Hill Rd., Menlo Park, California, 94025, USA*
[3]*Department of Material Science and Engineering, 496 Lomita Mall, Stanford University, Stanford, 94305, USA*
[4]*Linac Coherent Light Source, SLAC National Accelerator Laboratory, 2575 Sand Hill Rd., Menlo Park, California, 94025, USA*

* The authors acknowledge support by the U.S. Department of Energy, Office of Basic Energy Sciences.

Abstract:

We report extension of the multiple-wavelength anomalous diffraction technique in crystallography to imaging non-periodic nanostructures. By measuring multiple diffraction patterns at different x-ray wavelengths and polarizations, we were able to extract the holographic relative phase between charge and anomalous scattering. Pure element and magnetization distribution can then be determined through an iterative phase retrieval algorithm [1] that features fast and reliable convergence.

We present image reconstruction of polystyrene spheres of size 300 and 90 nm via wavelength-tuning near the Carbon K edge [2]. We also show image reconstruction of the out-of-plane component of the magnetization of a Co/Pd multilayer thin film via polarization tuning with sub-100-nm resolution.

References:

[1] D. Zhu, B. Wu, R. Rick et al., Opt. Lett. **34**, 2604 (2009).
[2] A. Scherz, D. Zhu, R. Rick et al., Phys. Rev. Lett. **101**, 076101 (2008).

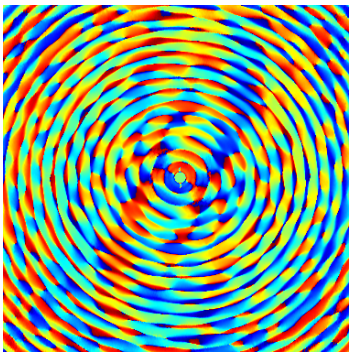

Figure 1: The calculated holographic relative phase for the polystyrene sphere reconstruction.

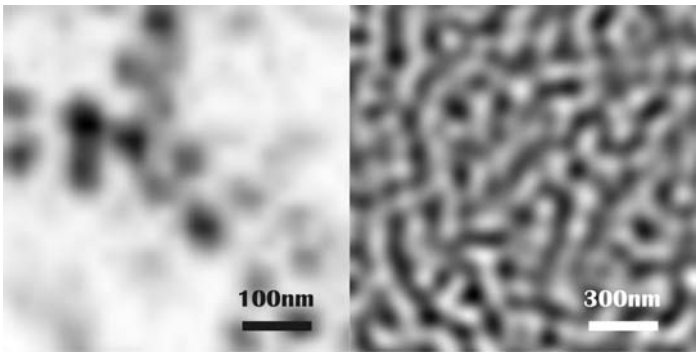

Figure 2: Reconstruction of the polystyrene spheres (left) and the worm domain formation of the Co/Pd multilayer thin film (right).

Generalization of DEI Methods into Grating-Interferometer-Based Phase-Contrast Imaging

P.P. Zhu[1], X.S. Liu[1], W.X. Huang[1], Q.X. Yuan[1], Z.L. Wang[1], K. Zhang[1], Y.L. Hong[1], Z.Z Zhu[1], Z.Y. Wu[1,,2]

[1]*Beijing Synchrotron Radiation Facility, Institute of High Energy Physics, Chinese Academy of Sciences, Beijing 100049*

[2]*National Synchrotron Radiation Laboratory, University of Science and Technology of China, Hefei 230026, China*

Abstract:

X-ray grating interferometer based phase contrast imaging (GPI) has been attracting attention as a new phase sensitive X-ray imaging method since 2006 [1,2]. A contrast corresponding to the wave-front deflection caused by the X-ray refraction at a sample can be probed. However, several constraints hamper the application of the existing approaches as possible methods for clinical based medical imaging. One of the major limitations is that almost all methods require at least three projective images to extract the refraction angle image. It makes the use of the same acquisition procedure of the conventional absorption CT impossible. According to the existing physical, mathematical, and methodological similarities between diffraction enhanced imaging (DEI) and GPI, here we report a way in which DEI methods may be generalized for GPI.

In this contribution, first we introduce the shift curve in GPI in analogy to the rocking curve in DEI [3-5], then we establish the GPI equation as the DEI equation. Afterwards the low angle image and the high angle image can be obtained by positioning the analyzer grating at the low angle half slope at first and then at the high angle half slope on the shift curve, respectively, to derive quantitative formulae of the absorption and the refraction angle image. In order to further simplify the method and avoid the background difference between the low angle and the high angle images, the high angle image was replaced with the first collected with the sample upside down. In conclusion, this novel method represents a major step forward in hard X-ray phase tomography, providing all of the advantages associated with conventional X-ray CT, in addition to yielding both phase and absorption information through only one set of projective image data with a full sample rotation.

References:

[1] A. Momose, S. Kawamoto, I. Koyama et al., Jpn. J. Appl. Phys **42**, L866 (2003).
[2] F. Pfeiffer, M.Bech, O. Bunk et al., Nat. Mater. **7**, 134 (2008).
[3] P.P. Zhu, J. Y. Wang, Q.X. Yuan et al., Appl. Phys. Lett. **87**, 264101 (2005).
[4] J. Wang, P. Zhu, Q. Yuan et al., Phys. Med. Biol. **51**(14), 3391 (2006).
[5] K. Zhang, P. Zhu et al., Phys. Med. Biol. **53**(20), 5757 (2008).

Conjugation of Fe_3O_4@TiO_2 Core-Shell Nanoparticles to Doxorubicin Improves Localization and Cytotoxicity in Drug-Resistant Ovarian Carcinoma

H. Arora[1], A. Wu[2], T. Paunesku[1], G. Woloschak[1]

[1]*Northwestern University, 303 E. Chicago Avenue, Ward Building 13-002, Chicago, IL, USA*
[2]*Ningbo University, Ningbo, Zhejiang, China*

Abstract:

Our laboratory investigates TiO_2 as a building material for nanoconjugates (NCs) for bio-nanotechnology applications. TiO_2 is particularly useful because of its semiconductor and nanocrystalline properties. The surfaces of TiO_2 molecules < 20 nm in diameter develop "corner defects" allowing covalent binding of ligands to the nanoparticle surface. Excitation of TiO_2 nanomaterials by photons carrying energy greater than the 3.2-eV band gap results in a charge separation that can be transferred to a covalently bound molecule [1]. Addition of a Fe_3O_4 core to NCs allows imaging by magnetic resonance without affecting surface properties of TiO_2 molecules (Fe_3O_4@TiO_2). To such NCs we bound the chemotherapeutic doxorubicin (DOX).

Nanoconjugates were synthesized so that 35% of the 8-nm nanoparticle surface was bound with DOX (DOX-NP). Two ovarian carcinoma cell lines were used: OVCAR-8 and NCI/ADR-RES (an isogenic cell line over-expressing the multi-drug-resistant transporter p-glycoprotein). Flow cytometry analysis showed increased DOX uptake in DOX-NP-treated NCI/ADR-RES cells, compared to DOX alone. DOX uptake in OVCAR-8 cells was not appreciably affected by conjugation. Differences in cytotoxicity were not found until 24 hours post-treatment; nanoparticle conjugation led to a slight increase in cell death in NCI/ADR-RES, but not OVCAR-8 cells. Confocal microscopy of NCI/ADR-RES cells showed nuclear localization of DOX when conjugated to NCs, but no intracellular signal with un-conjugated DOX. Elemental mapping by X-ray fluorescence microscopy confirmed the presence of Ti in cytoplasm and nuclei of both sensitive and resistant cell types, indicating cellular and nuclear uptake and stability of Fe_3O_4@TiO_2 NCs.

Conjugation of DOX to Fe_3O_4@TiO_2 nanocomposites results in increased uptake and cytotoxicity in a drug-resistant model of ovarian carcinoma. Previous work in other cancer models showed increased DNA damage and up-regulation of DNA repair mechanisms with DOX-NP compared to DOX alone, inviting further study into mechanisms underlying the advantages of DOX-NP conjugation.

References:

[1] T. Paunesku, T. Rajh, G. Wiederrecht et al., Nat. Materials **2**, 343 (2003).

Nanoparticle Uptake Study by Transmission X-ray Microscopy

C.-C. Chien[1], Y. S. Chu[3], J. Yi[2], K. S. Liang[3], Y. Hwu[1†]

[1]*Institute of Physics, Academia Sinica, Taipei 115, Taiwan*
[2]*Advanced Photon Source, Argonne National Laboratory, Argonne, IL 60439, USA*
[2]*National Synchrotron Radiation Research Center, Hsinchu 300, Taiwan*
[†]Corresponding author:phhwu@sinica.edu.tw

Abstract:
Full-field x-ray microscopy using zone-plate optics reached 20-nm resolution with Zernike contrast. With a high-brightness synchrotron source, fast image acquisition is possible for biology specimens. We took advantage of these newly available capabilities and studied in detail the uptake of nanoparticles of biology systems. Specifically, we image with high resolution to detect the presence of nanoparticles and their location in cells with respect to the cellular organelles with various cancer cell lines. Such results corroborate the quantitative measurements and identify the differences in the uptake behavior. We also took advantage of the high penetration of 8-keV x-ray photons and investigate the nanoparticle distribution in mice after injection via veins or arteries. Coupling this information with phase-contrast imaging at a lower resolution on live animals, we were able to provide a complete and comprehensive picture of the biological interaction of the nanoparticles and establish the possible use of x-rays as a means to study pharmacokinetics.

X-ray Microscopy of Primary Dopaminergic Neurons: Trace Elements Distribution and Oxidative State

T. Dučić[1], P. Lingor[2], L. Barski[2], T. Salditt[3], M. Salomé[4], A. Meents[1]

[1]*HASYLAB – DESY, Notkestrasse 85, D-22607 Hamburg, Germany*
[2]*Department of Neurology, Robert-Koch-Str. 40, D-37075 Göttingen, Germany*
[3]*Institute for x-ray Physics, Friedrich-Hund-Platz 1, D-37077 Göttingen, Germany*
[4]*ESRF, 6 rue Jules Horowitz, F-38043 Grenoble, France*

Abstract:

The considerable recent progress in x-ray sources, beamlines, and instrumentation has paved the way to establish synchrotron (SR)-based techniques as a promising tool for neuroscience in general. A novel P11 bio-imaging beamline at the high-brilliance storage ring PETRA III will provide sample environment and handling capabilities ideal for neuroscience applications. In particular, cryogenic imaging and *in situ* optical microscopy will be possible. The P11 beamline is designed to provide a broad range of experimental nanoprobe techniques, such as fluorescence mapping, absorption, and phase contrast imaging in 2-D and 3-D.

For establishing the experimental system, we studied primary dopaminergic neurons (PDN) isolated from midbrain mice, as a model for Parkinson's disease (PD) at ID21 at ESRF. PD is the second most frequent neurodegenerative disease [1]. Transition metals have been suggested to play a pivotal role in the pathogenesis of PD and other neurodegenerative disorders [1]. Redox trace metals are involved in the generation of free radicals via the Fenton reaction, which results in increased oxidative stress triggering mitochondrial dysfunction, lipid membrane peroxidation, DNA damage, and dopaminergic neuron death [1,2].

We used an advanced high-resolution analytical study based on the recent progress in x-ray imaging based on SR. In particular, we used x-ray fluorescence (XRF) spectroscopy to map the elemental distribution in cells and tissues with a spatial resolution on the order of 100 nm, including information on the redox state by spectromicroscopy. A novel cryo stage at ID21 allows us to image frozen hydrated cells without the need for invasive preparation and specimen sectioning. The first results show that Mn accumulates in particular small patches on the periphery of the PDN (Figure 1).

A joint synergistic effort of several groups combining different expertise is necessary to follow neuro-pathogenic development and complexity by using several model systems of PD and different methods, especially new SR techniques. Besides a much-focused contribution of molecular scale pathologies in neurology, we expect that this kind of experiments will also serve to better link up the recent technical developments at bioimaging beamlines at the PETRA III synchrotron with neuroscience applications at large.

References:

[1] D. Weintraub C.L. Comella, S. Horn, Parkinson's disease: pathophysiology, symptoms, burden, diagnosis, and assessment, Part 1 14, S40 (2008).

[2] P. Lingor, K. Unsicker, K. Krieglstein, Exp Neurol **163**, 55 (2000).

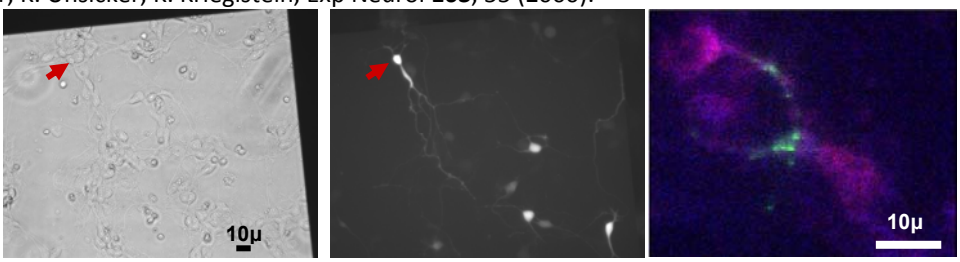

Figure 1: Light (A), fluorescence (B), and x-ray fluorescence (C) microscopy of primary dopaminergic neurons (PDN) grown on Si_3N_4 membrane. Dopaminergic neuron is marked by arrows in A and B. The overlapping image in C indicates distribution of Mn-green, P-red, and S-blue after Mn^{2+} treatment. Note that P and S indicate cell bodies of PDN. Image 40 x 45 µm, pixel size 0.3 µm, with dwell time 150 ms.

Switchable Cell Trapping Using Superparamagnetic Beads*

P. Fischer[4], M. T. Bryan[1], K. H. Smith[2], M. E. Real[2], M. A. Bashir[1], P. W. Fry[3], M.-Y. Im[4], T. Schrefl[1,5], D. A. Allwood[1], J. W. Haycock[2]

[1]*Department of Engineering Materials, University of Sheffield, Sheffield, UK*
[2]*The Kroto Research Institute, University of Sheffield, Sheffield, UK*
[3]*Centre for Nanoscience and Technology, University of Sheffield, Sheffield, UK*
[4]*Center for X-ray Optics, Lawrence Berkeley National Laboratory, Berkeley, California, USA*
[5]*St. Poelten University of Applied Sciences, St. Poelten, Austria*

* This work was supported by the BBSRC (grant BB/F015844/1), the EPSRC (grant EP/D056683/1) and by the Director, Office of Science, Office of Basic Energy Sciences, Materials Sciences and Engineering Division, of the U.S. Department of Energy under Contract No. DE-AC02-05-CH1123. DAA acknowledges an Advanced Research Fellowship from the EPSRC (grant GR/T02942/01).

Abstract:

Superparamagnetic beads and wires are widely used within bioscience to separate, organize, and manipulate biomolecules and cells [1,2]. The beads can be incorporated into biological cells without affecting cellular viability and are attracted towards magnetic poles.

We have investigated permalloy ($Ni_{81}Fe_{19}$) microwires as the basis of a switchable template for positioning magnetically labeled neural Schwann cells. Magnetic transmission X-ray microscopy and micromagnetic modeling show that magnetic domain walls can be created or removed in zigzagged structures by an applied magnetic field [3]. Schwann cells containing superparamagnetic beads are trapped by the field emanating from the domain walls. The design allows Schwann cells to be organized on a surface to form a connected network and then released from the surface if required (Figures 1 and 2). As aligned Schwann cells can guide nerve regeneration, this technique could benefit studies on the treatment of peripheral nerve injuries

References:

[1] E. Mirowski, J. Moreland, S. Russek et al., J. Magn. Magn. Mater. **311**, 401 (2007).
[2] M. Tanase, E.J. Felton, D.S. Gray et al., Lab on a Chip, **5**, 598 (2005).
[3] M.T. Bryan, K.H. Smith, M.E. Real et al., IEEE Magnetics Letters **1**, 1500104 (2010); doi: 10.1109/LMAG.2010.2046143.

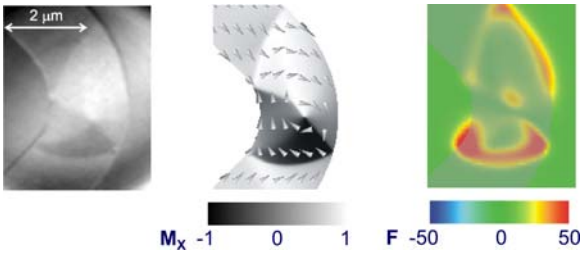

Figure 1: Switch ON configuration. Left: X-ray microscopy image of the domain wall, Center: micromagnetic simulations, Right: Calculated force F in pN.

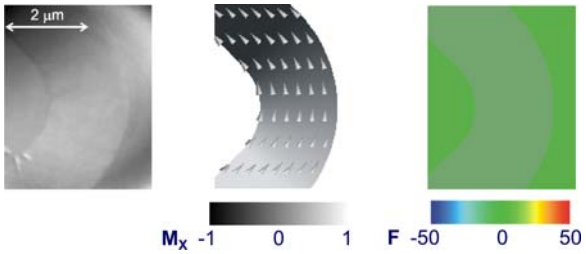

Figure 2: Switch OFF configuration. Left: X-ray microscopy image of the domain wall, Center: micromagnetic simulations, Right: Calculated force F in pN.

Comparative Cranial Osteology of Darwin's Finches Based on Micro-CT Scanning: Preliminary Results

A. Genbrugge[1,2], M.N. Boone[3], A. Herrel[4,5], L. Van Hoorebeke[3], J. Dirckx[1], P. Aerts[5,6], D. Adriaens[2]

[1]*Laboratory of Biomedical Physics, University of Antwerp, Groenenborgerlaan 171, B-2020 Antwerpen, Belgium*
[2]*Evolutionary Morphology of Vertebrates, Ghent University, K.L. Ledeganckstraat 35, 9000 Ghent, Belgium*
[3]*UGCT, Department of Physics and Astronomy, Ghent University, Proeftuinstraat 86, 9000 Ghent, Belgium*
[4]*Département d'Ecologie et de Gestion de la Biodiversité, Museum National d'Histoire Naturelle, 57 rue Cuvier, Case postale 55, 75231, Paris Cedex 5, France*
[5]*Department of Biology, University of Antwerp, Universiteitsplein 1, 2610 Antwerpen, Belgium*
[6]*Department of Movement and Sports Sciences, Ghent University, Watersportlaan 2, 9000 Ghent, Belgium*

Abstract:

Darwin's finches are the textbook example of adaptive evolution. All fourteen species are considered having evolved a different beak morphology corresponding to their food preferences. Unfortunately, little is known about the details on the relation between the beak design and its performance.

In continuation of the work of Bowman [1], we aim to unravel this causal link by comparing the osteological variation in beak design of the different Darwin's finches with that of a model organism, the Java sparrow (*Padda oryzivora*, a large-beaked species not closely related to Darwin's finches), and link this to mechanical capacities of the upper beak for dealing with mechanical stress. It is hypothesized that the beak morphology reflects the performance in seed cracking.

Based on micro-CT scanning of 12 different species, including species with long, pointed beaks (e.g., *Certhidea olivacea* and *Camarhynchus pallidus*) to species with deep, broad beaks (e.g., *Geospiza* magnirostris and *Padda oryzivora*), three-dimensional models of the beak have been made. With these models it was possible to study and compare the cranial skeletal elements to evaluate the adaptive nature of the observed skeletal variation with respect to dealing with hard seeds.

References:

[1] R.I. Bowman, Univ. Calif. Publ. Zool. **58**(1), 302 (1961).

Figure 1: 3D rendering of *Padda oryzivora* showing the jaw bones (yellow) through the beak parts (lateral view).

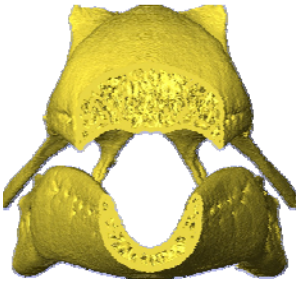

Figure 2: Cross section of the upper and lower beak of *Padda oryzivora* (frontal view).

3D Imaging of Whole, Unstained Cells by Using X-ray Diffraction Microscopy

H. D. Jiang[1], C. Y. Song[2], C. C. Chen[1], R. Xu[1,2], K. S. Raines[1], B. P. Fahimian[1], C. H. Lu[3], T. K. Lee[3], A. Nakashima[4], J. Urano[4], T. Ishikawa[2], F. Tamanoi[4], J. Miao[1]

[1]*Department of Physics and Astronomy, University of California, Los Angeles, CA 90095, USA*
[2]*RIKEN SPring-8 Center, 1-1-1, Kouto, Sayo, Hyogo 679-5148, Japan*
[3]*Institute of Physics, Academia Sinica, Nankang, Taipei 11529, Taiwan*
[4]*Department of Microbiology, Immunology, and Molecular Genetics, University of California, Los Angeles, CA 90095, USA*

Abstract:
Coherent diffraction microscopy (also termed coherent diffractive imaging) is a lensless imaging technique in which the coherent diffraction pattern of a non-crystalline specimen or a nanocrystal is measured and then directly phased to obtain an image. The well-known phase problem is solved by using the oversampling method in combination with the iterative algorithms. Since its first experimental demonstration in 1999, coherent diffraction microscopy has been applied to imaging a wide range of materials science and biological specimens such as nanoparticles, nanocrystals, biomaterials, cells, cellular organelles, viruses, and carbon nanotubes by using synchrotron radiation, high harmonic generation and soft X-ray laser sources, free electron lasers, and electrons [1,2]. Here we apply coherent X-ray diffraction microscopy to quantitative 3D imaging of a whole, unstained yeast spore at a resolution of 50–60 nm [3]. We identified the 3D morphology and structure of cellular organelles including spore wall, vacuole, endoplasmic reticulum, mitochondria, granules, nucleus, and nucleolus inside a yeast spore cell. Furthermore, we observed a 3D structure protruding from the reconstructed yeast spore, suggesting the spore germination process. Hence this work paves a way for nondestructive 3D characterization of a wide range of biological specimens at nanometer-scale resolutions that are too thick for electron microscopy.

References:

[1] J. Miao, P. Charalambous, J. Kirz et al., Nature **400**, 342 (1999).
[2] J. Miao, T. Ishikawa, T. Earnest et al., Annu. Rev. Phys. Chem. **59**, 387 (2008).
[3] H. D. Jiang, C. Song, C. C. Chen et al., submitted.

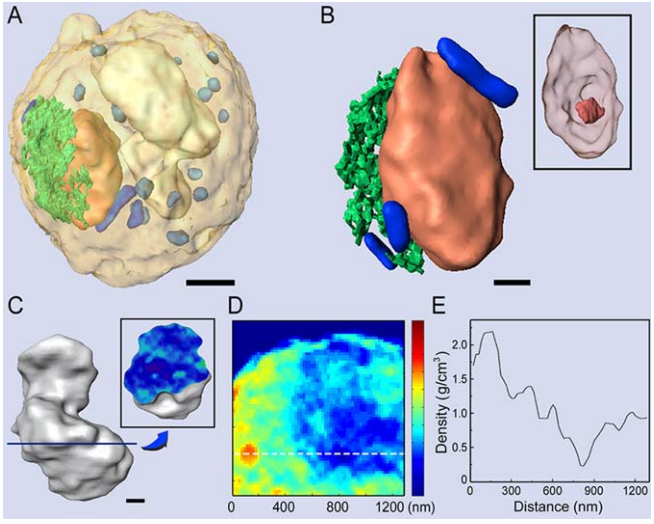

Figure 1: (A) 3D volume rendering of the reconstructed yeast spore, showing nucleus (orange), ER (green), vacuole (white), mitochondria (blue) and granules (light blue). Scale bar is 500 nm. (B) Zoomed view of the 3D morphology and structure of the nucleus, ER and mitochondria. Inset shows the nucleolus (orange). Scale bar is 200 nm. (C) 3D morphology and structure of the vacuole. Inset shows a cross-sectional image of the vacuole. Scale bar is 200 nm. (D), (E) A thin slice of the reconstructed yeast spore and a line scan along the dashed line, showing the density variation across a mitochondrion and the vacuole.

Cellular Imaging with SR-Based Soft X-ray Microscopy

S.P. Jiang, L. Chen, W.R. Zhang, S.X. Xu, J.W. Yan

National Synchrotron Radiation Laboratory, University of Science and Technology of China, Hefei, China

Abstract:

Soft x-ray microscopy is one of the most important research fields at the National Synchrotron Radiation Laboratory. The full-field transmission soft x-ray miroscope based on the Hefei Light Source has been already developed and will be continuously improved. Now imaging spatial resolution of the X-ray microscope is better than 70 nm [1].

Imaging experiments of some biological specimens were performed on the x-ray microscope, and we will present some x-ray images of the cells including *chlamydomonas* and diatoms.

References:

[1] S.P. Jiang, L. Chen, J. Phys.: Conf. Ser. **186**, 012008 (2009).

Observation of Organelles in Leydig Cells by Contact Soft X-ray Microscopy with a Laser Plasma X-ray Source*

M. Kado[1], M. Ishino[1], S. Tamotsu[2], K. Yasuda[2], M. Kishimoto[1], M. Nishikino[1], Y. Kinjo[3], K. Shinohara[4]

[1]*Japan Atomic Energy Research Agency, 8-1 Umemidai, Kizugawa-shi, Kyoto, Japan*
[2]*Nara Women's University, Kitauoyahigashi-machi, Nara-shi, Nara, Japan*
[3]*Tokyo Met. Industrial Tech. Research Institute, 2-11-1, Fukazawa, Setagaya-ku, Tokyo, Japan*
[4]*Waseda University, 3-4-1, Okubo, Shinjuku-ku, Tokyo, Japan*

* This research was partially supported by the Ministry of Education, Science, Sports and Culture, Grant-in-Aid for Scientific Research (C), 21540517, 2009.

Abstract:

Contact x-ray microscopy has achieved a single-shot imaging of wet biological specimens in natural condition and succeeded in imaging live mouse macrophages [1,2] with hair-like structures, which was not observed before. It is very important to identify obtained features in the x-ray images, since x-ray microscopes have potential to image features that have not been visualized yet. Here, we demonstrate to image the same biological specimens both by confocal laser microscopy and soft x-ray microscopy.

Staining biological specimens with well-established techniques makes easy to identify features in the fluorescence images obtained with confocal laser microscope. Comparing the x-ray images of the specimens with the fluorescence images, features found in the fluorescence images could also be identified in the x-ray images. Shown in Fig. 1 and Fig. 2 are fluorescence images and x-ray images of the hydrated Leydig cells stained with Phalloidin to label actin filaments. Comparing the x-ray images to the fluorescence images, fine structures of the actin filaments in the x-ray images were identified.

References:

[1] M. Kado, M.C. Richardson, J.M. Rajyaguru et al., Proc. of Experimental Biology and Medicine **220**, 27 (1999).
[2] M. Kado, H. Daido, Y. Yamamoto et al., Proc. of 8th Int. Conf. X-ray Microscopy, IPAP Conf. Series **7**, 41 (2006).

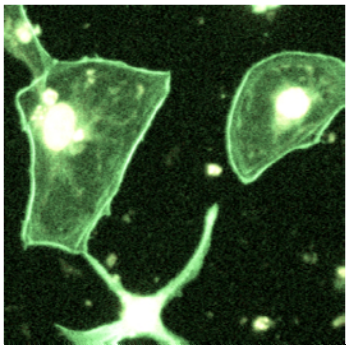

Figure 1: Fluorescence images of Leydig cells observed with a confocal laser microscope.

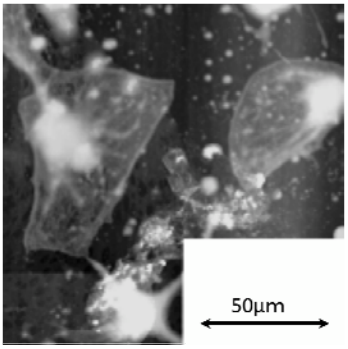

Figure 2: X-ray images of the same Leydig cells observed with the confocal laser microscope.

Investigating Selectivity in Algal Biomineralization of Barium and Strontium with X-ray Fluorescence Microscopy*

M. Krejci[1], S. Vogt[2], D. Joester[1]

[1]Department of Materials Science *and Engineering,* Northwestern *University, 2220 Campus Drive, Evanston, IL, USA*

[2]*X-Ray Science Division, Argonne National Laboratory, 9700 S. Cass Avenue, Argonne, IL, USA*

* This work was supported by a Laboratory Graduate Appointment with Argonne National Laboratory and The Initiative for Sustainability and Energy at Northwestern University (ISEN).

Abstract:

There is currently no cost-effective and selective separation method available to remove radioactive ^{90}Sr from either nuclear waste or the environment. The difficulty is caused by the chemical similarity of Ca^{2+}, Sr^{2+}, and Ba^{2+} cations, which also leads to indiscriminate transport (and incorporation into bone) in most animals. [1] However, desmid green algae of the genus Closterium have the ability to selectively precipitate $(Ba,Sr)SO_4$ crystals within vacuoles in a Ca-rich environment, indicating that they possess a unique capability for Sr and Ba selective transport. [2]

We are currently investigating the basic methods of Sr and Ba selectivity and transport in these organisms, using synchrotron x-ray fluorescence microscopy (SXRF) elemental mapping to identify routes of uptake and locations of selectivity filters. With this technique, we have verified the uptake and sequestration of Ba and Sr into crystals and have observed time-dependent changes in intracellular Sr concentrations. The kinetics of uptake and efflux of Sr appear to be dependent on external Ca concentrations, and Sr and Ca show similar cellular localization. This suggests that selectivity for Sr versus Ca may not occur at the whole cell level. Instead, high S levels detected in the vacuole may indicate a selective precipitation mechanism at the vacuolar level. We propose a "sulfate trap" model, in which high sulfate levels in the vacuole leads to preferential precipitation of $BaSO_4$ and $SrSO_4$ due to their low solubilities relative to $CaSO_4$. An elucidation of the mechanisms of selectivity in these organisms will enable and inspire innovation of chemical and bioremediation approaches to ^{90}Sr cleanup operations.

References:

[1] O. Raabe, Radiat. Res. **131**(1), 112 (1992).

[2] J. Wilcock et al., P. Roy. Soc. Lond. B Bio. **256**, 203 (1989).

Nanotechnology and X-ray Optics for Reproduction of the Three-Dimensional Structure of a Damaged Rat Spinal Chord after Gene Therapy

A.V. Kuyumchyan[1,2,3], V.L. Arvanian[4], D. A.Kuyumchyan[5], V.V. Aristov[1], E.V. Shulakov[1]

[1] *Institute of Microelectronics Technology, RAS, 142432, Chernogolovka, Russia*
[2] *American NanoScience and Advanced Medical Equipment, Inc., CA 91206, USA*
[3] *ORP Inc, Seattle, WA 98103, USA,*
[4] *SUNY Stony Brook, NY 11794, USA*
[5] *Riverside Community Colleges, 4800 Magnolia Avenue, Riverside, CA 92506-1299, USA*

Abstract:

X-ray microscopy is a powerful imaging method for life, materials, and environmental sciences. High-resolution 3D images of nano-size and biological samples are currently made by zone plate (ZP) X-ray microscopy, transmission electron microscopy, and atomic-force microscopy. The wave front reconstruction process was first proposed by Gabor [1] and subsequently enhanced by Leith and Upatnieks. As was shown [2], reproduction of X-ray holograms by means of the crystal ZP is possible.

In this paper, we describe a new special geometry for recording hard X-ray holograms using crystal ZP. Two objects have been tested in this study: one for the development of nanotechnology and the second for visualization of images of the damaged spinal cord of an adult rat. The first objects consisted of the word combination “X-Ray Fourier hologram”. They were prepared on the silicon crystal membranes by electron-beam lithography and ion-plasma etching. The second object was the damaged spinal cord of an adult rat, with and without treatment with neurotrophin NT3 secreted from a genetically engineered fibroblast. We recorded the FIB image of the damaged spinal cord after different gene therapies. The experimental resulting 3D FIB image of the damaged spinal cord is shown in Figures 1a and b.

References:

[1] D. Gabor, Proc. Roy. Soc. (London) A **197**, 454 (1949).
[2] A. Kuyumchyan, A. Souvorov, T. Ishikawa et al., Proc. 8th Int. Conf. X-ray Microscopy, IPAP Conf. Series 7, 417 (2006).

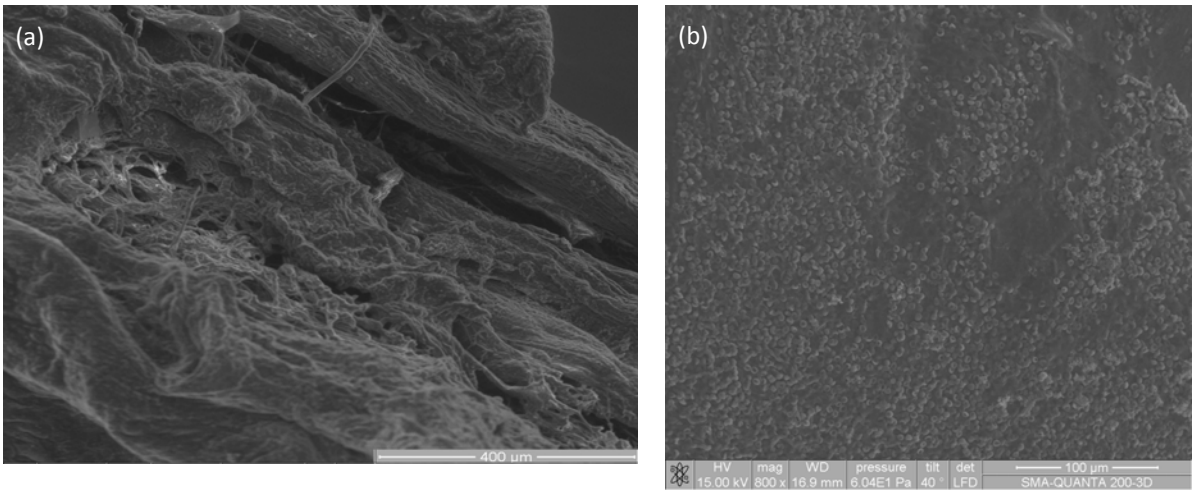

Figure 1: FIBM image of the damaged spinal cord (a) without treatment and (b) with treatment.

Combined X-ray Microfluorescence and Atomic Force Microscopy Studies of Mg Distribution in Cells

S. Lagomarsino[1], S. Iotti[2], G. Farruggia[3], F. Wolf[4], A. Cedola[1], V. Trapani[4], M. Fratini[1], I. Bukreeva[1], L. Mastrototaro[4], I. McNulty[5], S. Vogt[5], D. Legnini[5], J.A.M. Maier[6]

[1]*IFN-CNR - V. Cineto Romano, 42 00156 Roma - Italy*
[2]*Dipartimento di Medicina Interna, dell'Invecchiamento e Malattie Nefrologiche Università di Bologna, Via Massarenti, 9 40138 Bologna - Italy*
[3]*Dipartimento di Biochimica « G. Moruzzi » Università di Bologna, Via Irnerio, 48 40126 Bologna - Italy*
[4]*Istituto di Patologia Generale - Università Cattolica del Sacro Cuore - Facoltà di Medicina "A. Gemelli" L.go F. Vito, 1 00168 Roma – Italy*
[5]*Argonne National Laboratory, 9700 South Cass Avenue, Argonne, Illinois 60439, USA*
[6]*Dipartimento di Scienze Cliniche, Università di Milano, Via GB Grassi 74, Milano 20157 – Italy*

Work supported by PRIN project.

Abstract:

Magnesium (Mg) is an abundant intracellular cation essential for cellular processes such as proliferation and death [1,2]. Though reduced Mg availability and/or increased excretion are associated with some common diseases, such as diabetes, hyperlipemia, hypertension and neuropsychiatric disorders, an accurate description of the regulatory mechanisms of Mg at the cellular level and of its intracellular distribution among different sub-compartments is still lacking [3].

In this work we present x-ray microfluorescence measurements aimed at giving the intracellular Mg distribution with a submicron spatial resolution. These studies were combined with atomic force microscopy (AFM) measurements to normalize the x-ray fluorescence intensity according to the real thickness of the cell under study, which provides a concentration map of Mg quite different from the fluorescence intensity map obtained without thickness normalization. Based on the same principle, from the x-ray transmitted intensity through the cell and the AFM measurements, we were also able to recover a map of the x-ray linear absorption coefficient (“mu”), which can provide useful information about local electronic density. Mammary mouse epithelial HC11 cells were fixed and dehydrated in acetone/methanol 1:1. The x-ray microfluorescence measurements were carried out at beamline 2-ID-B of APS (Argonne, USA), with an incident beam of 1.5 keV, i.e., relatively close to the Mg absorption edge (1.3 keV). This innovative methodology can also be applied to other components and other elements in a straightforward way and shows that an interdisciplinary approach is necessary to successfully apply physical methods to the elucidation of biological issues.

References:

[1] F. Wolf and A. Cittadini, Mol. Aspects Med. **24**, 3 (2003).
[2] H. Rubin, Magnesium Res. **18**, 268 (2005).
[3] F. Wolf and V. Trapani, Clinical Sci. **114**, 27 (2008).

In situ Coherent Diffraction Imaging of Cellulose Crystals*

J. Lal[1], L. Makowski[1], I. Robinson[2], R. Harder[3]

[1]*Biosciences Division, Argonne National Laboratory, Argonne, IL 60439*
[2]*Physics and Astronomy Department, University College London, UK WC1E 6BT*
[3]*Advanced Photon Source, Argonne National Laboratory, Argonne, IL 60439*

Abstract:
Cellulose is perhaps the most abundant renewable source of organic molecules on earth. The vast majority of it is present as microcrystals, fibrils or fibers embedded within plant cell walls. Technically, it is a major challenge to efficiently tease out the individual molecules in order to make them amenable to degradation into small organic molecules suitable as chemical feedstocks. One stumbling block is the difficulties involved in imaging the fibrils *in situ*. Without this capability, it is difficult to monitor the effects of pretreatments required. Here we will outline our adaptation of coherent diffraction imaging for visualizing cellulose crystals *in situ*. This method, still in development, is capable of producing images of individual crystalline domains even when the cellulose is embedded within opaque plant material. Preliminary images suggest that the large-scale organization of the crystalline fibrils is dependent on the position in the plant (primary vs secondary plant cell walls); the hydration of the material and the maturity of the plant.

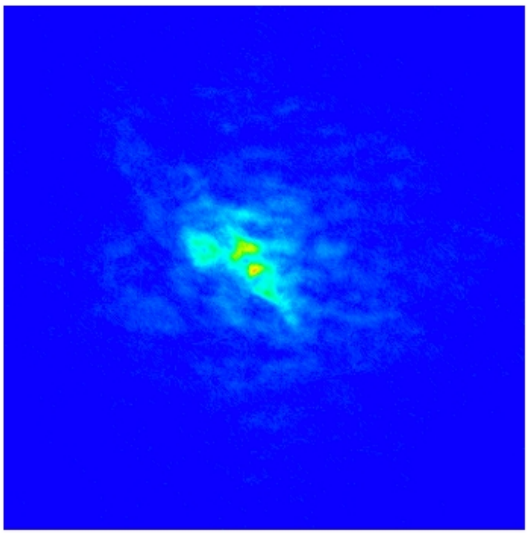

Figure 1: This is a section through the (2 0 0) reflection from a cellulose microcrystal. The fringes about this reflection were used to reconstruct the image of the crystal shown in Figure 2.

Figure 2: This is a reconstruction of a cellulose microcrystal from vascular bundles of maize (dried corn stalk). The crystal is about 857 x 498 x 72 nm. The fingers projecting from the bottom are about 25 nm in diameter.

In-Line Phase Contrast for High-Resolution Laboratory X-ray Imaging in Thick Tissue

U. Lundström, P. Skoglund, P. Takman, H. M. Hertz

Biomedical and X-Ray Physics, Department of Applied Physics, Royal Institute of Technology, SE-106 91 Stockholm, Sweden

Abstract:

We investigate how in-line phase contrast [1] can be applied to pre-clinical medical imaging using a laboratory x-ray source. In-line phase contrast has the distinct advantage over other phase-contrast imaging techniques in that it does not require any sophisticated and absorbing x-ray optics. On the other hand, it places higher demands on the x-ray source and detector. Recently, a liquid-metal-jet-anode high-brightness microfocus source [2] demonstrated laboratory-scale high-resolution phase-contrast imaging of thin samples with adequate exposure times [3]. In the present paper, we investigate its applicability to biomedical imaging of thicker samples. The main challenges in applying this to biomedical imaging is to keep the dose and exposure time low while making use of the harder x-rays required to penetrate thicker tissue.

A detailed simulation tool has been developed to find optimal imaging conditions and to allow prediction of the types of samples that can be imaged successfully. Simulations show excellent agreement with experiments, as shown in Figures 1 and 2, where a nylon thread has been imaged and simulated. For tissue of typical thickness for preclinical applications (2 cm) our simulations show that <20 μm size features can be visible with about 20 mGy radiation dose. We are currently acquiring images in a well-controlled environment to verify these simulations and to show that high contrast and high resolution can be obtained in thick soft tissue.

References:

[1] R A Lewis, Phys. Med. Biol. **49**, 3573 (2004).
[2] O. Hemberg, M. Otendal, and H. M. Hertz, Appl. Phys. Lett. **83**, 1483 (2003).
[3] T. Tuohimaa, M. Otendal, and H. M. Hertz, Appl. Phys. Lett. **91**, 074104 (2007).

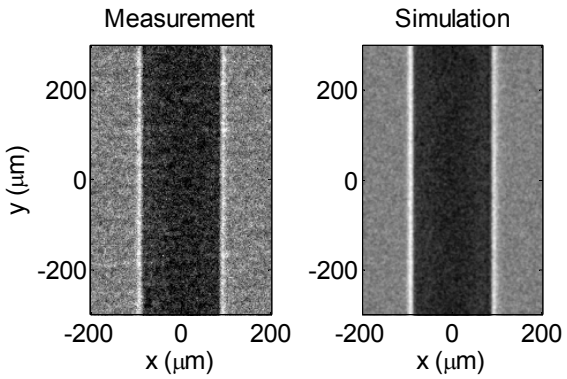

Figure 1: X-ray image of a nylon thread compared to simulation. The bright lines on the edges of the thread indicate the presence of in-line phase contrast.

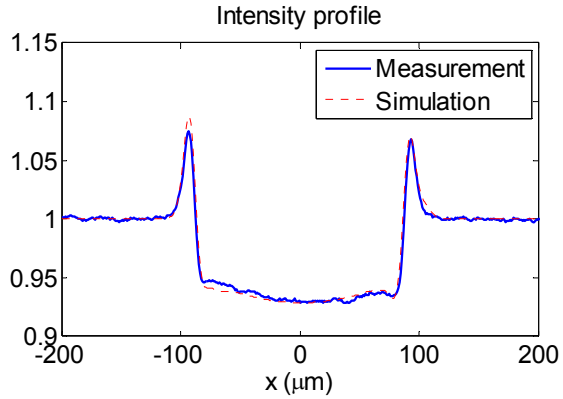

Figure 2: The images in Figure 1 integrated along the direction of the thread. The asymmetries in the line profiles are ascribed to a slight asymmetry in the source emission profile.

Nano-resolution X-ray Tomography for Deciphering a Wiring Diagram of the Mammalian Brain

H. Mizutani[1], H. Sagara[2], A. Takeuchi[3], T. Ohigashi[4], W. Yashiro[5], K. Uesugi[3], Y. Suzuki[3], A. Momose[5], T. Takagi[1]

[1]*Science Integration Program, Organization for Interdisciplinary Research Projects, University of Tokyo, 5-1-5 Kashiwa-no-ha, Kashiwa, Chiba, Japan*
[2]*Institute of Medical Science, University of Tokyo, 4-6-1 Shirokanedai, Minato, Tokyo, Japan*
[3]*Japan Synchrotron Radiation Research Institute / SPring-8, 1-1-1 Kouto, Sayo, Hyogo, Japan*
[4]*Research Organization of Science & Engineering, Ritsumeikan University, 1-1-1 Noji Higashi, Shiga, Japan*
[5]*Department of Advanced Materials Science, Graduate School of Frontier Sciences, University of Tokyo, 5-1-5 Kashiwa-no-ha, Kashiwa, Chiba, Japan*

Abstract:
Neural circuits in the central nervous system are the substrate of various high-order brain functions. Anatomical and functional graph structures of neural networks with actual connections will provide us with perspectives to elucidate the brain complex system. Here, we aim to develop a three-dimensional mouse brain atlas of neural circuits using high-resolution x-ray tomography by synchrotron radiation. It will not only identify a large number of synapses but also clarify the structure of neuronal networks for understanding the most complicated organ in the body. In this study, we observed individual neurons of the mouse brain using hard x-ray Talbot-type phase-contrast micro-tomography with 1-µm resolution at SPring-8 [1,2]. Furthermore, a nano-resolution hard x-ray Zernike-type phase-contrast microscope revealed nerve fibers and organelles, including mitochondria and synapses, in the neural tissue (Figure). In the near future, we will utilize this information to begin deciphering the wiring diagram of the brain by using the nano-resolution x-ray tomography.

References:
[1] Y. Takeda et al., Appl. Phys. Exp. **1**, 117002 (2008).
[2] H. Mizutani et al., J. Physics: Conf. Series **186**, 012092 (2009).

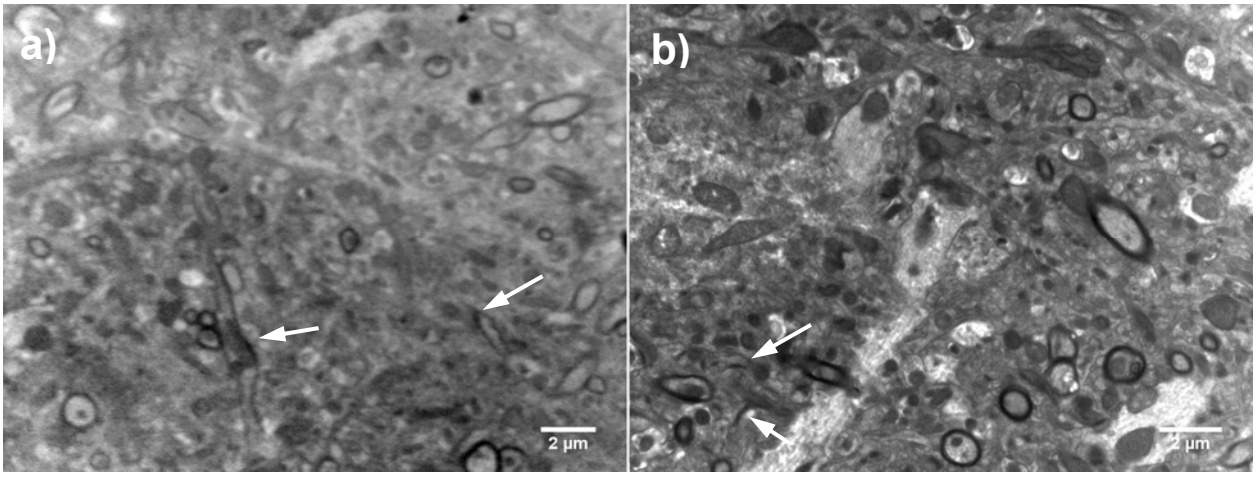

Figure : Two different micrographs of the mouse brain slice tissue stained by heavy metals 200 nm in thickness. They were observed by using a) Zernike-type x-ray phase-contrast microscopy (8 keV) and b) transmission electron microscopy (120 kV). Arrows indicate the synapses, the connection sites of neurons.

Microtomographic Analysis of Human Brain Circuits*

R. Mizutani[1], A. Takeuchi[2], K. Uesugi[2], S. Takekoshi[3], R.Y. Osamura[3], Y. Suzuki[2]

[1]*Dept. of Applied Biochemistry, School of Engineering, Tokai University, Kanagawa 259-1292, Japan*
[2]*Research and Utilization Division, JASRI/SPring-8, Hyogo 679-5198, Japan*
[3]*Department of Pathology, Tokai University School of Medicine, Kanagawa 259-1193, Japan*

* This study was supported in part by Grants-in-Aid for Scientific Research from the Japan Society for the Promotion of Science (no. 21611009).

Abstract:

Neuronal circuits, which are essential for brain functions, are built up by neurons as a three-dimensional network, so tracing the three-dimensional neuronal network of human cerebral cortex is the first step to understanding the mechanism of human brain functions.

The cortical microstructures were visualized by microtomographic imaging of adult frontal-cortex tissue stained with metal impregnation [1,2]. Skeletonized wire models were built by tracing the three-dimensional distribution of absorption coefficients (Figure 1). The model building procedures were similar to those reported for crystallographic analyses of macromolecular structures, while neuronal processes were traced by using a three-dimensional Sobel filter. Possible neuronal circuits were analytically resolved from the skeletonized wire models. The operating mechanism of the resolved circuits is discussed on the basis of neurotransmission in the circuits [3].

At present the primary method for visualizing three-dimensional structures of biological tissues is confocal light-microscopy. However, absorptive and refractile nature of ultraviolet, visible, and infrared lights with respect to biological tissues makes it difficult to visualize three-dimensional structures of block samples. In contrast, the transparency of biological tissues to hard x-rays facilitates three-dimensional visualization of the brain tissue. Our results indicate that x-ray microtomography is a potential method of revealing three-dimensional structures in neuroscience, like x-ray crystallography in molecular biology.

References:

[1] R. Mizutani et al., Brain Res. **1199**, 53 (2008).
[2] R. Mizutani et al., Tissue Eng. C **14**, 359 (2008).
[3] R. Mizutani et al., Cereb. Cortex, in press; doi: 10.1093/cercor/bhp237.

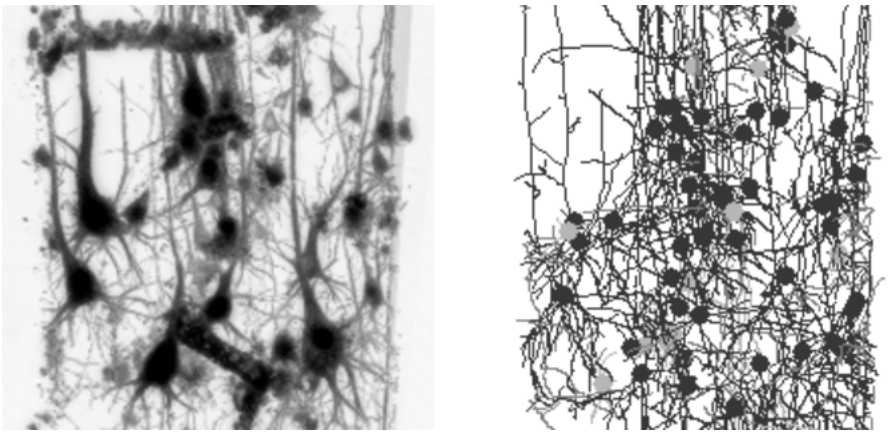

Figure 1: Left: microtomographic structure of external pyramidal layer of human frontal cortex. Right: skeletonized three-dimensional model of the same region. Circles indicate cell body coordinates.

Micro-CT of Porous Apatite Fiber Scaffolds Studied by Projection X-ray Microscopy

J. Moriya[1], M. Aizawa[2], H. Yoshimura[1]

[1]*Dept. of Physics, Meiji University, 1-1-1 Higashimita, Tama-Ku, Kawasaki, 214-8571, Japan*
[2]*Dept. of Applied Chemistry, Meiji University, 1-1-1 Higashimita, Tama-Ku, Kawasaki, 214-8571, Japan*

Abstract:

Hydroxyapatite (HAp) has been widely used as a scaffold for repairing fractured bone. For bone regeneration, the morphology of apatite scaffold, and in addition composition, crystal structure, and crystal orientation of HAp are considered to be important. The apatite scaffold constructed by single-crystal fibers with pores showed good result for cellular response. Specially, apatite fiber scaffold (AFS) with large pores, 100 to 250 μm, was found to enhance the cell activities, such as cell proliferation and differentiation *in vitro* [1]. The porous APS was prepared by heating apatite fiber crystals with spherical carbon beads at 1300 °C for 5 h in a steam atmosphere. The carbon beads evaporated during the heating process and spherical pores remained in the AFS. The fiber orientation and pore structure in AFS seems to be essential for growth of cells. In this point of view, we have investigated the three-dimensional (3-D) structure of AFS non-destructively by X-ray micro CT using a SEM modified projection X-ray microscope [2]. A 1-μm-thick platinum film was used as a metal target with an electron beam accelerating voltage of 18 keV. In this condition, the characteristic X-ray of platinum Lα (0.13 nm) was the dominant X-ray in the emission. The 3-D structures of AFS are reconstructed from a series of 120 X-ray projection images taken around a single rotation axis using the Feldkamp-based cone-beam reconstruction method. Cross sections of AFS extracted from the reconstructed 3-D data are shown in Figures 1 and 2. Thicknesses of the sections were about 50 μm in Figure 1 and 100 μm in Figure 2. Pores according to the carbon beads appeared as dark circles in the images. The distribution of pores and high density areas were not homogeneous in the preparation of large carbon beads. The reason is not clear, though buoyancy force working on the carbon beads may disturb homogeneous distribution of the carbon beads in the apatite fiber slurry.

References:

[1] M. Aizawa, F.S. Howell, K. Itatani et al., J. Ceram. Soc. Jpn. **108**, 249 (2000).
[2] A. Tanisako, A. Hori, A. Okumura et al., J. Electron Microsc. **54**, 379 (2005).

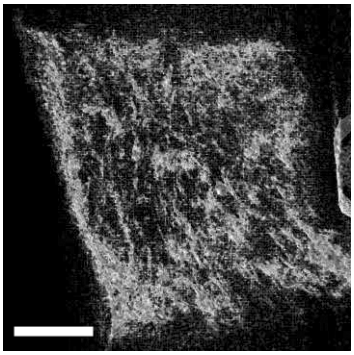

Figure 1: Cross section of AFS obtained from CT reconstruc-tion; AFS fabricated using 20 μm carbon beads. Scale bar shows 100 μm.

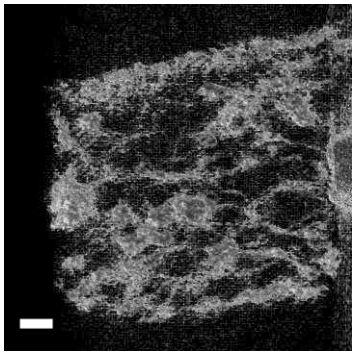

Figure 2: Cross section of AFS obtained from CT reconstruc-tion; AFS fabricated using 20 μm carbon beads. Scale bar shows 100 μm.

Differential Phase-Contrast Tomography of Amyloid Plaques in Alzheimer Mouse Models

B. Pinzer[1], M. Cacquevel[2], S. McDonald[3], P. Modregger[1], M. Stampanoni[1,4], P. Aebischer[3]

[1]*Swiss Light Source, Paul Scherrer Institut, 5232 Villigen PSI, Switzerland*
[2]*Lab. for Neurodegenerative Disorders, BMI, EPF Lausanne, 1015 Lausanne, Switzerland*
[3]*Materials Science Centre, University of Manchester, Manchester, United Kingdom*
[4]*Institute for Biomedical Engineering, University and ETH Zürich, 8092 Zürich, Switzerland*

Abstract:
Differential phase contrast (DPC) imaging has proven to be a powerful method to distinguish different biological tissues. Combined with tomography, three-dimensional reconstructions of biological samples can be obtained non-destructively [1]. A particular challenge is the characterization of depositions of amyloid β-peptides in plaques in brain tissue, which are supposed to be responsible for neurodegeneration in Alzheimer's disease [2]. Using the grating interferometer setup at the TOMCAT beamline of the Swiss Light Source [3], we were able to visualize the three-dimensional distribution of Aβ plaques in the brains of transgenic mice with a nominal voxel size of 7.4 µm. Comparison with histological sectioning indicates that the image features were indeed Aβ plaques. The high quality of the measurements allows for automated extraction of quantitative data like volumetric plaque density, plaque burden, or density differences between Aβ plaques and surrounding brain tissue. This is an important step towards systematic studies of the mechanisms and dynamics of Aβ plaque genesis and deposition.

References:

[1] T. Weitkamp, A. Diaz, C. David et al., Opt. Express **13**(16), 6296 (2005).
[2] J. Hardy and D. J. Selkoe, Science **297**, 5580 (2002).
[3] S.A. McDonald, F. Marone, C. Hintermuller et al., J. Synchrotron Radiat, **16**, 562 (2009).

Nitrogen Detection in Foods via Energy-Dispersive Spectroscopy

V.L. St. Jeor

Cargill Incorporated, Global Food Research, Advanced Analytics,
2500 Shadywood Rd., Excelsior, MN 55331

Abstract:

Standard-based energy dispersive spectroscopy (SB-EDS) is one way of detecting and quantifying nitrogen (N) within some sample materials, but not the only way. Other methods such as Kjeldahl, Dumas, or LECO (pyrolysis-based methodologies), have been accepted as industry standards in foods and feeds for decades [1]. In addition to the study itself, we compare EDS methodology to the pyrolysis-based methods in example materials. However, for EDS, nitrogen is being evaluated against carbon (C) and oxygen (O) only, in this evaluation. These conditions are the worst possible, for EDS nitrogen detection; so the system's sensitivity has been optimized to nitrogen.

By a strict definition [2], total nitrogen concentration, in the presence of large carbon and oxygen peaks, can be resolved and quantified, via our EDS system software, down to about 4.8 percent. One can detect nitrogen in the spectra at lower concentrations, but not quantify it. Nitrogen resolution and quantification under the above conditions is almost entirely dependent upon relative amounts of N when comparing to defined amounts of both C and O (but more specifically C). With reduced amounts of C, nitrogen becomes more easily defined and quantified.

Many food additives, such as soy flour, soy protein, and gluten contain more than 5% N, meaning they are good candidates for this methodology. A primary advantage for EDS in these applications is that pyrolysis-based methods underestimate total N by 16-30% (when compared to that predicted by the molecular formula). Standard-based EDS methods match molecular formula predictions within a small margin for error. The obvious limitations for standard-based EDS nitrogen detection is that quantification is limited below 5% N content (for C, N, and O exclusive systems) because of non-resolvable [2] N peaks by quantification software routines. EDS is also limited by the number of samples that can be analyzed in a given period of time.

References:

[1] P. Williams, D. Sobering, J. Antoniszyn, Proc. of the Wheat Protein Symposium, Canadian Grain Commission, p. 37 (1998).

[2] J. Anzelmo, ICDD, Clinic on Practical X-ray Fluorescence Spectrometry (2009).

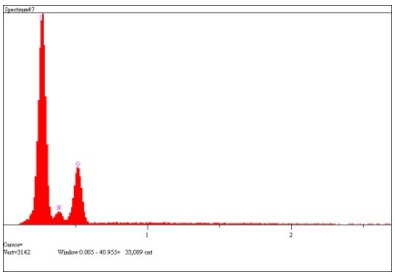

Figure 1: EDS X-ray spectra indicating quantifiable nitrogen.

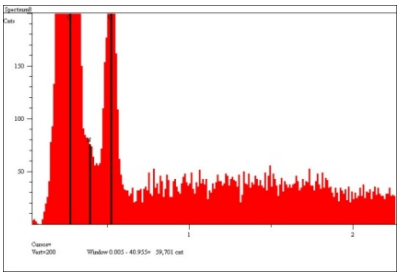

Figure 2: Expanded EDS spectra indicating non-quantifiable N.

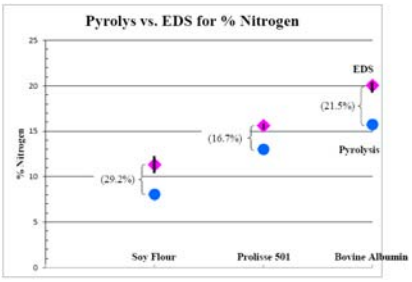

Figure 3: Standard-based EDS vs pyrolysis, total N analyses.

Micro-X-ray Fluorescence in Food Forensics

V.L. St. Jeor, A.R. Muroski, C. McGuire, A.D. Lape

Cargill Incorporated, Global Food Research, Advanced Analytics,
2500 Shadywood Rd., Excelsior, MN 55331

Abstract:

Food forensics has become a significant component of what Cargill does, both for its own needs, and for those of our customers. It is a field of science within Cargill that has developed over time as need arose. In the larger sense, it sports much of the same instrumentation used by those in criminal forensics. However, there are three basic objectives in food forensics: 1) identifying foreign material, or chemicals [1]; 2) genomics to track or identify genetically modified organisms and to trace the origins of seeds, food, or food ingredients [2]; and 3) answering "what went wrong" with some food or food system. For the latter it may be off color, off odor, the wrong viscosity, watering-off, the wrong texture, enzymatic or micro-contamination, the presence of sediment, a broken emulation, or any other of a nearly endless list of possibilities.

For example, a customer made the discovery of an odd, off-color anomaly within a batch of their chicken hotdogs. Because of a few iron filings discovered on a magnet (designed to remove such impurities from dried ingredients) and customer experience, it was assumed by the customer that iron filings must be at the heart of the discoloration. The customer was so certain of this conclusion that we were asked to do a forensics evaluation on their product *a third time*, when the first two evaluations turned up negative for iron filings. This presentation is the results of that third evaluation.

Here we identify, using micro-x-ray fluorescence (XRF), micro-XRF x-ray mapping, and visible spectroscopy, that iron is at least partly causal; but not iron in the form of iron filings as predicted by our customer. Rather, "heme" from myoglobin (bone marrow), an ingredient in the hotdog, seems to interact with iodine (possibly from the added salt) plus heat, to form the odd, green and red bull's-eye-shaped anomaly that proved so bothersome to our customer.

References:

[1] V.L. St. Jeor et al., Microsc. Microanal. **14**, Suppl. 2. 1120 (2008).
[2] M. Woolfe, S. Primrose, Trends Biotechnol. **22**(5**)**, 222 (1 May 2004).

Figure 1: Chicken hotdog with Red and Green anomaly.

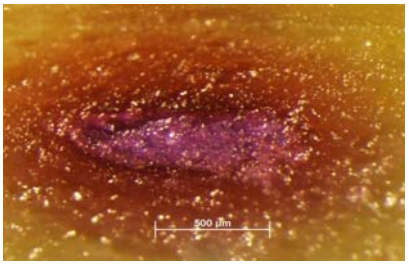

Figure 2: Anomaly in cross-section. Bar = 500µm.

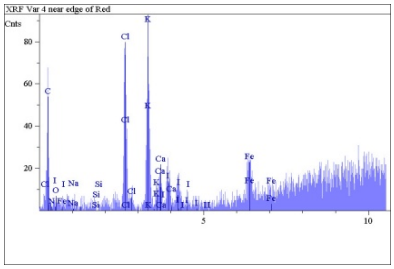

Figure 3: XRF results for the anomaly.

Ultrastructure of Frozen Hydrated *Chlamydomonas* Cells as Revealed by X-ray Tomography Using XM-2

A.D. Stead[1], C. Knoechel[2], D. Parkinson[2], C. Larabell[2]

[1]*School of Biological Sciences, Royal Holloway (Univ. London), Egham, Surrey, UK*
[2]*National Center for X-ray Tomography, Advanced Light Source, Berkeley, CA, USA*

Abstract:
Previous work using both soft x-ray contact microscopy [1,2] and transmission x-ray microscopy using XM-1 at the ALS [3] has revealed the presence of x-ray absorbing spherical structures within the cytoplasm of *Chlamydomonas* cells. The composition and function of these structures, which are not seen by transmission electron microscopy and are destroyed both by the commonly used EM fixatives and radiation damage [4], has remained a mystery although we have speculated that they may be related to the polyphosphate granules previously reported by some workers [5,6] or, as has recently been suggested, acidocalcinosomes [7,8]. Curiously, the limited elemental data we had obtained on the composition of the spheres, using XM-1, supports the idea that these structures are similar to acidocalcinosomes [9].

To obtain further information on the size and distribution of these structures we have employed tomography using XM-2 at the Advanced Light Source, Berkeley. Cells were encouraged into fine glass capillaries and rapidly frozen; after alignment, approximately 93 images were recorded through a 360^{o} rotation of the frozen specimen using the XM-2 microscope. In all, eight cells were imaged and reconstructions were made from these data sets. The reconstructions show the x-ray dense spheres are randomly distributed throughout the cell and are up to 2 μm in diameter; estimates suggest they may occupy up to 25% of the cell volume. Although structures believed to be the nucleus, chloroplast, and pyrenoid were identified, there seems to be no specific spatial relationships revealed between these organelles and the spheres; further improvements in aligning the images, coupled with segmentation by hand, might facilitate the identification of other sub-cellular organelles that are involved in the deposition or breakdown of these spheres, especially if they are polyphosphate granules.

In the future it is planned to image such cells across the phosphorus absorption edge and/or image cells grown under different nutrient regimes to try and determine the composition and function of these spheres. Such imaging may contribute to our understanding of the function of acidocalcinosomes that have proved impossible to study by conventional electron microscopy.

References:

[1] T.W. Ford, A.D. Stead, W. Myring et al., *X-Ray Microscopy II*, 403 (Berlin: Springer-Verlag, 1988).
[2] A.D. Stead, A.M. Page, T.W. Ford, Proc. SPIE **2523**, 40 (1995).
[3] T.W. Ford, W. Meyer-Ilse, A.D. Stead, AIP Conf. Proc. **507**, 119 (2000).
[4] T.W. Ford, A.M Page, W. Meyer-Ilse et al., *X-Ray Microscopy and Spectromicroscopy II*, 185 (Berlin: Springer-Verlag, 1998).
[5] M. Siderius, A. Musgrave, H. van den Ende et al., J. Phycol. **32**, 402 (1996).
[6] F.A. Ruiz, N. Marchesini, M. Seufferheld et al., J. Biol. Chem. **276**, 46196 (2001)
[7] K. Miranda, C.O. Rodrigues, J. Hentchel et al., Microsc. Microanal. **10**, 647 (2004).
[8] R. Docampo, P. Ulrich, S.N.J. Moreno, Philos. T. Roy. Soc. **365**, 775 (2010).
[9] K. Miranda, R. Docampo, O. Grillo et al., Protist **155**, 395 (2004).

Feasibility Study of X-ray Imaging with Near Carbon K-Shell Edges on *Deinococcus radiodurans*

K. Takemoto[1], I. Narumi[2], K. Satoh[2], T. Ohigashi[3], H. Kihara[1]

[1]*Department of Physics, Kansai Medical University, Hirakata, Japan*
[2]*Quantum Beam Science Directorate, Japan Atomic Energy Agency, Takasaki, Japan*
[3]*Ritsumeikan University Research Organization of Science and Engineering, Kusatsu, Japan*

Abstract:
In order to actually observe a cell in the living state using X-ray microscopy, an observation method needs to be optimized. We propose a new method for observing cells in the "carbon window" region (4.4 nm < λ < 5 nm), with energy slightly lower than that of the K-absorption edges of carbon, instead of the "water window" region (2.3 nm < λ < 4.4 nm) [1].

Using an antifreeze solution instead of water, it is possible to decrease the temperature of biological specimens to subzero temperature without freezing. The low temperature promises reduction of radiation damage to the biological specimens. Since organic matters are quite transparent in the carbon window region, a ***contrast enhancing labeling*** technique is applied. Using this method, the label material binding site is clearly visualized like the fluorescence of optical microscopy observation. In addition, since *Deinococcus radiodurans* has been known to withstand radiation levels up to 1,000 times the level that would kill normal human cells, X-ray imaging that makes *D. radiodurans* an observation object will be closer to living conditions.

The purpose of the study is to determine the feasibility of using X-ray microscopy in the carbon window region. Here, we will start with a simple case to consider the possibility of applying a material as a specific marker of the living *D. radiodurans* in the antifreeze solution monitored by X-rays. However, it is not yet clear whether *D. radiodurans* exhibits the radiotolerance at the carbon window region. We will also describe the radiotolerance of *D*. *radiodurans* at the carbon window region.

References:

[1] I.A. Aryukov, A.V. Vinogradov, Yu.S. Kas'yanov et al., Quant. Electron. **34**, 691 (2004).

Observations of Biological Specimens at Cryo Temperatures with Soft X-ray Microscopy at the SR Center of Ritsumeikan University

K. Takemoto[1], M. Kimura[1], K. Usui[2], T. Ohigashi[3], H. Namba[2], H. Kihara[1]

[1]*Department of Physics, Kansai Medical University, Osaka, Japan*
[2]*Department of Physical Science, Ritsumeikan University, Shiga, Japan*
[3]*Ritsumeikan University Research Organization of Science and Engineering, Shiga, Japan*

Abstract:

Soft X-ray microscopy is expected to be one of the promising tools for observing living cells with nm order resolution. However, in order to observe living cells, there are several problems to be solved. The most serious problem is radiation damage. Cryo-temperature X-ray microscopy is now accepted as the most useful tool for directly imaging living cells because the cryogenic technique promises reduction of radiation damage of bio-specimens.

Since 1996, we have been operating a transmission X-ray microscope at the SR center of Ritsumeikan University, Kusatsu, Japan [1]. It is capable of imaging specimens of several micrometers thickness. Our aim is also to observe living cells with the X-ray microscope. To reduce the damage from irradiation by X-rays, we have developed and installed a cryogenic sample chamber system to the X-ray microscope. This cryogenic system has been designed for observing bio-specimens at temperatures between 273 and 110 K. The details of the setup of the cryogenic system were reported at XRM 2008.

Using this system, we have successfully observed the first X-ray microscopic images of biological samples at cryo temperatures. However, we found several problems needed to be improved in order to achieve the satisfactory performance of the cryo-microscopy.

In this poster, we will show first cryogenic images of biological specimens, and we will report several problems of the present cryogenic system.

References:

[1] A. Hirai, K. Takemoto, K. Nishino et al., Jpn. J. Appl. Phys. **38**, 274 (1999).

Phase-Contrast Micro-CT for Studying Small-Animal Tumor Models

A. Tapfer[1], M. Bech[1], M. Willner[1], K. Achterhold[1], I. Zanette[2], T. Weitkamp[2], S. Stangl[3], G. Multhoff[3], M. Molls[3], C. David[4], J. Kenntner[5], J. Schulz[5,6], M. Walter[6], T. Grund[5], J. Mohr[5], F. Pfeiffer[1]

[1]*Department of Physics, Technical University Munich, 85748 Garching/ Munich, Germany*
[2]*European Synchrotron Radiation Facility, 38043 Grenoble, France*
[3]*Klinikum rechts der Isar, Technical University Munich, 81675 Munich, Germany*
[4]*Paul Scherrer Institut, 5232 Villigen-PSI, Switzerland*
[5]*Karlsruhe Institute of Technology, 76344 Eggenstein-Leopoldshafen, Germany*
[6]*Microworks, 76137 Karlsruhe, Germany*

Abstract:
One of the main limitations of absorption-based x-ray imaging of biomedical samples is the weak soft-tissue contrast. This limitation can be addressed by phase-sensitive imaging methods that provide considerably improved soft-tissue contrast. During the last decades various approaches have been investigated—amongst them grating-based interferometric imaging methods. Such a grating interferometer measures differential phase-contrast projection images and can be combined with quantitative computer tomography. The method can be applied to both synchrotron- and lab-based x-ray sources, which potentially allows for adapting the method to pre-clinical and clinical biomedical imaging applications. Here, we will report on recent laboratory- and synchrotron-based x-ray phase-contrast micro-CT results that investigate particularly the feasibility of visualizing and studying small-animal tumor models (in mice).

References:

[1] A. Momose, S. Kawamoto, I. Koyama et al, Jpn. J. Appl. Phys. **42**, L866 (2003).
[2] T. Weitkamp, A. Diaz, C. David et al, Optics Express **13**, 6296 (2005).
[3] F. Pfeiffer, T. Weitkamp, O. Bunk et al., Nature Physics **2**, 258 (2006).
[4] F. Pfeiffer, O. Bunk, C. David et al., Phys. Med. Biol. **52**(23), 6923 (2007).
[5] M. Bech, T.H. Jensen, R. Feidenhans'l et al., Phys. Med. Biol. **54**(9), 2747 (2009).

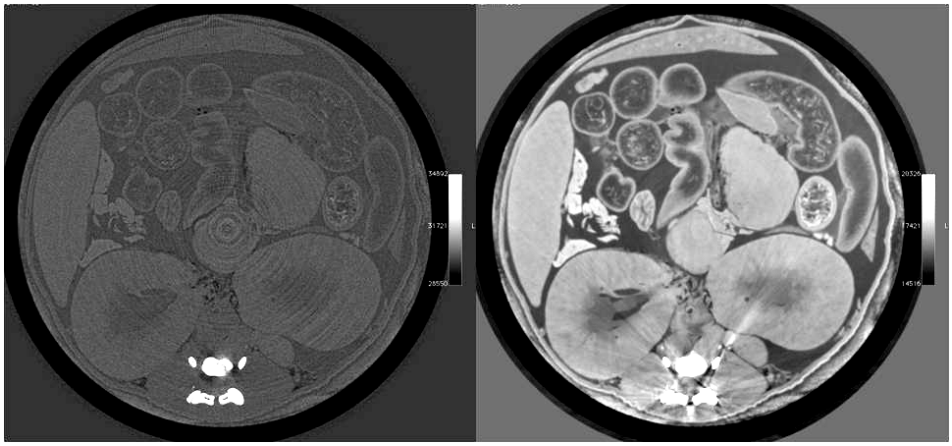

Figure 1: Axial slice through a reconstructed micro-CT scan of an *ex vivo* tumor-mouse at 35 keV (ID19, European Synchrotron Radiation Facility) demonstrating improved soft-tissue contrast for the phase image over the absorption image. Left: Standard absorption, right: Phase-contrast.

Structural and Quantificational Analysis of Eukaryotic Cells Using Soft X-ray Tomography

M. Uchida[1,2], G. McDermott[1,2], M. LeGros[2,3], C. Knoechel[1,2], C. Larabell[1,2,3]

[1]*Department of Anatomy, University of California San Francisco, San Francisco, CA, USA*
[2]*National Center for X-ray Tomography, Advanced Light Source, Berkeley, CA, USA*
[3]*Physical Biosciences Division, Lawrence Berkeley National Laboratory, Berkeley, CA, USA*

Abstract:
XM-2 at the Advanced Light Source of Lawrence Berkeley National Laboratory is the world's first soft X-ray microscope designed specifically for applications in cell biology. This new microscope produces 3D reconstructions of cells in a near native state at 50 nm isotropic resolution or better. To date, we have imaged a wide variety of specimens from bacteria, yeast to mammalian cells (e.g., *E. coli*, budding/fission yeast, T cells, and red blood cells) [1]. Here, we report the two examples of quantitative, high-resolution 3-dimensional imaging analyses of eukaryotic cells: 1) an evaluation of the cellular consequences of treating the fungal pathogen, *Candida albicans*, treated with candidate drug molecules [2] and 2) a study of organelle growth in relation to the cell growth during cell cycle in the budding yeast, *Saccharomyces cerevisiae* [3].

References:

[1] G. McDermott et al., Trends Cell Biol. **19**, 587 (2009).
[2] M. Uchida et al., Proc. Natl. Acad. Sci. USA **106**, 19375 (2009).
[3] M. Uchida et al., in preparation.

Figure 1: Segmented *C. albicans* hypha [1]. This is a pathogenic form of *C. albicans*. The one shown here is about 47 µm long. Unlike electron tomography, sectioning was not required to obtain the data set. Instead, five constitutive data sets were collected and stitched together.

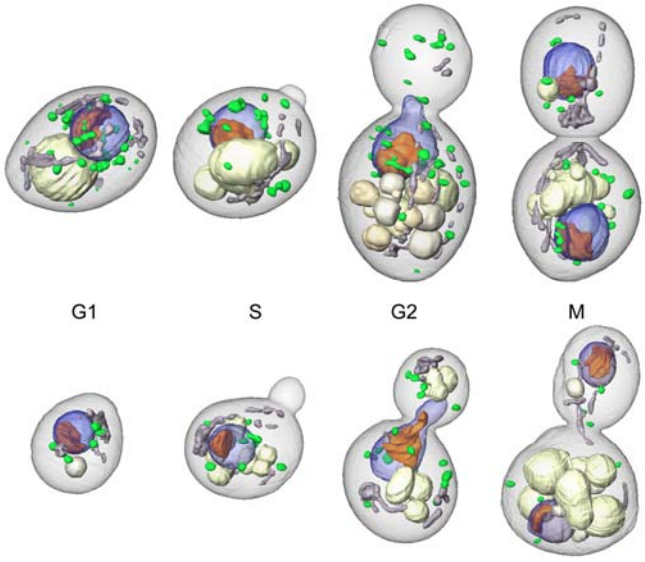

Figure 2: Representative of *S. cerevisiae* cells shown at different phase of cell cycle [3]. Top row represents diploid cells, and the bottom row represents haploid cells. Organelles are color-coded: nucleus, blue; nucleolus, orange; vacuoles, ivory; mitochondria, gray; lipid bodies.

Soft X-ray Tomography: A High-Resolution Modality for 3-D Biological Imaging

M. Uchida[1,2], D. Parkinson[1,2], C. Knoechel[1,2], M. Myllys[3], M. LeGros[2,4], M. Facciotti[5], G. McDermott[1,2], V. Sarafis[6], C. Larabell[1,2,3]

[1]*Department of Anatomy, University of California San Francisco, San Francisco, CA, USA*
[2]*National Center for X-ray Tomography, Advanced Light Source, Berkeley, CA, USA*
[3]*Department of Physics, University of Jyväskylä, Finland*
[4]*Physical Biosciences Division, Lawrence Berkeley National Laboratory, Berkeley, CA, USA*
[5]*Department of Biomedical Engineering, University of California at Davis, Davis, CA, USA*
[6]*Institute of Physical Biology, University of South Bohemia, Nove Hrady, Czech Republic*

Abstract:
Soft x-ray tomography is an exciting new modality for quantitatively imaging cell morphology and sub-cellular organization at high spatial resolution. Cells can be imaged intact, unstained, and fully hydrated. The resultant images are highly representative of the cells in their native, functional state. The contrast mechanism in soft x-ray tomography allows precise structural and quantitative analyses to be carried out. We will present data from a number of recent soft x-ray tomographic studies analyzing both prokaryotic and eukaryotic cells.

References:
G. McDermott, M.A. Le Gros, C.G. Knoechel et al., Trends Cell Biol. **19**, 587 (2009).

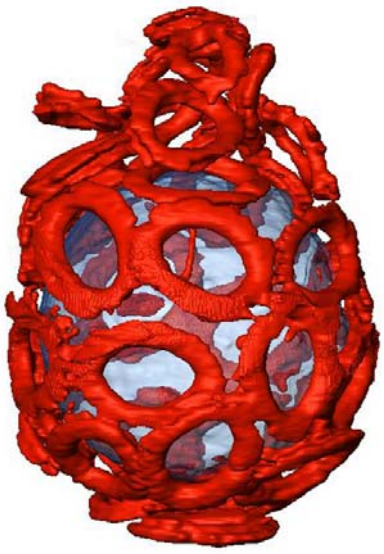

Figure 1: This image shows a segmented volume of *Emiliania huxleyi*. *E. huxleyi* is a marine unicellular alga (shown in blue) that is surrounded by the complex structures called coccoliths (shown in red). The size of *E. huxleyi* shown here is about 6 μm in diameter.

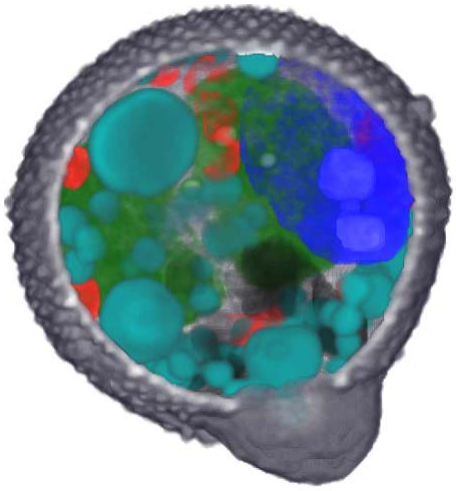

Figure 2: Volume rendered view of *Dawsonia superba*. The size of this spore shown here is about 8.0 μm in diameter. *D. superba* is known to be one of the largest mosses in the world. Inside of this reproductive structure, nucleus (blue), chloroplasts (green), lipid bodies (turquoise), and vacuoles (gray, orange) are visible.

X-Ray Fluorescence Imaging of Chelator-Treated Erythrocytes Infected with the Malaria Parasite *Plasmodium falciparum*

J. Ward[1], R. Marvin[2], S. Vogt[3], T.V. O'Halloran[2], J.E. Penner-Hahn[1]

[1]*Department of Chemistry, University of Michigan, Ann Arbor, MI, 48109, USA*
[2]*Department of Chemistry, Northwestern University, Evanston, IL, 60206, USA*
[3]*Advanced Photon Source, Argonne National Laboratory, Argonne, IL, 60439, USA*

Abstract:

Malaria is a blood-borne illness caused by protozoan parasites of the *Plasmodium* genus, the most deadly of which is *Plasmodium falciparum*. The disease causes 1-3 million deaths annually, mostly in impoverished nations [1]. Quinoline-based antimalarials such as chloriquine have enjoyed widespread use due to their low cost and high efficacy. However, the development of resistance to these antimalarials has driven research into alternative treatment routes.

Erythrocytes infected with *P. falciparum* are known to accumulate zinc 2-3 fold as the parasite matures [2]. We hypothesized that this zinc plays an essential role in the parasite's growth and survival, and that sequestering this zinc through the use of chelators would be an effective treatment strategy. Chelator treatment revealed that while membrane-impermeable chelators had little effect on parasite survival, membrane-permeable chelators caused a decrease in viability in proportion to their zinc-binding affinity.

X-ray fluorescence imaging was employed to determine the effect these chelators had on the zinc contents and distribution within the parasite. The X-ray maps reveal that both the membrane-permeable chelator TPEN and the membrane-impermeable chelator EDTA abolish zinc uptake, with a possible re-localization of zinc in the TPEN-treated case. Subsequent extended x-ray absorption fine structure (EXAFS) analyses of chelator-treated cultures reveal differences in zinc speciation between EDTA- and TPEN-treated conditions. Thus, while the parasite appears to be able to survive under low-zinc conditions, treatment with membrane-permeable chelators is associated with a dysregulation of zinc that may contribute to parasite mortality.

References:

[1] J.G. Breman, Am. J. Trop. Med. Hyg. **64**, 1 (2001).
[2] H. Ginsburg, R. Gorodetsky, M. Krugliak, Biochimi. Biophys. Acta, **886**, 337 (1986).

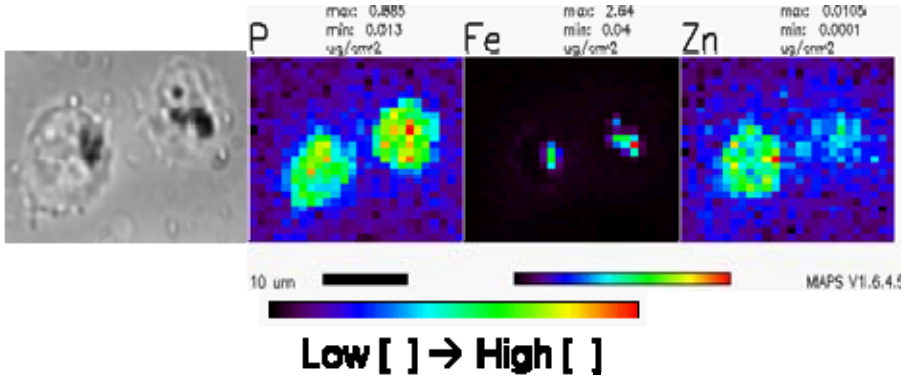

Figure 1: Typical X-ray fluorescence map of two erythrocytes infected with schizont-stage *P. falciparum*.

Application of X-ray Phase Contrast Microscopy to Xylem Cavitation and Water-Refilling in Plants*

Y. L. Xue, T. Q. Xiao**, C. Chen, Y. Q. Ren, Y. J. Tong, G. H. Du, H. J. Xu

Shanghai Institute of Applied Physics, CAS, 239 Zhang Heng Road, Pudong District, Shanghai, China

* Supported by the State Key Development Program for Basic Research of China (Grant No. 2010CB834301), the External Cooperation Program of the Chinese Academy of Sciences(Grant No. GJHZ09058), the National Natural Science Foundation of China (Grant Nos. 10805071, 10705020), and the Key Program for Basic Research of the Science and Technology Committee of Shanghai, China (Grant No. 08JC1411900).

** Corresponding author. E-mail: tqxiao@sinap.ac.cn.

Abstract:

Water transportation in plants and xylem cavitation and embolism are significant to the growth or even survival of plants. However, the mechanisms of these phenomena still remain unclear. Nowadays, it is a hot topic in the field of plant physiological and eco-physiology [1-3]. X-ray microscopy in phase contrast (XPCM) based on synchrotron radiation, owing to its high temporal and spatial resolution, has essential advantages over other methods in the investigation of water transport and xylem cavitation and embolism non-destructively and *in situ*. In this report, the dynamic processes of cavitation (shown in Figure 1) and water-refilling (shown in Figure 2) in rice and bamboo leaves were investigated utilizing XPCM at the Shanghai Synchrotron Radiation Facility (SSRF). The experiments revealed the mechanism of cavitation occurrence for the first time. It also gave two different processes of water-refilling under different kinds of drought stress. The results demonstrated that XPCM is a promising method to reveal the mystery of water transport and xylem cavitation and embolism in plants, which will be very beneficial to the research of the drought-resistant property of different crops and trees.

References:

[1] T. Hölttä, T. Vesala, E. Nikinmaa, J. Theor. Biol. **249**, 111 (2007).
[2] F. Y. Shen, R. F. Gao, W. J. Liu et al., Tree Physiol. **22**, 655 (2002).
[3] S.-J. Lee, Y. M. Kim, Ann. Bot. **101**, 595 (2008).

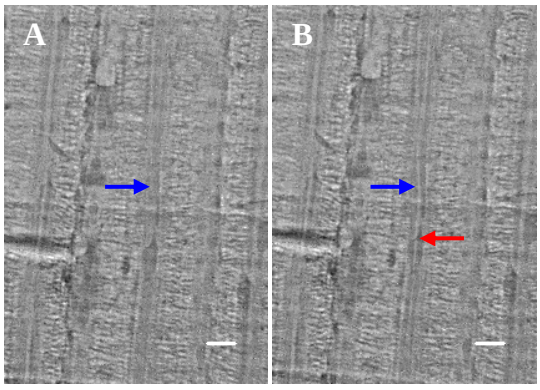

Figure 1: XPCM images of cavitation process. Scale bar=50 μm. A, B are two images recorded in sequence with an exposure time of 600 ms, in which the blue arrows indicate the contrast change after cavitation, while the red arrow points out the wall between two adjacent vessel elements.

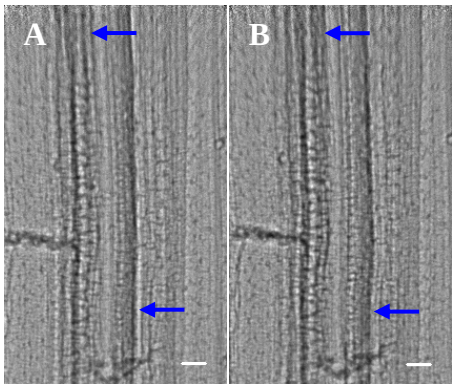

Figure 2: XPCM images of water-refilling process. Scale bar=50 μm. A, B are two images showing contrast changes of vessels after refilling, in which the arrows indicate the contrast change after water-refilling (air could enhance the contrast while water would blur it).

Uptake Mechanisms of EGFR-Targeted Nanoparticles

Y. Yuan[1], T. Paunesku[1], H. Arora[1], J. Ward[2], S. Raha[1], S. Vogt[2], G. E. Woloschak[1]

[1]*Northwestern University, 303 E. Chicago Ave., Chicago, IL, USA*
[2]*Argonne National Laboratory, 9700 S. Cass Ave., Argonne, IL, USA*

Abstract:
We are developing TiO_2 nanoconjugates (NCs) that can be used as therapeutic and diagnostic agents. Nanoscale TiO_2 can be surface conjugated with various molecules and has the unique ability to induce reactive oxygen species after radiation activation. The two major questions that we wish to answer are (1) how are NCs internalized by cells and (2) is targeting of NCs using a small peptide achievable. To address these questions, we have created NCs targeted to epidermal growth factor receptor (EGFR), which is enriched in many cancers of epithelial origin. Since EGFR is rapidly endocytosed upon ligand binding, we predict that targeting NCs to EGFR will increase internalization by certain cancer cells.

Previous reports have shown that a part of epidermal growth factor (EGF) known as the B-loop domain is required for binding EGFR. Therefore, we have selected eleven amino acids from this region and synthesized FITC-labeled, dopamine-conjugated peptides. These peptides were then used to treat HeLa cells as well as two isogenic colon cancer cell lines, one with high EGFR expression (SW480) and one with low EGFR expression (SW620). Immunofluorescent imaging of treated cells showed that FITC-labeled peptides colocalized with EGFR labeled with fluorescent antibodies on the cell surface and within the cytoplasm.

The synthetic EGF peptides were then conjugated to NPs via dopamine to create EGFR targeted NCs. These NCs also colocalized with EGFR in treated cells by immunofluorescence imaging. In addition, we used nano-gold labeled antibodies to target the cytoplasmic domain of EGFR. Finally, using x-ray fluorescence microscopy (XFM) we looked for overlap of gold and titanium. This was possible because XFM allows for direct detection of titanium as well as gold. These images showed that gold nanoparticles conjugated with anti-EGFR antibodies colocalized with titanium from TiO_2-EGF peptide nanoparticles at the cell surface.

Nanoparticles are a promising vehicle for the delivery of therapeutic and diagnostic agents to different cell types. Conjugating biomolecules that promote specific uptake and retention in tumor cells will allow for controlled drug delivery. As a first step, we have shown by light microscopy and XFM that EGFR targeted NCs can indeed bind to cell surface EGFR.

3D Visualization of the Microstructure of *Amphizoa davidi Lucas* Using Micro-CT

K. Zhang[1], D.-e Li[3], W. Huang[1], Q. Yuan[1], P. Zhu [1], H. Zhou[3],
J. Gelb[4], A. Tkachuk[4], W. Yun[4] , Z. Wu[1,2]

[1] *Institute of High Energy Physics, Chinese Academy of Science, Beijing 100049, China*
[2] *National Synchrotron Radiation Laboratory, University of Science and Technology of China, Hefei 230026, China*
[3] *Key Laboratory of Zoological Systematics and Evolution, Institute of Zoology, Chinese Academy of Sciences, Beijing 100101 China*
[4] *Xradia Inc., 4075A Sprig Drive, Concord, CA 94520, USA*

Abstract:

The investigation of the internal morphology of insects is usually performed using classical microtomy yielding optical micrographs of stained thin sections. It is time-consuming to obtain high quality cross-sections from microtomy, and sections can be damaged. This approach, therefore, is often impractical for those who need quick acquisition of three-dimensional structural information. Recently, x-ray micro-tomography (Micro-CT) as a potential tool for the morphologic classification of insects with sufficient spatial resolution was applied to observation and identification of the features of *Amphizoa davidi Lucas* at the cellular length scale, which provides a valuable new and non-destructive approach for the better understanding the three-dimensional structural information of biological organization [1,2]. The pilot experiments presented in the paper clearly revealed the differentiation of fine structural and morphologic details such as the abdomen with the intestine and the genital organs of the *Amphizoa davidi Lucas* with the full three-dimensional structure, and the alimentation system was also investigated and described in order to better understand to the evolution of the beetle .We can concluded that the spatial resolution and contrast condition of micro-CT imaging are quite promising for the new approach of zoological insect classification, especially for the classification of rare and precious insect specimen.

References:

[1] G. Hounsfield, Brit. J. Radiol. **46**, 1016 (1973).
[2] F. Peyrin, M. Salome, P. Cloetens et al., Technol. Health Care **6**(5-6), 391 (1998).

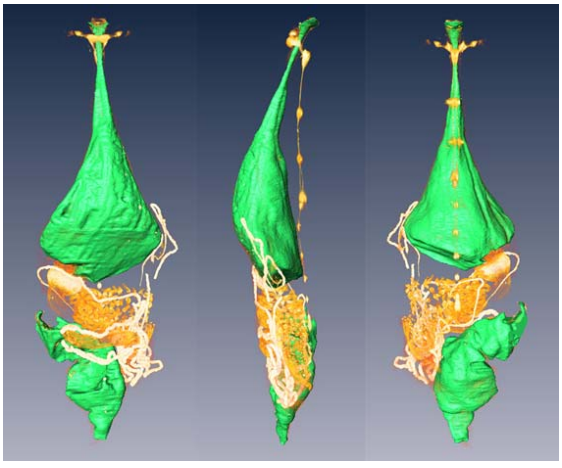

Figure 1: The alimentation system was reconstructed firstly.

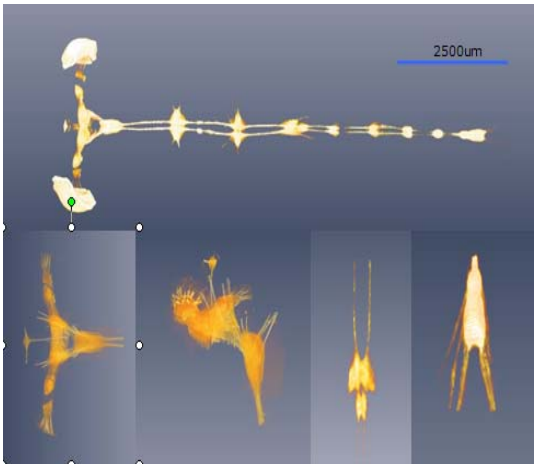

Figure 2: The nervous system of *Amphizoa davidi Lucas*.

Soft X-ray Spectromicroscopy to Study of Rubbery Polymer Nanocomposites

T. Araki, K. Fukumori, N. Suzuki, T. Mitsuoka

Toyota Central R&D Labs., Inc., Nagakute, Aichi 480-1192, Japan

Abstract:
Hydrogenated nitrile-butadiene rubber (HNBR) is widely used in the automotive industry for leak-free seals, gaskets, and hoses where resistance to aggressive chemicals and extreme temperature is required. To achieve the above demanding performance, HNBR is modified with cross-linking and the addition of fillers and additives used as polymer nanocomposites. It is important to study: 1) distribution of each component in the HNBR matrix and 2) cross-linking density to understand how the concentrations of cross-linker, fillers, and additives affect the physical properties of the rubbery polymer nanocomposites.

Scanning transmission x-ray microscopy (STXM) can provide images with both the high spatial resolution achieved by zone plate optics and the chemical sensitivity provided by NEXAFS spectroscopy [1]. Carbon-black-filled HNBR elastomers vulcanized with sulfur or peroxide cross-linkers was prepared and the STXM measurement of the cryo-microtomed thin section samples was carried out to obtain a quantitative compositional map. Preliminary STXM results of samples prepared with varying concentrations of cross-linker and carbon black will be presented.

References:

[1] H. Ade and A. P. Hitchcock, Polymer **49**, 643 (2008).

3D Laue Microscopy of Local Dislocation Densities and Elastic Strain Gradients in the Two-Phase Composites*

R.I. Barabash[1,2], G.E. Ice[2], W. Liu[3]

[1] *Materials Science and Technology Div., Oak Ridge National Laboratory, Oak Ridge, TN,USA*
[2] *Materials Science and Engineering Department, University of Tennessee, Knoxville, TN*
[3] *Advanced Photon Source, Argonne, IL, USA*

* Research supported by the Division of Materials Sciences and Engineering, U.S. Department of Energy. Data collection was carried out on beamline ID-34-E at the Advanced Photon Source.

Abstract:

To understand the small-scale mechanical behavior of composite materials, it is critical to develop techniques to characterize their defect distributions at appropriate length scales. Recently x-ray beams have become available with beam sizes down to ~100 nm. These small penetrating beams can be used to probe very small volumes of materials to determine local strain gradients and defect states. We show how 3D spatially-resolved polychromatic microscopy can be used to nondestructively obtain depth-dependent elastic strain gradients and dislocation densities in the constituent phases of a directionally solidified NiAl–Mo eutectic composite consisting of ~500-800 nm Mo fibers in a NiAl matrix [1-3]. Measurements were made before and after the composite was compressed by 5 and 11%. The Mo fibers were analyzed both in their embedded state and after the matrix was etched back to expose them as pillars. In the as-grown composite, due to thermal expansion mismatch, the Mo phase is under compression and the NiAl phase is in tension (Fig. 1). After the pre-strains, the situation is reversed with the Mo phase in tension and NiAl matrix in compression. The dislocation density in both the Mo and NiAl phases is found to increase after pre-straining (Fig. 2).

References:

[1] R. I. Barabash, H. Bei, Y. F. Gao et al., J. Mater. Res. **25,** 2, 199 (2010).
[2] H. Bei, R.I. Barabash**,** G.E. Ice et al., Appl. Phys. Lett. **93**, 071904 (2008).
[3] G.E. Ice, R.I. Barabash, in *Dislocations in Solids*, Eds. F.R.N. Nabarro and J.P. Hirth, Elsevier, **13**, 79, pp. 500-601, (2007).

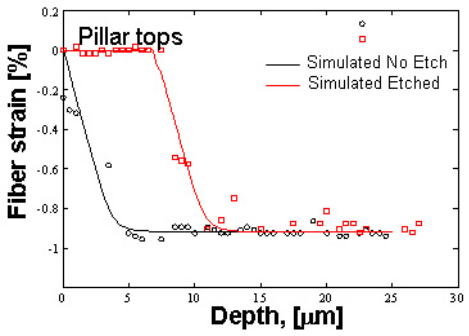

Figure 1: Measured by X-ray microscopy (symbols) and simulated (solid lines) strain in exposed and embedded Mo fibers

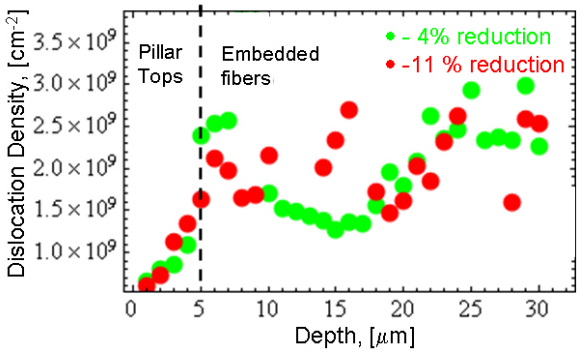

Figure 2: Dislocation density in exposed and embedded part of Mo fibers after 4% and 11% compression.

Soft X-ray Microscopic Investigation on Self-Assembling Nanocrystals

M. Benk[1], K. Bergmann[1], A. Querejeta[2], S. Srivastava[2], N. A. Kotov[2], D. Schaefer[3], T. Wilhein[3]

[1]*Fraunhofer Institute for Laser Technology, Aachen, Germany*
[2]*Department of Chemical Engineering, Materials Science and Engineering, and Biomedical Engineering, University of Michigan, Ann Arbor, Michigan, USA*
[3]*Institute for X-Optics (IXO), RheinAhrCampus, Remagen, Germany*

Abstract:

The assembly of nanoparticles to larger agglomerates is important to a variety of fields like environmental and colloidal science or nanoelectronics. Hyperbranched nanocrystals, for example, exhibit unique electronic and photonic properties. These properties enable realizing novel materials for future electronics and photonic devices [1]. High carrier mobility of these structures offers increase of efficiency and low cost production of hybrid solar cells [2]. A promising simple approach to produce hyperbranched nanocrystals and nanorods is spontaneous self-assembly from individual nanoparticels within a liquid media.

Variation in particle size and branching structure affect the performance of semiconductor material. Production of efficient nanostructures demands deep understanding of the underlying process.

Real-time imaging of self assembly and destruction of hyperbranched nanocrystals and nanorods in the liquid media can provide new information, complementary to static TEM images. Soft x-ray microscopy is a promising candidate to give this information by means of large penetration depth of soft x-rays into the liquid media, in comparison to electrons.

Within the scope of a preliminary experiment CdTe nanowires and hyperbranched PbS nanocrystals are imaged by means of soft x-ray microscopy applying a gas-discharge light source. Follow up experiments aim at time-resolved imaging of the growth of the structures in the liquid media using a table top setup with a wet specimen chamber.

References:

[1] Z. Tang, N. A. Kotov, M. Giersig, Science **297**, 237 (2002).
[2] I. Gur, N. A. Fromer, C.-P. Chen et al., Nanoletters **7**(2), 409 (2007).

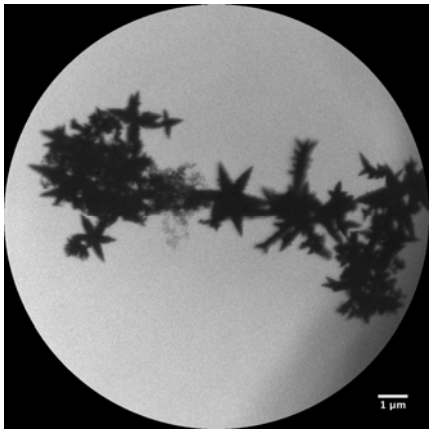

Figure 1: Self assembled hyperbranched PbS nanocrystals.

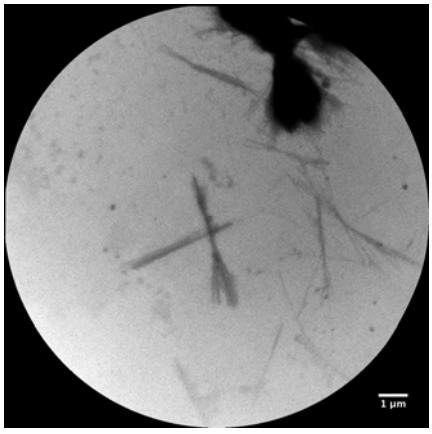

Figure 2: Self assembled CdTe nanowires.

Internal Strain Mapping of Zeolite Microcrystals by Coherent X-ray Diffraction Imaging*

W. Cha[1], S. Song[1], N. C. Jeong[2], R. Harder[3], K. B. Yoon[2], I. K. Robinson[4,5], H. Kim[1]

[1]*Department of Physics & Interdisciplinary Program of Integrated Biotechnology, Sogang University, Seoul 121-742, Korea*
[2]*Department of Chemistry, Sogang University, Seoul 121-742, Korea*
[3]*Advanced Photon Source, Argonne National Laboratory, Argonne, IL 60439, USA*
[4]*Department of Physics and Astronomy, University College, London WC1H 0AH, UK*
[5]*Diamond Light Source, Harwell Campus, Didcot, Oxford OX11 0DE, UK*

* This work was supported by National Research Foundation of Korea (Nos. 2010-0000112 and R15-2008-006-01001-0), Seoul Research and Business Development Program (10816), and Sogang University Research Grant (2009).

Abstract:

We measured coherent x-ray diffraction (CXD) on zeolite microcrystals in order to get information on internal density distribution and to learn about the strain developed during the synthesis and attachment process onto the substrate. Zeolites are a class of crystalline aluminosilicates having uniform and regularly spaced pores with the dimension of 0.3-1.5 nm. They have been widely used in industry as catalysis, ion exchangers, and adsorbents [1]. For such applications, zeolite crystals are used as membranes [2] and as an agglomerated form into small beads using inorganic binders.

When the object is illuminated by coherent x-rays, the oversampled diffraction pattern can be inverted to give real space images of the sample [3]. The experiments were performed at beamline 34-ID-C of the Advanced Photon Source, USA and employed monochromatic radiation with x-ray energy of 9 keV. The diffraction patterns were obtained at (200) and (020) Bragg condition with unfocused beam. From the distortion and asymmetry of the diffraction pattern, the strain field distribution is estimated. We inverted the diffraction patterns from a less strained crystal to obtain the three-dimensional image of the shape and internal strain fields using error reduction and hybrid input-output phase retrieval algorithms. We also show a few examples of characteristic distortion modes relevant to coherent x-ray diffraction of zeolites [4].

References:

[1] M.E. Davis, Nature **417,** 813 (2002).
[2] J.S. Lee, Y-J. Lee, E. Lee Tae et al., Science **301**, 818 (2003).
[3] M.A. Pfeifer, G.J. Williams, I.A. Vartanyants et al., Nature **442**, 63 (2006).
[4] W. Cha, S. Song, N.C. Jeong (unpublished).

Three-Dimensional High-Resolution Imaging of Nanoporous Gold Using Fresnel and Bragg Coherent X-Ray Diffraction Imaging

Y. K. Chen[1, 2], S. Kim[2], R. Harder[2], E. Lima[3], I. McNulty[2], D. C. Dunand[1]

[1]*Department of Materials Science and Engineering, Northwestern University, Evanston, IL, USA*
[2] *Advanced Photon Source, Argonne National Laboratory, Argonne, IL, USA*
[3] *National Synchrotron Light Source II, Brookhaven National Laboratory, Upton, NY, USA*

Abstract:

Nanoporous gold, with a large specific area and biocompatibility, has numerous potential applications ranging from catalysts, sensors, and electrodes to coatings for medical devices [1]. Nanoporous gold is created by a simple dealloying method, where silver from a silver-gold alloy is dissolved in an acid solution. The resulting sponge-like nanoporous structure consists of a network of nearly pure gold ligaments 5-30 nm in size [2].

Understanding the morphology of nanoporous gold provides information on the kinetics of pore formation and the materials properties. X-ray coherent diffractive imaging (CDI) provides the high spatial resolution necessary to study these complex structures. We studied the pore structure in 3D by Fresnel coherent diffractive imaging (FCDI) combined with tomography. To study the local 3D strain induced by dealloying, we imaged nanocrystals of silver-gold alloy using CDI in the Bragg geometry. The crystals were imaged before dealloying and at the early dealloying stage. The results from both methods will be discussed.

References:

[1] Y. Ding and M. Chen, MRS Bull. **34**, 8 (2009).
[2] J. Erlebacher, M. J. Aziz, A. Karma et al., Nature **410**, 450 (2001).

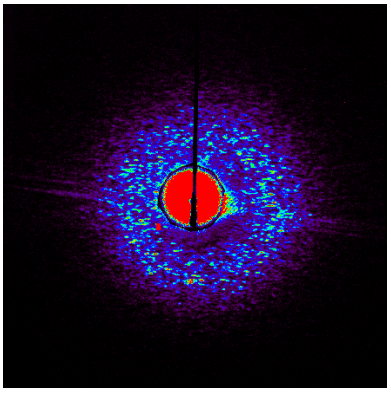

Figure 1: A Fresnel x-ray coherent diffraction pattern from a 1-μm nanoporous gold tip.

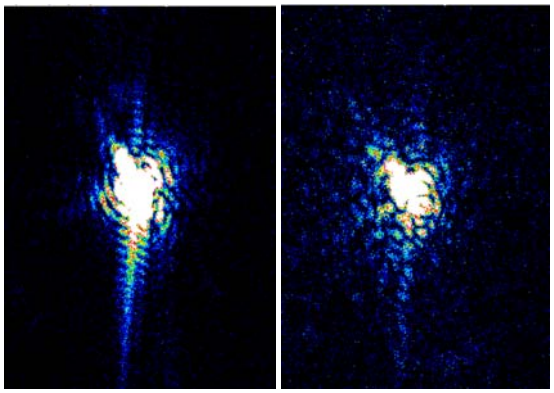

Figure 2: X-ray coherent diffraction patterns taken at Bragg geometry from a silver-gold nano-crystal before dealloying (left) and after 20 sec dealloying (right).

In situ Dynamics at the Advanced Photon Source X-ray Imaging Beamlines*

F. De Carlo[1], X. Xiao[1], K. Fezzaa[1], N. Chawla[2], F. Fusseis[3]

[1]*X-ray Imaging Group, Advanced Photon Source, Argonne National Laboratory, Argonne, IL*
[2]*School of Mechanical, Aerospace, Chemical, and Materials Engineering, Arizona State University, Tempe, AZ*
[3]*School of Earth & Environment, The University of Western Australia, Crawley, WA, Australia*

*Use of the Advanced Photon Source is supported by the U. S. Department of Energy, Office of Science, Office of Basic Energy Sciences, under Contract No. DE-AC02-06CH11357.

Abstract:

X-ray imaging at synchrotron facilities provides fast imaging with exposure times ranging from hundreds of milliseconds to 150 ps and for 2D and 3D spatial resolution ranging from a few microns to 30 nm.

In this poster we present the instrumentation available at the x-ray imaging beamlines of the Advanced Photon Source and the material science applications where the high-resolution, fast imaging systems were instrumental to extract *in situ* 4D dynamic information focusing on the study of deformation of SiC-particle-reinforced Al alloy matrix composites and on the formation of secondary porosity in natural rock samples. We will also present some examples of studies done with exposure time down to 100 ps and repetition rate up to ~ 0.5 million fps. These include fluid dynamics singularities [1,2], fuel injector inner dynamics [3], and rapid gasless reactions propagation [4].

The characterization of damage in materials is often conducted by mechanical testing followed by laborious cross-sectioning. X-ray tomography provides a perfect tool to characterize damage in materials non-destructively. In this talk, we report a novel methodology that addresses the critical link between microstructure and deformation behavior, by using the three-dimensional virtual microstructure obtained by x-ray tomography. The approach involves capturing the microstructure by *in situ* tensile testing, performing x-ray tomography, and incorporating the microstructure into a powerful finite-element modeling code for simulation. We will present a case study based on uniaxial tensile deformation of SiC-particle-reinforced Al alloy matrix composites. In particular, the evolution of damage in the form of particle fracture, interfacial debonding, and void growth will be described.

The fast x-ray imaging capability combined with *in situ* heating allowed us to investigate the formation of secondary porosity in natural rock samples [5]. By controlling the sample time-temperature history, we determined the effects of thermal expansion cracking on porosity in granite during progressive heating. The analysis of complex displacement fields in the acquired time-series dataset using a cross-correlation algorithm showed how cracks formed along grain boundaries and within grains, and interconnected during heating. A second set of heating experiments aimed at documenting the porosity evolution and fluid escape pathways during the dehydration of gypsum to basanite demonstrates how a permeable pore network formed and stabilized as the reaction progressed from the outside towards the center of a cylindrical sample.

References:

[1] Y. Wang K.-S. Im, K. Fezzaa, Phys. Rev. Lett. **100**, 154502 (2008).
[2] K. Fezzaa and Y. Wang, Phys. Rev. Lett. **100**, 104501 (2008).
[3] Y. Wang, X. Liu, K.-S. Im et al.. Nature Physics **4**, 305 (2008).
[4] R.V. Reeves, J.D.E. White, E.M. Dufresne et al., Phys. Rev. B. **80**, 224103 (2009).
[5] F. Fusseis, K. Regenauer-Lieb, J. Liu et al., Nature **459**, 974 (2009); DOI: 10.1038/nature08051.

Study the Relationship between Microstructure and Performance of Solid-Oxide Fuel-Cell Anode Using Nano-CT

Y. Guan[1], W. Li[1], Y. Gong[2], G. Liu[1], X. Zhang[1], J. Chen[1], Y. Xiong[1], H. Wang[2], Y. Tian[1]

[1]*National Synchrotron Radiation Laboratory, University of Science and Technology of China, Hefei, Anhui 230029, People's Republic of China*
[2]*Hefei National Laboratory for Physical Sciences at Microscale, University of Science and Technology of China, Hefei, Anhui 230026, People's Republic of China*
Email: ychtian@ustc.edu.cn

Abstract:
Solid Oxide Fuel Cells（SOFCs）are an exciting energy technology because of their high-energy conversion efficiency, environmental safety, and flexible fuel types. The ability to visualize the 3D dimensional micro-structure of an SOFC electrode is very important to understand the relationship between its complex microstructure and performance. This study details the utilization of a nano computed tomography (nano-CT) technique to image the 3D microstructures of a porous nickel-yttria-stabilized zirconia (Ni-YSZ) composite anode substrate based on the Ni K-absorption edge. Five samples of Ni-YSZ anode substrates were chosen to perform the thermal cycle to change its microstructure. The anode substrate was heated to 750oC, then kept at 750°C for 2 hours in a hydrogen atmosphere and finally cooled down to room temperature. The five chosen samples were exposed to 2, 4, 6, 8, and 10 times thermal cycles, respectively. The volume ratio of three phases (Ni, YSZ, and pore), volume-specific three-phase boundary, and other key structural parameters were obtained using the 3D reconstructions with 50 nm resolution. The volume percentages of Ni increased significantly from 11.1% (4 times thermal cycle) to 20.4% (8 times) while volume-specific TPB changed from 1.04×106 m/cm^3 to 2.66×105 m/cm^3. The effect of anode microstructures on performance can be explored and then used to optimize the performance of SOFC.

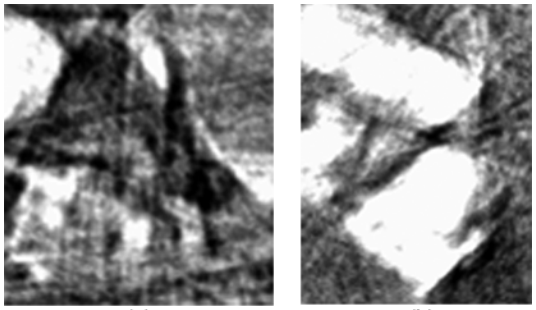

Figure 1: 2D slice image of anode substrates. (a) 4 times thermal cycle; (b) 8 times thermal cycle. The white portion is Ni.

Full-field X-ray Microscopy of TiO_2-Based Nanostructures

P. Guttmann[1], S. Heim[1], C. Bittencourt[2], X. Ke[3], G. Van Tendeloo[3], P. Umek[4], D. Arcon[4], C.P. Ewels[5]

[1]*Helmholtz-Zentrum für Materialien und Energie GmbH, Dep. Microscopy, Albert-Einstein-Str. 15, 12489 Berlin, Germany*
[2]*LCIA, University of Mons, Av. Nicolas Copernic 1, Mons, Belgium*
[3]*EMAT, University of Antwerp, Groenenborgerlaan 171, Antwerp, Belgium*
[4]*Institute Jozef Stefan, Jamova 39, Ljubljana 1000, Slovenia*
[5]*IMN, CNRS UMR6502, Université de Nantes, BP 32229, Nantes, France*

Abstract:
Low dimensional TiO_2-based materials have been successfully synthesized. These novel nanostructures bring to reality the possibility for fine tuning of chemical reactivity, as the system structure and the occupation of the outermost energy levels can be controllably tuned by changing preparation parameters.

In this work, electronic properties of individual $(Na,H)_xTi_3O_7$ nanoribbons (NR) (Fig.1) and $(Na,H)_xTi_3O_x$ nanoscrolls (NS) prepared through hydrothermal treatment of anatase TiO_2 were studied using TXM-NEXAFS at beamline U41-FSGM at BESSY II, Berlin [1]. For comparison reference samples (TiO_2 anatase and rutile, $SrTiO_3$) were used as models for the interpretation of the spectroscopic signatures. Ti $L_{2,3}$-edges were recorded in two experimental geometries: $\bar{E}$ parallel and perpendicular to the principal axis of the nanostructure (Fig. 2). This structure results from transitions to final state that are sensitive to deviations from Ti O_h symmetry [2]. The absence of splitting of e_g states suggests that for nanoribbon Ti occupies sites with high O_h symmetry in contrast to sites with distorted O_h symmetry in TiO_2-anatase. The electronic structure of the materials is discussed in terms of the crystal field splitting, and the hybridization between the transition metal and the ligand anions.

[1] S. Heim, P. Guttmann, S. Rehbein et al., Journal of Physics: Conference Series **186**, 012041 (2009).
[2] J. P. Crocombette, J. Phys.: Condens. Matter **6**, 10811 (1994).

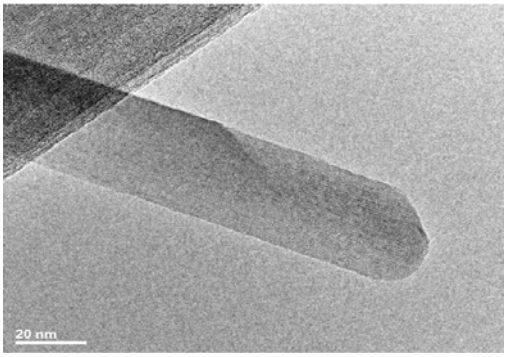

Figure 1: TEM image of an isolated TiO_2-based Nanoribbon showing the layered structure – Exposure to an electron beam leads, after a few minutes, to the collapse of the initial structure.

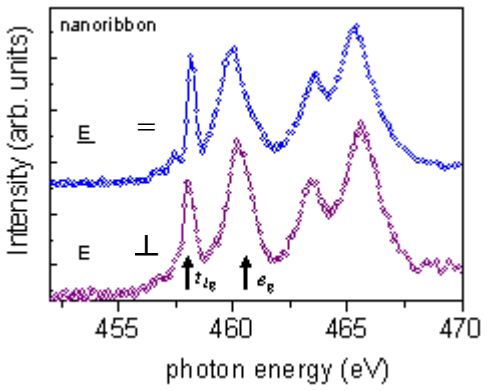

Figure 2: The Ti *L*-edges spectrum of the TiO_2-based nanoribbon recorded in two experimental geometries: E vector parallel (E∥) or perpendicular (E⊥) to the principal axis of the nanostructure.

STXM Investigations of *in situ*-Operated OFETs

C. Hub[1], S. Wenzel[1], J. Raabe[2], B. Watts[2], R. Fink[1]

[1]*Univ. Erlangen-Nürnberg, Egerlandstr.3, D-91058 Erlangen, Germany*
[2]*Paul Scherrer Institut, SLS, CH-5232 Villigen, Switzerland*

We acknowledge financial support from the BMBF (contract 05KS7WE1) and ICMM.

Abstract:
Ultrathin pentacene-based organic field-effect transistors (OFETs) on commercially available silicon nitride membranes suitable for transmission x-ray experiments were investigated. The devices produced by high-vacuum deposition show excellent electronic performance (μ = 0.6 cm² V^{-1} s^{-1}, $I_{on/off}$ = 10^6) comparable to state-of-the-art OFETs. STXM-experiments recorded with the PolLux-STXM at the Swiss Light Source [1] correlate structural and electronic properties at highest spatial and spectral resolution.

Local NEXAFS spectra were used to analyze the different orientations of the pentacene nanocrystals. We can prove that the NEXAFS contrast for individual microcrystals is due to azimuthal orientations of the crystallites. Since the overall thickness of the device is sufficiently thin, we can study the electronic properties of the device while it is in operation. Spectral changes during OFET operation can, however, hardly be detected with the current setup. We discuss potential reasons of this finding. Most probably, the local excitations (core-excitonic states) are not sensitive enough to the polarized state when the gate voltage is switched on. In addition, the applicable currents affect only 10^{-2} of the molecules located at the interface to the dielectric.

References:

[1] J. Raabe, G. Tzvetkov, U. Flechsig et al., Rev. Sci. Instrum. **79**, 11370 (2008).

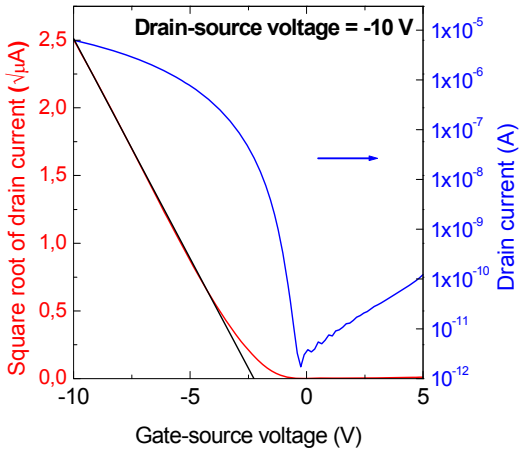

Figure 1: Device characteristics for a pentacene-based OFET using Si_3N_4 as dielectric thus allowing *in situ* STXM analysis.

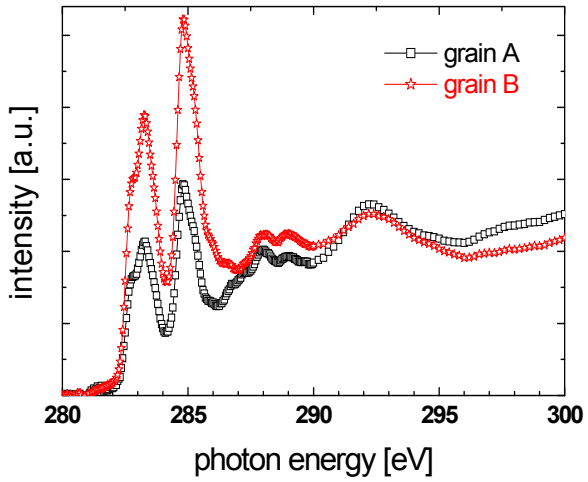

Figure 2: NEXAFS linear dichroism of individual crystallites of the pentacene-OFET. The effect is due to azimuthal orientations.

Selective Adsorption of Bbenzoic Acid Species on Patterned OH/Si(100) Surface

K. Ihm[1], K.-J. Lee [2], T.-H. Kang[1], S. Chung[2]

[1]*Pohang Accelerator Laboratory, Pohang, Kyungbuk 790-784, Korea*
[2]*Department of Physics, POSTECH, Pohang, Kyungbuk 790-784, Korea*

Abstract:
It has recently been observed that benzoic acid strongly reacts with OH group on the silicon surface. Here, by defining the area in which OH group is adsorbed on the Si surface, selective adsorption of benzoic acid species was attempted. The patterned OH/Si surface was prepared by irradiating the 0th order beam from the bending magnet of the synchrotron facility through the gold mesh placed in front of the OH/Si sample. For discerning the selectively adsorbed molecule by x-PEEM (x-ray photoelectron emission microscopy) at N k-edge, 4-NBA (4-nitro benzoic acid) was utilized instead of benzoic acid. NEXAFS (near-edge x-ray absorption fine structure) spectra at carbon and oxygen k-edges were in good accord with the previous results obtained from the BA (benzoic acid) system. The x-PEEM images around N k-edge clearly showed that the molecules adsorb only on the area in which OH groups remain.

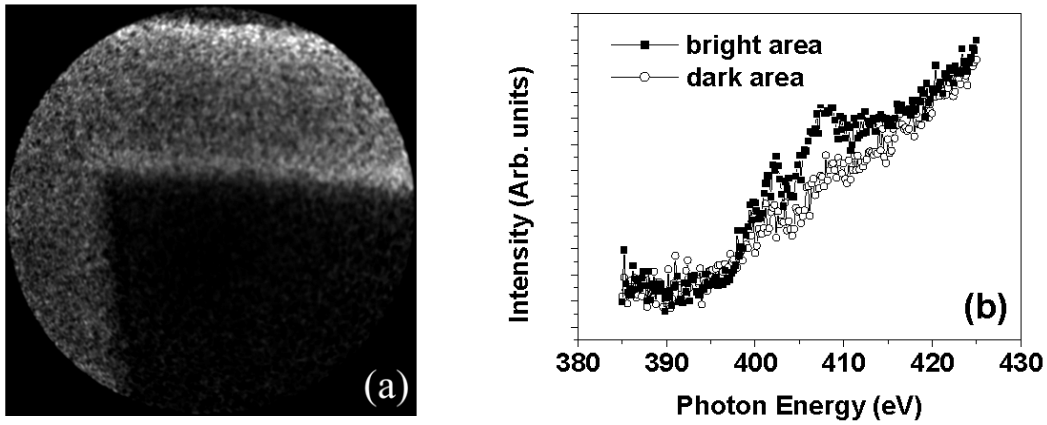

Figure 1: (a) X-PEEM image acquired by subtracting the image taken at 385 eV from the image taken at 408 eV. The field of view of the image was 20 μm. The bright region in the image shows the shape of a half part of mesh unit. (b) Spatially resolved absorption spectra around N k-edge acquired by extracting the intensity value from the images taken at the corresponding photon energies. The spectra represented by filled square and empty circle were extracted from the bright region and dark region, respectively.

Three-Dimensional Mapping of Pore Structure in Nanoporous Gold by Fresnel Coherent Diffractive Imaging

S. Kim[1], Y.K. Chen[2,1], X. Xiao[1], E. Lima[3], D. Vine[4,5], D.C. Dunand[2], I. McNulty[1]

[1]*Advanced Photon Source, Argonne National Laboratory, Argonne, IL, 60439, USA*
[2]*Department of Materials Science, Northwestern University, Evanston, IL USA*
[3]*Brookhaven National Laboratory, Upton, NY USA*
[4]*School of Physics, University of Melbourne, Melbourne, VIC Australia*
[5]*ARC Centre of Excellence for Coherent X-ray Science, Melbourne, VIC Australia*

* Use of the Advanced Photon Source is supported by the U.S. Department of Energy, Office of Science, Basic Energy Sciences, under contract No. DE-AC02-06CH11357.

Abstract:

Nanoporous metallic foams have potential applications as surface-chemistry-driven actuators, chemical sensors, catalytic conversion systems, and voltage-tunable components [1-2]. We investigated the porosity and density of dealloyed nanoporous gold by x-ray Fresnel coherent diffractive imaging at length scales inaccessible to lens-based x-ray imaging methods [3]. Use of a complex constraint in the reconstruction algorithm [4] enables quantification of the sample pore size distribution and density profile, parameters necessary to understand the kinematic mechanisms controlling formation and coarsening of nanoporous metals. Three-dimensional imaging by Fresnel coherent diffractive imaging is possible by combining a tomographically acquired series of two-dimensional FCDI reconstructions. This approach will give a complete picture of the nanofoam architecture—including pore curvature, distribution, shape, connectivity, and faceting—providing a deeper understanding of the formation and properties of metallic foams at the nanoscale.

References:

[1] J. Biener et al., Nature Mater. **8**, 47 (2009).
[2] J. Weissmuller et al., Science **300**,312 (2003).
[3] G.J. William et al., Phys. Rev. Lett. **97**, 025506 (2006).
[4] J.N. Clark et al., Opt. Express, **18**(3), 1981 (2010).

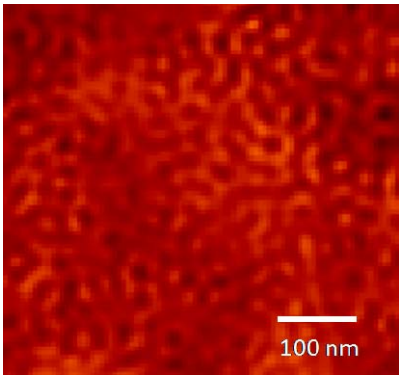

Figure 1: Pore structure in a dealloyed nanoporous gold sample imaged by **FCDI**.

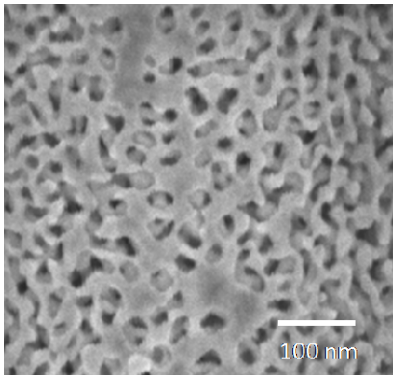

Figure 2: Sample surface imaged by Scanning Electron Microscopy (**SEM)**

A Powerful Tool for Nano Materials Structure Characterization

W. Li[1], J. Chen[1], Y. Guan[1], C. Wu[2], G. Liu[1], X. Zhang[1], Z. Wu[1], S. Yu[2], L. Guo[3], Y. Tian[1]

[1]*National Synchrotron Radiation Laboratory, University of Science and Technology of China, Hefei, Anhui 230029, P. R. China*

[2]*Division of Nanomaterials & Chemistry, Hefei National Laboratory for Physical Sciences at Microscale, University of Science and Technology of China, Hefei, Anhui 230026, P. R. China*

[3]*School of Materials Science and Engineering, Beijing University of Aeronautics and Astronautics, Beijing 100083, P. R. China*

Email: ychtian@ustc.edu.cn

Abstract:

It has been shown that x-ray nano-computed tomography (nano-CT), which combines the large penetration depth of hard x-rays with tomographic techniques [1,2], is a powerful tool to study the interior structures of microscale and nanoscale materials. Here, we report that the nanocomputed tomography (nano-CT) with 50 nm resolution at National Synchrotron Radiation Laboratory (NSRL) was used to reconstruct the three-dimensional (3D) structures of nanoscale materials and then offer important 3D information by the quantitative analysis of reconstructed data. For example, by the 3D reconstruction of copper sulfide crystals we understand that it is the cuboctahedron structure which has 14 faces comprising of six squares and eight triangles. Nano-CT is also suitable for imaging the interior of optically opaque nanomaterials such as polycrystalline hollow zinc oxide microspheres. Moreover, the reconstructed data can be used to quantitatively calculate the diameter, volume, porosity, and surface area of ZnO microspheres. 3D reconstruction of one nanomaterial sample (see Figure 1) clearly shows that the basic unit of their structure is the pyramid. Two pyramids make an octahedron while some pyramids grow and form the star-shaped structure. Some parameters such as the vertex angle and side length of the octahedron, volume of irregular snow-shaped structure, and surface area can be obtained based on the reconstructed data. These results indicate that nano-CT is a useful characterization method for analyzing internal structures of various nanomaterials.

References:

[1] J. Chen, C.Y. Wu, J.P. Tian et al., Appl. Phys. Lett. **92**, 233104 (2008).

[2] W.J. Li, N. Wang, J. Chen et al., Appl. Phys. Lett. **95**, 053108 (2009).

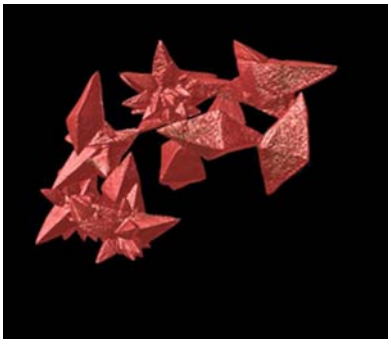

Figure 1: Three dimensional rendering of the 3-D tomographic reconstruction of sample.

X-Ray Linear Dichroism in Single-Walled Carbon Nanotube Bundles

E. Najafi[1], J. Wang[1], A. P. Hitchcock[1], J. Guan[2], S. Denommee[2], O. Bourne[2], B. Simard[2]

[1]*Brockhouse Institute for Materials Research, McMaster University, Hamilton, Ontario L8S 4 M1, Canada*
[2]*Steacie Institute for Molecular Sciences, National Research Council of Canada, Ottawa, ON*

Abstract:

The X-ray linear dichroism (XLD) of individual carbon nanotubes (CNT) [1] has been examined using scanning transmission X-ray microscopy (STXM) at the Canadian Light Source. The CLS STXM is sourced with an elliptically polarizing undulator (EPU) capable of orienting the E-vector of the light from –90° to +90° which allows high quality XLD imaging. Multi-walled CNT exhibit a very large XLD at 285 eV, the C 1s → π* transition, with strongest signal when E is perpendicular to the tube axis [1]. MWCNT have large diameters (40-80 nm) and thus are approximately rectangular arrangements of graphene sheets. This XLD signal correlates with structural defects and thus maps of its intensity can be considered as maps of sp^2 defects [1]. In contrast to MWCNT, single walled CNT have 1-2 nm diameter and thus very strong curvature. In fullerene, where there is also strong curvature, the local π-σ bonding and π*-σ* antibonding symmetry mixing is large [2]. Due to the large curvature of single-walled carbon nanotubes (SWCNT) and thus expected strong π-σ mixing, we had expected only a weak X-ray linear dichroism (XLD). However, C 1s STXM of SWCNT bundles (Figs 1 & 2) shows a strong XLD, of comparable intensity to that observed for MWCNT [3]. This suggests π*-σ* mixing in SWCNTs is much smaller than that in fullerenes.

STXM measurements were carried out at the SM beamline at the Canadian Light Source, which is supported by the Canada Foundation for Innovation (CFI), NSERC, Canadian Institutes of Health Research (CIHR), National Research Council (NRC) and the University of Saskatchewan. We thank Chithra Karunakaran, Martin Obst and Jian Wang for their expert support of the CLS STXM.

References:

[1] E. Najafi, D. Hernández Cruz, M. Obst et al., Small, **4**, 2279 (2008).
[2] S.M. Azami, R. Pooladi, M. H. Sheikhi, J. Mol. Struc.-Theochem. **901**, 153 (2009)
[3] E. Najafi et al., J. Am. Chem. Soc. (submitted).

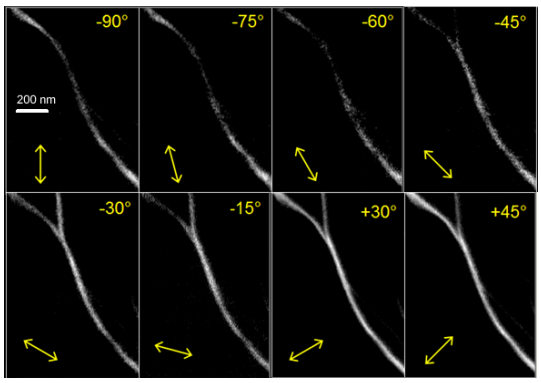

Figure 1: Images of the C 1s →π* intensity recorded for various polarization angles by STXM. The arrows indicate the orientation of the E-vector.

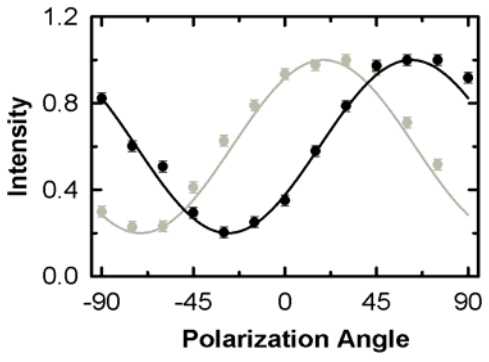

Figure 2: Continuum normalized C 1s →π* intensities derived from XLD stacks of SWCNT (gray) and MWCNT (black). The solid lines are fits to the XLD polarization function.

Coherent Synchrotron-Based Micro-Imaging Employed for Quantitative Studies of Micro-Gap Formation in Dental Implants

T. Rack[1], S. Zabler[2], A. Rack[3], M. Stiller[1], H. Riesemeier[4], K. Nelson[1]

[1]*Charité, Campus Virchow Clinic, D-13353 Berlin, Germany*
[2]*Technical University, Straße des 17. Juni 135, D-10623 Berlin, Germany*
[3]*European Synchrotron Radiation Facility, BP220, F-38043 Grenoble, France*
[4]*Bundesanstalt für Materialforschung und –prüfung, D-12200 Berlin, Germany*

Abstract:
The success rate of dental implants is often reported as "of the order 100%". Yet, this number only states that no revision was necessary within the first 5 years after implantation. On the long term a variety of failure scenarios are known which can cause a revision and / or implant loosening. Due to production limitations for these small devices, the joint between implant and abutment is characterized by a small micro-gap. Design, micro-gap and geometrical tolerances have a tremendous impact on the fatigue lifetime and on the cyclic deformation of dental implants under non-axial load.

Therefore, we investigated micro-gap formation at the implant-abutment interface of two-piece dental titanium implants *in vitro* under different mechanical loads. The aim of this study was to display the occurrence of micro-gaps for different two-piece dental implant designs with conical connections. Furthermore, the micro-gaps under different loads were studied in a quantitative manner, allowing for a correlation with, e.g., leak-proof tightness [1].

Experiments were carried out using high resolution radiography in combination with hard X-ray synchrotron radiation. Synchrotron-based radiography yields high spatial resolution together with high contrast even when exploiting micro-sized features in highly attenuating objects. Due to the coherence of the synchrotron light, even structures below the resolution limit of the imaging system can be detected by means of X-ray phase contrast. Adapted numerical routines are used to retrieve the real spatial dimensions of those features [2].

Several sets of radiographic projection images were acquired at the BAM*line* (BESSY-II light source, Helmholtz Zentrum Berlin, Germany). A micro-gap was detectable for all four different design systems under study. Its size naturally depends on the force as well as the angle under which the load is applied [3].

The existing designs for two-piece dental implants need to be enhanced in order to guarantee leak-proof tightness and therefore avoid microbial colonization of the internal cavity of the implant–abutment complex. Hence, there is room to further increase the success for two-piece dental implants [4].

References:

[1] A. Rack, T. Rack, M. Stiller et al., J. Synchrotron Radiat. **17**, 289 (2010).
[2] S. Zabler, H. Riesemeier, P. Fratzl et al., Opt. Express **14**, 8584 (2006); http://www.opticsexpress.org/abstract.cfm?URI=oe-14-19-8584.
[3] A. Rack, S. Zabler, B.R. Müller et al., Nucl. Instrum. Methods A **586**, 327 (2008).
[4] W. Semper, S. Kraft, T. Krüger et al., J. Dent. Res. **88**, 725 (2009).

Effect of Temperature on the Stability of Ga in ZnO

J. A. Sans[1], G. Martínez-Criado[1], J. Pellicer-Porres[2], J. F. Sanchez-Royo[2], A. Segura[2], J. Susini[1]

[1]*European Synchrotron Radiation Facility, 38043 – Grenoble, France*
[2]*Departamento de Física Aplicada-ICMUV, MALTA Consolider Team, Universidad de Valencia, 46100- Burjassot, Valencia, Spain*

Abstract:
Temperature can produce a drastic change in the electrical and optical properties of ZnO:Ga thin films during the deposition or during *ex situ* thermal annealing. The electron concentration drops by four orders of magnitude at 420°C (Figure 1) and the optical absorption edge recovers the undoped ZnO features. The phase diagram between ZnO-Ga_2O_3 proposed by G.B. Palmer and K.R. Poeppelmeier [1] showed the existence of an intermediate compound of cubic spinel $ZnGa_2O_4$. Temperature-dependent x-ray absorption spectroscopy and extended x-ray absorption fine structure were used in order to study the influence of the thermal annealing under oxidizing conditions. The results exhibited the increase of the proportion of Ga in the octahedral coordination [2]. Furthermore, x-ray linear dichroism spectroscopy (Figure 2) and extended x-ray absorption fine structure studies were carried out to examine the effect of the growth temperature in the crystalline structure. The use of these techniques allowed assigning the unexplained variations of the electrical and optical properties to the formation of a mixture of intergrowth phases of cubic spinel $ZnGa_2O_4$ and ZnO:Ga. This argument can be applied to the increase of Ga content in the octahedral coordination obtained from the thermal annealing under oxidizing conditions.

References:

[1] G. B. Palmer and K. R. Poeppelmeier, Solid State Sci. **4**, 317 (2002).
[2] J. A. Sans, G. Martínez-Criado, J. Pellicer-Porres et al., Appl. Phys. Lett. **91**, 221904 (2007)
[3] J. A. Sans, G. Martínez-Criado, J. Pellicer-Porres, J. F. Sánchez-Royo, and A. Segura (sent to Appl. Phys. Lett.).

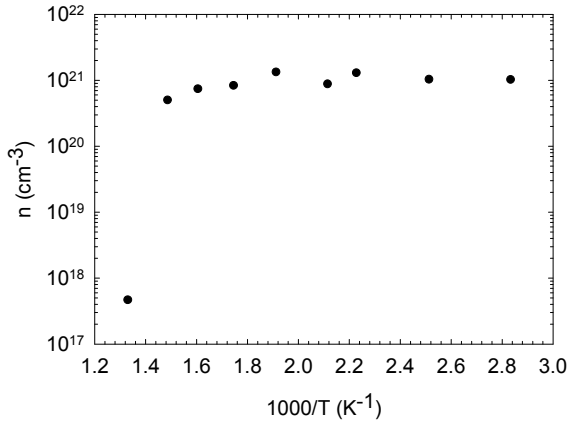

Figure 1: Carrier concentration versus annealing temperature.

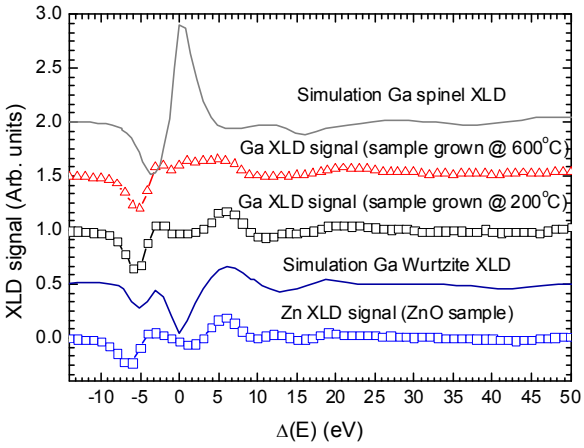

Figure 2: XLD signals at Ga and Zn K-edge of samples grown at low and high temperature. Theoretical simulations (FEFF code) of Ga in Wurtzite and spinel structure were included.

Interfacial Diffusion in ZnO Grown on Sapphire

J. A. Sans[1], G. Martínez-Criado[1], J. Szlachetko[1,2], M. Feneberg[3], K. Thonke[3], G. Almonacid[4], A. Segura[4]

[1]*European Synchrotron Radiation Facility, 38043 – Grenoble, France*
[2]*Institute of Physics, Jan Kochanowski University, Kielce, Poland*
[3]*Institut für Halbleiterphysik, Universität Ulm, 89069- Ulm, Germany*
[4]*Departamento de Física Aplicada-ICMUV, MALTA Consolider Team, Universidad de Valencia, 46100- Burjassot, Valencia, Spain*

Abstract:
Unintentional doping of samples can introduce undesired results in the manufacture of thin films-based optoelectronic devices. For instance, the incorporation of Al into ZnO coming from sapphire substrate has recently triggered the attention of several studies [1,2]. Thin ZnO films with and without a GaN buffer layer were deposited on sapphire substrates by a modified chemical vapor deposition process at low and high temperatures. Cathodoluminescence measurements along the cross-section showed a red-shift of the emission peak close to the ZnO/GaN interface [3]. Such variation was explained by the Ga diffusion into ZnO. However, there is no unambiguous evidence so far about the chemical composition. In the present experiment, the wavelength dispersive spectrometer of beamline ID21 of the ESRF was used to examine spatially the investigated interfaces. The spectral resolution was about 20 eV in the energy range from 1 keV to 1.5 keV. Figure 1 shows the inclusion of Al inside the ZnO thin film going through the GaN buffer layer for the sample grown at high temperature. The use of high spectral resolution is justified in Figure 2, where it was necessary in order to resolve unequivocally the overlapping x-ray fluorescence lines of Zn, Ga, and Al. The effect of the deposition temperature is displayed in the inset of Figure 2, an increase in the amount of Al diffused into the ZnO layer is observed when the growth temperature increases.

References:

[1] G.-Y. Huang, C.-Y. Wang, J.-T. Wang, J. Appl. Phys. **105**, 073504 (2009).
[2] R. S. Wang and H. C. Ong, J. Appl. Phys. **104**, 016108 (2008).
[3] R. Schneider, M. Schirra, A. Reiser et al., Appl. Phys. Lett. **92**, 131905 (2008).

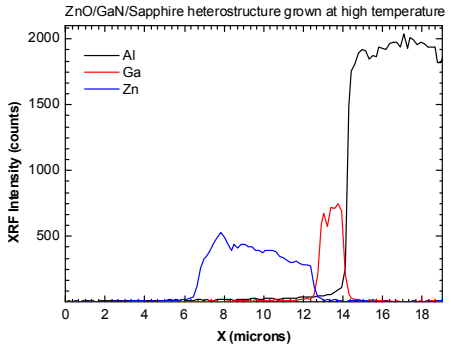

Figure 1: Distribution of XRF signals along the cross-section of the sample with buffer layer grown at high temperature.

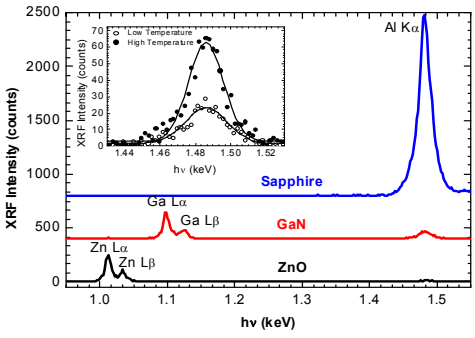

Figure 2: XRF spectrum measured in the different materials that compose the heterostructure. Inset: Comparison between Al signal inside ZnO for sample grown at high (●) and low (○) temperatures.

Seeing and "Feeling" Polymer Blends on a Nano-Scale

I. Schmid[1], J. Raabe[1], R. Fink[3], S. Wenzel[3], H. Hug[2], C. Quitmann[1]

[1]*Swiss Light Source, Paul Scherrer Institut, 5232 Villigen – PSI, Switzerland*
[2]*Empa, Überlandstrasse 129, 8600 Dübendorf, Switzerland*
[3]*Univ. Erlangen-Nürnberg, Egerlandstrasse 3, 91058 Erlangen, Germany*

Abstract:

NanoXAS is a novel x-ray microscope combining laterally resolved soft x-ray spectroscopy and scanning probe microscopy. We report on first results from thin polymer blend films and magnetic materials.

The instrument uses Fresnel zone plates to focus x-rays (100 – 1800 eV) onto a semi-transparent sample which is raster scanned through the beam. As in a STXM the transmitted x-rays are measured by a photodiode providing a transmission image.

As a novelty a scanning probe microscope (SPM) is looking on the downstream side of the sample. It provides additional morphological information by imaging sample topography, the so-called phase contrast, which mainly arises from viscoelastic and adhesion sample-tip interaction. Furthermore the SPM tip can be used to collect the photoelectrons produced upon x-ray absorption in the sample [1].

As a first example (Fig. 1) we show results for a polymer blend (80% PMMA, 20% PS, spin cast onto SiN membrane, annealed 170°C / 1 h). All images were taken on the same sample *in situ*. The x-ray transmission image (left) shows PS islands (yellow) embedded in the PMMA-matrix. These islands have a height of about 45 nm as seen from the SPM topography (center).

Combining spectroscopic information from the x-rays with SPM data provides detailed information about the self-organization in such phase separated blends, in particular on defects, which are seen as dark spots on top of the PS islands (center) and differences between the bulk (STXM) and surface structure (SPM).

Experience detecting photoelectrons with the SPM tip as well as local conductance map results will be presented for polymer blends and for mesoscopic magnetic structures.

References:

[1] I. Schmid et al., Ultramicroscopy (submitted).

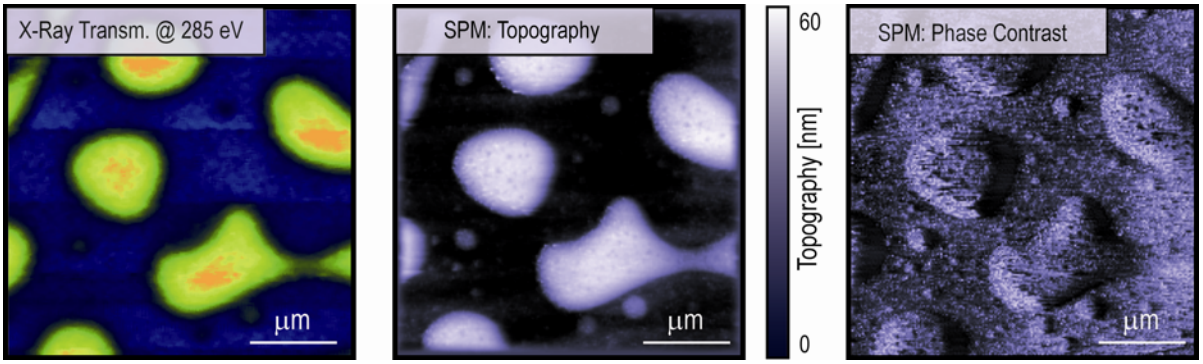

Figure 1: Polymer blend imaged in the NanoXAS instrument showing x-ray transmission (left), SPM topography (center) and SPM-phase contrast (right). All images were taken *in situ*.

Characterization of Microstructured Optical Arrays (MOAs)

M. T. Shand[1], G. R. Morrison[1], A. G. Michette[1], D. Hart[1], S. J. Pfauntsch[1], T. Stevenson[2], W. Parkes[2], C. Dunare[2], R. Willingale[3], C. Feldman[3], T. Button[4], C. Meggs[4], D. Rodriguez-Sanmartin[4]

[1]*King's College London, Department of Physics, Strand, London, UK*
[2]*Scottish Microelectronics Centre, University of Edinburgh, Edinburgh, UK*
[3]*The University of Leicester, Department of Physics and Astronomy, Leicester, UK*
[4]*The University of Birmingham, Department of Metallurgy and Materials, Birmingham, UK*

Abstract:
Microstructured optical arrays (MOAs) are currently in development as part of the UK Smart X-ray Optics consortium [1]. The active area of an MOA consists of a 1-D array of channels, each only a few microns wide, etched through a silicon wafer [2]. Single grazing-incidence reflections from the internal walls of the channels can be used to redirect X-rays to a focus, providing 1-D line focusing. Curvature can be introduced across the wafer by using piezoelectric actuators bonded to the surface, leading to active control of the grazing angle and therefore the focal length. Reflections from two arrays operated in tandem will enhance the focused flux by reducing the grazing angle for each reflection, allowing channels at the outer edges of the active area to contribute more effectively to the focus [3]. The reflective nature of MOAs also suggests a microprobe can be formed using a broadband source, further increasing the focused flux.

The performance of single-reflection, unactuated MOAs can be evaluated by tracing the ray path from a point source of X-rays through the channel structure onto a linear CCD array. Translation of either the MOA wafer or CCD along the optical axis provides valuable information about the focusing properties. Simulations of the intensity profile projected from a point source on to the CCD plane allow the relative contributions of the reflected and unreflected components to be distinguished, which greatly aids the interpretation of experimental observations. This is especially useful when considering the focusing behavior of the MOA for an extended object, where there is an asymmetry in the reflected component for off-axis object points

References:

[1] A.G. Michette et al., J. Phys.: Conf. Ser. **186**, 012067 (2009).
[2] C. Dunare et al., Proc SPIE **7360**, 736015 (2009).
[3] A.G. Michette et al., Proc SPIE **6705**, 670502 (2007).

Specific Stainless Identification Using Micro-X-ray Fluorescence

V.L. St. Jeor, A.D. Lape

Cargill Incorporated, Global Food Research, Advanced Analytics,
2500 Shadywood Rd., Excelsior, MN 55331

Abstract:

Nothing is worse than finding contaminating foreign material (FM) in the food we eat. Food producers, food ingredient producers, and processers go to great lengths to prevent foreign materials from entering food and food ingredients. And, should something find its way into the food, great efforts and expense are used to identify it, remove it, and to trace the source to eliminate future contamination. These efforts amount to a significant portion of the total costs required to bring food to market.

The four most often asked *customer* questions for Metal FM are:

What is the FM? Example response: Metal (via SEM backscattered mode).

What metal is it? Example response: Stainless steel (via EDS).

Which stainless steel? Answered via micro-XRF and submitted known potentials.

Where did it come from? This usually means "your facility or ours?"

Question #3 has traditionally been the most difficult to answer. Generally speaking, metal FM is a very small (<1 mm) fleck, with most examples being on the order of 50-100 µm. Most traditional tests used to identify specific metals [1] are of no use with such small examples. However, x-ray fluorescence holds the potential to identify minor components within the metal including relative amounts, which can help identify a specific source. And, although more traditional x-ray fluorescence is often too bulk-oriented to be of value with these small flecks, we have found that micro-x-ray fluorescence can frequently provide the needed sensitivity, when comparing the unknown FM to a collection of possible known sources obtained from the customer. Advances in the technology, such as being able to bring a stream of x-rays to a focal point, are invaluable. The small probe sizes associated with x-ray tubes used for micro-XRF usually allow clean spectra from very small unknowns without the background associated with EDS and often without interference from surrounding materials.

References:

[1] http://www.astm.org

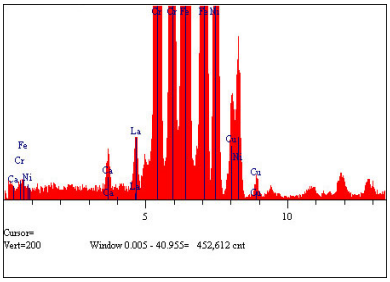

Figure 1: A micro-XRF spectrum of an unknown Stainless fleck.

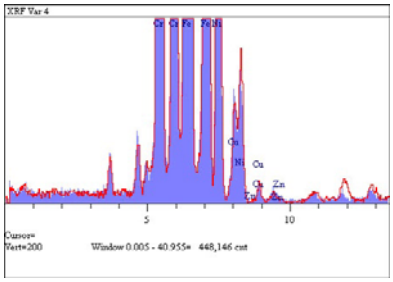

Figure 2: Unknown overlaying a customer-provided known.

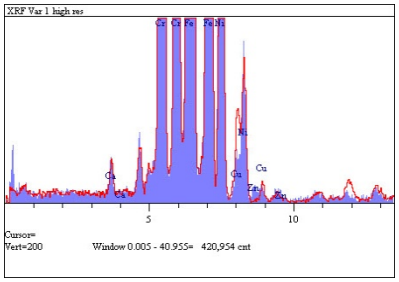

Figure 3: Unknown overlaying a 2nd customer-provided known.

Figure 2 is more consistent with the unknown than Figure 3.

Elastic Strain Relief in a Single Lithographic SiGe Nanostructure by Nanobeam X-ray Diffraction

A. Tagliaferri[1,3], D. Chrastina[2], G. M. Vanacore[1,3], M. Zani[1,3], M. Bollani[2,3], S. Schroder[4], M. Burghammer[4], P. Boye[5], G. Isella[2,3], R. Sordan[2]

[1]*Dipartimento di Fisica, Politecnico di Milano, Piazza Leonardo da Vinci 32, I-20133 Milano, Italy*
[2]*L-NESS, Dipartimento di Fisica del Politecnico di Milano, Polo Regionale di Como, Via Anzani 42, I-22100 Como, Italy*
[3]*CNISM, Via della Vasca Navale, 84 - 00146 Roma*
[4]*European Synchrotron Radiation Facility, B.P. 220, F-38043 Grenoble Cedex, France*
[5]*Institute of Structural Physics, TU Dresden, D-01062 Dresden, Germany*

Abstract:

Nanofabrication techniques such as electron-beam lithography (EBL) are able to define $Si_{1-x}Ge_x$/Si MOSFET channel widths down to the limit for carrier confinement (~5 nm). In this regime, the channel strain depends also on the lateral boundary conditions due to elastic and plastic relaxation, resulting in uniaxial strain and even higher mobility enhancements [1]. X-ray diffraction (XRD), the conventional method for accurately determining composition and strain in $Si_{1-x}Ge_x$ heterostructures, usually averages over several square mm [2] and is therefore not sensitive to such nm-scale variations of strain. Recently, the use of refractive lenses and synchrotron sources [3,4] has allowed nanoscale XRD of self-assembled $Si_{1-x}Ge_x$ quantum dot structures [4,5].

We present nanoscale XRD on single $Si_{1-x}Ge_x$/Si nano-ridges (x=12% and width between 1 and 2 hundred nm) and on steps fabricated by EBL. We made use of innovative refractive x-ray optics for the characterization of single nanostructures in a "top-down" approach. The experiment has been performed at the Nanofocus extension of the ID13 beamline at the ESRF, with an x-ray spot size of 100 nm. The setup allows us to determine the lattice parameter inside the nano-ridges and as a function of the position across the steps, thus investigating the lateral variations in strain, i.e., the elastic strain relief within the structures. The comparison of the data with kinematical simulations performed on data extracted from finite element modeling (FEM) of the nanostructures (based on their actual geometries as measured by atomic force microscopy) allows a stringent validation of the FEM and a complete mapping of the elastic strain relief resulting from the nano-patterned geometry.

The measured degree of elastic relaxation is quantitatively significant (~50%) in the nano-ridges, and extends on a spatial length of about 1 micron from the edge of the steps. This result is important in view of the exploitation of $Si_{1-x}Ge_x$/Si nanostructures as channels and controlled strain substrates in the electronics industry.

References:

[1] L. Yeh, M.H. Liao, C.H. Chen et al., IEEE T. Electron Dev. **56**, 2848 (2009).
[2] T. Mizutani, O. Nakatsuka, A. Sakai et al., Solid State Electron. **53**, 1198 (2009).
[3] C.G. Schroer, P. Boye, J.M. Feldkamp et al., Phys. Rev. Lett. **101**, 090801 (2008).
[4] M. Hanke, M. Dubslaff, M. Schmidbauer et al., Appl. Phys. Lett. **92**, 193109 (2008).
[5] M.S. Rodrigues, T.W. Cornelius, T. Scheler et al., J. Appl. Phys. **106**, 103525 (2009).

In Situ Study of Energy Materials and Microelectronics by Transmission X-ray Microscopy (TXM)

J. Wang[1], Y. S. Chu[1], K. Evans-Lutterodt[1], A. Lanzirotti[1], J. Dvorak[1], L. Berman[1], S. Hulbert[1], C.-C. Kao[1], M. Feser[2], A. Tkachuk[2]

[1]*Brookhaven National Laboratory, Upton, NY 11973, USA*
[2]*Xradia, Inc., Concord, CA 94520, USA*

Abstract:
In recent years, hard x-ray imaging has found tremendous application in many scientific disciplines. The increasing scientific demand for 2D and 3D x-ray imaging is primarily related to the use of higher spatial resolution, higher energies for larger penetration depths, higher sensitivity using differential absorption and phase contrast, and faster imaging for investigation of dynamics [1]. At the National Synchrotron Light Source (NSLS), in collaboration with Xradia Inc., we are developing a transmission x-ray microscope (TXM) for 2D and 3D x-ray imaging at the nanometer scales. The microscope will perform tomography with both absorption and Zernike phase-contrast capabilities, operating in the energy range of 5 keV to 11 keV with spatial resolution down to ~30 nm. This new imaging capability is expected to find a broad range of applications for solving important problems in energy storage materials, biofuels, and microelectronics systems. The new TXM will be an excellent match to the NSLS-II mission and will be moved to NSLS-II in the future.

In this paper, we present the conceptual design of the new TXM and its integration with the X8C at NSLS. Expected performance of the instrument at NSLS-II will also be presented, along with several potential application examples.

References:
[1] Y. S. Chu et al., Appl. Phys. Lett. **92**, 103119 (2008).

Elemental Mapping of Ancient Glass Eye-Bead Using SRXRF *

Z. Xie[1], X. X. Zhang[2], X. C. Zhang[2], Z. Y. Pan[1,†], Y. H. Peng[1], F. C. Hu[1],
X. H. Yu[3], K. Yang[3], Z. Y. Jin[2,†]

[1]*National Synchrotron Radiation Laboratory, University of Science and Technology of China, HeZuoHua South Road 42#, 230029, Hefei, P.R. China*
[2]*Archaeometry Lab, University of Science and Technology of China, JinZhai Road 96#, 230026, Hefei, P.R. China*
[3]*Shanghai Institute of Applied Physics, Chinese Academy of Sciences, 201204, Shanghai, P.R. China*

† Corresponding Co-authors: zyjin@ustc.edu.cn, zhypan@ustc.edu.cn

* This work was supported by the National Natural Science Foundation of China (No. 20701036, 10635060) and China Postdoctoral Science Foundation (No. 20070410222).

Abstract:

Due to its high spatial and elemental resolving power, synchrotron radiation x-ray fluorescence (SRXRF) imaging is particularly suitable to mapping distributions of elements with low concentration in a small area. This method has been widely used in chemistry, electronics, and material science [1,2]. Recently, it has also proved to be an effective and powerful technique to study archaeological samples [3,4].

A glass eye-bead dating to the Warring States Period (475 B.C to 221 B.C.) unearthed from the Danjiangkou site in Hubei Province, China, was studied by synchrotron radiation x-ray fluorescence imaging. The eye-bead sample shows a multi-layered structure: the body, the pupil, and the inlaid colored layers. Figure 1 is the optical micro-image of the sample, which is a patchwork due to the limitation of the field of view. The distribution information of Pb, Ba, Fe, and Hg elements is obviously viewed by their SR-XRF images. From Fig. 2, we can see that all five layers contain Ba, Hg is mainly distributed in the left blue layer and the right light brown layer, while Pb can be found only in the former and Fe is concentrated in the latter. This suggests that these compounds for the five layers come from the partly melted materials.

References:

[1] G. Martinez-Criado, A. Somogyi, A. Homs et al., Appl. Phys. Lett. **87**, 061913 (2005).
[2] M. Podgorczyk, W.M. Kwiatek, W.M. Zajac et al., X-Ray Spectrom. **38**, 557 (2009).
[3] M.J. Anjos, R.C. Barroso, C.A. Perez et al., Nucl. Instrum. Methods B **213**, 569 (2004).
[4] R.R. Martin, S.J. Naftel, A.J. Nelson et al., J. Archaeol. Sci. **34**, 936 (2007).

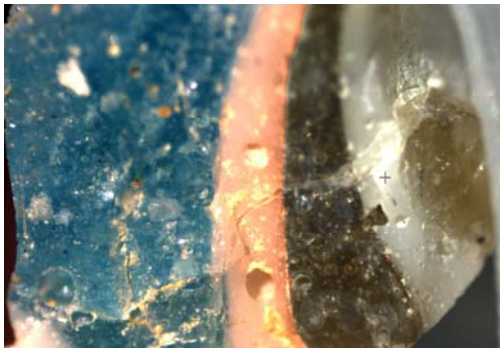

Figure 1: Optical image of ancient glass eye-bead (patchwork).

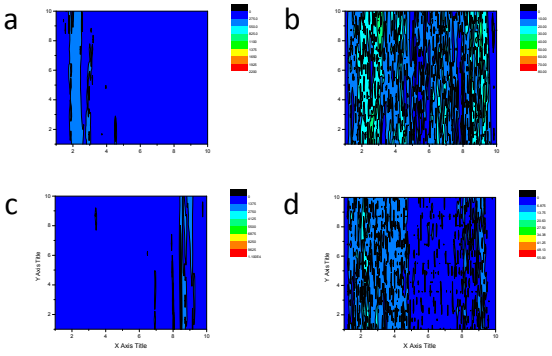

Figure 2: SR-XRF images for (a) Pb, (b) Ba, (c) Fe, and (d) Hg in ancient glass eye-bead.

Author Index

NOTES

NOTES

Welcome Reception — 3rd Floor (street level)

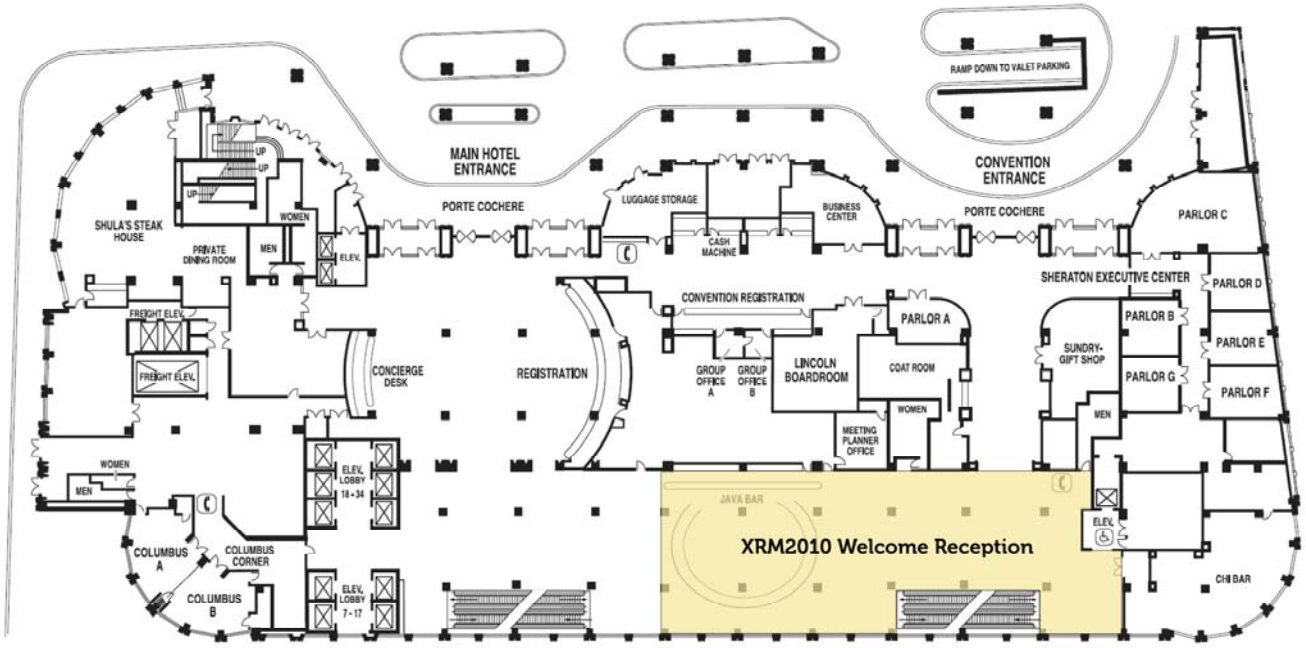

Registration Desk, Oral Talks, Posters, and Vendors — 4th Floor

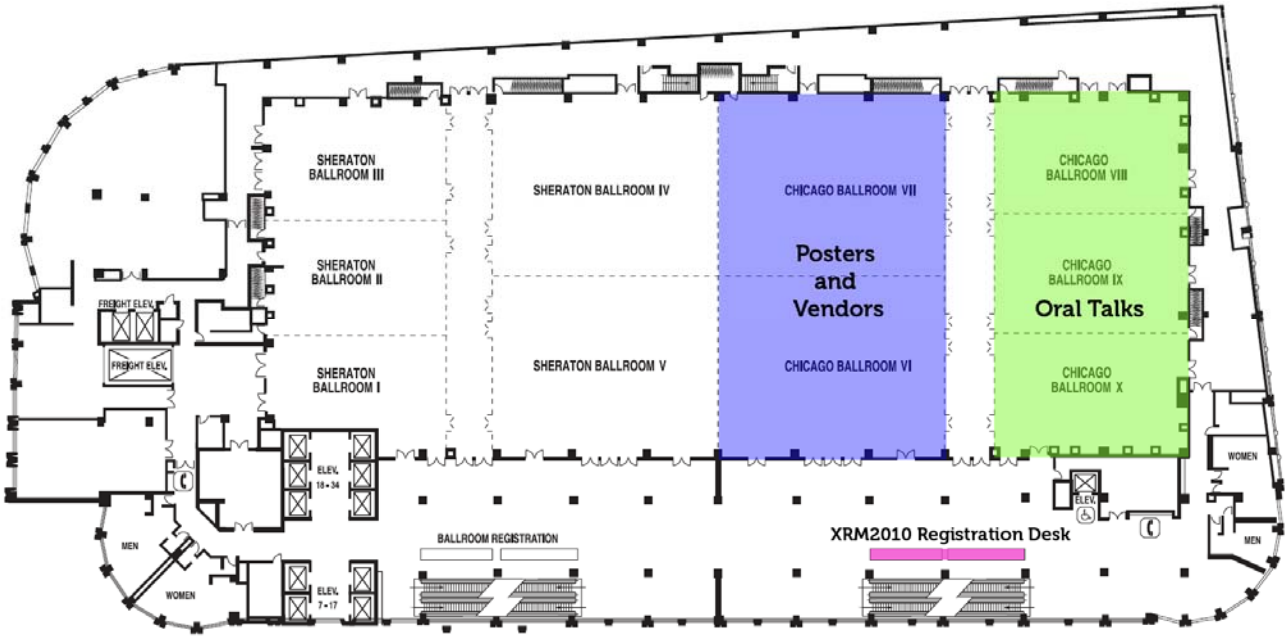

XRM 2010 Program-at-a-Glance

Welcome Reception—Sunday, August 15, 17:00-19:00, at the Sheraton Hotel and Towers

	Monday, August 16	Tuesday, August 17	Wednesday, August 18	Thursday, August 19	Friday, August 20
7:30	Registration	Registration	Registration		
8:15	**Opening and Welcome: Eric Isaacs** ◊				
8:30	**Mo1: X-ray Facilities, Instruments, and Optics I** ◊ **Chair: David Attwood** KAZUTO YAMAUCHI: Sub-10-nm Focusing of Hard X-rays Using Mirrors ANDERS HOLMBERG: Towards 10-nm Zone-Plate Fabrication **Takahisa Koyama**: Development of Multilayer Laue Lenses **Hanfei Yan**: Toward One-Nanometer Hard X-Ray Microscopy Using MLLs	**Tu1: X-ray Microscopy Methods I** ◊ **Chair: Janos Kirz** AMANDA PETFORD-LONG: Electron Microscopy of Nanomaterials **Jian Wang**: 3D Chemical and Elemental Imaging by STXM **David Paterson**: Ultrafast X-ray Fluorescence Microscopy **Andreas Scherz**: MAD Holography	**We1: X-ray Facilities, Instruments, and Optics III** ◊ **Chair: Peiping Zhu** WEILUN CHAO: Ultra-High-Resolution Soft X-ray Zone Plate Microscopy HONGJIE XU: X-ray Microscopy Beamlines at the SSRF **Andrea Somogyi**: The Nanoscopium Nanoprobe at Synchrotron Soleil **Burkhard Kaulich**: Nano and Life Sciences with TwinMic at Elettra	**Th1: Biological and Biomedical Science** ◊ **Chair: Chris Jacobsen** JOSE CARRASCOSA: X-ray and Electron Microscopy of Vaccinia Virus TANJA PAUNESCU: Elemental Mapping of Contrast Agents for Medical Imaging **Gang Li**: 3D Structures of the Oldest Found Embryo Fossils **Johannes Schittny**: Sub-micron Particles in Unstained Lung Parenchyma	**Fr1: Panel Discussion: Nanometer Resolution in X-ray Microscopy** ◊ **Chair: Qun Shen** **Panelists:** Christian David Chris Jacobsen Jörg Maser Hidekazu Mimura Keith Nugent Ian Robinson Christian Schroer Gayle Woloschak
10:20	Exhibits & Refreshments ‡	Exhibits & Refreshments ‡	Exhibits & Refreshments ‡	Exhibits & Refreshments ‡	Refreshments ‡
10:45	**Mo1 continues** ◊ **Chair: Mau-Tsu Tang** CHRISTIAN KNOECHEL: Correlative X-ray Tomography and Light Microscopy **Christian David**: Fabrication of Diffractive Optics for X-ray Sources **Timm Weitkamp**: X-ray Talbot Interferometry at ESRF	**Tu1 continues** ◊ **Chair: Murray Gibson** JOHANNA NELSON: X-ray Diffraction Microscopy of Frozen Hydrated Yeast **Klaus Giewekemeyer**: Lensless Biological Imaging with Waveguides **Fucai Zhang:** Wavefront Modulation Coherent Diffractive Imaging	**We2: X-ray Microscopy Methods III** ◊ **Chair: Günter Schmahl** BO HUANG: Pushing the Resolution Limit of Visible Light Microscopy **Lukas Helfen**: Holographic and Fluorescence Laminography for 3D Imaging	**Presentations for XRM 2012** ◊ **Vote for XRM 2012**	**Presider: Alan Michette** **WMI and Student** ◊ **award presentations** **XRM 2012 winner** **XRM2010 closeout**
11:40					
12:00	Lunch	Lunch	Lunch	Lunch	Box lunch pickup for tour
12:30					Buses depart for APS tour
13:00					
13:30	**Mo2: X-ray Facilities, Instruments, and Optics II** ◊ **Chair: Hans Hertz** STEFAN REHBEIN: Zone Plate Development at H-Z Berlin **Rajmund Mokso**: Following Dynamic Processes by X-ray Tomography **Ivan Vartaniants**: Coherence and CDI Experiments at FLASH	**Tu2: X-ray Microscopy Methods II** ◊ **Chair: Keith Nugent** ANDREAS MENZEL: Scanning Small-Angle X-ray Scattering of Bio Tissues **Christian Schroer**: Scanning Microscopy with Diffraction Contrast **Christian Holzner**: Scanning Hard X-ray Phase Contrast X-ray Microscopy	**We3a: X-ray Microscopy Meth. IV** § **Chair: Hyun-Joon Shin** **Luca Gregoratti**: Chemical Imaging of Nanodevices with SPEM **Gema Martinez-Criado**: Luminescence Imaging of Nano-LEDs **Paul Fenter**: Imaging Interfacial Topography and Reactivity **Marco Stampanoni**: Hard X-ray Phase-Contrast Nano-tomography **Chris Ryan:** Maia X-ray Detector Array at the Australian Synchrotron **We3b: Magnetism and Magnetic Materials** ¤ **Chair: Christoph Quitmann** MI-YOUNG IM: Imaging Spin States in Magnetic Nanostructures OLEG SHPYRKO: Probing Magnetic Domain Structure via CDI **Hendrik Ohldag**: Crystal and Magnetic Domains in Co/NiO(001) **Bartel Van Waeyenberge**: Vortex and Vortex Core Dynamics	**Th2a: Biological and Biomedical Science II** § **Chair: Sadao Aoki** JIM MCNALLY: 3D Cellular Fine Structure Resolved by TXM **Keith Nugent**: Cryo Transmission X-ray Imaging of the Malaria Parasite **Enju Lima**: Cryogenic Diffraction Microscopy for Biological Samples **Th2b: Materials and Condensed Matter** ¤ **Chair: Maya Kiskinova** EMIEL DE SMIT: *In situ* Nanoscale Chemical Imaging of Catalysts **Wilson Chiu**: Elemental Mapping of Solid Oxide Fuel Cells by TXM **Yu-chen Chen**: Dealloying and Coarsening of Nanoporous Gold	**APS Tour**
15:00	Exhibits & Refreshments ‡	Exhibits & Refreshments ‡	Exhibits & Refreshments ‡	Exhibits & Refreshments ‡	
15:30	**Mo2 continues** ◊ **Chair: Jean Susini** SASA BAJT: Multilayer-Based Optics for High-Brightness X-ray Sources **Fernando Brizuela**: Full-Field Microscope for EUVL Masks **Michael Bertilson**: Laboratory Soft X-ray Tomography of Cryo-Fixated Cells	**Tu2 continues** ◊ **Chair: Alan Michette** ANDREW PEELE: Fresnel Coherent Diffractive Imaging **Yukio Takahashi**: High-Resolution Hard X-ray Diffraction Microscopy **Stephan Hruszkewycz**: Coherent Bragg Diffraction via <100 nm Beams	**We4a: Emerging Fields** § **Chair: Graeme Morrison** ZIYU WU: Low-Dose Single-Step Method for Phase-Contrast Imaging ANTON BARTY: Femtosecond X-ray Imaging Using Free Electron Lasers **Marine Cotte**: Cultural Heritage Science at the ESRF **Akira Saito**: One-Nanometer-Scale Elemental Analysis by SR-STM **We4b: Environ., Earth, and Space** ¤ **Chair: Adam Hitchcock** ANNA BUTTERWORTH: STXM Analysis of Impact Tracks in Stardust Aerogel PAULO MONTEIRO: High-Resolution Imaging of Construction Materials **Joy Andrews**: Hard X-ray Imaging of Mercury Accumulation in Plants **Antonio Lanzirotti**: Fluorescence Tomography in Geo/Cosmo/Bio-chem	**Th2a continues** § **Chair: Gerd Schneider** PETER LAY: Application of XRM to Human Disease and Therapies **Martina Ralle**: Subcellular XFM of Metal-Induced Pathologies **Lydia Finney**: Visualizing a Role for Zinc in Stem Cell Differentiation **Th2b continues** ¤ **Chair: Michael Feser** ROSS HARDER: Coherent Diffraction Imaging of Strain on the Nanoscale **Jon Tischler**: Submicron-Resolution 3D Polychromatic Microdiffraction **Pice Chen**: Imaging and Structural Analysis of Ferroelectric Domains	
17:30	Poster Session 1 setup ‡ (all day)	Exhibits & Poster Session 1 ‡ (to 19:30)	Poster Session 2 setup (all day) ‡	Exhibits & Poster Session 2 ‡ (to 19:30)	Buses depart to Chicago
18:30			Banquet (to 22:00) – Navy Pier		Tour buses return

Location Key:

◊ **Chicago Ballrooms IX and X**

‡ **Chicago Ballrooms VI and VII**

§ **Chicago Ballroom VIII**

¤ **Chicago Ballroom X**